

ANNUAL REVIEW OF NUCLEAR SCIENCE

JAMES G. BECKERLEY, *Editor*
Schlumberger Well Surveying Corporation

ROBERT HOFSTADTER, *Associate Editor*
Stanford University

LEONARD I. SCHIFF, *Associate Editor*
Stanford University

VOLUME 7

1957

PUBLISHED BY
ANNUAL REVIEWS, INC.
IN CO-OPERATION WITH THE
NATIONAL RESEARCH COUNCIL
OF THE NATIONAL ACADEMY OF SCIENCES

ON SALE BY
ANNUAL REVIEWS, INC.
PALO ALTO, CALIFORNIA, U.S.A.

Engin. Library

QC
770
.A65
V.7

ANNUAL REVIEWS, INC.
PALO ALTO, CALIFORNIA, U.S.A.

© 1957 BY ANNUAL REVIEWS, INC.
ALL RIGHTS RESERVED

Library of Congress Catalog Card Number: 53-995

FOREIGN AGENCY

Maruzen Company, Limited, 6
Tori-Nichome Nihonbashi, Tokyo

PRINTED AND BOUND IN THE UNITED STATES OF AMERICA BY
THE GEORGE BANTA COMPANY, INC.

PREFACE

The present volume begins with mesons and ends with mesons. The hundred pages devoted to mesons reflect in part the fact that no specific review of meson work has been presented since Volume 4 of this series; they also reflect the "ripeness" of the topic for review. (In fact, a book based on the last chapter will appear next year.)

Similarly, the allocation of almost a third of the present volume to high-energy electron reactions and to collective model theories for nuclei indicates the state of these respective fields of endeavor. We believe that these chapters are timely and that the number of pages is justified by the significance of the reviewed material.

The balance of the present volume is more nearly consistent with the pattern of previous volumes. In view of the recent accumulation of a great mass of data on moments and spins of radioactive isotopes, a lengthy chapter on this subject has been included. Short chapters on radiochemical separations and associated equipment, as well as a longer chapter on high-energy particle reactions, conclude the coverage of physical science topics.

Radiobiology chapters include an extensive review of biochemical effects arising from exposure to ionizing radiation as well as reviews of lethal actions and the pathology of radiation exposure. As in past volumes, the extensive activities of the cellular radiobiologists are reviewed.

The chapters of this volume have been produced as a consequence of lengthy and devoted labor by the individual authors. We appreciate these efforts and believe the resulting volume is of commensurate value.

The patience and capabilities of the Editorial Assistant, Mrs. Tove Hunchar, are gratefully acknowledged.

* * *

The Committee notes with deep regret the untimely death of Dr. Alberto F. Thompson in Washington on June 18, 1957. As recorded in the preface to Volume 1 of this series, Dr. Thompson was the principal individual responsible for founding the *Annual Review of Nuclear Science*. This effort, as well as his leadership in technical information work for the Atomic Energy Commission and the National Science Foundation, is evidence of Dr. Thompson's substantial and valuable public service.

J.G.B.
C.L.C.
L.F.C.
T.P.K.
E.S.
R.E.Z.



CONTENTS

	PAGE
MU-MESON PHYSICS, <i>J. Rainwater</i>	1
RADIOCHEMICAL SEPARATIONS BY ION EXCHANGE, <i>K. A. Kraus and F. Nelson</i>	31
EQUIPMENT FOR HIGH LEVEL RADIOCHEMICAL PROCESSES, <i>N. B. Garden and E. Nielsen</i>	47
CELLULAR RADIobiology, <i>E. L. Powers</i>	63
BIOCHEMICAL EFFECTS OF IONIZING RADIATION, <i>B. E. Holmes</i>	89
VERTEBRATE RADIobiology (LETHAL ACTIONS AND ASSOCIATED EFFECTS), <i>V. P. Bond and J. S. Robertson</i>	135
VERTEBRATE RADIobiology (THE PATHOLOGY OF RADIATION EXPOSURE), <i>C. C. Lushbaugh</i>	163
THE COLLECTIVE MODEL OF NUCLEI, <i>F. Villars</i>	185
NUCLEAR AND NUCLEON SCATTERING OF HIGH-ENERGY ELECTRONS, <i>R. Hofstadter</i>	231
COLLISION OF ≤ 1 BEV PARTICLES (EXCLUDING ELECTRONS AND PHOTONS) WITH NUCLEI, <i>S. J. Lindenbaum</i>	317
THE MEASUREMENT OF THE NUCLEAR SPINS AND STATIC MOMENTS OF RADIOACTIVE ISOTOPES, <i>W. A. Nierenberg</i>	349
HYPERONS AND HEAVY MESONS (SYSTEMATICS AND DECAY), <i>M. Gell-Mann and A. H. Rosenfeld</i>	407

Annual Reviews, Inc., the National Research Council, and the Editors of this publication assume no responsibility for the statements expressed by the contributors of this *Review*.

MU-MESON PHYSICS¹

By J. RAINWATER

Department of Physics, Columbia University, New York, New York

INTRODUCTORY SURVEY OF NEW DEVELOPMENTS

Earlier summaries of μ -meson interactions and properties are given in references (1 to 7). We shall confine our attention in this paper principally to recent developments. The most exciting development in this field is but a few months old at the time of this writing. It is the experimental verification by Garwin, Lederman & Weinrich (8) of the predictions of Yang & Lee (9a) of the polarization of μ -mesons with respect to their emission direction following $\pi^\pm \rightarrow \mu^\pm + \nu$ decay, and of the front-back anisotropy of the electrons with respect to muon spin direction on $\mu^\pm \rightarrow e^\pm + \nu + \bar{\nu}$ decay. The same theory seems to have been independently formulated by Landau (9b) and by Salam (9c), but their work was not known to the experimental groups until after the basic discoveries had been made. The meson experiments were preceded and inspired by the success of Wu, *et al.* (10) on the observation of a front-back asymmetry in the electron emission from magnetically polarized super-cooled Co⁶⁰ nuclei. The effects are now subject to very concentrated experimental study by many different groups and the experimental situation should be greatly clarified by the time this article appears in print. At the time of this writing the *Bulletin of the American Physical Society* for the 1957 Washington meeting has announced that Session M (11) is to be devoted to contributed papers on this subject, and Session N is devoted to a Symposium of invited papers on the subject of parity nonconservation.

The observed effects in π and μ decay require that the final states should not be eigenstates of either the parity operator P , or the charge conjugation operator C . So far as is now known, however, they can be eigenstates of the product CP of the two, which is related (12) to the time reversal operator T of Wigner. The predictions of Lee & Yang relating to μ -mesons came from an extension of their earlier work relating to the puzzling K-meson ($\tau - \theta$) problem, where they assume the existence of mixed parity states for such particles (13, 14). In particular they consider the possibility that the weak Fermi-type interactions involve the breakdown of parity invariance in a manner similar to that where the electromagnetic interaction involves a breakdown of strict charge independence for the strong couplings. In treating the $\pi \rightarrow \mu + \nu$ decay, and the nuclear and muon beta decay process, they have mainly considered the two component neutrino theory (9, 15). This extremely simple (and therefore esthetically favored) model for the neutrino had been discussed by Pauli (15) in 1933, but had been generally rejected on the ground that it did not give eigenstates of the parity operator. Parity conservation had been generally assumed to be one of the most sacred of the

¹ The survey of literature pertaining to this review was completed in April, 1957.

general invariance principles for theories of fundamental particles. The theory requires that the neutrino spin (axial vector) always be parallel to its momentum (polar vector), and the antineutrino spin always be antiparallel to its momentum. The parity operator leaves a neutrino as a neutrino and reverses the momentum, but not the spin, to give a nonallowed state (with similar results for the antineutrino). The theory could have reversed the definition of neutrino and antineutrino, but this choice, combined with the principle of conservation of light particles, fits the observed beta decay experiment asymmetry for $n + \nu \rightarrow p + e^-$. The charge conjugation operator changes a neutrino to an anti-neutrino without changing the spin or momentum directions, which again leads to a nonallowed state.

Many consequences of the existence of polarized μ -meson beams and the front-back $\mu \rightarrow e + \nu + \bar{\nu}$ decay anisotropy are being rapidly exploited. Perhaps the most important of these is the possibility of a high precision measurement of the magnetic moment of the μ -meson. The μ -mesonic x-ray spectra in $2p \rightarrow 1s$ transitions in lead of Fitch & Rainwater (16) required that the moment be within ~ 15 or 20 per cent of the Dirac value since any anomalous part would give a double strength contribution to the fine structure splitting of the $2p$ level. The initial experiments of Garwin, Lederman, & Weinrich (8) consisted of stopping μ^+ mesons in a carbon block and viewing the decay electrons with a counter telescope at $\sim 90^\circ$ to the incoming beam direction. They used a delayed coincidence gate of 1.25 μ sec. duration starting 0.75 μ sec. after the incident meson traversed the initial telescope. By applying a magnetic field of variable strength perpendicular to the horizontal plane of the two telescopes, the μ -meson spin could be caused to rotate through variable mean angles in the horizontal plane. The counting rate showed an oscillatory variation with respect to applied field, from which it was determined that the gyromagnetic ratio must be 2.00 ± 5 per cent. Later preliminary experiments by Garwin and his co-workers, (17) give $g = (2.0064 \pm 0.005)$ using a resonance radio frequency flipping field. This agrees with the predicted value for only electromagnetic effects; $g = 2[1 + \alpha/2\pi - 1.89\alpha^2/\pi^2]$, given independently and simultaneously by Suura & Wichmann (18a) and by Petermann (18b).

The front-back asymmetry should increase with increasing positron energy. This increase has been seen by Coffin, *et al.* (11) using different thicknesses of graphite between the counters in the final telescope. A large liquid scintillation telescope and pulse height analyser were used by Rainwater, Edelstein, & Frati (unpublished) in cooperation with the above group to replace the final detection telescope for the positrons. The asymmetry was observed as a function of pulse height in the final large liquid scintillator to try to detect the energy dependence of the asymmetry. Both experiments to date have shown a maximum asymmetry ratio of ~ 3.0 to 4.0 at the high energy end and a minimum asymmetry of ~ 1.3 in the same direction at lower energies. The two component theory predicts a unique result corresponding to a reversal of the sense of the asymmetry at low energies. The

effect of bremsstrahlung complicates the experimental measurement of this effect since it tends to degrade the energy of the more energetic positrons and thus "dilute" the contribution of the less abundant low energy positrons with a high energy type asymmetry contribution.

An additional recent development has been the relatively precise determination of the charged π and μ -meson masses using the precise mesonic x-ray results for the lower limit on the μ -mass and the upper limit on the π -mass, with the μ -meson range in the $\pi^+ \rightarrow \mu^+ + \nu$ decay determining the $\pi - \mu$ mass difference. Koslov, Fitch, & Rainwater (19) found that $3d \rightarrow 2p$ μ -mesonic x-rays for phosphorus are of energy above the lead K absorption edge. Stearns, *et al.* (20) found that the $4f \rightarrow 3d$ π -mesonic x-ray energy for aluminum lies below the energy of the K absorption edge for antimony. When these transition energies are computed taking account of all known effects, including vacuum polarization, the K absorption edge energies determine limits on the meson masses. In a recent review of this subject, Cohen, Crowe, & Du Mond (21) evaluate these limits as $(206.77 \pm 0.04) m_e$ for the lower limit on the μ -meson mass, and $(273.51 \pm 0.04) m_e$ as the upper limit on the π -mass. This difference $(m_\pi - m_\mu) \leq (66.74 \pm 0.06) m_e$ may be compared with the result of Barkas, Birnbaum, & Smith (22) $(m_\pi - m_\mu) = (66.41 \pm 0.07) m_e$. Cohen, Crowe, & Du Mond place a larger uncertainty of $0.10 m_e$ on $(m_\pi - m_\mu)$. Since the upper limit for $(m_\pi - m_\mu)$ is very close to the directly measured value, Cohen, Crowe, & Du Mond select the values

$$m_\pi = (273.34 \pm 0.13) m_e$$

$$m_\mu = (206.93 \pm 0.13) m_e$$

assuming that the positive and negative mesons of each type have identical masses. The directly determined mass values of Barkas *et al.* (22) are

$$m_{\pi^+} = (273.3 \pm 0.2) m_e$$

$$m_{\pi^-} = (272.8 \pm 0.3) m_e$$

$$m_\mu^+ = (206.9 \pm 0.2) m_e$$

Cohen, Crowe, & Du Mond select as final weighted values, assuming exact mass equality for positive and negative mesons,

$$m_\pi = (273.25 \pm 0.12) m_e$$

$$m_\mu = (206.84 \pm 0.12) m_e$$

This value is a weighted average of the above experimental results plus the result $m_{\pi^-} = (272.74 \pm 0.40) m_e$ determined by Crowe & Phillips (23) in 1954 from a measurement of the energy of the π^- meson capture gamma in hydrogen.

Another indication that the μ -meson behaves as a normal charged Dirac spin $\frac{1}{2}$ particle is provided by the measurements of Masek, Lazarus, & Panofsky (24) on the pair production cross section in aluminum and lead using 600 Mev bremsstrahlung. Rawitscher (25) finds that the experimental results, when analysed to test the maximum anomalous moment $\mu = (1 + \lambda)e\hbar/2 mc$

RAINWATER

requires that $-0.4 < \lambda < 0.2$. The smallness of the cross section for Pb is interpreted as providing information that the nuclear scattering of fast μ -mesons is much smaller than Coulomb scattering by a point nucleus. This latter observation is relevant to the experiments on the anomalous scattering of high energy cosmic ray μ -mesons. Cooper & Rainwater (26) reviewed the experimental results prior to 1955. Subsequent measurements of Lloyd & Wolfendale (27) support the results of McDiarmid (28) in indicating that the large angle multiple scattering distribution corresponds much more closely to that expected for point, rather than extended nuclei. The anomalous term goes as Z^2 , which suggests that it is a coherent effect. Fowler (29) has recently suggested that the inelastic (incoherent) processes in the interaction of fast μ -meson with nuclei may alter the elastic scattering enough to account for the observations without invoking strong interactions of μ -mesons with nuclei of other than electromagnetic origin.

Hirokawa, Kamori, & Ozawa (30) have recomputed the expected results for the frequency of high energy bursts due to the extremely high energy μ -mesons in cosmic rays. They obtain predicted results for spin $\frac{1}{2}$ which are only slightly different from those of Christy & Kusaka (31). They are in excellent agreement for spin $\frac{1}{2}$ with no anomalous moment, while there is appreciable disagreement for the anomalous term $|\lambda| \leq 0.6$. Since the fractional correction for $\lambda \neq 0$ has its leading term vary as λ^2 , a result $|\lambda| \leq 0.3$ is indicated. Coupled with the recent r.f. resonance spin flip experiment which shows that $|\lambda| < 0.006$, this may be taken as a confirmation of the burst theory for spin $\frac{1}{2}$ particles.

George & Evans (32) have studied the stars produced in nuclear emulsions underground due to penetrating μ -mesons. These and many other experiments investigating the moderate energy inelastic interactions of μ -mesons with nuclei have been analysed using the semi-classical Williams-Weizsäcker method of virtual photons, which gives results in order of magnitude agreement with experiment. Recently Fowler (33) gave arguments to show that the Williams-Weizsäcker method should not be valid, and estimated that a proper treatment would give appreciably smaller predicted cross sections. This conclusion has been disputed by Kessler & Kessler (34) who reach the following conclusions:

We have thus shown that the application of the Williams-Weizsäcker method to the present problem agrees with the field theoretic point of view in the sense of (their derived equation) and the subsequent discussion. Needless to say this method is valid for any electromagnetic interaction of a relativistic fermion.

George's interpretation of the nuclear interaction of μ -mesons seems therefore to be correct, as the predicted and experimental cross sections are in fairly good agreement, and there is no need for the introduction of a new kind of interaction of the μ -meson with the nucleus.

There is agreement of the nuclear size predictions, assuming only electromagnetic interactions, from the measurements of Fitch & Rainwater (16) of

the $2p-1s$ transition energy for a μ^- -meson about a lead nucleus, and the Stanford electron scattering results. This shows that there is no large anomalous nuclear interaction in that case, even though the μ -meson K orbit is largely inside the nucleus.

In addition to the μ -meson interactions mentioned above, there are additional processes involving μ -mesons in weak coupling interactions. These include the studies of Steinberger and his students of the upper limit for the frequency of occurrence of competing processes that might be expected to occur. These various results are discussed in the following sections.

Alvarez, *et al.*, (35) recently reported a very interesting and unexpected nuclear reaction in which μ^- -mesons stopping in a liquid hydrogen bubble chamber catalyzed the nuclear fusion reactions $H+D+\mu^- \rightarrow He^3 + \mu^-$ and $D+D \rightarrow H^3 + H^1$. A ten in. liquid hydrogen bubble chamber was exposed in a magnetic field of 11,000 gauss to stopping K^- mesons from the Berkeley Bevatron. The beam contained a large μ^- -meson contamination and 2500 μ^- -meson stopping were observed in 75,000 photographs. The μ^- -meson stoppings could be distinguished from π^- -meson stoppings from the curvature in the magnetic field of the last-10 cm. of path. In 15 cases a μ^- -meson came to rest and then gave rise to a secondary negative particle of 1.7 cm. range (a 4.1 Mev μ -meson from $\pi \rightarrow \mu + \nu$ decay has 1.0 cm. range) which subsequently decayed by emitting an electron. The energy distribution of the electron energies was just that expected from μ decay. Assuming that the secondary particle was the μ -meson ejected in an Auger (or K capture) process following catalysis of the reaction $D+H \rightarrow He^3$, the meson's kinetic energy of 5.4 Mev is the amount expected from the energy release in the reaction. The hypothesis is that the μ^- -meson is initially captured into a K orbit about a proton (orbit radius \approx Bohr electron radius/186) and this neutral system drifts until the μ -meson decays, or until the system encounters a deuteron. The reduced mass effect on the meson binding is 135 ev larger for $D^++\mu^-$ than for $H^++\mu^-$ so the D robs the μ^- from the H and this new system drifts until the next event. This may be the μ -decay, or a $D-\mu-H$ molecular ion may form. This structure places the D and H about 200 times closer than for an ordinary hydrogen molecular ion and seems to lead to a large probability for induced fusion. The authors (35) have performed this experiment with natural hydrogen (0.02 per cent D), a mixture having 0.3 per cent D, and a mixture having 4.3 per cent D. For each of the three cases the number of observed fusion reactions and free μ^- -decays were as follows: (a) normal hydrogen showed 15 fusions for 2541 decays (0.6 per cent), (b) the 0.3 per cent enriched mixture showed 57 fusions for 2950 decays (2 per cent), (c) the 4.3 per cent enriched mixture showed 32 fusions for 1269 decays (2.5 per cent). In addition a few events $D+D \rightarrow H^3 + H^1$ were observed, and one event where a μ^- catalysed the $He^3 + \mu^-$ twice for the more highly concentrated deuterium mixture. If the μ^- -meson were not an unstable particle, or if its lifetime were several orders of magnitude larger

than is the case, this process might be the answer to the practical exploitation of nuclear fusion for power purposes. As it is, however, it seems only to represent an intriguing effect of no commercial application.

THE $\pi \rightarrow \mu + \nu$ AND $\mu \rightarrow e + \bar{\nu}$ PROCESSES

In the ordinary theory of nuclear beta decay (36) the interaction Hamiltonian can be written as

$$H_{\text{int.}} = \sum_m (\psi_p^\dagger \gamma_4 O_{Hm} \psi_n) (C_m \psi_e^\dagger O_{Lm} \psi_\nu) + \text{conj. comp.} \quad 1.$$

where O_{Hm} and O_{Lm} are similar Dirac operators for the nuclear (written here for one neutron \rightarrow proton) and the electron-neutrino fields. $m = 1, 2, 3, 4, 5$ for the interactions S, V, T, A, P which have O_m respectively of the form 1, $\gamma_\mu - (i/2\sqrt{2})(\gamma_\mu\gamma_\nu - \gamma_\nu\gamma_\mu)$, $-i\gamma_\mu\gamma_5$ and γ_5 . The fermion Hamiltonian for no interactions is taken, for each field separately, as

$$H_0 = \alpha \cdot \vec{p} + \beta m \quad (\hbar = c = 1) \quad 2.$$

If σ is the 2×2 Pauli spin matrix, the usual representation has

$$\alpha = \begin{pmatrix} 0 & \sigma \\ \sigma & 0 \end{pmatrix}, \quad \alpha_4 = i \quad 3a.$$

$$\beta = \begin{pmatrix} 1 & 0 \\ 0 & -1 \end{pmatrix} \quad 3b.$$

$$\gamma = -i\beta\alpha, \quad \gamma_4 = \beta \quad 3c.$$

$$\gamma_5 = \gamma_1\gamma_2\gamma_3\gamma_4 = - \begin{pmatrix} 0 & 1 \\ 1 & 0 \end{pmatrix} \quad 3d.$$

For a plane wave state $e \exp. i\vec{p} \cdot \vec{r}$ the space dependence is multiplied by a column vector to give

$$\psi_1 = N \begin{pmatrix} E + m \\ 0 \\ p_z \\ p_+ \end{pmatrix} e^i \exp. i\vec{p} \cdot \vec{r} \text{ for } E > 0, \quad \sigma_z = 1/2 \text{ (N.R.)} \quad 4a.$$

$$\psi_2 = N \begin{pmatrix} 0 \\ E + m \\ p_- \\ -p_z \end{pmatrix} e^i \exp. i\vec{p} \cdot \vec{r} \text{ for } E > 0, \quad \sigma_z = -1/2 \text{ (N.R.)} \quad 4b.$$

$$\psi_3 = N \begin{pmatrix} -p_z \\ -p_+ \\ m \\ |E| + 0 \end{pmatrix} e^i \exp. i\vec{p} \cdot \vec{r} \text{ for } E < 0, \quad \sigma_z = 1/2 \text{ (N.R.)} \quad 4c.$$

$$\psi_4 = N \begin{pmatrix} -p_- \\ p_z \\ 0 \\ |E| + m \end{pmatrix} e^i \exp. i\vec{p} \cdot \vec{r} \text{ for } E < 0, \quad \sigma_z = -1/2 \text{ (N.R.)} \quad 4d.$$

where $p_+ = p_x + i p_y$ and $p_- = p_x - i p_y$ and (N.R.) means nonrelativistic. In their paper (13) "Question of Parity Conservation in Weak Interactions," June 1956, Lee & Yang suggest that the interaction operator should be modified in the electron neutrino part by replacing $C_m \psi_s \gamma_5 O_{Lm} \psi$, with

$$\psi_s \gamma_5 O_{Lm} (C_m + C'_m \gamma_5) \psi, \quad 5.$$

where the extra application of the odd parity operator γ_5 gives a mixture C_m of ordinary parity and C'_m of opposite parity. If time reversal invariance is preserved in β decay, all of the C_m and C'_m are real. In their later paper (9) Lee & Yang essentially choose $C'_m = -C_m$ to give a maximum front-back asymmetry in the decay of a polarized nucleus. This gives results the same as for the two component theory with right hand screw neutrinos. The alternate choice for a two component neutrino theory is $C'_m = C_m$ to have the neutrino behave as a left hand screw. This is seen by setting $m = p_x = p_y = 0$ and $|E| = |p_z|$ in equations 4a-d. For p_z positive the operator $(1 - \gamma_5)$ on ψ_1 gives 2ψ , while $(1 - \gamma_5)\psi_2 = 0$. An antineutrino with momentum p_z and E positive corresponds to an empty negative energy state having p_z and E negative. For this case $(1 - \gamma_5)\psi_3 = 2\psi_3$ while $(1 - \gamma_5)\psi_4 = 0$. Thus the negative energy state has $\sigma_z = \frac{1}{2}$ (opposite to p_z). The corresponding antineutrino has positive p_z and $\sigma_z = -\frac{1}{2}$ (again opposite to p_z). Instead of having $(1 - \gamma_5)$ operate to the right on ψ_s , it can be made to operate to the left on ψ_s . γ_5 anticommutes with each γ_μ . Thus for interactions S, T, and P, we have $\gamma_5 O_{Lm} (1 - \gamma_5) = (1 + \gamma_5) \gamma_5 O_{Lm}$, while for V and A we have $\gamma_5 O_{Lm} (1 - \gamma_5) = (1 - \gamma_5) \gamma_5 O_{Lm}$. Operating to the left, $(1 - \gamma_5)$ again produces a state having only spin parallel to the momentum.

To obtain the simpler form of the two component theory we note that equation 2 for $m \neq 0$ requires a set of four anticommuting operators (α, β). For $m = 0$, however, only three anticommuting operators are required and the Pauli spin matrices are known to form such a set. Thus one can try the form (15, 9)

$$H = \mathbf{d} \cdot \mathbf{p} \quad 6.$$

This has \mathbf{d} parallel to \mathbf{p} for the positive energy state ($E = p$) and \mathbf{d} antiparallel to \mathbf{p} for the negative energy state. This two component theory can also be expressed using four component state vectors and 4×4 operators. The operators of equation 3a-d are for a representation diagonal in σ_z and β . Lee & Yang (9) choose a representation diagonal in σ_z and α_z .

$$\alpha = \begin{pmatrix} \mathbf{d} & 0 \\ 0 & -\mathbf{d} \end{pmatrix}, \quad \alpha_4 = \quad 7a.$$

$$\beta = \begin{pmatrix} 0 & 1 \\ 1 & 0 \end{pmatrix} \quad 7b.$$

$$\gamma = -i\beta\alpha, \quad \gamma_4 = \beta \quad 7c.$$

$$\gamma_5 = \gamma_1 \gamma_2 \gamma_3 \gamma_4 = \begin{pmatrix} -1 & 0 \\ 0 & 1 \end{pmatrix} \quad 7d.$$

For the Hamiltonian of equation 2 this gives as the states corresponding to those of equations 4a-d.

$$\psi_1 = N \begin{pmatrix} E + p_z \\ p_+ \\ m \\ 0 \end{pmatrix} e \exp. ip \cdot r \text{ for } E > 0, \quad \sigma_z = 1/2 \text{ (N.R.)} \quad 8a.$$

$$\psi_2 = N \begin{pmatrix} 0 \\ m \\ -p_- \\ E + p_z \end{pmatrix} e \exp. ip \cdot r \text{ for } E > 0, \quad \sigma_z = -1/2 \text{ (N.R.)} \quad 8b.$$

$$\psi_3 = N \begin{pmatrix} -m \\ 0 \\ |E| + p_z \\ p_+ \end{pmatrix} e \exp. ip \cdot r \text{ for } E < 0, \quad \sigma_z = 1/2 \text{ (N.R.)} \quad 8c.$$

$$\psi_4 = N \begin{pmatrix} -p_- \\ |E| + p_z \\ 0 \\ -m \end{pmatrix} e \exp. ip \cdot r \text{ for } E < 0, \quad \sigma_z = -1/2 \text{ (N.R.)} \quad 8d.$$

These correspond to electron or μ -meson plane wave states. For the neutrino states the added requirement $\gamma_5 \psi_\nu = -\psi_\nu$ makes $\mathbf{d} \cdot \mathbf{p}$ equivalent in its effect to $\mathbf{\alpha} \cdot \mathbf{p}$.

For a neutrino with \mathbf{p} in the $+z$ direction only states corresponding to ψ_1 and ψ_4 are used.

$$\psi_{1\nu} = \begin{pmatrix} 1 \\ 0 \\ 0 \\ 0 \end{pmatrix} e \exp. ipz \text{ for } E > 0, \quad \sigma_z = 1/2 \quad 9a.$$

$$\psi_{4\nu} = \begin{pmatrix} 0 \\ 1 \\ 0 \\ 0 \end{pmatrix} e \exp. ipz \text{ for } E < 0, \quad \sigma_z = -1/2 \quad 9b.$$

A final state antineutrino has its energy, momentum, and spin equal but opposite to those of the empty negative energy state.

In $\pi \rightarrow \mu + \nu$, the π has spin zero and the relative motion orbital angular momentum must be zero, or be perpendicular to their line of emission. Thus the μ and ν (or $\bar{\nu}$) must both have their spins parallel to their motion if ν , or both antiparallel if $\bar{\nu}$. If one assumes conservation of light particles, then either μ^+ or μ^- can be taken as the particle. Three possible choices for μ^- decay are

$$\mu^- \rightarrow e^- + \nu + \bar{\nu} \quad 10a.$$

$$\mu^- \rightarrow e^- + 2\bar{\nu} \quad 10b.$$

$$\mu^- \rightarrow e^- + 2\nu \quad 10c.$$

Equation 10a treats μ^- and e^- as the particles and μ^+ as an antiparticle. Equation 10b treats μ^- as the antiparticle and μ^+ and ν as particles. Equation 10c treats μ^- and ν as antiparticles, where $\bar{\nu}$ is defined to be the left hand screw particle. Equation 10b and 10c can be ruled out on the grounds that the predicted Michel parameter (37) $\rho = 0$ for the shape of the electron energy spectrum. The experimental results indicate $\rho > 0.5$. The predicted spectrum shape for Equation 10a has $\rho = 0.75$, which is slightly higher than the experimental results, but which is probably not inconsistent with them when one notes that systematic errors (such as bremsstrahlung effects) would probably tend to make the experimental ρ values too small.

If equation 10a is accepted as correct, then the μ^- is the particle and the μ^+ the antiparticle. The question still remains as to whether ν or $\bar{\nu}$ is the particle for the neutrino field. Since the choice for ν was taken to agree with the result for nuclear beta decay, one should probably take

$$\pi^+ \rightarrow \mu^+ + \nu \quad 11a.$$

and

$$\pi^- \rightarrow \mu^- + \bar{\nu} \quad 11b.$$

in which case the μ^+ from the decay of a π^+ at rest has its spin parallel to its motion, while a μ^- would have its spin anti-parallel to its motion. For equation 10a Lee & Yang (9) chose the charge retention form of the interaction

$$H_{\text{int.}} = f_v(\psi_v^\dagger \gamma_5 O_A \psi_\mu)(\psi_\nu^\dagger \gamma_5 O_A \psi_\nu) + f_A(\psi_v^\dagger \gamma_5 O_A \psi_\mu)(\psi_\nu^\dagger \gamma_5 O_A \psi_\nu) + \text{conj. comp.} \quad 12.$$

since S, T, and P type couplings cannot contribute in this case. Professor Lee has pointed out that this is the most general form for the choice of the interaction using their two component theory. If a coupling scheme

$$\sum_i C_i (\psi_v^\dagger \gamma_5 O_i \psi_\nu)(\psi_\nu^\dagger \gamma_5 O_i \psi_\mu) + \text{conj. comp.}$$

were used instead, the coefficients C_i in either scheme are definite linear combinations of those in the other scheme, so that the net effect of using a different scheme is to feature different couplings, with no change in the final result. Such a change might be desired if one wanted to fit all weak interactions using a common Universal Fermi interaction.

For a μ^- meson at rest with $\sigma_z = +\frac{1}{2}$, the electron distribution is given by (9)

$$dN = 2x^2[(3 - 2x) + \xi \cos \theta(1 - 2x)]dx d\Omega_e (4\pi)^{-1} \quad 13.$$

where

- $x =$ the ratio of the electron's momentum p to p_{\max}
- $\theta =$ electron emission angle with respect to the muon spin direction
- $\xi = (f_v f_A^* + f_A f_v^*) (|f_v|^2 + |f_A|^2)^{-1}$

The total decay probability per unit time is

$$\text{Rate} = m^6(|f_A|^2 + |f_v|^2)/(3 \cdot 2^8 \pi^2) \quad 15.$$

where m = meson mass. The experimental results are consistent with $f_A = -f_v$. Both are real if T invariance holds. For nonpolarized muons the expectation value of $\cos \theta$ is zero for any electron direction, so the term involving $\cos \theta$ in equation 13 becomes zero to give the shape $x^2(3-2x)$ for the electron spectrum. For completely polarized muons the angular distribution for electrons of energy E is of the form $(1+a \cos \theta)$, where $|a|$ is a maximum for $x=1$ (the upper end of the spectrum) where $\alpha = -\xi$. For $x=\frac{1}{2}$ the asymmetry parameter is zero, and for $x < \frac{1}{2}$ it changes sign, reaching a maximum value $\alpha = \xi/3$ for $x=0$. For the integrated spectrum $\alpha = -\xi/3$. If the peak to valley ratio is taken for $\theta = 0^\circ$ and 180° , this ratio is $(1+|\xi|)(1-|\xi|)^{-1}$ at $x=1$, and is $(1+|\xi|/3) \cdot (1-|\xi|/3)^{-1}$ for $x=0$ and also for the integrated spectrum.

The measurements (8, 17, 18) using the μ^+ mesons from the Nevis Cyclotron show a maximum for emission in a direction opposite to the motion of the μ^+ . For the electron detection telescope in the horizontal plane at 100° with respect to the incident meson direction, and using a one in. thick graphite stopping target for the μ^+ mesons, decay positrons were counted between 0.75 and 2.00 μ sec following the arrival of the μ^+ meson. The carbon block has a solenoidal winding to produce a variable vertical magnetic field within the graphite. A double shield of sheet iron removed the main effects of the cyclotron fringing magnetic field. The counting rate at the electron telescope as a function of current in the coil is shown in Figure 1. The peak rate at 0.19 amps. corresponds to a condition where the meson moment precessed through $180^\circ - 100^\circ = 80^\circ$ during a time of $\sim 1.3 \mu$ sec after the meson was stopped. If the time gate width were sufficiently small relative to the delay, and if all stopping mesons in the target were in an effective field of the same strength, Figure 1 would be expected to show a continuing sinusoidal oscillation as a function of vertical magnetic field. The large fractional spread in time delays accepted has the effect of making the amplitude decay with increasing cycles of net precession. The solid curve of Figure 1 is the predicted curve for $\alpha = -\frac{1}{3}$ after taking account of the above effect and the effect of the angular spread of the telescope. The direction of precession was established by changing the angle of the positron telescope and noting the direction of shift of the resulting curve relative to that of Figure 1. The analysis showed that the precession was that expected for $\alpha \approx -\frac{1}{3}$ and the normal value for the moment. Since $|\xi| \leq 1$ in Equation 14, and $\alpha = -\xi/3$ for the integrated spectrum, this indicates that essentially the maximum possible integrated spectrum asymmetry was obtained. For μ^+ the sign of ξ in terms of f_v and f_A is reversed. Therefore, (a) $-f_v \approx f_A$ is required and the result is consistent with both f_v and f_A being real and of opposite sign and (b) the μ^+ beam must be very nearly 100 per cent polarized. (f_v and f_A must be real if time reversal invariance holds.)

It is far from obvious why the muons should be almost 100 per cent polarized in these experiments. Without prior knowledge of the experimental observation, in fact, it is not hard to convince oneself that almost zero net

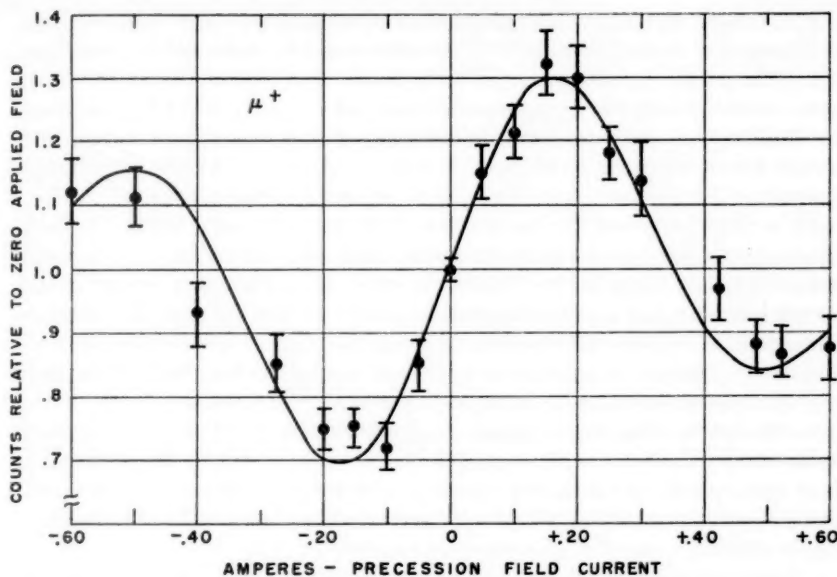


FIG. 1. Variation of the delayed gated counting rate for the positrons from $\mu^+ \rightarrow e^+ + \nu$ decay as a function of the current through a vertical solenoid enclosing the graphite slab in which the μ^+ mesons are stopped. The mean precession angle of the muon spin before decay is proportional to the vertical magnetic field. From (8).

polarization should be observed, even though the μ -mesons are completely polarized in their direction of motion in the pion center of mass system. The arguments are as follows: (a) The μ -mesons selected are formed by π -meson decays in flight near their point of production within the cyclotron. The selected μ -mesons have ~ 100 Mev kinetic energy in the lab system, but only ~ 4 Mev kinetic energy in the pion c.m. system. In the relativistic transformation from the pion c.m. system to the lab system the neutrino spin follows its momentum, but the μ -meson spin direction is relatively little changed. Thus one might expect the final μ -meson beam to have large contributions from decays in which the c.m. emission direction was at an appreciable angle with respect to the lab direction. The rapid fall off of the pion spectrum in this energy region would favor cases where the decay was near the forward direction, but it is not easy to see in a quantitative fashion that the effect would be so large. (b) Even if the μ -mesons are completely polarized with respect to their motion in the laboratory frame, they have a long history of events before they finally decay in the stopping sample. First they are bent $\sim 90^\circ$ in the fringing field of the cyclotron. For a normal Dirac moment this offers no problem, since the spin precesses in a magnetic field at the same frequency as the orbital motion. (c) In the slowing down process they pass through eight inches of graphite. If there was any appreciable tendency for

the μ^+ mesons to pick up a single electron during the slowing down, or after stopping, the muonium system so formed would be expected to cause considerable muon depolarization. Furthermore, if a stable triplet muonium atom were formed after stopping, the observed g factor should be dominated by the larger electron moment. When the positive muon stops in a solid it would be expected to be subject to local magnetic fields due to adjacent atoms (nuclear or electron). It would be expected to have its charge neutralized by electrons, and thus be subject to their depolarizing fields. The large observed polarization in graphite shows that these effects do not occur in graphite to any large degree. However, graphite contains only atoms having no nuclear spin and an even number of electrons. The μ^+ probably occupies some definite lattice position after stopping, and shares one electron with the surrounding atoms in a covalent type bond such that the electron has zero net moment averaged over times which would be important for a precession. Materials other than graphite might be expected to give more depolarization for μ^+ and it would be expected that μ^- -mesons will be largely depolarized before decay since they go through a series of Bohr orbits about a nucleus eventually reaching a 1s state. Both of these expectations are found to apply (8, 11).

Reported peak to valley asymmetry ratios for μ^+ are: Carbon, 1.80 ± 0.08 ; Al, 2.00 ± 0.20 ; Ca, 1.66 ± 0.10 ; bromoform (CHBr_3), ≈ 1.8 give large polarizations. Sulfur, 1.0 ± 0.1 ; Na Cl, 1.0 ± 0.15 ; Si O₂ (fused), ≈ 1.0 ; Si O₂ (crystal), ≈ 1.0 give almost no polarization asymmetry. Nuclear emulsion, 1.38 ± 0.09 ; H₂O, 1.41 ± 0.10 ; teflon, 1.47 ± 0.10 ; liquid propane, 1.44 ± 0.05 give intermediate asymmetries. The reason for the small effect in sulfur is not instantly apparent since, like carbon, it has even Z and even A. It does have an unusually large number of stable crystal lattice structures below the melting point, which may offer a clue to its large depolarizing effect.

Friedman & Telegdi (38), observing $\pi^+ \rightarrow \mu^+ \rightarrow e^+$ processes in nuclear emulsion (subjected to < 1 gauss magnetic field) obtain essentially the same peak to valley ratio with respect to the muon direction (in the pion at rest decay) as was observed by the Nevis experiment replacing the graphite with nuclear emulsion. This offers additional evidence that the Nevis μ^+ -meson beam is almost 100 per cent polarized.

When μ^- -mesons were used in place of μ^+ -mesons, with graphite as the stopping material, a small anisotropy in the decay was still observed (8) with a ~ -0.05 . The experiments were able to show that the μ^- moment is also the expected one (to poorer accuracy) and that its angular distribution is also peaked in the backward direction with respect to the meson motion. Lee & Yang (9) obtain the general theoretical result that even if all three invariance principles C (charge conjugation), T (time reversal), and P (parity) are not conserved, the e^+ angular distribution in $\pi^+ \rightarrow \mu^+ \rightarrow e^+$ decay is exactly the same as the e^- angular distribution in $\pi^- \rightarrow \mu^- \rightarrow e^-$ decay. The only difference is that the μ^+ and μ^- have opposite polarization with respect to their motion. The electron angular distribution is the same, however, with respect to the direction of the muon motion.

The counter experiments have, at the time this article was written, failed to show the reversal of the asymmetry direction for the low energy end of the spectrum. Pless *et al.* (11), however, report that they observe essentially an isotropic distribution for low energy positrons from $\mu^+ \rightarrow e^+$ decays in a propane bubble chamber. The chamber was magnetically shielded and exposed to the external μ^+ beam of the University of Chicago Synchrocyclotron.

One interesting observation of Lattes, and his co-workers (11) concerns the value of the asymmetry factor for $\pi^+ \rightarrow \mu^+ \rightarrow e^+$ decays observed in nuclear emulsions exposed to cosmic rays at high altitudes. They observe an asymmetry parameter $a = 0.0 \pm 0.07$ in contrast to $a = 0.18 \pm 0.03$ for the accelerator experiments. By the time this article appears in print this matter should be largely clarified as to whether the difference is associated with the physics of the upper atmosphere mesons, or with the physics of the emulsion exposure. If the mesons are the cause, this suggests unexpected complications in the family of elementary particles. The energy dependence of the positron spectrum for μ^+ decay has been studied by a large number of investigators. The results, expressed in terms of the Michel parameter ρ , mainly vary from $\rho \approx 0.5$ to 0.7. The possible curves form a family which starts as the phase space factor x^2 (where $x = \text{electron momentum}/\text{maximum momentum}$) for the low energy end (treating the electron mass as negligible). For $\rho = 0$, the curve goes to zero as $x \rightarrow 1$. For $\rho > 0$ the curve has a discontinuity at $x = 1$, with the value at $x = 1$ an increasing function of ρ . The comparison of the results of Sargent, *et al.* (39) with the various predicted curves, after correcting the theoretical curves for the experimental resolution, is shown in Figure 2. They obtain $\rho = 0.64 \pm 0.10$. These results, however, must be corrected (40) for bremsstrahlung and other effects which tend to decrease the observed value of ρ by about 0.04 or 0.03 in this range of ρ (40) to give $\rho \approx 0.68 \pm 0.11$. Sagane, Dudziak, & Vedder (41) obtained

$$\rho = 0.23 \begin{array}{l} + 0.03 \\ - 0.05 \end{array}$$

using a spiral orbit spectrometer. They obtained a relatively sharp break in the spectrum at the upper energy end at an energy in close agreement with the expected value. They have since discovered a serious systematic error due to pole piece saturation at high fields and now favor $\rho = 0.62$. Rosenson (42) reports a value $\rho = 0.68 \pm 0.05$ after corrections (40) for inner bremsstrahlung, etc. Bonetti, Setti, Panetti, Rossi, & Tomansini (43) obtain $\rho = 0.57 \pm 0.14$ and review earlier published results. Kinoshita & Sirlin (40d) recently gave the theoretical correction that should apply for the two component theory.

MUON LIFETIME IN MATTER

Bell & Hinks (44) found a mean lifetime of (2.22 ± 0.02) μsec . for stopped μ^+ mesons. The lifetime of stopped μ^- mesons should be smaller due to the competition between decay and nuclear capture in the reaction $\mu^- + p \rightarrow n + \nu$. Tiomno & Wheeler (7) predict that the ratio of capture to free decay

from the K shell should vary as Z^4 . This is a low Z approximation based on the observation that the K shell orbit radius varies as Z^{-1} in a point nucleus approximation. The probability density for the muon at the nucleus thus varies as Z^3 , and there are Z protons available for the reaction. Figure 3 gives the experimental results of Meyer (45) for the capture rate. These results are in essential agreement with those of Weinrich & Lederman (46). For $Z < 30$ the predicted Z^4 dependence roughly holds, with equal capture and decay rates for $Z \approx 11$. For $Z > 40$ the results show only a slight variation with Z . This is in agreement with a more exact analysis as is shown by the comparison of the experimental and calculated points in Figure 3. One reason for the decreased Z dependence is the finite nuclear size effect for large Z which greatly decreases the binding energy and the compactness of the K shell wave function from those expected from point nucleus theory. A second effect results from the relatively low energy available to the nucleus in the decay, since most of the capture energy is carried off by the neutrino. The magnitude of the nuclear matrix element must be examined more closely for possible transitions. In analogy to nuclear beta decay the modified initial state function would be expected to give poorer overlap with possible final state functions as the nuclear size increases.

Steinberger & Wolfe (47) have looked for the high energy electrons that

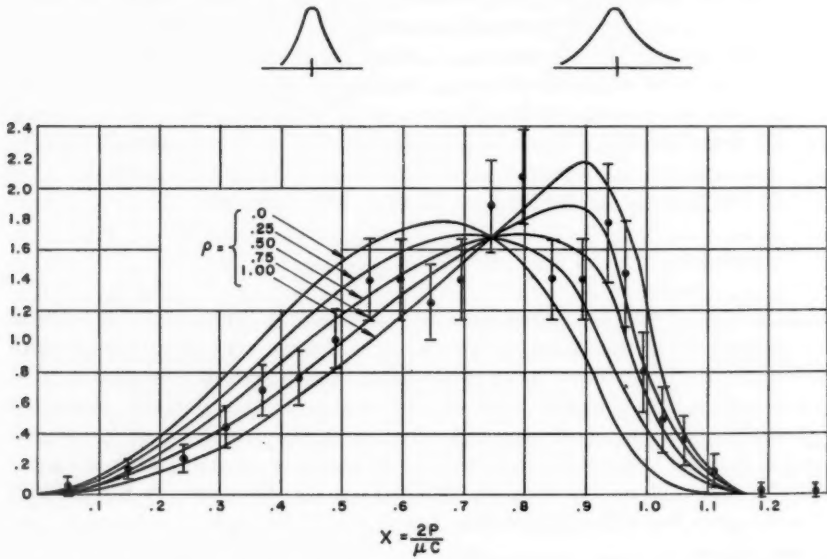


FIG. 2. The $\mu^- \rightarrow e^- + \nu + \bar{\nu}$ positron decay spectrum as observed (39) using a hydrogen filled diffusion cloud chamber in a 7750 gauss magnetic field. The theoretical Michel curves have the experimental resolution function folded in for comparison with experiment.

would result if μ^- capture by nuclei occasionally took place via the alternative processes



or



The electron energy for these reactions would be almost double the upper limit for the muon free decay spectrum, so the experiment consisted of using a counter telescope with many alternating counters and absorbers to discriminate strongly against the lower energy decay electrons, while giving a reasonable sensitivity (~ 50 per cent) for electrons from capture. No events were found and an upper limit $\sim 5 \times 10^{-4}$ was set for the relative rate of electron to neutrino emission on capture. The importance of such results does not become fully clear until one attempts to explain the existence and relative rates of various energetically permitted reactions using field theory with universal weak couplings between the various light and heavy particle fields. Such theories must then not only account for the observed reactions, but

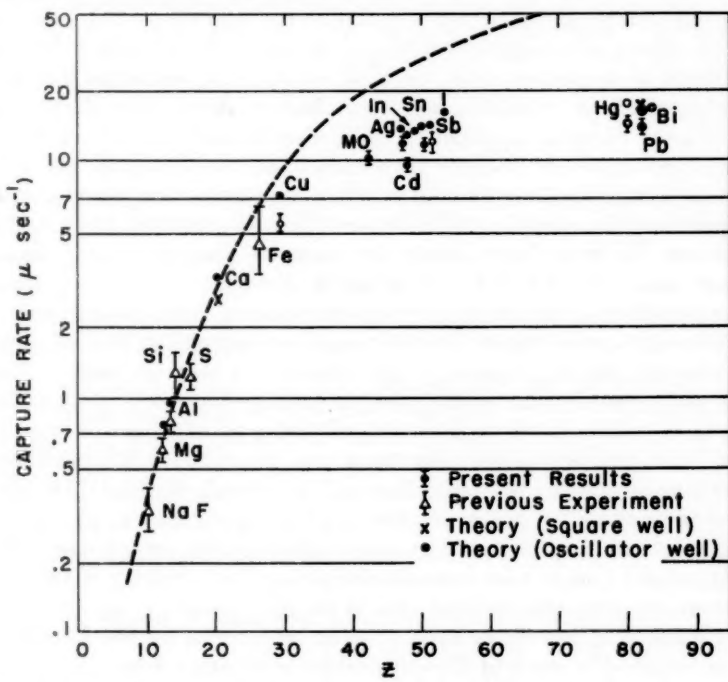


FIG. 3. Meyer's results (45) for the capture rate for μ^- mesons in K shell orbits about nuclei versus Z . The dashed curve corresponds to a Z^4 dependence which gives a relatively good fit for low Z . The dots and crosses are the predicted values using less crude assumptions.

must be consistent with the low observed upper limits for the rates of these other processes to the main ones.

ABSENCE OF OTHER DECAY MODES FOR π AND μ -MESONS

Friedman & Rainwater (48) found for 1419 momentum selected π^+ mesons ending in nuclear emulsion only one possible case which did not end in a $\pi^+ \rightarrow \mu^+$ decay. This one case could easily have been a μ^+ meson instead, so the result was zero or one decay in 1419 other than $\pi^+ \rightarrow \mu^+$. Lokanathan & Steinberger (49) looked for the high energy electrons from the specific process $\pi^+ \rightarrow e^+ + \nu$ by methods similar to those used to look for $\mu^- + p \rightarrow p + e^-$. They set an upper limit $\sim 10^{-4}$ for this process. In the same paper they give an upper limit of 2×10^{-5} for the fraction of μ^+ decays proceeding via the process $\mu^+ \rightarrow e^+ + \gamma$ determined by using a photon and electron telescope in coincidence. There was some question as to whether coupling schemes which predict a low ratio of $\pi \rightarrow e + \nu$ to $\pi \rightarrow \mu + \nu$ would also necessarily predict a low rate for $\pi \rightarrow e + \nu + \gamma$. Lokanathan & Steinberger (50) set an upper limit of $\sim 3 \times 10^{-6}$ for this process. The exact value for the upper limit depends on the assumed form of the angular correlation between the e^+ and γ directions.

The theory of competing modes of decay of the π^+ meson have been considered by a number of theorists (51 to 56). It is concluded that the observed low rate of (radiative and nonradiative) decay with electron emission to $\pi \rightarrow \mu$ decay is expected for axial vector coupling, using a universal Fermi coupling which proceeds via a nucleon-antinucleon pair. The $\pi \rightarrow \mu + \nu$ decay is permitted for both axial vector and pseudoscalar Fermi couplings. For pseudoscalar coupling the $\pi \rightarrow e + \nu$ process is predicted to be much too important. The $\pi \rightarrow e + \nu + \gamma$ decay via tensor coupling of amount present in nuclear beta decay is found by Treiman & Wyld (51) to lead to a predicted ratio of 0.025 or larger for $\pi \rightarrow e + \nu + \gamma$ to $\pi \rightarrow \mu + \nu$. There are so many ways that one may a priori choose the weak coupling interactions to apply between particles that the calculations, to the extent that they are correct, may be taken mainly as allowing or excluding certain specific models. The failure to observe $\pi \rightarrow e + \nu$ relative to $\pi \rightarrow \mu + \nu$ could also be explained in terms of a direct weak interaction between the π and the (μ, ν) fields, with no corresponding interaction between the π and (e, ν) fields. Similarly, the absence of $\mu^- + (n \text{ or } p) \rightarrow e^- + (n \text{ or } p)$ relative to $\mu^- + p \rightarrow n + \nu$ may again represent a direct weak coupling in the latter case, but not in the former case. The observations of so many new weak coupling reactions involving K mesons and hyperons suggests that caution should be used in specifying exactly what direct weak coupling terms exist. This is heightened by the formal divergences obtained in many of the calculations involving intermediate steps.

Since the preceding section was written, Cassells has reported (*Seventh Annual Rochester Conference on High Energy Physics*) an upper limit of 5×10^{-6} for the relative frequency of the process $\pi \rightarrow e + \nu + \gamma$ from an experiment similar to that of Lokanathan & Steinberger.

THE SPIN OF THE MUON

It is becoming more difficult to assign other than spin $\frac{1}{2}$ to the μ -meson. The burst production results are in excellent agreement with the predictions of spin $\frac{1}{2}$ theory with no anomalous moment, as shown in Figure 4. The predictions for spin 1 theory are very much above the spin $\frac{1}{2}$ theory predictions as is shown in Figure 4. The spin $\frac{3}{2}$ theory predictions are even further from the experimental values. Mathews (57) has considered the theory of *Compton Scattering and Bremsstrahlung of Spin $\frac{3}{2}$ Particles*. He finds that the predicted burst production is greater than ten times that for spin $\frac{1}{2}$ theory for 10^{11} ev and over.

The gyromagnetic ratio for the muon has now been measured (17) and shown to be 2.00 to within $\frac{1}{2}$ per cent or less. The predicted g factor for higher spin is inversely as the spin (58). Thus $g = \frac{1}{2}$ is predicted for spin $\frac{1}{2}$. The known cases where the g factor for spin $\frac{1}{2}$ particles is very different from 2.00 are the nucleons. In this case their known strong coupling to the π meson field leads to the expectation that the pions should contribute large effects to the nucleon moments. The μ -meson, however, has no known strong couplings of a nonelectromagnetic type to other fields. The magnetic moment would thus be expected (18) to be that predicted by a full, correct, treatment of its interaction with the electromagnetic field, $g = 2/[1 + \alpha/2\pi - 1.89\alpha^2/\pi^2]$.

MU MESONIC X-RAYS

The theory of the energy of bound states for a μ^- -meson about a nucleus of charge $Z e$ is basically given by the Dirac theory as if the meson were just a heavy electron. Figure 5 shows the nonrelativistic energies for the $2p \rightarrow 1s$, $3d \rightarrow 2p$, $4f \rightarrow 3d$, and $5g \rightarrow 4f$ transitions. The corrections due to relativistic, fine structure, finite nuclear size, and vacuum polarization effects can either be expressed in energy units, or in terms of meson mass change in the non relativistic theory required to give the same change in the transition energy. Figures 5 to 8 and most of the discussions of this section, are due to Koslov, Fitch, & Rainwater (19a) and are taken from the Doctoral thesis of Samuel Koslov (19b). Figure 6 gives the increase in the effective mass coefficient m , and thus of the transition energy due to relativistic and fine structure effects. All of these figures give poor approximations for $|E| < 2$ mev for the K shell. Figure 7 shows the correction due to nuclear penetration, finite nuclear size, and acts to decrease the transition energy. The Dirac point nucleus binding energy in Sommerfeld approximation is

$$E = \frac{1}{2} mc^2 \left(\frac{Z\alpha}{n} \right)^2 \left[1 + \left(\frac{Z\alpha}{n} \right)^2 \left(\frac{n}{|k|} - \frac{3}{4} \right) \right] \quad 16.$$

where

$$|k| = \begin{cases} = l + 1 & \text{for } j = l + 1/2 \\ = l & \text{for } j = l - 1/2 \end{cases}$$

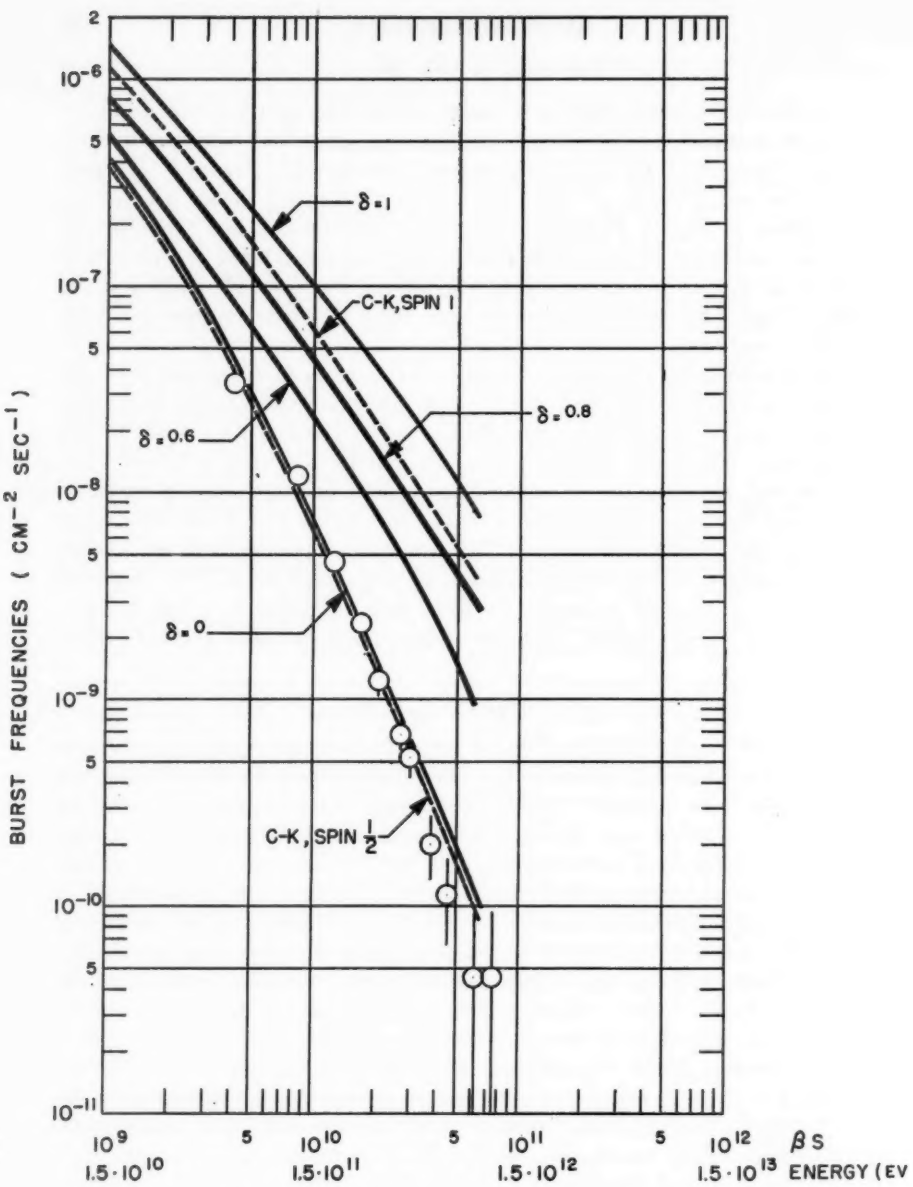


FIG. 4. A plot of the frequency versus energy of large cosmic ray bursts versus their size. The solid curves are the predicted frequency assuming only electromagnetic interactions of μ -mesons with nuclei. The dashed lines are given by Christy & Kusaka (31) for spin $\frac{1}{2}$ and spin 1 theories. The remaining curves are given by Hirokawa, Komori & Ogawa (30) for spin $\frac{1}{2}$ theory in which the magnetic moment is $(1+\delta)$ times the normal Dirac moment. Agreement is obtained for spin $\frac{1}{2}$ and no anomalous moment.

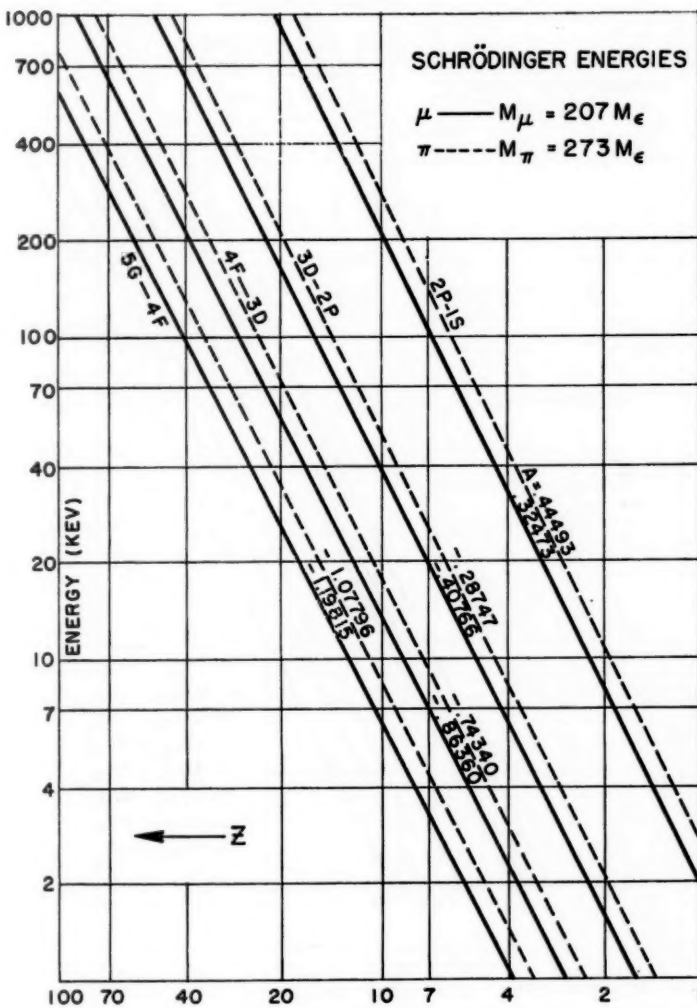


FIG. 5. Schrodinger energies of mesonic transitions. These energy values assume the transitions to take place between Bohr orbits of $l=n-1$ and are uncorrected for the effects of relativity, spin, etc. The lines are of the form $\log_{10}E = A + 2 \log_{10}Z$, where E is in Kev and A is shown for each curve.

RELATIVISTIC
 &
 FINE STRUCTURE
 CORRECTION
 SOMMERFELD APPROX.
 $m_\mu = 207 m_e$

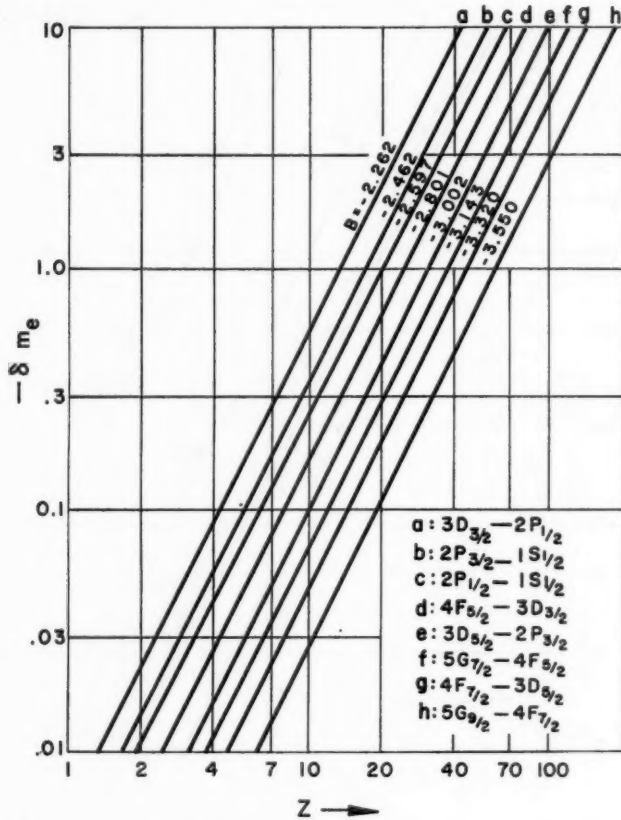


FIG. 6. Relativistic and fine structure effect for μ^- mesonic transitions. The correction is calculated in the basis of the "Sommerfeld approximation" and expressed in terms of electron mass units (assuming $m_\mu^- = 207 m_e$). This term increases the transition energy and thus decreases the mass calculated from the Schrodinger energy. The lines are of the form $\log_{10}(-\delta m_e) = B + 2 \log_{10}Z$. B is shown for each curve.

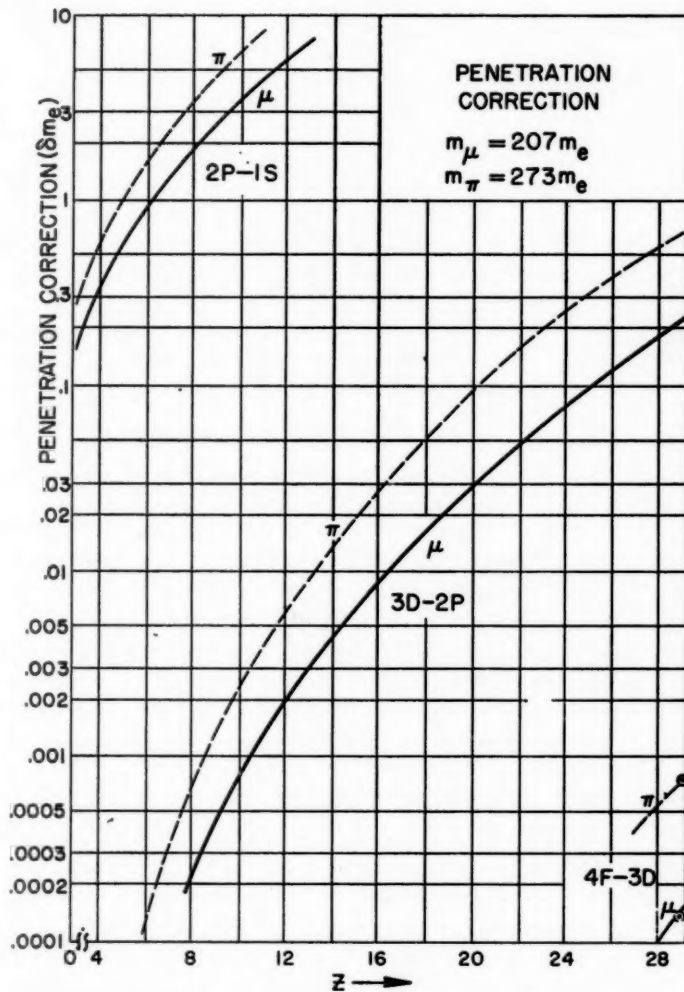


FIG. 7. Effect of nuclear penetration on transition energies. The effect tends to decrease the transition energy and was calculated as a first order perturbation of the point nucleus energy, using a nuclear radius of $1.2A^{1/3} \times 10^{-13}$.

and $\alpha = e^2/\hbar c$. For $l=n-1$ and small r , the electron radial wave function $\psi_e = C(Z, n, 1)r^{l+1}$. The change in the Coulomb interaction energy due to nuclear size is

$$\Delta V_e = \frac{C^2(Z, n, l)}{(2l+2)(2l+3)} \int_0^\infty \rho(r) r^{2(l+1)} r^2 dr \quad 17.$$

where

$$\int_0^\infty \rho(r) r^2 dr = Ze$$

and

$$C^2(Z, n, l) = \left[\frac{2Z\mu}{(l+1)a_0 m_e} \right]^{2l+3} \frac{1}{(2l+2)!} \quad 18.$$

with a_0 = Bohr radius for hydrogen. For a constant charge density to $r=R$, and $\rho=0$ for $r>R$, this gives a fractional change in the binding energy E of

$$\frac{\Delta V_e}{|E|} = \frac{12(l+1)}{(2l+2)(2l+5)(2l+3)!} \left[\frac{2Z\mu R}{(l+1)a_0 m_e} \right]^{2l+2} \quad 19.$$

For high Z and $l=0$ or 1 this approximation may be poor and a more exact solution of the Dirac equation is necessary (16, 5).

The vacuum polarization correlation is based on the theory of Uehling (60a) and of Serber (60b). Foldy & Eriksen (61) and Mickelwait & Corbin (62) give the results of calculations of the vacuum polarization effects for mesonic atoms. The following analysis of this effect is from the Doctoral thesis of S. Koslov (19b) and is applicable for cases where the meson spends only a small fraction of its time within the nucleus.

The additional potential V_p produced by the vacuum polarization is given in terms of the *Uehling Integral* (60).

$$V_p(r) = \frac{-\alpha}{2\pi} \frac{Ze}{r} f(\rho) \quad 20a.$$

where

$$f(\rho) = \int_0^1 \frac{2v^2(1-v^2/3)}{(1-v^2)} e^{-2\rho/(1-v^2)^{1/2}} \quad 20b.$$

where $\rho=r/b$, $d=\hbar/m_e c = \hbar_{ce}$ and $\alpha^{-1} \approx 137$. Wichmann & Kroll (63) have shown that this lowest order theory result is a very good approximation to the result of the theory to all orders. Neglecting the nuclear size effect, the meson radial function for $n=l+1$ is

$$r\psi = \phi = Cr^{l+1}e^{-r/a} \\ a = yb = [137m_e(l+1)/Z\mu]b \quad 21a.$$

Then

$$\frac{\langle V_p \rangle}{\langle E \rangle} = \frac{\alpha}{\pi} \frac{\langle \frac{f(\rho)}{r} \rangle}{\langle 1/r \rangle} = \frac{\alpha}{\pi} G_1(y) \quad 21b.$$

where

$$G_l(y) = \frac{2}{3} \int_0^1 \left[\frac{(x^2 + 2)(1 - x^2)^{1/2}}{x} \right] \left[\frac{x}{x+y} \right]^{2l+2} dx \quad 21c.$$

This may be rapidly evaluated with good accuracy using the following expression based on Simpson's rule

$$G_l(y) \approx \sum_i w(X_i) \left(\frac{X_i}{X_i + y} \right)^{2l+2} \quad 21d.$$

The values of X_i used and the corresponding w , in parentheses, are 0.5 (1.78), 0.1 (0.444), 0.15 (0.592), 0.2 (0.332), 0.3 (0.591), 0.4 (0.220), 0.5 (0.346), 0.6 (0.140), 0.7 (0.226), 0.8 (0.088), and 0.9 (0.121). The results obtained by this simple method are in excellent agreement with those obtained using a more elaborate analysis. When the nuclear size is small compared to the dimensions of the meson wave function, Rockmore (64) has explicitly shown that finite nuclear size corrections are negligible for most purposes.

When the size of the meson orbit is not large compared to the nuclear size, as for the K and L shells of lead, a different method must be used (65).

For low energy transitions there is competition between radiative and Auger transitions. This is discussed by Burbridge & De Borde (66). Figure 8 shows the ratio of radiative to Auger transition rates for a series of transitions of interest. Further discussion of this subject is given by De Borde (67) & Demeur (69). Recently Stearns & Stearns (68) have directly measured the relative radiative yields of the μ -meson K and L series transitions for $Z=3$ to 19. For the K shell transitions, they find a dropping yield for $Z < 6$ which is not expected from the above theory for the competition of Auger with radiative transitions. A dropping of the L yield occurs for $Z < 12$. Both results can be expressed by the factor $Z^4/(C+Z^4)$ where $C_1=450$ for the K series and $C_2=2 \times 10^4$ for the L series transitions (68).

In evaluating mesonic x-ray transition energies for $n \leq 5$, $l \leq 4$, the electron shielding effect is negligible, although the gross level shift may not be negligible. This is seen by noting that the meson electrostatic potential energy is constant inside a spherically symmetric electron charge distribution (that part of V due to the electrons), so only the electron charge within the meson orbit affects the transition energy by changing the effective nuclear charge. The K shell electrons give the main contribution to the electron density near the nucleus, where their total charge density is $\rho/Ze = (2/a_0)^3 Z^2$. Here $r^2 \rho dr$ is the charge between r and $r+dr$. For a meson in an $l=4$, $n=5$ Bohr orbit the orbit radius is $25 a_0/Z(\mu/m_e)$, which gives a fractional reduction in Z of $(50 m_e/\mu)^3/3Z$. The requirement $\Delta E \geq 20$ Kev for a $5g-4f$ transition requires that $Z \geq 18$ for a μ meson and this fractional change is $\sim 3 \times 10^{-4}$. Wheeler (70) has shown that hyperfine effects due to the nuclear magnetic moment are very small.

The results of level calculations for lead are given by Fitch & Rainwater (16) and by Ford & Hill (5). A rather interesting effect which has not yet

been observed experimentally is the expected elaborate splitting of the $2p$ levels due to interactions with collective nuclear modes. These effects have been investigated theoretically by Wilets (71) & by Jacobsohn (72). These effects grossly alter the fine structure of the levels for heavy nuclei not near closed shells. This is true for even-even nuclei as well as for odd A nuclei.

One of the important results from the study of μ -mesonic x-ray spectra was the determination of the smaller effective nuclear radii (16, 5) which has since been so thoroughly confirmed by the Stanford electron scattering measurements. Another has been the use of K -edge filters to establish upper

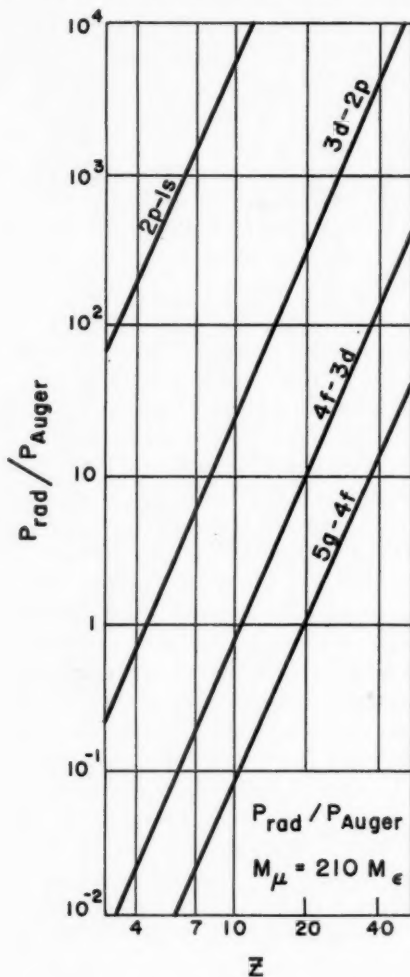


FIG. 8. Relative probability of a radiative transition to an Auger transition (for $m_\mu = 210 m_e$). The figure is based upon calculations by Burbridge and De Borde for $Z = 6, 7, 8, 35$, and 47 .

or lower limits for various mesonic x-ray transition energies. Table I, which was prepared by Koslov (19b), gives the limit value which would be determined for the μ^- -meson mass by observation of various favorable x-ray transitions using the indicated element for a K -edge filter. The nonrelativistic energies are given and must be corrected for all of the effects discussed above. The transitions which have been tested (19, 21) are the Carbon $2p \rightarrow 1s$, the phosphorus $3d \rightarrow 2p$, and the silicon $4f \rightarrow 3d$. The most interesting result is that for phosphorous, which has been discussed in the introductory part of this paper. The lower limit for the μ^- mass (21) before including the vacuum polarization correction is mass $\geq 207.54 m_e$. This is so far above the value determined by independent methods (21, 22) as to unmistakably demonstrate the existence of vacuum polarization effects for mesonic atoms.

K MESON DECAYS INVOLVING μ -MESONS

μ -Mesons normally are observed as by products of $\pi \rightarrow \mu$ decay. The heavier K mesons also have decay processes involving the μ -meson in compe-

TABLE I

MASS OF THE μ^- MESON CORRESPONDING TO MESONIC X-RAY ENERGIES EQUAL TO THE K ABSORPTION EDGE ENERGY FOR SELECTED TRANSITIONS

μ mass	Atom Target	Transition	Filter	Energy (kev)
209.31	Cu 29	5G-4F	Ds 66	53.792
209.30	Br 35	5G-4F	Pt 78	78.379
209.19	C 6	2P-1S	Ir 77	76.123
209.09	F 9	3D-2P	Te 52	31.811
209.14	Na 11	5G-4F	CO 27	7.709
209.07	Cu 29	4F-3D	U 92	116.083
209.06	Se 34	5G-4F	Os 76	73.882
209.02	Zn 30	5G-4F	Er 68	57.486
209.01	Ca 20	5G-4F	Ag 47	25.518
208.79	As 33	5G-4F	W 74	69.503
208.70	Ga 31	5G-4F	Yb 70	61.303
208.67	Al 13	4F-3D	Rh 45	23.225
208.66	Ge 32	5G-4F	Hf 72	65.313
208.52	F 9	4F-3D	Ge 32	11.103
207.88	p 15	3D-2P	Pb 32	88.065
207.71	Mn 25	4F-3D	Te 81	85.674
207.55	O 8	5G-4F	Ca 20	4.038
207.40	Sc 21	5G-4F	In 49	27.929
207.03	Ne 10	2P-1S	La 57	38.933
206.91	Si 14	4F-3D	Cd 48	26.713
206.73	N 7	3D-2P	Nb 41	18.988

These values are based on the Schrodinger energy of mesonic orbits (for the reduced mass) uncorrected for relativistic effects, fine structure, penetration, and vacuum polarization.

tition with other decay modes involving π mesons and electrons. The primaries for all of these decay processes are, at present, believed to be the same particle since they have, to within experimental errors, (73 to 81) the same mass values and mean lives for decay. Peterson (76) gives (966.7 \pm 1.1) m_μ as the K mass. The common lifetime is $\sim 1.2 \times 10^{-8}$ sec. There are five basic divisions for the decay of K^+ mesons. (a) $K_{\mu 2}$ (~ 58 per cent) has $K^+ \rightarrow \mu^+ + \nu$ (b) $K_{\pi 2}$ (~ 29 per cent) has $K^+ \rightarrow \pi^+ + \pi^0 \equiv \theta^+$ (c) $K_{\pi 3}$ (~ 7 per cent) has $K^+ \rightarrow 2\pi^+ + \pi^- \equiv \tau^+$ and $K^+ \rightarrow \pi^- + 2\pi^0 \equiv \tau'^+$ (d) $K_{\mu 3}$ (~ 3 per cent) has $K^+ \rightarrow \mu^+ + 2$ neutrals. One of the neutrals may be a π^0 and the other a neutrino. (e) $K_{\pi 3}$ (~ 3 per cent) has $K^+ \rightarrow e^+ + 2$ neutrals. The results are similar for K^- mesons that decay in flight, but those that stop produce reactions with nuclei (81). The subject of heavy mesons and hyperons is beyond the scope of this review, and the reader is referred to the article by Gell-Mann & Rosenfeld (in this volume) for a more thorough presentation of this subject.

NEUTRON PRODUCTION BY FAST AND STOPPED μ -MESONS

The nuclear processes produced by fast cosmic ray μ -mesons were described in the introduction as probably being consistent with only electromagnetic interactions. Without giving an exhaustive review of all experimental work, the general experimental situation as summarized by Stearns, *et al.* (82) is given below.

The mean cross section-neutron multiplicity product ($\langle \sigma m \rangle$) for sea level μ -mesons ($p_c > 1$ Bev) traversing Pb has been measured, a thermalized neutron being detected in delayed coincidence with a penetrating particle. A magnet cloud chamber above the producer and a hodoscope-absorber array below it serve to identify μ -meson interactions, $\langle \sigma m \rangle = (22 \pm 8) \times 10^{-29} \text{ cm.}^2/\text{nucleon}$. Theoretical calculations using the photoneutron yields of Jones & Terwilliger (83) $\langle \sigma m \rangle = 15 \times 10^{-29} \text{ cm.}^2/\text{nucleon}$ for the yield resulting from knock-on showers and $\langle \sigma m \rangle = 9 \times 10^{-29} \text{ cm.}^2/\text{nucleon}$ for the direct yield from equivalent photons of the μ -meson field. This theory also agrees with the results of underground measurements at higher average momenta [Annis, Wilkins, & Miller (84)]. There is no evidence of scattering in excess of Coulomb scattering.

TABLE II

Observed	α -particle model	Predicted Fermi gas model	
		$M_{eff} = M$	$M_{eff} = M/2$
f(0)	0.315 ± 0.098	0.319	0.515
f(1)	0.506 ± 0.064	0.362	0.474
f(2)	0.146 ± 0.027	0.184	0.010
f(3)	0.019 ± 0.015	0.080	0
f(4)	0.009 ± 0.006	0.034	0
f(5)	0.002 ± 0.002	0.014	0
f(6)	0.002 ± 0.002	0.005	0

When stopped μ^- mesons are absorbed by nuclei the neutrino carries off most of the energy in $\mu^- + p \rightarrow n + \nu$. The stars produced are thus relatively small compared, say, with those produced when π^- mesons are absorbed. Kaplan, Moyer, & Pyle (85) present the following results in an abstract for the 1957 Washington meeting of the American Physical Society.

Neutron Multiplicities from μ^- capture in Pb and Ag have been observed with a cadmium-loaded liquid scintillator tank. The observed distributions previously reported have been compared with the distributions predicted by a Fermi gas model (with both the effective nucleon mass, $M_{\text{eff}} = M_n$ and $M_{\text{eff}} = M_n/2$), and an α particle model. Assuming a boil off neutron spectrum, the observed distribution for Pb compare with the predicted distributions as shown in Table II. In the lower multiplicities, where the statistics are better, the Fermi model with $M_{\text{eff}} = M/2$ seems to give the best fit. The distribution from Ag will also be discussed.

Jones (86) measured the average multiplicity of neutrons produced by stopped μ -mesons in Mg (0.6 ± 0.2), Na (1.0 ± 0.4), and Pb (1.7 ± 0.3). The results agree with those of Conforto & Sard (87). Jones (86) gives references to the earlier experimental work on this subject and to the theoretical considerations.

LITERATURE CITED

1. Marshak, R. E., *Meson Physics* (McGraw-Hill Book Co., New York, N.Y., 378 pp., 1952)
2. Thorndike, A. M., *Mesons—A Summary of the Experimental Facts* (McGraw-Hill, Book Co., New York, N.Y., 237 pp., 1952)
3. Rossi, B., *High Energy Particles* (Prentice-Hall Inc., New York, N.Y., 569 pp., 1952)
4. Bethe, H. A., and de Hoffmann, F., *Mesons and Fields*, 2, *Mesons* (Row, Peterson and Co., Evanston, Ill., 449 pp., 1955)
5. Ford, K. W., and Hill, D. L., *Ann. Rev. Nuclear Sci.*, 5, pages 25–72 (1955)
6. Sard, R. D., and Crouch, M. F., *Progress in Cosmic Ray Physics*, II (Interscience Publishers, New York, N.Y., 1954)
7. Tiomno, J., and Wheeler, J. A., *Rev. Mod. Phys.*, 21, 153 (1949)
8. Garwin, R. L., Lederman, L. M., and Weinrich, M., *Phys. Rev.*, 105, 1415 (1957)
- 9.(a) Yang, C. N., and Lee, T. D., *Phys. Rev.*, 105, 1671 (1957) (b) Landau, L., *Nuclear Phys.*, 3, 127 (1957) (c) Salam, A., *Nuovo Cimento*, 5, 299 (1955)
10. Wu, C. S., Ambler, E., Hayward, R. W., Hopfes, D. D., and Hudson, R. P., *Phys. Rev.*, 105, 1413 (1957)
11. *Bull. Am. Phys. Soc.* [II], 2, Session M, 204–06 (1957)
12. Lee, T. D., Oehme, R., and Yang, C. N., *Nevis Cyclotron Laboratories Report* 36, (Columbia Univ. Phys. Dept., January, 1957)
13. Lee, T. D., and Yang, C. N., *Phys. Rev.*, 104, 254 (1956)
14. Lee, T. D., and Yang, C. N., *Phys. Rev.*, 104, 822 (1956)
15. Pauli, W., *Handbuch Der Physik*, 24, 226–27 (Springer Verlag, Berlin, Germany, 853 pp., 1933)
16. Fitch, V. L., and Rainwater, J., *Phys. Rev.*, 92, 782 (1953)
17. Garwin, R. L., Lederman, L. M., Sachs, A., Coffin, T., and Penman, S., *Seventh Annual Rochester Conference on High Energy Physics*.
- 18.(a) Suura, H., and Wichmann, E. H., *Phys. Rev.*, 1005, 1930 (1957) (b) Petermann, A., *Phys. Rev.*, 105, 1931 (1957)
- 19.(a) Koslov, S., Fitch, V. L., and Rainwater, J., *Phys. Rev.*, 95, 291, 625 (1954); (b) Koslov, S., "Studies of Low Energy Mesonic X-Ray Transitions and Vacuum Polarization Effects in Mesonic Atoms" (Doctoral Thesis, Columbia Univ., New York, N.Y., 1956)
- 20.(a) Stearns, M. B., Stearns, M., De Benedetti, S., and Leipuner, L., *Phys. Rev.*, 97, 240 (1955); 96, 804 (1954) (b) Stearns, M. B., and Stearns, M., *Phys. Rev.*, 103, 1522 (1956)
21. Cohen, E. R., Crowe, K. M., and Du Mond, J. W. M., *Phys. Rev.*, 104, 266 (1956)
22. Barkas, W. H., Birnbaum, W., and Smith, F. M., *Phys. Rev.*, 101, 778 (1956)
23. Crowe, K. M., and Phillips, R. H., *Phys. Rev.*, 96, 470 (1954)
24. Masek, G. E., Lazarus, A. J., and Panofsky, W. K. H., *Phys. Rev.*, 103, 374 (1956)
25. Rawitscher, G. H., *Phys. Rev.*, 101, 423 (1956), G. W. Rawitscher, Doctoral Thesis, Stanford University, Palo Alto, Calif., 1956
26. Cooper, L. N., and Rainwater, J., *Phys. Rev.*, 97, 492 (1955)
27. Lloyd, J. L., and Wolfendale, A. W., *Proc. Phys. Soc. A.*, 68, 1045 (1955)
28. McDiarmid, I. B., *Phil. Mag.*, 45, 933 (1954)
29. Fowler, G. N., *Nuclear Phys.*, 3, 121 (1957)
30. Hirokawa, S., Komori, H., and Ozawa, S., *Nuovo Cimento*, 4, 736 (1956)
31. Christy, R. F., and Kusaka, S., *Phys. Rev.*, 59, 405 and 414 (1941)

32. George, E. P., and Evans, J., *Proc. Phys. Soc. A*, **63**, 1248 (1950); **64**, 193 (1951); **68**, 829 (1955)
33. Fowler, G. N., *Proc. Phys. Soc. A*, **68**, 945 (1955)
34. Kessler, D., and Kessler, P., *Nuovo Cimento*, **4**, 601 (1956)
35. Alvarez, L. W., et al., *Phys. Rev.*, **105**, 1127 (1957)
36. Rose, M. E., in *Beta and Gamma Ray Spectroscopy* 271-91 (Interscience Publishers, New York 1955)
37. Michel, L., *Proc. Phys. Soc. A*, **63**, 514 (1950), *Nature*, **163**, 959 (1949)
38. Freedman, J. I., and Telegdi, V. L., *Phys. Rev.*, **105**, 1681 (1957)
39. Sargent, C. P., Rinehart, M., Lederman, L. M., and Rogers, K. C., *Phys. Rev.*, **99**, 885 (1955)
- 40.(a) Lenard, A., *Phys. Rev.*, **90**, 968 (1953) (b) Finkelstein, R. J., and Behrends, R. E., *Phys. Rev.*, **97**, 568 (1955) (c) Behrends, R. E., Finkelstein, R. J., and Sirlin, A., *Phys. Rev.*, **101**, 866 (1956) (d) Kinoshita, T., and Sirlin, A., *Bull. Am. Phys. Soc.*, [II], **2**, 191 (1957)
41. Sagane, R., Dudziak, W. F., and Vedder, J., *Phys. Rev.*, **95**, 863 (1954); *Bull. Am. Phys. Soc.*, [II], **1**, 174 (1956)
42. Rosenson, L., *Bull. Am. Phys. Soc.*, [II], **2**, 2 (1957)
43. Bonetti, A., Setti, R. L., Panetti, M., Rossi, G., and Tomansini, G., *Nuovo Cimento*, **3**, 33 (1956)
44. Bell, W. E., and Hinks, E. P., *Phys. Rev.*, **84**, 1243 (1951)
45. Meyer, A. J., *Princeton University Palmer Physical Laboratory and Naval Ordnance Laboratory Technical Report No. 16*. (Doctoral Thesis, Princeton Univ., Princeton, N. J., 83 pp., 1954)
46. Weinrich, M., and Lederman, L. M., *Bull. Am. Phys. Soc.*, [II], **1**, 174 (1956)
47. Steinberger, J., and Wolfe, H. B., *Phys. Rev.*, **100**, 1490 (1955)
48. Friedman, H., and Rainwater, J., *Phys. Rev.*, **81**, 644 (1951)
49. Lokanathan, S., and Steinberger, J., *Phys. Rev.*, **98**, 240 (1955)
50. (a) Lokanathan, S., *Nevis Cyclotron Laboratories Report No. 30*. (Doctoral Thesis, Columbia Univ., New York, N. Y., 49 pp., 1957) (b) Lokanathan, S., and Steinberger, J., *Nuovo Cimento*, **2**, 151 (1955)
51. Treiman, S. B., and Wyld, H. W., Jr., *Phys. Rev.*, **101**, 1552 (1956)
52. Eguchi, T., *Phys. Rev.*, **102**, 879 (1956)
53. Ross, M., *Phys. Rev.*, **104**, 1736 (1956)
54. Bludman, S. A., and Ruderman, M. A., *Phys. Rev.*, **101**, 910 (1956)
55. Ogawa, S., *Progr. Theoret. Phys. (Kyoto)*, **13**, 367 (1955)
56. Oneda, S., and Wakasa, A., *Nuclear Phys.*, **1**, 445 (1956)
57. Mathews, J., *Phys. Rev.*, **102**, 270 (1956)
58. Moldauer, P. A., and Case, K. M., *Phys. Rev.*, **102**, 279 (1956)
59. Ulehla, I., *Mat. fyz. časopis*, **4**, 11 (1954)
60. (a) Uehling, E. A., *Phys. Rev.*, **48**, 55 (1935) (b) Serber, R., *Phys. Rev.*, **48**, 49 (1935)
61. Foldy, L. L., and Eriksen, E., *Phys. Rev.*, **95**, 1048 (1954)
62. Mickelwait, A. B., and Corben, H. C., *Phys. Rev.*, **96**, 1145 (1954)
63. Wichmann, E., and Kroll, N. M., *Phys. Rev.*, **96**, 232 (1954)
64. Rockmore, R. (Unpublished data)²

² I wish to thank Dr. Rockmore for carrying out these calculations in connection with our low energy mesonic x-ray measurement program.

65. Cooper, L. N., and Henley, E. M., *Phys. Rev.*, **92**, 801 (1953)
66. Burbridge, G. R., and De Borde, A. H., *Phys. Rev.*, **89**, 189 (1953)
67. De Borde, A. H., *Proc. Phys. Soc. A*, **67**, 57 (1954)
68. Stearns, M. B., and Stearns, M., *Phys. Rev.*, **105**, 1573 (1957)
69. Demeur, M., *Nuclear Phys.*, **1**, 516 (1956)
70. Wheeler, J. A., *Phys. Rev.*, **92**, 812 (1953)
71. Wilets, L., *Dan. Mat. Fys. Medd.*, **29**, (1954)
72. Jacobsohn, B. A., *Phys. Rev.*, **96**, 1637 (1954)
73. Ritson, D. M., Pevsner, A., Fung, S. C., Widgoff, M., Zorn, G. T., Goldhaber, S., and Goldhaber, G., *Phys. Rev.*, **101**, 1085 (1956)
74. Alvarez, W., and Goldhaber, S., *Nuovo Cimento*, **2**, 344 (1955)
75. Widgoff, M., Shapiro, A. M., Schluter, R., Ritson, D. M., Pevsner, A., and Henry, V. P., *Phys. Rev.*, **104**, 811 (1956)
76. Peterson, J. R., *Phys. Rev.*, **105**, 693 (1957)
77. Hoang, T. F., Kaplan, M. F., and Yekutieli, G., *Phys. Rev.*, **102**, 1185 (1956)
78. Orear, J., Harris, G., and Taylor, S., *Phys. Rev.*, **104**, 1463 (1956) *Bull. Am. Phys. Soc. [II]*, **2**, 20 (1957)
79. Hornbostel, J., Salant, E. O., and Zorn, G. T., *Bull. Am. Phys. Soc. [II]*, **2**, 20 (1957)
80. Fitch, V., and Motley, R., *Phys. Rev.*, **101**, 496 (1956)
81. Barkas, W. H., Dudziak, W. F., Giles, P. C., Heckman, H. H., Inman, F. W., Mason, C. J., Nickols, N. A., and Smith, F. M., *Phys. Rev.*, **105**, 1417 (1957)
82. (a) Stearns, B. F., Sard, R. D., Jones, D. R., and De Pagter, J. K., *Bull. Am. Phys. Soc. [II]*, **2**, 5 (1957) (b) Stearns, B. F., "Technical Report No. 21, Contract N6-ONR-202, Task Order III" (Doctoral Thesis, Washington University, Saint Louis, Mo., 1956)
83. Jones, L. W., and Terwilliger, K. M., *Phys. Rev.*, **91**, 699 (1953)
84. Annis, M., Wilkins, H. C., and Miller, J. D., *Phys. Rev.*, **94**, 1038 (1954)
85. Kaplan, S. N., Moyer, B. J., and Pyle, R. V., *Bull. Am. Phys. Soc. [II]*, **2**, 194 (1957)
86. Jones, D. R., *Phys. Rev.*, **105**, 1591 (1957)
87. Conforto, A. M., and Sard, R. D., *Phys. Rev.*, **86**, 465 (1952)

RADIOCHEMICAL SEPARATIONS BY ION EXCHANGE¹

BY KURT A. KRAUS AND FREDERICK NELSON

Chemistry Division, Oak Ridge National Laboratory, Oak Ridge, Tennessee

During the past few years ion exchange has become firmly entrenched as a separations tool. Its great popularity stems from its theoretical and practical simplicity, its insensitivity to concentration, its versatility and broad applicability, its rapidity for obtaining materials of extremely high purity and, of course, from the ready availability of reasonably stable ion exchange materials. Ion exchange is ideally suited for separations at the trace concentration so typical for radiochemical work and, indeed, ion exchange and radiochemical developments have been closely allied. Further, because ion exchange columns are simple to operate, easily shielded and adaptable to remote control, their use is attractive, even at relatively high activity levels.

The war-time work on the Manhattan project on the separation of rare earth and other fission products is generally considered the starting point of the present great interest in the use of ion exchangers for inorganic and radiochemical separations. Since then, application of ion exchangers to radiochemical problems has increased enormously and now includes such widely different fields as analysis, process control, isolation of tracers from target materials, discovery, identification and study of new elements, separation of activities in neutron activation analysis, general investigations of the chemistry of solutions, "hot atom" chemistry, production of radioisotopes, and waste disposal. The isolation of uranium from low grade ores is, in principle, also a radiochemical separation and has become the largest application of ion exchangers outside the water conditioning field.

The flood of ion exchange papers originating in many laboratories throughout the world is now so large as to preclude adequate coverage in the limited space of this review, even if attention is confined, as will be done here, to inorganic separations. Complete restriction of the paper to radiochemical applications, although implied by the title, seemed inappropriate since except at highest radiation densities, there is essentially no difference between separations of active or inactive materials. The field to be covered is thus extremely large and, in order to stay within bounds, citation of references had to be severely restricted, and selections often be made on an arbitrary basis. Fortunately, the field is frequently reviewed and a number of recent books (e.g., refs. 1 to 9) and review articles (e.g., refs. 10 to 21) are available. In addition, it is hoped that sufficient individual citations have been made to provide an adequate introduction to recent developments in the field.

¹ The survey of literature pertaining to this review was completed in March, 1957.

MATERIALS

Ion exchangers may be defined as three-dimensional networks to which either positive or negative charges are affixed. Electrical neutrality is preserved by mobile or displaceable ions of the opposite charge (counter ions) which may be exchanged for others in the surrounding medium. As implied by this broad definition, a large number of organic and inorganic materials have ion exchange properties, as discussed, for example, in a review article by Deuel & Hutschneker (11). Many adsorbents listed in the extensive bibliography of Deitz (7) presumably also act as ion exchangers though this may not be explicitly stated.

The ion exchange materials currently used most extensively for separations are the synthetic organic resins, particularly those derived from copolymerization of styrene with the cross-linking agent, divinylbenzene. Their ion exchange properties arise through incorporation of charged groups, such as quaternary amines (anion exchangers) or sulphonic acids (cation exchangers). They have high capacities, good chemical stability and show fairly rapid exchange rates. Their limited radiation stability prevents their use at extremely high radiation levels (22, 23). However, as discussed by Parker *et al.* (22), at radiation densities where resin destruction occurs, other radiation-induced problems arise, such as bubble formation in the columns or destruction of organic complexing agents.

These resins show little selectivity for ions of the same charge type and structure and separation factors are often small. Larger separation factors can often be obtained with more highly cross-linked resins, but unfortunately, usually at the expense of a decrease in exchange rates. To meet the need for more selective exchangers, resins have been synthesized which contain special functional groups such as those derived from dipicrylamine, EDTA (ethylenediaminetetraacetic acid), 8-hydroxyquinoline, etc. As reviewed by Deuel & Hutschneker (11) and Hale (24). These resins have higher selectivities for some elements or groups of elements than the "standard" resins, but are still in the developmental stage and presently not generally available for separations.

The clay minerals and related materials have, of course, long been known to have ion exchange properties. A summary of the recent status of the field may be found in many books [e.g., Grim (25)]. Presumably their poor chemical stability limits their use for separations. However, because of their expected radiation stability there is a resurgence of interest in these materials. A number of recent papers discuss their ion exchange properties (26 to 31) and their possible application to radioactive waste disposal problems (32 to 35).

In a search for radiation stable and nonsiliceous inorganic ion exchange materials, hydrous zirconium oxide and a number of other insoluble hydrous oxides were found to exhibit anion exchange and cation exchange properties in acidic and basic solutions respectively (36). Acid salts such as zirconium

phosphate, tungstate, and molybdate behave as cation exchangers (37, 38). These materials have reasonably high capacities, good exchange rates and selectivities, and along with the "classical" adsorbent, activated alumina, should find many applications in inorganic and radiochemical separations.

The term "liquid ion exchange" is currently being introduced by some to describe metal extractions with long-chain amines in suitable diluents such as nitrobenzene, chloroform, and kerosene. Acid uptake by these amine solutions is formally very similar to that of weakly basic anion exchangers [Smith & Page (39)]. Further, extraction of metals by these amines is remarkably similar to adsorbabilities by anion exchange resins as becomes immediately apparent from a comparison of typical anion exchange (14) and extraction data (40, 41, 42). Hence knowledge gained from anion exchange studies appears directly transferable to amine salt extractions, and conversely their study should help elucidate the properties of anion exchangers. Use of the long-chain amines for recovery of uranium, vanadium, and thorium from acidic ore leach liquors [Brown & co-workers (43, 44)] promises to become of considerable importance.

TECHNIQUES

Adsorption by ion exchangers can be considered a two-phase equilibrium just like solvent extraction with which ion exchange shares more than superficial similarity (45). From a practical point of view, ion exchange and solvent extraction differ principally in the ease with which they can be employed in multi-stage and continuous processes. Multi-stage solvent extraction is comparatively easy on an industrial scale, e.g., with counter-current extraction columns, but cumbersome on a laboratory scale. Until the recent introduction of new moving bed (22, 46, 47, 48) and resin-in-pulp methods (49) the reverse seemed to be true for ion exchange chromatography. Even small stationary columns are equivalent to a large number of repetitive contacts and the effective height of a theoretical plate under favorable circumstances may be as small as a few diameters of the exchanger particles [Glueckauf (50)]. Hence most laboratory scale separations can usually be made with columns only a few cm. long, which in turn implies short separation times.

To effect separations in a minimum amount of time and with minimum solution volumes, conditions should be available so that the ions to be separated show large adsorbability ratios or separation factors. Further, the ion to be eluted should show low adsorbability so that it can be removed from the columns within a few column volumes of eluent. For the resolution of mixtures this implies a change of eluent after elution of each element. For difficult separations, where the separation factors are relatively small, e.g., in the separation of rare earths, continuous variation of eluting conditions (gradient elution) (51 to 55) may be found advantageous.

Detailed knowledge of chromatographic theory is generally not a prerequisite for devising separations when the separation factors are large, but

it becomes invaluable when they are small. Excellent discussions of column theory may be found in the recent papers of Glueckauf (50, 56). Said (57) extended the theory to columns which do not necessarily contain a large number of "theoretical plates."

While most ion exchange separations are best carried out by standard column techniques, other methods, of course, may be employed. Batch equilibrations though rarely satisfactory for separations, are widely used for the determination of distribution coefficients which are needed in the search for optimum separations conditions and in a study of the solution chemistry of the solutes.

Rapid elution techniques with shallow resin beds permit separation of short-lived daughter activities from long-lived parents. A typical example, separation of 0.8 sec. Pb^{207m} from Bi^{207} has been discussed by Campbell & Nelson (58) who point out that diffusion theory and decay rate considerations indicate applicability of the technique to the separation of daughter activities with half-lives in the millisecond region.

Paper chromatography of electrolytes is also, in a sense, an ion exchange technique. This relationship has become more obvious with the recent introduction of ion exchange papers made from specially treated cotton fibers (59), and of papers containing ion exchange resin particles (60, 61). Although paper chromatography and its variants, including chromatography with cellulose columns, are extensively used in radiochemical separations, they will not be discussed here.

Excellent separations may sometimes be achieved by a technique often called precipitation chromatography where an exchange column is pre-treated with a reagent which causes precipitation of the ions to be removed. This method is particularly effective for fission product clean-up since, e.g., an anion exchanger in the hydroxide form will remove essentially all metals except the alkalis and alkaline earths (62, 63, 64). The technique also seems adaptable to separation of daughter activities from their parents (65, 66) and has been used by Tokiyama & Suito (67) for group separations in a qualitative analysis scheme. More complete references, particularly to earlier work, may be found in the reviews of Schubert (20) and Finston & Miskel (65).

SEPARATIONS

It has become trivial to state that ion exchange methods can be used to separate essentially all elements of the periodic table from each other. Rather, the problems presently seem to revolve around decreasing the time necessary for separations, controlling elution order, and developing techniques for operation under extreme conditions such as very high temperatures or high radiation levels. Considerable progress along these lines will be made in the future, no doubt, through development of new ion exchange materials, probably an essential prerequisite for work at very high temperatures and radiation levels. Exploitation of complexing reactions of the elements presently

seems to be the most popular approach for decreasing separation times and controlling elution order. The latter is of considerable importance since for best utilization of exchange capacity adsorption of the trace rather than macro component is desired, and for minimizing radiation damage the minor rather than the major activity should be retained.

Through selection of either a cation or anion exchanger one can often control elution order or, better, which ion is adsorbed and which one not. This applies not only to separation of nonmetallic elements from metals, but also to the separation of metals from each other. Adsorbability of a metal by a cation exchanger is normally decreased by complex formation, while the reverse is often the case with anion exchangers. Application of this important feature may be illustrated with the separation of Zn(II), Cd(II), and Hg(II) in chloride solutions. With cation exchangers the most strongly complexed element [Hg(II)] is eluted first at low chloride concentrations and its adsorption can readily be prevented under conditions where Zn(II) and Cd(II) are strongly adsorbed. Cadmium(II) may be eluted at higher chloride concentrations, followed by Zn(II) at still higher concentrations. If the separation is carried out with anion exchangers the three elements could first be adsorbed at relatively high chloride concentrations, Zn(II) and then Cd(II) removed by stepwise decrease of chloride concentration, while Hg(II) would remain adsorbed. Actually, Hg(II) is difficult to remove unless chloride ions are also displaced from the resin with another eluting medium from which Hg(II) does not adsorb.

Thus, anion and cation exchange techniques are often complementary and, except for elution order, there is little reason to prefer one over the other. However, in the opinion of the authors, anion exchange techniques are often clearly superior. Of the many reasons for this preference, the following may be cited: (a) Organic anion exchangers have extraordinary selectivity for some complexes which make separations and concentrations possible at high ionic strength where cation exchange techniques often fail. As a consequence anion exchange techniques often permit exploitation of "unusual" differences between elements. (b) Many metals must be complexed, often to negative ions, to remain in solution and these can be adsorbed only by anion exchangers. (c) Many metal complexes which are adsorbed on anion exchangers can be eluted without consumption of reagents, e.g., with water or dilute electrolyte solutions.

However, irrespective of whether anion or cation exchange techniques are preferred for a given separation, complexing reactions are, as mentioned, of paramount importance. For this reason the following discussion is organized according to ligands used rather than elements or groups of elements. The references cited are to be taken as illustrations; an exhaustive review of the literature was not attempted. Indeed, even complete coverage of the literature would not do justice to this field. Many separations which have not previously been published may be deduced almost immediately from an examination of the adsorption functions of the elements and many adsorp-

tion functions may be estimated with considerable degree of confidence from the known complexing properties of the elements.

Chlorides.—Hydrochloric acid solutions are attractive media for small scale ion exchange separations, not only because HCl is readily available and causes little difficulties in subsequent operations, such as evaporation, but also because most metals are soluble in HCl and many of these form complexes with chloride ions. In addition, a large number of metals are extremely strongly adsorbed by anion exchangers from chloride solutions. The adsorption functions often differ widely, even for so-called "similar" elements. Hence, anion exchange in chloride solutions appears to be an effective and broadly applicable separations technique and the system has received a large amount of attention in a number of laboratories. A comprehensive study of most metals has been carried out during the last several years at the Oak Ridge National Laboratory with a strongly basic, quaternary amine anion exchanger. Much of this information (for elements up to uranium) has been summarized from a separations point of view in recent review articles (14, 16). Japanese workers have made extensive use of anion exchange in chloride solutions as may be illustrated by the work of Sasaki (68) on the separations Se—Te—Po and Te—Sb—Sn and of Yoshino (69) on the separation of P, As, and Ge. In a study of a large number of elements with an imino-type anion exchanger Jentzsch and co-workers (70) found results, which though generally similar to those obtained with quaternary amine resins differed from them considerably for a few elements.

The earlier results with uranium and the transuranic elements have been reviewed by Hyde (13). These elements are strongly adsorbed at moderate HCl concentrations when present in oxidation states +4 and +6 but show little adsorption in their +3 oxidation states. This difference may be utilized for the separation of uranium, neptunium and plutonium from each other, from the transplutonic elements (71), and from thorium and rare earths, which are not adsorbed (72, 73, 74). In saturated HCl the transcurium elements show sufficient adsorbability to permit their separation from the lanthanides (71).

Because of the inherent simplicity of the method, Horton, Thomason & Kelley (75) have utilized anion exchange for remote control separation of uranium and corrosion products from highly radioactive fuel solutions. Horton & Thomason (76) used anion exchange in HCl for the purification of Al(III) (nonadsorbed) from many elements which interfere with its colorimetric determination.

The anion exchange behavior of a number of metals is sufficiently unique in HCl solutions to permit their separation from practically all other elements by a single adsorption-elution cycle. Zn(II) is a particularly favorable example (77) and its separation from other metals has been exhaustively studied by Miller & Hunter (78, 79) and by Rush & Yoe (80).

While anion exchange in HCl solutions leads to many excellent separations, some important exceptions should be noted: (a) A considerable num-

ber of elements cannot be adsorbed at any chloride concentration and other media or cation exchange techniques are necessary for their separation from each other. (b) Several elements, particularly in the fourth and fifth groups of the periodic table, hydrolyze readily even at high acidities and their reproducible handling necessitates the use of stronger complexing agents, e.g., HF or HCl-HF (see next section). (c) Elements which form extremely strong chloride complexes, such as those of the platinum group, are difficult to remove from anion exchangers unless special eluting conditions are employed.

Fortunately many of these strongly complexed elements are not adsorbed by cation exchangers [MacNevin & Crummet (81)] and in this way may be separated from the many elements which normally are adsorbed. Similar cation exchange methods were used by Butler (82) for the removal of base metals from platinum and rhodium and by MacNevin & Lee (83) for the removal of mercury from gold.

Metals which form moderately stable chloride complexes can be removed from cation exchangers in the inverse order of the stability of their chloride complexes by increasing the chloride concentration of the eluent. Essentially such techniques were used by Wickbold (84) and by Yoshino & Kojima (85) for separation of zinc and cadmium and by Klement & Sandmann (86) for separation of gallium, indium, and germanium. Carleson (87) attempted the separation of Co(II), Ni(II) and Cu(II), but—in contrast to the anion-exchange method—found it to be poor. Considerable improvement resulted by the use of mixed solvents for elution, a device which has been successfully employed for a variety of separations [see e.g., Burstall, *et al.* (88), Okuno, Honda & Ishimori (89), Kember, MacDonald & Wells (90), Davies & Owen (91)].

When the metals are not complexed by chloride ions or if complex formation occurs only at very high HCl concentrations, cation exchange separations may be based on the specificity of the resins for the elements to be separated and on the effect of the eluting ion concentration on the exchange equilibrium. From the mass action effect one predicts, ideally, a decrease of adsorbability (distribution coefficients) with eluting ion concentration, the rate of decrease depending on the ratio of the charges of the ions involved. However, Diamond, Street & Seaborg (92) found that Y(III) and some lanthanides show adsorbability minima at moderately high HCl concentrations beyond which the distribution coefficients increase substantially. Since the actinides do not show minima in their adsorption functions this high ionic strength effect may be utilized for separation of trivalent actinides from lanthanides. Similar high ionic strength effects are described by Diamond (93) for alkali metals and alkaline earths. These examples illustrate the desirability of further extending cation exchange studies to high supporting electrolyte concentrations. Ion exchange theory has not yet advanced to the point where predictions can safely be made regarding relative adsorbabilities under such conditions and many surprising results may be anticipated. As

an example, we have found [Kraus, Coombe & Nelson (157)] that Au(III) as the negatively charged complex AuCl_4^- is extremely strongly adsorbed from concentrated chloride solutions by a cation exchanger (Dowex-50) under conditions where a typical cation, such as cesium, is not adsorbed.

HCl-HF mixtures.—Many elements, particularly those of the fourth, fifth and, to some extent, of the sixth group, form hydrolytic polymers or precipitate even in very acidic solutions. The difficulties resulting from these hydrolytic reactions may be circumvented by formation of strong fluoride complexes and effective separations involving these elements have been carried out with HCl-HF mixtures by anion exchange techniques (94 to 97). Fluoride ions have also been used to improve some otherwise marginal separations (72, 98). In view of the effectiveness of anion exchange in HCl-HF mixtures, a large number of elements, including Fe(III) and the soluble elements of groups 3 to 6, were systematically studied in 1 M HF over a broad HCl concentration range and the results were recently summarized (16).

Separations in fluoride-containing media are of course also feasible by cation exchange. The following examples illustrate the attractiveness of the method and the desirability of much further work: Freund & Miner (99) separated aluminum from zirconium; Hettel & Fassel (100) concentrated rare earths at low concentrations and separated them from large amounts of zirconium; the authors, in collaboration with Day (158), separated tracer V^{4+} from titanium oxide cyclotron targets dissolved in 6 M HF.

Other inorganic anions.—Ion exchange in bromide and iodide solutions has so far received little attention. Herber & Irvine (101) found that the anion exchange behavior of a number of transition elements in HBr was very similar to that in HCl. Iodide solutions have been found useful for the separation of zinc and cadmium (78, 102) and for eluting certain elements through reduction to nonadsorbable ions (13, 71).

Anion exchange of a number of metals in cyanide solutions has been discussed by Burstall & Wells (ref. 4, p. 83), though principally in connection with gold recovery. A typical cation exchange separation in cyanide solutions, iron from titanium, has been described by Yoshino & Kojima (103).

Thiocyanate complexing has been used for the separation of iron from aluminum (104), gallium (105) and chromium (106) by anion exchange, and of iron, manganese, and nickel from chromium by cation exchange (107). The trivalent actinides and lanthanides may be adsorbed from thiocyanate solutions by strongly basic anion exchange resins (108). An interesting application is the separation of gram amounts of americium from rare earths (109).

Anion exchange in nitrate solutions has been found useful in a number of applications. Huffman, Oswalt & Williams (110) found that perrhenate and pertechnitate could be removed from anion exchangers more readily with HNO_3 than with HCl as one might expect from the higher selectivity of the

exchangers for nitrate than for chloride ions (111). Thorium (IV), which is not adsorbed from chloride solutions is strongly adsorbed from nitrate solutions and in nitric acid may be separated from rare earths (16, 112), uranium (16, 113) and iron (16). Although adsorption of a few other elements such as Bi(III) (114) and Ce(IV) (16) has been described, it is not expected that anion exchange in nitrates will have as broad applicability as anion exchange in chlorides. Further, nitric acid at high concentrations tends to destroy the resin, a disadvantage which limits the useful nitric acid concentration range.

Use of polyvalent inorganic ions for separations has received surprisingly little attention except in applications relating to recovery of uranium from ore leach liquors. As mentioned earlier, this has become the largest application of ion exchangers outside of the water conditioning field. While isolation of uranium from carbonate and phosphate solutions is feasible, most processes involve isolation from sulfate solutions as has been discussed by various authors at the 1955 Geneva Conference on the Peaceful Uses of Atomic Energy. These methods are based on the fact that uranium in dilute sulfate solutions is strongly adsorbed by anion exchangers under conditions where most other elements show negligible adsorbability. Removal of uranium from the exchangers may be achieved either at high sulfuric acid concentrations or by converting the sulfate form exchangers to some other form (nitrate or chloride) whereupon elution may be achieved at low electrolyte concentrations.

Of the other elements known to be adsorbed from sulfate solutions Th(IV) might be mentioned since it is of special interest in radiochemical applications. The adsorption function of Th(IV) in sulfate solution parallels that of U(VI) closely, although its distribution coefficients are generally lower by a factor of a hundred (16).

The use of phosphate media has received relatively little attention. Recently, however, Holroyd & Salmon (115) showed that a number of trivalent metals were significantly adsorbed by anion exchangers from phosphoric acid solutions under conditions where several divalent elements were essentially not adsorbed. Genge, Holroyd, *et al.* (116) utilized this difference for separations and observed inverted elution order with cation exchangers.

Pyrophosphate media permit interesting separations as demonstrated, for example, by Ryabchikov & Osipova (107) who, using a cation exchanger, separated Fe(III), Cr(III) and Mn(II) by controlling ligand concentration and acidity. Ryabchikov & Osipova (107) and Vasilev, *et al.* (117) also found thiosulfate solutions useful for a number of separations.

Organic ligands.—Organic reagents form complexes with most metals. They were introduced as eluting agents about ten years ago in the now classical cation exchange separations of rare earths and fission products (118) and their popularity has remained high. For example, Buser (119) improved separation (cation exchange) of the alkali metals by elution with uramil-diacetic acid; Lerner & Rieman (120) used lactic acid for the separation of alkaline earths, while Honda (121) used acetate and ethylenediaminetetra-

acetic acid (EDTA); Bovy & Duyckaerts (122) separated barium and strontium with EDTA.

Studies aimed at improving separation of rare earths and trivalent actinides have been very numerous and many eluting agents have been suggested other than the citrates which were used first. The reagents investigated include lactate (52, 71, 123, 124 to 127), malonate (126), glycolate (126, 128, 129), EDTA (126, 130 to 133), and other amino polyacetic acids (134); tartrate (124), and α -hydroxyisobutyrate (135 to 141). Each of these, of course, has special advantages. The reagents of choice presently seem to be lactate, EDTA, and α -hydroxyisobutyrate. Gradient elution has been used for separation of rare earths and of actinides. A gradient technique based on continuous variation of operating temperature has recently been suggested by Stewart (141), who believes that the temperature coefficient of the acid constant of the complexing agent is utilized.

In view of the success of cation exchange separations with organic ligands, anion exchange methods tended to be neglected. However, many excellent separations are feasible by anion exchange as demonstrated particularly by Samuelson and his co-workers, who also describe separations in which the complexing agent is adsorbed on the exchanger and not added to the solution. Using exchangers in citrate, acetate, or EDTA forms, they separated the alkali metals and alkaline earths from many other elements (142 to 146). Separation of alkaline earths from alkali metals was effected through control of the acidity of the eluent or with alcoholic solutions (143). The authors utilized anion exchange for the separation of lithium from sodium and other alkali metals (147) and for the separation of the alkaline earths from each other (148) in EDTA and citrate solutions respectively. Anion exchange separation of rare earths in citrate solutions has also been demonstrated (149).

Because of their excellent complexing properties, oxalates should be effective ligands for ion exchange separations. The following anion exchange separations involving oxalates are representative: Sn—Sb—Te (150); Fe—Ga (151); Mo—W (152); Nb—Ta (153); Nb—Zr (154).

Separations schemes.—General separations schemes based exclusively on ion exchange methods now appear feasible though so far such schemes have not been proposed and tested. Of course, as in conventional analysis, radiochemical problems rarely require a scheme for separating all elements. The largest group of elements normally encountered by radiochemists are those contained in gross fission product mixtures. These may readily be divided into sub-groups, e.g., by cation exchange methods as described by Parker, *et al.* (22). More detailed schemes for isolating individual fission products as well as some heavy elements were described by Japanese workers (155) in connection with their interesting analyses of "Bikini Ashes" which fell on the fishing boat "Fukuryu Maru." Crouch & Cook (156) also describe a general scheme for fission product analysis. A discussion of anion exchange of fission products has been given by the authors (14).

Schemes for group separations, of course, are not limited to the fission products and, indeed, ion exchange techniques, either by themselves or in conjunction with standard analytical methods, presently appear extremely attractive for such purposes. While exploitation of ion exchange for general analysis is still largely in the future, ion exchange techniques presently are most highly developed for routine and rapid removal of a large number of elements from mixtures, for isolation of elements with unique adsorption properties, for separations involving relatively few elements, and—an application not sufficiently recognized—for identification of radioactive tracers.

LITERATURE CITED

1. Samuelson, O., *Ion Exchangers in Analytical Chemistry* (John Wiley and Sons, Inc., New York, N. Y., 291 pp., 1953)
2. Ion Exchange Resins in Medicine and Biological Research, *Ann. N. Y. Acad. Sci.*, **57**, 61 (1953)
3. Broda, E., and Schönfeld, T., *Handbuch der Mikrochemischen Methoden*, **2** (Springer Verlag, Vienna, Austria, 423 pp., 1955)
4. *Ion Exchange and Its Applications* (Collected papers) (J. Soc. Chem. Ind. London, England, 173 pp., 1955)
5. Lederer, E., and Lederer, M., *Chromatography* (Elsevier Publishing Company, 2nd English Ed., Amsterdam, The Netherlands, 711 pp., 1957)
6. Osborn, G. H., *Synthetic Ion Exchangers* (Chapman and Hall Ltd., London, 194 pp., 1955)
7. Deitz, V. R., *Bibliography of Solid Adsorbents* (Nat'l. Bur. of Standards Circular 566, 1528 pp., 1956)
8. Nachod, F. C., and Schubert, J., Eds. *Ion Exchange Technology* (Academic Press, Inc., New York, N. Y., 660 pp., 1956)
9. Bruce, F. R., Fletcher, J. M., Hyman, H. H., and Katz, J. J., Eds., *Process Chemistry, Progress in Nuclear Energy*, **III** (McGraw-Hill Book Co., Inc., New York, N. Y., 407 pp., 1956)
10. Buser, W., Graf, P., and Grutter, W. F., *Chimia (Switz.)*, **9**, 73 (1955)
11. Deuel, H., and Hutschneker, K., *Chimia (Switz.)*, **9**, 49 (1955)
12. Griessbach, R., *Chem. Tech. (Berlin)*, **9**, 12 (1957)
13. Hyde, E. K., *Proc. Intern. Conf. Peaceful Uses Atomic Energy*, **7**, 281 (1956)
14. Kraus, K. A., and Nelson, F., *Proc. Intern. Conf. Peaceful Uses Atomic Energy*, **7**, 113, 131 (1956)
15. Kraus, K. A., In *Symposium on Trace Analysis* (John Wiley and Sons, In press)
16. Kraus, K. A., and Nelson, F., In *Symposium on Ion Exchange and Chromatography* (Am. Soc. Testing Materials, June 1956, In press)
17. (a) Kunin, R., et al. (yearly reviews), e.g., *Anal. Chem.*, **27**, 1191 (1955); **28**, 729 (1956); (b) *Ind. Eng. Chem.*, **47**, 565 (1955); **48**, 540 (1956); **49**, 507 (1957)
18. Rupp, A. F., and Binford, F. T., *J. Appl. Phys.*, **24**, 1069 (1953)
19. Schindewolf, U., *Mass. Inst. Technol., Lab. Nuclear Science Tech Rept.*, No. 68 (December 1955); *Angew Chem.*, **69**, 226 (1957)
20. Schubert, J., *Ann. Rev. Phys. Chem.*, **5**, 412 (1954)
21. Thomas, H. C., and Frysinger, G. R., *Ann. Rev. Phys. Chem.*, **7**, 137 (1956)
22. Parker, G. W., Higgins, I. R., and Roberts, J. T., in *Ion Exchange Technology* (Academic Press Inc., New York, N. Y., 660 pp., 1956)
23. Cathers, G. I., In *Process Chemistry, Progress in Nuclear Energy*, **III** (McGraw-Hill Book Co., Inc., New York, N. Y., 407 pp., 1956)
24. Hale, D. K., *Research*, **9**, 104 (1956)
25. Grim, R. E., *Clay Mineralogy* (McGraw-Hill Book Company, Inc., New York, N. Y., 384 pp., 1953)
26. Gaines, G. L., Jr., and Thomas, H. C., *J. Chem. Phys.*, **21**, 714 (1953); **23**, 2322 (1955)
27. Faucher, J. A., and Thomas, H. C., *J. Chem. Phys.*, **22**, 258 (1954)
28. Barrer, R. M., and Sammon, D. C., *J. Chem. Soc. (London)*, 2838 (1955); 675 (1956)

RADIOCHEMICAL SEPARATIONS BY ION EXCHANGE 43

29. Barrer, R. M., and Falconer, J. D., *Proc. Roy. Soc. (London), A*, **236**, 227 (1956)
30. Amphlett, C. B., *British Report, AERE C/R-1862* (1956)
31. Amphlett, C. B., and McDonald, L. A., *J. Inorg. & Nuclear Chem.*, **2**, 403 (1956)
32. Hatch, L. P., *Am. Scientist*, **41**, 410 (1953)
33. Ginell, W. S., Martin, J. J., and Hatch, L. P., *Nucleonics*, **12**, 14 (December 1954)
34. Manowitz, B., and Hatch, L. P., *Chem. Eng. Progr. Symposium Series*, **50**, (12) 144 (1954)
35. Hatch, L. P., Regan, W. H., Mnaowitz, B., and Hittman, F., *Proc. Intern. Conf. on the Peaceful Uses of Atomic Energy*, **9**, 648, United Nations (1956)
36. Kraus, K. A., and Phillips, H. O., *J. Am. Chem. Soc.*, **78**, 249 (1956)
37. Kraus, K. A., and Phillips, H. O., *J. Am. Chem. Soc.*, **78**, 694 (1956)
38. Kraus, K. A., Carlson, T. A., and Johnson, J. S., *Nature*, **177**, 1128 (1956)
39. Smith, E. L., and Page, J. E., *J. Soc. Chem. Ind. (London)*, **67**, 48 (1948)
40. Leddicotte, G. W., and Moore, F. L., *J. Am. Chem. Soc.*, **74**, 1618 (1952)
41. Ellenberg, J. Y., Leddicotte, G. W., and Moore, F. L., *Anal. Chem.*, **26**, 1045 (1954)
42. Mahlman, H. A., Leddicotte, G. W., and Moore, F. L., *Anal. Chem.*, **26**, 1939 (1954)
43. Brown, K. B., Crouse, D. J., Coleman, C. F., *Some New Solvent Extraction Processes for Use in the Hydrometallurgical Treatment of Uranium, Thorium and Vanadium Ores* (Presented at the Ann. Inst. Mining Eng. Meeting, New Orleans, La., February 1957)
44. *Chem. Eng. News*, **34**, 2590 (1956)
45. Kraus, K. A., Nelson, F., and Smith, G. W., *J. Phys. Chem.*, **58**, 11 (1954)
46. Hutcheon, J. M., *Ion Exchange and Its Application*, 101, (Soc. Chem. Ind., London, England, 173 pp., 1955)
47. Higgins, I. R., and Roberts, J. T., *Chem. Eng. Progr. Symposium Series*, **50** (14), 87 (1954)
48. Arehart, T. A., Bresee, J. C., Hancher, C. W., and Jury, S. H., *Chem. Eng. Progr.*, **52**, 353 (1956)
49. Hollis, R. F., and McArthur, C. K., *Proc. International Conference on the Peaceful Uses of Atomic Energy*, **8**, 54, United Nations (1956)
50. Glueckauf, E., *Ion Exchange and Its Applications*, **34** (Soc. Chem. Ind., London, England, 173 pp., 1955)
51. Alm, R. S., Williams, J. P., and Tiselius, A., *Acta. Chem. Scand.*, **6**, 826 (1952)
52. Freiling, E. C., and Bunney, L. R., *J. Am. Chem. Soc.*, **76**, 1021 (1954)
53. Nervik, W. E., *J. Phys. Chem.*, **59**, 690 (1955)
54. Freiling, E. C., *J. Am. Chem. Soc.*, **77**, 2067 (1955)
55. Piez, K. A., *Anal. Chem.*, **28**, 1451 (1956)
56. Glueckauf, E., *Trans. Faraday Soc.*, **51**, 34 (1955)
57. Said, A. S., *Am. Inst. Chem. Eng. Journal*, **2**, 477 (1956)
58. Campbell, E. C., and Nelson, F., *J. Inorg. & Nuclear Chem.*, **3**, 233 (1956)
59. Kember, N. F., and Wells, R. A., *Nature*, **175**, 512 (1955)
60. Hale, D. K., *Chem. Ind.*, 1147 (1955)
61. Lederer, M., *Anal. Chim. Acta*, **12**, 142 (1955); **15**, 226 (1956)
62. Dalton, J. C., and Welch, G. A., *Anal. Chim. Acta*, **15**, 317 (1956)
63. James, R. H., and Welch, G. A., *Nature*, **177**, 183 (1956)

64. Woodhead, J. L., Fudge, A. J., and Jenkins, E. N., *Analyst*, **81**, 570 (1956)
65. Finston, H. L., and Miskel, J., *Ann. Rev. Nuclear Science*, **5**, 269 (1955)
66. Perkins, R. W., *Anal. Chem.*, **29**, 152 (1957)
67. Tokiyama, K., and Suito, E., *Japan Analyst*, **4**, 8 (1955); *Chem. Abstracts*, **50**, 4699a (1956)
68. Sasaki, Y., *Bull. Chem. Soc. Japan*, **28**, 89, 615 (1955)
69. Yoshino, Y., *Bull. Chem. Soc. Japan*, **28**, 382 (1955)
70. Jentzsch, D., et al., *Z. anal. Chem.*, **146**, 88 (1955); **147**, 20 (1955); **148**, 321, 325 (1955-56); **150**, 241 (1956); **152**, 134 (1956)
71. Thompson, S. G., Harvey, B. G., Choppin, G. R., and Seaborg, G. T., *J. Am. Chem. Soc.*, **76**, 6229 (1954)
72. Kraus, K. A., Nelson, F., and Moore, G. E., *J. Am. Chem. Soc.*, **77**, 3972 (1955)
73. Kraus, K. A., Moore, G. E., and Nelson, F., *J. Am. Chem. Soc.*, **78**, 2692 (1956)
74. Ishimori, T., and Okuno, H., *Bull. Chem. Soc. Japan*, **29**, 78 (1956)
75. Horton, A. D., Thomason, P. F., and Kelley, M. T., *Anal. Chem.*, **29**, 388 (1957)
76. Horton, A. D., and Thomason, P. F., *Anal. Chem.*, **28**, 1326 (1956)
77. Kraus, K. A., and Moore, G. E., *J. Am. Chem. Soc.*, **75**, 1460 (1953)
78. Miller, C. C., and Hunter, J. A., *Analyst*, **79**, 483 (1954)
79. Hunter, J. A., and Miller, C. C., *Analyst*, **81**, 79 (1956)
80. Rush, R. M., and Yoe, J. H., *Anal. Chem.*, **26**, 1345 (1954)
81. MacNevin, W. M., and Crummett, W. B., *Anal. Chem.*, **25**, 1628 (1953)
82. Butler, C. K., *Ind. Eng. Chem.*, **48**, 711 (1956)
83. MacNevin, W. M., and Lee, I. L., *Anal. Chim. Acta*, **12**, 544 (1955)
84. Wickbold, R., *Z. anal. Chem.*, **132**, 401 (1951)
85. Yoshino, Y., and Kojima, M., *Japan Analyst*, **4**, 311 (1955); *Chem. Abstracts*, **50**, 12737d (1956)
86. Klement, R., and Sandmann, H., *Z. anal. Chem.*, **145**, 325 (1955)
87. Carleson, G., *Acta Chem. Scand.*, **8**, 1673 (1954)
88. Burstall, F. H., Forrest, P. J., Kember, N. F., and Wells, R. A., *Ind. Eng. Chem.*, **45**, 1648 (1953)
89. Okuno, H., Honda, M., and Ishimori, T., *Japan Analyst*, **2**, 428 (1953); *Chem. Abstracts*, **48**, 6320^o (1954)
90. Kember, N. F., Macdonald, P. J., and Wells, R. A., *J. Chem. Soc.*, 2273 (1955)
91. Davies, C. W., and Owen, B. D. R., *J. Chem. Soc.*, 1676 (1956)
92. Diamond, R. M., Street, K., Jr., and Seaborg, G. T., *J. Am. Chem. Soc.*, **76**, 1461 (1954)
93. Diamond, R. M., *J. Am. Chem. Soc.*, **77**, 2978 (1955)
94. Kraus, K. A., and Moore, G. E., *J. Am. Chem. Soc.*, **73**, 9, 13, 2900 (1951)
95. Huffman, E. H., and Lilly, R. C., *J. Am. Chem. Soc.*, **73**, 2402 (1951)
96. Forsling, W., *Arkiv Kemi*, **5**, 489, 503 (1953)
97. Hague, J. L., Brown, E. D., and Bright, H. A., *J. Research Natl. Bur. Standards*, **53**, 261 (1954)
98. Kraus, K. A., and Moore, G. E., *J. Am. Chem. Soc.*, **77**, 1383 (1955)
99. Freund, H., and Miner, F. J., *Anal. Chem.*, **25**, 564 (1953)
100. Hettel, H. J., and Fassel, V. A., *Anal. Chem.*, **27**, 1311 (1955)
101. Herber, R. H., and Irvine, J. W., Jr., *J. Am. Chem. Soc.*, **76**, 987 (1954)
102. Baggott, E. R., and Willcocks, R. G. W., *Analyst*, **80**, 53 (1955)
103. Yoshino, Y., and Kojima, M., *Bull. Chem. Soc. Japan*, **23**, 46 (1950)
104. Teicher, H., and Gordon, L., *Anal. Chem.*, **23**, 930 (1951)

105. Korkisch, J., and Hecht, F., *Mikrochim. Acta*, 1230 (1956)
106. Venturello, G., and Gualandi, C., *Ann. Chim.*, **46**, 229 (1956); *Chem. Abstracts*, **50**, 12739^a (1956)
107. Ryabchikov, D. I., and Osipova, V. E., *J. Anal. Chem. U.S.S.R.* **11**, (3) 285 (1956)
108. Surls, J. P., Jr., and Choppin, G. R., *J. Inorg. & Nuclear Chem.*, **4**, 62 (1957)
109. Coleman, J. S., Penneman, R. A., Keenan, T. K., Lamas, L. E., Armstrong, D. E., and Asprey, L. B., *J. Inorg. & Nuclear Chem.*, **3**, 327 (1956)
110. Huffman, E. H., Oswalt, R. L., and Williams, L. A., *J. Inorg. & Nuclear Chem.*, **3**, 49 (1956)
111. Wheaton, R. M., and Bauman, W. C., *Ind. Eng. Chem.*, **43**, 1088 (1951)
112. Chen, Y., Lin, C., and Chen, T., *J. Chinese Chem. Soc. [2]*, **2**, 111 (1955) (in English); *Chem. Abstracts*, **50**, 9220^a (1956)
113. Carswell, D. J., *J. Inorg. & Nuclear Chem.*, **3**, 384 (1957)
114. Nelson, F., and Kraus, K. A., *J. Am. Chem. Soc.*, **76**, 5916 (1954)
115. Holroyd, A., and Salmon, J. E., *J. Chem. Soc.*, 269 (1956)
116. Genge, J. A. R., Holroyd, A., Salmon, J. E., and Wall, J. G. L., *Chem. Ind. (London)*, 357 (1955)
117. Vasilev, A. M., Toropova, V. F., and Busygina, A. A., *Uchenye Zapiski Kazan. Gosudarst. Univ. im. V. I. Ul'yanova-Lenina*, **113**, (8) 91 (1953); *Referat. Zhur. Khim.*, 1954 (44488) *Chem. Abstracts*, **50**, 724^b (1956)
118. (Collected papers), *J. Am. Chem. Soc.*, **69**, 2769-881 (1947)
119. Buser, W., *Helv. Chim. Acta*, **34**, 1635 (1951)
120. Lerner, M., and Rieman, W., *Anal. Chem.*, **26**, 610 (1954)
121. Honda, M., *Japan Analyst*, **3**, 132 (1953); *Chem. Abstracts*, **48**, 9868^a (1954)
122. Bovy, R., and Duyckaerts, G., *Anal. Chim. Acta*, **11**, 134 (1955)
123. Cunningham, J. G., et al., *J. Inorg. & Nuclear Chem.*, **1**, 163 (1955)
124. Glass, R., *J. Am. Chem. Soc.*, **77**, 807 (1955)
125. Wish, L., Freiling, E. C., and Bunney, L. R., *J. Am. Chem. Soc.*, **76**, 3444 (1954)
126. Mayer, S. W., and Freiling, E. C., *J. Am. Chem. Soc.*, **75**, 5647 (1953)
127. Bunney, L. R., Freiling, E. C., McIsaac, L. D., and Scadden, E. M., *Nucleonics*, **15**, (2) 81 (1957)
128. Stewart, D. C., *Anal. Chem.*, **27**, 1279 (1955)
129. Stewart, D. C., and Faris, J. P., *J. Inorg. & Nuclear Chem.*, **3**, 64 (1956)
130. Spedding, F. H., Powell, J. E., and Wheelwright, E. J., *J. Am. Chem. Soc.*, **76**, 612 (1954)
131. Cornish, F. W., Phillips, G., and Thomas, A., *Can. J. Chem.*, **34**, 1471 (1956)
132. Loriers, J., *Compt. rend.*, **240**, 1537 (1955)
133. Fuger, J., *Bull. soc. chim. Belges*, **66**, 151 (1957)
134. Holleck, L., and Hartinger, L., *Angew. Chem.*, **66**, 586 (1954)
135. Ghiorso, A., Harvey, B. G., Choppin, G. R., Thompson, S. G., and Seaborg, G. T., *Phys. Rev.*, **98**, 1518 (1955)
136. Milsted, J., Beadle, A. B., Glover, K. M., and Fremlin, J. H., *AERE-C/R-1951* (May 1956)
137. Smith, H. L., and Hoffman, D. C., *J. Inorg. & Nuclear Chem.*, **3**, 243 (1956)
138. Milsted, J., and Beadle, A. B., *J. Inorg. & Nuclear Chem.*, **3**, 248 (1956)
139. Choppin, G. R., and Silva, R. J., *J. Inorg. & Nuclear Chem.*, **3**, 153 (1956)
140. Choppin, G. R., Harvey, B. G., and Thompson, S. G., *J. Inorg. & Nuclear Chem.*, **2**, 66 (1956)

141. Stewart, D. C., *J. Inorg. & Nuclear Chem.*, **4**, 131 (1957)
142. Samuelson, O., Lundén, L., and Schramm, K., *Z. anal. Chem.*, **140**, 330 (1953)
143. Samuelson, O., and Sjöström, E., *Anal. Chem.*, **26**, 1908 (1954)
144. Samuelson, O., *Chim. anal.*, **37**, 191 (1955)
145. Samuelson, O., Sjöström, E., and Forsblom, S., *Z. anal. Chem.*, **144**, 323 (1955)
146. Samuelson, O., and Sjöberg, B., *Anal. Chim. Acta*, **14**, 121 (1956)
147. Nelson, F., *J. Am. Chem. Soc.*, **77**, 813 (1955)
148. Nelson, F., and Kraus, K. A., *J. Am. Chem. Soc.*, **77**, 801 (1955)
149. Huffman, E. H., and Oswalt, R. L., *J. Am. Chem. Soc.*, **72**, 3323 (1950)
150. Smith, G. W., and Reynolds, S. A., *Anal. Chim. Acta*, **12**, 151 (1955)
151. Blasius, E., and Negwer, M., *Z. anal. Chem.*, **143**, 257 (1954)
152. Meloche, V. W., and Preuss, A. F., *Anal. Chem.*, **26**, 1911 (1954)
153. Gillis, J., et al., *Mededel. Koninkl. Vlaam. Acad. Wetenschap. Belg.*, **15**, No. 13, 3 (1953); *Chem. Abstracts*, **48**, 9862^d (1954)
154. Wacker, R. E., and Baldwin, W. H., *U. S. AEC Report, ORNL 637* (1950); *Nuclear Sci. Abstr.*, **4**, 469 (1950); *Brit. Abstr.*, C244 (1951)
155. Kimura, K., et al., *Japan Analyst*, **3**, 335 (1954); See also K. Kimura, *Proc. Intern. Conf. Peaceful Uses Atomic Energy*, **7**, 196 (1956)
156. Crouch, E. A. C., and Cook, G. B., *J. Inorg. & Nuclear Chem.*, **2**, 223 (1956)
157. Kras, K. A., Coombe, D. C., and Nelson, F. (Unpublished data)
158. Hettesl, H. J., Fassel, V. A., and Day, R. A. (Unpublished data)

EQUIPMENT FOR HIGH LEVEL RADIO-CHEMICAL PROCESSES¹

BY NELSON B. GARDEN AND ELMER NIELSEN

University of California Radiation Laboratory, Berkeley, California

At first glance it might appear that the major portion of the subject of this review would be covered adequately and easily through reference to "Chemical Processing and Equipment; Selected Reference Material, U. S. Atomic Energy Program," a recent survey (1) prepared primarily for the Geneva, Switzerland International Conference on the Peaceful Uses of Atomic Energy in 1955. By combining with the Geneva publication a few other (2 to 7) selected references a sufficient cross section can be obtained to show the development of the art and to illustrate the divergent tendencies which have existed.

However, anyone venturing into the field of high level radiochemical processing for the first time may easily become confused by the magnitude and diversity of the associated problems presented in the literature. It is hoped that this review may assist in clarifying the interrelation of the many factors which should properly be considered in choosing the most advantageous equipment for undertaking high level radiochemistry.

In this survey wherever opinions are expressed or implied they are based on the viewpoint that safety is given foremost importance. Along with this, however, must be combined the practical considerations dealing with efficiency and expense.

BASIC FACTORS IN EQUIPMENT DESIGN

In the early days, processors of radioactive materials approached the hazard problems in about the same way, i.e., giving them minimum consideration. With advances in the radiological field the importance of these problems became recognized and various corrective approaches were taken leading to the development of different, mutually incompatible types of equipment for radiochemical processing.

One redeeming feature is that of these different approaches, one appears to be gaining in popularity. In fact, it is conceivable that we will shortly reach the period when under such a single approach considerable standardization of equipment for high level radiochemical processes will be achieved and much of this equipment will be as commercially available as similar equipment for nonradioactive chemical operations.

The design of processing equipment should start by considering and making decisions regarding the factors enumerated in Table I.

The factors in Table I are not as independent of one another as the tabulation might imply. For instance, the type of shielding used usually

¹ The survey of literature pertaining to this review was completed in March, 1957.

TABLE I
FACTORS AFFECTING EQUIPMENT DESIGN

-
1. Area selected to be subject to contamination
 - a. As a basic processing area
 - b. As dispersion from airborne physical transfer
 1. From planned processed steps
 2. From normal transfer operations into or out of working area
 3. From required repair, modification, or replacement operations
 4. From waste disposal operations
 5. From demolition operations, upon termination of process operations
 2. Shielding and Viewing
 3. Material Damage—Decontamination
-

dictates the type of manipulator one must use and this in turn might influence the efforts to control and limit the area of contamination. Keeping in mind that such interrelationships do exist, the above factors will be discussed, particularly in the manner in which they have a bearing on the equipment that has been developed for high level radiochemical processes.

There will also be some discussion of facilities developed for operations such as metallurgical tests which involve radioactive materials, but which are not primarily chemical operations. Considerable shielding and auxiliary handling equipment were originally developed for metallurgical tests and studies, but became applied to or closely duplicated for the more contamination-spreading, corrosive, and equipment-damaging chemical operations.

AREA OF CONTAMINATION

In the opinion of the authors, the major factor affecting the design of radiochemical processing equipment is the choice of the area wherein contamination is to be controlled. The stricter the control, the greater the ingenuity required to assure that the desired area of contamination limits are met. Conversely, the design of the radiochemical processing equipment can determine the area of contamination. The extent of the area of contamination may not always be immediately apparent, being determined possibly from equipment repair or modification operations (8), decontamination operations, or transfer operations (9), or arising from insidious, sometimes unsuspected, accumulations (10, 11).

For practically any operation the area of contamination need be no more than the interior of small, mobile enclosures (12 to 16) or multiples thereof. Without enclosure controls it may extend over the entire operating areas (17 to 19) including air exhaust plenums, buried drain lines, and personnel-occupied areas. The latter case is usually associated with provisions for change rooms, special protective clothing, special "hot" laundries, rigid rules against eating or smoking in operating areas, and frequent urine analysis and other medical checks on operating personnel.

The point to examine in any installation is the nature of the contamination barrier and its weaknesses. In many cases there are provisions for an adequate contamination barrier for a given process if it is not necessary to penetrate the barrier (*a*) for process manipulations, (*b*) for repair, modification or replacement of equipment, (*c*) for removal of product or waste, or (*d*) for disposal of equipment upon termination of the process.

At one time, most organizations chemically processing radioactive materials were on common ground. Recognition of the toxicity of radioisotopes caused the operations to be undertaken in fume hoods (20, 21) in accordance with the long-established practice for handling nonradioactive, toxic, or noxious chemicals. If radioactivity levels were high enough to warrant shielding, lead or steel bricks were stacked in the hood between the operator and his work, and operations were viewed with mirrors. Operations were performed around the shielding, with the hands or by means of tongs (22, 23). Tongs were also developed (24) for operating through the shielding wall. One of the earliest specialized pieces of equipment was remote pipetting apparatus (25, 26) used in such installations.

The contamination barrier was a dynamic one: an air flow passing by the operator into the hood and up the stack. The intended area of contamination was the inside of the hood with lesser degrees of contamination in the stack and outside environment. Steps were taken to limit the area of contamination to the hood itself by installing filters in the exhaust stack, concurrent with studies (27) to find better filtering media. The area of contamination however was also found to extend into the personnel-occupied laboratory area, a situation attributable to poor air flow characteristics at the hood face, aggravated by movements in front of the hood (28) and also to penetrations of the contamination barrier for reasons previously stated.

The varying solutions to this problem led to divergent corrective measures that in turn affected the design of operating equipment. In some cases, studies were made for high air velocities; hood entrance designs and exhaust patterns (28, 29) that would alleviate the poor characteristics of an air stream as a dynamic contamination barrier. Hood face velocities of 100 to 150 ft/min. combined with laminar flow design were found to be necessary. The impact of this on the size of filters, blowers, and general building ventilation and heating can be appreciated (18).

Another companion-correction was to redesign hoods (30, 31) to have smaller openings while processing material, thus achieving the higher air flows but with smaller, less expensive filters and blowers. The hood construction permitted large openings when installing or removing equipment for a process but the lower air flow became a hazard when dismantling contaminated equipment. Many hot cells, presently in use, can be considered as falling in this category.

A different approach was to eliminate almost completely the dependence on the air flow as a contamination barrier by completely enclosing an operation in a fairly tight mobile enclosure (12), that had only the air through-put

(10 to 30 cfm) necessary for removing chemical fumes and mists. Operations were performed inside such enclosures through rubber gloves if penetrating radiation were not involved. If shielding were required, it was placed around the enclosure (13) and operations were carried out by mechanical means usually involving to some extent through-the-shielding manipulators. It should be emphasized that the shielding was separate and distinct from the enclosure. The shielding did not also serve as the contamination barrier, and thus never became contaminated.

Certain operational and design criteria as stated in Table II are the essence of the shielded-enclosure approach to controlling the contamination spread from radiochemical operations.

The enclosure and its exhaust train up to a closely placed filter defined quite specifically and limited the area of contamination. By planning the process equipment within the enclosure, with the understanding that repair, maintenance, replacement, decontamination, and eventual disposal of equipment as well as removal of product and waste must be possible without destroying the integrity of the contamination barrier, one has the assurance that the area of contamination will be within the desired limits.

Having the process equipment within mobile enclosures permits the disposal and replacement of the entire enclosure and its equipment as a possible alternative to the lengthy and costly decontamination operations otherwise required in order to repair, replace or just remove a piece of equipment.

TABLE II
OPERATIONAL AND DESIGN CRITERIA FOR RADIOCHEMICAL,
SHIELDED-ENCLOSURE OPERATIONS

-
1. Enclosure
 - a. Sized for ready disposal without disassembly.
 - b. Mobility (not a fixed installation).
 - c. Possible to interconnect and disconnect several enclosures even when contaminated inside.
 - d. Standardization.
 2. Equipment
 - a. Engineered to permit remote assembly from and disassembly into units that can be introduced into or removed from the enclosure without violation of the contamination barrier.
 - b. Engineered to permit decontamination and reuse if expensive, or made inexpensive enough to justify disposal after use.
 - c. As much equipment as possible, particularly of the type that is expensive or requires frequent maintenance, designed to be outside the contamination barrier and, if possible, outside the shielding.
 - d. Standardization for commercial production as is similar equipment for nonradioactive, nonremote operations.
 3. Planned operations, including waste disposal, equipment repair and replacement, and decontamination or final demolition.
 4. Cold practice runs of planned operations.
-

Recent work (16, 32) has shown that presently developed filters are not adequate contamination barriers for high-level radiochemical operations. Very tight enclosures have been developed for such operations wherein the air exhaust rates are 0.01 to 0.02 cfm, with a 10-20 cfm recirculating system for removing fumes and mists.

Mention should also be made of completely tight enclosures that developed mainly from the need for inert or dry atmospheres or both in handling or processing pyrophoric or hygroscopic materials (33, 34).

It was stated earlier that of the different approaches for handling the factors in Table I, one appears to be gaining ground. More frequent use can be noted (35 to 38) of enclosures instead of hoods as the contamination barrier for operations not involving penetrating radiation. There is also an increasing use of enclosures inside of shielding facilities (39 to 43).

In some cases (44 to 46), involving existing caves, provisions are being made for the use of hoods inside such caves to minimize contamination of the shielding or for the use of separate enclosures if particularly contaminating operations are to be run. At first glance, it might appear that existing cave construction and type of manipulators in use would make difficult the transition to a completely separate contamination enclosure. However, successful applications (41 to 43) involving similar caves and manipulators indicate otherwise. There would be a loss of the horizontal travel, presently enjoyed by some manipulator installations (44, 45).

There is a growing awareness appearing in print (47 to 50) of the problems involved, such as downtime of facility use and radiation burn-up of available manpower, when the shielding serves also as the contamination barrier. One also finds (51 to 55) more recognition and planning for operations beyond the process itself such as the introduction of material, replacement of equipment, removal of product, samples and waste. The removal of liquid product, sample or waste is not too difficult. Vacuum or gravity systems can be used for their transfer outside the enclosure and shielding to suitably shielded receivers and if heat-sealable plastic tubing is used, disconnects should present no problem.

It is the transfer of solids, including bottled liquids, that presents difficulty if the spread of contamination is undesirable. Drawer-type arrangements operating through shielding walls are described (56, 57), but they appear to take only radiation protection into consideration. A design (58) for sealing a container to an opening in a cave wall is indicative of a considerable amount of attention and ingenuity to the contamination control aspects of a transfer operation. A motorized dolly for receiving material from the bottom of a separately shielded enclosure is described (39), having provisions for some degree of control of the spread of contamination. There is an excellent system (34, 59) for unshielded high level operations involving the use of heatsealable, plastic bags attached to the process enclosure. There is some indication (16, 41) also of its use for shielded operations.

With regard to the replacement, removal or final disposition of process equipment, a trend can be noted towards having such equipment simple and

inexpensive (48, 60, 61), thus justifying disposal rather than decontamination, and towards minimizing the equipment (62, 63) in the contaminated area. In this connection one also notes increasing use (64 to 67) of the term "unitization." Unitization can be defined as the design of equipment for a process in such a way that any part or unit is reasonable in size with respect to its disposal and can be easily inserted and removed remotely for a complete assembly. It is in these phases of equipment development that the greatest progress is yet to come.

SHIELDING AND VIEWING

In discussing shielding, one should differentiate between shielding for gammas and shielding that must, in addition, be adequate for neutrons. The latter type of shielding is particularly necessary for nuclear reactors and particle accelerators. For reasonable size, such shielding must contain the better neutron moderators and absorbers. Much of the development work on concrete shields has been directed at applications involving high neutron flux attenuation.

In radiochemical processing, the neutron shielding problem is confined to those few places processing high levels of alpha-emitters in intimate proximity to materials having significant cross sections for alpha-neutron reactions and to those processing the higher actinides for which spontaneous fission rates are significant. Since such neutron shielding is still a limited problem, it will not be considered in this discussion.

The necessity for shielding to protect personnel from radiation is one of the major basic requirements leading to the continuous development work still underway for equipment to perform operations remotely and for means to view those operations. Regardless of what the shielding material is or whether it is one inch or ten feet thick, it might appear that a given remote operation problem could be solved with the same equipment, that is, the type of shielding used would be determined solely by the cost of the various shielding materials. This is not the case at the present time.

Basically the problem is to transmit direction, force, and energy into an area one dare not enter, and generally cannot enter. What one might otherwise do—if radioactivity were not involved—with one's hands must be done by other means. It is possible to design equipment for an operation and control the equipment from any reasonable distance by electrical or hydraulic means, or, in some cases such as valves, by simple handle extensions. If this could be done, the type or thickness of shielding would not be pertinent to the design of the equipment.

But, if unforeseen equipment repairs are needed, or equipment or process changes are desired after a run is underway, the steps involved to do these things can be difficult, time-consuming and extremely hazardous (8, 68). Conceivably, all such problems could be foreseen and designed for, using electrical or hydraulic systems to carry out the operations. An alternative, however, would be to have a mechanical extension of the hands that could perform a multitude of operations as needed or desired.

Very versatile, though both complicated and expensive, forms of an extension of the hands are the mechanical master-slaves (69 to 73) which operate over the top of a front-shielded cave (74) or through a top opening (41, 64) or over-the-head front wall opening (42, 54, 75) in a completely shielded cave. The master-slave was designed originally for metallurgical studies in caves of the shielded-hood type for which the shielding also formed part of the contamination barrier. Its purpose was not just to handle some unforeseen operations, but any operation. Its development stemmed (69, 76) from the feeling that modification of standard laboratory instruments and apparatus for remote control was sometimes costing many times that of the original equipment and that this was being done for each and every test. The intent was to provide the scientists with easily controllable mechanical arms so that he could operate existing standard laboratory equipment behind shielding barriers with minimum modification and at the same time be prepared for unpredictable requirements and emergencies.

In the early installations using master-slave manipulators, the slave portion of the manipulator was completely in the contaminating environment. Maintenance of such an involved piece of machinery would thus require either personnel entry into a contaminating and high radiation area or involve the removal of the contaminated manipulator into the operating area.

More recent designs (71, 73), however, take this problem into consideration and provide means for booting or covering the slave portion of the manipulator and many applications (41 to 43) show it so used. It appears (77) that earlier booting served to protect the manipulator from contamination but had to be withdrawn together with the manipulator, when manipulator repairs were required. This should contaminate the operating area as well as the shielding-wall sleeve supporting the manipulator. However, there is a recent description (78) of a booting for these manipulators that need not be withdrawn with the manipulator.

The master-slave mechanical manipulators as presently developed have come a long way towards meeting the versatility design criteria (69, 76) but must still (62) be supplemented by planning and designing process equipment. They have the advantage that they impose no limitation on the type or thickness of shielding that can be used. If the spread of contamination is not considered a problem, they have the advantage of large area coverage, particularly in the carriage mounted mechanical type (44, 45) or the more recent electrically-controlled type (79).

A less versatile and appreciably less expensive type of manipulator is a fairly simple tong operating directly in ball and socket (13, 15, 60, 80) or "castle" (16, 39, 60) mounts in the front wall of a shield. However, the practical limitations on the weight of a ball and socket mount has limited its application to a six-inch shielding wall (13) while the "castle" mount has been used in shielding walls up to nine inches thick (39). To use such manipulators requires the section of front shielding wall containing the manipulators to be made of steel, lead, or denser materials. Booting for such manipulators (16, 81) is fairly simple.

The use of such manipulators requires more specific planning for the operations to be performed as discussed earlier under the section headed Area of Contamination. These manipulators have proven (15) to be a sufficient supplement to such planned operations.

Returning to the shielding, several alternatives can be seen. By completely planning an operation, including all possible events, no supplementary manipulators are needed and no restrictions on shielding material or thickness are imposed. With fairly complete planning of proposed operations, one can use simple, inexpensive, through-the-wall manipulators to handle some emergency and unforeseen events. However, such manipulators require use of the denser, more expensive shielding materials in that part of the shielding wall containing the manipulators. With the more intricate and expensive master-slaves, less specific planning of proposed operations is required beyond that necessary for contamination control during equipment repair or replacement and waste disposal and no restriction is imposed on the type and thickness of shielding.

For the shielding of gammas in the range of 1 to 3 Mev the thickness of material needed for a given shielding application varies almost inversely as the density of the material (55, 82). For a shielding wall, this gives practically the same weight of shielding, regardless of shielding material. For shielding lower energy gammas, the higher atomic weight materials have a greater efficiency than that indicated by their density. The weight of a shielding wall would then be less if made of the denser, higher atomic weight materials. When a given volume must be surrounded by shielding, there can be a considerable saving in weight, floor area and shielding volume by using denser materials.

It is almost axiomatic that the cost per unit weight of shielding materials increases rapidly with density. Thus, unless some other factor dictates, one might expect that the least dense of the common shielding materials (ordinary concrete) would be used, and that this would probably be the shielding material for caves utilizing master-slaves as manipulators, since the master-slaves impose no restriction on thickness of shielding.

Actually many caves utilizing master-slaves are constructed not from ordinary concrete but from the more costly, denser concretes [barytes concrete (44, 56), magnetite concrete (45), ferrophosphorus concrete (75, 83)], which can probably be attributed to the desire to be as close as possible for direct general viewing of operations.

Thus viewing becomes another parameter entering into the design of high level facilities. Viewing can be direct, through a sufficient thickness of glass (84), high density liquids such as zinc bromide (45, 56) high-density lead-glass (16, 39) or combinations of these (44) or it can be indirect, as with periscope-mirror combinations (85 to 87) or completely remote as with television viewing. The use of television can still be considered to be in the development stage. There are excellent reports (88 to 90) on the various direct and indirect viewing means, discussing their advantages and limitations.

Examination of the literature reveals that there are in use quite a few combinations of types of viewing windows and types of shielding walls. For the front concrete shielding walls, the trend appears to be towards the less-thick high density concretes. The corresponding windows are changing from the all glass, or zinc bromide solution windows to the combination (non-browning glass, zinc bromide solution, and high-density lead glass) or to the all lead-glass types that have the same density as the concrete.

The closest viewing approach to operations is obtained with all high density ($\rho = 6.2 \text{ gm./cm.}^3$) lead glass windows and these are usually used in conjunction with steel or lead shielding walls at radiation levels that do not give serious darkening of the inner part of the lead glass. Very high levels of radiation would require some nonbrowning glass ahead of the lead glass.

Besides the relationship between the type and thickness of shielding used and the type of viewing windows there is a relationship between the size or number of windows and the type of manipulator used. Large or numerous windows (41, 89) are required to utilize the maximum coverage and versatility of the mechanically-linked master-slave. This problem of course does not exist with the electrically controlled manipulators.

Other points that might be considered in choosing a shielding material are the eventual disposal costs and any salvage value that there might be. Generally, none of the material costs of concrete shielding can be recovered. Disposal costs would depend on the degree to which the concrete was contaminated. The use of tapes and strip coats to cover the concrete reduce the possibility of contamination but they are subject to chemical and radiation damage failure (68) and once contamination reaches the concrete, it is extremely difficult to remove (91). Better protection is afforded the concrete when it is covered with steel (44, 45) though care would have to be taken at the time of demolition to be sure contamination is not transferred from the steel to the concrete.

Steel shielding should have the normal salvage value of steel scrap if separate contamination barrier enclosures were used. However, if the shielding walls also served as the contamination barrier, disposal as contaminated waste might be more economical.

Lead shielding walls should have very good salvage value. Depending upon the design, the salvage value can amount to more than half of the initial construction cost, provided, however, that separate enclosures served as the contamination barrier.

It is possible that the future will see greater use of the more expensive but denser shielding materials such as tungsten, the more machineable tungsten-copper alloy or uranium.

MATERIAL DAMAGE, DECONTAMINATION

High level radiochemical operations have radiation damage (68) as an inherent problem as well as the usual chemical corrosion problems. In addition, there is the desire to decontaminate and recover equipment. Modern plastics have been developed that provided excellent corrosion resistance.

Many studies have been made on the radiation resistance (92, 93) of these materials and on the decontaminability of many materials (91, 94) including such plastics.

Ideally one would like a material that has excellent corrosion resistance stability against radiation damage, abrasion resistance, and decontaminability, and one that meets the necessary mechanical requirements and is economical. No material has all the characteristics desired; fortunately, not every application requires all these properties. Nevertheless, even among the desired characteristics required for a particular application, compromises must be made and these can have a bearing on the design of equipment. For instance, it might be more desirable to design equipment as cheap throwaways after use than to decontaminate the more expensive components that must then have the characteristics of high corrosion resistance, radiation damage stability, and decontaminability. Other possible examples are quite numerous but a few might serve to illustrate the situation.

Stainless steel once found quite widespread application because of its general corrosion resistance to many chemicals except the halogen containing acids and salts and because of its good decontaminability. However, care must be taken (95) to assure welds that are equally corrosion resistant. Its decontaminability is not universally (96, 97) regarded as sufficient to justify its cost. By coating ordinary steel with some of the plastic finishes now available better corrosion resistance, cheaper construction, and at least equal decontaminability has been achieved within the range in which the plastic withstands radiation damage.

However, plastic coatings on steel are of no value on moving parts where mechanical abrasion can occur, and the galling that can occur on mating parts may rule out stainless steel for both components. All plastic components or substitution of plastics for some of the components are possible solutions.

Glassware in spite of its fragility is used for many equipment components both because of its ease of fabrication and because it permits viewing chemical processes. However, sufficient radiation will darken glass to the point of making further viewing impossible. This possibility should be anticipated and provisions made for replacement of such parts.

Teflon, because of its excellent corrosion resistance to almost all chemicals, would appear to be excellent for remote-operation equipment. A long life-time of usage before failure should occur. However, it has one of the lowest tolerances to radiation damage (92, 93) among modern plastics. Its use must therefore be limited to operations in which the total exposure is expected to be below the radiation damage level or else provision should be made for the ready and simple replacement of teflon parts.

If close-fitting tolerances are required on metal parts of a piece of equipment, one might as well expect to discard the parts when heavily contaminated. Thorough decontamination can remove enough material to bring dimensions outside the permissible tolerance, making the parts unusable.

This forms an especially strong argument for trying to avoid in a design the necessity for close tolerances or, if unavoidable, to have such parts outside the contamination barrier. An example might be a motor and gear system used to drive a piece of process equipment. Repair and maintenance will be simpler and the usable lifetime greater if placement of the motor and gear system in the contaminable process area can be avoided.

OPERATIONAL EQUIPMENT

As can be seen, high level radiochemical processing has many considerations other than the mere placing of a contamination barrier and shielding around equipment that would otherwise be assembled for a nonradiochemical operation. The problems which one must anticipate and make provisions for extend considerably beyond the process itself. Before considering the process equipment itself, one must make fundamental decisions on the policy or philosophy that will govern the operations.

Is it desired to limit with some assurance the spread of contamination or just try to detect it as it comes and then decontaminate or live with some contamination in personnel-occupied areas? The answer to this question will determine whether the enclosure type, the high-air-flow hood type or intermediate cave type installations should be used. The same decision can determine the magnitude of the exhaust blowers and filters, building ventilation requirements, whether special clothing, change rooms and "hot" laundries are necessary, and how extensive a medical surveillance program is needed.

Shall the shielding also be the contamination barrier or shall a separate enclosure serve as the contamination barrier? This decision will affect the provisions for repair or replacement of equipment or for modifying the operation, or for using the shielding in an entirely different operation. The manner and ease with which one can handle and set-up equipment before radioactivity is involved no longer exists after radioactive materials have been introduced into the system.

What type of shielding should be used—ordinary concrete, high density concrete, steel, lead, or other high density materials? Should the same type of shielding be used on all sides of the process area or can they be different? Costs alone would dictate ordinary concrete, but available space and desired closeness for viewing of operations make the denser materials advantageous at least for the front or operational face of the shield. As pointed out earlier in this article, the decision on shielding is interrelated with the decision on manipulators and on contamination control.

What means of viewing operations shall be used: mirrors, periscopes, liquid, nonbrowning glass, ordinary glass, lead glass, composite windows, or television-type remote viewing? Cost, level of radiation, and type of shielding will be the parameters generally dictating the answer to this question.

Shall external general manipulators be used and, if so, what type? If one decides to use no manipulators or one of the various master-slave type of

manipulators, the type of shielding is not important. Through-the-wall manipulators require steel, lead or denser materials as shielding on that wall. With the mechanically operated master-slave, much standard equipment, not specifically designed for radiochemical operations, can be used, and many unplanned or unforeseen events can be handled. Repair, removal, or introduction of such standard equipment into a process area may require provision for large openings, with a corresponding increase of ventilation to minimize the spread of contamination. No manipulators, or direct through-the-wall manipulators, require more careful planning of proposed operations.

How shall one handle liquid waste? Shall it run through piping from the process area to some waste handling area or shall provisions be made to handle it batch-wise from the processing area? If piped, what provisions are needed for possible leaks and for making any repairs to or replacement of contaminated pipe lines?

How shall one remove the final product, analytical samples, or solid wastes, including replaced equipment? Will these operations spread contamination? Will personnel entry, preceded by decontamination operations be necessary for equipment repair or replacement?

Having made all the foregoing decisions one is then ready to consider the process itself. Depending upon the nature of those decisions, process equipment will or will not require special consideration because of the radioactive materials involved. While each installation working with radioactive materials has devised gadgets for remote operations, many of these are peculiar to the particular operation and a particular policy and philosophy of operation. Universality is still a goal for the future.

The best that one, newly entering this field can do, is to establish a basic policy of operation and to derive the resultant design criteria which process equipment designers must then meet. If previously designed equipment can meet those criteria, the best recent compilation of equipment for such reference is that (1) cited in the first paragraph of this article.

LITERATURE CITED

1. *U. S. Atomic Energy Commission Report, TID-5276*, 74-302 (1955)
2. *Ind. Eng. Chem.*, **41**, 227-50 (1949)
3. *U. S. Atomic Energy Commission Report, NP-3875*, (1952)
4. *Nucleonics*, **12**, (11) 35-100 (1954)
5. "Fourth Annual Symposium on Hot Laboratories and Equipment," *U. S. Atomic Energy Commission Report, TID-5280*, 383 pp. (1955)
6. "Fourth Annual Symposium on Hot Laboratories and Equipment," *U. S. Atomic Energy Commission, Report, TID-5280 Suppl. 1*, 123 pp. (1956)
7. *Fifth Hot Laboratories and Equipment Conference* (American Society of Mechanical Engineers, New York, N. Y., 383 pp., 1957)
8. Miller, L. F., and Kinderman, E. M., *Nucleonics*, **12**, (11) 82-83 (1954)
9. Gould, J. R., *U. S. Atomic Energy Commission Report AECD-3885*, 18 pp. (1952)
10. Dismuke, S., *Nucleonics*, **12**, (11) 89-90 (1954)
11. Rupp, A. F., *Oak Ridge Natl. Lab. Rept., ORNL-2064*, 22 pp. (1955)
12. Garden, N. B., *Ind. Eng. Chem.*, **41**, (11) 237-38 (1949)
13. Nielsen, E., *Oak Ridge Natl. Lab. Rept., ORNL-52-10-230* (1953) (Classified)
14. Garden, N. B., *U. S. Atomic Energy Commission Rept. NP-3875*, 55-64 (1952)
15. Ruehle, W. G., Jr., *Nucleonics*, **12**, (11) 84-85 (1954)
16. Garden, N. B., *U. S. Atomic Energy Commission Rept. TID-5280*, 338-346 (1956)
17. Tomkins, P. C., *Ind. Eng. Chem.*, **41**, 231-44 (1949)
18. Bagnall, K. W., and Spragg, W. T., *Atomics*, **6**, 71-78 (1955)
19. Rupp, A. F., and Benford, F. J., *J. Appl. Phys.*, **24**, 1069-81 (1953)
20. *Argonne Natl. Lab. Rept. ANL-4146*, 60 pp. (1948)
21. Guest, G. H., and Cook, L. G., *Chalk River Lab. Rept. CRHR-368*, 13 pp. (1948)
22. Boddington, P., *Brit. Atomic Energy Research Establishment Rept. AERE-E/M-30*, 32 pp. (1950)
23. Apperly, A., *Brit. Atomic Energy Research Establishment Rept. AERE-E/R-1291*, 45 pp. (1953)
24. Ritchie, A. B., and Spragg, W. T., *J. Sci. Instruments*, **28**, 214-16 (1951)
25. Tubis, M., Doan, C., and Libby, R. L., *Science*, **110**, 431-32 (1949)
26. Weber, J., Jr., and Dewell, E., *Ames Lab. Rept.*, (6) *ISC-112*, 5 pp. (1950)
27. Bralove, A. L., *Nucleonics*, **8**, (4) 37-54; (5) 60-67; 15-23, 33 (1951)
28. Detwiler, C. G., *Knolls Atomic Power Lab. Rept. KAPL-864*, 12 pp. (1954)
29. Schulte, H. F., Hyatt, E. C., Jordan, H. S., and Mitchell, R. N., *U. S. Atomic Energy Commission Report, AECU-2859*, 20 pp. (1953)
30. Fitzpatrick, J. P., Bohlin, N. B., and Gold, S. S., *U. S. Atomic Energy Commission Report AECU-617*, 9 pp. (1949)
31. Swartout, J. A., *Ind. Eng. Chem.*, **41**, 233-36 (1949)
32. Thaxter, M. D., Cantelow, H. P., and Burk, C., *Fifth Hot Laboratories and Equipment Conference*, 111-20 (American Society of Mechanical Engineers, New York, N. Y., 383 pp., 1957)
33. Meadors, O. L. (Private communication 1952)
34. Kelman, L. M., Wilkinson, W. D., Shuck, A. B., and Goertz, R. C., *Nucleonics*, **14**, (3) 61-65; (4) 65-71; (5) 77-82 (1956)
35. Christopherson, E. W., *Nucleonics*, **12**, (11) 94-95 (1954)
36. Meinke, W. W., Emmons, A. H., and Gomberg, H. J., *Nucleonics*, **13**, (11) 76-79 (1955)
37. Bagnall, K. W., and Spragg, W. T., *Atomics*, **6**, 125-29, 133 (1956)

38. Kaulitz, D. C., and Roake, W. E., "A Sectional Gloved Box," *Hanford Atomic Products Operation Rept.*, HW-26500, 17 pp. (1955)
39. Dykes, F. W., Fletcher, R. D., Turk, E. H., Rein, J. E., and Shank, R. C., *Anal. Chem.*, **28**, 1084-91 (1956)
40. Feirstein, H. E., *Nucleonics*, **12**, (11) 40-41 (1954)
41. Foltz, J. R., Gardner, W. J., and Rosen, F. D., *Atoms Intern. Rept.*, NAA-SR-1227, 67 pp. (1956)
42. Caverly, M. R., and Snyder, M. D., *U. S. Atomic Energy Commission Rept. TID-5280*, 327-37 (1956)
43. Sullivan, L. O., *U. S. Atomic Energy Commission Rept. TID-5280 Suppl. I.*, 107-23 (1956)
44. Bartz, M. H., and Burnham, J. B., Jr., *Nucleonics*, **12**, (11) 42-43 (1954)
45. Rylander, E. W., and Blomgren, R. A., *Nucleonics*, **12**, (11) 98-100 (1954)
46. Kittle, J. H., *Nucleonics*, **12**, (11) 60 (1954)
47. Calkins, G. D., and Whitney, J. E., *Fifth Hot Laboratories and Equipment Conference*, 59-66 (American Society of Mechanical Engineers, New York, N. Y., 383 pp., 1957)
48. Doe, W. B., *Fifth Hot Laboratories and Equipment Conference*, 73-81 (American Society of Mechanical Engineers, New York, N. Y., 383 pp., 1957)
49. Schwartz, E. S., *Fifth Hot Laboratories and Equipment Conference*, 91-97 (American Society of Mechanical Engineers, New York, N. Y., 383 pp., 1957)
50. Hancock, F. E., and Castner, S. V., *Fifth Hot Laboratories and Equipment Conference*, 380-83 (American Society of Mechanical Engineers, New York, N. Y., 383 pp., 1957)
51. Farmakes, J. R., Blomgren, R. A., and Schraadt, J. H., *U. S. Atomic Energy Commission Rept. TID-5280*, 121-32 (1956)
52. Youngquist, C. H., *U. S. Atomic Energy Commission Rept. TID-5280*, 318-325 (1956)
53. Youngquist, C. H., *Fifth Hot Laboratories and Equipment Conference*, 375-79 (American Society of Mechanical Engineers, New York, N. Y., 383 pp., 1957)
54. Stearns, R. F., *Knolls Atomic Power Laboratory Report KAPL-1406*, 19 pp. (1955)
55. Dunster, H. J., *Nuclear Eng.*, **1**, (4) 144-48 (1956)
56. Frederick, E. J.; *Nucleonics*, **12**, (11) 36-37 (1954)
57. Angel, C. W., and Ring, F., Jr., *Nucleonics*, **11**, (9) 69 (1953)
58. Blomgren, R. A., and Bohlin, N. J. G., *U. S. Atomic Energy Commission Rept. TID-5280 Suppl. I.*, 61-72 (1956)
59. Moulthrop, H. A., *Hanford Atomic Products Operation Rept.*, HW-25108, 74 pp. (1952)
60. Schuman, R. P., and Jones, M. E., *Fifth Hot Laboratories and Equipment Conference*, 128-32 (American Society of Mechanical Engineers, New York, N. Y., 383 pp., 1957)
61. Reynolds, M. B., *Fifth Hot Laboratories and Equipment Conference*, 243-50 (American Society of Mechanical Engineers, New York, N. Y., 383 pp., 1957)
62. Kelley, M. T., and Fisher, D. J., *Fifth Hot Laboratories and Equipment Conference*, 105-10 (American Society of Mechanical Engineers, 29 W. 39th St., New York, N. Y., 383 pp., 1957)

63. Schuck, A. B., and Mayfield, R. M., *Argonne Natl. Lab. Rept.*, ANL-5499, 160 pp. (1956)
64. Hughes, D. C., *U. S. Atomic Energy Commission Rept.* TID-5280, 107-20
65. Conboy, J. T., Hunter, K. R., Reynolds, H. W., and Truran, W. H., *Fifth Hot Laboratories and Equipment Conference*, 98-104 (American Society of Mechanical Engineers, 29 W. 39th St., New York, N. Y., 383 pp., 1957)
66. Morgan, J. R., *Fifth Hot Laboratories and Equipment Conference*, 176-84 (American Society of Mechanical Engineers, New York, N. Y., 383 pp., 1957)
67. Feldman, M. J., *U. S. Atomic Energy Commission Rept.* TID-5280, 208-24 (1956)
68. Coplan, B. V., and Smith, D. J., *Nucleonics*, 12, (11) 92-93 (1954)
69. Goertz, R. C., *Nucleonics*, 10, (11) 36-42 (1952)
70. Field, R. E., and Gifford, J. F., *Hanford Atomic Products Operation Rept.*, HW-26175, 24 pp. (1952)
71. Goertz, R. C., *Nucleonics*, 12, (11) 45-46 (1954)
72. Howell, L. N., and Tripp, A. M., *Nucleonics*, 12, (11) 48-49 (1954)
73. Carlson, W. D., *U. S. Atomic Energy Commission Rept.*, TID-5280, 11-25, 123 pp. (1955)
74. Fisher, R. W., and Winders, G. R., *Nucleonics*, 12, (11) 44 (1954)
75. Calkins, G. D., Lush, E. C., and Asanovich, G., *U. S. Atomic Energy Commission Rept.*, TID-5280, 91-106 (1955)
76. Hull, H. L., *Nucleonics*, 10, (11) 34-35 (1952)
77. Smith, S. C., *Fifth Hot Laboratories and Equipment Conference*, 67-72 (American Society of Mechanical Engineers, New York, N. Y., 383 pp., 1957)
78. Wehrle, R. B., *Fifth Hot Laboratories and Equipment Conference*, 211-19 (American Society of Mechanical Engineers, New York, N. Y., 383 pp., 1957)
79. Thompson, W. M., and Goertz, R. C., *U. S. Atomic Energy Commission Rept.* TID-5280, 1-10 (1955)
80. Stang, L. G., Jr., *U. S. Atomic Energy Commission Rept.* TID-5280, 35-45 (1955)
81. Leith, W. H., *U. S. Atomic Energy Commission TID-5280*, 300-10 (1955)
82. Rockwell, T., 3rd, *U. S. Atomic Energy Commission Rept.*, AECD-3352, 29 pp., (1950)
83. Roberts, C. J., *Fifth Hot Laboratories and Equipment Conference*, 17-30 (American Society of Mechanical Engineers, New York, N. Y., 383 pp., 1957)
84. Blomgren, R. A., and Hagemann, F., *Argonne National Laboratory Rept.*, ANL-4426, 12 pp. (1950)
85. Winsche, W. E., Stang, L. G., Jr., Strickland, G., Richards, P., Selvin, G. J., Horn, F., and Bennett, G., *U. S. Atomic Energy Commission Rept.*, TID-5020, 17 pp. (1951)
86. Lumbert, A. R., *Nucleonics*, 12, (11) 38-39 (1954)
87. Silvester, A. G., *Nucleonics*, 13, (11) 80-81 (1955)
88. Remote Control Engineering Division, *Argonne National Laboratory Rept.*, ANL-4903, 44 pp. (1952)
89. Ferguson, K. R., *U. S. Atomic Energy Commission Rept.*, TID-5280, Suppl. 1, 73-94
90. Ferguson, K. R., *Nucleonics*, 10, (11) 46-51 (1952)
91. Watson, C. D., *Fifth Hot Laboratories and Equipment Conference*, 36-58 (American Society of Mechanical Engineers, New York, N. Y., 383 pp., 1957)

92. Bressee, J. C., Flandry, J. R., Goode, J. H., Watson, C. D., and Watson, J. S., *Nucleonics*, **14**, (9) 75-81 (1956)
93. Harrington, R., *Nucleonics*, **14**, (9) 70-74
94. *Nucleonics*, **9**, (5) C12-15 (1951)
95. Glen, H. J., *Fifth Hot Laboratories and Equipment Conference*, 299-306 (American Society of Mechanical Engineers, New York, N. Y., 383 pp., 1957)
96. Tomkins, P. C., and Bissell, O. M., *Ind. Eng. Chem.*, **42**, 1469-75 (1950)
97. Lamb, E., *Fifth Hot Laboratories and Equipment Conference*, 311-17 (American Society of Mechanical Engineers, New York, N. Y., 383 pp., 1957)

CELLULAR RADIobiology^{1,2,3,4}

E. L. POWERS

Division of Biological and Medical Research, Argonne National Laboratory, Lemont, Illinois

This review will deal with the papers published during the calendar year 1956 concerning the effects of low and high energy radiations on experimental cellular systems. Since the two previous reviews in this series [Mortimer & Beam (1) and Gray (2)] consist of comprehensive discussions of the literature of recent years, only a few papers covered by these authors will be cited in this report. The subjects covered in this paper are concerned for the most part with single cell systems. As the literature on chemical protection is being treated elsewhere (3) in this volume, it is also omitted. Certain recognizable cellular effects, such as effects on tissue cells and genetic and cytological changes in the cells of higher organisms, are not being described. Because of the large literature in these areas, they should be treated separately and *in extenso*.

EFFECTS OF ULTRAVIOLET RADIATION

ACTION SPECTRUM STUDIES

Since many compounds of biological importance show specific absorption of electromagnetic radiations, *a priori* it should be possible to relate effects included in biological systems by ultraviolet and visible radiations to initial interactions between the radiations and cellular constituents. A source of nearly monochromatic radiant energy is necessary for studies of this kind; also necessary are careful measurements of irradiance in order to compare the extent of biological effect at different wavelengths. Correct inferences, moreover, depend very strictly upon the fulfillment of two important conditions: the response to a wide range of wavelengths of narrow spectral breadth from 2200 Å through the visible must be measured and the available irradiance must be high so that iso-response action curves can be constructed for even the least efficient spectral regions. When only low dosage rates (or irradiances) are available, moreover, it is necessary to ascertain that reciprocity (the Bunsen-Roscoe hyperbolic relationship) obtains, that all constant products of time and irradiance induce constant biological result.

¹ The survey of literature pertaining to this review was completed in January, 1957.

² The following abbreviations are used in this chapter: HVL (Half-Value Layer), LET (Linear Energy Transfer), RNA (Ribonucleic Acid), TMV (Tobacco Mosaic Virus).

³ This work performed under the auspices of the U. S. Atomic Energy Commission.

⁴ I thank Elaine Katz Bernstein and Jane Murphy for assistance in the preparation of this paper.

Many studies of action spectra suffer for not having fulfilled these conditions.

Several machines have been constructed to give high irradiancy over a broad portion of the spectrum. The quartz water-prism monochromator of Fluke & Setlow (4) has made possible a number of recent ultraviolet action spectrum studies. The biological spectrograph described by Monk & Ehret (5) provides a better compromise of high resolution, low scattered radiation and high irradiance. The latter spectrograph employs a ruled grating in place of the prism; it provides a continuous spectrum of radiant energy up to 50 ergs/sec./mm.² for an 8.5 in. specimen, 450 ergs/sec./mm.² for a 0.75 in. specimen in the near ultraviolet, over a wide range (from 2200 to about 8000 Å); it gives high and linearly uniform dispersion of 1 Å/mm. These two machines together with the proven one at Beltsville (6) constitute, to this author's knowledge, the high energy monochromators of importance in the United States. In France (7) there is one that performs especially well in the ultraviolet region of the spectrum.

A straightforward inactivation of biologically active material was performed by Setlow & Doyle (8). Paramecin, a substance secreted by kappa-containing *Paramecium aurelia*, var. 4, is toxic to some organisms not containing the kappa particle, and earlier investigations of van Wagendonk (9) had indicated the possibility that this material was a DNA-like substance. The action spectrum calculated by Setlow & Doyle (8) using the water-prism spectrograph shows that the material gives a spectrum resembling the absorption spectrum of a trypsin-like protein rather than that of DNA or a DNA protein. The inactivation of influenza virus (Melbourne) has been studied in the same manner [Powell & Setlow (10)] by measuring both the disappearance of the ability of the virus to interfere with the liberation of hemagglutinants and by measuring the loss of infectivity. The authors assume simple exponential inactivation of the virus and calculate inactivation constants. Action spectra based on these constants show that for the interfering property of the virus there is a broad peak between 2600 and 2800 Å, indicating to the experimenters that a protein is involved in this activity of the virus. On the other hand, infectivity is lost as the wavelength changes in a manner which would indicate absorption of the energy by pure nucleic acid. A similar study has been presented [Fluke (11)] on the action spectrum for loss of plaque-forming capacity of the coliphage T1, with the added refinement of measurements of the spectrum both at normal and at very low temperatures. At normal temperatures there is a peak at 2800 Å; the author interprets this to indicate that action of the radiation might be mediated through protein. When the action spectrum is taken at 90°K. the broad peak is not refined. It is of some theoretical interest to note that the absorption spectrum of coliphage T1 follows throughout the observed action spectrum at the longer wavelengths, meaning that quantum efficiency in this region remains constant. At the lowest region measured, 2250 Å, the quantum efficiency drops to a relative value of 0.25 compared to the 1.4 observed at the longer wavelengths (approximately 2600 Å). It is noted further that the

inactivation curves observed are of so-called multi-target variety, the wet coliphage giving a more extreme result in this respect than the dry coliphage.

The action of ultraviolet in bringing about cellular effects was measured at three spectral regions by Six (12) in the alga *Acetabularia*. In this marine organism it is possible to irradiate the cytoplasm while shielding the nucleus, and to measure subsequently several biological capabilities. [See below, Hämmerling (26).] Monochromatic ultraviolet at 254, 281 and 297 m μ was used on the nucleus-free portion, thus giving pure cytoplasmic irradiation. The average length of life after irradiation, as well as the ability to differentiate, was measured. The author notes that 254 m μ has the greatest efficiency with 297 m μ showing very little or no effect. He concludes that there is a relation between the purines and pyrimidines in the cytoplasm and the damage induced by the ultraviolet. Although absorption of the ultraviolet energy by purines and pyrimidines is allowed by the three points, such a conclusion must be considered premature until a complete action spectrum has been obtained.

Another study of ultraviolet damage has been presented by Goldman & Setlow (13). Immediately after fertilization the zygotic nucleus of the *Drosophila* egg migrates to the center of the yolk mass, and there it is effectively shielded from external ultraviolet irradiation. After seven or eight cell divisions, the daughter nuclei become peripherally located and can at that time be exposed to ultraviolet. Utilizing these facts, the authors attempted to distinguish between nuclear and cytoplasmic damage. Irradiations of late eggs (presumably nuclear damage) resulted in early permanent inhibition of development, while damage induced early (presumably cytoplasmic damage) resulted in later effects, i.e., morphogenetic movements are altered, but differentiated larvae appear showing various abnormalities. The authors calculated the action spectrum from inactivation constants based on simple exponential inactivation assumption, and then concluded that the RNA in the cytoplasm is involved in the initial absorption of the energy of the ultraviolet in the cytoplasmically damaged eggs. This study offers two difficulties to the reviewer. In the first place the evidence for reciprocity failure in the study was not presented. Reciprocity is assumed to hold from the range 8 ergs/sec./mm.² to 170 ergs/sec./mm.². We should note that Giese *et al.* (14) working with *Didinium* showed a definite reciprocity failure in the region below 10 ergs/sec./mm.². Christensen & Giese (15) showed that while reciprocity holds for the region from 5 to 15 ergs/sec./mm.² in *Tetrahymena*, the relationship fails at higher or lower rates. Secondly, a comparison of these results in *Drosophila* with those reported by von Borstel & Moser (16) in *Habrobracon* shows that the response is approximately the same in magnitude, but that the *Habrobracon* inactivation curve, based on many more points, has a definite shoulder to about 1000 ergs/mm.². It seems to the reviewer that the simple exponential inactivation assumption is an illegitimate oversimplification, for the dose-effect curves of *Drosophila* reported by Goldman & Setlow (13) can be interpreted to be of the multi-target type.

STRAIN DIFFERENCES

A number of mutants in microorganisms and viruses assist in the analysis of mechanisms of ultraviolet damage to cells. As noted in the next section the heminless mutant of *Escherichia coli*, utilized by Ogg *et al.* (17) and by Latarjet & Beljanski (18), allowed the demonstration of a relationship between ultraviolet sensitivity and the presence of an enzyme or enzymes or an enzyme system or systems. Payne *et al.* (19), using *E. coli* B, *E. coli* B/r, and *E. coli* B/F, the latter two being radiation-resistant mutants, examined the cytological effects of ultraviolet radiation. Following ultraviolet treatment the chromatinic bodies in all three varieties aggregate, but this effect is reversed early in the two radiation resistant cultures. The authors proposed that primary damage is the same in the three strains, but that repair of the injury proceeds much more quickly in the two resistant strains. Differential absorption of ultraviolet energy is not responsible for the differences in the effect, but rather the repair of an injured condition that appears to be similar in all cells. Goucher and his colleagues (20) used four species of *Azotobacter* to investigate the role of genetic determination in ultraviolet damage. They noted that *Azotobacter chroococcum* is inactivated in a simple exponential fashion by ultraviolet light and then is easily photoreactivated. *Azotobacter agile* strain 44 is also inactivated in a simple exponential fashion, but photo-reversibility occurs to a lesser extent. *Azotobacter Q* shows very little photo-reversibility and is inactivated in a multi-target fashion, while *Azotobacter vinelandii*, showing sigmoid inactivation, demonstrates no photo-reversibility. In none of these cases was a simple dose reduction of ultraviolet by visible light demonstrated.

Differences in ultraviolet sensitivity related to genetic constitution have been investigated in coliphage T2 and T4 by Striesinger (21). Differences in sensitivity within the tobacco mosaic virus have also been investigated [Siegel, Wildeman & Ginoza (22)]. Two strains, U1 and U2, demonstrate a 5½-fold difference in sensitivity to germicidal lamp irradiations. When the nucleic acid is separated from the protein in the two viruses, both are equally sensitive to ultraviolet irradiations, showing a sensitivity equal to that of the more sensitive virus (U2). When these two nucleic acids are reunited to protein, the reconstituted viruses are now equivalent in sensitivity, again equal to the more sensitive one. The experimenters believe that in the native intact viruses there is a difference in the binding between nucleic acid and the protein portions of the virus. In the U1 virus, energy absorbed by the nucleic acid can be transmitted to the protein where it is less effective in bringing about inactivation. This explanation of differences in sensitivity is different in principle from that offered by Payne *et al.* (19) for the differences shown in the three strains of *E. coli* in which, after similar initial damage, a biological repair mechanism operates but at different rates.

Different sensitivities within the same cell in the same general system were recorded by Tessman (23). The capacity of *E. coli* to support phage growth is sensitive to ultraviolet irradiation, but the sensitivity differs from phage to phage. Phage T2 is produced after doses to the host cell that

markedly reduce that capacity of the cell to produce T1 and T3. The T1 capacity is more sensitive than that for T3.

SITE OF ACTION IN CELL

In attempts to pinpoint the effects of ultraviolet irradiation on cellular materials, several authors have reported on differential irradiation of the nucleus and the cytoplasm. von Borstel & Moser (16) reported roughly exponential inactivation of developing *Habrobracon* when the nucleus-containing side of the egg is irradiated. Death generally occurs before the eighth fission. When the cytoplasmic side is irradiated a sigmoid type survival curve, with death occurring late in development, is generally seen. These results are to be compared with those described above by Goldman & Setlow (13). In the case of *Habrobracon* the authors maintain that nuclear damage is photoreversible, whereas the cytoplasmic damage is not. Powers & Ehret (24) present a general review on this subject, including a description of this effect in *Paramecium*. In analyzing the results of several other authors, Powers & Ehret concluded that a large portion of the ultraviolet effect seen in many experiments is cytoplasmic in nature, that some of it is probably nuclear, and that most of the damage reversible by visible light is of the nuclear type.

During this same period Brandt & Giese (25) described their results after irradiating *Paramecium caudatum*. These authors believe that 226 m μ does not penetrate far enough into the cytoplasm to affect the nucleus while 267 m μ ultraviolet does. The loss of motility occurs at 226 m μ at dosages 1/15 that necessary at 267 m μ for the same effect. The animals irradiated at 226 m μ recover, those at 267 m μ do not. When irradiated at 239 m μ the organisms exhibit division delay and then generally die. After complete immobilization at 226 m μ , division delay sometimes is seen and sometimes is not. Whenever delay is present, it is partially photoreversible by simultaneous illumination of the organism; the immobilization effect appears to be resistant to the photoreversing action of visible light. Brandt & Giese believe that the division delay phenomenon is nuclear in origin, while the immobilization effect is based on cytoplasmic damage, with the action spectrum for immobilization being similar to the absorption spectrum of protein and lipide. Their proposal that division delay is of nuclear origin is consistent with the photoreversible effects observed in *Habrobracon* in that it is at least partially reversible.

Hämmerling (26) attempted to distinguish between nuclear and cytoplasmic damage in *Acetabularia*. He saw that capacity for differentiation in nucleus-free cytoplasm sinks sharply after pure cytoplasmic absorption of energy, while nucleated pieces retain the capacity after much higher dosages. The interpretation is made that cytoplasmic absorption of ultraviolet energy does bring about loss of differentiation capacity [see also Six (12)]. Yost and co-workers (27) isolated mitochondria from rats and noted a distinct loss in cytochrome oxidase activity, believing that a peak for efficiency exists in the neighborhood of 260 m μ . The irradiation technique used, how-

ever, does not allow critical evaluation of this latter point. It seems clear, though, that this biochemical activity of cytoplasmic particulates is affected, and the authors' suggestion that some ultraviolet damage might be brought about because of this is not unreasonable.

Errera & Ficq (28) irradiated the starfish oocyte with ultraviolet and then measured the metabolism. Adenine-8-C¹⁴ (incorporated into nucleic acids) and phenylalanine-2-C¹⁴ (incorporated into proteins) were offered the eggs after irradiation. The authors believe that ultraviolet of 254 m μ wavelength inhibits synthesis of protein. Because there is very little ultraviolet absorption in the sap, a low effect was brought about. Related to the results of these two papers are the findings of Ogg, Adler & Zelle (17), who investigated a radiation-resistant mutant of *E. coli* that cannot synthesize hemin. A 15 per cent difference in dose is necessary to cause a biological effect equivalent to that induced in a wild-type cell. The heminless coli have no catalase and no cytochrome activity, and addition of hemin abolished the differences in sensitivity. Ordinary cells have catalase and cytochrome activity and addition of hemin to these cells makes no difference. About the same time, Latarjet & Beljanski (18) reported on sensitivity of the *coli* H mutant (of the same origin) to ultraviolet, but did not claim that the sensitivity is affected by the presence or absence of hemin. To this reviewer, however, the inactivation curves of the latter authors at the low end of the spectrum agree approximately with those of Ogg *et al.* (17). When the organisms exhibited high survival levels, the two sets of authors reported very different types of inactivation curves: Ogg *et al.* (17) showed a standard multi-target type of curve, while Latarjet & Beljanski (18) showed a complex convex downward relationship, sometimes interpreted as indicating two populations in the culture differing in sensitivity. Dosages in the two sets of experiments cannot be compared. James & Chaplin (29) measured the selective advantage of a presumably nuclear effect induced in diploid cells of yeast with ultraviolet. The survival of heterozygotes with radiation-induced lethals was less than that observed in lethal-free cells.

DARK RECOVERY STUDIES

Several authors have presented evidence concerning the spontaneous or thermally-dependent reactivation that occurs in the dark following ultraviolet damage to cells. Charles & Zimmerman (30) noted that strain B of *E. coli* held in saline at different temperatures after being treated with 300 ergs/min./mm.² in the dark for different periods of time showed increases in survival with increases in temperature, as well as with increases in time to a maximum at about 12 hr. Under the conditions of their experiments, this effect was not additive with light reactivation; that is, light treatment or time treatment exhausted the reactivation capability. A radiation-resistant strain did not show reactivation to this extent. Barner & Cohen (31) performed similar experiments on dark recovery. They held *E. coli* in a glucose-containing mineral medium lacking thymine, a medium not allowing division in the strain (15T⁻) used. It was found that the number of viable cells re-

recoverable from the suspension increased by about a factor of five over a period of 20 min.; then, there was a gradual decline of the number of survivors recoverable. The nonauxotrophic parent strain of *E. coli* (15) was also tested in this way and it was observed to be restored approximately fourfold during the first 20 min. After this time the restored cells died and the viable count was that eventually expected on the basis of the number of survivors of the irradiation. The degree of recovery was fixed by plating.

Buzzell (32) investigated dark recovery of *E. coli* B after ultraviolet, paying particular attention to the kinetics of reactivation. As a consequence of the reactivations observed during the so-called slow recovery period, this author proposed that a number of sites must be reactivated in order to completely restore a bacterium. The thermal reactivation of each position is first order, and the variable is the number of sites available for reactivation under different conditions. For example, a bacterium in the resting state (a very radiation-resistant one) has a small number of equally sensitive targets. Stein & Laskowski (33) also investigated the so-called thermal reactivation of *E. coli* B after ultraviolet. Reactivation was temperature-dependent, with high temperature incubation giving dose reduction factors up to 4:1. Similar to the results of Barner & Cohen (31) are those of Bruce & Maaløe (34) who irradiated synchronously dividing *Salmonella typhimurium*. When these organisms are held under conditions not allowing growth, there is a recovery with time. Under favorable plating conditions, the degree of recovery found at the time of plating can be stabilized. In this brief paper, the authors found that the increase in survival proceeded during the first hour, and gave results roughly similar to those described by Barner & Cohen (31) with the thymineless mutant. They attempted to relate ultraviolet sensitivity to a stage in the division cycle, but did not successfully demonstrate any change in sensitivity as division proceeded through the mitotic period. The authors further recognized that the changes in temperature from 25° to 37°C. necessary to bring about division synchrony may be the reason for the change in radiation sensitivity.

The dependence upon temperature of the chemical reactions leading to initial injury has been analyzed in the ciliate protozoan *Didinium* by Giese et al. (14). When continuous ultraviolet light was used, they found a slight increase in time to the fourth division in the region from 5° to 30°C. When, however, the ultraviolet radiation was flashed, there was considerable rise in the injury with increases in temperature. For instance, with a .0246 sec. dark period, injury increased from 22 hr. to 41 hr. mean time to fourth division in the 5° to 30°C. spread. When the dark interval was increased to 0.532 sec., the rise was from 22 hr. to 93 hr. The authors compared this response to the dark chemical reactions seen in photosynthesis, the difference in *Didinium* being that the asymptotic or peak region was never realized. The results indicate that in very short periods of time after absorption of ultraviolet by *Didinium*, temperature-dependent chemical reactions occur. These reactions are easily distinguishable from the ones involved in the temperature-dependent recovery reactions described above. The latter reactions have high

temperature coefficients and long time constants (peak efficiencies occurring 20 to 30 min. after damage), whereas the reactions described in *Didinium* are obviously much more rapid.

Mutation frequency in *Drosophila* after ultraviolet irradiation of the polar cap of the egg was shown to be influenced by postirradiation treatment with light, temperature, and oxygen [Meyer (35)]. Postirradiation light decreased mutation frequency in the moderate ultraviolet dosage range (~ 400 ergs/mm.²), but not at higher dosages (~ 700 ergs/mm.²). Warm postirradiation treatment temperatures as well as oxygenation also reduced mutation frequency.

Another environmental factor has been shown to be important in the dark period following ultraviolet irradiation of *E. coli* B. Weatherwax (36) showed that the hydrogen ion concentration of the plating medium significantly changed the degree of survivorship observed after germicidal lamp irradiation. Survival increased 1000-fold as the hydrogen ion concentration of an M9 medium was changed from pH 8 to pH 5 following any given dose. As in the case of "heat" activation, the reactions involved were also time-dependent; recovery increased up to about 2 hr. after irradiation and then decreased during the next 2 hr. Thus another variable has been added to the wealth of factors that are known to influence the survival of bacteria before, during and after ultraviolet irradiation. One variable that does not, apparently, influence survival is contact among irradiated cells. Galperin & Errera (37) show that irradiated *E. coli* B have no mutual effect on each other.

The ultraviolet sensitivity in *Astasia longa* was shown by Schoenborn (38) also to be dependent upon metabolic factors. This organism grows in inorganic medium in the presence of selected organic metabolites. A number of substances such as cystine, tryptophan, adenine, cytidylic acid, uracil, and sodium pyruvate afforded protection if they were added before irradiation. None of these compounds were effective in reducing sensitivity when they were added after irradiation. In the case of cysteine, cells had to be grown in its presence for some time before protection was afforded; i.e., mere presence of cysteine in the solution was not sufficient.

LIGHT RECOVERY STUDIES

The role of visible light in reversing ultraviolet damage after ultraviolet exposure was the subject of a number of investigations. Photoreactivation of substances *in vitro* (e.g., the pneumococcus-transforming factor) could not be accomplished by Latarjet & Cherrier (39); an *in vivo* set of reactions seems to be required. The results reported by Zamenhof *et al.* (40) are similar: the transforming principle of *Hemophilus influenzae* inactivated by ultraviolet could not be photoreactivated *in vitro*. Weatherwax (41) was able to desensitize *E. coli* B to ultraviolet by pre-irradiating with graded amounts of visible light. The survival curves following ultraviolet exposure differed for different amounts of visible light. At low dosages the protection was much greater than at high dosages of ultraviolet, suggesting to the re-

viewer the possibility of two types of damage in *E. coli*. As noted elsewhere in this review, there seems to be a difference in photoreversibility of cytoplasmic and nuclear damage in other systems. It is of interest to note that Kelner (42) could not desensitize strain B/r with previous exposures to visible light. Postirradiation reversal of ultraviolet damage with visible light has been extended to mammalian cells by Kelner & Taft (43). These authors measured the tumor-producing efficiency for different wavelengths of ultraviolet, and found 2537 Å to be most effective in producing skin carcinomas, and the region from 2800 to 3100 Å to be most efficient for the production of sarcomas (with a few carcinomas also produced). When light reactivation was attempted, the frequency of carcinomas was somewhat reduced, but that of sarcomas was not. The authors, however, were not satisfied that reversibility by light has been critically demonstrated.

Rieck & Rudich (44) demonstrated that acute lethality of ultraviolet to intact albino mice is also photoreversible. Death in this strain ensues in 15 to 20 days after 5×10^7 ergs/cm.² if the animals are held in the dark between periodic exposures. When the animals are exposed to bright light in these intervals, the lethality curve shows a lower slope. Histological studies showed that the mice held in darkness exhibited epithelial thickening of the ear epidermis eight times that of normal, while those exposed to visible light between ultraviolet exposures showed epithelial thicknesses only twice normal.

The effect of genetic constitution on photoreversibility in single cells (*Azotobacter*) [Goucher *et al.* (20)] has been discussed in this review (above). Some strains are easily photoreversible; others show no photoreversibility. In the four instances studied, those strains with multi-target type survival curves showed little photoreversibility. Similarly, Stuy (45) demonstrated that the strains of *Bacillus cereus* differ in photoreversibility; of fifteen tested, only two were easily reversible. The spores of these two, moreover, could not be photoreactivated. Stuy (46) also studied the photoreversibility of germinating *B. cereus* spores (not seen by reviewer).

Latarjet (47) reviewed recent studies of photoreactivation of *E. coli* with especial attention to the results of the Paris laboratories. The possibility of using mutants lacking energy-transmitting molecules as aids in understanding postirradiation reactions is being appreciated. Latarjet & Beljanski (18) showed that the H mutant (lacking hemin and catalase) is not different in its photoreversibility from the porphyrin-containing parent strain. They concluded that "the porphyrins do not appreciably act as chromophores" in photorestoration. This system does not seem to be involved in the chemical reactions leading to reversal of ultraviolet damage. The action spectrum of visible light in restoring viability to *E. coli* B/r presented by Jagger & Latarjet (48) (3130 to 4900 Å) does not suggest a chromophore to them. They think, however, that it might be DNA.

Brandt & Giese (25), studying *Paramecium caudatum*, demonstrated that immobilization of the cells after exposure to 226 m μ is not photoreversible, whereas delay in division induced at 239 m μ is partially photoreversible. As

we noted above, these authors think that the photoreversible portion of the response is that which occurs in the nucleus, while the nonphotoreversible damage is cytoplasmic. This agrees with the general explanations of sites of ultraviolet damage in insects.

Some clues concerning the chemical nature of the reversing action of visible light on division in *Tetrahymena pyriformis* were presented by Christensen & Giese (15). A photoreversing amount of energy given continuously at 4350 Å is more effective at low intensity than at very high intensities. Reciprocity, in other words, does not hold in the photoreversing actions. When the light at high intensity was flashed, however, the efficiency rose. From experiments in which the dark and light periods were varied, the authors inferred that there is a series of dark reactions of the order of few hundredths of a second duration. Another ciliate, *Colpidium colpoda*, also reacted in the same way; photoreversal was much more pronounced when a given amount of visible light was delivered in frequent flashes rather than continuously. We should note that in the *Tetrahymena* experiments, at least, the division delay measured was that which occurs immediately after irradiation. This delay is to be distinguished from the very much longer delay common in these ciliates after the third or fourth division has taken place. In any case, it appears that the photoreversal period can be subjected to the same kind of physical tests found valuable in the study of other photochemical reactions.

Another study of pertinence to the subject of the transfer and use of photoreactivating energy was described by Kaplan & Kaplan (49). Using strain K of *Serratia marcescens*, they induced and photoreactivated color "mutants" under different conditions of humidity. In 95 per cent R.H. the cells show only 1/20 the sensitivity as at 33 per cent. Conclusions from this unexpected result have to be tempered with the fact that about 75 per cent of the cells die during the drying and remoistening processes. Color mutants, moreover, are most numerous in the dry state. When change is induced in the dry state, however, no photoreversibility can be accomplished in regard to color strains or survival. When the ultraviolet irradiation is done in the wet state, photoreversibility for lethality is possible in the wet state but not in the dry. The number of color mutants can be reduced by visible illumination in either the wet or dry state.

The metabolic nature of photorestoration was stressed by Newcombe (50) who measured in *Streptomyces* the disappearance of reversibility after injury by ultraviolet. For a period of time equal to about half a division interval, mutations are photoreversible; then they become light stable. A delay in nuclear division results in prolonged photoreversibility.

Another demonstration of the modification of photoreactivating light within a strain by changing environmental conditions was provided by Durham & Wyss (51). Cells inactivated to 10 per cent survival can be fully restored if a salt-broth medium is used for growth; equivalent cells grown in nutrient broth are reactivated to only 20 per cent by similar amounts of light.

EFFECTS OF IONIZING RADIATIONS

THEORETICAL RADIobiOLOGY

The development of target theory by Lea (52) and by Timoféeff-Ressovsky & Zimmer (53) provided useful and valuable models for the design of cellular experiments in radiobiology. Since these proposals appeared, some change in outlook has occurred among some radiobiologists, with simple target theory becoming gradually modified [Zirkle (54) and Tobias (55)]. Zimmer (56) recently has briefly reviewed the current status of target theory, pointing out that although it will continue to be useful, it is clear that single explanations are highly unlikely for radiation effects in biological systems. A valuable recent summary of the status of target theory was presented also by Alper (57) who examined the evidence on modifications of "direct" actions. It is her view that the role of free radicals and peroxides may be interpreted in such a way as to support, rather than weaken, target theory as presented originally. Butler (58), in a review, attempted to account for the large, biological effects resulting from small radiation energy inputs in terms of a few changes in the DNA-histone relationships in the cell.

Other authors have underlined the essential complexity of living systems, even when the components can be isolated to a large extent. In *Achromobacter fischeri*, for example, the light emitted is influenced by x-irradiation. Hug & Wolff (59) attempt to present a general theory to describe this response in terms of recovery processes of a biological nature that depend upon two or more sequential events involving participants of different radiation sensitivities. Even in this simple system involving a limited number of substances, fitting of observed fact to theory is difficult.

Simple mathematical descriptions for the presumably genetically induced death in microorganisms are possible however. Wijsman (60, 61) presented a relatively simple theory that describes lethality induced in yeast by radiations of different specific ionizations (LET). His basic assumptions are that all sensitive sites occur within the nucleus, and that diffusion lengths of substances intermediary between the ionization event and the sensitive target are long compared to nuclear dimensions. Survival curves in yeast after treatment with α -particles of different energies fit a simple mathematical formulation containing a parameter that specifies the LET within a typical cylindrical ionization track. The value of this parameter varies with the mass and energy of the particle.

A contribution to the empirical analysis of survival curves was made by Gurian (62) who improved the Kimball method of fitting so-called multi-target survival curves of microorganisms. The modification gives appropriate weights to different survival values, the weight depending on sampling errors and on the transformation used in fitting the curves. Epstein (63) applied the now familiar multi-target hypothesis as a model for irradiation effects on bacterial capacity to support phage growth.

The discussion of Hoffmann *et al.* (64) of applying computer methods to the analysis of populations of dividing cells could be of value in cellular

radiobiology. Intermitotic times are of varying lengths, each mean length having values distributed about it. The next intermitotic time after the first will have a similar distribution. The calculation of sequential times is a problem, then, of multiple probabilities for each daughter cell (the Monte Carlo random problem). The authors developed a machine method and show that it applies to observed numbers. For example, the mitotic index for a population of cells derived from a single cell stabilizes only after nine generations. Although the case of exponential growth considered by these authors had previously been treated analytically by Kendall (65), the Monte Carlo method has promise in application to situations where mathematical analysis becomes very difficult.

Extension of these methods to radiation experiments will be of interest. If radiosensitivity varies with position within the intermitotic interval, estimates of the distribution of radiation sensitivities might then be made by these methods. The value of such information in heterogeneous cell systems (e.g., tissue cultures and microorganisms in exponential growth) is obvious.

CELLULAR EFFECTS

Cell division studies.—Several general reviews pertinent to radiation effects on cell division appeared during the year. Anderson (66) offered a hypothesis concerning the events leading to the initiation of cell division; he described the biochemical and biophysical evidence supporting this. The review of Klein (67) describes the origin, characteristics, and responses of ascites tumors, a test system which is becoming more popular in radiation studies.

Shepard *et al.* (68), using the ciliate *Didinium nasutum*, measured the delay in division caused by x-rays. With starved specimens, they measured the increase in time to the fourth division. As in many other protozoan forms, delay in division increases as radiation dosage is increased. At 100,000 r fission delay of the treated samples was 15 hr. beyond control levels, at which dosage death of cells began to occur. The division delay produced in yeast was examined in detail by Burns (69), the patterns produced being as follows. In mature diploid cells radiation was followed by a short delay, which in turn is succeeded by a much longer delay. Most frequently the next intermitotic interval is not delayed. The large delay seen in the second division is related to dose in an exponential fashion ($1 - e^{-kd}$). The first delay observed is not correlated with the second and, therefore, is uncorrelated with dose. This pattern is reversed when diploid cells are irradiated during the budding process. In such cases, the first delay is usually very long and the second delay is either short or nonexistent. Unlike lethality, division cannot be easily related to the ploidy of the cells and thus appears to be a phenomenon independent of the nuclear condition. The author presents a tentative hypothesis relating these effects to the lethality effects observed by others in yeast.

Ord & Danielli (70) continued their investigation of the sites of damage in

Amoeba caused by x-rays using *Amoeba proteus*. In these forms, treated or untreated nuclei can be transferred to treated or untreated cytoplasm of the same species, making possible the recognition of the relative importance of damage to each of the sites (nucleus versus cytoplasm). Although it is probable that nuclei can be damaged directly by x-rays, there is evidence that irradiated cytoplasm can damage unirradiated nuclei, making a test of direct action of x-rays on nuclei very difficult. Direct action on cytoplasm and the reversible nature of this damage could be demonstrated by the authors. The relative overall sensitivities, based on lethality studies, are in the proportion 2.4:1, the LD₅₀ being in the ratio of 120,000 r (nuclei) to 290,000 r (cytoplasm).

A similar investigation in *Pelomyxa illinoiensis*, another ameboid form, was reported by Daniels (71). By micro methods he injected unirradiated protoplasm into x-irradiated cells and thus prevented death. The cytoplasm was centrifuged and the effectiveness of different strata in preventing death was tested. His preliminary results show that some component which migrates toward the centrifugal pole is necessary for recovery in the ameboid form; however, at the present time no morphological entity can be recognized as the agent. The evidence on fission delay in *Paramecium aurelia* was reviewed and interpreted by Powers & Ehret (24). Fission delay by x-rays and other agents is temperature-dependent and is related in magnitude to other effects (one likely nuclear effect) and to dosage in such a way as to favor the interpretation that the cytoplasm is the important site of damage. Using the ciliate *Tetrahymena*, Ducoff (72) induced x-irradiation fission block in fission synchronized cultures. This was done to study both the DNA content at the time of damage in the fission block and effect of damage on DNA synthesis. He found that the length of the fission block is proportional to dosage, but does not appear to be related to the amount of DNA present in the cells at the time of damage. He further found that synthesis of DNA continues even though fission block was induced by x-rays. This result is commonly found in microorganisms.

Freyman (73) measured effects of single doses of total body x-rays on rats on cell division in the Yoshida ascites tumor. He equated the mitotic rate with mitotic index (the number of cells observed in mitosis per unit number of cells counted). According to his analysis and interpretation, 425 r total body x-ray completely inhibits mitosis of these cells for 3 hr. and recovery from the fission block takes place over the next twenty hours. The general problems surrounding the analysis of cells, their growth rates, length of intermitotic times, etc. are discussed fully by Hoffman (74).

The effects of continuous radiation by beta particles on tissue culture cells with particular emphasis on effects on mitosis were described by Stroud (75). Tissue cultures of chick embryo skeletal muscle were incubated with tritium, an emitter of β -particles of low energy. The effects were recorded both with cinematographic techniques and direct observation. One of the significant results was that mitosis itself is considerably prolonged by radiation, meta-

phase being particularly prolonged, resulting in an accumulation of metaphases in the tissue culture. Data which depend upon the use of the mitotic index as a measure of cell division rate should be evaluated considering this result. The observations on the behavior of the cleavage furrow are also of interest. In these cultures under constant irradiation, the cleavage furrow loses its position in both time and space. Many irregularities were observed, indicating that under these circumstances it is independent of the spindle and chromosomes.

The sensitivity of the cell in various stages of the mitotic process was briefly reported by Nakao (76). Using the amphibian egg, he found that x-ray sensitivity varies at different stages following insemination. Sensitivity is high at the time of insemination; it is lowest when pronuclei are fusing; it rises at the time of the first cleavage, and is still below the maximum observed at insemination.

Several papers dealt with the effects of x-rays on the mitotic process in *Vicia faba*. Hornsey (77) analyzed the contribution of lengthening of the mitotic time to the observed reduction in growth rate in root tips. Her conclusion, based on the fact that the number of aberrant micronuclei present three days after irradiation is that expected if mitosis is proceeding at a normal rate, is that the observed reduction in growth at the time of the count is not caused by a prolongation of the time of mitosis. Pelc & Howard (78) measured the effect of fractionation of x-rays on DNA synthesis and total growth in the roots of *Vicia*. When 140 r is given continuously there is a significant reduction in the number of cells containing P^{32} in the chromosomes (counted from squash preparations measured by radioautograph) compared to controls. When this dosage is broken into four 35-r periods with six hours between each, the number of cells labeled is intermediate between that found with continuous radiation and the control, indicating that a biological repair of some sort takes place in the cells. The relative efficiency of 31-Mev x-rays and 180-kvp x-rays was measured by Fritz-Niggli (79) in the same plant. Qualitatively the two radiations had the same effect, but quantitatively 31 Mev x-rays were much less efficient than 180-kvp x-rays. At 250 r for instance, the values observed (per cent of cells in division) were almost at control levels after the high energy x-rays, but were consistently different in the case of 180-kvp x-rays.

Survival studies.—In this section we shall review the papers appearing during 1956 dealing with the biological and physical factors affecting the survival of cells after irradiation. [See Holmes (3), Hollaender & Stapleton (80) and Hollaender & Kimball (81) for more general discussion of studies of radiation protection.] Gunter & Kohn (82) re-examined the effect of cell concentrations on the survival of certain bacteria after x-irradiation. In the concentration region between 10^2 and 10^9 cells per ml., cell concentration played no part in determining radiation sensitivity for *E. coli*, *Rhodopseudomonas*, *Pseudomonas* and haploid *Saccharomyces*. The survival of *Azotobacter* and diploid *Saccharomyces* became greater in concentrations above approxi-

mately 10^8 cells per ml. These authors think that oxygen concentration and respiratory activity of the cells are related to this effect. Goucher *et al.* (83) also examined radiation sensitivity with reference to cell concentration in *E. coli* B/r and showed that concentrations from 10^4 to 10^9 cells per ml. have no effect on survival after irradiation, a result essentially the same as reported by Gunter & Kohn (82). Goucher *et al.* (83) discuss fully these results in relation to earlier reports of others which were contrary. In the same study they examined the role of respiratory activity in determining radiation sensitivity of these organisms. Incubation with succinate before exposure gives no protection to *E. coli* B/r unless the exposure system is such that oxygen equilibration with air is prevented. In these experiments, moreover, malonic acid did not affect the irradiation protection given by incubation with succinate under the proper conditions. Here, also, results were different from others previously reported by other authors; this difference is discussed.

Several authors presented studies on the nature and significance of survival curves after irradiation in cell systems. It was shown [Gunter & Kohn (84)] that survival curves of a number of bacteria, unlike irradiated diploid yeast cells, are not affected by heterogeneity in colony size.

Gunter & Kohn (85) also describe the kinds of survival curves demonstrated in a number of microorganisms: *Azotobacter*, *Rhodopseudomonas*, *E. coli*, *Pseudomonas* and haploid and diploid yeast. They recognize at least three types of survival curves after irradiation. All of these are either interpreted as simple exponentials or in terms of a single simple exponential. There is a rather full discussion of the literature on this subject.

Pittman (86) analyzed the mutation induction curves observed in yeast that demonstrated a peak effect similar to that seen in several other microorganisms. When the number of adenine-deficient cells induced by x-rays in a dissimilated heterozygous culture of *Saccharomyces* is plotted against dose as a fraction of the number of survivors, there is an initial rise at low doses and, then, with increasing dosage there is a decrease in the fraction. Pittman proposed that the cultures consist partly of a number of budding cells, and that these budding cells are resistant, not only to the lethal effects of x-rays as described by Beam *et al.* (87), but also to the mutagenic action of x-rays. The plot of mutants per unit number of survivors, consequently, goes down as dosage increases.

This type of response curve also appears in other forms. When the number of phage centers observed in cultures of the lysogenic bacterium K12 (λ) is plotted against dosage, there is an increase in the number of induced colonies to a maximum, and then a decrease with increasing dosage. Marcovich (88) offered two explanations for the phenomenon: x-rays induced conversion of prophage to the vegetative phage leading to visible colonies of phage and, simultaneously, damaged the capacity of the host bacterium to carry out phage synthesis; or, alternatively, a system activated by one event may be destroyed if two occur, e.g., the production of several levels of oxidizing and reducing substances. (With the last general explanation, a good

fit of the data to the second term of the Poisson series was obtained.) Both explanations are alike in that two competing results occur simultaneously, but at different rates. The induction process itself [Marcovich (89)] is a single-hit process, dose-rate independent, and insensitive to oxygen. The characteristics of this lysogenic system in a constant flux of γ -radiation were described also [Marcovich (90)].

The development of techniques that allow manipulation of mammalian cells in ways similar to those successfully used with microorganisms allows more sensitive measurements of their radiosensitivity. Puck & Marcus (91), using the HeLa carcinoma cell, demonstrated that ability to form colonies is a radiation-sensitive capacity of the cell. The response curve is of the multi-target variety with a shoulder extending to about 200 r. The exponential region of the response curve indicates an inactivation coefficient of 0.0104 r^{-1} —relatively high radiation sensitivity for these cells. The authors fitted this curve by assuming that the Y intercept is at two. Some of the cells that cannot form colonies continue their growth without division and become very large, a property commonly seen in irradiated microorganisms.

Microorganisms as test objects for the measurement of biological efficiency of photons of widely different energies were investigated in a series of papers [Gunter, Kohn, Tyree *et al.* (92), Kohn & Gunter (93) and Kohn & Gunter (94)]. The sensitivity of haploid yeast to 180-kvp x-rays (half value layer, $=0.75 \text{ mm. Cu}$, 700 rads/min., $\text{LET} \leq 2000 \text{ ev}/\mu$) was compared to that of the yeast to 22.5 Mvp x-rays ($\text{LET} \leq 200 \text{ ev}/\mu$) produced by a betatron in two μ sec. pulses at 180 pulses per sec. Response curves were essentially simple exponentials. The slopes of the inactivation curves were in the ratio of 1.06, with the high energy x-rays being the more efficient. The authors discuss the errors inherent in the total measurement and conclude that the 1.06 value cannot be considered to be different from 1.00. The conceivable contribution of pulsing was mentioned. In the two other studies, Kohn & Gunter (93, 94), measuring the relative efficiency of 1000-kvp x-rays (HVL 8–9 mm. Cu) and 250-kvp x-rays (HVL 1.6 mm. Cu), obtained an opposite result. At a dose rate of 150–200 r/min. cell suspensions of *Saccharomyces* (haploid and diploid) exhibited survival curves having a ratio of 0.879 (1000/250). Two bacteria, *Rhodopseudomonas sphaeroides* and *E. coli* B/r, showed sensitivities in the ratio of about 0.9 for the same two radiations.

The role of lethal genetic changes in determining death in irradiated yeast cells was investigated further by Owen & Mortimer (95). They mated irradiated haploid and diploid cells of various combinations and observed survival, comparing them to expectation. Although there are apparent unexpected consequences of the mating experiments, the authors believe that the lethal chromosome change theory is supported by their results. The lethal chromosome change theory is extended to include the possible contributions to the effect of the damage of nonchromosomal cellular constituents that increase with increasing ploidy.

The lethal effects of x-rays and nitrogen mustards in *Paramecium aurelia* were reviewed and analyzed by Powers & Ehret (24). They proposed that the lethal effects of x-rays as well as of ultraviolet in this organism are principally cytoplasmic, because, primarily, more likely nuclear effects measured in the same cell have quite different relations to dosage. A contrary attitude was presented by Gray (96) who reviewed lethality studies in a number of other forms. In his opinion the evidence points in the cases reviewed mostly to the nucleus as the site of primary damage. Also, the theory of radiation sensitivity of Schjeide *et al.* (97) proposed that damage is the result of oxidants produced by irradiation in the nucleus principally. However, the evidence from *Paramecium*, *Pelomyxa*, and *Amoeba*, and the apparent growing awareness among investigators using other forms that the simple nuclear damage assumption is not adequate, will probably result in wider inquiry into this important radiobiological matter. The technique of selectively irradiating parts of cells, reviewed last year by Zirkle, Bloom & Uretz (98), will be valuable in contributing answers to these questions of sites of damage in the cell, and their relative importance in bringing about observed effect.

In *Paramecium aurelia* evidence on this point was contributed by Kimball & Gaither (99). They measured growth behavior of exconjugant animals that were amicronucleate at the time of irradiation, but which then received nuclei from an unirradiated conjugant. At the dose level used (35 kr) no effects were observed on growth or survival. [We note that this dose is below those used in the experiments analyzed by Powers & Ehret (24).] On the other hand, when crosses were made that ensured reciprocal exchange of pronuclei, differences were observed between the exconjugants. Kimball & Gaither believe that an incompatibility reaction, and not a radiation effect, is being observed in this case. The point is open. In these experiments also, behavior of pronuclei at conjugation was inferred from the presence or absence of genetic markers in exconjugants. It appears that irradiation influences the successful production, or transfer, or fusion, of the male pronucleus. Further, radiation effects induced in successful male pronuclei are permanent, while at the same time expected chromosomal aberrancies are not observed. Earlier in the year Bachofer (100) also reported effects of x-rays on pronuclear fusion time in *Ascaris lumbricoides suum*, a phenomenon probably related to the effects described by Kimball & Gaither. On the other hand, in *Tetrahymena pyriformis* conjugation was disturbed by high dosages of x-rays, but most animals, even those in the 300-kr groups, revealed no disturbance in nuclear behavior at conjugation [Elliott & Clark (101)].

Changes in microorganisms after x-rays that may be interpreted as nuclear changes were described by several authors. Newcombe (102) investigated the separate and combined actions of cold and x-rays in *Streptomyces* in causing death and some undescribed changes called "mutations." Mutations are induced at different rates by the two agents, they are only partly additive, and the relations between cell death and mutations are

such that the author concludes that while some steps in the mutation process are similar after the treatments, there are some that are different. Kimball *et al.* (103) observed that nuclear changes in Paramecium can be increased by treatment of the cells after x-irradiation and before the first division following irradiation. The changes are not fixed for at least two hours after irradiation. Unstable forms of *Streptomyces venezuelae* were the largest class of "mutants" after x-irradiation, the stable forms being of lowest frequency [Gwatkin & Gottlieb (104)].

Several papers appeared that described the sensitivity of microorganisms encountered in food sterilizing operations. [For a fuller discussion of progress in food sterilization by radiations, the reader is referred to Holmes (3).] Pertinent to our consideration are several investigations which showed the following: (a) the dosages necessary to produce complete freedom of the culture from microorganisms (an indeterminant end point in many cases) were compared, and yeast seemed to be more resistant to ionizing radiation than molds [Bridges, Olivo & Chandler (105)]; (b) some spores are more resistant than vegetative cells [Pepper, Buffa & Chandler (106)]; (c) survivors of high dosage radiation produce colonies which are no more resistant than the parent colony, i.e., the radiations did not produce radiation-resistant mutant cells [Koh, Morehouse & Chandler (107)]; (d) in another paper (108) the same authors present the sensitivities of a number of different microorganisms.

Temperature effects.—The importance of varying temperatures in the low temperature range in investigating the mechanism of action of x-rays is becoming more widely appreciated by biologists. During 1956 several investigations were reported. Stapleton & Edington (109) reduced the temperature of suspensions of *E. coli* B/r in buffered salt solution and observed the usual sharp change in sensitivity near the freezing point. In an oxygen-saturated system, there is sensitivity change with decreasing temperature below 0°C.; and, they believe their results indicate that, in contrast to the oxygen-saturated system, there is temperature independence below 0°C. in a nitrogen-saturated system. In consideration of the size of the errors, this author believes that their claim is unwarranted. The slopes of the response curves in all environments tested (O_2 , N_2 , $Na_2S_2O_4$) behave qualitatively the same as temperature is reduced; conclusions based on the error analysis are weak because of the uncertainties, pointed out by the authors themselves, that surround the original estimates of the slopes. Their results allow that the temperature dependence reported in an oxygen-free system is the same except in magnitude as that observed for the oxygen-saturated system.

Houtermans (110) tested for changes in sensitivity of spores of *Bacillus subtilis* to x-rays and α particles as affected by water content and temperature during the irradiation period. The sensitivity of wet spores to x-rays (50 kvp through a Be window with no added filtration) is a smooth, almost linear function of temperature from room temperature to $-184^{\circ}C.$, with a small acceleration between 0° and -50° ; in dry spores the sensitivity shows

a somewhat sharper decrease in this latter region. The response of dry spores to α rays is like that to x-rays, whereas the response of wet spores is different, demonstrating temperature independence to -184°C . In all instances when a difference in sensitivity existed, dry spores showed greater sensitivity than wet spores. Superficially, at least, this result is different from that reported in yeast by Wood (111). In this work, sensitivity to x-rays was always higher in yeast in the liquid state than it was in the solid, but not dry, state. Wood (111) accounts for the decrease in sensitivity by the disappearance of free water from the system, and such an interpretation is consistent with that proposed by Stuy (46) who observed increases in sensitivity of spores of *B. cereus* to ultraviolet and x-rays during the germination period. Stuy proposed the amount of water taken up during germination as the reason for the change in sensitivity in such spores. While other mechanisms may be operative (physiological changes), it is clear that there are differences in sensitivity.

VIRUSES AND MACROMOLECULES

The results of several studies on the radio sensitivity of different viruses have appeared during the year. Jordan & Kempe (112) measured sensitivity to cobalt 60 gamma rays of St. Louis encephalitis virus, western equine encephalitis, vaccinia, and poliomyelitis virus. Lauffer *et al.* (113) attempted to explain inactivation of x-rays of tobacco mosaic virus (TMV). Because RNA from irradiated TMV has a viscosity different from normal, they believe that breakage of the long rods is the mechanism of inactivation. They acknowledge the difficulty caused by the difference between the lethal dosages and those required to bring about changes in viscosity.

Attempts to define size and shape of sensitive areas in viruses and large molecules by irradiating dry preparations with agents producing different specific ionizations were described in several papers. Jagger & Pollard (114) used deuterons, α particles, and electrons to change infectivity and hemagglutination properties in two strains of influenza A virus. One of these, MEL, appears to have two regions of sensitivity, one high and one low. General sensitivity is apparently determined by a very small part of the total influenza virus particle, and seems to be inactivated by single events. The hemagglutinating property, on the other hand, is radiation-resistant, needing three ion pairs per particle for inactivation, according to the calculations of these authors. Powell & Pollard (115) measured changes in the interfering property of the influenza virus after irradiations with the same agents. Changes in the capacity of the virus to interfere with the production of hemagglutinins, infective virus and complement fixation antigen are such that a molecular weight of 1.6×10^6 is indicated for the portion of the virus responsible. This value is near the 1.4×10^6 calculated for the coliphages T1 and T2 by Pollard & Setlow (116) for the mutual exclusion of one by the other in mixed infections. In the same study the sensitive volume for the attachment property of T1 to *E. coli* was calculated as an equivalent

mol. wt of 326,000. The value for T2 gave an equivalent mol. wt of 183,000. The cross reactivation property of T1 was described by Till & Pollard (117) as involving about sixty per cent of the genetic portion based on deuteron inactivations. Also, Brinton (118) estimated the molecular weight of an antiphage against T4 in the dry and wet state; the value being between 50,000 and 120,000. Ginoza & Norman (119) estimated the molecular weight of tobacco mosaic virus RNA from measurement of x-irradiated samples in the frozen state as between 1.5 and 6×10^6 . They believe the whole molecule is the infectious unit.

Other characteristics of coliphages were investigated in radiation experiments. Weigle & Bertani (120) examined the phenomenon of "multiplicity reactivation" in T2 after ionizing radiations. Sensitivity to both ultraviolet and ionizing radiations is measured by the number of infected bacterial cells that can produce progeny phage. When only one treated particle per host-cell is ensured in the mixture of phage and bacteria, the sensitivity is greater than that seen when more than one treated particle (multiplicity infection) is ensured for each host bacterial cell, i.e., multiplicity results in reactivation. Weigle & Bertani (120) showed that this reactivation is seen after gamma irradiation of isolated T2. When soft x-rays are used, however, sensitivity is changed only after irradiation of the phage absorbed on the host cell. The authors think that the damage in the virus that can be substituted for by another damaged particle is probably genetic in nature like that after ultraviolet, although they allow for a difference between ultraviolet and x-ray damage.

Harm (121) reported similar experiments with ultraviolet in the T4 phage and pointed up a difficulty in the pure genetic substitution hypothesis. As in the usual multi-target type of inactivation, one would expect that the slope of the inactivation curve finally attained as dosage increases would be equal to that seen after single infection tests. This has not been observed [Dulbecco (122)] and Harm (121), even after eliminating cells of varying surface areas, also is unable to approach the theoretical curves. Harm suggested that different kinds of genetic damage occur, only some of which can be reactivated by multiplicity infections. Cross-reactivation of two strains of irradiated influenza virus was reported by Gotlieb & Hirst (123). A neurotropic (w^+) and a nonneurotropic (M^-) strain can form recombinants. After ultraviolet irradiation, survival was increased by mixture of the two strains. Heat, certainly a nonspecific damage, affected these viruses in the same way.

The radiation-sensitive volume of the adrenocorticotropic hormone molecule in the dry state was estimated [Child *et al.* (124)]. Assuming exponential inactivation the authors calculate an inactivation molecular weight of about 2500.

EFFECTS OF RADIOACTIVE ISOTOPES

During the year the effects of some radioactive isotopes of biological interest were measured in a number of cellular systems. The use of tritium as

a source of continuous radiation in tissue cultures has been described (75). Tritium was also used by Davydoff (125) who measured the efficiency of this soft beta emitter relative to that of the gamma emitter Ir¹⁹² in inducing lethality in *Serratia indica*. She reported a relative efficiency of 0.87, which is very near that of 0.82 reported by the original workers using *Paramecium* (126). In another study Spalding *et al.* (127) measured the efficiency of tritium in *Vicia faba* that shows an efficiency for root growth of 1.0.

These studies were of effects caused directly by the β -particles emitted from the nuclei of the unstable isotopes. There are other effects of radioactive decay in cell systems which many authors think are visible effects of the transmutation of atoms from one biologically important entity into another. (For instance, the transmutation of P³² into S³² at the time of the emission of the negative electron from the atomic nucleus.)

Powers (128) reviewed the literature in this area up to 1956, and described results found in *Paramecium aurelia*. Post-autogamous death is regarded as a likely measure of micronuclear change brought about by the treatment. There is evidence that P³² incorporated into the protoplasm of the animal is much more efficient in bringing about this effect than Sr⁸⁹, Sr⁹⁰ mixtures at similar radiation dosage levels. The latter elements are not incorporated into protoplasm at critical sites such as expected in the case of phosphorus, and the difference in efficiency is thought to be related to the difference in position of the atoms in question. Interpretation is complicated by the fact that the organism concentrates phosphorus to levels much above that of the medium resulting in higher radiation levels in the cell. There is a review of all of the published considerations of point source geometry, and the methods of application are exemplified for the *Paramecium* case. Even when concentration up to 200X is taken into consideration, phosphorus is more efficient than strontium, suggesting that transmutation of phosphorus has an effect above and beyond that of the radiation to which the cells are exposed.

In *Neurospora crassa*, using lethality of conidia as a measure, Strauss *et al.* (129) recorded the efficiency of P³² and S³⁵ in inducing effect. Lethality is in a straight-line relation to decay of the radioactive elements. Because of the geometry and the relationship of the effect to decay, they suggest that both sulfur and phosphorus are in such positions in the conidium of *Neurospora* as to make a change in some of these atoms lethal. The importance of change in the sulfur and phosphorus atoms are thought to be of approximately the same magnitude.

In *E. coli*, Fuerst & Stent (130) measured the importance of disintegration of P³² incorporated into the protoplasm of the organism. Cells were allowed to incorporate P³² at 16 mc. per mg. for five to six fissions. These cells were stored at -196°C. and survival was measured as a function of time. Under these conditions *E. coli* B/r is inactivated in a multi-target (three in number) manner, the straight-line exponential portion of the survival curve being linearly related to the number of decaying P³² atoms. The explanation is given that there are three units in the cell that have to

be inactivated before death occurs, and that on this basis approximately two per cent of all P^{32} disintegrations are effective in inactivating a unit. This is about the efficiency measured in coliphage. When the thymineless strain ($15T^-$) is used a slightly different result is observed. This organism, not synthesizing DNA in the absence of thymine, showed a much greater resistance to P^{32} . Such resistance is regarded as an indication that the important sites of phosphorus to give this effect are DNA molecules, agreeing with the earlier conclusion of Rubin (131) for genetic effects induced in this manner.

Two investigations described the analysis of coliphage by P^{32} disintegrations. Stent & Fuerst (132) used the method to reveal the fate of DNA in phage infections. These authors used a lytic phage (the direct lysis of the host cell by the infecting bacteriophage) and a lysogenic phage (lysis induced by other treatment, as ultraviolet, in host cells containing nonactive but multiplying phage many cell divisions after infection). They measured the sensitivity of the phages at short times after infection of the cell. Immediately after infection the viruses are sensitive to P^{32} decay, but a short time later, at about the same time both become resistant. When bacteria highly labeled with P^{32} was used as the host, the reproduction of the lysogenic λ was more sensitive to P^{32} decay than the lytic T2 and the sensitivity of the former lasted longer. Stahl (133) using the coliphage T4 measured the sensitivity of five different genetic characters. According to his results, phosphorus decaying in the DNA portion of the phage particle inactivated the genetic characteristic. While interpretation at the atomic level will be difficult (128), the method in general shows promise as a means of precise analysis of the role of substances in cells.

LITERATURE CITED

1. Mortimer, R. K., and Beam, C. A., *Ann. Rev. Nuclear Sci.*, **5**, 327-68 (1955)
2. Gray, L. H., *Ann. Rev. Nuclear Sci.*, **6**, 353 (1956)
3. Holmes, B., *Ann. Rev. Nuclear Sci.*, **7**, 89 (1957)
4. Fluke, D. J., and Setlow, R. B., *J. Opt. Soc. Am.*, **44**, 327-30 (1954)
5. Monk, G. S., and Ehret, C. F., *Radiation Research*, **5**, 88-106 (1956)
6. Parker, M. W., Hendricks, S. B., Borthwick, H. A., and Scully, N. J., *Botan. Gaz.*, **108**, 1-26 (1946)
7. Wihlm, H., *Rev. opt.*, **33**, 425-54 (1954)
8. Setlow, R. B., and Doyle, B., *Biochim. et Biophys. Acta*, **22**, 15-20 (1956)
9. van Wagendonk, W. J., *J. Biol. Chem.*, **173**, 691-704 (1948)
10. Powell, W. F., and Setlow, R. B., *Virology*, **2**, 337-43 (1956)
11. Fluke, D. J., *Radiation Research*, **4**, 193-205 (1956)
12. Six, E., *Z. Naturforsch.*, **11b**, 463-70 (1956)
13. Goldman, A. S., and Setlow, R. B., *Exptl. Cell Research*, **11**, 146-59 (1956)
14. Giese, A. C., Shepard, D. C., Bennett, J., Farmanfarmaian, A., and Brandt, C. L., *J. Gen. Physiol.*, **40**, 311-26 (1956)
15. Christensen, E., and Giese, A. C., *J. Gen. Physiol.*, **39**, 513-26 (1956)
16. von Borstel, R. C., and Moser, H., *Progress in Radiobiology*, 211-15 (Oliver and Boyd Ltd., London, England, 557 pp., 1956)

17. Ogg, J. E., Adler, H. I., and Zelle, M. R., *J. Bacteriol.*, **72**, 494-99 (1956)
18. Latarjet, R., and Beljanski, M., *Ann. inst. Pasteur*, **90**, 127-32 (1956)
19. Payne, J. I., Hartman, P. E., Mudd, S., and Phillips, A. W., *J. Bacteriol.*, **72**, 461-72 (1956)
20. Goucher, C. R., Kamei, I., and Kocholaty, W., *J. Bacteriol.*, **72**, 184-88 (1956)
21. Streisinger, G., *Virology*, **2**, 1-12 (1956)
22. Siegel, A., Wildman, S. G., and Ginoza, W., *Nature* **178**, 1117 (1956)
23. Tessman, E. S., *Virology*, **2**, 679-88 (1956)
24. Powers, E. L., and Ehret, C. F., *Proc. Internat. Conf. Peaceful Uses Atomic Energy*, **11**, 266-72 (United Nations, New York, N. Y., 402 pp., 1956)
25. Brandt, C. L., and Giese, A. C., *J. Gen. Physiol.*, **39**, 735-51 (1956)
26. Häammerling, J., *Z. Naturforsch.*, **11b**, 217-20 (1956)
27. Yost, H. T., Robson, H. H., and Spieglerman, I. M., *Biol. Bull.* **110**, 96-106 (1956)
28. Errera, M., and Ficq, A., *Progr. in Radiobiology*, 3-6 (Oliver and Boyd Ltd., London, England 557, pp., 1956)
29. James, A. P., and Chaplin, C. E., *Radiation Research*, **5**, 162-66 (1956)
30. Charles, R. L., and Zimmerman, L. N., *J. Bacteriol.*, **71**, 611-16 (1956)
31. Barner, H. D., and Cohen, S. S., *J. Bacteriol.*, **71**, 149-57 (1956)
32. Buzzell, A., *Arch. Biochem. Biophys.*, **62**, 97-108 (1956)
33. Stein, W., and Laskowski, W., *Z. Naturforsch.*, **11b**, 643-53 (1956)
34. Bruce, V. G., and Maaløe, O., *Biochim. et Biophys. Acta*, **21**, 227-33 (1956)
35. Meyer, H. U., *Caryologia, Suppl.*, 893-894 (1954)
36. Weatherwax, R. S., *J. Bacteriol.*, **72**, 329-32 (1956)
37. Galperin, H., and Errera, M., *Protoplasma*, **46**, 210-12 (1956)
38. Schoenborn, H. W., *J. Protozool.*, **3**, 97-99 (1956)
39. Latarjet, R., and Cherrier, N. (Unpublished data)
40. Zamenhof, S., Leidy, G., Hahn, E., and Alexander, H. E., *J. Bacteriol.*, **72**, 1-11 (1956)
41. Weatherwax, R. S., *J. Bacteriol.*, **72**, 124-25 (1956)
42. Kelner, A., *J. Bacteriol.*, **58**, 511-22 (1949)
43. Kelner, A., and Taft, E. B., *Cancer Research*, **16**, 860-66 (1956)
44. Rieck, A. F., and Rudich, E. C., *Radiation Research*, **5**, 592 (1956)
45. Stuy, J. H., *Biochim. et Biophys. Acta*, **22**, 238-40 (1956)
46. Stuy, J. H., *Biochim. et Biophys. Acta*, **22**, 241-46 (1956)
47. Latarjet, R., *Strahlentherapie*, **101**, 580-98 (1956)
48. Jagger, J. J., and Latarjet, R. (Unpublished data)
49. Kaplan, R. W., and Kaplan, C., *Exptl. Cell Research*, **11**, 378-92 (1956)
50. Newcombe, H. B., *Brookhaven Symposium in Biology*, No. 8, 88-102 (1956)
51. Durham, N. N., and Wyss, O., *J. Bacteriol.*, **72**, 95-100 (1956)
52. Lea, D. E., *Actions of Radiations on Living Cells* (Macmillan Co., New York, N. Y., 402 pp., 1947)
53. Timoféeff-Ressovsky, N. W., and Zimmer, K. G., *Das Trefferprinzip in der Biologie* (S. Herzel Verlag, Leipzig, Germany, 317 pp., 1947)
54. Zirkle, R. E., *Symposium on Radiobiol.*, 333-56 (Wiley and Sons, New York, N. Y., 465 pp., 1952)
55. Tobias, C. A., *Symposium on Radiobiol.*, 357-84 (Wiley and Sons, New York, N. Y., 465 pp., 1952)
56. Zimmer, K. G., *Acta Radiol.*, **46**, 595-602 (1956)
57. Alper, T., *Radiation Research*, **5**, 573-86 (1956)
58. Butler, J. A. V., *Radiation Research*, **4**, 20-32 (1956)

59. Hug, O., and Wolff, I., *Progress in Radiobiology*, 23-30 (Oliver and Boyd Ltd., London, England, 557 pp., 1956)
60. Wijsman, R. A., *Radiation Research*, 4, 257-69 (1956)
61. Wijsman, R. A., *Radiation Research*, 4, 270-77 (1956)
62. Gurian, J. M., *Biometrics*, 12, 123-26 (1956)
63. Epstein, H. T., *Bull. Math. Biophys.*, 18, 265-70 (1956)
64. Hoffman, J. G., Metropolis, N., and Gardiner, V., *J. Natl. Cancer Inst.*, 17, 175-88 (1956)
65. Kendall, D. G., *Biometrika*, 35, 316-30 (1948)
66. Anderson, N. G., *Quart. Rev. Biol.*, 31, 169-99 (1956)
67. Klein, G., *Z. Krebsforsch.*, 61, 99-119 (1956)
68. Shepard, D. C., Giese, A. C., and Brandt, C. L., *Radiation Research*, 4, 154-57 (1956)
69. Burns, V. W., *Radiation Research*, 4, 394-412 (1956)
70. Ord, M. J., and Danielli, J. F., *Quart. J. Microscop. Sci.*, 97, 29-37 (1956)
71. Daniels, E. W., *Radiation Research*, 5, 604-5 (1956)
72. Ducoff, H. S., *Exptl. Cell Research*, 11, 218-20 (1956)
73. Freyman, J. G., *Cancer Research*, 16, 930-36 (1956)
74. Hoffman, J. G., *The Size and Growth of Tissue Cells* (Charles C Thomas, Publisher, Springfield, Ill., 102 pp., 1953)
75. Stroud, A. N., *Ann. N. Y. Acad. Sci.*, 67, 11-34 (1956)
76. Nakao, Y., *Progress in Radiobiology*, 363-69 (Oliver and Boyd Ltd., London, England, 557 pp., 1956)
77. Hornsey, S., *Exptl. Cell Research*, 11, 340-45 (1956)
78. Pelc, S. R., and Howard, A., *Progress in Radiobiology*, 8-10 (Oliver and Boyd Ltd., London, England, 557 pp., 1956)
79. Fritz-Niggli, H., *Naturwissenschaften*, 43, 112-13 (1956)
80. Hollaender, A., and Stapleton, G. E., *Proc. Internat. Conf. on the Peaceful Uses of Atomic Energy*, 11, 311-14 (United Nations, New York, N. Y., 402 pp., 1956)
81. Hollaender, A., and Kimball, R. F., *Nature*, 177, 726-30 (1956)
82. Gunter, S. E., and Kohn, H. I., *J. Bacteriol.*, 72, 422-28 (1956)
83. Goucher, C. R., Kamei, I., and Kocholaty, W., *Arch. Biochem. Biophys.*, 65, 522-33 (1956)
84. Gunter, S. E., and Kohn, H. I., *J. Bacteriol.*, 71, 124-25 (1956)
85. Gunter, S. E., and Kohn, H. I., *J. Bacteriol.*, 71, 571-81 (1956)
86. Pittman, D. D., *J. Bacteriol.*, 71, 500-1 (1956)
87. Beam, C. A., Mortimer, R. K., Wolfe, R. G., and Tobias, C. A., *Arch. Biochem. Biophys.*, 49, 110-22 (1954)
88. Marcovich, H., *Ann. Inst. Pasteur*, 90, 303-19 (1956)
89. Marcovich, H., *Ann. l'Inst. Pasteur*, 90, 458-81 (1956)
90. Marcovich, H., *Progress in Radiobiology*, 236-40 (Oliver and Boyd Ltd., London, England, 557 pp., 1956)
91. Puck, T. T., and Marcus, P. I., *J. Exptl. Med.*, 103, 653-66 (1956)
92. Gunter, S. E., Kohn, H. I., Tyree, E. B., Laughlin, J. S., Ovadia, J., Shapiro, G., and Thompson, P., *Radiation Research*, 4, 326-38 (1956)
93. Kohn, H. I., and Gunter, S. E., *Radiation Research*, 5, 674-87 (1956)
94. Kohn, H. I., and Gunter, S. E., *Radiation Research*, 5, 688-92 (1956)
95. Owen, M. E., and Mortimer, R. K., *Nature*, 177, 625-26 (1956)

96. Gray, L. H., *The Ciba Foundation Symposium on Ionizing Radiations and Cell Metabolism*, 255-74 (Little, Brown and Company, Boston, Mass., 318 pp., 1956)
97. Schjeide, O. A., Mead, J. F., and Myers, L. S., *Science*, **123**, 1020-22 (1956)
98. Zirkle, R. E., Bloom, W., and Uretz, R. B., *Proc. Internat. Conf. on the Peaceful Uses of Atomic Energy*, **11**, 273-282 (United Nations, New York, N. Y., 402 pp., 1956)
99. Kimball, R. F., and Gaither, N., *Genetics*, **41**, 729-42 (1956)
100. Bachofer, C. S., *Science*, **123**, 139-40 (1956)
101. Elliott, A. M., and Clark, G. M., *J. Protozool.*, **3**, 181-87 (1956)
102. Newcombe, H. B., *Radiation Research*, **5**, 382-89 (1956)
103. Kimball, R. F., Gaither, N., and Wilson, S. M., *Radiation Research*, **5**, 485 (1956)
104. Gwatin, B., and Gottlieb, D., *J. Bacteriol.*, **71**, 328-32 (1956)
105. Bridges, A. E., Olivo, J. P., and Chandler, V. L., *Appl. Microbiol.*, **4**, 147-49 (1956)
106. Pepper, R. E., Buffa, N. T., and Chandler, V. L., *Appl. Microbiol.*, **4**, 149-52 (1956)
107. Koh, W. Y., Morehouse, C. T., and Chandler, V. L., *Appl. Microbiol.*, **4**, 153-55 (1956)
108. Koh, W. Y., Morehouse, C. T., and Chandler, V. L., *Appl. Microbiol.*, **4**, 143-46 (1956)
109. Stapleton, G. E., and Edington, C. W., *Radiation Research*, **5**, 39-45 (1956)
110. Houtermans, T., *Z. Naturforsch.*, **11b**, 636-42 (1956)
111. Wood, T. H., *Radiation Research*, **5**, 602 (1956)
112. Jordan, R. T., and Kempe, L. L., *Proc. Soc. Exptl. Biol. Med.*, **91**, 212-15 (1956)
113. Lauffer, M. A., Trkula, D., and Buzzell, A., *Nature*, **177**, 890 (1956)
114. Jagger, J., and Pollard, E. C., *Radiation Research*, **4**, 1-19 (1956)
115. Powell, W. F., and Pollard, E. C., *Virology*, **2**, 321-36 (1956)
116. Pollard, E., and Setlow, J., *Radiation Research*, **4**, 87-101 (1956)
117. Till, J. E., and Pollard, E. C., *Arch. Biochem. Biophys.*, **63**, 260-62 (1956)
118. Brinton, C., *Progress in Radiobiology*, 373-78 (Oliver and Boyd Ltd., London, England, 557 pp., 1956)
119. Ginoza, W., and Norman, A., *University of California at Los Angeles Report, UCLA-377* (October 3, 1956)
120. Weigle, J. J., and Bertani, G., *Virology*, **2**, 344-55 (1956)
121. Harm, W., *Virology*, **2**, 559-64 (1956)
122. Dulbecco, R., *J. Bacteriol.*, **63**, 199-207 (1952)
123. Gotlieb, T., and Hirst, G. K., *Virology*, **2**, 235-48 (1956)
124. Child, R. G., Moyer, A. W., Pollard, E. C., and Cox, H. R., *Arch. Biochem. Biophys.*, **61**, 291-98 (1956)
125. Davydoff, S., *Comptes rend.*, **243**, 1455-57 (1956)
126. Powers, E. L., and Shefner, D., *Proc. Soc. Exptl. Biol. Med.*, **78**, 493-97 (1951)
127. Spalding, J. F., Langham, W. H., and Anderson, E. C., *Radiation Research*, **4**, 221-27 (1956)
128. Powers, E. L., *U. S. Atomic Energy Commission Report, TID-7512*, 17-29, 416 pp. (1956)
129. Strauss, B. S., Vaharu, T., Frickey, P., and Matheson, J., *Radiation Research*, **5**, 25-38 (1956)
130. Fuerst, C. R., and Stent, G. S., *J. Gen. Physiol.*, **40**, 73-90 (1956)

131. Rubin, B. A., Perry, M. F. C., and Thanassi, F. Z., *Bacteriol. Proc.* 32, (1953)
132. Stent, G. S., and Fuerst, C. R., *Virology*, 2, 737-52 (1956)
133. Stahl, F. W., *Virology*, 2, 206-34 (1956)

CONFERENCES AND THEIR PUBLICATIONS

- Ionizing Radiations and Cell Metabolism (Ciba Foundation, London, England, March 6 to 9, 1956) *Ionizing Radiations and Cell Metabolism* (Wolstenholme, G. E. W., and O'Connor, C. M., Eds., Little, Brown and Co., Boston, Mass., 318 pp., 1956)
- Fourth International Conference on Radiobiology (University of Cambridge, Cambridge, England, August 14 to 17, 1955) *Progress in Radiobiology* (Mitchell, J. S Holmes, B. E., and Smith, C. L., Eds., Oliver and Boyd Ltd., London, England 560 pp., 1956)
- A Conference on Radioactive Isotopes in Agriculture (Argonne National Laboratory and the U. S. Atomic Energy Commission, East Lansing, Michigan, January 12 to 14, 1956) "Radioactive Isotopes in Agriculture," *U. S. Atomic Energy Commission Report, TID-7512* (U. S. Government Printing Office, Washington, D. C., 416 pp., 1956)
- Symposium in Biology, Mutation (Brookhaven National Laboratory and the U. S. Atomic Energy Commission, Upton, New York, June 15 to 17, 1955) "Mutation," *Brookhaven National Laboratory Report, No. 8, BNL-350(C-22)*, (U. S. Department of Commerce, Washington, D. C., 231 pp., 1956)
- Symposium on Structure of Enzymes and Proteins (Oak Ridge National Laboratory and the U. S. Atomic Energy Commission, Gatlinburg, Tennessee, April 4 to 6, 1955) *J. Cellular Comp. Physiol., Suppl.*, 47, 1-286 (1955)
- International Conference on the Peaceful Uses of Atomic Energy (United Nations, Geneva, August 8 to 20, 1955) *Proceedings of the International Conference on the Peaceful Uses of Atomic Energy*, 10, 544 pp., "Radioactive Isotopes and Nuclear Radiations in Medicine," 11, 402 pp., "Biological Effects of Radiation," 12, 553 pp., "Radioactive Isotopes and Ionizing Radiations in Agriculture, Physiology and Biochemistry," (United Nations, New York, N. Y., 1956)
- Conference on Tissue Fine Structure (National Institutes of Health, Harriman, New York, January 16 to 18, 1956) *J. Biophys. Biochem. Cytol., Suppl.*, 2, Part 2, Baltimore, Md., 454 pp. (1956)
- Basic Mechanisms in Radiobiology, IV. Cellular Aspects (National Academy of Sciences, National Research Council, Bear Mountain, New York, May 12 to 14, 1955) "Cellular Aspects of Basic Mechanisms in Radiobiology," Nuclear Science Series Report, No. 18, Publ. No. 450 (Patt, H. M., and Powers, E. L., Eds., National Academy of Sciences, National Research Council, Washington, D. C., 190 pp., 1956)
- Radiation Research Society, Fourth Annual Meeting (Chicago, Illinois, May 17 to 19, 1956) *Radiation Research*, 5, 466-91 and 587-611 (1956)
- Society of Nuclear Medicine, Third Annual Meeting (Salt Lake City, Utah, June 21-23, 1956) *Internat. J. Appl. Radiation and Isotopes*, 1, 123-42 (1956)
- Eighth International Congress of Radiology (Sociedad Mexicana de Radiología, Mexico City, Mexico, July 22 to 28, 1956)

BIOCHEMICAL EFFECTS OF IONIZING RADIATION^{1,2}

BY BARBARA E. HOLMES

Department of Radiotherapy, University of Cambridge, Cambridge, England

The radiation biochemist's obvious aim, to understand the biochemical mechanisms underlying the radiation effects which can be clinically and histologically seen, is still very far from attainment.

The primary event which eventually leads to inhibited growth or to death of the cell can only be guessed at and cause and effect are undoubtedly often confused. Nevertheless, increasing knowledge of the physico-chemical reactions caused by irradiation, as well as accumulating experience of the type of response to be expected in the cell, are gradually changing both the empirical and hit-or-miss nature of the biochemical investigations. The recent realization, for instance, that the presence or absence of oxygen in a system undergoing irradiation is likely to have a profound effect on the final result, is already of great value to radiobiologists. Knowing the important role of oxygen, radiobiologists are able to make a more reasoned judgement when comparing the radiosensitivities of various systems and to have a better basis for the planning of their own experiments.

Because of an obvious practical necessity, increased attention has been given lately to the results of whole body irradiation, including many metabolic effects. Many of these are completely beyond interpretation at present because of the complexity of the systems involved. This is particularly true when supralethal doses are given or when a long interval has elapsed between the irradiation and the collection of experimental data. The observer is faced with the results of endocrine inhibition and stimulation, disorders due to loss of function of particular tissues and other disorders which may be due to death and autolysis of cells in all tissues. Nevertheless, great advances in our knowledge of the effect of irradiation on the haemopoietic system and of protection and the mechanisms of protection against irradiation have been gained by work with whole animals.

In this review it is not possible to include all work on the metabolic effects of whole body or localized irradiation or on the modification of irradiation results by protectors or by oxygen, but an attempt has been made to discuss those papers which give an indication of the biochemical mechanisms directly involved. Such an indication is obviously more easily found when

¹ The review of literature pertaining to this review was completed in December, 1956.

² The following abbreviations are used in this chapter: ATP (Adenosinetriphosphate); BAL (2,3-dimercaptopropanol); DNA (Deoxyribonucleic Acid); DNAP (Deoxyribonucleic Acid Phosphorus); DNP (Deoxyribonucleoprotein); RNA (Ribonucleic Acid); DPN⁺ and DPNH (oxidised and reduced diphosphopyridinenucleotide).

immediate effects rather than only late effects of the irradiation are investigated; in fact, it may be important to detect changes of metabolism which persist only during the time of irradiation and disappear afterwards. Work describing the effects on substances in solution has fortunately been reviewed lately by Collinson & Swallow (1) and only very recent experiments with substances of biological interest need be mentioned here.

The recent review by Gray (2) on cellular radiobiology summarizes much biochemical work. Reviews of work on radiation biochemistry, including recent publications dealing with the inhibition of DNA synthesis by irradiation are included in two recent papers by Hevesy (3, 4). It is therefore only necessary to discuss the very recent work on the nucleic acids in this review.

WHOLE BODY IRRADIATION

Fat Metabolism.—There is considerable confusion in the results obtained by measuring metabolic processes after whole body irradiation. Differences in dose, time interval and in the fed or fasting condition of the animals, alter the results given by different workers.

There is some agreement, however, on the changes produced by irradiation on the fat metabolism of the various tissues. Coniglio, McCormick & Hudson (5), found that incorporation of acetate into the liver fatty acids was increased and into those of the wall of the intestine was decreased after 750r. Goldwater & Entenman (6) found that, with either x-rays or nitrogen mustard treatment, the liver weight, glycogen content and lipogenesis were increased above the normal fasting levels; the serum lipide levels also rose. Morehouse & Searcy (7, 8) also found that irradiation increased the *in vivo* incorporation of acetate into liver fatty acids and glycogen and that, after 1500r given to fasting rats, the phospholipide synthesis rate was doubled and the amount of neutral fat very much increased, while there was a 50 per cent reduction in the incorporation into the phospholipides of the wall of the intestine. It is of particular interest to note that *in vitro* studies supported these findings. The same authors (9) gave di-oleylpalmitin acid labelled with ^{14}C to rats after 1000r to 1500r total body radiation by mouth and found increased retention of material in the stomach and increased amount of unabsorbed material in the intestinal lumen. The decreased incorporation in the intestinal wall, which was found at the same time, they attributed to radiation injury and destruction of cells, since there was at the same time increased incorporation in the phospholipide of the liver. Coniglio, *et al.* (10) using monkeys 12 days, 96 days and 22 days after exposure to 325r, 400r and 650r of whole body irradiation found no defect in absorption and found liver lipide levels to be the same as those of pair-fed controls. The interval between radiation and killing was unusually long and probably accounts for the difference between these results and others which have been quoted.

Gould (11) found that 24 hours after a dose of 2400r given to the whole animal, cholesterol synthesis in the liver was ten times higher and 48 hours

after was twenty-five times higher than in unirradiated controls. The effect of the irradiation was not immediately visible. The rate of synthesis was measured by ^{14}C acetate and was shown not to be due simply to acetate diversion. In most tissues the rate of synthesis was unchanged and in the spleen it was lower than in the control. Gould, Bell & Lilley (12) found that while the normal rate of cholesterol synthesis was diminished by adrenalectomy, the rise in rate produced by irradiation was not. The authors found a decreased amount of cholesterol in the liver in spite of the high rate of synthesis and considered that irradiation must have increased the turnover rate of the cholesterol. This conclusion was supported by the increased rate of disappearance of cholesterol which had been labelled with ^{14}C some days before the irradiation. Fatty acid synthesis was also increased.

Popjak (13) showed that irradiation *in vitro* of liver slices produced an immediate accelerating effect on the synthesis of fatty acid and cholesterol from ^{14}C acetate. The effect was more marked in slices from foetal liver, which has a higher metabolic rate, than in slices from adult liver. The slices were irradiated in air and at room temperature.

Hevesy & Forssberg (3) pointed out that there is an increase in serum lipoproteins after irradiation and that, in samples taken 30 hr. after whole body irradiation, there was excellent correlation between the raised lipoprotein levels and the subsequent death of the animal.

Bernheim, Ottolenghi & Wilbur (14) found that there was an increase in the linoleic, linolenic, and total fat content in the bone marrow of rabbits after irradiation. They also showed a strange change of properties of the bone marrow homogenates. Homogenates from normal rabbits do not form fatty acid peroxides as do those from some other tissues; moreover they inhibit peroxide formation in liver homogenates and protect succinoxidase against fatty peroxides. They appear to contain, therefore, an antioxidant and a protective compound, perhaps sulphhydryl-containing. Homogenates made from bone marrow taken 48 hr. after irradiation of the whole rabbit with 1400r, contain some fatty acid peroxide and form more on incubation. After 800r they are less effective in protecting succinoxidase against these peroxides. There is, of course, a possibility that these effects may be the result of changes in cell population.

An excellent summary of work dealing with the effect of irradiation on fats and lipides *in vivo* and *in vitro* was given in a paper of Chevallier & Burg (15).

Carbohydrate metabolism.—Some work has been carried out on the effect of whole body irradiation on liver glycogen and blood sugar levels.

These experiments are not easy to interpret, as the results obviously depend a great deal on direct or indirect stimulation of the pituitary glands and pancreas. A paper by McKee & Brin (16) in which they describe the effect of irradiating fasted rats with doses up to 1500r x-rays illustrates this point well. For a time, the liver glycogen content fell in both irradiated and normal rats, but 50 hr. after irradiation it rose to a considerable peak in the

exposed rats and fell to a very low level at 75 to 80 hours after. Even small doses (250r) were to some extent effective. These results of irradiation were not found in adrenalectomized or hypophysectomized rats. In a parabiont pair, of which one was irradiated, this one gave the usual result and the unirradiated partner showed a smaller but definite effect.

Hevesy (3) points out that experiments (except those with very large doses) have, at least, shown that the livers of irradiated rats are capable of accumulating glycogen. He quotes a number of authors, including fairly recent papers of Loureau (17) and Fischer (18).

Sherman & Dwyer (19) gave a dose of 600r to the whole body of fed mice. A rise in blood sugar levels was found shortly after irradiation. This agreed with earlier work of Thompson & Steadman (20). A rise in the content of sugar and glycogen (glycogen soluble in cold trichloroacetic acid) in the liver was also found, especially at 30 to 60 minutes after irradiation.

Keilina (21) studied glycogen metabolism of rat livers two days after 500r of x-ray irradiation and decided glycogen was broken down mostly by "hydrolysis" whereas, in normal livers, it was broken down by phosphorolysis. The work of Perkinson & Irving (22) may agree with this. They gave what may be considered as whole body irradiation to rats by injecting them with 5 μ c. of ^{32}P per gr. of body weight and investigating the metabolism of the liver from two hours after injection. At 24 hours after injection respiration was reduced by 35 per cent and anaerobic glycolysis by 50 per cent in excised liver tissue.

Hevesy & Forssberg (24) found that when labelled glucose was given just before irradiation there was a 20 per cent depression of the usual output of $^{14}CO_2$. Thus the changes in liver glycogen found after irradiation may, perhaps, be to some extent due to changes in the metabolic activities of the liver itself.

Loureau-Pitres (25) has suggested that part of the extra formation of glycogen found in the irradiated animal may come from the products of protein metabolism, which has been found to be accelerated by exposure to x-rays. Kay, Harris & Entenman (26) noticed that 24 hours after 450r or 2500r x-rays, the plasma level of nonglycogenic amino acids was increased, but not the level of glycogenic amino acids; the content of liver glycogen was high and the glycogenic amino acids had presumably been used for synthesis.

Tissue proteins.—It is generally accepted that irradiation of the whole body of an animal leads to protein breakdown and often to appearance of the breakdown products in the serum and urine. That this may represent the death and autolysis of protein in sensitive tissues has now been more definitely shown by Altman, and his co-workers (27) who gave ^{14}C glycine to animals before an LD₅₀ dose of x-rays and followed the tissue glycine content and labelling and urinary hippuric acid labelling for two days after irradiation. Their data indicated a ten-fold increase in protein breakdown when compared with controls. Correlation of the specific activity of hippuric acid glycine with that of the tissue glycine suggested that labelled

glycine is transported from the sensitive tissues to the liver and that endogenous glycine synthesis in the liver is inhibited after irradiation.

Kay *et al.* (28) showed an increase in the excretion of taurine, sulfate, and urea after small doses of irradiation in rats. The effect could be seen with 75r and increased up to 250r but with higher doses increased no further. This confirmed the results of Hempelmann, Lisco & Hoffman (29) who found excretion of taurine after as little as 35r in human cases. Kay *et al.* followed the hourly taurine and urine excretion curve after irradiation with 600r and found that the increase was definite after 3 hr. and reached its peak at 5 hr. when it was nearly four times as great as in control animals. The excretion rate then fell rapidly. The increase in urea and sulfate excretion during the first 24 hours can be prevented by adrenalectomy but this does not affect the excretion of taurine, which probably, therefore, comes from another source. The fact that the maximum excretion was achieved with doses below the fatal level suggests that the substance of origin was, in a sense, expendable. It is also possible that in losing this sulfur-containing substance, the animals lost something that could have been a protective substance.

Other irradiation results suggest changes in the proteins circulating in the blood. Winkler & Paschke (30) found that doses of 400r and over caused a decrease γ -globulin level in rat serum; larger doses gave an earlier and more marked effect. Leone (31) examined the sera of chickens by turbidimetric precipitative tests with antisera prepared in rabbits. After a dose of 990r (approximately the LD₅₀ dose) there appeared to be an actual qualitative change in the β -globulin fraction and an increase in the amount of albumin. An attempt to find a change in the synthesis of the proteins by examining liver fractions was not successful, and experiments designed to test for auto-antibodies by adding plasma from irradiated birds to chick tissues in culture, gave inconsistent results. Fricke, Leone & Landman (32) after irradiating ovalbumin *in vitro* with large doses found that their serological data suggested the formation of new molecular species and not only a destruction of antigenic sites. In an anaphylactic test, with a challenging dose of 1.0 mg. of native ovalbumin, a medium sensitizing dose was 2 μ gr. of the native protein but only 0.05 μ gr. of protein, which had been irradiated in air-saturated solution. The clotting power of fibrinogen seems also to be impaired by irradiation. Smith & Lewis (33) showed a marked delay in the clotting time of withdrawn rat and hamster peritoneal fluid when the animals had been exposed to a dose of 600r. The delay appeared one day after irradiation and persisted for some time. The addition of a small amount of protamine sulfate resulted in the immediate appearance of fibrin strands, which suggested that the delay was due to a heparin-like substance. Rieser (34) and Rieser & Rutman (35) irradiated solutions of fibrinogen *in vitro* and found a clotting delay with small doses of x-rays. A linear relationship was obtained with doses of 25r to 500r. The effect could be overcome by increasing considerably the amount of thrombin used to produce the clot, but there appeared to be a decreased amount of normally activated fibrino-

gen. The amount of peptide liberated on clotting was 30 per cent less than normal, although the amount of clottable protein was the same. The presence of cysteine or glutathione during irradiation did not protect the fibrinogen and themselves delayed clotting. The authors suggested that this irradiation effect, interesting because of the small doses involved, was not due to the oxidation of sulphydryl groups. They suggested that such a group might be concerned in the actual polymerization, since cysteine, glutathione, and thiourea did protect fibrinogen against the loss of ability to clot at all, even with thrombin addition. This effect needed very large irradiation doses and was demonstrated by Scheraga & Nims (36).

Ascorbic acid of tissues, water and salt balance.—Studies on the ascorbic acid content of the tissues after whole body irradiation have been made by various authors. Klein, Handen & Swick (37, 38) found no change within the first 72 hours after 600r of x-rays in the ascorbic content of rat liver, brain, pancreas, muscle, or kidney. There was a fall in concentration in the thymus, lymph nodes and spleen which was definite 4 hr. after irradiation and marked at 27 hours after. The depletion in ascorbic acid shown by these tissues was very nearly as great after 300r. The authors found that it was related to weight changes in the tissues and considered that it might be due to a change in cell populations. The intestinal mucosa of the rats showed a sharp rise in ascorbic content 4 hr. after irradiation of the animal; the level then fell slowly but was still high at 24 hours. The changes were not accounted for by hydration of the tissues.

Considerable attention has been given to loss of ascorbic acid from the suprarenals themselves. Wexler, Pencharz & Thomas (39) show that half-body irradiation of rats with 625r caused a bigger depletion, followed by a more rapid repletion, of adrenal ascorbic acid than when the irradiation was given to the whole body. Whole body irradiation they therefore considered as giving so extreme an effect that the fullest reaction could not take place. Nims & Geisseloder (40) found that whole body irradiation caused adrenal hypertrophy (this was indirect and due to starvation) and a decrease in adrenal ascorbic acid and cholesterol. They considered that irradiation stimulated the pituitary-adrenal system. Bacq, Fischer & Beaumariage (41) showed that morphine and nembutal, used as inhibitors of the pituitary-adrenal response to stress, could inhibit this early fall in ascorbic acid and cholesterol after a lethal dose of x-rays, but could not prolong life. Cysteamine, a protector against radiation, could not inhibit the early fall of cholesterol, but prevented the later fall in cholesterol and ascorbic acid level of the adrenals and caused the animals to survive. Bacq, Martinovitch *et al.* (42) also showed that newborn rats, which did not show a fall in adrenal ascorbic acid in response to adrenalin or cold, also showed no fall after irradiation.

The work of Nims & Sutton (43) demonstrated once more the complexity of the effects of whole body irradiation. They showed responses which are partly due to fasting and partly due to stimulation of the pituitary-

adrenal system. To this stimulation are attributed the early increase in water uptake and decrease in adrenal cholesterol. Fasting for two days can, by itself, cause changes in water consumption and liver glycogen levels, but these do not take place in hypophysectomized rats. Smith & Tyree (44) also showed that the polydipsia which is found immediately after irradiation is prevented by previous adrenalectomy.

The early polydipsia produced by irradiating the whole body is also mentioned by Edelman (45) who found an accompanying increase in excretion of Na, K, and Cl. Glenn & Boss (46) did not find any change in Na excretion or Na serum level for the first 96 hours after a dose of 500r or 1000r. There was, however, a significant and real loss of K through the kidney on the first day after 500 to 1000r units. Serum K levels were high during the first 24 hours, especially at 2 hr. after irradiation. The electrolyte metabolism of rats after irradiation with 700r was also investigated by Caster & Armstrong (47) who found that, within the first 3 to 12 hr. there was a movement of tissue chloride, acid and water into the gastric contents. Four days after irradiation the plasma chloride became high and the total-body chloride balance became negative. Changes in tissue potassium varied with the sensitivity of the tissue but the total body potassium loss was directly correlated with loss of muscle mass.

Intense local irradiation to the limbs (up to 79,000r units) led to extra-cellular edema in the muscles but not to loss of K per unit dry weight. The muscles were not subjected to great activity but could still function up to 22 hr. after the exposure. [Wilde & Sheppard (48).]

Bruce & Stannard (49) found that, in yeast, 60,000r of x-ray irradiation lessened K uptake and increased the leakage. When the yeast was placed in solutions containing two and three carbon members of the glycolytic cycle the leakage was increased.

Prodi & Miceli (50) found that intradermally injected India ink or diphtheria toxin spread with unusual rapidity through the skin immediately after it had been exposed to 500r or more. The authors consider this to be due to a change in the hyaluronic acid in the skin.

Haemoglobin formation.—The sensitivity of the blood forming tissues to irradiations has long been recognized and the fact that the destruction of the cells of the marrow and spleen is one of the chief causes of death in the animal. The use of ^{59}Fe as a detector of haemoglobin formation has given a clear picture of the post irradiation events. Hennessey & Huff (51) found that the injection of ^{59}Fe was a sensitive indicator of damage to the bone marrow. They measured the labelling of red blood cells in control and irradiated animals. By putting in the iron at various intervals after irradiation they found that little immediate effect could be found, but that after 24 hr. even doses of 5r and 25r could be shown to have decreased the labelling.

Belcher, Gilbert & Lamerton (52) also showed that the uptake of iron by red blood cells was reduced by irradiation, particularly if the ^{59}Fe was injected 24 or 48 hours after the irradiation. They could show an effect of

50r at 24 hours and after 100r inhibition was nearly complete at this time. Baxter, *et al.*, (53) were able to demonstrate by ^{59}Fe labelling, the part played by the spleen in recovery after irradiation. Belcher, Harriss & Lamerton (54) showed depression of ^{59}Fe uptake in the blood forming tissues of rats by 450r units of whole body irradiation. The uptake of storage iron into the liver is not depressed, which is in agreement with the work of Giuliano, mentioned below. Shielding of one hind limb reduces the effect of the irradiation on haemoglobin formation and allows the spleen to become active again at an earlier time after the irradiation.

Gilbert, Paterson & Haigh (55) used ^{59}Fe to study the life cycle of red blood cells in the monkey. The red blood cells had a finite life span of about 100 days; doses LD₅₀ levels do not seem to affect this life span of cells in circulation although they almost completely inhibit erythropoiesis. ^{59}Fe from the labelled cells passed into the plasma at the end of their life span. The peak of radioactivity in the plasma was at about 100 days after the labelling injection of the iron in both control and irradiated animals, although the amount of radioactivity was much smaller in the latter.

Giuliano (56) used plasma taken from a rabbit which had been injected with inorganic iron one hour before as a source of protein-bound "transferrin" iron. When this was injected intravenously into another rabbit it disappeared from the plasma with a half-value time of 2 hr. Irradiation of the rabbit with 800r of x-rays depressed the rate at which "transferrin" iron left the plasma, probably because haemoglobin formation had been partly inhibited. When inorganic iron, which is probably stored and not converted directly into haemoglobin, is injected intravenously, about 70 per cent to 80 per cent is lost from the plasma in one minute. This rapid disappearance is not affected by x-rays. Bonnichsen & Hevesy (57) found that the effect on "transferrin" iron was much more marked when it was injected two days after the irradiation than when it was injected within half an hour. They interpreted this as indicating that red corpuscles already in advanced stages of maturation can complete their haemoglobin content even after exposure to x-rays (to which they are very resistant) and can pass out into the circulation. The formation of new cells by mitosis is prevented and the further formation of haemoglobin is thus strongly inhibited; many of the marrow cells are actually destroyed and one day after irradiation the total number of marrow cells may be reduced to one half of its normal value.

The formation of haemoglobin is thus very definitely connected with cell division. The formation of cytochrome-*b* and catalase in the liver [Hevesy & Bonnichsen (58)] was not affected by x-rays, while that of myoglobin was reduced to a half between 6 to 18 hr. after 1400r. Since haem formation as such had proved to be not very sensitive to x-rays, this suggested that myoglobin synthesis might also be connected with cell division. This is discussed further by Hevesy (3, 4) and by Bonnichsen, Hevesy & Akeson (59) who point out that one dividing cell in 3,000,000 cells could provide the amount of new myoglobin observed.

Other workers quoted by Hevesy have seen that, after irradiation, red cells leak into tissue interspaces and into the lymph where they are probably destroyed. Fedorov (60) demonstrated increased destruction of haemoglobin, by making an anastomosis between the gallbladder and the ureter in dogs and finding out an increase in tetra-pyrro-bilirubin excretion starting two days after whole body irradiation of 200 to 400r.

These experiments on haemopoiesis demonstrate the necessity, in radio-biochemical work, of looking for immediate as well as late effects. What might have been taken to be an inhibition of haemoglobin formation proved to be, in fact, an inhibition of blood-cell formation. This is demonstrated also by work with bone marrow *in vitro*. Lajtha & Suit (61) and Suit, *et al.*, (62) have shown that doses of 300r to 5000r given to human bone marrow in culture, do not inhibit the uptake of ^{59}Fe . This was demonstrated by autoradiographic methods. The iron uptake, which *in vitro* took place mainly in the early normoblasts, was compared in the irradiated and control cultures in the first 6 or 8 hr. after irradiation and, in another series, during the first 24 hours after irradiation. Only cells which had survived the irradiation were, of course, included and many of these must have been fatally damaged and likely to die within a day or two, but in the survivors the uptake of ^{59}Fe was normal. The same result was obtained when 1000r was delivered to a field immediately above the manubrium just before the manubrium marrow was collected for culture, or when 100r whole body irradiation was given one to four days before collecting the marrow. When the ^{59}Fe was given *in vivo* 24 to 72 hr. (but not when given immediately) after 100r whole body irradiation there was delay in the appearance of the iron in the circulating erythrocytes.

EFFECTS ON ENZYMES

The determination of the response of cellular enzymes to irradiation has proved a difficult matter. Dale (63, 64) has carried out many observations on the irradiation of enzymes in solution and their protection by other dissolved substances and has established fundamental facts concerning the response of enzymes as such. He (65) has pointed out the difficulties of applying this knowledge to a consideration of what happens *in vivo* and entered a plea for thinking particularly of the effects on the enzyme systems actually at work in the cell at the time of irradiation. The total amount of enzyme in a cell might be greater than the part of it which was active at any moment; an irradiation effect on a small active part might well be missed in an estimation of the total activity extractable from the cell. Geographical distribution of enzymes and protective substances might also cause inequalities in sensitivity. An irradiation effect on an enzyme system during activity might alter reaction velocities and upset the sequence of metabolic steps and the steady state of the concentration of reacting substances which has been established in the cell.

Krebs (66) pointed out that the "pacemaker" reactions, which control

the rates of metabolic processes, were more vulnerable than others to interference by extraneous agents because the enzymes responsible for them must work at full capacity under physiological conditions. Any change in the "pacemaker" reaction would alter the steady-state level of intermediate metabolites. A few examples of such alterations will be mentioned later in this section. As a general rule such an alteration might be temporary and the metabolism would revert to its normal course when the irradiation was over, but it is possible that the accumulation or lack of a given intermediate might have a harmful effect on the cell which would not be put right so quickly.

Okada & Fletcher (67) suggested the possibility of an amplification of radiation effects, through the action of the irradiation on one or more parts of a chain of enzyme reactions in which, for instance, the product of one system serves as the substrate for the next. They cited the aldolase-phosphoglyceraldehyde system. In a personal communication, Dr. Okada pointed out that, where a system containing many enzymes and co-factors is concerned, an almost undetectable inactivation of each enzyme considered separately, could lead to a large decrease in the amount of the final product.

An interesting example of the effect of geographical distribution on enzyme sensitivity was given by Cotzias (68) who found that the irradiation dose-activity curve of cholinesterase from various tissues suggested the presence of a more and a less sensitive fraction of the enzyme. Ultracentrifugation gave quantitatively the same fractionation, the part of enzyme attached to particles being less sensitive, in fact behaving like a dry enzyme. The author was able to use this technique to decide the degree of dryness and wetness of enzymes within the cell and found that, with some enzymes, a large fraction appeared to be out of contact with water and a smaller fraction wet.

The estimation of enzyme activities in irradiated tissues has often shown a rise in activity, at least as a first effect. Pirie (69) in her extremely useful summary of the effect of irradiation of tissue enzymes, mentioned several examples of this rise. Another recently discovered instance was an increase in glucose-6-phosphate activity after irradiation of exteriorized salivary glands [English (70)]. Feinstein (71), himself using phospho-protein phosphatase as a test object (but quoting many other examples from the literature) showed that the apparent increase in activity of the enzyme was due to loss of organ weight, in the case of the spleen, or of protein content of the tissue, as in the case of the intestine. The calculations were based on the wet weight or on the protein content of the tissue.

These tissue changes may be due to the effect of whole body irradiation and are not always found on local irradiation of the tissue itself. Petersen, Fitch & Dubois (72) showed that local irradiation of the spleen with 800r, with the rest of the body shielded, prevented the large increase (already noticeable at 6 hr. after irradiation and marked after 72 hr.) found in the activity of spleen adenosinetriphosphatase and β -nucleotidase after whole

body radiation. Loss of DNA phosphorus was also found to be slight 24 hours after local irradiation but to be about 44 per cent of the total after whole body irradiation and the histological changes after 800r locally, resembled those caused by 100r to the whole body; the spleen and the rest of the body could be irradiated separately with a 12 hr. interval between them and the still give a result like the whole body irradiation. The authors do not believe that the differences are caused entirely by uninjured cells from outside wandering into the spleen after local irradiation. Boiron, Paoletti & Tubiana (73) who carried out similar experiments using 1000r, found that the loss of weight and change of histological appearance of the spleen was much less after local irradiation only.

Petersen *et al.* also found that the inhibition of citrate synthesis (as demonstrated by estimation of fluorocitrate after the injection of fluoracetate) did not occur when the irradiation was restricted to the spleen only, although after whole body irradiation Dubois, Cochran & Doull (74) had obtained a marked inhibitory effect.

Another example of a generalized effect of whole body irradiation on enzyme activity is given by the work of Brin & McKee (75), who showed that irradiation raised the transaminase activity of the liver. Transaminase activity was also increased by starvation (often found after irradiation) and by cortisone and nitrogen mustard injection.

Whole body irradiation with 600r had no effect on the adenosine deaminase or nucleoside phosphorylase during the first ten days after irradiation [Eichel (76)].

Weiss & Tabachnik (77) gave a large dose (6800 rep) of β -radiation to the skin and found no change in the phosphatase, ribonuclease or even deoxyribonuclease during the first 40 days after the irradiation.

The increase in deoxyribonuclease after irradiation is often much greater than the nonspecific enzyme increases, which have just been discussed.

Kowlessar, Altman & Hempelmann (78, 79) showed an increased urinary excretion and plasma concentration of both deoxyribonuclease enzymes after irradiation with 700r. Deoxyribonuclease I (pH optimum at 7.5) had already increased ten times in the serum at 18 hours after irradiation. The authors believe that these enzymes came from the irradiated cells, but suggested that changes in the natural enzyme inhibitors must also be considered.

Bacq & Errera (80) developed the "enzyme release theory" of radiation effects on cells. They considered that enzymes which are attached to structures in the cell (deoxyribonuclease being mainly attached to the mitochondria) might pass into solution if the structure was broken down by the irradiation and attack their substrates in different parts of the cell. deoxyribonuclease might thus be able to penetrate the nucleus (perhaps particularly the irradiated nucleus) and attack the DNA. Goutier-Pirotte & Thonnard (81) and Goutier-Pirotte & Oth (82) demonstrated that, within half an hour of irradiation, an increased proportion of the deoxyribonuclease had passed into the supernatant fraction in centrifuged cell preparations.

Future work on the action of irradiation on the deoxynucleoproteins in the cell will have to decide which effects are attributable to deoxyribonuclease activity and which to more direct action.

In the spleen and thymus (though not in the liver and kidney) of rats which had received an LD₅₀ x-ray dose, an increase in deoxyribonuclease II activity per wet weight and a fall in DNA content was found by Gordon, Okada & Hempelman (83). One day after the irradiation acid soluble substances giving the Dische reaction and thought to be deoxypentose derivatives were found in the tissues. The fall in DNA content was thought by the authors to be due to decreased synthesis and to increased destruction by the enzyme (full papers in press in the *Archives of Biochemistry and Biophysics*).

The increased activity of deoxyribonuclease must also be considered when preparations of deoxynucleoprotein are being made from irradiated cells. There is always danger of enzyme contamination of the product.

It should be noted that irradiated silkworm eggs could induce genetic changes in sperm cells which were introduced 2 to 4 hr. after the irradiation [Nakao (84)].

Some inhibitory effects of irradiation on metabolic processes can be shown. An inhibition of methionine uptake into the nuclei of the columnar epithelium of the trachea of mice 16 and 24 hr. after whole body irradiation with 200 or 1000r, was demonstrated by Pelc (85) using radioautographic methods. Neither the observed nuclear uptake of labelled methionine nor the effect of the x-rays upon it was connected with mitosis.

Burn, Kordik & Mole (86) found an increased sensitivity to acetylcholine and a slight fall in pseudo-cholinesterase in isolated loops of gut taken from rats 24 hr. after a dose of 1000r.

Pirie was able to demonstrate that irradiation, given to one eye only, caused a fall in glutathione content, in the activity of glutathione reductase and in the protein content of the lens long before any clinical signs of cataract were visible [Pirie, van Heyningen & Boag (87), Pirie (88)]. With very young rabbits a fall in reduced glutathione content could be seen after two or three days.

Another interesting result of a strictly localized irradiation was the loss of alkaline phosphatase from mouse bone demonstrated by Woodard & Spiers (89). No detectable loss occurred *in vitro* after 20,000r, but *in vivo* all doses from 900 to 2500r, caused a fall in activity detectable after 24 hr. and maximal after 12 to 25 days. Wilson (90) followed the uptake of ³²P into the bone of six-week-old mice, and considered that the depression of uptake, which appeared a week after irradiation with 2000r, depended on the death of the cells, particularly the osteoblasts and reflected a depression of alkaline phosphatase content of the bone.

To determine the action of irradiation on cell enzymes themselves it is necessary to make observations immediately after irradiation. Any effects which develop only after a time interval are likely to be secondary to other

destructive processes going on in the cell. This was well brought out by Pirie (69) who discussed radiation effects on many cellular enzymes *in situ*.

When this restriction is observed, it is usually found that any inhibitory effect of x-rays on the glycolytic or oxidative enzymes of the cell requires doses so large compared to the lethal dose for the cell, that it is difficult to imagine that destruction of these enzymes plays a causative part in cell death.

This is, perhaps, partly because we know most about the lethality of x-rays to specially sensitive cells like lymphocytes and thymocytes (which are easily destroyed by various agents) or to cells undergoing mitosis. Cells in division have a specially radiosensitive mechanism concerned with the reduplication of their nuclear material; the dose required to kill cells in a nondividing tissue in sufficient numbers for us to notice the destruction, is probably much nearer than which could be expected to show an effect on their general metabolism. (That a few cells in a nondividing tissue are killed by moderate doses was demonstrated by Nagai, *et al.* (91) who found cell fragments and pyknotic nuclei in adult mouse liver 6 hr. after 600r total body irradiation).

Where enzymes are freely distributed about the cell, our chance of seeing an irradiation effect from a small dose is slight. When they are organized in a system like the mitochondria we might hope to see the effects of disorganizing this particle, even when the individual enzymes, tested separately and with cofactors duly supplied in the reaction mixture, show no appreciable loss of activity. van Bekkum, Jongepier, *et al.* (92) gave a dose of 1100r whole body irradiation to rats, killed them 4 hr. later and prepared the mitochondria from the spleen. They were able to show that the respiration of the mitochondria was somewhat depressed and the phosphate uptake considerably more so when succinate was used as substrate. The oxidative phosphorylation brought about by the mitochondria was definitely depressed. Van Bekkum and collaborators carried out a series of experiments which have been summarized by van Bekkum (93) recently. Four hours after the dose given in the first experiments many dead and degenerating cells were already present in the spleen. With a dose of 700r, nuclear degeneration was obvious in a few cells after 1 hr., whereas no change in oxidative phosphorylation was definite until after 2 hr. Diminution of mitotic frequency was seen after 15 min. On the other hand, at 2 hr., the percentage inhibition of oxidative phosphorylation in mitochondria and the percentage of cells, showing nuclear degeneration was much the same.

In less radiosensitive tissues, such as liver, mouse tumors, and regenerating liver, much greater doses fail to produce this mitochondrial change after a 4 hr. interval. Localized irradiation to the spleen is as effective as whole body irradiation as regards mitochondrial oxidative phosphorylation.

The mitochondrial experiments with succinate were usually done in the presence of added adenylic acid and cytochrome-c. Omission of cytochrome-c caused a 50 per cent fall in both phosphate and oxygen uptake in the

control preparations, whereas in the irradiated preparations the fall was much greater, particularly four hours after the irradiation, when the phosphate uptake was particularly low. This marked cytochrome-*c* deficiency of the irradiated particles may have been due to a leakage or may have been caused by a radiation-induced alteration in the cytochrome.

Goldfeder (94) isolated liver mitochondria after medium doses of x-rays to the whole body in mice. She found a decrease in ATP synthesis in the mitochondria from male but not from female mice. The fall in P/O ratio was less in the mitochondria from female mice than in those from the males. The actual interval between irradiation and death of mice after a dose of 700r was longer in the females.

Isolated mitochondria present a quite different irradiation problem. Van Bekkum found that he could not reproduce his results on isolated mitochondria even with 20,000r. Ord & Stocken (95) found that 960r, given under well oxygenated conditions, had no immediate effect on oxidative phosphorylation. The mitochondria were prepared in 0.25M sucrose and cytochrome-*c*, ATP, glucose, hexokinase, and succinate as substrate were added to the reaction mixture, and were present during irradiation.

Van Bekkum also irradiated the mitochondria in a well-oxygenated medium containing cytochrome-*c*, adenylic acid, glucose, hexokinase, ethylene-diamine tetracetate, and succinate as substrate; the particles were kept on ice for 4 hr. before testing.

It is extremely difficult to reconcile these results with those of Fritz-Niggli (96, 97) who found that, with mitochondria prepared in 5.75 per cent mannitol, an effect on the oxygen uptake with pyruvate, α keto glutarate, fumarate and citrate was produced by irradiating the mitochondrial suspension with doses as low as 50r. If the irradiation was given when the mitochondria were suspended in a 2.88 per cent mannitol and K phosphate buffer mixture they were much more sensitive and, with citrate as substrate, oxidation was inhibited with 0.1r. This inhibition was obvious 30 and 60 min. after irradiation and was apparently as great with 0.1r as with 50r, but was not obtained when succinate was used as substrate. Cytochrome was not added to the reaction mixture during the respiration measurements; ATP, citrate and MgSO₄ were added, but not until after the irradiation was completed.

Fritz-Niggli found that succinate oxidation was not so sensitive and that definite results were not obtained with 50r. Succinate oxidation is known not to be so much affected as the other enzymes by injury to the structure of the mitochondria and she suggested that the small doses of x-rays might have produced their inhibiting effect by inducing alterations in this structure. The mannitol protection is certainly unlike ordinary chemical protection against x-rays in that its protective power fell so abruptly when the 5.75 per cent solution was diluted to 2.88 per cent, which is not a very weak solution. The mitochondria appeared unaltered after the irradiation, however, and it still remains difficult to account for the extreme difference in

sensitivity shown by her experiments and those of other authors, even though they were using succinate as substrate. In Fritz-Niggli's experiments there were no substrates present during irradiation, but the mitochondria were kept cold.

We know something of irradiation effects on other steps of the Krebs cycle and respiratory carrier systems. Gardella & Lichtler (98) showed that coenzyme A activity was not affected by 10,000r given to Yoshida tumor cells *in vitro* and no change could be found 8 hr. after giving 1600r total body irradiation to the animal.

Mee & Stein (99) showed that when cytochrome-c was irradiated in the absence of oxygen and in the presence of alcohols or hydrogen an unusual reduction product was formed which could not function in the respiratory chain. In the presence of benzoate or succinate the normally occurring reduction product only was formed, even when the x-ray dose was much increased. Laser (100) showed that ferri-cytochrome-c was first reduced by irradiation and, on readmission of air after the irradiation, was oxidized to a green product which could not be reduced by the usual enzymes. Barron & Talmadge (101) showed the reduction of ferri-cytochrome-c by irradiation in the absence of air was increased by iso-citrate, lactate, pyruvate, alamine, and malate. Once again an unusual product was formed which they suggested might be oxyporphyrin. Succinate and alpha ketoglutarate had no effect on the yield of the unnatural product; glucose, glucose-6-phosphate, and butyrate inhibited it.

Swallow (102) showed that coenzyme I (DPN^+) was hardly affected by x-irradiation in the absence of oxygen unless alcohol or one of several other substrates was present, in which case it was reduced to a form which could not react with the usual enzyme systems; this reduced form was thought to be a dimer.

It is plain that, although changes which give a certain percentage of inactivation can be produced in the respiratory carriers, the doses required are very great and can probably not account for inhibition of the respiratory or phosphorylating systems of the mitochondria which have been described.

Another case of producing an effect (this time in the opposite sense) on an enzyme by irradiation of the larger structure to which it is bound, is described by Aronson, Fraser & Smith (103). They irradiated yeast and found, after a few hours irradiation, a sevenfold increase of catalase activity. The calculated sensitive volume corresponded to a molecule of weight between 1.5 and 2 million and the authors suggested that the catalase was released from association with this large particle by the irradiation. Further irradiation of such an activated enzyme suggested that its molecule weight was now about 250,000, which agrees with the known molecular weight of other catalases. The enzyme was now more easily inactivated by heat and the activation energies for the catalase — H_2O_2 reaction were lower.

The idea that the effects of irradiation on systems in a steady-state condition might be investigated by detecting changes during irradiation, or by

preventing further reaction of the system directly the irradiation has been completed, has not yet been pursued by many experimenters. The work of Hug & Wolf (104) with luminescent bacteria gives an extremely interesting example of the possibilities of this approach. *Achromobacter fischeri* was cultivated and irradiated when the emitted light intensity had remained at a constant level for several hours. This implied that luciferin was being produced at the same rate as it was undergoing irreversible oxidation. Light intensity was reduced immediately irradiation was begun; light emission stopped altogether after a time, depending on the dose rate. If irradiation was stopped before the light intensity reached zero, the intensity began to rise again immediately, reaching a new level which was below the original one. The intensity at which this new level is established had an exponential relationship to the x-ray dose; the mean recovery time after any dose was of the order of minutes. The irradiation thus appears to have two effects on light emission, one is irreversible and the other, which seems to have the higher hit probability, is completely reversible. Bacteria in a nonnutritive medium do not show this recovery from irradiation and are known not to be able to form their light-producing matter. The irreversible effect which leads to the final lowering of light intensity was probably due to the destruction of an enzyme.

Strehler, *et al.* (105) suggested the possibility that bacterial luciferin might be reduced flavine mononucleotide. In *Achromobacter* extracts, functioning without the addition of DPNH, either reduced riboflavin or reduced flavine mononucleotide will support luminescence. The presence of oxidized riboflavin actually inhibited luminescence of bacterial extracts when DPNH was added. The authors suggested that it might act as a competitor inhibiting the reduction of the flavin mononucleotide. It seems possible, therefore, that the reversible inhibition of luminescence found by Hug might be due to the formation of (or failure to remove) some such oxidized inhibitor through the action of the radiation, or to a lowering of the amount of reduced as compared with oxidized DPN or to any such change, brought about by oxidizing radicals, which might tend to inhibit the reduction of flavin mononucleotide. A certain amount of color is given to these suggestions by the work of Tahmisan & Wright (106) who irradiated grasshopper eggs and killed them by bringing them into contact with boiling water. Eggs killed while actually under the x-ray beam showed a DPN/DPNH ratio higher than in the controls. If they were killed a few minutes after irradiation had ceased, the ratio was still high but was falling.

What may be a curious example of changes which disappear shortly after radiation ceases is given by the formation of methaemoglobin by irradiation. Dowlen & Walker (107) gave whole body irradiation to rats and took samples of blood from the tail during the irradiation. By the time the irradiation dose had reached 6000r the percentage of methaemoglobin in the blood was about seven. The irradiation was then stopped and another sample taken one hour later, by which time the methaemoglobin level was prac-

tically normal. The oxidation was presumably not enzymic and could be obtained in irradiated haemoglobin solutions, whereas the rereduction must have been so. Klein (108) irradiated rats with 5000r, anaesthetised the animal directly after the irradiation was over and took blood from the heart. The blood was kept cold until fractionation with ammonium sulfate was complete. No methaemoglobin was found.

Höhne and his co-workers (109) showed inhibitory effects of 20,000r on anaerobic and aerobic glycolysis and smaller effects on respiration. They attempted to find the actual site of the irradiation block by determining the steady state concentration of metabolites. Perchloric acid was added to the cells after 60 min. measurement of their metabolism in glucose. When compared with normal cells it was found, in agreement with the decrease of lactic acid formation observed before killing the cells, that there was a considerable decrease in pyruvic acid content. The concentrations of fructose diphosphate and dihydroxy-acetone phosphate were very much increased. These changes occurred during aerobic and anaerobic glycolysis and during respiration and indicated a definite inhibition of the step in the glycolysis cycle following the formation of the triosephosphates. The authors obtained some evidence that this was due to inhibition of the phosphoglyceraldehyde dehydrogenase.

Ungar *et al.*, (110) irradiated the adrenal gland of the calf during a perfusion with blood containing ACTH. The irradiation and perfusion were continued for 2 to 3 hr. and the dose at the end of the experiment was about 2000r. The adrenal steroids were then estimated in the blood and it was found that the irradiation had much diminished their formation when compared with an unirradiated preparation Rosenfeld *et al.* (111) added various steroid precursors to the perfusing blood and were able to show that several hydroxylations were inhibited by the irradiation and so also was the oxidation of the $\Delta 5$ - 3β -hydroxyl group to the $\Delta 4$ -3-ketone group. It would be most interesting if this experiment could be carried out in some way that would allow time for recovery.

An example of an enzyme system extremely sensitive to irradiation is afforded by the auxin-producing system examined by Gordon (112). This work has been summarized by Pirie (69) and by Gray (2) in his review and need not be discussed in detail. It is particularly puzzling that the effects of even small doses of irradiation are so long-lasting (one week, after 25r) since the formation of cytoplasmic proteins in general [Hevesy (113), Holmes & Mee (114), Forssberg (115), Butler, Cohn & Crathorn (116)] and of enzymes in particular [Hokin & Hokin (117)] has been shown to be somewhat insensitive to irradiation, and it would be supposed that the auxin-forming enzyme could be quickly replaced.

Forssberg (118) found an inhibitory effect of x-rays on the elongation of the sporangiophore of Phycomycetes. This elongation is a lengthening of the structure and not a process of cell division. Doses as small as 0.0005r can be observed to have an inhibiting effect on the steady increase in length of the

sporangiophore and a dose of 1r gives a maximal effect. The inhibition is quickly reversible when irradiation is stopped; very much larger doses are needed to produce a permanent effect (about 5000r) and about 50,000r is needed to kill the mould. It is not known whether growth is, in this case, mediated by auxin.

Several authors have attempted to distinguish between the different activities of enzymes which have more than one activity, by their sensitivity to irradiation. The rennet and protease activities of chymotrypsin were equally and simultaneously destroyed by x-rays and the results were independent of hydrogen ion concentration from pH 9 to pH 5 [Moore & McDonald (119)]. Aronson, Mee & Smith (120) on the other hand, showed that the protease activity of chymotrypsin was much less sensitive to x-rays than was the esterase activity, which was tested by its ability to hydrolyse *n*-acetyl tyrosine ethyl ester. Biochemical evidence does not support the idea that two active centers are involved. The authors suggested that it is likely that there are differences in the attachment of the two substrates to the enzyme molecule, and that perhaps the protein substrate may be attached at many points and less likely to be affected by damage to one point in the enzyme surface.

The hypoxanthine and aldehyde oxidizing activities of xanthine oxidase were examined by Fluke (121) with regard to their destruction in the dry state by bombardment with α -particles and other ionizing radiations. The two activities showed the same sensitivity to irradiation, although the target mass appeared to be definitely smaller than the whole enzyme molecule. According to a personal communication from the author, the third enzyme activity, oxidation of reduced DPNH, is destroyed at the same rate as the others.

EFFECTS ON NUCLEIC ACID METABOLISM AND ON NUCLEOPROTEINS

During the last twelve years very many studies have been made on the relation of deoxynucleic acid synthesis to cell division and the effect of irradiation on this synthesis. Much of this work is discussed in the two reviews already mentioned and some further points have been summarized by Howard (122) this year.

It is now commonly agreed that the new DNA which is necessary for cell division is synthesized before the division takes place. In many tissues, there is a pause after one division of the cell, then synthesis is renewed and continues for some hours and is followed by a second pause before actual mitosis begins. This is probably the usual course of events in cells that divide once in every 24 hr. or so, though the time spent in each stage naturally varies. Gaulden (123) has recently described a course rather different from this in the grasshopper neuroblast, a tissue with a rather brief mitotic cycle and which could be directly observed throughout. ^{14}C -labelled thymidine was added when the cell entered a given stage of mitosis and was fixed at the end of a given stage, and the staining and radioautograph technique carried

out. Thymidine was found in the DNA fraction only. Uptake of thymidine began in middle telophase and continued into very early prophase and was most active during late telophase and interphase. In the experiments of Lajtha, Oliver & Ellis (124) however, in which the authors used labelled formate, which passed almost entirely into the DNA thymine of human bone marrow cells in culture, the usual pauses were found.

When the inhibition or delay of DNA synthesis is taken as the criterion of x-ray effect, the sensitive period for cells showing the usual cycle has been found by most workers to be during interphase, before the onset of the synthesis itself. During this period, small doses of x-rays are effective, although their effect can, obviously, not be seen until synthesis does start in the controls. Lajtha, Oliver & Ellis (124) confirmed the fact that this period is the sensitive one and stated in discussion that irradiation at the time very shortly before synthesis gave the most marked results. Other workers, using the first outburst of mitosis in the regenerating liver as their experimental material, found that this particular moment was not the most sensitive and that irradiation at all times before DNA synthesis began, including even the time immediately before the partial hepatectomy which gave the stimulus to the mitosis, were equally effective, although the shape of the recovery curve was somewhat different [Holmes & Mee, quoted by Holmes (23)].

There is a general agreement that when DNA synthesis is actually in progress, a much larger dose of x-rays is needed to inhibit it. This was originally shown in the pioneer work of Howard & Pelc (125) using autoradiographs.

In Gaulden's experiments with neuroblasts, a material showing no interval between one mitosis and the synthesis of DNA for the next, she was able to show that the most sensitive period for irradiation (when mitosis-blocking was the criterion), was during middle and late prophase, when DNA synthesis was not occurring. She also concluded that the dose needed for inhibiting mitosis was much less than that needed for interference with thymidine incorporation into DNA. Other authors have shown that small doses of x-rays can inhibit mitosis very shortly before it is due to occur, when the DNA synthesis is already complete.

The relationship of the inhibition of DNA synthesis to the death of the cell and the relationship of both these phenomena to direct damage of a nucleoprotein molecule by the irradiation, is not sufficiently understood as yet and is a central problem for anyone considering this type of x-ray effect.

Pelc & Howard (126) found that doses of x-rays (50r to 200r) had the effect of reducing the number of cells synthesising DNA to 60 per cent of the normal during the subsequent 12 hours and interpreted this as meaning that sensitivity to inhibition or delay of DNA synthesis is greatest in cells in the first part of interphase.

Howard (122) discussed evidence for the theory that changes in rate of synthesis are actually caused by radiation-induced changes in the cell population. These might be attributable to a shift in the proportion of cells in syn-

thesis (as discussed above) or to the death of cells. The death of cells could be caused by alteration in the genetic material and would then occur at the next metaphase or anaphase or soon after mitosis, but might also be caused by other injuries which lead to death in the same interphase, or when the cell attempted to enter mitosis. This latter type of death could occur not long after the irradiation. That changes in amount of DNA or rate of DNA synthesis seen many hours after irradiation were likely to be due to death of many of the cells has been recognized for some time and does not affect the present argument.

Kelly & Jones (127) followed the 2 hr. incorporation of ^{32}P in Ehrlich ascites tumor cells at various intervals after 800r x-ray irradiation to the mouse. They found no significant depression till 24 hrs. after irradiation; at 12 and 20 hr. the average cell volume, the total nucleic acid per cell and the DNA per cell increased steadily in irradiated and unirradiated cells. In the irradiated cells at 48 hr. the cell volume and total nucleic acid per cell had continued to increase even further, but the DNA per cell had not. The maximum DNA content reached was approximately the octoploid value, which was the ordinary premitotic content in this tumor strain. The irradiated tumor cells were unable to enter mitosis and the DNA remained at about this level while the normal cells had completed their mitosis.

It is recognized that doses of x-irradiation from about 1000r to 2000r reduce the rate of DNA synthesis by 50 per cent immediately and that increasing the dose considerably does not increase the effect. Ord & Stocken (128) made a most important contribution when they showed that this 50 per cent inhibition was already apparent 3 min. after a dose of 1000r and was not increased beyond 50 per cent 2 hr. after the irradiation of rat thymus cells *in vivo*.

It is plain that a dose of x-rays which is able to cause an immediate inhibition of DNA synthesis must be able to cause this inhibition during the synthetic period itself, which small doses do not do. It is very likely that a dose of this size will cause death of the affected cells and perhaps of most of the other cells eventually. Ord & Stocken's (128) experiment showed that 50 per cent inhibition of synthesis was one of the first effects of the lethal injury, and, since it was not any greater 2 hr. after the irradiation, was not a secondary process due to breakdown of the cell. As to what this lethal injury is, we have no definite evidence. The authors were not able to show changes in the DNA prepared from rat thymus at 2 hr. after irradiation; they examined the molecular weight, heat sensitivity base ratios and the titration curves obtained between pH 5.5 and 2.7. At 24 hr. after irradiation, when many dying cells must have been present, many changes in the DNA were found.

Attention has been focused on the deoxynucleoprotein molecule as one of the main targets of ionizing radiations partly because of its large size and the large area occupied by deoxynucleoprotein in the nucleus and also because of the very noticeable genetic effects, failures of mitosis and breakage of chromosomes that are produced by irradiations.

Experiments have been carried out with prepared DNP irradiated *in*

vitro. Bernstein (129) prepared DNP from nuclei and found a gradual spontaneous depolymerization in watery solutions which involved loss in intrinsic viscosity. Acceleration of loss of viscosity proportional to the dose given was found if the DNP was irradiated with doses from 250 to 5000r, but the loss of intrinsic viscosity was not increased. The capacity of isolated nuclei to swell in water was markedly decreased by a dose of 1000r.

Fibers of DNP newly made by precipitation from a solution in molar NaCl and irradiated with 5000 to 10,000 released a considerable amount of DNA into solution. This effect could not be imitated with nitrogen mustard [Rozenaal, Bellamy and Baldwin (130)]. Cole & Ellis (131) found that DNP prepared from mouse spleen was altered by 850r of x-ray irradiation in such a way that DNA was much more rapidly liberated by tryptic digestion of the irradiated than of the control material. Swelling in distilled water was also much decreased if the material was first incubated for one half hr. after the irradiation; control material was incubated for the same time for comparison. The swelling of DNP could be decreased by prior treatment with molar NaCl, which would cause some dissociation of the protein and the DNA.

That irradiation caused some dissociation of protein and DNA had been suggested by Kaufman, McDonald & Bernstein (132) who found an immediate effect of 1000r in reducing the capacity of thymus nuclei to swell in water. *Drosophila* salivary gland cells showed a loss of the usual capacity to swell in water after treatment with trypsin and electrolyte solutions, if taken about 2 hr. after irradiation with doses from 250 to 4000r. Onion roots exposed to 16,000r did not show a change of methyl green stainability, which argued against depolymerization of DNA, but dissociation of nucleoprotein was suggested as the cause of changes found in the fast-green and pyromin staining.

The next step, that of attempting to show effects of irradiation of DNP *in vivo*, has been undertaken by several workers. Drew (133) found that if pneumococcus cells were irradiated in heart broth with the totally lethal dose of 100,000r, the transforming factor was left intact. Deoxynucleoprotein was separated from the spleens of mice immediately after they had received a whole body dose of 81Or [Ellis & Cole (134)]; the capacity of the DNP to swell and form gels in distilled water was not altered. Unlike material from normal mice, these gels lost their gel-like properties and viscosity and formed some insoluble matter when incubated from 1 to 2 hr. at 37°C. Cole & Ellis (135) were able to show changes in the nucleoproteins of the mouse spleen taken 1 hr. after irradiation with a lethal dose of x-rays. Part of the deoxy-polynucleotide had become soluble in 0.14 M.NaCl. The soluble proportion of the total DNA increased up to four or six hours after irradiation and the insoluble part, apparently the usual DNP, decreased correspondingly. It was thought that this was due to the action of catheptic enzymes in the cell. Broken cell preparations (not diluted) of normal spleen liberate the soluble deoxynucleotide on incubation.

Calcium is known to be present in DNP preparations and is thought to

provide a link between individual DNA molecules. Steffansen (136) has been able to show that *Tradescantia* plants grown in the presence of a sub-optimal amount of calcium have an unusually high rate of spontaneous chromosome breakage. They also have an unusually large number of aberrations (distinguishable from the spontaneous ones) after x-irradiation.

Many other puzzles concerning DNA synthesis remain outstanding. To mention only one, irradiation *in vitro* is often very much less effective as an inhibitor of DNA synthesis than is irradiation *in vivo*. In the past, this has often been due to lack of oxygenation *in vitro*, but work has been done [Ord & Stocken (137)] which suggested that the process or extent of synthesis was not exactly the same *in vitro* as it was *in vivo* and that this could account for the apparent lack of irradiation effect.

OXYGEN EFFECT

Since the work of Mottram (138), who showed that bean root tips were less sensitive to x-rays and γ -radiation in the absence of oxygen and of Thoday & Read (139), who found that, in the root tip cells, the proportion of anaphases showing bridges and fragments was three times larger in oxygenated water than in oxygen-free, the question of the "oxygen effect" has become one of great importance in any consideration of the mode of action of radiations on living material.

Many papers have been written showing the effect of oxygen on the radiosensitivity of different materials. Read (140) comparing the mean growth of irradiated roots to the growth of a control group, showed that a dose given with 20 cc. oxygen per liter of the water in which the roots were immersed had the same effect as three times the dose given in oxygen-free water. He also found that oxygen supplied directly after an irradiation on oxygen-free water had no effect. Giles & Riley (141) and Giles & Beatty (142) studied the effect of oxygen in increasing the x-ray production of chromosome aberrations in *Tradescantia*. Dowdy, Bennett & Chastain (143) irradiated rats in an atmosphere containing only 5 per cent of oxygen and found that the mean lethal dose was more than that in air. Patt (144) has reviewed the literature up to 1953. Since then many more papers describing the effect of irradiating biological materials in the presence or absence of oxygen have been written. In most types of living cell the presence of oxygen caused an increase in radiosensitivity and, as Read (145) pointed out, the dose required to produce a given injurious effect in the absence of oxygen was usually two to three times that needed under conditions of normal aeration. Since the biological materials and the effects looked for were very varied, this constancy suggested that the oxygen effect must be connected with the actual ionization process.

For several years it was considered that a probable explanation was the formation of HO_2 from the interaction of the oxygen with the H atom formed by the irradiation of water. It was considered that HO_2 would have oxidizing properties. However Swallow (102), speaking at the 4th International Con-

ference on Radiobiology in 1955 and supported by Weiss and by Uri [who himself had drawn attention to the same point (146)] stated that, in the normal range of biological pH, HO_2 is largely dissociated into H^+ and O_2^- and will therefore have reducing properties and is not likely to account for the effects which are seen.

Attention was also given to H_2O_2 as a possible oxidizing agent which was likely to be formed in greater amount in presence of oxygen. On investigation, it appeared that many systems showing an oxygen effect were not very sensitive to H_2O_2 . Kimball, & Gaither (147) showed that when Paramecia are irradiated with large doses of x-rays and in the absence of large numbers of bacteria, the division-delaying and lethal effects may be due to H_2O_2 and to other fairly stable substances found in the medium after irradiation. Mutagenic effects, however, could not be produced by H_2O_2 . Paramecia are known to contain catalase and it was thought at first that the H_2O_2 did not penetrate readily as far as the micronuclei. In later work [Hearon & Kimball (148)] the amount of externally applied H_2O_2 reaching the micronucleus was calculated on the basis of the cell dimensions and the measure of consumption rate of H_2O_2 by whole cells. It was shown that the ratio of the micronuclear concentration of H_2O_2 to that in the medium was the same when the cells were placed in an H_2O_2 -containing medium as when the H_2O_2 was produced by irradiation. Precise comparisons could therefore be made. Kimball, Hearon & Gaither (149) found no mutagenic effect after exposure to concentrations of 5.6×10^{-4} per liter or 0.1 mole per liter and concluded that H_2O_2 formation could be regarded as a means of harmlessly dissipating x-ray energy.

It is, naturally, quite possible that, in systems lacking catalase, H_2O_2 could be a factor in producing x-ray effects, and, in this case, an oxygen effect would be found. Evans (150) showed ten years ago that heavily irradiated seawater could affect the sperm of *Arbuta punctata*, reducing its survival time and delaying the first cleavage after fertilization. The chief agent was, apparently, H_2O_2 , since the toxicity could be removed by catalase and the same effects could be produced by adding H_2O_2 . Feinstein, Cotten & Hampton (151) tested this possibility using mice and showed that H_2O_2 intraperitoneally injected was toxic to mice. The toxicity was much increased by adding Na azide (a catalase inhibitor) but not by hydroxylamine, which is a very strong catalase inhibitor, but is perhaps not stable in the animal body. Prior irradiation of the mice increased the lethality of H_2O_2 . On the other hand prior treatment with azide diminished the 30 day lethal effect of whole body irradiation very considerably, which is very difficult to explain if catalase is regarded as a protective agent.

Baxendale and Smithies (152) have investigated the rates of reaction of O_2 and some organic molecules with H atoms and have shown that many organic substances react sufficiently fast to compete with the small amount of oxygen usually present in solutions. Under normal conditions the cell contains little dissolved oxygen and it is thus very likely that organic radicals

will be formed there by irradiation and will afterwards react with the oxygen to form peroxides. Whether these are likely to be more effective than H_2O_2 , or whether they are more or less likely to escape breakdown by peroxidase or catalase in the cell we cannot say. Horgan & Philpot (153) suggested that the x-ray induced autoxidation in the mouse might involve squalene or similar substances.

Latarjet (154) found that succinic peracid and commercial cumene hydroperoxide would imitate the effects of irradiation in the inactivation of bacteria or bacteriophage; some mutagenicity was observed for the peracid with *Escherichia Coli* B, but not all possible mutations were produced. The peracid but not the hydroperoxide, inactivated a pneumococcal transforming factor (streptomycin resistance) and gave an inactivation curve resembling that given by x-irradiation. The transforming factor was purified and could be regarded as pure DNA. It was remarkable that when it was irradiated in solution in yeast extract, a condition where the indirect effect of irradiation was thought to be dominant, the sensitivity was not influenced either by oxygen or by hydrogen and gave the same result after oxygen saturation, oxygen removal, or hydrogen saturation.

In addition to any possible reactions between H or OH and dissolved oxygen, the presence or absence of oxygen has, of course, a more direct effect on the chain of respiratory carriers in the cell, in that it determines to what extent they will be in an oxidized or reduced form. It is of great interest to discover how much this affects their radiosensitivity. In other words, we wish to know whether the "oxygen effect" is attributable to the actual presence of oxygen or to the utilization of oxygen in the cellular respiratory system. Some very interesting experiments have been carried out with this in view. Laser (155) used several strains of bacteria, aerobes, and anaerobes and some yeasts. These were washed and suspended in phosphate buffer containing glucose (but no nitrogen source for growth) which was in equilibrium with N_2 , H_2 , or O_2 during the irradiation. The bacteria or yeasts were removed into fresh medium immediately afterwards and various metabolic processes and the growth rate measured. All growing cells showed an "oxygen effect," usually a threefold increase in sensitivity. A strictly anaerobic organism was unaffected by a dose of 6500r in N_2 but growth was almost completely inhibited by this dose in O_2 . *Sarcina lutea* also showed a typical oxygen effect, but if the respiratory poisons CO, KCN, hydroxylamine, and azide were present during irradiation, the oxygen had no effect and a dose of 26,000r unit of x-rays caused no more growth inhibition than it would have if given in N_2 . All these respiratory inhibitors interfere with cytochrome oxidase and leave the other respiratory carriers in the reduced form. Urethane, which leaves all the carriers in their oxidized form, did not protect against the presence of oxygen. This suggested that at least some of the respiratory chain molecules had to be in their oxidized form in order to show full radiosensitivity, which suggested that the inhibitory effect of x-rays might be due to a reduction process. Tahmisian & Devine (156) also demonstrated that CO could protect

to some extent against sensitization by oxygen, by replacing the nitrogen of the atmosphere with CO before irradiating grasshopper eggs. The irradiation effect was lessened, but this protection was effective only in the dark, as would be expected if it produced its protection through combination with cytochrome oxidase. Bellamy & Lawton (157) found that washed *Streptococcus faecalis* cells were sensitive to irradiation in air, but were partly protected by glucose. If glucose and methylene blue were added together, there was no protection from air. These organisms are anaerobic and lack the ordinary aerobic respiratory system; methylene blue is able to transport hydrogen to the oxygen of the air. The authors therefore concluded that the protection offered by the glucose was due to reduction of some enzymes on constituents of the cells. They believed that the effect of oxygen in making enzyme systems radiosensitive, must be superimposed on a genetic effect of the presence of O₂ during irradiation. Laser (158) also showed that fresh spores, when irradiated in phosphate buffer, showed the same sensitivity as the vegetative form of *B. subtilis* and about the same oxygen effect. If the spores were first washed and freeze-dried, they were less radiosensitive and showed no oxygen effect. When the yeast *Candida utilis* was starved of nitrogen reserve and had a low resting metabolism at the time of irradiation, it showed no irradiation oxygen effect, in complete contrast to the behaviour of the normally nourished yeast cells.

Alper & Howard-Flanders (159) have objected to the idea that radiosensitivity of the organism as a whole depends on the state of the respiratory enzymes, since much more oxygen is required to reach the half-value of oxygen sensitization of *E. coli* than to reach the half of their full respiration rate.

It is characteristic of the "oxygen" effect that it is much less marked when densely ionizing radiations are used. (A recent example of this was given by Howard-Flanders, Moore, & Wright (160) who used the growing mouse tail as a test object and compared the effect of fast neutrons and of x-rays in anoxia and oxygenated conditions). It would be useful to make such a comparison in experiments like those described by Laser (155). In many cells the respiratory carriers are attached to cell structures and function most efficiently when the structure is intact. It seems possible that densely ionizing radiation might have a very destructive effect on this structure even if the carriers were in a reduced state. If this were the case, the oxygen effect would be less striking with densely ionizing radiation than with the x-rays that were actually used.

Very little work has so far been done on the oxygen effect when using enzyme activity, *in vivo* or *in vitro*, as the criterion of radiosensitivity. When such work is done in the future, it should certainly include an estimate of the relative biological efficiencies of different types of irradiation in the presence and absence of oxygen.

So far cases have been considered in which the oxygen effect might be attributed to reactions of the radicals from irradiated water with dissolved

oxygen, or to the reaction of oxygen with respiratory carriers in such a way as to make them more radiosensitive. Another possibility is skillfully argued by Alper (161) in a lecture entitled "The Modification of Damage caused by Primary Ionization of Biological Targets." According to this suggestion, one of the primary products, H and OH, from irradiated water may react directly with the important molecule under consideration, forming an organic radical which will then itself react with dissolved oxygen to form a peroxide and may finally undergo degradation. If this organic molecule is vital to the life of the cell and if, in the absence of oxygen, the radical formed by interaction with H or OH may have an opportunity of returning to its normal state, the presence of oxygen will have made the irradiation more lethal.

It seems certain that one of the important molecules of the cell which is affected by irradiation is the deoxynucleoprotein. Work on DNA, protein and bacteriophage particles in which an oxygen effect could be demonstrated is described below.

The irradiation of purified DNA in watery solution was shown by several workers [Butler & Conway (162), Conway (163) and Scholes & Weiss (164)] to produce an immediate slight loss of viscosity; this loss was certainly just as great in nitrogen as in oxygen. During the 48 hr. after irradiation in oxygen there was a further progressive loss of viscosity, which was finally very marked, but which was very much less if oxygen had not been present during the irradiation. This aftereffect was accounted for by the formation of labile intermediates of various sorts and by the fact that irradiated DNA was susceptible to attack by H_2O_2 and by irradiation products present in the solution.

Wilkinson & Williams (165) and Scholes & Weiss (166) irradiated simple phosphate esters in oxygen and were agreed that hydroxyperoxides or peroxy radicals of these esters were formed as intermediates; some inorganic phosphate was released during irradiation and a further amount as an aftereffect when the unstable products were broken down. Scholes & Weiss could demonstrate that some similar reactions occur when ribonucleic acid is irradiated and believed that the first effect is an attack on the pentose.

In the cases described so far it appeared that the first reaction, unaffected by the presence of oxygen, could be brought about by either H atoms or OH radicals, either of which could cause the formation of a DNA radical. In the case of the bacteriophages there was apparently a preferential effect of either the H atom or the OH radical according to the bacteriophage used.

Andersen (167) showed that when pepsin was irradiated, either in the presence of the absence of oxygen, there was some immediate loss of enzyme activity, which was much the same in both cases. If the enzyme solutions were allowed to stand, there was a further fall in activity which was strongly temperature dependent and was more marked when the irradiation had taken place in the presence of air. The progressive fall in activity appeared to be due to a change which had been produced in the protein molecule itself, as the rate was not altered by a twenty-five-fold dilution in the solution. It is very

interesting that Loiseleur (168) who worked for many years on the effects of oxygen on the irradiation of substances in solution, showed that an irradiation-produced darkening of a tyrosine solution increased after irradiation had stopped. He suggested the formation of a peroxide intermediate.

Alper (169) used S 13 bacteriophage and found that, while some of the particles were inactivated at once, some were part-inactivated and liable to become inactive later. Thus the phage titre continued to fall after irradiation, particularly if the particles were left in contact with the irradiated medium. Part-inactivation did not occur in suspensions that were highly protected against the action of water decomposition products; radiation energy absorbed within the phage particle itself brought about immediate inactivation only. The agents which acted destructively on the part-inactivated phage after irradiation were of a reducing nature (ascorbic acid, for instance), and H_2O_2 could be considered as having a reducing action here. The immediate indirect effect of irradiation appeared also to be of a reducing nature; OH radicals did not produce this part-inactivated state and the presence of oxygen at the moment of irradiation had a protective effect.

Bachofer & Pottinger (170) using T1 'phage, also found some protective effect of oxygen at the time of irradiation, but, as they got no increased effect from using a hydrogen instead of a nitrogen atmosphere, concluded that the primary reaction was not with the H atom but with the OH radical from water and confirmed this by using OH produced from H_2O_2 . They suggested that O_2 might make a stabilizing complex with the phage "radical" at the reaction site. 'Phage that had been stored at 4° C was not much protected by oxygen and 'phage dissolved in phosphate buffer containing magnesium and NH_4Cl was less protected than samples dissolved in distilled water.

It is obviously of great interest to examine the known cases where the presence of oxygen does not increase the effects of irradiation. Nakao (171) irradiated toad eggs at various times between insemination and first cleavage and when the control embryos had reached the tail-bud stage, the experimental embryos were examined for irradiation injury. The irradiation was given, while the eggs were in air or in a vacuum, at 30 min., 1 hr., 10 min., 2 hr., 30 min. and 3 hr., 30 min. after insemination. Only at 30 min. could any protective effect of anoxia be seen, although there is no reason to believe that oxygen did not reach the embryo at all stages equally. At 2 hr., 20 min. the embryos were all more resistant to x-rays, but at 3 hr., 30 min. they were once more radiosensitive, both in oxygen and *in vacuo*. Nakao (172) had previously shown that reduction of sensitivity by anaerobiosis applied only to the eggs and not to the spermatozoa when the production of developmental anomalies was the criterion.

Mendelsohn (173) used the ability of rabbit kidney cortex slices to develop a concentration gradient for *p*-aminohippurate as his test object. The presence or absence of oxygen during the time of irradiation did not affect the dose required for a 50 per cent decrease in the concentration ratio as compared with unirradiated controls.

Wolff & Luippold (174) showed that anoxia affects the irradiated chromosome in two different ways, which makes interpretation of results more complicated. Chromosome breakage was lessened by anoxia, but the rejoining of breaks, an energy requiring process, was much slower and the number of two-hit aberrations to this extent increased.

Patt (175) in discussing the radiosensitivity of mammalian cells described a very curious effect. In a suspension of thymus cells, the marked protective effect of hypoxia was partly annulled by chilling the suspension to 0.2° C for 15 min. after the x-ray. If the suspensions were chilled before irradiation there was no protective effect of hypoxia (about 0.1 per cent O₂ in N₂). The author discussed work by other experimenters, which also seemed to show that some effect could be obtained by changing the conditions after irradiation.

In the examples quoted above there is no reason to suppose that the lack of oxygen effect was due to a failure of the oxygen to reach the inside of the cells. This is, however, a great difficulty in some tissues and in coarse suspensions of tissue or in thick slices.

Hall (176) observed that the x-ray sensitivity of tumor fragments in air was an inverse function of their size. The most probable explanation was that the oxygen did not reach the center of the large fragments. It has very often been noticed that tissues irradiated *in vitro* are much less radiosensitive than those irradiated *in vivo* and it is certain that at least part of this lack of sensitivity is caused by lack of oxygen in the cells not directly in contact with the air.

Scott (177) has devised a neat model system for determining the thickness of cell layers needed to render those furthest away from the oxygen supply insensitive to irradiation. He used the growth of Ehrlich ascites tumor cells *in vivo* as his criterion of x-ray effect and separated them, during irradiation *in vitro*, from their oxygen supply by compact layers of respiring but nongrowing cells. He found that if the layer of respiring cells was 250 microns thick, the tumor cells became anoxic within a few minutes and became much more resistant to irradiation.

In tissues in the body, although there is every reason to believe that the cells will be deprived of oxygen when a low-oxygen atmosphere is breathed and will probably receive a little more than usual when a high oxygen atmosphere is breathed, quantitative comparisons cannot as yet be made. Phillips & Cater (178) found a large rise in oxygen tension as measured by platinum electrodes lying between the cells in rat tissues, when the animal breathed pure oxygen. Phillips (179) also pointed out that the importance of the small extra amount of oxygen dissolved in the serum in animals breathing pure oxygen will have a relatively greater significance in a tissue with a small utilization of oxygen.

Gray, *et al.* (180) showed that, in solid tumors growing in animals, there was a difference in radiation response of the tumor cells at different distances from the blood supply. Thomlinson & Gray (181) made histological examina-

tions of many carcinomata (chiefly carcinoma of the bronchus) arising from sites where stratified squamous epithelium is found. Such tumors, they showed, often grew in solid rods, which appeared in transverse section as circular areas surrounded by stroma, but with no capillaries visible among the tumor cells. When the cords were above a definite thickness, necrotic areas were found in the centers. Measurements were made on 160 sections and it was established that there was no tumor cord more than 200μ in radius which was without central necrosis and that the surrounding sheath of tumor cells never exceeded 180μ , so that no intact tumor cell was seen more than 180μ from the stroma. No central necrosis was seen in any tumor cord less than 160μ in radius. It was therefore assumed that O_2 (and possibly other nutrients) could not penetrate through more than 200μ of solid tissue. The deepest living layer of cells must have been to some extent anoxic and therefore would be more radioresistant and perhaps able to live and grow after the death of the outer cells following irradiation. The authors pointed out that an increased oxygen tension at the periphery of such a cord would be likely to secure a greater differential irradiation damage to these tumor cells than to the cells of well oxygenated normal tissues.

Howard Flanders & Wright (182) and Howard Flanders, Moore & Wright (160) irradiated the growing mouse tail when the mice were breathing gas mixtures with various partial pressures of oxygen. The dividing cartilage cells of growing bone are separated from capillary blood by the zone of hypertrophic cartilage which was found to be 100μ thick in the mouse tail. The oxygen tension of the dividing cells must have been well below that of the cells nearest to the capillaries. It was found that the radiosensitivity was increased by nearly 30 per cent when the animals were breathing pure oxygen instead of air, the criterion of radiation effect being the subsequent growth of the tail.

PROTECTION AGAINST RADIATION

The subject of chemical protection against ionizing radiations, as a result of much experimental work and some increase in our knowledge of the possibilities involved, has reached the interesting stage which enables the claims of different theories to be debated.

Patt and coworkers (183) first demonstrated the protective effect of cysteine in animals, and discussed the possible mechanism of sulphydryl protection against mammalian radiation injury. Bacq first showed that cysteamine gave very good protection (Gerebtzoff & Bacq (184)). Recently (185) when considering the mode of action of cysteamine and its derivatives and collecting the evidence from many sources, he came to the conclusion that no one theory could account for all the effects of these chemical protectors.

The protective effect of molecules containing $-SH$ during the irradiation of substances in solution is probably often due to its competition for the radicles formed by the irradiated water. At first it was thought that the protective effect in animals was due to the same cause, though it was difficult to

understand why a little additional cysteine or glutathione should have so much effect in tissues already full of them. It became plain that the mechanism was not so simple when it was found that many —SH compounds (notably thioglycollic acid and BAL) protected only very slightly. It was pointed out by Eldjarn & Pihl (186) that in a biological medium, the ability of cysteine (a very good protector in the animal) to inactivate radicals was not high enough to account for its protective effect.

Koch & Hagen (187) and Doherty & Burnett (188) substituted various groups in the cysteamine molecule and found that the NH₂ group was also necessary for protection in the animal. Koch and Hagen tried the effects of substituting in the amino group and found that as their products became more protective they also became more toxic. They felt that this must indicate a more specific reaction than simply the capture of radicals.

Van Bekkum & de Groot (189) also found that with a number of biological amines, protection is only given by doses which induce toxic symptoms. In order to distinguish between a generalized effect and actual protection of cells, these authors compared the protection effect of some compounds on mice and on thymocytes. Cysteine, glutathione, cysteamine and di-ethyl-dithiocarbamate could protect against lethal doses of x-rays in both systems but various biological amines that protected mice had no effect on thymocytes.

These results alone are, perhaps, not enough to show any specificity of protection. Amines might work through a generalized pharmacological effect, and the NH₂ group or a substituted NH₂ group might merely increase the penetration of cysteamine derivatives into the cell. Hollaender and co-workers (190) showed that the cysteamine did pass into or become firmly attached to the bacterial cell (*E. coli*) since the radio-resistance conferred on the bacteria by being placed in cysteamine solution could not be removed by careful washing.

Naturally, the ability of the protecting compound to arrive at the required place is one of its prerequisites. Some of the differences in type of action shown by various protectors, may be due to their being concentrated in one or another tissue and exerting their chief protective action there. An example of this is given by Jennings & Tessmer (191) and concerns protection conferred by glutathione against whole body irradiation in mice. The glutathione reached a fairly high concentration in liver and spleen 30 minutes after injection. If the mice were already protected by spleen shielding, glutathione did not give any extra protection; if the spleen had been removed beforehand, there was no protective effect of glutathione.

There is now much evidence that the sulphydryl radiation-protection substances do react with definite chemical groups in the body and may exercise their protective function by this means.

Eldjarn & Pihl (192) demonstrated that *in vitro* and *in vivo* cysteamine and cystamine reacted with —SH groups to form mixed disulfides. This happened both with soluble substances, such as glutathione and with the —SH

groups of proteins. They considered it possible that this might be a mechanism for the protection of an essential —SH, or even, to protect the protein molecule as a whole, if the rupturing of the new disulfide bond served as a nondestructive form of energy dissipation after energy-transfer from neighboring parts of the molecule. Pihl & Eldjarn (193) made a further investigation and found that interaction of the S—S compounds, such a cystine and cystamine, with biological —SH compounds and of cysteamine, cysteine and glutathione with biological S—S compounds occurred readily when these were incubated together. If this mechanism were to act as a protector of vital groups, it was obviously necessary that the reaction of the protecting substance with them must not be permanent. Koch (194) showed the β -isomers of homocysteine and cysteine (isocysteine) were actually radiation sensitizing agents and suggested as a possible reason that they might form the same compounds *in vivo* as the α -isomers, but that the compounds might persist for too long a time.

The suggestion made by Eldjarn & Pihl that there might be transfer of the effect of the irradiation reaction from other parts of the molecule to the disulfide bond is in agreement with the work of Gordy, Ard & Shields (195), who found strong evidence for the idea that when radiation knocked out an electron to create a hole or vacancy at some point in a protein molecule, the hole or vacancy would quickly be filled by an electron borrowed from a cystine group. This mechanism would probably greatly diminish the irradiation damage in the protein, but might strengthen rather than weaken the disulfide bond, which, in that case, would have to be broken eventually by reduction to restore the original molecule. An example of the protection of a long molecule by the insertion of a reactive group is given by Alexander & Charlesby (196). They showed that the irradiation energy required to cause cross-linkages in long chain hydrocarbons did not depend on the molecule weight. The addition of a naphthyl group (especially in the center of the molecule) much increased the amount of energy required, though other, equally bulky, groups did not.

Lefort & Ehrenberg (197) as well as Caldecott (198) showed a protective action on seeds of hydration up to a given water content. Ehrenberg (199) using carboxymethyl starch ether for viscosity measurements, showed a minimum starch breakdown when irradiation was done when the moisture content was about 20 per cent of water. Apparently when the water content increases towards that point, an increased fraction of the absorbed energy can be carried off. Potassium iodide added to potato starch was oxidized by the x-irradiation. This oxidation was greatest where the starch decomposition was least, at 20 per cent water content.

Where transfer of irradiation effect occurs in a molecule, whether by electron transfer or other mechanism, it will naturally not always appear as a protective action but may increase the chances of a decomposition of a biologically vital group by the irradiation. In either case it is obviously a possibility that must be carefully considered in explanation of cellular irradiation

effects. Svedberg & Brohult (200), when irradiating the huge haemocyanine molecule with α -particles, found that the irradiation always caused a breaking of the molecule into two equal parts. One α -particle per molecule was enough to do this.

A biologically very important instance is given by Setlow & Doyle (201) who showed that hyaluronidase, when dried together with its substrate hyaluronic acid was more sensitive to the direct action of irradiation by 3.8 Mev deuterons than when irradiated alone. An ionization in the substrate could inactivate the enzyme. When the substrate and enzyme were dried under conditions which prevented their reacting together, the increased sensitivity was not found; the data indicate that it depends on the specific combination of enzyme and substrate and must be due either to a transfer of energy from the substrate to the enzyme or an alteration of the substrate which causes it to remain bound to the enzyme during the subsequent estimation of activity.

It is conceivable that a result such as that obtained by Cox, *et al.* (202) with increasing doses of γ -rays on solutions of Na deoxyribonucleate, might be due to transfer of irradiation effects from other parts of the molecule to the apparently most sensitive points. The first effect found was the rupture of the crosslinking hydrogen bonds, those linking the adenine-thymine pair probably being more rapidly broken than those linking the guanine-cytosine pair. Higher doses are needed to cause any appreciable change in intrinsic viscosity and still larger to cause degradation of the bases.

Other methods of protection must now be considered. Hagen & Koch (203) showed that iodo-acetate sensitized animals to radiation, confirming the work of Feinstein, Cotten & Hampton (151) and also that iodo-acetate itself could produce tissue injuries not unlike radiation injuries. Iodo-acetate reacted rapidly with the protective —SH compounds (cysteine, cysteamine, N. Dimethyl cysteamine) and slowly with the poorly protective —SH compounds (thioglycollic acid, thioglycol, and BAL) which suggested that its toxic action might be selective in the same sense.

Since the protective effect of anoxia against x-irradiation became plain, various workers have considered the possibility that the —SH and other chemical protectors were chiefly useful as oxygen removers. Lacassagne, Duplan & Buu-Hoi (204) acting on this idea, used pyrogallol derivatives to protect mice against LD₁₀₀ doses and were able to reduce the 30 day mortality rate.

Bonet-Maury & Patti (205) and Konecci, Taylor & Wilks (206) did experiments using carbon monoxide as a protective agent in animals, using it to lower oxygen transport in the blood. The first authors found that a concentration of 4×10^{-3} CO in the atmosphere caused 67 per cent of mice to survive the otherwise lethal dose of 800r. Konecci *et al.* gave 500r (an LD₁₀₀) to guinea pigs and found that pre-treatment with CO gave a 50 per cent survival and that even post-treatment had some protective effect.

Hollaender & Kimball (207) found that even glucose, succinate, and

some glycols and alcohols can give some protection to microorganisms by causing them to use up the oxygen in solution more rapidly.

Gray (208) described the measurement of small amounts of oxygen by the Hirsch cell, a method which could be used to detect changes in amounts of dissolved oxygen in biological fluids. He showed that, when a small amount of commercial cysteine (not specifically purified to free it from metals) was added to water or buffer solution, it could denude the water of dissolved oxygen in 10 minutes at pH 6.5. The experiments of Forssberg & Nybom (209) on the protection of Allium roots with cysteine and of Bacq & Herve (210) on the protection of pea roots by 1/5000 cysteamine were repeated. It was shown that very little oxygen was present in the water surrounding the roots and that the protection was probably due to anoxia. Gray considered that anoxia must also have played an important part in the protection by cysteine of bacteria, [Stapleton *et al.* (211)] and of thymocytes [Patt *et al.* (212)] when these were irradiated. Van Bekkum, on the other hand, obtained good protection of thymocytes with small concentrations of cysteamine which did not appreciably alter the concentration of oxygen in the suspending medium. Phillips (178) and Cater (213) in discussion stated that when making measurements with platinum electrodes *in vivo*, they found very little reduction in oxygen tension as a result of injecting cysteine, though a marked fall in the oxidation-reduction potential.

Bacq, *et al.* (214) quoted experiments showing that cystamine produces a slowing of the circulation in rats, which leads to a marked desaturation of the venous blood and probably a deficient supply of oxygen to the tissues. The experiment was done under barbiturate anaesthesia; control animals showed a 70 per cent oxygen saturation while those with cystamine showed only a 40 per cent saturation. The same authors showed that cysteamine protected mice against oxygen poisoning; it was five times more effective in this than cysteine.

Salerno, Uyeki & Friedell (215) carried out some experiments with cysteine. Liver slices from cysteine treated rats had a greatly increased oxygen uptake and the authors considered that this caused the 50 per cent reduction of oxygen content that they found in venous blood. *p*-aminopropiophenone reduced the amount of oxygen carried in the arterial blood by conversion of haemoglobin to methaemoglobin. When the cysteine and *p*-aminopropiophenone were given together very good protection against irradiation was afforded, but this was abolished when oxygen under pressure was breathed by the animal.

To a limited extent the effect of the —SH protectors and the effect of anoxia are additive. Experiments by Devik & Lothe (216) found that four mice out of 20 survived and a dose of 1000r of x-irradiation in 8.4 per cent oxygen and 2 out of 21 survived this lethal dose if 5 mg. of cystamine was injected before they were irradiated; if the low oxygen tension and the cystamine treatment were combined, 13 out of 18 animals survived. However Lothe & Devik (217) find only a very slight additional protection by

cysteamine when the ear of a rabbit is made entirely anoxic before irradiation.

It would be very interesting to test the theory that irradiation under anoxic conditions fails to attack just those vital groups which are protected by the active —SH compounds. Auerbach (218) reported that anoxia reduced the mutation rate in *Drosophila* but that cysteamine did not. There is a danger, in such comparisons, that the cysteamine may not penetrate sufficiently into the cells; Nakao, Tazima & Sugimura (219), however, also report a lack of protection against mutagenic and lethal irradiation effects in the silkworm, both when the female received cysteamine or cysteine before mating, and when the eggs were immersed in solutions of the protectors before irradiation. It is possible that in the case cited by Auerbach there is a real difference between the two mechanisms.

The development of techniques for the chilling and later recovering of animals has made it possible to test the effect of the lowered temperatures on radiosensitivity. Lacassagne (220), Hempelmann, Trujillo & Knowlton (221), Storer & Hempelmann (222) and also Baclesse & Marios (223) showed that, in newborn rats and mice and in adult rats, reducing the body temperatures below about 18° C at the time of irradiation made the animals definitely less sensitive to it. Storer & Hempelmann concluded that the degree of anoxia was an important factor in the increased survival of infant mice irradiated at 3°–7° C. Placing them in an atmosphere of N₂ after chilling produced no additional protection, but an atmosphere of O₂ decreased the survival rate considerably.

Hornsey (224) showed the effect of anoxia and of cold in the protection of newborn mice by placing litter-mates in a stream of N₂ and, when breathing ceased, irradiating one group directly and the other after packing in ice for five minutes; the dose given was 1500r. No difference was found in the subsequent growth rate of the young mice between those irradiated in the anoxia state and those irradiated while under anoxia and hypothermia. No unprotected mouse of this strain survived 900r.

Adult mice were cooled to between 0° and 0.5° C. while keeping them in an atmosphere of low oxygen tension. 100 per cent of these mice survived doses of 900r to 1500r.

A different result seems to be obtained when hibernating animals are used. Künkel, Höhne & Maass (225) subjected dormice to a dose of 700r while these were in hibernation at a temperature of +4° C. These animals appeared to be uninjured, but when brought back to room temperature 21 days later showed signs of radiation sickness. The death-rate 30 days after the end of hibernation was the same as the death-rate 30 days after irradiation in animals irradiated while in a waking condition at room temperature. The 21 days of hibernation after irradiation seemed to be an inert period but not a recovery period.

Cysteine injected into animals irradiated at room temperature was an excellent protective agent but useless for promoting recovery when injected

after irradiation. It was astonishing that, in the hibernating animals, the cysteine afforded perfect protection when given 21 days after the irradiation. It appeared that the irradiation injury was not completed while the animals were in the hibernating state.

The lack of protection from low temperatures during hibernation suggests that the hibernating animal, with its metabolism slowed by hormonal control, does not use its oxygen quickly and is not really anoxic. An experiment is reported (*the New Scientist*, 1957, p. 5) with bats, which were brought by starvation to a state resembling hibernation before irradiation; these bats showed no radiation injury until they were later fed and warmed, after which they died.

RECOVERY FROM RADIATION

Although it was known that the animal body had some power to recover from radiation injury and could, therefore, tolerate small, repeated irradiation doses better than one large one, this recovery seemed to be mostly a question of regrowth of the intestinal mucosa and replacement of dead cells in the bone marrow and spleen by division of the remaining ones. The disturbance of pituitary-adrenal function, and the metabolic changes associated with it also disappeared gradually. The replacement of these important tissues could, of course, only take place when sufficient cells had been left alive in the very radiosensitive spleen, bone marrow and intestinal mucosa.

Recovery after a truly lethal dose was demonstrated to occur after injection of pulps from spleen and bone marrow [Jacobson *et al.* (226)] but a series of exciting researches [Ford, Hamerton, Barnes & Loutit (227)] proved that the recovery of the irradiated animal was, in a sense, indirect, and depended on the replacement of its own blood forming tissues by growth of the foreign cells.

Recovery of bacteria had been shown by Stapleton, Billen & Hollaender (228) to be increased when the irradiated bacteria were kept at temperatures not optimal for growth. It was thought that the lower temperature discouraged mitosis and gave the damaged organisms a chance of restoration of their normal metabolism.

It is only very lately that a few indications of the possibility of encouraging recovery by known chemical compounds have appeared. Hollaender & Doudney (190) quoted experiments of Stapleton, Sbarra & Hollaender in which *E. coli* B/R grown aerobically in nutrient broth, recovered from x-ray effects to a considerable degree (that is the number of survivors was much increased) if they were plated after irradiation on agar containing spleen, beef, or yeast extract. A synthetic medium containing glutamine, uracil, and guanine in addition to salts and glucose was equally effective. This treatment no doubt enables bacteria to survive which have lost their power to synthesize glutamine, uracil, and guanine. In fact may pick out the mutant bacteria of this type. It is remarkable that the full effect of cysteamine protection during irradiation [Hollaender & Doudney, (190)] could only be seen if the

bacteria are afterwards plated on the same special media. Cysteamine apparently did not protect very successfully against this particular injury to the metabolism or genetic makeup of the bacteria. Bacteria placed at sub-optimal temperatures after irradiation did, however, show a marked effect of cysteamine protection, without the addition of special nutrients to the media, and bacteria protected by mercapto-ethanol rather than cysteamine during irradiation showed a very marked effect of this protection even when they and the unprotected controls were grown on a minimal medium after irradiation. Bacteria which had been grown on a simple glucose and salt medium before irradiation and which had, presumably, formed the necessary enzymes to do so, did not need the special nutrients after irradiation [Hollaender (229)].

This type of recovery, whether due to recovery of individual cells or to the selection of mutants or both, demonstrates principles which can probably not be applied at all directly in the case of an irradiated animal, although it must be remembered that Forssberg (230) showed that the addition of DNA to the ascitic fluid of mice led to a quick resumption of DNA synthesis after irradiation of the Ehrlich ascites tumor. Stapleton, Woodburg & Hollaender (231) however have now isolated an RNA polynucleotide fraction from *E. coli* B/R which is very active in stimulating recovery of the same strain of bacteria if amino acids are supplied at the same time. Preliminary experiments suggest that this compound, when some difficulties of toxicity have been overcome, may give an increased survival rate in mice after an LD₅₀ dose of x-rays. Fractions of the same sort prepared from mouse tissues will no doubt be tried later by these authors. Kumta, Gurnami & Sahasrabudhe (232) found that 24 hr. after 600r whole body irradiation the free methionine in the liver had fallen markedly. This suggested that the administration of methionine after irradiation might modify irradiation injury. Nerurka *et al.* (232a) have found that this procedure reduced the post-irradiation loss of DNA (that is to say, of cells) from spleen and bone marrow.

An unexpected result was obtained by Kimball, Gaither & Wilson (233) who found they could prevent a proportion of mutational changes produced in paramecia by irradiation by giving H₂O₂ after the irradiation. This could be given as much as two hours later, provided no mitosis had intervened.

An agent which is found in yellow bone marrow and is thought to be useful in stimulating recovery from leucopenia and granulocytopenia is the alloxyglycerol, batyl alcohol.

Sandler (234) found that the substance in unsaponifiable bone marrow fat which could protect against benzene poisoning was batyl alcohol or an ester of this. Purified batyl alcohol was equally useful as a protector. An alloxyglycerol ester given by mouth was found by Brohult & Holmburg (235) to relieve a fairly long-standing irradiation leucopenia. At the same time Edlund (236) found that synthetic batyl alcohol given to adult mice in small doses subcutaneously every other day after irradiation produced a significant increase in 30 day survival rate after 750r.

Brohult (237) found that administration of shark liver oil, which contains 50 per cent of alkoxyglycerol esters, was very effective in preventing a fall in white cell count during irradiation, an optimal dose being 1.2 g. per day given by mouth. The possibility could not be excluded that some other substance in shark liver oil was responsible for this and trials of purified and synthetic batyl alcohol and other alkoxyglycerols are in progress.

STERILIZATION OF FOODS

Since it became plain that large amounts of radioactive material would become available from the waste products of nuclear reactors, much attention has been drawn to the possibility of sterilizing food by irradiation instead of by heating. Before food sterilized by irradiation can be supplied to the public its nutritive value must be tested and the possibility of the formation of toxic products by the irradiation must be investigated. A large amount of work has already been carried out in the United States and in England along these lines.

Johnson & Motta (238) gave three million r units of γ -radiation to frozen raw foods. The loss in nutritive value of the proteins was not more than that caused by the usual heating processes. The loss of biological value of milk protein could be fully restored by adding cystine.

The effect of three million r units upon the water-soluble vitamin content of raw beef was tested by Alexander, *et al.* (239), who found that thiamine was decreased by between 60 per cent and 70 per cent, pyridoxine by 25 per cent, riboflavin by about 10 per cent and niacin, choline and folacin were unaltered. When added to diets, menadione and, to a smaller extent vitamins K₁ and K₂, were found by Richardson, Woodworth & Coleman (240) to be radiosensitive, but comparatively little vitamin K was lost when natural foodstuffs were irradiated. Irradiation of fat is known to cause oxidation and formation of peroxides [see Hannan and Shepherd (241) (242)]. The toxicity of oxidized soy bean oil and of *t*-butyl hydroperoxide when added to the diet was investigated by Andrews, Mead & Griffith (243). MacKinney (244) decided, after comparative experiments, that where destruction of carotenoids occurs it is as a result of products of other reactions, probably those taking place in the lipides. The loss of carotenoids in whole tomatoes is very slight, although the internal structure of the tomato is lost, suggesting the breakdown of pectin.

Kertesz, and associates (245) tested the effects of irradiation on pectin. The viscosity of pectin in solution could be reduced by x-rays, but the presence of sugars protected the pectin against this effect. Actual jellies of pectin and sucrose were very insensitive. It is plain that the results of irradiating pectin in different foodstuffs will give very variable results.

Tappel (246) found that the irradiation of meat in an atmosphere of nitrogen eliminated the formation of peroxides, but that carbonyl compounds were formed in oxygen or nitrogen. He discussed the effect of high irradiation doses on vitamins, haematin compounds, carotenoids, and enzymes.

Hannan & Shepherd (241, 242) made a detailed study of the irradiation of fats and the formation of fatty peroxides. These experiments are summarized in a report by Hannan (247) on the use of ionizing radiation for food preservation. He found that, when fat was irradiated in air the peroxide value was maximum at a dose of about 5×10^6 reps and was greatest in fats irradiated at low temperatures. After low temperature irradiation, peroxide formation continued for about five days if the fat was kept cold all the time. When the fat was irradiated in the absence of oxygen no peroxides were produced, but if the irradiation was carried out in the cold and the fat afterwards held at low temperatures, peroxides were formed as soon as oxygen was admitted, even if this was several months after irradiation. It appears that a reactive group was formed by the irradiation which disappeared if the fat was warmed but was stable for a long time at low temperatures and which reacted with oxygen to form peroxide. The effect of low temperature was almost certainly due to the solid state of the fats; the aftereffect fell from a maximum value to zero over the temperature range where the fat changed from a hard solid to a liquid.

Carotenoid pigments dissolved in the fat were partially bleached during the irradiation, provided that the fat is not molten, and more completely bleached during low temperature aftereffect and peroxide formation. The anti-oxidants (mainly tocopherols) which are often present in natural fats are also destroyed, either by the peroxides or by the reactive precursor.

Schweiger *et al.* (248) examined the color changes occurring in irradiated meat. They found that myoglobin was much less stable in crude or purified extracts than it was in the meat itself. A green color was formed during the irradiation which appeared to be due to a change in the porphyrin nucleus of myoglobin.

Doty & Wachter (249) showed that there was little, if any, inactivation of the proteinase in beef at a dosage of 0.5×10^{-6} reps. The survival of this enzyme would obviously be a disadvantage during storing unless refrigeration was used. The irradiation reduced the amount of tyrosine extractable from the beef.

Green (250) determined the effect of the sterilizing irradiation doses on the enzymes in foodstuffs and found that they were disappointingly radio-resistant and that the threat of food spoilage by enzyme action would always be present unless the inactivation of enzymes could be accomplished by other means. A dose of 2×10^6 reps, which was sufficient to kill the majority of microorganisms gave only a 29 per cent reduction of activity of the proteolytic enzymes in beef heart.

Batzer & Doty (251) showed that the odors developed during the irradiation of beef, which are one of the great drawbacks to irradiation sterilization of many foods, were partly due to sulfur containing compounds, one of which was H_2S itself. Another may have been methyl mercaptan, but it is possible that a more complicated compound was formed which released H_2S and methyl mercaptan during the estimation procedures. Determinations of

glutathione content showed a considerable loss of this compound (or other compound estimating as glutathione) as a result of irradiation.

It will be appreciated that the papers quoted here are a sample from a very large number of papers and reports which are now appearing on the subject of irradiation of foodstuffs. Journals to be consulted are *Food Technology*, *Food Research*, *Journal of Agricultural and Food Chemistry*, *Journal of Science of Food and Agriculture* and *Chemistry and Industry*.

LITERATURE CITED

1. Collinson, E., and Swallow, A. J., *Chem. Revs.*, **56**, 61 (1956)
2. Gray, L. H., *Ann. Rev. Nuclear Sci.*, **6**, 353 (1956)
3. Hevesy, G., and Forssberg, A., *Proc. Intern. Congr. Biochem., Brussels, 3rd Congr. 1955*, 479 (Academic Publishers Inc., New York, N.Y., 1956)
4. Hevesy, G., *Brit. J. Radiol.*, **29**, 465 (1956)
5. Coniglio, J. G., McCormick, D. D., and Hudson, G. W., *Am. J. Physiol.*, **185**, 577 (1956)
6. Goldwater, W. H., and Entenman, C., *Radiation Research*, **4**, 243 (1956)
7. Morehouse, M. G., and Searcy, R. L., *Federation Proc.*, **15**, 316 (1956)
8. Morehouse, M. G., and Searcy, R. L., *Science*, **122**, 158 (1955)
9. Morehouse, M. G., and Searcy, R. L., *Radiation Research*, **4**, 175 (1956)
10. Coniglio, J. G., Darby, W. J., Efner, J. A., and Fleming, J., *Am. J. Physiol.*, **184**, 113 (1956)
11. Gould, R. G., *Progress in Radiobiology*, 71 (Oliver & Boyd Ltd., Edinburgh, Scotland, 557 pp., 1956)
12. Gould, R. G., Bell, V. L., and Lilley, E. H., *Radiation Research*, **5**, 609 (1956)
13. Popjak, G., *Progress in Radiobiology*, 71 (Oliver & Boyd Ltd., Edinburgh, Scotland, 557 pp., 1956)
14. Bernheim, F., Ottolenghi, A., and Wilbur, K. M., *Radiation Research*, **4**, 132 (1956)
15. Chevallier, A., and Burg, C., *Radiobiology Symposium, 1954*, 1 (Butterworth and Co. Ltd., London, England, 362 pp., 1955)
16. McKee, R. W., and Brin, M., *Arch. Biochem. Biophys.*, **61**, 390 (1956)
17. Loureau, M., *Compt. rend.*, **236**, 422 (1953)
18. Fischer, P., *Arch. intern. physiol.*, **63**, 134 (1954)
19. Sherman, F. G., and Dwyer, F. M., *Federation Proc.*, **15**, 169 (1956)
20. Thompson, H. E., and Steadman, L. T., *A.E.P.-152* (University of Rochester, Rochester, N.Y., 1950)
21. Keilina, R. Y., *Biokhymia*, **20**, 420 (1955); *Nuclear Science Abstracts*, Vol. 10, Abstract 535 (1956)
22. Perkinson, J. D., and Irving, C. C., *Radiation Research*, **5**, 589 (1956)
23. Itzhaki, S., (as quoted by B. E. Holmes) *Ciba Foundation Symposium on Ionizing Radiations and Cell Metabolism*, 318, 225 (1956)
24. Hevesy, G., and Forssberg, A., *Nature*, **168**, 692 (1951)
25. Loureau-Pitres, M., *Arkiv. Kemi.*, **7**, 211 (1954)
26. Kay, R. E., Harris, D. C., and Entenman, C., *Am. J. Physiol.*, **186**, 175 (1956)
27. Altman, K. I., Haberland, G. L., Schreier, K., and Hempelmann, L. H., *Radiation Research*, **5**, 466 (1956)
28. Kay, R. E., Early, J. C., and Entenman, C., *USN RDL-TR-98 NM006-015* (Naval Med. Research Inst., 1956)

29. Hempelmann, L. H., Lisco, H., and Hoffman, J. C., *Ann. Internal. Med.*, **36**, 444 (1952)
30. Winkler, C., and Paschke, G., *Radiation Research*, **5**, 156 (1956)
31. Leone, C. A., *U. S. Atomic Energy Commission Document AECU-3133* (1955)
32. Fricke, H., Leone, C. A., and Landman, W., *Radiation Research*, **5**, 478 (1956)
33. Smith, E. S., and Lewis, Y. S., *Progress in Radiobiology* (Oliver & Boyd, Edinburgh, Scotland, 557 pp., 1957)
34. Rieser, P., *Proc. Soc. Exptl. Biol. Med.*, **91**, 654 (1956)
35. Rieser, P., and Rutman, R. J., *Nature*, **178**, 257 (1957)
36. Scheraga, H. A., and Nims, L. F., *Arch. Biochem. Biophys.*, **36**, 336 (1952)
37. Klein, P. D., Handen, D. T., and Swick, R. W., *Proc. Soc. Exptl. Biol. Med.*, **90**, 204 (1955)
38. Klein, P. D., Handen, D. T., and Swick, R. W., *Radiation Research*, **3**, 333 (1955)
39. Wexler, B. C., Pencharz, R., and Thomas, S. F., *Am. J. Physiol.*, **183**, 71 (1955)
40. Nims, L. F., and Geisseloder, J. L., *Radiation Research*, **5**, 58 (1956)
41. Bacq, Z. M., Fischer, P., and Beaumariage, M., *Bull l'acad. roy. med. Belg.*, (VI) **19**, 399 (1954)
42. Bacq, Z. M., Martinovitch, M. M., Fischer, P., Shaditch, G. S., Pavlovitch, R., and Radivojivitch, D. V., *Bull. de l'acad. roy. med. Belg.* (VI) **22**, 328 (1956)
43. Nims, L. F., and Sutton, E., *Am. J. Physiol.*, **177**, 51 (1954)
44. Smith, D. E., and Tyree, E. B., *Am. J. Physiol.*, **184**, 127 (1956)
45. Edelman, A., *Federation Proc.*, **8**, 39 (1949)
46. Glenn, J. L., and Boss, W. R. F., *Federation Proc.*, **15**, 75 (1956)
47. Caster, W. O., and Armstrong, W. D., *Radiation Research*, **5**, 189 (1956)
48. Wilde, W. S., and Sheppard, C. W., *Proc. Soc. Exptl. Biol. Med.*, **88**, 249 (1955)
49. Bruce, A. K., and Stannard, J. N., *Radiation Research*, **5**, 471 (1956)
50. Prodi, G., and Miceli, R., *Proc. Soc. Exptl. Biol. Med.*, **88**, 472 (1955)
51. Hennessey, T. J., and Huff, R. L., *Proc. Soc. Exptl. Biol. Med.*, **73**, 436 (1959)
52. Belcher, E. H., Gilbert, I. G. F., and Lamerton, L. F., *Brit. J. Radiol.*, **27**, 387 (1954)
53. Baxter, C. F., Belcher, E. H., Harriss, E. B., and Lamerton, L. F., *Brit. J. Haematol.*, **I**, 86 (1955)
54. Belcher, E. H., Harriss, E. B., and Lamerton, L. F., *Progress in Radiobiology*, 303 (Oliver & Boyd, Edinburgh, Scotland, 557 pp., 1956)
55. Gilbert, C. W., Paterson, E., and Haigh, M. V., *Progress in Radiobiology*, (Oliver & Boyd, Edinburgh, Scotland, 557 pp., 1957)
56. Giuliano, R., *Arkiv Kemi*, **8**, 481 (1955)
57. Bonnichsen, R., and Hevesy, G., *Acta Chem. Scand.*, **9**, 569 (1955)
58. Hevesy, G., and Bonnichsen, R., *Biochemistry of Nitrogen*, 295 (Helsinki, Finland, 1955)
59. Bonnichsen, R., Hevesy, G., and Akeson, A., *Acta Physiol. Scand.*, **34**, 345 (1955)
60. Fedorov, N. A., *Progress in Radiobiology*, 310 (Oliver and Boyd, Edinburgh, Scotland, 557 pp. 1956)
61. Lajtha, L. G., and Suit, H. D., *Brit. J. Haematol.*, **I**, 55 (1955)
62. Suit, H. D., Lajtha, L. G., Ellis, F., and Oliver, R., *Progress in Radiobiology*, 506 (Oliver and Boyd, Edinburgh, Scotland, 557 pp., 1956)
63. Dale, W. M., *Biochem. J. (London)*, **37**, 80 (1942)
64. Dale, W. M., Gray, L. H., and Meredith, W. J., *Phil. Transactions* **242A**, 33 (1949)

65. Dale, W. M., *Ciba Foundation Symposium on Ionizing Radiations and Cell Metabolism*, 25 (J. & A. Churchill Ltd., London, England, 318 pp., 1956)
66. Krebs, H. A., *Ciba Foundation Symposium on Ionizing Radiations and Cell Metabolism*, 103 (J. & A. Churchill, Ltd., London, England, 318 pp., 1956)
67. Okada, S., and Fletcher, G. L., *Radiation Research*, **5**, 588 (1956)
68. Cotzias, G. C., *Progress in Radiobiology*, 41 (Oliver & Boyd Ltd., Edinburgh, Scotland, 557 pp., 1956)
69. Pirie, A., *Ciba Foundation Symposium on Ionizing Radiations and Cell Metabolism*, 38 (J. & A. Churchill Ltd., London, England, 318 pp., 1956)
70. English, J. A., *Research Report NM 006 012 04 100* (Naval Med. Research Inst., 1956)
71. Feinstein, R. N., *Radiation Research*, **4**, 217 (1956)
72. Petersen, D. F., Fitch, F. W., and Dubois, K. P., *Proc. Soc. Exptl. Biol. Med.*, **88**, 394 (1955)
73. Boiron, M., Paoletti, C., and Tubiana, M., *Compt. rend.*, **241**, 1231 (1955)
74. Dubois, K. P., Cochran, K. W., and Doull, J., *Proc. Soc. Exptl. Biol. Med.*, **76**, 422 (1951)
75. Brin, M., and McKee, R. W., *Arch. Biochem Biophys.*, **61**, 384 (1956)
76. Eichel, H. J., *Proc. Soc. Exptl. Biol. Med.*, **88**, 155 (1955)
77. Weiss, C., and Tabachnik, J., *Federation Proc.*, **15**, 538 (1956)
78. Kowlessar, O. D., Altman, K. I., and Hempelmann, L. H., *Arch. Biochem. Biophys.*, **52**, 362 (1954)
79. Kowlessar, O. D., Altman, K. I., and Hempelmann, L. H., *Arch. Biochem. Biophys.*, **54**, 355 (1955)
80. Bacq, Z. M., and Errera, M., *Preliminary Report of the Radiations Committee of U. N. Document A/AC-82/1210* (1956)
81. Goutier-Pirotte, M., and Thonnard, A., *Biochim. et Biophys. Acta*, **22**, 396 (1956)
82. Goutier-Pirotte, M., and Oth, A., *Biochim. et Biophys. Acta*, **22**, 394 (1956)
83. Gordon, E. P., Okada, S., and Hempelmann, L. H., *Radiation Research*, **5**, 479 (1956)
84. Nakao, Y., *Nature*, **172**, 625 (1953)
85. Pelc, S. R., *Nature*, **178**, 359 (1956)
86. Burn, J. H., Kordik, P., and Mole, R. H., *Brit. J. Pharmacol.*, **7**, 58 (1952)
87. Pirie, A., van Heyningen, R., and Boag, J. W., *Biochem. J. (London)*, **54**, 682 (1953)
88. Pirie, A., *Progress in Radiobiology*, 18, (Oliver & Boyd Ltd., Edinburgh, Scotland, 557 pp., 1956)
89. Woodard, H. Q., & Spiers, F. W., *Brit. J. Radiol.*, **26**, 38 (1953)
90. Wilson, C. W., *Brit. J. Radiol.*, **29**, 86 (1956)
91. Nagai, S., Matsuda, H., Akita, K., and Kasue, T., *Med. J. Osaka Univ.*, **5**, (1954)
92. van Bekkum, D. W., Jongefrier, H. J., Nieuwerkerk, H. T. M., and Cohen, J. A., *Brit. J. Radiol.*, **27**, 127 (1954)
93. van Bekkum, D. W., *Ciba Foundation Symposium on Ionizing Radiations and Cell Metabolism*, 77 (J. & A. Churchill, Ltd., London, England, 318 pp. 1956)
94. Goldfeder, A., *Progress in Radiobiology*, 70 (Oliver & Boyd Ltd., Edinburgh, Scotland, 557 pp., 1956)
95. Ord, M. G., and Stocken, L. A., *Brit. J. Radiol.*, **28**, 279 (1954)
96. Fritz-Niggli, H., *Naturwissenschaften*, **42**, 585 (1955)

97. Fritz-Niggli, H., *Naturwissenschaften*, **43**, 113 (1956)
98. Gardella, J. W., and Lichtler, E. J., *Federation Proc.*, **15**, 70 (1956)
99. Mee, L. K., and Stein, G., *Biochem. J. (London)*, **62**, 377 (1955)
100. Laser, H., *Nature*, **176**, 361 (1955)
101. Barron, E. S. G., and Talmadge, P., *Radiation Research*, **5**, 468 (1956)
102. Swallow, A. J., *Progress in Radiobiology*, **317** (Oliver & Boyd Ltd., Edinburgh, Scotland, 557 pp., 1956)
103. Aronson, D. L., Fraser, M. J., and Smith, C. L., *Radiation Research*, **5**, 225 (1956)
104. Hug, O., and Wolf, L., *Progress in Radiobiology*, **23**, (Oliver & Boyd, Ltd., Edinburgh, Scotland, 557 pp., 1956)
105. Strehler, B. L., Harvey, E. N., Chang, J. J., and Cormier, M. J., *Proc. Natl. Acad. Sci., U. S.*, **40**, 10 (1954)
106. Tahmisian, T. N., and Wright, B. J., *Federation Proc.*, **15**, 184 (1956)
107. Dowlen, R. N., and Walker, J. K., *Proc. Soc. Exptl. Biol. Med.*, **90**, 398 (1955)
108. Klein, J. R., *Proc. Soc. Exptl. Biol. Med.*, **91**, 630 (1956)
109. Höhne, G., Kunkel, H. A., Maass, H., and Rathgen, G. H., *Progress in Radiobiology* (Oliver & Boyd Ltd., Edinburgh, Scotland, 557 pp., 1957)
110. Ungar, F., Rosenfeld, G., Dorfman, R. I., and Pincus, G., *Endocrinology*, **56**, 30 (1955)
111. Rosenfeld, G., Ungar, F., Dorfman, R. I., and Pincus, G., *Endocrinology*, **56**, 27 (1955)
112. Gordon, S. A., *Progress in Radiobiology*, **44** (Oliver & Boyd Ltd., Edinburgh, Scotland, 557 pp., 1956)
113. Hevesy, G., *Nature*, **164**, 269 (1949)
114. Holmes, B. E., and Mee, L. K., *Brit. J. Radiol.*, **25**, 273 (1952)
115. Forssberg, A., *Ciba Foundation Symposium on Ionizing Radiations and Cell Metabolism*, 212 (J. & A. Churchill, Ltd., London, 318 pp., 1956)
116. Butler, J. A. V., Cohn, P., and Crathorn, A. R., *Progress in Radiobiology*, (Oliver & Boyd Ltd., Edinburgh, Scotland, 557 pp., 1957)
117. Hokin, M. R., and Hokin, L. E., *J. Biol. Chem.*, **219**, 85 (1956)
118. Forssberg, A., *Acta Radiol.*, Suppl. 49, P. E. Norstedt & Sons, Stockholm, Sweden, 143 pp., 1943)
119. Moore, E. C., and McDonald, M. R., *Radiation Research*, **3**, 38 (1955)
120. Aronson, D. L., Mee, L. K., and Smith, C. L., *Progress in Radiobiology*, **61** (Oliver & Boyd Ltd., Edinburgh, Scotland, 557 pp., 1956)
121. Fluke, D. J., *Brookhaven National Laboratory Quarterly Progress Report*, Jan 1 March 31 (1956)
122. Howard, A., *Ciba Foundation Symposium on Ionizing Radiations and Cell Metabolism* 196 (J. & A. Churchill, Ltd., London, England, 318 pp., 1956)
123. Gaulden, M. E., *Records Genetic Soc. Am.*, No. 25, 651 (1956)
124. Lajtha, L. G., Oliver, R., and Ellis, F., *Progress in Radiobiology*, **54**, (Oliver & Boyd, Edinburgh, Scotland, 528 pp., 1957)
125. Howard, A., and Pelc, S. R., *Heredity, Suppl.* **6**, 216 (1953)
126. Pelc, S. R., and Howard, A., *Radiation Research*, **3**, 135 (1955)
127. Kelly, L. S., and Jones, H. B., *Federation Proc.*, **15**, 108 (1956)
128. Ord, M. G., and Stocken, L. A., *Progress in Radiology*, **65** (Oliver & Boyd Ltd., Edinburgh, Scotland, 557 pp., 1957)
129. Bernstein, M. H., *Nature*, **174**, 463 (1954)
130. Rozendaal, H. M., Bellamy, W. D., and Baldwin, T. H., *Nature*, **168**, 694 (1951)

131. Cole, L. J., and Ellis, M. E., *Radiation Research*, **5**, 252 (1956)
132. Kaufman, B. P., McDonald, M. R., and Bernstein, M. H., *Ann. N. Y. Acad. Sci.*, **59**, 553 (1955)
133. Drew, R., *Radiation Research*, **3**, 116 (1955)
134. Ellis, M. E., and Cole, L. J., *Radiation Research*, **4**, 477 (1956)
135. Cole, L. J., and Ellis, M. E., "Research and Development Technical" Report USN RDL-TR-114 (1956)
136. Steffansen, D., *Radiation Research*, **5**, 597 (1956)
137. Ord, M. G., and Stocken, L. A., *Biochem. J. (London)*, **63**, 3 (1956)
138. Mottram, J. C., *Brit. J. Radiol.*, **8**, 32 (1935)
139. Thoday, J. M., and Read, J., *Nature*, **160**, 608 (1947)
140. Read, J., *Brit. J. Radiol.*, **24**, 635 (1951)
141. Giles, N. H., and Riley, H. P., *Proc. Natl. Acad. Sci., U. S.*, **35**, 640 (1949)
142. Giles, N. H., and Beatty, A. V., *Science*, **112**, 643 (1950)
143. Dowdy, A. H., Bennett, L. R., and Chastain, S. M., *Radiology*, **55**, 879 (1950)
144. Patt, H. M., *Physiol. Revs.*, **33**, 37 (1953)
145. Read, J., *Brit. J. Applied Phys.*, **2**, 331 (1951)
146. Uri, N., *Chem. Rev.*, **50**, 375 (1952)
147. Kimball, R. F., and Gaither, N., *Proc. Soc. Exptl. Biol. Med.*, **80**, 525 (1952)
148. Hearon, J. Z., and Kimball, R. F., *Radiation Research*, **3**, 283 (1955)
149. Kimball, R. F., Hearon, J. Z., and Gaither, N., *Radiation Research*, **3**, 435 (1955)
150. Evans, T. C., *Biol. Bull.*, **92**, 99 (1947)
151. Feinstein, R. N., Cotter, G. J., and Hampton, M. M., *Am. J. Physiol.*, **177**, 156 (1954)
152. Baxendale, J. H., and Smithies, D. H., *Z. physik. Chem. (Neue Folge)*, **7**, 242 (1956)
153. Horgan, V. J., and Philpot, J. St. L., *Radiobiology Symposium, 1954*, 26 (Butterworth & Co., London, England 362 pp., 1955)
154. Latarjet, R., *Ciba Foundation Symposium on Ionizing Radiations and Cell Metabolism*, 275 (J. & A. Churchill, Ltd., London, England, 318 pp., 1956)
155. Laser, H., *Nature*, **174**, 753 (1954)
156. Tahmisan, T. N., and Devine, R. L., *Radiation Research*, **3**, 182 (1955)
157. Bellamy, W. D., and Lawton, E. J., *Ann. N. Y. Acad. Sci.*, **59**, 595 (1955)
158. Laser, H., *Ciba Foundation Symposium on Ionizing Radiations and Cell Metabolism*, 106 (J. & A. Churchill, Ltd., London, England, 318 pp., 1956)
159. Alper, T., and Howard-Flanders, P., *Nature*, **178**, 978 (1956)
160. Howard-Flanders, P., Moore, D., and Wright, E. A., *Progress in Radiobiology*, 456 (Oliver & Boyd Ltd., Edinburgh, Scotland, 557 pp., 1956)
161. Alper, T., *Radiation Research*, **5**, 573 (1956)
162. Butler, J. A. V., and Conway, B. E., *J. Chem. Soc.*, **3418** (1950)
163. Conway, B. E., *Brit. J. Radiol.*, **27**, 42 (1954)
164. Scholes, G., and Weiss, J., *Brit. J. Radiol.*, **27**, 47 (1954)
165. Wilkinson, R. W., and Williams, T. F., *Progress in Radiobiology*, 82 (Oliver & Boyd Ltd., Edinburgh, Scotland, 557 pp., 1956)
166. Scholes, G., and Weiss, J., *Progress in Radiobiology*, 93 (Oliver & Boyd Ltd., Edinburgh, Scotland, 557 pp., 1956)
167. Andersen, R. S., *Brit. J. Radiol.*, **27**, 50 (1954)
168. Loiseleur, J., *Ann. Inst. Pasteur*, **84**, 1601 (1953)
169. Alper, T., *Brit. J. Radiol.*, **27**, 50 (1954)
170. Bachofer, G. S., and Pottinger, M. A., *J. Gen. Physiol.*, **40**, 289 (1956)

171. Nakao, Y., *Progress in Radiobiology*, 363 (Oliver & Boyd, Edinburgh, Scotland, 557 pp., 1956)
172. Nakao, Y., *Annot. Zool. Jap.*, **25**, 187 (1952)
173. Mendelsohn, M. L., *Am. J. Physiol.*, **180**, 599 (1955)
174. Wolff, S., and Luippold, H. E., *Progress in Radiobiology*, 217 (Oliver & Boyd, Ltd., Edinburgh, Scotland, 557 pp., 1956)
175. Patt, H. M., *Ann. N. Y. Acad. Sci.*, **59**, 649 (1955)
176. Hall, B. V., *Cancer Research*, **12**, 268 (1952)
177. Scott, O. C. A., *Brit. J. of Cancer*, **11**, 130 (1957).
178. Phillips, A. F., and Cater, D. B., *Progress in Radiobiology*, 275 (Oliver & Boyd, Edinburgh, Scotland, 557 pp., 1956)
179. Phillips, A. F., *Progress in Radiobiology*, 459 (Oliver & Boyd, Ltd., Edinburgh, Scotland, 557 pp., 1956)
180. Gray, L. H., Conger, A. D., Ebert, M., Hornsey, S., and Scott, O. C. A., *Brit. J. Radiol.*, **26**, 638 (1953)
181. Thomlinson, R. H., and Gray, L. H., *Brit. J. Cancer*, **9**, 539 (1955)
182. Howard-Flanders, P., and Wright, E. A., *Nature*, **175**, 428 (1955)
183. Patt, H. M., Straub, R. L., Blackford, M. E., and Smith, D. E., *Am. J. Physiol.*, **163**, 740 (1950)
184. Gerebtzoff, M. A., and Bacq, Z. M., *Experientia*, **10**, 341 (1954)
185. Bacq, Z. M., *Progress in Radiobiology*, 160 (Oliver & Boyd Ltd., Edinburgh, Scotland, 557 pp., 1957)
186. Eldjarn, L., and Pihl, A., *J. Biol. Chem.*, **223**, 341 (1956)
187. Koch, R., and Hagen, U., *Progress in Radiobiology*, 246 (Oliver & Boyd, Edinburgh, Scotland, 557 pp., 1956)
188. Doherty, D. G., and Burnett, W. T., *Proc. Soc. Exptl. Biol. Med.*, **89**, 312 (1955)
189. van Bekkum, D. W., and de Groot, J., *Progress in Radiobiology*, 243 (Oliver & Boyd Ltd., Edinburgh, Scotland, 557 pp., 1956)
190. Hollaender, A., and Doudney, C. O., *Radiobiology Symposium, Liege 1954*, 112 (Butterworth & Co., London, England, 362 pp., 1955)
191. Jennings, F. L., and Tessmer, C. F., *Radiation Research*, **5**, 606 (1956)
192. Eldjarn, L., and Pihl, A., *Progress in Radiobiol.*, 249 (Oliver & Boyd Ltd., Edinburgh, Scotland, 557 pp., 1956)
193. Pihl, A., and Eldjarn, L., *Progress in Radiobiology*, 147 (Oliver & Boyd Ltd., Edinburgh, Scotland, 557 pp., 1957)
194. Koch, R., *Progress in Radiobiology* (Oliver & Boyd, Edinburgh, Scotland, 557 pp., 1957)
195. Gordy, W., Ard, W. B., and Shields, H., *Proc. Natl. Acad. Sci., U.S.*, **41**, 1983 (1955)
196. Alexander, P., and Charlesby, A., *Radiobiology Symposium, 1954 (Liege)*, 49, (Butterworth & Co., London, England, 362 pp., 1955)
197. Lefort, M., and Ehrenberg, L., *Ark. Botan.*, **3**, Article 7, 121 (1955)
198. Caldecott, R., *Radiation Research*, **3**, 316 (1955)
199. Ehrenberg, L., *Progress in Radiobiology*, 114 (Oliver & Boyd Ltd., Edinburgh, Scotland, 557 pp., 1956)
200. Svedberg, T., and Brohult, S., *Nature*, **143**, 938 (1939)
201. Setlow, R. B., and Doyle, B., *Radiation Research*, **2**, 15 (1955)
202. Cox, R. A., Overand, W. G., Peacocke, A. R., and Wilson, S., *Nature*, **176**, 919 (1955)

BIOCHEMICAL EFFECTS OF IONIZING RADIATION 133

203. Hagen, U., and Koch, R., *Progress in Radiobiology*, 257 (Oliver & Boyd Ltd., Edinburgh, Scotland, 557 pp., 1956)
204. Lacassagne, A., Duplan, J. F., and Buu-Hoi, N. P., *Compt. rend.*, **238**, 1279 (1954)
205. Bonet-Maury, P., and Patti, F., *J. Radiol. Electrol.*, **35**, 851 (1954)
206. Konecci, E. B., Taylor, W. F., and Wilks, S. S., *Radiation Research*, **3**, 157 (1955)
207. Hollaender, A., and Kimball, R. F., *Nature*, **177**, 726 (1956)
208. Gray, L. H., *Progress in Radiobiology*, 267 (Oliver & Boyd, Edinburgh, Scotland, 557 pp., 1956)
209. Forssberg, A., and Nybom, N., *Physiol. Plantarum*, **6**, 78 (1953)
210. Bacq, Z. M., and Herve, A., *Bull. acad. roy. méd. Belg.*, (6), **17**, 13 (1952)
211. Stapleton, G. F., Billen, D., and Hollaender, A., *J. Bacteriol.*, **63**, 805 (1952)
212. Patt, H. M., Blackford, M. E., and Straube, R. L., *Proc. Soc. Exptl. Biol. Med.*, **80**, 92 (1952)
213. Cater, D. B., *Progress in Radiobiology*, 276, (Oliver & Boyd Ltd., Edinburgh, Scotland, 557 pp., 1956)
214. Bacq, Z. M., Cuypers, Y., Evrard, E., and Soetens, R., *Compt. rend. soc. biol.*, **149**, 2014 (1955)
215. Salerno, P. R., Uyeki, E., and Friedell, H. L., *U. S. Atomic Energy Commission Document NYO 4924* (1955)
216. Devik, F., and Lothe, F., *Acta Radiol.*, **44**, 243 (1955)
217. Lothe, F., and Devik, F., *Brit. J. Radiol.*, **44**, 206 (1955)
218. Auerbach, C., *Progress in Radiobiology*, 277, (Oliver & Boyd, Ltd., Edinburgh, Scotland, 557 pp., 1956)
219. Nakao, Y., Tazima, Y., and Sugimura, T., *Radiation Research*, **3**, 400 (1955)
220. Lacassagne, A., *Compt. rend.*, **215**, 231 (1942)
221. Hempelmann, L. H., Trujillo, T. T., and Knowlton, N. P., *A.E.C.U. 239* (1949)
222. Storer, J. B., and Hempelmann, L. H., *Am. J. Physiol.*, **171**, (1952)
223. Baclesse, F., and Marios, M., *Compt. rend.*, **238**, 1926 (1954)
224. Hornsey, S., *Progress in Radiobiology* 248 (Oliver & Boyd Ltd., Edinburgh, Scotland, 557 pp., 1957)
225. Künkel, H. A., Höhne, G., and Maass, H., *Progress in Radiobiology*, 176 (Oliver & Boyd Ltd., Edinburgh, Scotland, 557 pp., 1957)
226. Jacobsen, L. O., Simons, E. L., Marks, E. K., Robson, M. J., Berthard, W. F., and Gaston, E. O., *J. Lab. Clin. Med.*, **35**, 746 (1950)
227. Ford, C. E., Hamerton, J. L., Barnes, D. W. H., and Loutit, J. F., *Nature*, **177**, 452 (1956)
228. Stapleton, G. E., Billen, D., and Hollaender, A., *J. Cellular Comp. Physiol.*, **41**, 345 (1953)
229. Hollaender, A., *Bull. Atomic Scientists*, **12**, 76 (1956)
230. Forssberg, A., *Progress in Radiobiology*, 171 (Oliver & Boyd Ltd., Edinburgh, Scotland, 557 pp., 1956)
231. Stapleton, G. E., Woodburg, D. H., and Hollaender, A., *Radiation Research*, **5**, 598 (1956)
232. Kumta, U. S., Gurnami, S. U., and Sahasrabudhe, M. N., *Current Sci. (India)*, 362 (1955)
- 232a. Nerurka, M. K., Baxi, A. J., Ranadive, N. S., Nerurka, M. V., and Sahasrabudhe, M. B., *Nature*, **180**, 193 (1957)

233. Kimball, R. F., Gaither, N., and Wilson, S. M., *Radiation Research*, **5**, 486 (1956)
234. Sandler, O. E., *Acta Med. Scand.*, Suppl. 225 (1949)
235. Brohult, A., and Holmberg, J., *Nature*, **174**, 1102 (1954)
236. Edlund, T., *Nature*, **174**, 1102 (1954)
237. Brohult, A., *Progress in Radiobiology*, 241 (Oliver & Boyd Ltd., Edinburgh, Scotland, 457 pp., 1957)
238. Johnson, B. C., and Motta, V. C., *Federation Proc.*, **15**, 907 (1956)
239. Alexander, H. D., Day, E. J., Sauberlich, H. E., and Salmon, W. D., *Federation Proc.*, **15**, 921 (1956)
240. Richardson, L. R., Woodworth, P., and Coleman, S., *Federation Proc.*, **15**, 924 (1956)
241. Hannan, R. S., and Shepherd, H. J., *Trans. Faraday Soc.*, **49**, 326 (1953)
242. Hannan, R. S., and Shepherd, H. J., *Brit. J. Radiol.*, **27**, 36 (1954)
243. Andrews, J. S., Mead, J. F., and Griffith, W. H., *Federation Proc.*, **15**, 918 (1956)
244. Mackinney, G., *Project No. 7-84-0-002 Contract DA-19-129-Gm-254* (1956)
245. Kertesz, Z. I., Morgan, B. H., Tuttle, L. W., and Lanvin, M., *Radiation Research*, **5**, 372 (1956)
246. Tappel, A. L., *Report, P.B.-121307* (U. S. Dept. of Commerce, Washington, D. C., 1956)
247. Hannan, R. S., *Special Report*, 61 (Dept. Sci. Ind. Research, Food Invest., London, 1955)
248. Schweigert *et al.*, *P.B.-121309* (1956)
249. Doty, D. M., and Wachter, J. F., *Agricultural and Food Chemistry*, **3**, 61 (1955)
250. Green, D. E., *Project No. 7-84-01-002* (Quartermaster Food and Container Institute for the Armed Forces, Chicago) (1955)
251. Batzer, H., and Doty, D. M., *Agricultural and Food Chemistry*, **3**, 64 (1955)

VERTEBRATE RADIOBIOLOGY (LETHAL ACTIONS AND ASSOCIATED EFFECTS)^{1,2,3,4}

V. P. BOND AND J. S. ROBERTSON

Medical Department, Brookhaven National Laboratory, Upton, L.I., New York

This review is confined principally to works which deal with physical and biological factors of importance in attempts to quantify the complex lethal and associated actions of ionizing radiations in mammals. The related subjects of physiological and biochemical mechanisms of action of ionizing radiation are dealt with extensively in other reviews (1 to 5). Additional general sources of information have been published recently. Among these are two excellent books on radiobiology (6, 7). The report of the International Conference on the Peacetime Uses of Atomic Energy (8), held in Geneva in 1955, makes available data from many countries. Reports of other international meetings (9 to 13), and the monograph of Rajewsky [in German (14)], are pertinent. Reports of early work on the Manhattan and other Projects, previously available only as individual government documents, have now been collected in book form (15, 16, 17). Reports on the effects of the atomic bombs detonated in Japan have now been published in book form (18, 19). An exhaustive treatise by the Japanese on bomb radiations and their effects has been published (20), as has the complete report on the Marshallese accidentally exposed to fallout radiations in March, 1954 (21). Reports on human beings involved in reactor accidents are now readily available (8, 22). The American (23) and British (24) reports on the biological effects of atomic radiations reflect the general concern regarding, and attempt to evaluate, the possible health hazards associated with various uses of nuclear and x-radiations. A preliminary statement of revised maximum permissible radiation exposures to man is now available (25). Radiation exposures from necessary medical and dental procedures are assumed to have no effect on one's tolerance status. The United Nations Scientific Committee on Effects of Atomic Radiation has outlined the responsibilities of the medical profession with regard to the use of x-rays and other ionizing radiation (26). It has been proposed that complete records of cumulative exposure be kept for each individual (27).

¹ The survey of literature pertaining to this review was completed in February, 1957.

² Research was supported by the U. S. Atomic Energy Commission.

³ The authors are indebted to Marjorie Comstock, Brookhaven Research Library, for her excellent bibliographic assistance.

⁴ The following abbreviations are used in this chapter: HVL (half value layer), LET (lineal energy transfer), kvp (kilovolt peak), MEA (mercaptoethyl-amine), RBE (relative biological effectiveness), TSD (target to skin distance).

DOSIMETRY

Considerable emphasis continues to be placed on dosimetric problems, both from the standpoint of accurate evaluation and comparison of radiotherapy and radiobiological data, and for accurate hazard evaluation in man (28 to 36). The recent book by Hine & Brownell (37) makes available a unified presentation of facts, theories, and practical aspects pertinent to the determination of the amount of energy absorbed in a medium exposed to ionizing radiations. In this book, as in other recent radiobiological literature (28 to 32), the emphasis has been to express dose as recommended by the International Committee on Radiation Units (ICRU) in terms of the tissue dose in roentgens, or better, in terms of the absorbed dose in rads (38). The air dose, however, with insufficient data given with which to calculate rads or even the tissue dose or rads, is still the unit most commonly used by radiobiologists for expressing radiation dose. A number of papers provide the distribution of dose throughout the tissues in relative terms, yet give absolute values for the exposure in terms of air dose only with no air dose to tissue dose conversion factor provided. It is considered desirable initially to define dosimetric terms employed. Recommendations of the ICRU are followed as closely as possible; however some terms used in earlier (but not in the latest) recommendations of the committee have been retained for simplicity.

The *roentgen* retains its original definition in terms of a quantity of ionization in air (38). The *air dose* (termed exposure dose in air in NBS handbook 62) is expressed in roentgens and refers to the dose measured essentially free in air, in the absence of the biological specimen, exposure equipment or other scattering material. *Tissue dose* (termed exposure dose with scatter in NBS handbook 62) also expressed in roentgens, refers to the dose indicated by a roentgen meter embedded in the biological material (or equivalent phantom) at the site of interest. The tissue dose may differ greatly from the air dose because of buildup and scatter within the exposed materials. The tissue dose can be converted to *absorbed dose* in rads by means of tables or curves relating energy absorption in air to that in tissue (36 to 39). The conversion factor varies with beam energy and type of tissue, and the British (36) and American (37, 39) conversion factors differ by a few per cent. It is perhaps unfortunate that adoption of the rad was recommended before complete agreement on how to convert to rads in practice was achieved. Over the range of energies commonly used in mammalian radiobiological work, 200 kvp to 2000 kvp or Co⁶⁰ gamma radiation, the tissue dose (but not necessarily the air dose) is equal, within 5 per cent, to the absorbed dose in rads for soft tissue (36 to 39). Calorimetric methods are being employed to determine accurately the absorbed dose [(40, 41, 42), Adams *et al.* (8)].

The adoption of the rad represents a step forward in that, unlike the previous "rep" and "energy unit," it provides a physical unit for absorbed dose which (a) is clearly and arbitrarily defined, and (b) avoids the confusing implication in the use of the rep of being "equivalent" to the roentgen. How-

ever, it cannot be regarded as curing the many ills rightly or wrongly ascribed to use of the roentgen or rep. Most of the available monitoring instruments measure roentgens in air, and the factor for conversion to tissue dose, let alone absorbed dose, will be unknown under many practical circumstances. Even when tissue dose and absorbed dose can be considered to be known, it becomes difficult to decide, in a complex organism with markedly heterogeneous dose distribution, what number best describes "the" dose received by the organism. Thus the air dose, under many practical situations, may be the most sensible parameter to use.

Berger & Doggett (43) have used the methods of Spencer and Fano in the theoretical treatment of dose distribution within large masses of materials. Unfortunately, the specific geometry representing a human being has not been dealt with as yet (28). While depth-dose patterns in large phantoms for x-rays or various energies are easily available, such curves for only a very few γ -radiations have been determined (21, 28, 44).

Techniques for measurement of dose in neutron, and in neutron and gamma fields have been described (2, 45 to 50). Calculations of dose from threshold-detector measurement of flux, and from proportional counter and other measurements appear to agree favorably with estimates using tissue equivalent chambers (46, 47, 51). The specific energy loss from heavy particles in tissue has been considered further (52, 53, 54), and depth dose and flux curves for neutrons in tissue have been calculated and measured (31, 55 to 58).

ACUTE MORBIDITY AND MORTALITY

LD_{50} values.—Many LD_{50} values have been published since the last review by Thomson (1). Sufficient data now are available to allow tentative generalizations not previously obvious. A representative list of published $LD_{50}/30$ day values is presented in Table I. Additional references to LD_{50} values not listed in the table are: mice and rats (16, 17, 59, 60, 61), hamster (17), monkey (17, 62, 63), and dogs (17, 64, 65). Additional LD_{50} values for the guinea pig will be discussed subsequently.

Several conclusions can be derived from the table. Most striking, perhaps, is the apparently clear demarcation of LD_{50} values, expressed as mid-line absorbed dose, between small and large animals. The air doses, also listed in the table, do not reveal this relationship. The LD_{50} for all large species studied is approximately 250 rads or less for x-rays under conditions of uniform dose distribution in the tissues; that for small species is approximately double this value or greater.

The degree to which air dose distorts the relationship of LD_{50} values among species is accentuated by the fact that, as irradiations are usually carried out, the tissue dose is considerably greater than the air dose with small species (guinea pig or smaller), approximately equal with medium-sized species (rabbit, monkey), and considerably smaller with large species

TABLE I
LD₅₀ VALUES FOR MAMMALS*

Species	Radiation Used	Radiation Factors	LD ₅₀ Value		Ref. No.
			Air dose (r)	Absorbed dose (rad)	
Mouse	250 kvp x-ray	0.5 mm. Cu, 1 mm. Al HVL 1.6 mm. Cu	362† to 443†	521† to 638†	(66)
	200 kvp x-ray	0.25 mm. Cu, 1 mm. Al HVL 0.8 mm. Cu	405	558†	(67)
	Bomb gamma	High energy and dose rate	759	666†	(68)
Rat	200 kvp x-ray	0.45 mm. Cu, 1 mm. Al HVL 1 mm. Cu	665	815†	(69)
	200 kvp x-ray	0.5 mm. Cu, 1 mm. Al HVL 1.05 mm. Cu	640	796†	(70)
Ground Squirrel	250 kvp x-ray	0.25 mm. Cu, 1 mm. Al HVL 0.9 mm. Cu	700	>700†	(71)
Hamster	2000 kvp x-ray	HVL 5 mm. Pb	800	>800†	(72)
	250 kvp x-ray	0.5 mm. Cu, 1 mm. Al HVL 1.6 mm. Cu	460†	586†	(73)
	200 kvp x-ray	0.25 mm. Cu, 0.5 mm. Al HVL 1.5 mm. Cu	700	>700†	(74)
Guinea Pig	200 kvp x-ray	0.25 mm. Cu, 1.0 mm. Al HVL 0.8 mm. Cu	337	400†	(34)
	186 kvp x-ray	0.25 mm. Cu, 1.0 mm. Al HVL 0.8 mm. Cu (crossfire exposure)	400	380†	(75)
	Co ⁶⁰ gamma	Multiple sources	500	490†	(76)
	1.10 Mev (50%)	Dose rate 70 r/min (4x exposure)			
	1.33 Mev (50%)				
Rabbit	200 kvp x-ray	0.5 mm. Cu, 1.0 mm. Al HVL 0.98 mm. Cu (bilateral exposure)	800	735†	(16)
	250 kvp x-ray	3.25 mm. Cu HVL 3.4 mm. Cu (Multiport exposure)	805	751†	(32)
	250 kvp x-ray	Parabolic filter HVL 2.0 mm. Cu (Crossfire exposure)	700†	680†	(77)
	Co ⁶⁰ gamma 1.10 Mev (50%) 1.33 Mev (50%)	HVL 5.1 cm. Al Dose rate 50 r/hr (Multiple sources)	1094	911†	(78)
Monkey	250 kvp x-ray	HVL 1.6 mm. Cu Dose rate 3 r/min. (Bilateral exposure)	760†	546†	(79)
	250 kvp x-ray	0.5 mm. Cu, 1.0 mm. Al HVL 1.0 mm. Cu (Animals rotated)	550	522†	(80)
Dog	250 kvp x-ray	0.5 mm. Cu, 1.0 mm. Al HVL 1.5 mm. Cu (Bilateral exposure)	281	244†	(31)
	1000 kvp x-ray	HVL 2.0 mm. Pb (Bilateral exposure)	304	250†	(28)
	2000 kvp x-ray	HVL 4.3 mm. Pb (Bilateral exposure)	312	260†	(81)
	Co ⁶⁰ gamma 1.17 Mev (50%) 1.33 Mev (50%)	HVL 5.1 cm. Al (Bilateral exposure)	465†	303†	(82)
	250 kvp x-ray	14.2 mm. Al Parabolic filter, 0.5 mm. Cu HVL 2.15 mm. Cu (Unilateral exposure)	450	322†	(28)
	Bomb gamma	High energy and dose rate	271	250†	(83)

* See text for additional explanatory material relating to the table.

† Value not given in work cited. Calculated or estimated from data given.

TABLE I (Continued)

Species	Radiation Used	Radiation Factors	LD ₅₀ Value		Ref. No.
			Air dose (r)	Absorbed dose (rad)	
Swine	1000 kvp x-ray	HVL 2.0 mm. Pb (Bilateral exposure)	510	247†	(28)
	2000 kvp x-ray	HVL 4.3 mm. Pb (Bilateral exposure)	388	237†	(84)
	2000 kvp x-ray	HVL 4.3 mm. Pb (Unilateral exposure)	500	305†	(84)
	Bomb gamma	High energy and dose rate	225	187†	(85)
Sheep	Co ⁶⁰ gamma 1.17 Mev (50%) 1.33 Mev (50%)	HVL 5.1 cm. Al Dose rate 50 r/hr (Multiple sources)	618	242†	(86)
	Nb ⁹⁵ and Zr ⁹⁵ gammas 0.73 Mev (93%) 0.23 Mev (7%)	HVL 3.9 cm. Al Dose rate 20 r/hr (Multiple sources)	524	205†	(87)
Goat	200 kvp x-ray	0.5 mm. Cu, HVL 0.98 mm. Cu (Bilateral exposure)	350	237†	(88)
Burro	Co ⁶⁰ gamma 1.17 Mev (50%) 1.33 Mev (50%)	HVL 5.1 cm. Al Dose rate 50 r/hr (Multiple sources)	784	306†	(86)
	Ta ¹⁸² gamma 1.22 Mev (57%) 1.13 Mev (37%) 0.2 Mev (6%)	HVL 4.3 cm. Al Dose rate 20 r/hr (Multiple sources)	651	256†	(89)
	Nb ⁹⁵ -Zr ⁹⁵ gamma 0.73 Mev (93%) 0.23 Mev (7%)	HVL 3.9 cm. Al Dose rate 20 r/hr (Multiple sources)	585	229†	(87)
Man	Fallout gamma 1.5 Mev (19%) 0.75 Mev (51%) 0.1 Mev (24%)	Dose rate variable (Plane field)	350 (?)	300 (?)	(21)

† Value not given in work cited. Calculated or estimated from data given.

All dose rates used were of the order of 5 to 60 r/min., and all exposures were unilateral unless otherwise noted. The LD₅₀ values in rads represent the absorbed dose in soft tissue at the center (midline) of the animal. The dose in rads was estimated as follows: the tissue dose in r was first estimated, if not given, from the air dose by estimating all scattered radiations and taking into account the geometry of the exposure conditions used (28). Scatter can be approximated from standard depth-dose data (28, 35, 67, 90). The present authors duplicated as nearly as possible many of the experimental conditions and used the air/tissue dose ratio thus obtained. The tissue dose obtained represents the dose a dosimeter would indicate if it were embedded in tissue (or phantom material). The tissue dose in r was converted to absorb dose in rads, using the appropriate soft-tissue conversion factor (37, 38, 39). The conversion from air to tissue dose is an approximation made in many cases from incomplete physical data, and the conversion factors from tissue dose to rads are still open to question (see above). Additional details of the conversion used for any of the situations will be furnished on request. Total scatter varied with essentially full scatter, from less than 5 per cent of the air dose with Co⁶⁰ gammas to approximately 45 per cent with 250 kvp or lower energy x-rays (28, 90, 91). Ellinger quotes the LD₅₀/14 day value for guinea pigs, which is not significantly different from his LD₅₀/30-day value. Depth-dose measurements under the unusual geometrical conditions of the Oak Ridge multicurie γ -ray exposure field were made by the present authors in collaboration with Col. Bernard Trum. The large ratios, air dose/midline absorbed dose, obtained for burros, sheep, and swine result principally from geometrical factors (28). In most positions, occupied by the exposed large animals, over 50 per cent of the dose is received from a target to skin distance of less than 1.5 m.; thus inverse square fall off is appreciable. Large animals standing in the field receive much of the dose at the midpoint in the animal from the anterior or posterior directions, as opposed to the transverse (shorter) axis with bilateral irradiation in the laboratory (this would not apply to an upright man). All midline doses probably are maximal for an acute LD₅₀ value, since if the data for the effect of dose rate on LD₅₀ in the rat (92) apply to the larger species, the values should be further reduced by a factor of approximately 0.8 to allow comparison with radiation delivered in the course of minutes. The values should be also reduced further for comparison with x-ray LD₅₀ values because of the apparently reduced effectiveness of γ radiation relative to x-radiation (2). The LD₅₀ value for man can be considered only a rough approximation, since the dose is poorly known and there was no mortality in the exposed group (see below).

(dog or larger). The degree of discrepancy between air and tissue dose varies considerably with the exact geometry of the conditions used, but in general the discrepancy becomes larger as animal size becomes greater and the beam energy becomes lower.

The tissue dose LD₅₀ values for small animals presently available are all between the limits of approximately 400 and 800 rads for x-radiation, and between the limits of approximately 550 and 800 rads if the guinea pig is excluded. It is probable that the differences might be smaller if different species were irradiated such that the relative dose distributions through the body were identical. The monkey falls in the category of small animals, and thus cannot be considered, radiobiologically or hematologically (81), to be any "closer" to man than any other small species. It is difficult to simulate man quantitatively in total-body radiation studies with animals smaller than man [Table I and ref. 28]. The dog is not large enough for direct comparison. It is also clear from the table that if the LD₅₀ is desired for a given species under specific exposure conditions, the desired species and conditions must be adhered to rigidly to obtain meaningful quantitative results.

The LD₅₀ for the guinea pig appears to be higher than usually quoted, and the point requires further investigation. The mortality data on guinea pigs furnished by several previous investigators (16, 93 to 96) is often difficult to evaluate accurately regarding the LD₅₀ value in rads because of dosimetric and statistical difficulties, and the possible effects of animal strain and of possible disease in some of the animals used (16, 34, 76).

The data quoted in Table I strongly indicate that the guinea pig may not be the most sensitive of all mammals. It appears quite likely that man may be among the most sensitive. It appears also that the rabbit may not be the most resistant of mammals, but falls among the values for other small or medium-sized species in terms of sensitivity.

The uniformity of LD₅₀ values among strains and species is remarkable for large animals exposed under similar geometrical conditions. (Again, the higher LD₅₀ values for animals exposed to γ -radiations should be further adjusted for RBE and dose rate factors before strict comparisons with x-ray data are made.) This may result in part from the fact that large animals, unlike small, provide their own constant, maximum scatter situation.

Acute radiation effects in man.—If the data presented above for large animals apply also to man, one would expect the midline absorbed dose acute LD₅₀ for man to be of the order of 250 rads. This is in accord with the relatively low value estimated from the Marshallese exposed to fallout γ -radiation (21, 28), and would indicate that the value lies well below the 450 rad air dose commonly quoted. Recent data on patients treated with whole body radiation tend also to indicate this low value (28, 97, 98). Blair (99) has extrapolated from the same Marshallese data referred to above and concludes that the LD₅₀ (air dose) for man probably is not below 400 r. Both authors using the Marshallese findings employ data from animals in

the extrapolations and both emphasize the large uncertainty and possible error in the quantities deduced.

Data recently available on the effects of large doses of radiation on human beings have been referred to in the introductory section above (8, 18 to 22). In all instances, data are insufficient to allow an accurate estimate of the LD₅₀ for man (21, 100). The difficulties of evaluating and interpreting the complicated dosage situations with the reactor accidents have been discussed (22).

FACTORS AFFECTING THE DEGREE OF RESPONSE

Dosimetry.—The difficulties of measuring and properly recording radiation dose, on which the degree of response is highly dependent, have been dealt with above.

Energy dependence.—A true dependence of biological response on energy, resulting from differences in physical parameters such as specific ionization, can be determined only under conditions where accurate dosimetry is possible, and where the dose throughout the mammal is as uniform as possible. Kohn (30), fulfilling this condition in mice, has shown that 1000 kvp x-rays are less effective than 250 kvp x-rays by a factor of 0.8, using acute mortality in the mouse. This confirms earlier, less well-documented values indicating decreasing effectiveness for small animals over the range of 200 to 2000 kvp (2). There is evidence (Table I and ref. 2) that high energy γ -radiations in the laboratory may be even less effective (factor of approximately 0.6 or 0.7). A second type of dependence on energy, resulting from differences in penetrability is discussed below under "Pattern of dose deposition."

Geometry of exposure.—It has been shown (28) that with large animals the ratio of air dose to tissue dose will vary greatly depending on the precise conditions used. It is also shown that except for exposure with a "point source" from one side (unilateral exposure), all more complicated techniques (bilateral, multiport, rotational, crossfire, ring, "4 π " or plane field) produce, in terms of tissue dose, essentially the same dose distributions in a large tissue mass.

Pattern of dose deposition.—Radiations of even relatively high energy fall off rapidly in tissue and thus with unilateral exposure the exit tissue dose may be only a fraction of the incident tissue dose. This fall-off may be quite appreciable for an animal the size of the rabbit (16). Ellinger (67) has shown, in the mouse, that a more penetrating radiation given unilaterally results in a lower LD₅₀ (air dose, measured in identical way with both energies) than does a less penetrating radiation. The radiations compared were 200 and 140 kvp, for which no intrinsic or real energy dependence has been demonstrated. Michaelson *et al.* (quoted in ref. 28) compared 1000 and 250 kvp x-rays administered unilaterally and found little difference. The depth dose patterns in a dog phantom are remarkably similar with these radiations (101). Tullis (84) has shown that unilateral radiation in swine is less effective than the same radiations administered bilaterally in the swine. There is no

doubt that a less penetrating radiation (leaving some tissue on the distal side with relatively little exposure) is less effective than radiation with a more even tissue distribution. This would be anticipated from the known protective effect of relatively uninjured marrow (102).

The effect on LD_{50} of decreasing beam energy, under conditions of exposure such that the distribution of dose was as uniform as possible (but still not uniform with softer radiations) has been investigated systematically (32). The lower the energy, and the larger the species (mice and rabbits were used), the larger the LD_{50} , expressed as air or absorbed dose, becomes. A sharp rise in LD_{50} occurs at approximately 80 kvp in the mouse, and at higher energies for the rabbit (32) and dog (103). This "energy dependence" of effect, in terms of which the "RBE" of radiations is frequently quoted, is seen to be really an apparent energy dependence; if the radiation cannot penetrate to vital tissues, "energy dependence" of effect becomes essentially meaningless. The extreme of this phenomenon is represented with external β -radiation, with a very high LD_{50} value. It has nothing to do with true energy dependence of effect, with specific ionization, or with RBE in the stricter use of the term.

Because of the wide discrepancy of LD_{50} values in terms of monitored air dose under conditions of nonuniform dose deposition, a dose unit has been sought that might normalize LD_{50} values. Claims have been made that the integral dose (average tissue dose multiplied by the total grams of tissue exposed), or the exit tissue dose may normalize the LD_{50} values for such situations. Grahn, Sacher & Walton (32) have shown conclusively that integral dose is of no value in this regard (see below for further discussion of integral dose). Ellinger (67) has proposed the use of the exit tissue dose in this regard. He compared the effects of 140 and 200 kvp x-rays, which produced LD_{50} ratios for mice of 112/100 in terms of air dose, and produced relative exit tissue dose ratios of 100/121 when equal air doses for the two energies were compared. For the exit dose to be the normalizing parameter, one ratio should be equal to the reciprocal of the other. He considers the agreement "reasonable"; however, a comparison of other possible parameters, using his data, reveals the following (ratio of LD_{50} values for 140 and 200 kvp x-rays): air dose, 1.12; entrance tissue dose, 1.08; midline tissue, 1.0; exit tissue dose, 0.93. Very similar results were obtained with dogs exposed unilaterally to radiations of two different qualities (28). Potter (104) claimed advantages to the exit dose using lethality in rats. However, the data presented allow only qualitative, or semiquantitative interpretations at best. It would appear that, at present, the midline tissue dose is the best parameter in terms of which to express the dose delivered to a mammal (28).

The importance of the pattern of dose deposition in quantitative comparisons of LD_{50} values becomes of considerable importance when considering "total body" neutron exposures. It is apparent from the curves of Snyder & Neufeld (56) that most neutrons to be found in a fission spectrum do not

penetrate far in tissue and are like very soft x-rays in this regard. This lack of penetration would render them relatively ineffective for whole-body radiation effects, and this factor would probably more than offset any "RBE" factor determined with the uniformly-exposed mouse. In addition, the curves show a very large contribution to the total dose of γ -radiation generated by neutrons in tissue, particularly at the lower energies. This would render invalid the use of doses measured or calculated for mice (small mass, very little gamma) for a large animal the size of man. With the sizeable gamma contribution in large animals, the RBE for neutrons would be expected to be lower than with mice, and a lower RBE for dogs has been reported (31).

Type of radiation, RBE.—The subject of RBE has been reviewed recently (2, 105), and the myriad difficulties with the concept have been discussed. The Los Alamos group (106) has compiled a most comprehensive report dealing not only with their own extensive work on the acute RBE of various radiations in mammals, but with the published work of other authors on the subject as well. They have attempted to correlate RBE with LET, roughly equivalent in concept to the specific ionization of these radiations. Their own work covers the range from 4 Mev γ -radiations on the one extreme of LET to recoil fission fragments on the other. The data suggest a gradually increasing RBE with LET until a maximum is reached, at about 40 kev/ μ , followed by a decline. The authors carefully point out the many hazards in interpreting any such apparent correlation, although it is useful for practical purposes.

A point raised by examining the Los Alamos paper on RBE should be made. The authors ignored buildup and scatter in converting air dose to absorbed dose in rads, although conditions of minimal scatter with x- and γ -radiation were used. Under more usual conditions of greater scatter, the error will be quite large (up to approximately 45 per cent) if conversion to tissue dose in r is not made before the conversion to rads. It perhaps should be mentioned again that the conversion factor from tissue to absorbed dose varies with energy (36, 37, 39).

The following recent works on mammalian RBE values are also mentioned. A value of 0.6 to 0.7 has been determined for Co^{60} γ radiation relative to 250 kvp x-rays (107, 108). A difference in LD_{50} values for large animals exposed to different γ -radiations that cannot be readily explained on the basis of depth-dose or dose rate factors has been reported (cf. Table I). Vogel *et al.* (8, 109) report an RBE of 4.5 for fission neutrons using acute mortality in the mouse, and confirm earlier work indicating that the mechanism of death is different in neutron- and γ -irradiated mice. The difference between this value and that of 1.6 to 2.0 reported by others (107, 110) for fission neutrons exceeds that expected from experimental error, biological variation, or the fact that different "standard" radiations were used, and the dosimetry employed by the several investigators should be compared to clear up the reason for the apparent discrepancy. An RBE of approxi-

mately 1.6 for the heavy recoil particles from thermal neutron capture in B^{10} has been determined (106, 108). Further RBE values have been reported for high energy x- and β -radiations (111, 112), fast neutrons (31, 113, 114), thermal neutrons (108, 115) and alpha particles (116).

Modes of death with total body irradiation.—It has been shown abundantly [(2, 117), Quastler (8)], that death following acute total-body and regional exposure may result in a variety of syndromes, or modes of death, depending on the dose level, time after exposure, type of radiation used, and species involved. Some of these syndromes cannot be observed with total-body exposure because death may ensue from other syndromes with shorter survival periods. At very high doses death occurs in a matter of minutes or hours. This hyperacute syndrome has been studied in detail (118, 119), and is dependent on exposure of the brain. The precise order of events preceding death are dose-dependent. The marked symptomology related to brain dysfunction suggests that death may be from neurological damage. This type of death can be produced by irradiation of the head only [(120), Brace and Andrew (8)]. As the dose is reduced, survival time becomes larger until the three to four day "gastrointestinal" type of death is encountered. The shape of this well-known dose-survival time curve (117) has been examined using x-rays, thermal neutrons, and fission neutrons (121). The threshold for production of this type of death was lower for neutrons than for x-rays, as would be expected from the known difference in lethal patterns between x- and neutron-irradiated mice (114, 117). These authors (121) suggest that some of the difference observed between the effects of neutrons and γ -rays may be related to the relative "irreversibility" of heavy particle irradiation suggested by Blair (122). No such irreversible component was found, however, in mice initially irradiated with heavy particles from B^{10} capture of thermal neutrons, and challenged later with a second radiation exposure (123). The relatively shortened survival time with mice exposed to neutrons (114) has been found not to occur in dogs (31). A markedly shortened survival time has been observed in mice irradiated with the heavy particles from thermal neutron capture in boron, indicating that this type of death may be related to an unusual sensitivity of the gut to LET (124). The three to four day death is believed to result from damage to the intestinal tract (see under "Partial body irradiation" below for references). The "bone marrow" syndrome, encountered in the low-lethal dose ranges, has received attention (see also under "Partial body irradiation" and "Post-Protection"). There appears to be no doubt that the sequelae of pancytopenia (infection and hemorrhage) contribute to the demise; however, the relative contribution of these factors and the precise mechanism of death remains a subject for discussion (79, 125). Sporadic deaths occur in the few weeks following the "bone marrow" death period, when the marrow has essentially recovered. The cause of these deaths remains obscure.

Stohlmeyer, Cronkite & Brecher (126) showed that pre- and postirradiation bleeding and postirradiation administration of *p*-aminopropiophenone, both

anemia-inducing procedures, stimulated erythropoiesis in irradiated dogs and rats. Linman & Bethell (127) obtained an erythropoietic factor from the plasma of irradiated rabbits. Other hematological studies on total body irradiation are listed [(128 to 132), Hulse (10)].

An additional mode of death following acute total body exposure has been described. Austin *et al.* (133) believe that a 5 to 8 day death (as opposed to the 3 to 4 day gut death and the 8 to 15 day bone marrow death) occurs in mice. It can be argued, however, that these deaths are at the extremes of statistical variation around the 3 to 4 and 10 to 15 day deaths. Grounds for this are seen in the survival pattern of the large number of mice exposed to bomb γ -radiation (68). Survival time is inconstant at the dose levels producing the 5 to 8 day death (133, 125), and the occurrence of death at this time may mean that considerably less is known of the mechanism of the "gut" and "bone marrow" deaths than the names imply.

The realization that dose-dependent syndromes can occur is of considerable importance in quantitative radiobiology using mammals. It has been pointed out (114) that the apparent RBE for fast neutrons in mice will be quite different, depending on whether the doses to produce the 3 to 4 day gut death or the later marrow deaths are compared. It has been shown also [Clark *et al.* (8)], that neutrons producing death by different mechanisms may not be additive as far as that endpoint is concerned, but may be additive for other endpoints (134).

Partial body irradiation, the gram roentgen concept.—Quastler *et al.* (135) have reported deaths in approximately two weeks following irradiation of the head, jaw or tongue of the mouse at dose levels of 1500 r or greater. Death apparently cannot be attributed to starvation, respiratory embarrassment, or marrow aplasia, and the mechanism remains obscure. Similar deaths have been reported following 1500 r to the head of rats (136). Dogs given 1750 r to the head only apparently survived 5 months or longer (137). In the "total head (brain)" studies of Mason *et al.* (138), it appears likely from the survival time that the phenomenon described by Quastler (135) was responsible for death. These authors conclude that total-head irradiation does not induce death by a single means; it is a "cumulative effect upon the central nervous system and apparently other tissues without primary bacterial effects." An "oropharyngeal" syndrome, also similar to that described by Quastler, has been reported (139).

The gut syndrome, apparently identical if produced by either total-body irradiation or local irradiation of a large segment of bowel, has been reviewed in detail [(2, 140, 141, 117), Quastler (8)]. Resection of the irradiated intestine increases survival beyond the time when death from the gut syndrome would otherwise be lethal (142). That depletion of fluids contributes greatly as the immediate cause of death is indicated, since massive fluid replacement increases survival time (143). Death from this syndrome can be prevented in some animals by shielding only a small portion of the duodenum or ileum, but not by shielding the cecum or stomach (144). The authors feel that pro-

tection is operative through protection of some specific bowel function, rather than via a mechanism similar to that invoked for spleen or bone marrow protection (145).

The bone marrow syndrome also has been investigated by Lamerton *et al.* (146, 147, 148) using shielding. They show clearly the two phases of radiation injury by means of weight changes, and further confirm the fact that shielding of even a small portion of the bone marrow markedly reduces the degree of hematopoietic depression. Shielding of the skin failed to protect hematopoietic tissues. They also call attention to the importance of anemia in the acute bone marrow syndrome in the rat. The remarkable degree of protection afforded by marrow shielding, and the degree to which this may be masked by bowel damage, has been demonstrated in the studies of Swift *et al.* (102).

Bohr *et al.* (149) report protection against the lethal effects of whole body irradiation by shielding the exteriorized kidney alone. However, they used nonoperated controls. In the authors' and others' (150, 151) experience, operation alone will frequently account for an improved survival rate. Also, it is known (144, 102, 152) that shielding, or relative shielding of very small portions of the bowel or marrow will bring about small differences in mortality, and placement of even small pieces of lead adjacent to an animal will reduce significantly the amount of radiation from lateral and back scatter. The possibility that these factors may have influenced the results cannot be excluded. The kidney has been implicated in radiation death in chicks (153).

Maisin and his group in Belgium have worked extensively with shielding procedures. Their very large bibliography is given (3, 6, 8) and will not be duplicated in this review. They have concluded that there are at least two syndromes following total-body exposure, that shielding of the bone marrow or bowel is efficacious in enhancing survival, and that protection of the bowel and bone marrow by shielding act synergistically. These conclusions are in accord with those arrived at independently in this country and throughout the world (1, 2, 117, 144, 152).

The data of Kereiakes *et al.* (154, 155) on the effect of x-radiation delivered through grids are interesting, though difficult to interpret. The authors express dose in terms of volume dose, and conclude that

equal volume dose of x-radiation—through grids having various diameter hole sizes but a constant open area to closed area ratio resulted in increasingly greater survival as the grid hole sizes were decreased.

Volume dose was calculated by multiplying the total incident dose above the grid by the body weight and the ratio of open to closed area of the grid, assuming discrete cylinders of radiation beneath the open holes and negligible scatter beneath the shielded portion. The photographic evidence presented for discrete cylinders of radiation (154) results from the unscattered portion of the beam and does not necessarily indicate the absence of scatter. Depth-dose curves with grids indicate a sizeable degree of scatter beneath the

shielded areas (156, 157). Blair (158) has discussed the relationship of integral dose to mortality under these conditions. It is of interest that despite widely differing conditions (dose to some tissues beneath the open areas apparently varied from approximately 1000 to 6000 r), the effects could be regarded as being remarkably similar [extremes of survival rate between 13 and 84 per cent, achievable with the usual whole body radiation with dose differences of about 100 r (70)]. Thus the degree of protection afforded can receive different evaluations, depending on how dose is expressed and how the results are interpreted.

Court Brown and his group (159) have recalculated some of their earlier data on patients exposed in radiotherapy, and also have reported x-ray dose in terms of roentgens (integral dose only was reported previously). The re-analysis does not reveal a dependence of the degree of radiation sickness following single large exposures on the integral dose, as previously reported, but rather on the dose delivered in roentgens, the region of the body exposed and the body weight.

Blair (158) has advanced an interesting mathematical treatment relating partial-body to total-body exposure that appears to describe adequately some experimental data. The theory implies a "lethal effect" that is proportional to dose, but does not necessarily require that the gram-roentgen concept apply. The gram-roentgen concept has been shown to be invalid for predicting mortality with partial-body radiation (160), and with "total-body" irradiations of low penetrability (32). It appears likely that, while the gram-roentgen concept may be useful in clinical radiotherapy over limited ranges of integral dose to a specific area, and may allow better prediction of the degree of illness in radiation therapy, it is an oversimplification as far as the acute total body radiation syndrome is concerned. Lethality is a complex function of the dose in rads, the type of tissue irradiated, the type of tissue relatively shielded, and other factors such as dose rate, species, etc.

Search for a circulating "toxic factor" in irradiated animals continues. Muller (161) notes that a factor in normal rabbit serum that inhibits cell division is increased in amount following total-body irradiation. Edelmann (162) has published an abstract indicating a toxic factor in serum of irradiated rats assayed by injecting the material into adrenalectomized recipients. Campo *et al.* (163) and Lott *et al.* (164) were unable to demonstrate a circulating toxin.

Additivity of different radiation.—It has been shown (109) that total body gamma and fast neutron irradiation, administered in different proportions, are less than additive for acute mortality in mice. This was anticipated from the known differences in mechanism of death with the two radiations in mice. Additivity of thermal neutrons and γ -rays have been shown to be complete (165), however early deaths in mice are not as prominent with slow, as with fast, neutron irradiation.

Strain and age; cage effect.—Experiments have been carried out on the

variation in response to total body x-irradiation of different strains of mice with regard to body weight (166) and the acute LD₅₀ (66, 61). These papers quote and confirm definite differences observed by previous workers. The differences for the acute LD₅₀, though real, do not exceed 100 to 125 r. Earlier work on the variation of LD₅₀ value with age has been extended in systematic studies (167). The LD₅₀ increases with age from 37 to 105 days, and changes little up to the 709 days studied. The hypothesis of Blair (8) was not confirmed over the period studied; however, the extreme old age period was not studied in these experiments. An LD₅₀ of 600 r for 16-month-old rats was found, as contrasted with a value of 715 r for 6-month-old rats (60).

A significant difference in mortality rate among animals treated identically but housed in different cages has been demonstrated convincingly (168). The explanation for this phenomenon, which may account for many of the confusing results obtained when few animals in a single experiment are reported on, is not apparent.

Nutritional state.—Earlier work has been confirmed that a low protein diet prior to irradiation increases susceptibility (169). Severe protein deficiency after exposure apparently increases susceptibility (170). A fat deficient diet apparently increases the susceptibility to protracted, but not single x-ray exposure (171). The increased susceptibility may result from linoleate depletion (172). Attempts to alter the course of acute radiation illness with oral and parenteral feedings have not been uniformly successful (143, 173, 174, 175).

POST-PROTECTION

This subject was reviewed thoroughly up to July 1956 (3), including recent independent work by several groups (Lindsley *et al.*, Ford *et al.*, Nowell *et al.*, and Makinodan) indicating that the protection afforded by post-exposure injection of hematopoietic material, or by shielding of the spleen or other hematopoietic organs can result from transfer and "takes" of viable cells, rather than via a chemical recovery factor. Vos *et al.* (176), Russell *et al.* (177) and Mitchison (178) also have found regenerating hematopoietic tissue in irradiated, treated recipients to be those of the donor animal. Immunologic methods were used to distinguish between donor and recipient red cells, a histochemical method for leukocytes. Barnes *et al.* (10) gave irradiated mice spleen preparations containing varying proportions of intact cells and nuclei (techniques used allowed less than 0.5 per cent intact cells). Survival rate was independent of the nuclei count, and dependent on the count of intact cells, thus indicating that intact cells are required for protection. Nowell *et al.* (179) have demonstrated growth of injected rat marrow *in situ* in irradiated mice.

It has again been shown that autologous or isologous hematopoietic tissues afford greater protection than do homologous or, of course, heterologous materials (176, 177, 178, 180 to 183). Soska *et al.* in (10) have used

ingenious approaches to the problem, although it is regrettable that more animals, or more replicate experiments, were not used. Trentin (181) has questioned that deaths after three weeks in animals protected with heterologous material results from sloughing of the transplanted material after sufficient time has elapsed for antibodies against the foreign material to develop. In extending the work of Main & Prehn (182), he presents results indicating that while irradiated mice protected with isologous bone marrow did not tolerate skin homografts from an F_1 hybrid or foreign strain, mice protected with marrow from an F_1 or foreign strain mouse showed a high degree and long duration of tolerance to skin homografts from hybrid or other foreign strains. These results, coupled with the fact that animals dying late after heterologous protection frequently show normal blood counts, the author takes to indicate an induced immunological tolerance of any surviving antibody producing tissue of the irradiated host for tissue from the foreign donor. Doses as low as 110 r prevented sloughing of the foreign grafts (181). A further observation of interest was that, in two separate experiments, the survival rate and blood counts were lower in mice given 770 r and hybrid ("foreign") marrow, than in mice similarly treated at 550 r. No explanation for this is apparent. Jacobson *et al.* (184) have presented evidence that postirradiation protection against death with heterologous material may be possible without an appreciable degree of hematologic recovery as indicated by the peripheral blood. Maisin *et al.* (185, 186, 187) using radioactive iron, were able to demonstrate early function of homologous bone marrow injected intraperitoneally in irradiated hosts. Heterologous bone marrow could not be demonstrated to be functional by this technique. An interesting possible application of cell colonization in the irradiated host is seen in the studies of Barnes *et al.* (183), in which repopulation with normal donor hematopoietic tissues in leukemic mice made completely aplastic with high doses of radiation has been shown to be possible. This treatment is indicated appropriately by the authors to constitute a desperate measure. Cole *et al.* (188, 189) have continued studies on protection against radiation with isologous and heterologous bone marrow, and have reported a marked incidence of neoplasms and other late lesions in mice protected with spleen homogenates. Vogel *et al.* (190) were able to demonstrate protection with postirradiation implanted spleens against gamma-, but not against neutron-irradiated mice. This would be expected from the differences in mechanism of death in mice with the two irradiations (2).

Jacobson (191) continues to argue strongly in favor of the "humoral theory," and Loutit and his group (192) against it with equal vigor. The evidence becomes overwhelming in favor of cell transfer. Jaroslow & Taliaferro (193), Wissler *et al.* (194), Taliaferro & Taliaferro (195) and Sussdorf & Draper (196), in elaborate studies, demonstrated that shielding of various organs or body regions (spleen, appendix, leg, liver), and extracts of tissue and yeast preparations, afforded protection against x-ray depressed antibody formation. They do not feel, however, that the phenomenon in-

volved with extract-protection is the same as with protection by organ shielding. Makinodan *et al.* (197) report accelerated return of ability to produce agglutinins in x-irradiated mice treated with bone marrow.

Silverman *et al.* (198) have reduced the incidence of bacteremia in x-irradiated mice by means of post-exposure injections of spleen homogenate, and Shechmeister (199) demonstrated that spleen shielding during irradiation reduced susceptibility to intraperitoneally-injected *Escherichia coli*. Smith *et al.* (200) showed that following irradiation splenectomized mice had lower granulocyte counts and were more sensitive to bacterial challenge than were previously-normal irradiated mice. The same group (73) demonstrated that both streptomycin and marrow or spleen homogenate appreciably raised the LD₅₀ value of hamsters.

PRE-PROTECTION

Since the last review of this subject (3), a number of additional articles have become available. The recent works of Russian authors have become available [Graevsky (9)]. The extensive studies of Maisin and his colleagues on the protective action of mercaptoethyl-amine on total- and partial-body radiation effects have been summarized (3, 6, 8). Maldague *et al.* (201) report that MEA protects against the oropharyngeal syndrome described previously (135 to 139). Langendorff & Catsch (202) have reported that MEA protects with fractional total-body irradiation. The effects of MEA on tissue respiration following x-irradiation have been reported (203).

Van Bekkum & Cohen (8) have presented some of their work with pre-protective agents. Van Bekkum (204) has studied various dithiocarbonate compounds extensively, and concludes that the dithiocarbonate structure itself is the active portion. The mode of action of these compounds could not be determined from the studies. A variety of agents have been studied for protective effect, including quinoxaline 1,4-di-N-oxide (205), Megaphen (206), S, β -amino-ethylisothiouronium Br·HBr (207), sodium pentobarbital (208), and other anesthetic agents (209). Gessert & Phillips (210) made rats polycythemic with cobalt, and found these animals more susceptible to irradiation than normal controls. Similar results have been obtained by others (211). Gessett & Phillips conclude that "if dietary cobalt is capable of increasing the resistance of rats to whole body irradiation, as reported by Parr *et al.*" (212) "for mice after short-term feeding, it is not due to the polycythemia-inducing action of cobalt." Adaptation to trauma does not afford protection against total-body irradiation (213). The following works on oxygen and temperature effects are referenced in addition to those in (3). Gilbert *et al.* (214) have shown that the protective effect of previous irradiation against oxygen poisoning can be attributed to anorexia resulting from irradiation. Salerno *et al.* (215) present further evidence that many pre-protective agents (cysteine, cysteamine) may work indirectly by means of inducing tissue hypoxia. Friedberg (216) has demonstrated that rats whose

livers are made catalase-deficient by means of 3-amino-1,2,4-triazole are not more susceptible to x-irradiation.

Parkes (217) has demonstrated that irradiation of ovaries at -79°C . is less damaging than at room temperature, as determined from the number of "takes" of the transplanted tissue. Osborn & Kimeldorf (218) have studied the radiation response of bats exposed to warm and cold environments.

RECOVERY FROM LATENT INJURY

It is well established that for acute effects a given dose of radiation produces greater effects if delivered over a short period of time (minutes or hours) than if delivered slowly (over days or weeks). Or, to produce a given acute effect a larger dose of chronic than of acute radiation is required. There is less agreement about the effect of fractionating a given dose on late effects. The effect of the time over which radiation is delivered is attributed to recovery processes operating during the chronic irradiation procedures.

Mole (219) discusses the idea of recovery and its units of measurement. In a second report concerned with recovery during and after daily irradiation of mice, Mole (220) finds that a mouse can "neutralize" a dose of x-radiation of somewhere between 25 and 50 r daily. It is concluded that continued daily irradiation progressively damages the recovery process (220). The latter finding makes even more difficult the problem of interpreting the effects of chronic irradiation, as information about recovery rates derived from single large exposures is of little value. Although daily irradiation progressively damages the rate of recovery during the postirradiation period, the additional dose required to kill during the irradiation period is scarcely affected. Mole (220) speculates that two aspects of recovery are involved.

Paterson (221) gave 52 monkeys half an LD_{50} dose of x-rays followed seven days later or twenty days later by a second irradiation. With single irradiations, the LD_{50} was 570 r, that for the seven-day group was 736 r, and for the twenty-day group, 883 r, the animals in the twenty-day group apparently tolerating at the second irradiation a larger dose than the LD_{50} for a single exposure. The seven-day group's recovery rate, assuming exponential recovery, was at the rate of 14.6 per cent per day, a rate consistent with complete recovery in 20 days. Krebs & Storer (222) were unable to demonstrate an adaptation to total body irradiation.

Blair (223) found the half-time for repair of the injury as measured by lethality in the mouse to be 0.5 weeks, while in the dog it is about three weeks (224). Carsten (225) and Carsten & Noonan (226) found a 33 per cent per day recovery rate as measured by 30 day LD_{50} 's for lower body x-irradiated rats. This figure is considerably higher than any recovery rate reported for whole body irradiation. Some recovery processes such as repair of the acute depression of hematopoietic tissues can be described in histological terms, but the nature of the recovery processes affecting the latent injury has not been explained. In an attempt to develop a theory of recovery, Michie & Krohn

(227) describe mathematically the rate of recovery to be expected on the basis of detoxification of a postulated chemical toxin and show that this approach yields predictions consistent with the findings in some experiments with *Drosophila* eggs. Extrapolation to mammals is more difficult; a scheme for analyzing data with an electronic computer is suggested.

LATE EFFECTS

Animals which survive the acute effects of radiation and those which are exposed to doses or to dose rates too small to produce acute effects may develop any of a number of late effects. In some late effects there are definite lesions such as cataracts or cancer, but among the more subtle effects is a shortening of the life span without lesions directly ascribable to the effects of radiation. Brauer *et al.* (228) have reemphasized the importance of distinguishing the effects of sustained low-level irradiation from the delayed effects which follow 60 days or so after termination of radiation exposure.

Shortening of life span.—Berlin & Dimaggio (229) have discussed critically some of the theories relating the shortening of life span to radiation injury. The early theories have in common a linear or first-order dependence of effect on dose. Blair (99) reviews the data on shortening of life in mammals. With chronic irradiation at dose rates up to 120 r/day, shortening of life is about proportional to the total accumulated doses below three times the acute LD₅₀'s. Blair (8, 223) has developed a theory in which it is assumed that the injury from radiation is produced at a rate proportional to the dose rate and that recovery occurs at a rate proportional to the magnitude of the injury present except for an irreparable portion which accumulates in proportion to the total dose. Some of the survival data supporting Blair's theory was published by Sacher (Sacher, in ref. 11). In Blair's treatment (223), $I = S_0 - S$, where S_0 is the normal survival time and S is the survival time following irradiations. In surveys of published data of life span shortening in the mouse (223) and in the guinea pig, rat, and dog (224), Blair concluded that his theory could account for the data and that reparable and irreparable injury are additive in all proportions to produce lethality. In all species considered about 4 per cent of the acute injury from x-rays is irreparable (224). In a later paper (230) a figure of 7 per cent is given as the irreparable fraction in the mouse, irradiated with 250 kvp x-rays. Blair (122), and Stannard (8, 231) interpreted their early data as indicating that the injury from alpha-particles is 80 per cent irrecoverable. Bond *et al.* (108) irradiated mice with the heavy recoil particles from neutron capture in boron, and challenged the animals at intervals later with a second acute exposure to radiation. No residual effect of the heavy particle irradiation over that obtained with γ -radiation could be demonstrated.

Hursh *et al.* (232) report experiments designed to answer the question of whether the average reduction in survival is directly proportional to the total

radiation dose, regardless of the individual dose size for 250 kvp x-rays with rats. The results indicate that for single irradiations the mean survival time decreases roughly in proportion to the dose, excluding animals dying in the first 60-day period. The effect of a 600 r total dose is markedly reduced, however, when the dose is divided into 10 or 20 fractions delivered at daily intervals. Since the life shortening injury is regarded as being irreparable, several other possible causes of the reduced effect of fractionated doses are postulated and discussed.

Brues & Sacher (233) discuss the use of the Gompertz function (the logarithm of the rate of mortality) in relating the effects of radiation to the aging process. The Gompertz function is approximately linear with age for adult mammals. "The effect of a single exposure to radiation is an upward displacement of the function without change in slope, whereas that of constant exposure is to increase the slope of the subsequent functions" (233). In either case, the effect is comparable to an acceleration of aging, but the "consequences of irradiation may or may not represent processes identical qualitatively with normal aging processes," (233). Jones (234) also discusses the relationship of radiation injury to aging in terms of the Gompertz function.

Sacher (235, 236) has developed another approach to the life shortening problem with the hypothesis that "the unpredictability of mortality is a consequence of the uncertainty that is inherent in the dynamics of physiologic function." Assuming that fluctuations in physiologic function have Gaussian distributions, Sacher (235) shows that the Gompertz function can be predicted on a statistical basis, whereas it was originally described on an empirical basis. Death rates from chronic radiation are discussed in terms of shifts in the Gompertz function. The effect of fractionation on dose effects can be described by a first-power component of injury which accumulates additively at all time intervals, and a second-power component of injury which is additive over a period of a few days only. The results are compatible with the hypothesis that the irreversible injury has a genetic component.

Sacher (237) later re-examines the theories which assume a linear relationship between effect and dose and in the light of further data concludes that "the discrepancy between theory and experiment is too large to be ignored or minimized. . . . There is a serious flaw in the basic assumptions of first-order theories." Development of a revised theory, however, is deferred. Gowen & Stadler (238) gave 508 male mice acute doses of 20 r to 960 r of 98 kvp x-rays. The life span curves are analyzed in terms of linear and polynomial components, and are interpreted as indicating that at least two physiological systems are affected. Haley *et al.* (239) and Rust *et al.* (240) have extended their studies of chronic irradiation of the burro to 100 r, 50 r and 25 r (Co^{60}) daily. The differences in the sequence of effects seen is discussed (240). Combined with earlier studies of 400 r and 200 r daily, log survival appears to be linearly related to log dose rate.

Mole (241) discusses one of the problems of interpretation of the results of chronic irradiation experiments, the question of wasted radiation, or the radiation delivered to an animal which already has received a lethal dose of radiation.

The relation between dose rate and the dose required to kill mice is shown to be quite different between animals irradiated daily until death and those irradiated daily to a predetermined total dose. There was a continuous increase in the LD₅₀ as the daily dose was decreased from 800 r to 25 r in the latter experiment, whereas the LD₅₀ went through a minimum at about 100 r daily when irradiation continued until death.

LITERATURE CITED

1. Thomson, J. F., *Ann. Rev. Nuclear Sci.*, **4**, 377-400 (1954)
2. Cronkite, E. P., and Bond, V. P., *Ann. Rev. Physiol.*, **18**, 483-526 (1956)
3. Bond, V. P., and Cronkite, E. P., *Ann. Rev. Physiol.*, **19**, 299-34 (1957)
4. Edelman, A., *Ann. Rev. Nuclear Sci.*, **5**, 413-24 (1955)
5. Lorenz, E., and Congdon, C. C., *Ann. Rev. Med.*, **5**, 323-38 (1954)
6. Bacq, Z. M., and Alexander, P., *Fundamentals of Radiobiology* (Butterworth Scientific Publications, London, England, 389 pp., 1955)
7. Hollaender, A., Ed., *Radiation Biology*, 1, Pt. 1 and 2 (McGraw-Hill Book Co., Inc., New York, N.Y., 1269 pp., 1954)
8. *Proc. Intern. Conf. Peaceful Uses Atomic Energy*. Vol. 11, (United Nations, New York, N. Y., 402 pp., 1956)
9. *Conf. Acad. Sci. USSR Peaceful Uses Atomic Energy*. (In English translation, Available from the Superintendent of Documents, U.S. Gov't. Printing Office, Washington 25, D. C., 1956)
10. Nevesy, G., Forssberg, A., and Abbott, J. D., *Advances in Radiobiology*, (Oliver and Boyd, Edinburgh, Scotland, 557 pp., 1957)
11. Howard, A., and Ebert, M., *Nucleonics*, **11**, (12), 18 (1953); see also *Acta Radiol., Suppl.* **116** (1954)
12. Bacq, Z. M., and Alexander, P., Eds., *Proceedings of Radiobiology Symposium, Liège* (Butterworth Scientific Publications, London, England, 362 pp., 1955)
13. Mitchell, J. S., Holmes, B. E., and Smith, C. L., Eds., *Progress in Radiobiology* (Oliver and Boyd, Ltd., Edinburgh and London, England, 576 pp., 1956)
14. Rajewsky, B., *Strahlendosis und Strahlenwirkung* (George Thieme Verlag, Stuttgart, Germany, 184 pp., 1954)
15. Zirkle, R. E., Ed., *Biological Effects of External X- and Gamma Radiation* 1st ed., (McGraw-Hill Book Co., Inc., New York, N. Y., 530 pp., 1954)
16. Zirkle, R. E., Ed., *Biological Effects of External X- and Gamma Radiation*, Part 2, (U.S. AEC Technical Information Service, Document TID 5220, 477 pp., 1956)
17. Blair, H. A., Ed., *Biological Effects of External Radiation* 1st ed., (McGraw-Hill Book Co., Inc., New York, N.Y., 508 pp., 1954)
18. Oughterson, A. W., and Warren, S., *Medical Effects of the Atomic Bomb in Japan* (McGraw-Hill Book Co., Inc., New York, Toronto, London, 477 pp., 1956)
19. Neel, J. V., and Schull, W. J., *The Effect of Exposure to the Atomic Bombs on Pregnancy Termination in Hiroshima and Nagasaki* (National Academy of Sciences, Publication No. 461, Washington, D. C., 241 pp., 1956)

20. Committee for Compilation of Report on Research in the Effects of Radioactivity. *Research in the Effects and Influences of the Nuclear Bomb Test Explosions*, Vol. I and II. (Japan Society for the Promotion of Science, Veno, Tokyo, 823 and 1824 pp., 1956)
21. Cronkite, E. P., Bond, V. P., Conard, R. A., Shulman, N. R., Farr R. S., Cohn, S. H., Dunham, C. L., and Browning, L. E., *Atomic Energy Document TID 5358*, (1956), Gov't. Printing Office, Washington 25, D. C. (Shortened version in *J. Am. Med. Assoc.*, **159**, 430-34, 1955)
22. Hoffman, J. G., and Hempelmann, L. H., *Am. J. Roentgenol. Radium Therapy*, **77**, 144-60 (1957)
23. *The Biological Effects of Atomic Radiation*, (Summary Reports, National Research Council, Washington, D. C., 109 pp., 1956)
24. *The Hazards to Man of Nuclear and Allied Radiations*, (Report of the Medical Research Council, Great Britain, Her Majesty's Stationery Office, London, 128 pp., 1956)
25. "Maximum Permissible Radiation Exposures to Man," *Radiation Research*, **6**, 513-16 (1957)
26. United Nations Scientific Committee on Effects of Atomic Radiation, *Radiation Research* **6**, 517-19, (1957)
27. Poppel, M. H., Jacobson, H. G., Stein, J., and Jerry, G. H., *Am. J. Roentgenol. Radium Therapy Nuclear Med.*, **77**, 138-43 (1957)
28. Bond, V. P., Cronkite, E. P., Sondhaus, C. A., Iimirie, G., Robertson, J. S., and Borg, D. C., *Radiation Research* **6**, 554-72 (1957)
29. Kohn, H. I., and Gunter, S. E., *Radiation Research*, **5**, 674-87 (1956)
30. Kohn, H. I., and Kallman, R. F., *Radiation Research*, **5**, 693-99 (1956)
31. Bond, V. P., Carter, R. E., Robertson, J. S., Seymour, P. H., and Hechter, H. H., *Radiation Research*, **4**, 139-53 (1956)
32. Grahn, D., Sacher, G., and Walton, H., *Radiation Research*, **4**, 228-42 (1956)
33. Ellinger, F., Morgan, J. E., and Cook, E. S., *Radiology*, **64**, 210-18 (1955)
34. Ellinger, F., Morgan, J. E., and Cook, E. S., *Cancer*, **9**, 768-72 (1956)
35. Ellinger, F., Morgan, J. E., and Chambers, F. W., Jr., *Naval Med. Research Inst. Rept. NM006 012.04.43* (1952)
36. Symposium. "The Introduction of the Rad in Radiotherapy Practice," *Brit. J. Radiol.*, **29**, 353-69 (1956)
37. Hine, G. H., and Brownell, G. L., *Radiation Dosimetry* (Academic Press, New York, N. Y., 932 pp., 1956)
38. "Recommendations of the International Commission on Radiological Units," and Measurements (ICRU), *Radiology* **62**, 106-9 (1954); National Bureau of Standards Handbook 62 (U. S. Gov't. Printing Office, Washington, D. C., 1957)
39. Laughlin, J. S., and Pullman, I., *Preliminary Report to the Genetics Panel of the National Academy of Sciences Study of the Biological Effects of Atomic Radiation* (National Academy of Sciences, 1956)
40. Laughlin, J. S., Beattie, J. W., Henderson, W. J., and Harvey, R. A., *Am. J. Roentgenol. Radium Therapy Nuclear Med.*, **70**, 294-312 (1953)
41. Genna, S., and Laughlin, J. S., *Radiology*, **65**, 394-407 (1955)
42. McElhinney, J., Zendle, B., and Domen, S. R., *Radiation Research*, **6**, 40-54 (1957)

43. Berger, M. J., and Doggett, J. A., *J. Research Nat'l. Bur. Standards*, **56**, 89-98 (1956)
44. Brucer, M., *Am. J. Roentgenol. Radium Therapy, Nuclear Med.*, **75**, 49-55 (1956)
45. Tochilin, E., Ross, S. W., Shumway, B. W., Kohler, G. D., and Golden, R., *Radiation Research*, **4**, 158-73 (1956)
46. Rhody, R. B., *Radiation Research*, **5**, 495-501 (1956)
47. Hurst, G. S., Mills, W. A., Conte, F. P., and Upton, A. C., *Radiation Research*, **4**, 49-64 (1956)
48. Hurst, G. S., Harter, J. A., Hensley, P. N., Mills, W. A., Slater, M., and Reinhardt, P. W., *Rev. Sci. Instruments*, **27**, 153-56 (1956)
49. Sigoloff, S. C., *Nucleonics*, **14**, (10), 54-56 (1956)
50. Hurst, G. S., *Brit. J. Radiol.*, **27**, 353-57 (1954)
51. Rossi, H. H., Hurst, G. S., Mills, W. A., and Hungerford, H. E., *Nucleonics*, **13**, (4) 46-47 (1955)
52. Rossi, H. H., and Rosenzweig, W., *Radiology*, **64**, 404-10 (1955)
53. Snyder, W. S., and Neufeld, J., *Radiation Research*, **6**, 67-78 (1957)
54. Rossi, H. H., and Rosenzweig, W., *Radiation Research*, **2**, 417-25 (1955)
55. Barr, T. A., and Hurst, G. S., *Nucleonics*, **12**, (8), 33-35 (1954)
56. Snyder, W. S., and Neufeld, J., *Brit. J. Radiol.*, **28**, 342-50 (1955)
57. Tait, J. H., *Brit. J. Radiol.*, **23**, 282-86 (1950)
58. Stickley, E. E., *Am. J. Roentgenol. Radium Therapy, Nuclear Med.*, **75**, 609-18 (1956)
59. Catsch, A., Koch, R., and Langendorff, H., *Fortschr. Röntgenstrahl.*, **84**, 462-72 (1956)
60. Hursh, J. B., and Casarett, G., *Univ. of Rochester Rept.*, UR-403 (1955)
61. Grahn, D., and Hamilton, K. F., *Genetics*, (To be published)
62. Eldred, E., and Trowbridge, W. V., *Radiology*, **62**, 65-73 (1954)
63. Paterson, E., *J. Fac. Radiol.*, **5**, 189-99 (1954)
64. Prosser, C. L., Painter, E., and Swift, M. N., *Atomic Energy Commission Rept.*, MDDC-1272, CH-3738 (1946)
65. Gleiser, C. A., *Am. J. Vet. Research*, **14**, 284-86 (1953)
66. Kohn, H. I., and Kallman, R. F., *Radiation Research*, **5**, 309-17 (1956)
67. Ellinger, F., Morgan, J. E., and Chambers, F. W., Jr., *Naval Med. Research Inst. Rept.* MN006 012.04.44 (1952)
68. Cronkite, E. P., Bond, V. P., Chapman, W. H., and Lee, R. H., "Joint Report from Naval Medical Research Institute, Bethesda, Maryland, and U. S. N. Radiological Defense Laboratory, San Francisco, Calif.," *N.M.R.I. Rept.* NM-006-012.04.86, complete; condensed report published in *Science*, **122**, 148-50 (1955)
69. Buchanan, D. J., Darby, W. J., Bridgforth, E. B., Hudson, G. W., and Efner, J. A., *Am. J. Physiol.*, **174**, 335-40 (1953)
70. Clark, W. G., and Uncapher, R. P., *Proc. Soc Exptl. Biol. Med.*, **71**, 214-16 (1949)
71. Doull, J., and DuBois, K. P., *Proc. Soc. Exptl. Biol. Med.*, **84**, 367-70 (1953)
72. Rugh, R., Levy, B., and Sapadin, L., *J. Morphol.* **91**, 237-68 (1952)
73. Kohn, H. I., and Kallman, R. F., *Radiation Research*, **6**, 137-47 (1957)
74. Smith, W. W., Marston, R. Q., Gonshery, L., Alderman, I. M., and Ruth, H. J., *Am. J. Physiol.*, **183**, 98-110 (1955)

75. Lorenz, E., Congdon, C. C., and Uphoff, D., *Radiology*, **58**, 863-77 (1952)
76. Brecher, G., and Cronkite, E. P., (Personal communication)
77. Greenfield, M. A., Billings, M. S., Norman, A., and Lewis, A. E., *Univ. Calif. at Los Angeles Rept.*, UCLA-278 (1954)
78. Rust, J. H., Folmar, Jr., G. D., Lane, J. J., and Turm, B. F., *Am. J. Roentgenol. Radium Therapy Nuclear Med.*, **74**, 135-38 (1955)
79. Haigh, M. V., and Paterson, E., *Brit. J. Radiol.*, **29**, 148-57 (1956)
80. Schlumberger, H. G., and Vazquez, J. J., *Am. J. Pathol.*, **30**, 1013-48 (1954)
81. Cronkite, E. P., and Brecher, G., *Ann. New York Acad. Sci.*, **59**, 815-33 (1955)
82. Shively, J. N., Michaelson, S. M. and Howland, J. W., *Univ. of Rochester Rept.*, UR-465 (1956)
83. "Operation Greenhouse," *Scientific Directors Rept.*, Annex 2.2, Document WT-18 (Technical Information Service, Oak Ridge, Tenn., 1952)
84. Tullis, J. F., Chambers, F. W., Jr., Morgan, J. E., and Zeller, J. H., *Am. J. Roentgenol. Radium Therapy Nuclear Med.*, **57**, 620-27 (1952)
85. Tullis, J. L., Lamson, B. G., and Madden, S. G., *Radiology*, **62**, 409-15 (1954)
86. Rust, J. H., Trum, B. F., Wilding, J. L., Simons, C. S., and Comar, C. L., *Radiology*, **62**, 569-74 (1954)
87. *Report of UT-AEC Project 10, U.S. AEC Document ORO-145*, (Office of Technical Services, Dept. of Commerce, Washington 25, D. C. June, 1955)
88. Prosser, C. L., *Radiology*, **49**, 299-313 (1947)
89. Rust, J. H., Wilding, J. L., Trum, B. F., Simons, C. S., Kimball, A. W., and Comar, C. L., *Radiology*, **60**, 579-82 (1953)
90. Morgan, R. H., *Handbook of Radiology* (The Year Book, Publishers, Chicago, Ill., 518 pp., 1955)
91. Ellinger, F., *Radiology*, **44**, 125-42 (1945)
92. Thomson, J. F., and Tourtellotte, W. W., *Am. J. Roentgenol. Radium Therapy, Nuclear Med.*, **69**, 826-29 (1953)
93. Henshaw, P. S., *J. Natl. Cancer Inst.*, **4**, 485-501 (1944)
94. Haley, T. J., and Harris, D. H., *Science*, **111**, 88-90 (1950)
95. Rosenthal, R. L., *Blood*, **6**, 660-73 (1951)
96. Dauer, M., and Coon, J. M., *Proc. Soc. Expl. Biol. Med.*, **79**, 702-7 (1952)
97. Miller, L. S., Fletcher, G. H., and Gerstner, H. B., *Rep't 57-92, Seventh Air Univ. School of Aviation Medicine* (Randolph Air Force Base, Texas, 1957)
98. Collins, V. P., and Loeffler, R. K., *Am. J. Roentgenol. Radium Therapy, Nuclear Med.*, **75**, 542-47 (1956)
99. Blair, H. A., *Univ. of Rochester Report*, UR-442 (1956)
100. Wilson, R. R., *Radiation Research*, **4**, 349-59 (1956)
101. Roberts, C. J., and Dahl, A. H., *Univ. of Rochester Rept.*, UR-241 (1953)
102. Swift, M. N., Taketa, S. T., and Bond, V. P., *Radiation Research*, **4**, 186-92 (1956)
103. Jones, D. C., Alpen, E. P., and Bond, V. P., *Radiation Research*, **5**, 424 (1956)
104. Potter, J. C., *Radiology*, **37**, 724-26 (1941)
105. Bora, K. C., *Biology Division, Dept. of Atomic Energy, Indian Cancer Research Center*, Parel, Bombay 12 (1956)
106. Storer, J. B., Harris, P. S., Furchner, J. E., and Langham, W. H., *Radiation Research*, **6**, 188-288 (1957)

107. Upton, A. C., Conte, F. P., Hurst, G. S., and Mills, W. A., *Radiation Research*, **4**, 117-31 (1956)
108. Bond, V. P., Easterday, O. D., Stickley, E. E., and Robertson, J. S., *Radiology*, **67**, 650-63 (1956)
109. Vogel, H. H., Jr., Clark, J. W., and Jordan, D. L., *Am. J. Roentgenol. Radium Therapy Nuclear Med.*, **77**, 524-30 (1957)
110. Delihas, N., and Curtis, H., *Radiation Research*, (To be published 1957)
111. Fuller, J. B., Chen, I., Laughlin, J. S., and Harvey, R. A., *Radiation Research*, **3**, 423-34 (1956)
112. Moos, W. S., Fuller, J. B., Henderson, W. J., Dallenbach, F., and Harvey, R. A., *Radiation Research*, **3**, 44-51 (1955)
113. Riley, E. F., Evans, T. C., Rhody, R. B., Leinfelder, P. J., and Richards, R. D., *Radiology*, **67**, 673-85 (1956)
114. Carter, R. E., Bond, V. P., and Seymour, P. H., *Radiation Research*, **4**, 413-23 (1956)
115. Boone, I. U., Rogers, B. S., and Strong, V. G., *Radiation Research*, **5**, 459-65 (1956)
116. Basson, J. K., and Shellabarger, C. J., *Radiation Research*, **5**, 502-14 (1956)
117. Bond, V. P., Silverman, M. S., and Cronkite, E. P., *Radiation Research*, **1**, 389-400 (1955)
118. Langham, W., Woodward, K. T., Rothermel, S. M., Harris, P. S., Lushbaugh, C. C., and Storer, J. B., *Radiation Research*, **5**, 404-32 (1956)
119. Hicks, S. P., Wright, K. A., and Leigh, K. E., *Am. Med. Assoc. Arch. Pathol.*, **61**, 226-38 (1956)
120. Brace, K. C., Andrews, N. L., and Thompson, E. C., *Am. J. Physiol.*, **179**, 386-89 (1954)
121. Rothermel, S. M., Woodward, K. T., and Storer, J. B., *Radiation Research*, **5**, 433-40 (1956)
122. Blair, H. A., *Univ. of Rochester Rept.*, UR-274 (1953)
123. Bond, V. P., Cronkite, E. P., and Easterday, O. D. *Radiation Research*, Abstract, (Radiation Research Society Meeting, May 1957)
124. Bond, V. P., and Easterday, O. D., *Federation Proc.*, **15**, 21 (1956)
125. Mole, R. H., *Brit. J. Radiol.*, **26**, 234-41 (1953)
126. Stohlman, F., Cronkite, E. P., and Brecher, G., *Proc. Soc. Exptl. Biol. Med.*, **88**, 402-6 (1955)
127. Linman, J. W., and Bethell, F. H., *Blood*, **12**, 123-29 (1957)
128. Baum, S. J., Kimeldorf, D. J., and Jacobsen, E. M., *Blood*, **10**, 926-32 (1955)
129. Huang, K. C., and Bondurant, J. H., *Am. J. Physiol.*, **185**, 446-49 (1956)
130. Klein, J. R., *Proc. Soc. Exptl. Biol. Med.*, **91**, 630-32 (1956)
131. Dowben, R. M., and Walker, J. K., *Proc. Soc. Exptl. Biol. Med.*, **90**, 398-400 (1955)
132. Harris, P. F., *Brit. Med. J.*, **2**, 1032 (1956)
133. Austin, M. K., Miller, M., and Quastler, H., *Radiation Research*, **5**, 303-7 (1956)
134. Jordan, D. L., Clark, J. W., and Vogel, H. H., Jr., *Radiation Research*, **4**, 77-85 (1956)
135. Quastler, H., Austin, M. K., and Miller, M., *Radiation Research*, **5**, 338-53 (1956)
136. English, J. A., *Oral Surg. Oral Med. Oral Pathol.*, **9**, 1132-38 (1956)

137. English, J. A., Wheatcroft, M. G., Lyon, H. W., and Miller, C., *Oral Surg. Oral Med. Oral Pathol.*, **8**, 87-99 (1955)
138. Mason, H. C., Mason, B. T., and Moos, W. S., *Brit. J. Radiol.*, **28**, 495-507 (1955)
139. Dunjic, A., Maisin, J., Maldague, P., and Maisin, H., *Compt. rend. soc. biol.*, **150**, 587-92 (1956)
140. Quastler, H., *Radiation Research*, **4**, 303-20 (1956)
141. Conard, R. A., *Radiation Research*, **5**, 167-88 (1956)
142. Osborne, J. W., *Radiation Research*, **4**, 541-46 (1956)
143. Conard, R. A., Cronkite, E. P., Brecher, G., and Strome, C. P. A., *J. Appl. Physiol.*, **9**, 227-33 (1956)
144. Swift, M. N., and Taketa, S. T., *Am. J. Physiol.*, **185**, 85-91 (1956)
145. Ford, C. E., Lamerton, J. L., Barnes, D. W. H., and Loutit, J. F., *Nature* **177**, 452-54 (1956)
146. Belcher, E. H., Gilbert, I. G. F., and Lamerton, L. F., *Brit. J. Radiol.*, **27**, 387-92 (1954)
147. Baxter, C. F., Belcher, E. H., Harriss, E. B., and Lamerton, L. F., *Brit. J. Haematol.*, **1**, 86-103 (1955)
148. Lamerton, L. F., and Baxter, C. F., *Brit. J. Radiol.*, **28**, 87-94 (1955)
149. Bohr, D. F., Rondell, P. A., Palmer, L. E., and Bethell, F. H., *Am. J. Physiol.* **183**, 335-39 (1955)
150. Swift, M. N., (Personal Communication)
151. Restivo, S. R., and Mefford, R. B., *Radiation Research*, **6**, 153-66 (1957)
152. Taketa, S. T., Swift, M. N., and Bond, V. P., *Federation Proc.*, **13**, 523 (1954)
153. Stearner, P. S., Christian, E. J., and Brues, A. M., *Radiation Research*, **1**, 270-81 (1954)
154. Kereiakes, J. G., Parr, W. H., Storer, J. B., and Krebs, A. T., *Report No. 139, Army Med. Research Lab., Fort Knox, Kentucky* (1954); *Proc. Soc. Exptl. Biol. Med.*, **86**, 153-56 (1954)
155. Kereiakes, J. G., and O'Neill, T. A., *Report No. 178, Radiobiology Dept., Army, Med. Research Lab., Fort Knox, Kentucky* (1955)
156. Jacobson, L. E., *Am. J. Roentgenol. Radium Therapy, Nuclear Med.*, **69**, 991-1000 (1953)
157. Loewinger, R., *Radiology*, **58**, 351-60 (1952)
158. Blair, H. A., *Univ. of Rochester Rept., UR-462* (1956)
159. Court Brown, W. M., and Abbott, J. D., *Brit. J. Radiology*, **28**, 153-58 (1955)
160. Bond, V. P., Swift, M. N., Allen, A. C., and Fishler, M. C., *Am. J. Physiol.* **161**, 323-30 (1950)
161. Muller, J., *Nature*, **178**, 43-44 (1956)
162. Edelmann, A., *Federation Proc.*, **14**, 42 (1955)
163. Campo, R. D., Bond, V. P., and Cronkite, E. P., *Federation Proc.*, **16**, 18-19 (1957)
164. Lott, J. R., and Wilding, J. L., *Texas Univ. AF SAM 55-110* 5 pp. (1955)
165. Storer, J. B., and Harris, P. S., *U. S. Atomic Energy Commission Report LA-1502* (1953)
166. Grahn, D., *J. Exptl. Zool.*, **125**, 39-61 (1954)
167. Kohn, H. I., and Kallman, R. F., *Science*, **124**, 1078 (1956)
168. Raventos, A., *Brit. J. Radiol.*, **28**, 410-14 (1955)

169. Smith, W. W., Ackermann, I. B., and Alderman, I. M., *Am. J. Physiol.*, **169**, 491-98 (1952)
170. Schlesinger, M. J., *AEC Document UR-279* (1953)
171. Cheng, A. L. S., Kryder, G. D., Bergquist, L., and Deuel, H. J., Jr., *J. Nutrition*, **48**, 161-82 (1952)
172. Cheng, A. L. S., Ryan, N., Alfinslater, R., and Deuel, H. J., Jr., *J. Nutrition*, **52**, 637-43 (1954)
173. Smith, W. W., Ackermann, I., and Smith, F., *Am. J. Physiol.*, **168**, 382 (1952)
174. Jennings, F. L., *Proc. Soc. Exptl. Biol. Med.*, **80**, 10-13 (1952)
175. Smith, D. E., and Tyree, E. B., *Radiation Research*, **4**, 435-48 (1956)
176. Vos, O., Davids, J. A., Weyzen, W. W., and van Bekkum, D. W., *Acta Physiol. et Pharmacol. Nerrl.*, **4**, 482-86 (1956)
177. Russell, E. S., Smith, L. J., and Lauson, F. A., *Science*, **124**, 1076-77 (1957)
178. Mitchison, N. A., *Brit. J. Exptl. Pathol.*, **37**, 239-47 (1956)
179. Nowell, P. C., Cole, L. J., Roan, P. L., and Habermeyer, J. G., *J. Natl. Cancer Inst.*, **18**, 127-44 (1957)
180. Trentin, J. J., *Proc. Soc. Exptl. Biol. Med.*, **92**, 688-93 (1956)
181. Trentin, J. J., *Proc. Soc. Exptl. Biol. Med.*, **93**, 98-100 (1956)
182. Main, J. M., and Prehn, R. T., *J. Natl. Cancer Inst.*, **15**, 1023-29 (1955)
183. Barnes, D. W. H., Corp., M. J., Loutit, J. F., Neal, F. E., *Brit. Med. J.*, **2**, 626-30 (1956)
184. Jacobson, L. O., Marks, E. K., and Gaston, E. O., *Proc. Soc. Exptl. Biol. Med.*, **91**, 135-39 (1956)
185. Maisin, H., Maisin, J., Dunjic, A., and Maldague, P., *Compt. rend. soc. biol.*, **60**, 582-86 (1956)
186. Maisin, H., Dunjic, A., Maldague, P., and Maisin, J., *Compt. rend. soc. biol.*, **60**, 828-31 (1956)
187. Maisin, H., Dunjic, A., Maldague, P., Sempoux, D., and Maisin, J., *Comptes rend. soc. biol.*, **60**, 1031-35 (1956)
188. Cole, L. J., Habermeyer, J. G., and Nowell, P. C., *Naval Radiol. Defense Lab., USNRDL TR 104*, 26 p. (1956)
189. Cole, L. J., Nowell, P. C., and Ellis, M. E., *J. Natl. Cancer Inst.*, **17**, 435-46 (1956)
190. Vogel, H. H., Jr., Clark, J. W., Jordan, D. L., Bink, N., and Barhorst, R. R. (To be published)
191. Jacobson, L. O., *Progr. Hematol.*, **1**, 311-17 (1956)
192. Loutit, J. F., *J. Nuclear Energy*, **1**, 87-91 (1954)
193. Jaroslav, B. N., and Taliaferro, W. H., *J. Infectious Diseases*, **98**, 75-81 (1956)
194. Wissler, R. W., Robson, M. J., Fitch, F., Nelson, W., and Jacobson, L. O., *J. Immunol.*, **70**, 379-85 (1953)
195. Taliaferro, W. H., and Taliaferro, L. G., *J. Infectious Diseases*, **99**, 109-28 (1956)
196. Sussdorf, P. H., and Draper, L. R., *J. Infectious Diseases*, **99**, 129-42 (1956)
197. Makinodan, T., Gengozian, N., and Congdon, C. C., *J. Immunol.*, **77**, 250-56 (1956)
198. Silverman, M. S., Greenman, V., Ellis, M., and Cole, L. J., *Naval Radiol. Defense Lab. Rept. USNRDL TR 107* (1956)
199. Shechmeister, I. L., Paris, W. N., Krause, F. T., Paulissen, L. J., and Yunker, R., *Proc. Soc. Exptl. Biol. Med.*, **89**, 228-30 (1955)

VERTEBRATE RADIOBIOLOGY (LETHAL ACTIONS) 161

200. Smith, W. W., Alderman, I. M., and Ruth, H. J., *Am. J. Physiol.* **182**, 403-6 (1955)
201. Maldaque, P., Dunjic, A., Maisin, H., and Maisin, J., *Compt. rend. soc. biol.*, **150**, (To be published, 1956)
202. Langendorff, N., and Catsch, A., *Strahlentherapie*, **101**, 536-41 (1956)
203. De Schryver, A., *Arch. Intern. Physiol.*, **64**, 594-600 (1956)
204. Van Bekkum, D. W., *Acta Physiol. et Pharmacol. Nerrl.*, **4**, 508-23 (1956)
205. Haley, T. J., Flesher, A. M., Veomett, R., and Vincent, J., *Univ. Calif., Los Angeles, School of Med. Rept. UCLA* **384** (1956)
206. Klein, G., *Radiol. Clin.*, **25**, 65-72 (1956)
207. Benson, R. E., Michaelson, S. M., and Howland, J. W., *Univ. of Rochester Rept. UR* **452** (1956)
208. Fonner, R. L., and Laird, D., *Compt. rend.*, **239**, 832-34 (1954)
209. Wilson, J. E., *Anesthesiology*, **16**, 503-10 (1955)
210. Gessert, C. F., and Phillips, P. H., *Proc. Soc. Exptl. Biol. Med.*, **89**, 651-54 (1955)
211. Constant, M., and Phillips, P. H., *Proc. Soc. Exptl. Biol. Med.*, **85**, 678-81 (1954)
212. Parr, W., O'Neill, T., Bush, S., and Krebs, A. T., *Science*, **119**, (3091), 415-16 (1954)
213. McKenna, J. M., and Zweifach, B. W., *Radiation Research*, **6**, 126-36 (1957)
214. Gilbert, D. L., Greshman, R., and Fenn, W. O., *Am. J. Physiol.*, **181**, 272-74 (1955)
215. Salerno, P. R., Uyeki, E., and Friedell, H. L., *Western Reserve Univ. Report. NYO 4924* (1955)
216. Friedberg, W., *Proc. Soc. Exptl. Biol. Med.*, **93**, 52-53 (1956)
217. Parkes, A. S., *Nature*, **176**, 1216-17 (1955)
218. Osborn, G. K., and Kimeldorf, D. J., *Naval Radiol. Defense Lab. Report. USNRDL TR 76* (1956)
219. Mole, R. H., *Brit. J. Radiol.*, **29**, 563-69 (1956)
220. Mole, R. H., *Brit. J. Radiol.*, **30**, 40-46 (1957)
221. Paterson, E., Gilbert, C. W., and Haigh, M. V., *Brit. J. Radiol.*, **29**, 218-26 (1956)
222. Krebs, A. T., and Storer, J. B., *Army Med. Research Lab. Rept. No. 175, Fort Knox, Ky.* (1955)
223. Blair, H. A., *Univ. of Rochester Rept. UR-206* (1952)
224. Blair, H. A., *Univ. of Rochester Rept. UR-207* (1952)
225. Carsten, A. L., Masters Thesis "Determination of the Recovery from Lethal Effects of Lower Body Irradiation in Rats" Univ. of Rochester, Rochester, N.Y., 1956
226. Carsten, A. L., and Noonan, T. R., *Univ. of Rochester Rep UR-445*. (1956)
227. Michie, R. W., and Krohn, L. H., *Army Med. Research Lab., Rept. No. 202* (1955)
228. Brauer, R. W., Krebs, J. S., Murden, C. H., and Carroll, H. W., *U. S. Naval Radiol. Defense Lab. Rept. USNRDL-TR-80* (1956)
229. Berlin, N. I., and Dimaggio, F. L., *Armed Forces Special Weapons Rept. AFSWP-608* (1956)
230. Blair, H. A., *University of Rochester Report UR-312* (1954)
231. Stannard, J. N., Blair, H. A., and Baxter, R. C., *Univ. of Rochester Rept. UR-395* (1955)

232. Hursh, J. B., Noonan, T. R., Casarett, G., and Van Slyke, F., *Am. J. Roentgenol. Radium Therapy, Nuclear Med.*, **74**, 130-34 (1955)
233. Brues, A. M., and Sacher, G. A., *Analysis of Mammalian Radiation Injury and Lethality, Symposium on Radiobiology*, Nickson, J. J., Ed., John Wiley and Sons, New York, N. Y., 465 pp., 1952)
234. Jones, H. B., in *Conference on Mammalian Aspects of Basic Mechanisms in Radiobiology*. (Highland Park, Illinois, May, 1956, To be published)
235. Sacher, G. A., *Radiology*, **67**, 250-57 (1956)
236. Sacher, G. A., *J. Nat'l. Cancer Inst.*, **15**, 1125-44 (1955)
237. Sacher, G. A., *Science* **125**, 1039-40 (1957)
238. Gowen, J. W., and Stadler, J., *J. Exptl. Biol.*, **132**, 133-55 (1956)
239. Haley, T. J., McCulloch, E. F., McCormick, W. G., Trum, B. F., and Rust, J. H., *Am. J. Physiol.*, **180**, 403-7 (1955)
240. Rust, J. H., Trum, B. F., Lane, J. J., Kuhn, U. S. G., 3rd, Paysinger, J. R., and Haley, T. J., *Radiation Research*, **2**, 475-482 (1955)
241. Mole, R. H., *J. Natl. Cancer Inst.*, **15**, 907-14 (1955)

VERTEBRATE RADIOBIOLOGY (THE PATHOLOGY OF RADIATION EXPOSURE)^{1,2,3}

C. C. LUSHBAUGH

Los Alamos Scientific Laboratory, Los Alamos, New Mexico

No American review of the work reported during recent years has been attempted in the field of radiopathology since the extremely comprehensive one of Furth & Upton in 1953 (1). Lacassagne & Gricouloff, however, recently brought up-to-date their 1942 monograph (2), which reviews the literature in clinical and experimental gross and microscopic pathology of the effects of exposure to various kinds of radiation from its beginning in 1898 (3) to the present. In this book, still the most inclusive, critical treatise available on this subject, the authors have made a generous and adequate appraisal of recent advances from the points of view of past accomplishments and modern French radiotherapy. The enormous number of original papers from American and British sources, however, and the difficulty of obtaining them in France, apparently prevented their review from being as detailed and inclusive from 1942 to 1956 as it was up to 1942. The new edition, however, is still the only source today where the student can determine the factual origin of modern radiopathologic concepts and especially the antecedents of his own ideas. *The Histopathology of Irradiation* by Bloom and his associates (4), which was intended only as a compendium of the pathology portions of the biologic experiments of the Manhattan Project, continues as the radiopathology textbook for American radiobiologists, although it is now seriously outdated by the remarkable progress in this field in the last ten years.

In view of the enormous number of papers previously published on the histopathologic changes of exposure to ionizing radiations, it is surprising to find so many new contributions of importance being made. Staying abreast of them alone is almost as difficult as analyzing them. The present review attempts to bridge the gap in this regard between the time of the review of Furth & Upton (1) and March 1957. Although more than 300 papers were reviewed, some were undoubtedly inadvertently overlooked. A few were intentionally discarded because they were repetitious. Many are not reviewed here because they describe minor, interesting species differences in pathologic changes without shedding any light on the pathogenesis of radiation damage either in general or for a specific cell or tissue. The prejudices and

¹ The survey of literature pertaining to this review was completed in March, 1957.

² This review was written under the auspices of the U. S. Atomic Energy Commission which is not, however, responsible for the views the author expresses.

³ Grateful acknowledgement is made to Miss Dorothy Hale and Mrs. Betty Sullivan for unstinting aid in the literature search and preparation of the manuscript.

biases of the reviewer account for the omission of many which enabled the bibliography to be kept to a reasonable size.

RADIOSENSITIVITY OF CELLS

Little is known that can account for the differences in the radiosensitivity of various cells, tissues, and organs. Reviews by Patt (5) and Gray (6) illustrate well the shortcomings of our comprehension of this problem. A major cause of this lack of understanding is the scarcity of direct observations on the irradiated intracellular environment and on the manner in which it is modified by its extracellular fluid and cellular surroundings. A few recent advances here have been made by Stroud (7), Trowell (8) and Zirkle & Bloom (9). Trowell has recently corrected his conclusion that lymphocytes were only in slightly less radiosensitive *in vitro* than *in vivo*, by showing that the ED₅₀ was 1640 r *in vitro* and only 150 r *in vivo*. This observation makes indirect effects of the lymph node environment synergistic with the direct effects by a factor of eleven (8). The idea of the relative unimportance of direct "hits" in the mechanism of cellular damage in a particular cell is gaining wider acceptance through such experiments as those of Zirkle & Bloom (9), who found the mitotic process unaltered after direct proton bombardment of the centrosome and spindle, and the work of Stroud (7). After continuous irradiation of tissue cultures with tritium, Stroud failed to find structural chromosomal damage and concluded that the mitotic disturbances were related to primary physico-chemical changes which interfered with gelation and essential intracellular metabolic processes. This phenomenon of a degrading effect by ionizing radiation on gel states was recently seen as the rapid loss of jelly by irradiated sea urchin eggs (10). The radiosensitivity of morphologically identical cells is known to vary with the metabolic state of individual cells and the appearance of radioresistance among radiosensitive cells probably reflects only the destruction of the most susceptible cells of that type [Meldolesi (11)]. Environmental factors also may modify either cellular damage from radiation or the morphologic expression of this damage as shown by Langham *et al.* (12), and Lushbaugh & Hoak (13), who found in heavily irradiated rats and monkeys that damage to lymphocytes varied with the tissue in which the lymphocyte was located at the time of radiation, rather than with the total dose of radiation it received. There appeared to be a gradient through the body from the most sensitive lymphocytes in the intestinal mucosa to the most resistant ones in the thymus. This morphologic observation, however, may be an artefact since the time of appearance of pyknosis, karyorhexis, and lysis depends upon autolytic processes, and these apparent differences in radiosensitivity may reflect only local proteolytic activity. This explanation may also apply to the puzzling observation of Vogel & Ballin (14), who found that less cellular pyknotic fragmentation was apparent in the thymus 24 hr. after radiation with 20,000 r than after 400 r. After such high doses "fixation" necrosis of lymphocytes occurs and the only histologic ways such dead cells can be identified

microscopically is by their phagocytosis (13), stainability with eosin or loss of Brownian movement [Shrek (15)].

Much of the difficulty in developing a generalization concerning the meaning of "radiosensitivity" stems from there being no single unambiguous definition of the term. Many investigators feel that to be radiosensitive a cell must show immediate histologic signs of damage, such as pyknosis. In addition, however, morphological expression of cellular radiosensitivity may appear as mitotic inhibition, increased necrobiotic rate, nuclear vacuolization, increased nuclear fragmentation, micronucleation, nuclear gigantism, cytoplasmic differentiation [Friedman *et al.* (16); Glucksman (17)], over-production, or abnormal production of cytoplasmic processes (sclerosis), hypertrophy [Teir (18)], atrophy, hyperplasia, and carcinogenesis.

The finite radiosensitivity of an organ does not depend upon the various radiosensitivities of its component tissues but depends instead upon the radiosensitivity of an essential component tissue with either the least regenerative capacity or the most deleterious cytoplasmic response such as might lead to late sclerosis, atrophy, or infarction. The problem of radiosensitivity is further complicated by the variable time different tissues require after radiation exposure to develop the most irreparable morphologic and functional expression of damage. Thus, for example, the "radioresistant" kidney is in time the radiosensitive organ which limits the extent of radiotherapy of the whole abdomen (*vide infra*). Similarly, necrosis of the cerebral granular neurones can be shown to be a primary result of rapidly delivered massive doses of radiation without accompanying vascular effects, but the practical radiosensitivity of the brain or its therapeutic limits of radioresistance are defined by the radiosensitivity of its vascular structures.

HEMATOPOIETIC SYSTEM

The outstanding development in the pathology of radiation damage in the last four years was proving the correctness of the "cellular hypothesis" of the mechanism of splenic and marrow protection. Loutit (19), while not the first to point out the shortcomings of the theory of the soluble "recovery factor" [Storer (20); Storer *et al.* (21)], led the way, along with Barnes (22), in showing that the data which were considered by others to exclude the possibility of homologous cellular survival, failed to do so. They, along with many others, consistently pointed out that contamination by whole cells was the best explanation for the apparent successful radioprotection by sub-cellular homogenates of spleen and bone marrow [Cole *et al.* (23, 24); Brown *et al.* (25)]. For several years the experiments showing that irradiated mice could occasionally be protected by guinea pig or rat bone marrow [Lorenz *et al.* (26, 27, 28)] were used as the most potent arguments that the protective effect could be elicited only humorally, since it was difficult to presume that heterospecific cellular material would survive in even the irradiated host (19, 26, 27). Congdon & Lorenz's (28) interpretation of their own data that rat bone marrow can survive in the peritoneal cavity of the irradiated

mouse was used to the same end and the repopulation of the radiation-induced atrophic spleen and bone marrow was considered to be attributable to a humoral factor produced by these temporarily surviving intraabdominal implants [Congdon & Lorenz (28); Cole *et al.* (29)]. Actual proof that injected homologous marrow elements proliferate in irradiated hosts was first obtained by Main & Prehn (30), who showed that the irradiated animal injected with homologous marrow becomes tolerant of donor antigens to which it formerly would have reacted. Almost simultaneously, Lindsley *et al.* (31) showed by the use of an immunogenetic marker that homologous marrow in irradiated animals contributed as much as 80 per cent of the circulating erythrocytes for longer than 150 days postirradiation. Heterologous rat marrow was also shown to repopulate the marrow and spleens of irradiated mice by the histochemical demonstration of alkaline phosphatase positive myelogenous rat cells in mouse organs, which are histochemically alkaline phosphatase negative [Nowell *et al.* (32)]. This repopulation by transplanted homologous mouse marrow was shown to be apparently permanent in the heavily irradiated surviving mouse by the ingenious cytologic identification of the foreign cells by chromosome patterns which differed from that of the host [Ford *et al.* (33)]. Heterologous rat marrow was shown by this method to survive until the death of the mouse sixty to ninety days post-irradiation. These experiments failed to show any evidence that the repopulation of the recipient, irradiated mouse marrow was composed at all of the host's own cells. Rat serum proteins, however, could not be detected in the irradiated mouse [Makinodan (34)]. In spite of these observations, Jacobson (35, 36) continues to defend the "humoral theory," and further attempts to extract and concentrate the "protective principle" go on. Acceptance of the cellular hypothesis by others, however, has opened up a new field of such therapeutic possibilities as human bone marrow transplantation in idiopathic and iatrogenic aplastic anemias, acute and chronic leukemias, and the accidentally-produced acute radiation syndrome in man.

Among other hematologic studies carried out during this period, one showed that the rat hematopoietic system had a rapid recovery rate and that the extensive hematologic damage from 75 r per week was not cumulative [Baum *et al.* (37)]. Extremes of hematopoietic resistance to chronic irradiation are well illustrated by the experiments of Jacobson's group (38), which showed that no rabbits died from hematopoietic damage even after they had cumulative exposures up to 12,000 r at 8.8 r per week, while most of the guinea pigs died from aplastic anemia with accumulated doses of 700 to 6000 r. Cytochemical changes occurred in rat lymphocytes within two hr. after 600 r total body radiation [Ackerman *et al.* (39)]. Yoffey (40) and Harris (41) have found that before bone marrow regeneration occurs in the irradiated guinea pig, there is a phenomenal rise in numbers of lymphocytes in the marrow even though there is a coexisting peripheral lymphopenia. Their feeling that there is a direct relationship between this accumulation of

lymphocytes and the recovery of myeloid and erythroid cells appears to portend the development of another new concept in hematopoiesis. Latta & Waggener (42), however, failed to find any increase in lymphocytes in bone marrow following damage by P^{32} .

CONNECTIVE TISSUES

Skin.—Damage to the skin of the Marshallese natives and American military personnel in the Pacific area by radioactive fallout from an atomic test focused attention again on the problems and economic importance of acute and chronic radiodermatitis [Cronkite *et al.* (43)]. Further studies were made of the pathogenesis of these lesions in man [Gillman *et al.* (44); Griffith (45); Griffith *et al.* (46); Kulwin & Buley (47); Nodl (48, 49); Romanini & Chippa (50); Shaffer (51); Wachsmann (52); Witten & Sulzberger (53); Devik (54)]; in mice [Arvey *et al.* (55); Kroning & Sigmund (56)]; in rats [Upton & Gude (57); Ungar & Damgaard (58, 59); Lushbaugh *et al.* (60, 61, 62, 63, 64)]; in guinea pigs [Farris & Olivia (65); Pettersson (66)]; and in rabbits [Barth *et al.* (67); Meschan & Nettleship (68); Moritz & Henriques (69)]. The majority of these studies, and especially those of Lushbaugh (60) and Moritz (69) indicated that dermal necrosis is not the primary effect of radiation exposure, although it is still commonly considered so. Devik (54) has reviewed this subject extensively and reached the similar conclusion but feels that the whole process of radiodermatitis is dependent on epithelial damage. The epithelial changes seem to parallel those of the irradiated intestinal tract (*vide infra*). First there is cessation of mitosis, then differentiation occurs with disappearance of the basal layer, followed by further squamous metamorphosis with acanthosis, dyskeratosis, and parakeratosis. Ulceration results from failure of the necessarily continual replacement of the shedding epithelium to occur. A peculiar progressing chemical change of the collagen of the dermis either accompanies or leads to progressive ulceration of the dermis. While this change can be demonstrated histologically [Upton & Gude (57); Lushbaugh & Storer (60); Nerli (70)], its nature is unknown. Besides chronic ulceration, its presence is attended by severe functional deficiencies such as inability to heal surgical incisions [Lushbaugh & Storer (61); Merwin & Hill (71)]; inability to react to thermal burns and histamine activation [Ungar & Damgaard (58)]; and inability to resist bacterial invasion. When the radioulcer is deep, the defect is found to be effaced by a fibroplastic process that occurs below the injured but viable dermal structures and pushes them to the surface. This passive upward movement of relatively deep-lying vascular structures explains, at least in part, the rapid development of superficial telangiectasia in beta radiation burns. The resulting atopia of fat cells, muscle and dense collagen from the deep dermis is the probable basis for recurrent break-downs in epidermal integrity. The studies of Lushbaugh & Spalding (72) in sheep showed that the apparent hyperplastic "down growths" of acanthic epithelium which appear during

the repair of a beta burn and which resemble a cancerous change, according to Moritz (69), actually represent epithelial regeneration in surviving portions of hair follicles in the deep dermis. Since these shafts often lose their continuity with the surface, the common fate of these epithelial structures is the formation of epidermal inclusion cysts. Extremely few experimental investigations have attempted to search for a basis for these pathologic findings [Devik (54, 73); Kulwin & Buley (47)]. Devik (73) made the provocative observation that the epidermal cells within a heavily irradiated field bordering carefully shielded epithelium, were the ones that became extremely hyperplastic and, contrary to common opinion, the unirradiated bordering cells did not. He used this phenomenon as an example of cellular environment determining the response of cells to irradiation, since the central cells in the irradiated area differentiate and become dyskeratotic rather than undergo hyperplasia (54).

Recent advances in histochemistry are now being applied to this field. Dermal mast cell destruction [Pettersson (66); Arvey *et al.* (55); Upton & Gude (57)] has been found to be associated after local dermal irradiation with local increase in heparin, stainable acid polysaccharide, and changes in the connective tissue ground substance [Edgerly (74)]. A search for other biochemical and functional changes during the early morphologic latent period resulted in the observation that normal appearing skin, one to two days postirradiation, has a greatly enhanced glycolysis [Lushbaugh & Hale (63)], which it was postulated might result from alteration of local enzyme inhibitor systems or destruction of substances necessary for control of metabolic rates. This hypothesis, however, appears only partially correct in view of Ungar & Damgaard's experiments (58, 75), which show that proteolysis of locally irradiated skin is markedly inhibited in contrast to the remarkable enhancement of proteolysis which follows thermal injury of the skin (75). The reconciliation of these two observations does not seem possible on the basis of present knowledge. A similar postirradiation rise in inhibition of proteolytic enzyme activity was, however, recently found in rat intestines [Lushbaugh & Hughes (76)]. A completely bewildering observation is the one showing that intravenous splenic homogenates protect skin against 3000 rep beta [Ungar *et al.* (59)].

Studies on the effects of various sources and kinds of radiation on the skin showed: Co^{60} to be slightly more effective than radium [Meschan & Nettleship (68)]; that the atrophy and therapeutic usefulness of the thorium-x-alpha pastes are due to the penetration of the epidermis and its appendages by the vehicle carrying the thorium and not to unusual penetrability of the alpha particle [Witten & Sulzberger (53)]; and that thresholds of dermal radiation damage in the rabbit were for $\text{Sr}^{90}\text{-Y}^{90}$, and Y^{91} , 1500 to 2000 rep; for Cs^{137} , 2000 to 3000 rep; for Co^{60} , 4000 to 5000 rep; and for S^{35} , 20,000 to 30,000 rep [Moritz & Henriques (69)]. Lushbaugh & Spalding (72) found that the most radioresistant structure in the skin was the arrector pilorum muscle which was lost only if ulceration extended below it after as much as

20,000 rep of Sr⁹⁰-Y⁹⁰ beta radiation. Griffith (45) found 3-year-old β -ray dermatitis clinically less troublesome than originally comparable lesions from x rays.

CAPILLARIES AND CONNECTIVE TISSUE

The effects of radiation on capillaries and connective tissues were studied more from the physiological than morphological views [Nerli (70)], except for the extensive study by Devik (54). The numerous older studies on wound healing in irradiated areas have, in general, discouraged surgery there. Apparently, however, delay in elective surgical procedures is unnecessary beyond one week postirradiation even after 2000 r to the abdomen [Lawrence *et al.* (77)]. Final wound strength in previously irradiated areas is unaffected, although it takes longer to be achieved. Revascularization of thermal burns and exudates is delayed progressively by 500 to 1500 r in mice, and the number of new capillaries per unit area is progressively limited by doses above 700 r [Merwin & Hill (71)]. These effects are dependent upon a temporary failure of fibroblasts to differentiate in the irradiated field from the inflammatory exudate and a failure of these already present to proliferate [Lushbaugh & Storer (61)]. Capillary budding is similarly suppressed. The extent of this impairment is dependent on the amount of radiation exposure and can be quite complete but very superficial with β -irradiation (61). Brown & Fryer (78) recently reported excellent results in the surgical repair of several hands severely damaged by accidental β -irradiation seven months to four years previously.

The severe hypotension caused by whole body radiation is caused by the autonomic nervous system and is not due to a direct effect of the radiation on vascular structures [Brooks *et al.* (79); Heite & Schrader (80)]. Similarly the phenomenon of vascular sensitivity to epinephrine is not a local effect but is a measure of generalized postirradiation debility [Bohr *et al.* (81)]. While kidney shielding reduced this sensitivity, renal irradiation alone failed to cause it (81). Direct functional effects can be produced in blood vessels, as well as morphologic effects [Rieser (82)], as shown by the marked reduction in perfusion rate of the isolated rabbit ear after doses above 2000 r [Gerstner *et al.* (83)]. There is a rapid rise in protein content of these perfusates after irradiation. That all tissues have a threshold of radiosensitivity is seen in Gerstner's (83) observation that after 50,000 r striated muscle loses its functional ability within 24 hr. and the fibers swell and become progressively hyalinized [Lewis (84); Copeland (85)].

DIGESTIVE SYSTEM

Oral Tissues.—Because following oral radiotherapy the patient frequently suffers from xerostomia, loose teeth, and necrosis of the jawbone [MacLennan (86)], several experimental studies were made of irradiated oral tissues in the hope of defining the pathologic changes more accurately and thus affording a better pathologic basis for these clinical experiences. In this re-

gard, the salivary glands of rats and dogs were found to be sensitive to 1000 to 1750 r as evidenced by a marked increase in connective tissue, atrophy and metaplasia six or more months following their exposure [English (87); English *et al.* (88); Shafer (89)]. Fractionation appeared to increase the inflammatory fibrotic process. The commonly held opinion that morphologic changes do not occur in the salivary glands with sufficient severity to account for the clinical observation is apparently based on examination of the glands too soon after exposure. All are in accord that the submaxillary gland is more sensitive than the sublingual and parotid ones [Burstone (90)]. Radio-osteonecrosis was found to occur in monkeys with more than 4500 r. More than 6000 r were required to produce radio-osteitis and loose teeth [Medak & Burnett (91)]. The odontoblast is the most radiosensitive cell of the teeth, while the apparently morphologically similar cell, the ameloblast, is quite resistant [Burstone (90)].

GASTROINTESTINAL TRACT

Much of the confusion in the past concerning the pathology of the digestive tract following irradiation resulted from inaccurately labeling degenerative and reactive processes as necrosis and inflammation. Under the impetus of Friedman (92, 93), Quastler (94, 95) and later Lushbaugh (12, 13), the nature and importance of these changes have become better understood and it appears, as a result, that a logical concept of the pathogenesis of "radio-enteritis" is being formulated. As in most organs other than the lymphopoietic ones and those subjected to massive doses of irradiation, epithelial necrosis is actually a rare phenomenon in the digestive tract. The acidophilic parietal cell of the gastric mucosa of man [Goldgraber *et al.* (96)] and lower primates [Lushbaugh & Hoak (13)] appears to be the only cell type uniformly necrotic immediately following doses of irradiation approximating 1000 to 2000 r. More than 4500 r are required to cause gastric ulceration in man [Brick (97)]. The pathologic and physiologic changes [Detrick *et al.* (98); Littman *et al.* (99)] of the irradiated stomach of other species and the irradiated esophagus and intestinal tract of all animals appear to be the result of the cessation of mitosis in the basal layer of the esophageal epithelium, the gastric mucus neck cells, and indifferent reproductive cells of the intestinal crypts (92, to 95). The majority of intracryptic debris seen at this time is derived from necrosis of lymphoid cells of the lamina propria, the debris of which is apparently excreted through the lining epithelium [Lushbaugh & Hoak (13)]. As the result of this failure in production of new cells, the growth of the digestive epithelium stops [Friedman (92); LeBlond & Stevens (100); Quastler (95)]. Differentiation, however, is not only not prevented but it now occurs in anatomical areas where it is pathologic [Friedman (92); Montagna & Wilson (101); Lushbaugh & Hoak (13)]. Thus, in the esophagus, the basal cells become squamous, acanthic, and keratinized and as the superficial cells are desquamated the epithelial surface becomes progressively atrophic. If mitotic activity does not return soon enough, "ulcerative radio-esophagitis" (and "ruminal gastric ulceration" in rodents) occurs.

Similarly in the intestinal tract, cells in the crypts become mucus goblet cells [Friedman (92)], principal cells and, if the process is prolonged, become metaplastic squamous cells (95, 13). Ulceration of the intestinal tract is, however, the exception rather than the rule and occurs only when trauma from the fecal stream [Friedman (93)] exceeds the viability of the mucosal cells before their replacement can be effected. It may occur as a late complication of radiotherapy secondary to vascular sclerosis [Brick (97); Anderson *et al.* (102); Bock & Heyde (103)]. As squamous metaplasia proceeds, vacuolization, lipide accumulation and staining alterations are seen as evidence of cellular aging [Montagna & Wilson (101)].

With whole body doses in excess of 1000 r, but not more than 10,000 r, the survival time of the animal is fairly constant at three and one-half days, at which time the entire intestinal epithelium is often found denuded [Quastler (95)]. Shielding a portion of the duodenum or ileum [Swift & Toketa (104)] or irradiation of only the small intestine while shielding the rest of the abdominal contents [Osborne (105)] prolongs survival time after these supralethal doses by some unknown mechanism and delays the terminal mucosal denudation. Quastler (95) recently reviewed these intestinal changes and evaluated their importance in the syndrome of "acute intestinal death" from irradiation. He postulated that in the process of keeping the gastrointestinal lining intact, there are four feedback mechanisms: loss of superficial epithelium is the stimulus to mitotic activity, to decreased rate of "decay" of the principal cells, to their squamous metaplasia or "spreading," and to contraction of the villus muscle so that the area of the villus is reduced and the surface kept covered. It would appear, however, that following radiation exposure the situation is so altered from the normal that approaching the problem from the point of view of physiologic cybernetics is not entirely valid. The "stimulus" following exposure to ionizing radiation appears to be temporary or permanent failure of the generative mechanism of the crypts to supply new cells rather than primary loss of the mucosal barrier cells as in the normal physiologic state. The decreased rate of decay of the principal cells results logically from their remaining stationary since no new cells are being formed to push the old ones off the tip of the villus. It appears also that the "spreading" of the principal cells in this case is the result of irradiation damage, since radiation is known to cause metaplasia and squamous-like gigantism in epithelial cells deprived of their reproductive function [Glucksman (17); Lacassagne & Gricouloff (2)]. And lastly, while the decrease in villus size at first may be attributable to the contracture of the muscle of the villus, the progressive decrease in villus size beyond this point after irradiation is due principally to the loss of the lymphoid cells of the lamina propria and the condensation atrophy of the mucosal stroma. It would seem then that the preservation of an intact mucosa following exposure to large doses of radiation is fortuitously the result of various primary effects of irradiation, cancelling one another out, rather than the result of the orderly interplay of homeostatic feedback mechanisms. It would also appear that the terminal generalized denudation of the intestinal mucosa with

doses causing "acute intestinal death" marks the end of the "normal" life span of the metaplastic cryptic mucosal cell before its ability to generate new cells is restored. The morphologic changes of the gastrointestinal tract cannot be used in themselves to explain the mechanism of "acute intestinal death." Ulceration is not in itself the explanation for such a death, but the presence of ulceration or the persistence of the changes of so-called "radio-enteritis" are apparently the morphologic expressions of a still unknown local pathologic mechanism which causes death. The extirpation of a fatally irradiated stomach [Littman *et al.* (99)] or intestine [Osborne (105)] prevents death from such irradiation when it is otherwise inevitable. Beginning regeneration of intestinal mucosa was found three days after 1600 r in the irradiated partners of parabiotic rats by Sommers & Warren (106), possibly indicating the operation of a protective mechanism.

LIVER

The resistance of the liver to irradiation remains unexplained but received little attention in the past four years. The thesis that more than 12,000 r are needed to produce significant hepatic damage was shaken, however, by the experiments of White *et al.* (107, 108), which demonstrated that as little as 450 to 500 r total body irradiation was needed to act synergistically with a 6 per cent casein diet to produce a high incidence of severe nodular atrophic cirrhosis in rats. The low protein diet alone did not cause cirrhosis and a 15 per cent casein diet prevented the formation of cirrhosis with these doses of radiation. The synergistic action of inanition or malnutrition with x-irradiation may explain in fact the extensive local necrosis and biliary fibrosis of the left lobe of the liver found by Brick (97) in nine young but severely ill male adults who received about 5000 r locally to the midline region of the abdomen just below the xiphoid process as radiotherapy for metastatic testicular malignancy. Otherwise, this observation would seem to indicate that the liver of man is relatively radiosensitive in comparison with that of other mammals. Radiation-induced nutritional cirrhosis of the liver was observed in rats 145 days after exposure (107, 108), while in contrast, normal regenerative ability of the liver was found in rats exposed locally to 20,000 r immediately after partial hepatectomy [Gershbein (109)] and autopsied eleven days postirradiation. The widespread failure to observe morphologic liver damage following irradiation may reflect only the custom of studying animals dying shortly and up to 30 days after irradiation as in LD₅₀ studies. Upton *et al.* (110), for example, recently found striking increases in the incidence of hepatic damage and hepatoma production in mice 10 to 25 months after about 150 μ c of Au¹⁹⁸ (estimated as 3400 r). Hepatic damage from irradiation is more evident histochemically than by histologic stains [Lelievre *et al.* (111)].

PANCREAS

Like the liver, the pancreas is considered very radioresistant. The problem of the relative sensitivity of its various components was approached

morphologically by Spalding & Lushbaugh (112), who studied the islets of Langerhans of rats after massive doses of radiation delivered rapidly from a teleosource of barium-lanthanum. Pyknosis and necrosis of islet beta cells of monkeys that died within 200 hours following doses of 10,000 to 50,000 r of total body irradiation [Lushbaugh & Hoak (13)] were shown by these experiments to be primary rather than postmortem autolytic phenomena. The necrosis of the cells of the islet of Langerhans in the rat was evident within eight hours after 2500 to 5000 r. The alpha cells were more sensitive than the beta cells, their LD₅₀ being about 5000 r, as compared to 20,000 r for the beta cells. In the presence of such destruction, neither the blood vessels or the acinous cells of the pancreas showed any demonstrable morphologic change within the same time periods.

RENAL SYSTEM

The serious results of ill-defined definitions and concepts in radiobiology can be seen best in the fatal sclerosis of the irradiated "radioresistant" kidney. The entire history of the experimental and clinical development of the modern concept of "Radiation Nephritis" was recently reviewed by Grossman (113), who points out along with Carpender (114) that, although the threshold of radiosensitivity of the kidney is extremely well documented, it is generally unknown and particularly is not respected by the practicing radiotherapist. The human kidney develops sclerotic changes with doses above 2000 r. Unless at least one-third of a kidney is shielded during exposure to such a dose, this sclerosis reaches fatal proportions four to seven months afterwards [Grossman (113); Luxton (115)]. The nephrosclerosis of radiation consists of glomerular and arteriolar hyaline obliteration and scarring. In mice, the threshold of sensitivity is 500 r whole body radiation [Furth *et al.* (116)]. It is the major single cause of death in mice that survive 800 r with protection by splenic homogenates [Cole *et al.* (117)]. In rodents, the scarring is accompanied by atypical proliferation and dilation of the renal tubules. In man, radiation nephritis can be differentiated from the changes of malignant nephrosclerosis by almost all glomeruli being damaged, generalized interstitial fibrosis, and a thick fibrotic capsule [Luxton (115)]. In man, the renal tubules are atrophic rather than proliferative. Although kidney shielding increases survival of rats to 650 r, it appears that this effect is the result of a significant mass of the animal being shielded rather than a particular organ exerting a specific protective effect. If a small additional portion of the back of the rat is shielded at the same time the kidney is, the protection is greatly enhanced [Bohr *et al.* (118)].

GENERATIVE SYSTEM

Testis.—Eschenbrenner's concept [Eschenbrenner & Muller (119); Shaver (120)] that depletion of the spermatogonia is due to radiation-induced inhibition of mitosis rather than necrosis came under attack by Oakberg (121, 122), who pointed out with convincing experimental data that the reduction of both types of spermatogonia, A and B, was attribut-

able to their death and not to functional inhibition. Type B spermatogonia had an apparent LD_{50} of about 50 r, and type A 100 r. The spermatogonia known as type A must, however, have radiosensitive and radioresistant stages since type A cells do not disappear completely even after 1500 r, and all type B cells are gone after 200 r or more [Fogg (123)]. No necrotic type B cellular remnants are found 48 hr. after 600 r, while necrotic type A cells are found in varying numbers more than fifteen days after irradiation. Presumably the numerous necrotic type A cells, five to seven days after irradiation, represent delayed death occurring in the early stages of mitosis or late interphase, which delays further the repletion of the type B spermatogonia. All agree that the major factor in the ultimate atrophy of the germinal epithelium is continual loss of cells through progressive differentiation and maturation, although some spermatocytes do degenerate during meiosis. The apparent LD_{50} of the rat spermatocyte is roughly 600 r [Oakberg (121)]. Doses of more than 50,000 r failed to produce morphologic evidence of an effect on mature rat sperm while accelerating the rate of degeneration of the other tubular germinal elements [Spalding *et al.* (124)]. Shaver's (120) conclusion that local irradiation of the scrotum with 500 r produced no apparent testicular injury while total body irradiation with 500 r causes marked atrophy was shown to be erroneous [Kohn (125); Kohn & Kallman (126, 127)]. Necrosis of the germinal epithelium is a direct effect of radiation. No studies were made specifically of the effects of radiation on the interstitial cells, although these cells appeared normal 48 hours after 100,000 r in rats [Spalding (124)].

Ovary.—The extreme radiosensitivity of the ovary of the new born animal was demonstrated very cleverly by Rugh (128), who gave nursing mother mice 300 to 600 μ c of I^{131} , so that about 5 per cent of this dose was subsequently ingested in the milk by the suckling litter mates. All the female offspring were sterile by ten months, although they had received at most only 30 μ c of I^{131} . The males were not significantly affected. I^{131} in female adult rats caused temporary anestrus after 1000 and 2000 μ c intraperitoneally, but all animals subsequently produced viable, normal but small litters [Tillotson *et al.* (129)]. Although the thyroid gland was completely atrophic and hyalinized by this dose (estimated as 500,000 rep), multiple sections of the ovaries showed no changes (estimated maximum dose as 5,000 rep). By the injection of gonadotropins after 750 to 3000 r x-irradiation, Spalding *et al.* (130) were able to show that only the primitive ova and those of the secondary follicles were radiosensitive; the interphase ova of the primary follicles were radioresistant; and that the increased follicular atresia was an indirect effect secondary to generalized hormonal imbalance. Parthenogenetic maturation and cleavage of ova were seen in the mice two days after 3000 r. Complete sterility occurred with x-radiation eight weeks after single exposures above 100 r and after seven weekly exposures of 50 r.

Uterus.—The human endometrium is thicker than the penetrability of the beta particle of "filtered radium" and must be curetted out if the basal

layer is to be irradiated by this means [Von Massenbach & Czech (131)]. In the placenta, the maximum evidence of damage was seen at the junction of fetal and maternal tissue in locally irradiated pregnant rabbit uterine horns, five days after 1200 r [Foraker *et al.* (132)]. Histochemically, this damage was demonstrated as decreased dehydrogenase activity, diffuse granular alkaline phosphatase staining, reduction in periodic acid staining for glycogen—all nonspecific manifestations of cellular damage (132). This approach failed to alter the appraisal of morphologic changes as demonstrated with the routine hematoxylin and eosin staining procedure.

ENDOCRINE GLANDS

Rat pituitary basophiles are lost within 24 hours with 1000 r, possibly explaining the physiologic fall in TSH; while a progressive decrease in chromophobes in five days results in a relative increase in acidophiles which are the source of the postirradiation increase in ACTH according to Korson & Botkin (133), and Mateyko *et al.* (134). Interest in the thyroid gland was focused chiefly upon the effects of I^{131} [Marks *et al.* (135); Lindsay *et al.* (136); Dobyns *et al.* (137); Dailey *et al.* (138); Andrews & Knisely (139, 140)]. The lowest level of ingestion of I^{131} causing thyroid damage to sheep was 5 μ c per day but since the offspring of these sheep showed interfollicular thyroid edema at eight months of age, this dosage was considered higher than minimal. Between 80,000 and 200,000 rad over a six to eight-month period are required to produce complete fibrous obliteration of the gland in sheep [Marks *et al.* (134)]. Complete destruction of the normal human thyroid gland by I^{131} , as summarized by Andrews & Knisely (139, 140), does not appear to be producible with a single dose, but extensive epithelial necrosis, infarction, and fibrosis in normal glands can occur after 72 mc. Reliable, consistent radiologic changes can be found in hyperplastic glands [Dailey *et al.* (138)] after as little as 15 mc. Abnormal thyroid cells showing nuclear abnormalities typical of radiation damage have been found eight years after therapy, raising the questions of duration of life of a thyroid epithelial cell and of the possibility of propagating mutated forms [Dobyns *et al.* (137)]. No human case of thyroid carcinogenesis by I^{131} has yet been reported. Dailey found that the production of atrophic fibrotic glands is not secondary to radiovasculitis as previously thought (138). This study and that of Lindsay *et al.* (136) document thoroughly the histopathologic effects of the various types of radiation used therapeutically in thyroid disease. They found them qualitatively similar. Their observation that Hashimoto thyroiditis, a known precancerous disease, has a high incidence in irradiated hyperplastic glands may have an unfortunate prognosis. Follicular atrophy and fibrosis appear to follow therapeutic doses of gamma and x-radiation greater than 1000 r, but this change develops slowly during the ensuing year; epithelial necrosis follows doses greater than 10,000 r within two months of exposure [Lindsay *et al.* (136)].

Histologic changes were described in the adrenal cortex [Birkner *et al.*

(141); Haase & Kroning (142, 143); La Fargue *et al.* (144); Wexler *et al.* (145); Lushbaugh & Hoak (13)]. After doses of more than 50,000 r, the medulla was morphologically unaltered in monkeys, while the zona radiata of the cortex contained numerous foci of necrotic cells invaded by leukocytes (13). These changes were more evident with histochemical methods (141). With smaller doses around 800 r, the volume of the cortex increased (142, 144, 145), although necrotic cells were present. Haase & Kroning (142) felt that the extent of the adrenal changes correlated well with the incidence of leukemia in C₅₇ Black mice. Since 800 r in fractionated doses destroyed the ova without affecting the testicular interstitial cells, and both sexes developed the same degree of adrenal cortical damage, they felt the sexual glands were not involved in the generalized radiation-induced hormonal imbalance which was reflected in and contributed to the adrenal cortical changes (143).

NERVOUS SYSTEM

Brain and Spinal Cord.—Although theoretically there is a rate of exposure to ionizing radiation that can be tolerated without injury for a day or so by every tissue, this tolerance dosage rate is unknown for most tissues. In fact, most morphologic effects of radiation are considered to be independent of rate but dependent on total dose. Much of the confusion concerning the relative radiosensitivity of various cell types stems from the variable rates and energies used in delivering commonly used doses of radiation. Nowhere is this problem illustrated better than in the central nervous system. Injury of the brain or spinal cord with radiation of the energies and rates used commonly in radiotherapy is secondary to the damage of the cerebral blood vessels [Hicks *et al.* (146)]. Case reports of necrosis of the brain following improper therapy of skin tumors of the head illustrate this fact [Dugger *et al.* (147)]. On the other hand, primary destruction of the parenchyma of the central nervous system can occur primarily without accompanying vascular damage with high intensity x- and γ -rays [Arnold *et al.* (148); Haymaker (149); Brandenburg & Maurer (150)]. Extremely high intensity megavolt electrons cannot only destroy the parenchyma of the brain, but they can kill instantly [Hicks *et al.* (146); Haymaker (149)]. Although the precise mechanism of death is not yet fully worked out, it appears that such deaths (doses of 100,000 to 200,000 rep) are due to direct damage to the cardiorespiratory nuclei of the reticular substances and lower cranial nuclei of the medulla [Hicks *et al.* (146)]. The thresholds seem to be: 100 to 200 rep megavolt electrons per second cause necrosis of the subependymal embryonal cells of the brain; 1000 to 2000 rep cause a minimal amount of necrosis of the oligodendroglia cells; 5000 to 10,000 rep cause necrosis of the granule cell neurons; 20,000 rep cause necrosis of cortical neurons, oligodendroglia, and acute disintegration of the myelinated fibers of the striatum and hippocampal commissures [Hicks *et al.* (146)]. The peripheral nerves of coldblooded animals seem to be the most radioresistant viable animal structures, since their ac-

tion potentials only begin to decline at 180,000 r and 15 per cent still remain after 366,000 r [Gerstner (151)]. The spinal cord of *Macacus rhesus* monkeys can tolerate approximately 135 r of gamma (Ta^{182}) radiation per hr. for 24 hr. without morphologic or physiologic effect [McLaurin *et al.* (152)]. It would seem possible that such great tolerance to high voltage ionizing radiation would result in a wide differential of potential therapeutic usefulness between normal and malignant brain tissue. It appears though that the long delayed but inevitable sclerosis of connective tissue and vascular structures restricts the radiotherapy of the relatively more radiosensitive tumors embedded in "radioresistant" cerebral tissue to the damage threshold of the blood vessels, which appears to be about 4500 r delivered in fractions through multiple portals.

EYE

The principal attention in this field continued to be placed on the effects of ionizing radiation on the crystalline lens. The majority of the papers, however, were concerned with the comparative efficacy of such radiation as x-rays, beta-particles, betatron electrons, alpha-particles, neutrons, and mixed radiations from nuclear devices. A major contribution to this field was the analysis of the literature by Ham (153) based on the First, Second, Third, and Fourth Conferences on Radiation Cataracts held by the Committee on Radiation Cataracts from 1950 through 1953. From these conferences has come the concept, which, originally suggested by Poppe (154), is gaining wide acceptance, that cataract formation results from a primary effect upon the proliferating cells of the lens epithelium. This effect is seen as temporary cessation of mitosis and the continued formation of abnormal lens fibers and cellular monstrosities, such as balloon cells, which alter the transparency. Cataract formation depends upon the direct irradiation of the lens [Leinfelder *et al.* (155)]. The irradiated ciliary body may play a role when it is irradiated, but irradiation of the ciliary body is not necessary for cataractogenesis [Alter & Leinfelder (155); Leinfelder *et al.* (156, 157); Puntenney & Shochs (158)]. The failure of opacities to develop in portions of the lens shielded from irradiation appears to confirm this point (155, 157). The observation (158) that partial shielding of the lens prevents formation of a complete cataract in the irradiated portion even after 12,000 r is provocative. This phenomenon, the short penetration of the beta-particle, and the need for direct irradiation of the entire lens, would seem to explain the sharp localization of β -radiation opacities seen experimentally and clinically [MacDonald *et al.* (159); Haik *et al.* (160)] and to be the basis for the observation [Von Sallman *et al.* (161)] that more than 5000 rep of beta exposure are required to produce changes comparable to 1500 r of x-radiation.

It is widely agreed that all the different kinds of ionizing radiations cause the same lens changes without significant species differences. Although the exact numbers for the relative biological effectiveness (RBE) of these radia-

tions vary with the experimenter and his techniques, all agree that the greater the specific ionization of the radiation the greater its effectiveness [Cogan *et al.* (162); Moses *et al.* (163); Leinfelder *et al.* (156); Ham (153); Von Sallman *et al.* (164)]. Small daily exposures with neutrons are more effective than single ones, apparently doubling the RBE for cataractogenesis, indicating a poor recovery rate from such radiation damage. With increasing radiation energies damage is less pronounced [Leinfelder *et al.* (156)]. Of particular interest are these recent approximations of the radiosensitivity of the human lens: complete opacity with x-radiation, 2800 to 4000 r; partial 500 to 1000 r (156); minimal posterior sutural opacities with β -radiation, 2000 to 4000 rep applied to limbus, 20,000 to 40,000 rep applied to central cornea (MacDonald *et al.* (159)).

Pathologic effects of radiation on other portions of the eye were clarified further. Biegel (165) using the 20,000,000-v. betatron demonstrated that immediately following such irradiation of the eye, there is a transitory uveitis, followed by a keratitis. He found in rabbits that 3600 to 4500 r caused atrophy of the retinal bacillary layer. Mature cataracts were present after these doses, accompanied by a hypotony rather than a glaucoma as previously described. Pyknosis and autolysis of retinal rod nuclei leading to extensive atrophy were found following more than 2000 r whole body x-radiation in monkeys [Cibis and Brown (166); Brown *et al.* (167)]. The effect was a direct one. The rods were completely destroyed with 2000 r, but more than 30,000 r were needed to effect changes in all three types of neurons in the retina. Thirteen days after 6000 r of Co^{60} gamma radiation to the head of the animal, the outer nuclear layer of the retina contained only a single row of cone nuclei. These observations were extended recently by Kent & Swanson (168) in a histochemical evaluation of these changes in the rabbit retina after 6000 r of high intensity x-irradiation. The thirteen-and-one-half-day fetal mouse was found to be an ideal animal for studying radiosensitivity of the primitive components of the eye. Rugh & Wolff (169, 170) showed by this means that the neuroectoderm was very radioresistant, while the neuroblast derived from it was extremely radiosensitive, undergoing necrosis within four hr. after 150 r. The retina appeared normal 72 hr. after exposure because of prompt efficient phagocytosis of the debris. Such damage resulted, however, in microphthalmia. Recovery of irradiated neuroblasts was never seen. These cells were removed and the layer reconstituted by new neuroblasts from the neuroectoderm. Hitherto unknown effects of radiation were described by Benedict *et al.* (171) in LAF₁ mice with an inheritable iris atrophy. This effect, which consisted in an accelerated appearance of the defect, was considered, however, to be a reflection of advanced aging rather than a direct primary effect on the iris.

CONCLUSIONS

The progress in the understanding of the histopathogenesis of cellular damage from ionizing radiation has been remarkable in the last four years.

The outstanding major accomplishment appears, at this time, to be the establishment of the "cellular hypothesis" for radioprotection by hematopoietic homogenates. The possibility of developing new therapeutic methods for human diseases based on this technique looks most encouraging. Although little additional progress appears to have been made in defining further the mechanism of death at low doses of radiation, substantial progress was made toward better understanding the pathogenesis of damage and death from supralethal and rapidly delivered massive doses of radiation. The morphologic studies revealed hitherto unknown thresholds of damage for many tissues previously considered only as radioresistant. More observations of this kind are needed to understand the relative radiosensitivity of all tissues. The need is pointed out for more precise definitions of "radiosensitivity" and "resistance." The practical importance of evaluating organic radiosensitivity and degree of reparability and ultimately damaging sclerosis cannot be over-emphasized.

LITERATURE CITED

1. Furth, J., and Upton, A. C., *Ann. Rev. Nuclear Sci.*, **3**, 303-38 (1953)
2. Lacassagne, A., and Gricouloff, G., *L'Action des ionisantes Radiations sur l'organisme* (Maison et Cie, Paris France, 197 pp., 1956)
3. Stevens, L. G., *Brit. Med. J.*, 998 (1896)
4. Bloom, W., *Histopathology of Irradiation from External and Internal Sources* (McGraw-Hill Publishing Company, New York 18, N. Y., 808 pp., 1948)
5. Patt, H. M., *Ann. N. Y. Acad. Sci.*, **59**, 649-64 (1955)
6. Gray, L. H., *Brit. J. Radiol.*, **26**, 609-18 (1953)
7. Stroud, A. N., *Ann. N. Y. Acad. Sci.*, **67**, 11-34 (1956)
8. Trowell, O. A., *Brit. J. Radiol.*, **26**, 302-09 (1953)
9. Zirkle, R. E., and Bloom, W., *Science*, **17**, 487 (1953)
10. Evans, T. C., *Acta Radiol., Suppl.*, **116**, 441-47 (1954)
11. Meldolesi, G. E., *Arch. Radiol.*, **29**, 291-96 (1954)
12. Langham, W. H., Woodward, K. T., Rothermel, S. M., Harris, P. S., Lushbaugh, C. C., and Storer, J. B., *Radiation Research*, **5**, 404-32 (1956)
13. Lushbaugh, C. C., and Hoak, C., *Federation Proc.*, **14**, 1331 (1955)
14. Vogel, F. S., and Ballin, J. C., *Proc. Soc. Exptl. Biol. Med.*, **90**, 419-23 (1955)
15. Shrek, R., *Arch. Pathol.*, **63**, 252-59 (1957)
16. Friedman, N. B., Sargent, J. A., and Drutz, E., *Cancer Research*, **15**, 479-84 (1955)
17. Glucksman, A., *Brit. J. Radiol.*, **25**, 38-43 (1952)
18. Teir, H., *Acta Pathol. Microbiol. Scand.*, **32**, 337-47 (1953)
19. Loutit, J. F., *J. Nuclear Energy*, **1**, 87-91 (1954)
20. Storer, J. B., *Univ. Chicago Toxicity Lab. Quart. Progr. Rept.*, No. 6, 6-7 (July 1950)
21. Storer, J. B., Lushbaugh, C. C., and Furchner, J. E., *J. Lab. Clin. Med.*, **40**, 355-66 (1952)
22. Barnes, D. W. H., and Loutit, J. F., *Nucleonics*, **12**(5), 68-70 (1954)
23. Cole, L. J., Fishler, M. C., Ellis, M. E., and Bond, V. P., *Proc. Soc. Exptl. Biol. Med.*, **80**, 112-21 (1952)
24. Cole, L. J., Fishler, M. C., and Bond, V. P., *Federation Proc.*, **12**, 27 (1953)

25. Brown, M. B., Hirsch, B. B., Nozareda, C. S., Hochstetler, S. K., Faraghan, W. G., Toch, P., and Kaplan, H. S., *J. Natl. Cancer Inst.*, **15**, 949-73 (1955)
26. Lorenz, E., Congdon, C. C., and Uphoff, D., *Radiology*, **58**, 863-77 (1952)
27. Congdon, C. C., Uphoff, D., and Lorenz, E., *J. Natl. Cancer Inst.*, **13**, 73-107 (1952)
28. Congdon, C. C., and Lorenz, E., *Am. J. Physiol.*, **176**, 297-300 (1954)
29. Cole, L. J., Habermeyer, J. G., and Bond, V. P., *J. Natl. Cancer Inst.*, **16**, 1-9 (1955)
30. Main, J. M., and Prehn, R. T., *J. Natl. Cancer Inst.*, **15**, 1023-30 (1955)
31. Lindsley, D. L., Odell, T. T., Jr., and Tausche, F. G., *Proc. Soc. Exptl. Biol. Med.*, **90**, 512-15 (1955)
32. Nowell, P. C., Cole, L. J., Habermeyer, J. G., and Roan, P. L., *Cancer Research*, **16**, 258-61 (1956)
33. Ford, C. E., Hamerton, J. L., Barnes, D. W. H., and Loutit, J. F., *Nature*, **177**, 452-54 (1956)
34. Makinodan, T., *Proc. Soc. Exptl. Biol. Med.*, **92**, 174-79 (1956)
35. Jacobson, L. O., *Ann. Rev. Med.*, **7**, 345-52 (1956)
36. Jacobson, L. O., *Progress in Hematology* (Ed., Tocantins, L. M., Grune and Stratton, New York, N. Y., 344 pp., 1956)
37. Baum, S. J., Kimeldorf, D. J., and Jacobsen, E. M., *Blood*, **10**, 926-32 (1955)
38. Zirkle, R. E., Ed., *Biological Effects of External X and Gamma Radiation, Part I* (McGraw-Hill Book Company, Inc., New York, N. Y., 530 pp., 1954)
39. Ackerman, G. A., Bellios, N. C., Knouff, R. A., and Frajola, W. J., *J. Hematol.*, **9**, 795-803 (1954)
40. Yoffey, J. M., *J. Histochem. and Cytochem.*, **4**, 516-30 (1956)
41. Harris, P. F., *Brit. Med. J.*, **2**, 1032-40 (1956)
42. Latta, J. S., and Waggener, R. E., *Anat. Rec.*, **119**, 357-86 (1954)
43. Cronkite, E. P., Bond, V. P., Conard, R. A., Shulman, N. R., Farr, R. S., Cohn, S. H., Dunham, C. L., and Browning, L. E., *J. Am. Med. Assoc.*, **159**, 430-34 (1955)
44. Gillman, T., Penn, J., Bronks, D., and Roux, M., *Arch. Pathol.*, **59**, 733-49 (1955)
45. Griffith, H. D., *Arch. Geschwulstforsch.*, **6**, 305-11 (1954)
46. Griffith, H. D., Philip, J. F., and Swindell, G. E., *Brit. J. Radiol.*, **27**, 107-12 (1954)
47. Kulwin, M. H., and Buley, H. M., *Arch. Dermatol. u Syphilis*, **70**, 417-25 (1954)
48. Nodl, F., *Strahlentherapie*, **92**, 576-89 (1953)
49. Nodl, F., *Arch. Dermatol. u Syphilis*, **200**, 136-37 (1955)
50. Romanini, A., and Chippa, S., *Boll. soc. ital. biol. sper.*, **30**, 811-13 (1954)
51. Shaffer, R. N., *Transactions Am. Ophthalmol. Soc.*, **50**, 607-27 (1953)
52. Wachsmann, F., *Strahlentherapie*, **90**, 438-45 (1953)
53. Witten, V. H., and Sulzberger, W. B., *Am. J. Roentgenol.*, **74**, 90-97 (1955)
54. Devik, F., *Acta Radiol., Suppl.*, **119**, 1-72 (1955)
55. Arvey, L., Boiffard, J. A., and Gabe, M., *Compt. rend. soc. biol.*, **148**, 1189-91 (1954)
56. Kroning, F., and Sigmund, R., *Hautarzt*, **6**, 127-29 (1955)

57. Upton, A. C., and Gude, W. D., *Arch. Pathol.*, **58**, 258-64 (1954)
58. Ungar, G., and Damgaard, E., *Proc. Soc. Exptl. Biol. Med.*, **87**, 383-86 (1954)
59. Ungar, G., Damgaard, E., and Williams, F., *J. Appl. Physiol.*, **8**, 287-88 (1955)
60. Lushbaugh, C. C., Storer, J. B., and Hale, D. B., *Cancer*, **6**, 671-77 (1953)
61. Lushbaugh, C. C., and Storer, J. B., *Cancer*, **6**, 678-82 (1953)
62. Lushbaugh, C. C., and Hale, D. B., *Cancer*, **6**, 683-85 (1953)
63. Lushbaugh, C. C., and Hale, D. B., *Cancer*, **6**, 686-89 (1953)
64. Lushbaugh, C. C., and Hale, D. B., *Cancer*, **6**, 690-98 (1953)
65. Farris, G., and Olivia, L., *Giorn. Ital. dermatol. sifilol.*, **95**, 611-37 (1954)
66. Pettersson, T., *Acta Pathol. Microbiol. Scand. Suppl.*, **102**, 1-62 (1954)
67. Barth, G., Katrakis, G., and Wachsmann, F., *Strahlentherapie*, **92**, 644-48 (1953)
68. Meschan, I., and Nettleship, A., *Am. J. Roentgenol.*, **71**, 306-19 (1954)
69. Moritz, A. R., and Henriques, F. W., Jr., *Lab. Invest.*, **1**, 167-85 (1952)
70. Nerli, A., *Radioterap., radiobiol. e fis. med.*, **297**-315 (1954)
71. Merwin, R. M., and Hill, E. L., *J. Natl. Cancer Inst.*, **15**, 1031-37 (1955)
72. Lushbaugh, C. C., and Spalding, J. F., *J. Vet. Research* (In press 1957)
73. Devik, F., *Nord. Med.*, **50**, 964-66 (1953)
74. Edgerly, R. H., *Am. J. Physiol.*, **174**, 341-46 (1953)
75. Ungar, G., and Damgaard, E., *Proc. Soc. Exptl. Biol. Med.*, **87**, 378-83 (1954)
76. Lushbaugh, C. C., and Hughes, L. B. (Unpublished data 1957)
77. Lawrence, W., Jr., Nickson, J. J., and Warshaw, I. M., *Surgery*, **33**, 376-84 (1953)
78. Brown, J. B., and Fryer, M. P., *Surg., Gynecol. Obstet.*, **103**, 1-4 (1956)
79. Brooks, P. M., Gerstner, H. B., and Smith, S. A., *Radiation Research*, **4**, 500-9 (1956)
80. Heite, H. J., and Schrader, W., *Strahlentherapie*, **97**, 395-402 (1955)
81. Bohr, D. F., Rondell, P. A., Palmer, L. E., Baker, B. L., and Bethell, F. H., *Am. J. Physiol.*, **183**, 331-34 (1955)
82. Rieser, P., *Proc. Soc. Exptl. Biol. Med.*, **89**, 39-41 (1955)
83. Gerstner, H. B., Lewis, R. B., and Richey, E. O., *J. Gen. Physiol.*, **37**, 445-59 (1954)
84. Lewis, R. B., *Lab. Invest.*, **3**, 48-55 (1954)
85. Copeland, M. M., *Am. Acad. Orthopedic Surgeons Lectures*, **10**, 191-212 (1953)
86. MacLennan, W. D., *Proc. Roy. Soc. Med. (London)*, **48**, 1017-22 (1955)
87. English, J. A., *J. Dental Research*, **34**, 4-11 (1955)
88. English, J. A., Wheatcroft, M. G., Lyon, H. W., and Miller, C., *Oral Surg.*, **8**, 87-99 (1955)
89. Shafer, W. G., *J. Dental Research*, **32**, 796-806 (1953)
90. Burstone, M. S., *J. Am. Dental Assoc.*, **47**, 630-36 (1953)
91. Medak, H., and Burnett, G. W., *Oral Surg.*, **7**, 778-86 (1954)
92. Friedman, N. B., *J. Exptl. Med.*, **81**, 553-57 (1945)
93. Friedman, N. B., *Arch. Pathol.*, **59**, 2-4 (1955)
94. Quastler, H., Lanzle, E. F., Keller, M. E., and Osborne, J. W., *Am. J. Physiol.*, **164**, 546-56 (1951)
95. Quastler, H., *Radiation Research*, **4**, 303-20 (1956)
96. Goldgraber, M. B., Rubin, C. E., Palmer, W. L., Dobson, R. L., and Massey, B. W., *Gastroenterology*, **27**, 1-20 (1954)

97. Brick, I. B., *Arch. Internal Med.*, **96**, 26-31 (1955)
98. Detrick, L. E., Upham, H. C., Higby, D., Debley, V., and Haley, T. J., *Am. J. Physiol.*, **179**, 462-66 (1954)
99. Littman, A., Fox, B. W., Schoolman, H. M., and Ivy, A. C., *Am. J. Physiol.*, **174**, 347-51 (1953)
100. LeBlond, C. P., and Stevens, C. E., *Anat. Rec.*, **100**, 357-78 (1948)
101. Montagna, W., and Wilson, J. W., *J. Natl. Cancer Inst.*, **15**, 1703-35 (1955)
102. Anderson, R. E., Wilkowski, L. J., and Pontius, G. V., *Surgery*, **38**, 605-9 (1955)
103. Bock, K., and Heyde, W., *Zentr. Gynakol.*, **75**, 642-50 (1953)
104. Swift, M. W., and Taketa, S. T., *Am. J. Physiol.*, **185**, 85-91 (1956)
105. Osborne, J. W., *Radiation Research*, **4**, 541-46 (1956)
106. Sommers, S. C., and Warren, S., *Am. J. Digest. Diseases*, **22**, 109-11 (1955)
107. White, J., Congdon, C. C., David, P. W., and Ally, M. S., *J. Natl. Cancer Inst.*, **15**, 1155-63 (1955)
108. White, J., *J. Natl. Cancer Inst.*, **15**, 1617-18 (1955)
109. Gershbein, L. L., *Am. J. Physiol.*, **185**, 245-49 (1956)
110. Upton, A. C., Furth, J., and Burnett, W. T., Jr., *Cancer Research*, **16**, 216-21 (1956)
111. Lelievre, P., Betz, H., and Jehotte, J., *Compt. rend. soc. biol.*, **149**, 1077-79 (1955)
112. Spalding, J. F., and Lushbaugh, C. C., *Federation Proc.*, **14**, 1358 (1955)
113. Grossman, B. J., *J. Pediat.*, **47**, 424-33 (1955)
114. Carpenter, J. W. J., *Radiology*, **61**, 649-50 (1953)
115. Luxton, R. W., *Quart. J. Med.*, **22**, 215-42 (1953)
116. Furth, J., Upton, A. C., Christenberry, K. W., Benedict, W. H., and Moshman, J., *Radiology*, **63**, 562-69 (1954)
117. Cole, L. J., Nowell, P. C., and Ellis, M. E., *J. Natl. Cancer Inst.*, **17**, 435-46 (1956)
118. Bohr, D. F., Rondell, P. A., Palmer, L. E., and Bethell, F. H., *Am. J. Physiol.*, **183**, 335-39 (1955)
119. Eschenbrenner, A. B., and Muller, E., *Arch. Pathol.*, **50**, 736-49 (1950)
120. Shaver, S. L., *Am. J. Anat.*, **92**, 391-432 (1953)
121. Oakberg, E. F., *Radiation Research*, **2**, 369-91 (1955)
122. Oakberg, E. F., *J. Morphol.*, **97**, 39-54 (1955)
123. Fogg, L. C., and Cowing, R. F., *Exptl. Cell Research*, **4**, 107-15 (1953)
124. Spalding, J. F., Wellnitz, J. M., and Schweitzer, W. H., *Radiation Research*, **6** (In press 1957)
125. Kohn, H. I., *Radiation Research*, **3**, 153-56 (1955)
126. Kohn, H. I., and Kallman, R. F., *Brit. J. Radiol.*, **29**, 586-91 (1954)
127. Kohn, H. I., and Kallman, R. F., *J. Natl. Cancer Inst.*, **15**, 891-99 (1955)
128. Rugh, R., *Proc. Soc. Exptl. Biol. Med.*, **83**, 762-64 (1953)
129. Tillotson, G. W., Rose, R. G., and Warren, S., *Am. J. Roentgenol.*, **70**, 599-604 (1953)
130. Spalding, J. F., Wellnitz, J. M., and Schweitzer, W. H., *Fertility and Sterility*, **8**, 80-88 (1957)
131. Von Massenbach, W., and Czech, H., *Geburtsh. Frauenheilk.*, **14**, 317-22 (1954)
132. Foraker, A. G., Denham, W., and Mitchell, D. D., *Arch. Pathol.*, **59**, 82-89 (1955)
133. Korson, R., and Botkin, A. L., *Endocrinology*, **54**, 225-26 (1954)

134. Mateyko, G. M., and Edelmann, A., *Radiation Research*, **1**, 470-86 (1954)
135. Marks, S., Dockum, N. L., and Bustad, L. K., *AEC Research and Development Rept.*, HW-38758, 44 pp. (1955)
136. Lindsay, S., Dailey, M. E., and Jones, M. D., *J. Clin. Endocrinol. and Metabolism*, **14**, 1179-218 (1954)
137. Dobyns, B. M., Vickery, A. L., Maloff, F., and Chapman, E. M., *J. Clin. Endocrinol. and Metabolism*, **13**, 548-67 (1953)
138. Dailey, M. E., Lindsay, S., and Miller, E. R., *J. Clin. Endocrinol. and Metabolism*, **13**, 1513-29 (1953)
139. Andrews, G. A., Knisely, R. M., Bigelow, R. B., Root, S. W., and Brucer, M., *Am. J. Med.*, **16**, 372-81 (1954)
140. Andrews, G. A., and Knisely, R. M., in *Radioisotopes in Medicine*, Chap. 27, pp. 400-11 (U. S. Government Printing Office, 817 pp., 1953), Andrews, G. A., Brucer, M., and Anderson, E. B., Ed.
141. Birkner R., Suchowsky, G., and Trautman, J., *Strahlentherapie*, **94**, 506-26 (1954)
142. Haase, J., and Kroning, F., *Endokrinologie*, **32**, 8-23 (1954)
143. Kroning, F., and Haase, J., *Endokrinologie*, **32**, 264-80 (1955)
144. La Fargue, J., Schiller, J., Tyan, E., and Pitoy, S., *Ann. endocrinol. (Paris)*, **14**, 422-24 (1953)
145. Wexler, B. C., Pencharz, R., and Thomas, S. F., *Am. J. Physiol.*, **183**, 71-74 (1955)
146. Hicks, S. P., Wright, K. A., and Leigh, K. E., *Arch. Pathol.*, **61**, 226-38 (1956)
147. Dugger, G. S., Stratford, J. G., and Bouchard, J., *Am. J. Roentgenol.*, **72**, 953-60 (1954)
148. Arnold, A., Bailey, P., and Laughlin, J. S., *Neurology*, **4**, 165-78 (1954)
149. Haymaker, W., Vogel, F. S., Cammermeyer, J., Laqueur, G. L., and Nauta, W. J. H., *Am. J. Clin. Pathol., Suppl.*, **24**, 70 (1954)
150. Brandenburg, W., and Maurer, H. J., *Strahlentherapie*, **95**, 432-39 (1954)
151. Gerstner, H. B., *Am. J. Physiol.*, **184**, 333-37 (1956)
152. McLaurin, R. L., Bailey, O. T., Harsh, G. R. 3rd and Ingraham, F. D., *Am. J. Roentgenol.*, **73**, 827-35 (1955)
153. Ham, W. T., Jr., *Arch. Ophthalmol.*, **50**, 618-43 (1953)
154. Poppe, E., *Acta Radiol.*, **23**, 354-67 (1942)
155. Alter, A. J., and Leinfelder, P. J., *Arch. Ophthalmol.*, **49**, 257-60 (1953)
156. Leinfelder, P. J., Evans, T. C., and Riley, E., *Radiology*, **65**, 433-38 (1955)
157. Leinfelder, P. J., and Riley, E. F., *Arch. Ophthalmol.*, **55**, 84-86 (1956)
158. Puntenney, I., and Schoch, D., *Trans. Am. Ophthalmol. Soc.*, **51**, 285-300 (1953)
159. MacDonald, J. E., Hughes, W. F., Jr., and Pfeiffer, V. G., *A.M.A. Arch. Ophthalmol.*, **53**, 248-58 (1955)
160. Haik, G. M., Wood, L., Waugh, R. L., and Ellis, G., *Am. J. Ophthalmol.*, **38**, 465-70 (1954)
161. Van Sallman, L., Munoz, C. M., and Drungis, A., *Arch. Ophthalmol.*, **50**, 727-36 (1953)
162. Cogan, D. G., Donaldson, D. D., Goff, J. L., and Graves, E., *Arch. Ophthalmol.*, **50**, 597-602 (1953)
163. Moses, C., Linn., J. G., and Allen, A. J., *Arch. Ophthalmol.*, **50**, 609-12 (1953)

164. Von Sallman, L., Tobias, C. A., Anger, H. O., Welch, C., Kimura, S. F., Munoz, C. M., and Drungis, A., *Arch. Ophthalmol.*, **54**, 489-514 (1955)
165. Biegel, A. C., *Arch. Ophthalmol.*, **54**, 392-406 (1955)
166. Cibis, P. A., and Brown, D. V. L., *Am. J. Ophthalmol.*, **40**, 84-88 (1955)
167. Brown, D. V. L., Cibis, P. A., and Pickering, J. E., *Arch. Ophthalmol.*, **54**, 249-56 (1955)
168. Kent, S. P., and Swanson, A. A., *Radiation Research*, **6**, 111-20 (1957)
169. Rugh, R., and Wolff, J., *Arch. Ophthalmol.*, **54**, 351-59 (1955)
170. Rugh, R., and Wolff, J., *Proc. Soc. Exptl. Biol. Med.*, **89**, 248-53 (1955)
171. Benedict, W. H., Christenberry, K. W., and Upton, A. C., *Am. J. Ophthalmol.*, **40**, 163-69 (1955)

THE COLLECTIVE MODEL OF NUCLEI¹

By F. VILLARS

*European Organization for Nuclear Research (CERN),
Geneva, Switzerland²*

I. SURVEY

1. INTRODUCTION AND OUTLINE

A short time only after the introduction of the $j-j$ -coupling shell model in 1949 (1, 2), collective (cooperative) effects were brought back into the picture of the nucleus, in order to cope with the model's main difficulty: the explanation of the giant quadrupole moments (3). Since then, the systematic study of collective effects went almost parallel with the further development of the shell model. As a result, a synthesis of the two aspects of nuclear dynamics, single particle, and collective behaviour, has become one of today's most interesting problems of nuclear structure.

Collective aspects had for a long time dominated the thinking in nuclear physics, ever since in 1937 Bohr and Kalckar presented the liquid drop picture, and showed the implication of this and associated concepts for nuclear reactions, in particular. It is not in this form that the "collective model" has re-entered the scene in 1951. In fact, the original picture of collective motion attributable to very strongly interacting nucleons had to be considerably revised, since it has become clear that in moderate energy nuclear reactions the redistribution of excitation energy is a much slower process than one had previously assumed (4, 5, 6). This, together with the wealth of experimental evidence so neatly summed up in the shell model, is a clear indication that the idea of individual nuclear "orbits" (single particle quantum states) is a sensible concept up to excitation energies of 10 to 15 Mev. (For surveys of the shell model, see Refs. 7 to 11.)

Thus, if the "collective aspect" is revived today, it is not in the sense of questioning again all the results which point toward independent particle motion. The collective phenomena considered here are of a much more subtle type and, most essentially, they are intimately connected with the independent particle aspect of nuclear structure (12).

This independent particle aspect finds traditionally its expression in the Hartree-Fock equation, in which the single particle states of all nucleons co-operate to define a "self-consistent" one particle potential. In this non-linearity of the Hartree-Fock problem, we have already a typical collective effect: a truly self-consistent solution of these equations leads, indeed, to a potential, whose size, depth, shape, and deformation³ depends on the nature

¹ The survey of literature pertaining to this review was completed on March 1st, (1957).

² On leave of absence from Massachusetts Institute of Technology, Cambridge, Massachusetts.

³ We use the word "shape" to describe the radial dependence, the word "deformation" to describe the angular dependence of the well.

of the occupied states. Unfortunately, this collective aspect of the method cannot easily be exploited to display the collective dynamics. Most of the purely theoretical approaches to the problem of collective motion deal with this difficulty and with ways to overcome it.

The collective and unified models have been presented in various publications: condensed reviews by Bohr (13), by Bohr & Mottelson (14), and by Alder, *et al.* (15), a detailed account in the monograph by Bohr & Mottelson (16), and, with different emphasis, in the paper by Hill & Wheeler (12). This makes it possible here to emphasize more fully some developments which have not yet been adequately reviewed, and deal with the problem of a more detailed understanding of the fundamental assumptions of the model, of the role of single particle motion in the model, and of the outstanding problems still to be solved.

In the next two sections we shall give a short survey, presenting the unified model and the nature of the evidence supporting it.

Part II of this review is purely theoretical, and deals mainly with attempts to formulate collective motion in terms of particle concepts. The purpose of such theoretical attempts is twofold: first, they give insight into the nature and justification of the simplifying assumptions made in the construction of actual models; secondly, they are the starting point for new techniques of approach to the problem of finding self-consistent solutions of the Schrödinger equation. The achievement so far accomplished by these purely theoretical considerations is somewhat limited. But they have, for instance, helped to clear up the nature of the coupling of collective rotation and intrinsic motion, they have contributed to our understanding of the Inglis model, etc. They are presented here also as a temptation to stimulate further research along the lines sketched in that part.

In part III various models constructed to display collective aspects in nuclear structure are presented; an attempt is made to describe and to assess the nature of the assumptions involved in the construction of the model. Finally, definite statements made by such models are compared with the experimental evidence.

2. THE NATURE OF THE UNIFIED MODEL

Only very recently have there been any attempts to calculate a really self-consistent nuclear potential (17). Such attempts are discouraged by the unreliability of the approximation. The original Hartree-Fock approximation makes sense only for rather unrealistic types of two-body potentials [Bethe (18)]; more refined methods, expressing the energy in terms of the two-body scattering matrix [Brueckner & Levinson (19); Eden & Francis (20); Bethe & Goldstone (21)] have been used with a certain success by Brueckner, Eden & Francis (22), but are in a too preliminary stage to permit wholesale application. In addition, such methods were primarily designed to handle the problem of nuclear saturation (that is, determination of energy), whereas here the attention is focused on other properties: electric and magnetic moments, transition probabilities, moments of inertia. As Eden & Francis

have shown in an outline of a general "theory of models" (20), the correct evaluations of such quantities as mentioned above is a much more subtle problem than minimizing the energy. For the special case of magnetic moments, this difficulty has been illustrated by Bell, Eden & Skyrme (23). In this report we cannot but adopt a very elementary point of view and essentially ignore that problem; but this should not mean that we minimize its relevance for the questions to be discussed here.

Even apart from the questions of reliability, there is the formidable technical problem of carrying out a numerical Hartree-Fock calculation. As a consequence, all the thinking has been dominated by ready-made isotropic single particle potentials of given shape; their isotropy had at least the advantage of allowing the use of angular momentum eigenstates. The large quadrupole moments in the region $150 \leq A \leq 190$ and $A \geq 225$ have finally forced us to abandon this picture, and to admit nonspherical (deformed) potentials (3).

The introduction of deformed wells as a better approximation to self-consistency (from an energetic point of view) leads to states that cannot be *eigenstates* of the total angular momentum. But a similar situation has always been tacitly tolerated with respect to the total linear momentum. The total linear and angular momenta are collective dynamical variables, which cannot be properly taken care of in a self-consistent independent particle approximation; and it is certainly a step forward to recognize that nothing is gained by trying to sacrifice the flexibility of the Hartree-Fock method in an attempt to deal exclusively with angular momentum eigenstates. Overstating the case, we may say that both total linear and angular momentum are collective variables which have little to do with the internal structure, and are better discarded in a first approximation to the latter.

For the case of the angular momentum, Bohr, in a beautiful analysis (24), has shown how to interpret these states that do not conserve it: the angular momentum of the Hartree-Fock solution is an "intrinsic" angular momentum \mathbf{J} ; this latter differs from the (conserved) total angular momentum \mathbf{I} by a quantity $\mathbf{R} = (\mathbf{I} - \mathbf{J})$ representing the angular momentum of the precession of the nonspherical intrinsic structure about the axis \mathbf{I} . As this precession leaves the intrinsic structure relatively unaffected (see, however, part III), there exist, under suitable conditions, states of identical intrinsic structure, differing by the value of \mathbf{R} only. These states form the rotational spectrum of excitations.

Although this point of view strongly appeals to our intuition, its mathematical formulation presents difficult problems. The simplest approach is based on the assumption that a few nucleons only are responsible for the actual deformation of the well; these nucleons are then treated as individuals, and the remaining part of the nucleus is treated as a "soft" core, the dynamics of which is expressed in terms of a few suitable collective deformation parameters. The dynamic coupling between core and particles is introduced by the assumption that the density distribution $\rho(r, \theta, \varphi)$ of the core defines the well for the extra nucleons. Although this is a conceptually clean

scheme for constructing a unified model, it is subject to serious objections: (a) In order to obtain a workable "model" in the above mentioned way, the properties of the core, as defined here, should be either uniform or smoothly varying functions of the number of particles (N_c , Z_c) it contains. There is, however, every indication that if the number of extra nucleons is kept small (in the extreme limit: zero or two for even, one for odd nuclei), then the properties of the core show strong shell effects. It results that no purely collective model will reproduce the properties of such a core. (b) On the other hand, theoretical considerations, especially the results of the Inglis model (see part III), show that a relatively uniform behaviour may be expected for closed shell cores. But a division of the nucleus into a collectively described closed shell core and extra nucleons is hardly desirable either: First, the deformation of the core is then no longer a measure of the actual deformation of the nucleus. Second, since the number of extra nucleons may now be large, their direct interaction contributes significantly to the self-consistent potential, and they may be mainly responsible for the actual values of moments of inertia and deformation; just the most interesting collective aspects would then result from particles described individually. (c) To achieve self-consistency, one clearly needs a description which is symmetric in the particles, since they all contribute in a symmetric way to the definition of the single particle well. The only symmetric description of this kind which leads to a "model" is based on the method of Hill & Wheeler which is discussed in part II.2. This method gives a simple and straightforward way to superimpose the collective aspects upon the independent particle description of the nucleus, with the result that all quantities (inertial parameters, deformation potentials, collective flow pattern, electromagnetic moments) are determined by the underlying particle dynamics. A more ambitious and fundamental approach, which also describes all particles in a symmetric manner, is the method of redundant variables, presented in part II.4. This method is, however, still in its infancy.

3. ACHIEVEMENTS OF THE UNIFIED MODEL

The outstanding success of the unified point of view is of course the prediction and subsequent actual identification of rotational levels, together with an explanation of the rather well defined regions of their occurrence in the periodic table and the correlation between moments of inertia and intrinsic quadrupole moments. We now give a very short survey of this and other results of interest.

a) *Rotational levels.*—The number of rotational spectra, or of spectra with at least three levels fitting into a rotational band, is very considerable now (15, 25, 26). What characterizes these spectra so strikingly, even from a purely empirical point of view, is the accuracy with which they fit a one- (or two-, for $K=\frac{1}{2}$ bands) parameter formula. In adding a second (third) parameter in the form of a rotation-vibration coupling term, the levels can be reproduced with a really outstanding accuracy (see the examples given in Fig. 1). The one- (two-) parameter formulae are

$$E_I = \frac{\hbar^2}{2\mathfrak{J}} \{ I(I+1) + a\delta_{K,1/2}(-1)^{I+1/2}(I+1/2) \} \quad 1.$$

\mathfrak{J} being the effective moment of inertia and a the decoupling parameter (16, 27). K is the quantum number of the projection of the total angular momentum on the body fixed symmetry axis, and characterizes a rotational band:

$$\begin{array}{ll} I = 0, 2, 4, \dots; & K = 0: \text{even nuclei} \\ I = I_0, I_0 + 1, I_0 + 2, \dots; & K = I_0: \text{odd nuclei} \end{array}$$

Occasionally more than one band is observed in a nucleus, (W^{183}). All levels of a band have the parity of the ground state member.

The rotation vibration interaction adds a term

$$- \text{const } I^2(I+1)^2 \quad 2.$$

to the energy levels. The experimental value of the (positive) constant agrees in order of magnitude with what one expects on the basis of vibrational excitation energies. In Figure 1, we give an example, which illustrates three different types of rotational spectra.

The purity of the rotational level spacings leads us to interpret the dynamics in terms of a very simple coupling scheme: All particle motions are first coupled to the intrinsic symmetry axis, which in turn precesses, with an interpretation of adiabatic slowness, about the axis of the total angular momentum I .

b) *Quadrupole moments and E2-transitions.*—The giant quadrupole moments were, as already mentioned, the primary argument for the introduction of the collective viewpoint. Although the striking parallelism between magnitude of the intrinsic electric quadrupole moments Q_0 and the rotational moments of inertia \mathfrak{J} is qualitatively understood, we are still far from having a quantitative theory of the latter; this has in fact proven to be one of the most interesting problems to be solved yet, since the value of \mathfrak{J} depends so sensitively on the degree of residual internucleon coupling (See part III.2).

For strongly deformed nuclei, careful distinction must be made between intrinsic and "spectroscopic" quadrupole moments, the former measuring the deformation in the body fixed, the latter in the space fixed (laboratory) system. $E2$ -transition probabilities B_{E2} are directly expressible in terms of the intrinsic moments Q_0 , and the consistency between values of Q_0 from Q and B_{E2} measurements is reasonably good (25). This again indicates the basic correctness of the simple coupling scheme for large deformations.

For nuclei not displaying rotational levels, the situation may be rather complex. Generally, $E2$ -transitions appear to be strongly enhanced. It has been shown however that already a very small "contamination" of the rigorous shell picture with collective effects ("weak coupling") will enhance the $E2$ -transition rates, without otherwise affecting the intrinsic dynamics, which is still dominated by single particle level order and residual inter-

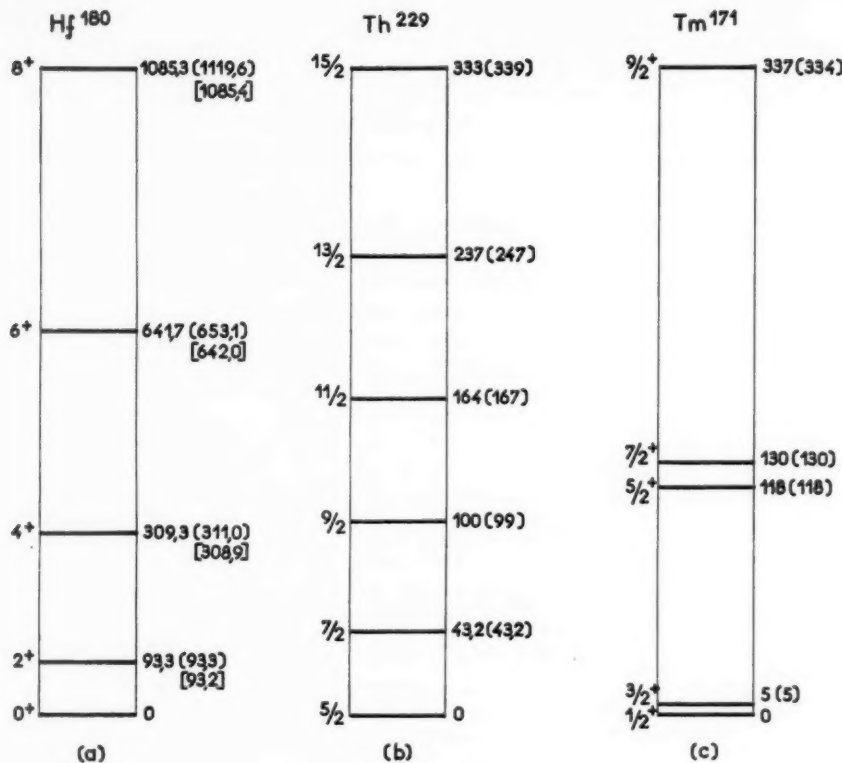


FIG. 1.

(a) Spectrum of an even nucleus:

$$E_I = (\hbar^2/2\mathfrak{J})I(I+1); \quad I = 0, 2, 4, \dots$$

Odd values of I are suppressed by the symmetry condition on the collective wave function. This example is discussed in detail in Refs. (13) and (15). To the left are spins and parities; to the right observed energies, calculated energies without, (), and with, [], rotation-vibration interaction. (b) Spectrum of an odd nucleus with $K \neq \frac{1}{2}$:

$$E_I = (\hbar^2/2\mathfrak{J})\{I(I+1) - I_0(I_0+1)\}; \quad I = I_0, I_0 + 1, \dots$$

This example is due to Goldin *et al.* (31), and found in the α -decay of U^{233} . (c) Spectrum of an odd nucleus with $K = \frac{1}{2}$:

$$E_I = (\hbar^2/2\mathfrak{J})\{I(I+1) + a(-1)^{I+1/2}(I+1/2)\}$$

This example is due to Johansson (32); the experimentally adjusted value of a is $a = -0.86$; the levels are found by β -decay of $E_{r^{171}}$.

particle couplings. This is so, at least, for odd nuclei. In many even nuclei, the frequently observed situations with $E_2/E_1 \approx 2$, together with 2^+ for E_1 , $2^+(4^+)$ for E_2 and the inhibition of the cross-over transition $E_2(2^+) \rightarrow E_0(0^+)$

seems to warrant a purely collective description in term of a harmonic oscillation. The situation is however not quite clarified yet, as no simple model covers all the facts in a quantitative way.

c) *Magnetic moments.*—The simple coupling scheme for strongly deformed nuclei again reduces the expression for μ to a two parameter formula (3 parameters for $K = \frac{1}{2}$):

$$\mu = \frac{1}{I+1} (g_{\alpha} I^2 + g_e I) \quad 3.$$

and an analysis consists in an interpretation of g_e and g_{α} , the g -factors for core precession and intrinsic motion, respectively [with $(g_{\alpha} - g_e)^2$ supplied by $M1$ -transition probabilities, see (16)]. Naively one would then expect g_e to be $= Z/A \sim 0.4$. Actually the experimental values deviate considerably from 0.4 (25), (15), even in cases where other evidence supports the coupling scheme.

One should, however, not necessarily consider this as a weakness of the theory. As may be seen in part II, all theoretical ("fundamental") approaches to the problem of collective rotation have stopped short of a complete decoupling of collective and intrinsic motion. In simple terms, this means that they have not found yet the "right" body fixed coordinate system: If we require the intrinsic motion, described in the body fixed system, to be decoupled from the rotation of that system, then that system is not defined by the kinematics of the nucleus alone, but is determined by the intrinsic dynamics too. The "right" intrinsic coordinate axes then depend not only on the distribution of nucleons, but on their momenta as well. In such a situation it cannot even be asserted that g_e should be equal to Z/A so that, until further notice, there is no question of a discrepancy. Investigations of these problems are only in their beginning (28).

d) *Fission.*—Space does not permit us to enter into this subject, but we wish to recall the work of Hill & Wheeler (12), Bohr (29), and Wheeler (30), in which the fission process is analyzed from the point of view of the unified model.

II. GENERAL THEORY

1. INTRODUCTORY COMMENTS

We have pointed out the collective aspects in the self-consistent independent particle approximation; but these features appear there merely in the form of collective (variational) parameters: size, shape, deformation (anisotropy), of the "self-consistent" potential well. It is particularly evident in the case of the well deformation that one would much prefer to consider these quantities as dynamical variables rather than as mere parameters; this would enable us to describe, through their time variation, the precession in space of the nonspherical potential well, and thus allow us to deal with eigenstates of the total angular momentum. This is clearly also a prerequisite for the possibility of describing collective (rotational) excitations,

that is, a class of states which differ, roughly speaking, mainly by the precession velocity of the well, but whose intrinsic structures are as similar as they can be under the circumstances.

There are essentially three methods with which this problem of describing the collective dynamics may be attacked. All these methods are more ambitious than a mere "collective model"; they aim at an understanding of the interdependence of collective and individual particle dynamics, and the results of these more fundamental approaches have a deeper interest than a ready-made model. a) In the first method [Hill & Wheeler (12), Griffin & Wheeler (33), and Peierls & Yoccoz (34, 35)], the starting point is an independent particle wave function, $\psi(x_1, \dots, x_A; \alpha)$, depending on one or several variational parameters α , for instance, the deformation of the single particle well, or the orientation of a nonspherical well in space. One then constructs the wave function

$$\phi(x_1, \dots, x_A) = \int d\alpha \chi(\alpha) \psi(x_1, \dots, x_A; \alpha) \quad 4.$$

and

$$\langle H \rangle = \int d\tau \phi^* H \phi = \int \int d\alpha d\alpha' \chi^*(\alpha) \chi(\alpha') h(\alpha; \alpha') \quad 5.$$

$$\langle N \rangle = \int d\tau \phi^* \phi = \int \int d\alpha d\alpha' \chi^*(\alpha) \chi(\alpha') n(\alpha; \alpha')$$

with an undetermined distribution amplitude $\chi(\alpha)$ of α . The variational problem $\delta(\langle H \rangle - \epsilon \langle N \rangle) = 0$ then leads to a "Schroedinger equation" for $\chi(\alpha)$, and an eigenvalue spectrum that obviously belongs to one single type of intrinsic structure. Centre of mass motion, collective rotations and vibrations may be described this way; in the two first cases the proper choice of the amplitudes, χ , makes ϕ eigenstates of total linear and total angular momentum, respectively, whereas the associated ψ do not have this property. b) In a second method one tries to isolate appropriate collective aspects by carrying out a (canonical) transformation of variables, thus replacing the original particle position coordinates by new variables, some of which directly represent the collective modes in question. A familiar example of this is the separation of the centre of mass; another example will be the separation of the total angular momentum. Total linear and total angular momentum are clearly the two most obvious collective variables for any system, and one might expect a general rule for their separation. Indeed, we shall show that, irrespective of the system, the kinetic energy of any system of N particles of mass m may be written as (36):

$$T = \frac{1}{2mN} P^2 + \frac{1}{2} \sum_{A,B} Q_{AB}(\xi)(L_A - L_A')(L_B - L_B') + \frac{1}{2} \sum_{\sigma,\tau} D_{\sigma\tau}(\xi) \pi_\sigma \pi_\tau, \quad 6.$$

P being the total linear momentum, L_A a component of the total angular momentum; ξ_σ , π_σ being "intrinsic" variables and their conjugate momenta,

and finally $L_A'(\xi_\sigma, \pi_\sigma)$ an intrinsic angular momentum, and $Q_{AB}(\xi)$ a reciprocal moment of inertia tensor. In contrast to P , L cannot be completely decoupled from the intrinsic motion; only in certain special cases is this approximately possible, making use of the specific properties of the system at hand.

A drawback of this method lies in the fact that it is not possible to identify the $(3N-6)$ variables, ξ_σ , with particle position coordinates; thus the description of the intrinsic motion in terms of "independent" particle states seems impossible by this method. Ways to overcome, at least partially, this difficulty will be indicated in the appropriate place. c) The third method was developed mainly with the idea to avoid to a certain extent the above mentioned difficulty. In order to be able to use "shell model" wave functions, the particle coordinates should be kept as independent variables. Now the introduction of collective dynamical variables may be viewed as a transformation $x_i \rightarrow x'_i$, α_s ($s = 1, \dots, f$), x_i being the original position coordinates, α_s the collective variables and the x'_i transformed position coordinates which, however, are subject to f conditions of constraint $F_s(x'_i) = 0$ ($s = 1, \dots, f$). The present method consists then of lifting this constraint temporarily, and to consider the F_s as dynamical variables alongside the x_i (method of redundant variables). Redundant variables without compensating subsidiary conditions have been introduced by various authors: (13, 37, 38). The reversible transformation, F_s , $x_i \rightleftarrows \alpha_s$, x'_i , can then be completed to a full canonical transformation: G_s , $p_s \rightleftarrows \pi_s$, p'_s , G_s being the momenta conjugate to the F_s : $[F_s, G_s] = -i\hbar\delta_{s,t}$. The original Hamiltonian, in the original variables, is independent of the F_s and G_s , and therefore commutes with both; this property is preserved also if H is written in terms of the new variables: $H(p_i; X_i) = \tilde{H}(p'_i, \pi_s; x'_i, \alpha_s)$. It follows that any function $\tilde{\psi}(x'_i, \alpha_s)$ is an eigenfunction of \tilde{H} if, in terms of the old variables, it takes the form

$$U(F_s)\psi_n(x_i) \quad 7.$$

ψ_n being an eigenfunction of H , and $U(F)$ an arbitrary function. Thus, all one seems to get so far is a spurious degeneracy of eigenstates introduced by the arbitrariness of the amplitudes U . However, for example, assume now that the structure of \tilde{H} is of type

$$\tilde{H} = H_1(\pi_s; \alpha_s) + H_2(p'_i, x'_i) + H_3(\alpha_s, x'_i)$$

with H_3 small, a situation which clearly suggests in lowest order of approximation the use of a wave function

$$\tilde{\psi}^{(0)}(\alpha_s, x'_i) = V(\alpha_s)\varphi(x'_i) \quad 7a.$$

This function does not reduce to type 7, if rewritten in terms of the old variables, and is therefore strictly speaking inadmissible; on the other hand, nothing prevents us from using 7a as a zero order approximation, to be improved by perturbation or variational methods. In this way, a completely new type of approximation technique may be formulated.

2. THE METHOD OF CONTINUOUS VARIATIONAL PARAMETERS

a) *Illustration of the method. Centre of mass motion.*—It is well known that in the Hartree-Fock approximation, the wave functions are not eigenfunctions of the total momentum. The expectation value of the Hamiltonian H contains therefore a spurious centre of mass energy $\langle(\sum p_i)^2\rangle/2Am$; in addition, there appear "ghost" levels, corresponding to an excited state of the centre of mass motion in the space fixed potential well (39).

Now, if $\psi(x_1, \dots, x_A)$ is such a wave function, it is easily seen that

$$\phi_P(x_1, \dots, x_A) = \int d\xi \exp(-iP \cdot \xi) \psi(x_1 + \xi, \dots, x_A + \xi) \quad 8.$$

is an *eigenfunction* of the total linear momentum P :

$$P_{op}\phi_P = -i\hbar \sum_i \partial\phi_P/\partial x_i = P\phi_P$$

ϕ_P is thus obtained from ψ by projecting out the component with total linear momentum P . We now discuss the improvement which is obtained by using ϕ_P instead of ψ in calculating expectation values: (a) Since all functions $\psi(x+\xi)$ give the same expectation value of the energy $\langle H \rangle = \int d\tau \psi^* H \psi$, this expectation value is infinitely degenerate with respect to the continuous displacement parameter ξ . As is well known in such cases [the classic example being the exchange energy obtained by (anti)symmetrization of a degenerate two particle wave function], a proper linear combination $\int d\xi \chi(\xi) \psi(x+\xi)$ of such degenerate states will lower the energy. In our case, we know that with $\chi(\xi) = \exp(-iP \cdot \xi)$ we construct *eigenstates* of P , and therefore with $P=0$ we get the lowest possible energy by eliminating the spurious centre of mass kinetic energy. (b) In connection with this last point, it is also seen that such a procedure eliminates all the ghost states: $\phi_{ghost} \equiv 0$ (34, 39, 41). (c) Choosing $\chi(\xi) = \exp(-iP \cdot \xi)$. ($P \neq 0$) we may compare the P dependence of

$$E_P = \frac{\langle H \rangle_P}{\langle N \rangle_P} = \frac{\int d\tau \phi_P^* H \phi_P}{\int d\tau \phi_P^* \phi_P} \quad 9.$$

with the known exact dependence of the energy on P :

$$E_P = E_{P=0} + \frac{P^2}{2Am}$$

In this way we get an estimate of the adequacy of the independent particle wave function ψ to determine a collective inertial parameter, here the total mass.

We carry out this comparison in some detail, since it is characteristic for the general method. We have, in Eq. 9:

$$\begin{aligned}\langle N_P \rangle &= \text{const.} \int d\xi \exp(-iP \cdot \xi) \int d\tau \psi^*(x) \psi(x + \xi) \\ \langle H \rangle_P &= \text{const.} \int d\xi \exp(-iP \cdot \xi) \int d\tau \psi^*(x) H \psi(x + \xi)\end{aligned}\quad 10.$$

Now the τ -integrals are 1 and \bar{H} , respectively, for $\xi = 0$, and drop off to zero for large values of ξ . For small ξ , one gets by expansion

$$1 - \frac{1}{2} \xi^2 \int d\tau \psi^*(x) (\sum p_i)^2 \psi(x) = 1 - \frac{1}{2} \xi^2 \bar{P}^2$$

and

$$\bar{H} - \frac{1}{2} \xi^2 \int d\tau \psi^*(x) H (\sum p_i)^2 \psi(x) = 1 - \frac{1}{2} \xi^2 \bar{H} \bar{P}^2$$

This suggests that the ξ -dependence of these integrals may be approximated by the Gaussians⁴

$$\exp(-\frac{1}{2} \xi^2 \bar{P}^2)$$

and

$$\exp(-\frac{1}{2} \xi^2 \bar{P}^2) (\bar{H} - \frac{1}{2} \xi^2 (\bar{H} \bar{P}^2 - \bar{H} \bar{P}^2) + \dots)$$

respectively. Clearly then, if in Eq. 10, P is assumed to be sufficiently small, $\exp(-iP \cdot \xi)$ is a slowly varying function and may be expanded; it follows by Eq. 9, that

$$E_P = \left(\bar{H} - \frac{\bar{H} \bar{P}^2 - \bar{H} \bar{P}^2}{2 \bar{P}^2} \right) + \frac{1}{2} P^2 \left(\frac{\bar{H} \bar{P}^2 - \bar{H} \bar{P}^2}{(\bar{P}^2)^2} \right) + \dots \quad 11.$$

defining a total mass

$$\frac{1}{M_{\text{tot}}} = \frac{1}{(\bar{H} \bar{P}^2 - \bar{H} \bar{P}^2) / (\bar{P}^2)^2} \quad 12.$$

The interpretation of the second term in Eq. 11, is simple and illuminating. Taking the coefficient of $\frac{1}{2} P^2$ in the last term as a "definition" of the total mass (Eq. 12), we have

$$E_{P=0} = \bar{H} - \frac{\bar{P}^2}{2 M_{\text{tot}}}$$

which shows that the method indeed cuts out the spurious centre of mass fluctuation energy.

b) *Collective rotations and moments of inertia.*—This method acquires a new dimension in connection with the application to rotational levels. A self consistent independent particle approximation will generally yield a nonspherical single particle well with arbitrary, but fixed orientation in space, and hence states which are not eigenstates of the total angular

⁴ For nonantisymmetrized wave functions the Gaussian dependence follows in the limit of large N .

momentum. Here again, we find a degeneracy of the expectation values of H with respect to the orientation in space; again, a proper linear combination of degenerate states will yield a better approximation. The particular linear combinations one must choose are, of course, just those which make the new trial functions ϕ eigenfunctions of the total angular momentum. Assuming a self consistent well with a symmetry axis Z' , we start with the functions $\psi_K(x')$, K being the value of $I_{Z'}$, and construct eigenfunctions ϕ_{IM} of I^2 and I_Z ;

$$\phi_{IM}(x) = \int d\Omega \mathcal{D}^{I^*}_{MK}(\Omega) \psi_K(x'(\Omega)) \quad 13.5$$

Ω gives the orientation of the body fixed coordinate system (X') in space, in terms of Euler angles θ, ψ, φ ; $d\Omega = \sin \theta d\theta d\psi d\varphi$ and the $\mathcal{D}^{I^*}_{MK}$ are the eigenfunctions of $I^2, I_Z, I_{Z'}$, to eigenvalues $I(I+1), M$ and K , respectively. It follows that

$$\begin{aligned} \langle H \rangle_I &= \sum_M \int d\tau \phi_{IM}^* H \phi_{IM} = \text{const. } \int d\Omega \mathcal{D}^{I^*}_{KK}(\Omega) \int d\tau \psi_K^*(x) H \psi_K(x'(\Omega)) \\ \langle N \rangle_I &= \text{const. } \int d\Omega \mathcal{D}^{I^*}_{KK}(\Omega) \int d\tau \psi_K^*(x) \psi_K(x'(\Omega)) \end{aligned}$$

The same arguments as in the centre of mass problem are now applied. If the self-consistent well is sufficiently anisotropic, the overlap between $\psi(x)$ and $\psi(x'(\Omega))$ will decrease rapidly with increasing angle θ between the Z - and the Z' -axes. Let us follow up the case $K=0$ (ground states of even-even nuclei). We have then, tentatively:

$$\int d\tau \psi_0^*(x) \psi_0(x'(\Omega)) \simeq \exp [-\frac{1}{2}\theta^2(\sum j)^2]$$

In addition, we make use of the small angle expansion

$$\mathcal{D}^{I_00}(\Omega) = P_I(\cos \theta) = 1 - \frac{1}{4}I(I+1)\theta^2 + \dots$$

Then, in straight analogy with the centre of mass problem, we get:

$$E_I = \frac{\langle H \rangle_I}{\langle N \rangle_I} = E_{I=0} + \frac{I(I+1)}{2J_{\text{eff}}} \quad 14.$$

$$\frac{1}{J_{\text{eff}}} = \frac{\overline{H J^2} - \overline{H} \overline{J^2}}{(\overline{J^2})^2} \quad 15.$$

j being $(\sum j)$.

This method makes it particularly apparent how the appearance of a rotational spectrum is tied to a sufficiently large deviation from spherical symmetry. Only then may we expect that the small angle expansion of $P_I(\cos \theta)$

⁵ We use here a definition of the eigenfunctions $\mathcal{D}^{I_{mm'}}$ of the symmetric top as given by Edmonds (41): $\mathcal{D}^{I_{mm'}}(\psi, \theta, \varphi) = e^{-im\psi} (jm|e^{-i\theta J_x}|jm') e^{-im'\varphi}$. Functions of type (13) have previously been used by Redlich & Wigner (42) in the calculation of β -decay matrix elements for deformed nuclei.

is reasonable, and that the series may be terminated at the I ($I+1$) term. Evaluation of the higher terms in principle allows to check the accuracy of the approximation.

Some preliminary numerical results have been obtained by Yoccoz, and agree reasonably well with experimental values. A result similar to Eq. 15 has been derived by Skyrme (40) based on a variational method closely related to the one presented here.

c) Electric quadrupole moments.—The improved wave functions ϕ_{IM} (Eq. 13), may be used to calculate other ground state properties of the nucleus. As an example we give here the expression for the spectroscopic electric quadrupole moment, represented by the tensor operator $Q_{20}(x)$. Q is the expectation value of Q_{20} for a state I , $M=I$. A straightforward calculation, using Eq. 13 and the properties of the \mathfrak{D}'_{KM} , gives

$$\begin{aligned} Q &= \int d\tau \phi_{IM}^* Q_{20} \phi_{IM} / \int d\tau \phi_{IM}^* \phi_{IM} |_{M=I} \\ &= \sum_m C_m(I, K) \frac{\int d\Omega \mathfrak{D}'_{K+m, K}(\Omega) \int d\tau \psi_K^*(x'(\Omega)) Q_{20}(x) \psi_K(x)}{\int d\Omega \mathfrak{D}'_{K, K}(\Omega) \int d\tau \psi_K^*(x'(\Omega)) \psi_K(x)} \end{aligned} \quad 16.$$

the $C_m(I, K)$ being a product of Wigner-coefficients. For $m=0$, $C_0(I, K)$ is the well-known projection factor of the strong-coupling theory (see part III.3d).

$$C_0(I, K) = \frac{3K^2 - I(I+1)}{(I+1)(2I+3)}$$

For strongly deformed states, only the term $m=0$ in (Eq. 16) contributes substantially, since $\mathfrak{D}'_{K+M, K} \propto (\sin \theta/2)^m$. The result, Eq. 16, has therefore some resemblance to the result of the Bohr-Mottelson model in the strong coupling limit:

$$Q = C_0(IK) Q_0(K); \quad Q_0(K) = \int d\tau \psi_K^*(x) Q_{20}(x) \psi_K(x) + \text{corr. terms.}$$

It is more general in the sense that the validity of Eq. 16 is not restricted to large deformations. In the limit of zero deformation, Eq. 16 properly reduces to $Q = Q_0(I)$.

No calculations using Eq. 16 seem to exist yet, and the same holds for magnetic moments.

Transition probabilities may also be calculated, provided the transitions occur within a given "rotational band" (fixed value of K). It must be remembered that wave functions belonging to same IM , but different K -values, are not orthogonal, in contrast to the corresponding wave functions in the Bohr-Mottelson model.

3. THE METHOD OF CANONICAL TRANSFORMATIONS⁶

a) *Systems with rotational levels.*—Any closed system of interacting particles has two obvious collective constants of motion: the total linear and the total angular momentum. We want here to answer the question: is it possible to write the Hamiltonian of the system in such a way as to display its dependence on these two constants of motion? This can indeed be done by a suitable transformation of variables. For the case of the angular momentum, it is necessary to define an "intrinsic" coordinate system (that is, a system defined by the relative positions of the particles in space) so that a common rotation of all can be considered as a rotation of this intrinsic frame (36, 43). The Euler angles of this intrinsic frame are then the collective variables, and the total angular momentum components their conjugate. The three Euler angles $\theta_s = (\psi, \theta, \varphi)$ define an orthogonal transformation $R_{A\alpha}(\theta_s)$ from space fixed components $x_{i\alpha}$ to body-fixed components x'_{iA} :

$$x_{i\alpha} = X_\alpha + R_{A\alpha}(\theta) x'_{iA} \quad 17.$$

In Eq. 17 we have isolated also the center of mass X_α . The x'_{iA} cannot be independent variables, but are subject to the conditions α): $\sum_i x'_{iA} \equiv 0$ (Definition of the centre of mass) β): three other, not yet specified conditions which will define the body-fixed frame: $F_s(x'_{iA}) \equiv 0$. We therefore write $x'_{iA}(\xi_s)$ in terms of (3N-6) independent, but unspecified, variables ξ_s . The condition β :

$$F_s(x'_{iA}) = F_s(R_{A\alpha}(\theta)(x_{i\alpha} - X_\alpha)) \equiv 0 \quad 18.$$

may be used to define the θ_s as functions of the $x_{i\alpha}$. From Eq. 17 it follows that the momentum is

$$p_{i\alpha} = \frac{1}{N} P_\alpha + \sum_\sigma \frac{\partial \xi_\sigma}{\partial x_{i\alpha}} \pi_\sigma + \sum_s \frac{\partial \theta_s}{\partial x_{i\alpha}} \Pi_s$$

π_σ and Π_s being the momenta conjugate to ξ_σ and θ_s . Π_s may be expressed in terms of the total angular momentum components L_{AB} (with respect to the body-fixed axes)

$$\Pi_s = \sum_{A < B} \left(\frac{\partial R_{A\gamma}}{\partial \theta_s} R_{B\gamma} \right) L_{AB} \quad 19.$$

and the intrinsic momentum split into two terms:

$$\sum_\sigma \frac{\partial \xi_\sigma}{\partial x_{i\alpha}} \pi_\sigma = R_{A\alpha} p'_{iA} - \sum_{A < B} \left(\frac{\partial R_{A\gamma}}{\partial x_{i\alpha}} R_{B\gamma} \right) L'_{AB}$$

L'_{AB} being the intrinsic angular momentum

$$L'_{AB} = \sum_i (x'_{iA} p'_{iB} - x'_{iB} p'_{iA})$$

⁶ There exist methods which are not so easily labelled; we mention here only Tomonaga's method of "approximately canonical" transformations (44, 45, 46), or a combination of canonical transformation and variational methods (47).

and

$$p'_{iA} = \sum_{\sigma\tau} \frac{\partial x'_{iA}}{\partial \xi_\sigma} c_{\sigma\tau}^{-1} \pi_\tau \quad c_{\sigma\tau} = \sum_{ia} \left(\frac{\partial x_{ia}}{\partial \xi_\sigma} \frac{\partial x_{ia}}{\partial \xi_\tau} \right)$$

It is thus possible to write the momentum p_{ia} in the form

$$p_{ia} = \frac{1}{N} P_a + R_{Aa} p'_{iA} + \sum_{A < B} \left(\frac{\partial R_{A\gamma}}{\partial x_{ia}} R_{B\gamma} \right) (L_{AB} - L'_{AB}) \quad 20.$$

It is now easily seen that the three terms of Eq. 20 are "orthogonal" to each other, that is, do not contribute any cross terms to the kinetic energy, which now simply becomes

$$T = \frac{P^2}{2mN} + \sum_{iA} \frac{p'_{iA}^2}{2m} + \frac{1}{2} \sum_{A,B} Q_{AB}(\xi) (L_A^2 - L'_A^2) (L_B^2 - L'_B^2) \quad 21.^7$$

where

$$mQ_{AB} = \sum_{ia} M_{ia,A} M_{ia,B}; \quad M_{ia,A} = \left(\frac{\partial R_{B\gamma}}{\partial x_{ia}} R_{C\gamma} \right) \quad 21a.$$

This result is completely general. We recall that neither x'_{iA} nor the p'_{iA} are independent variables, but we have with good purpose introduced a notation suggestive of an approximation one is tempted to try at this place, if the number of particles is sufficiently large: to consider at least some of the x'_{iA} and p'_{iA} in fact as independent variables, in which case they become conjugate pairs, of course. This approximation is the basis for the Hamiltonians as used in (37, 38).

As an illustration of Eq. 21 and 21a we use as definition of the body-fixed axes:

$$\sum_i x'_{iA} x'_{iB} = 0 \quad (A \neq B) \quad 22.$$

This relation has to hold identically in the independent variables ξ_σ . With Eq. 18 and 21a, we get:

$$M_{ia,AB} = (x'_{iA} R_{Ba} + x'_{iB} R_{Aa})$$

I_A being $\sum_i (x'_{iA})^2$. The inertia tensor Q_{AB} becomes diagonal, with eigenvalues

$$Q_{AA} = (I_B + I_C)/(I_B - I_C)^2 \quad 23.$$

This value is the equivalent of Bohr's result derived from irrotational liquid drop motion. (See part III.3d.)

Now let us consider what is gained by these results, both from the point of view of insight, and from the point of view of useful application: (a): Expression 21 for the kinetic energy shows to which extent the collective rotational motion may be decoupled from the intrinsic motion. The coupling terms express the fact that the intrinsic motion is described in a non-inertial frame and account for the centrifugal and Coriolis-forces acting on the in-

⁷ Whenever convenient, we use the notation $L_{BA} = L_A^2$ for axial vector components.

trinsic degrees of freedom. No purely kinematic argument for the choice of the body-fixed frame will remove these coupling terms. We must conclude from this that the choice (19) of the body-fixed frame is as good as any other, at least for nuclei (for molecules one is able to do considerably better, due to the quasi-rigidity of the system).⁸ (b): The effective moments of inertia, $\mathfrak{J}_{\text{eff}}$, which we shall define, for a system with rotational levels, by

$$E_I = E_0 + \frac{I(I+1)}{2\mathfrak{J}_{\text{eff}}},$$

cannot be found without solving the problem of the intrinsic motion to some extent at least. There is absolutely no reason to assume that $\mathfrak{J}_{\text{eff}}$ is directly related to the eigenvalues of the inertia tensor Q_{AB} , which are determined by the rather arbitrary choice of the body-fixed system. (c): To handle the intrinsic dynamics, clearly some "model" has to be made up. Such models will be discussed in part III. (d): In view of the observed shell structure in nuclei, it is often found convenient to single out some "valence nucleons" whose motion in the collective field created by the others (the "core"-nucleons) one is particularly interested in. It is then possible to carry out the transformation (Eq. 17, 18, 19) for the core-nucleons only, and to describe the motion of the extra particles in the body-fixed frame defined by the others. Calling x_r and p_r positions and momenta of the extra particles, we obtain an unsymmetric Hamiltonian:

$$H = \frac{P_c^2}{2mN_c} + H_{\text{intr}}(\pi_\sigma, \xi_\sigma) + \sum_{r,A} \left(\frac{p_{rA}^2}{2m} + \sum_{i=1}^{N_c} V(x_{rA} - x'_{iA}(\xi)) \right) + \sum_{r,s} V_{rs} \\ + \frac{1}{2} \sum_{A,B} Q_{AB} \left(L_A^{\widehat{A}} - L'^{\widehat{A}} - \sum_r l_{r,\widehat{A}} \right) \left(L_B^{\widehat{B}} - L'^{\widehat{B}} - \sum_r l_{r,\widehat{B}} \right) \quad 24.$$

In Eq. 24, the total angular momentum now includes the angular momentum of the valence nucleons; but it is still given by the operator (19). The form (Eq. 24) makes it of course impractical to include the exchange effects between the two groups of particles, but it is the adequate starting point for any approximation obtained by taking some kind of average over the intrinsic motion; in particular shall we be able to get a better understanding of the original Bohr model on the basis of Eq. 24.

N.B. to include the nucleon spin in Eq. 24, it is sufficient to make the substitution: $L_A^{\widehat{A}} - L'^{\widehat{A}} - \sum_r l_{r,\widehat{A}} \rightarrow L_A^{\widehat{A}} - J'_A - \sum_r j_{r,\widehat{A}}$ with $J'_A = L'_A + \frac{1}{2} \sum_i \sigma_{i,\widehat{A}}$; $j_{r,\widehat{A}} = l_{r,\widehat{A}} + \frac{1}{2} \sigma_{r,\widehat{A}}$. $L_A^{\widehat{A}}$ remains the same operator, but its interpretation changes to that of the total angular momentum of the total system. (e): It must thus be realized that a form like Eq. 21 or Eq. 24 will in no way tell directly whether rotational levels occur in a system. These expressions only furnish suitable starting points for approximations, or suggest models, in

⁸ Equation 21a may of course be applied to molecules as well. Due to the existence of equilibrium positions x_i^0 : $x_i' = x_i^0 + \delta x_i'$, there exists a more appropriate condition to define the body-fixed frame: $\sum_i (x_{iA}^0 \delta x'_{iB} - x_{iB}^0 \delta x'_{iA}) = 0$, from which the rigid body moments of inertia follow (36, 48).

which the programme of decoupling the total angular momentum from the intrinsic motion can be carried one step further; but in each case such a programme will have to take into account the intrinsic dynamics, or a model thereof. These questions will therefore be discussed in part III.

b) *Small amplitude collective vibrations.*—The transformation of the previous section (part II.3a) was appropriate for a situation, in which the mass distribution in the nucleus, say given by the tensor

$$I_{\alpha\beta} = \sum_i (x_{i\alpha} - X_\alpha)(x_{i\beta} - X_\beta) \quad 25.$$

is sufficiently anisotropic to define a nonspherical shape; this implies in particular that the eigenvalues I_A of $I_{\alpha\beta}$ show sufficiently small fluctuations:

$$\langle I_A^2 \rangle - \langle I_A \rangle^2 \ll \langle (I_A - I)^2 \rangle; \quad (I = \sum I_A / 3)$$

If this condition is not satisfied, then it is better to build up a formalism describing the fluctuations of $I_{\alpha\beta}$ about an isotropic average $I_0 \delta_{\alpha\beta}$. The best way to do this is to think of the actual distribution $I_{\alpha\beta}$ as arising from a fictitious isotropic distribution $I_0 \delta_{\alpha\beta}$ by action of a collective displacement field $\delta_\alpha(x) = w_{\alpha\beta} x_\beta$. The actual positions $x_{i\alpha}$ of the nucleons may then be viewed as the result of this displacement upon some "intrinsic" positions $x'_{i\alpha}$; that is

$$x_{i\alpha} = X_\alpha + (\delta_{\alpha\beta} + w_{\alpha\beta}) x'_{i\beta}(\xi) \quad 26.$$

X_α being again the center of mass.

The quantity $w_{\alpha\beta} x'_{i\beta}$ is then clearly a collective velocity field; in analogy to the original formulation of Bohr's model we assume this field to be irrotational and incompressible; this is equivalent to $w_{\alpha\beta} = w_{\beta\alpha}$; $\sum_\alpha w_{\alpha\alpha} = 0$; $w_{\alpha\beta}$ is thus a symmetric, traceless tensor, and may be written in terms of five independent parameters λ_μ :

$$w_{\alpha\beta} = \sum_{\mu=-2}^{+2} \lambda_\mu C_{\alpha\beta}^\mu \quad 26a.$$

the λ_μ thus chosen are complex and supposed to transform like the spherical harmonics $Y_{\mu\mu}^*$; it follows then that $\lambda_\mu^* = (-1)^\mu \lambda_{-\mu}$; the $C_{\alpha\beta}^\mu$ are normalized to $\sum_{\alpha\beta} C_{\alpha\beta}^* C_{\alpha\beta}^\mu = \delta_{\mu\nu}$. In order to introduce the λ_μ as dynamical variables, we must impose five restrictive conditions on the intrinsic positions (plus three others for the elimination of the center of mass). These are

$$\sum_i x'_{i\alpha} = 0 \quad 27a. \quad \sum_i x'_{i\alpha} x'_{i\beta} = I_0 \delta_{\alpha\beta} \quad 27b.$$

The meaning of this is clearly, as announced above, that the actual positions arise through a collective, five parametric displacement from an isotropic "intrinsic" distribution of positions.

Writing the momentum $p_{i\alpha}$ in the new variables, we have again

$$p_{i\alpha} = \frac{1}{N} P_\alpha + \sum_\sigma \frac{\partial \xi_\sigma}{\partial x_{i\alpha}} \pi_\sigma + \sum_\mu \frac{\partial \lambda_\mu}{\partial x_{i\alpha}} p_\mu$$

From here on all developments must be based on the assumed smallness of the λ_μ , in order to avoid extremely complicated expressions. A step analogous to the procedure in part II.3a, shows that

$$\sum_\sigma \frac{\partial \xi_\sigma}{\partial x_{i\alpha}} \pi_\sigma = p'_{i\alpha} + O(\lambda_\mu)$$

$p'_{i\alpha}$ being therein defined by $p'_{i\alpha} = (\partial x_{i\alpha}/\partial \xi_\sigma) c_{\sigma\tau}^{-1} \pi_\tau$, $c_{\sigma\tau}$ being the same matrix as there. The reason for introducing $p'_{i\alpha}$ is of course again its orthogonality to the two other terms in $p_{i\alpha}$. $\partial \lambda_\mu / \partial x_{i\alpha}$ is determined by the defining Eq. 26, 27b, which give, to order λ :

$$\partial \lambda_\mu / \partial x_{i\alpha} = C^*_{\alpha\beta} x'_{i\beta} / I_0$$

The kinetic energy is therefore approximately:

$$T = \frac{P^2}{2mN} + \sum_{i\alpha} \frac{p'_{i\alpha}^2}{2m} + \frac{1}{2mI_0} \sum_\mu p_\mu^* p_\mu \quad 28.$$

To construct the angular momentum, we need

$$\sum_i \left(x_{i\alpha} \frac{\partial \lambda_\mu}{\partial x_{i\beta}} - x_{i\beta} \frac{\partial \lambda_\mu}{\partial x_{i\alpha}} \right) \simeq i \sum_\nu \lambda_\nu (M_{\alpha\beta})_{\nu,\mu}$$

$(M_{\alpha\beta})_{\mu,\nu}$ being equal to the matrix element $(j\mu | J_{\alpha\beta} | j\nu) |_{j=2}$ of the angular momentum component $J_{\alpha\beta}$. The total angular momentum, referred to the center of mass, appears thus approximately as the sum of two terms

$$L_{\alpha\beta} = L_{C,\alpha\beta} + L'_{\alpha\beta}$$

with $L'_{\alpha\beta} = \sum_i (x'_{i\alpha} p'_{i\beta} - x'_{i\beta} p'_{i\alpha})$, the intrinsic angular momentum and $L_{C,\alpha\beta} = i \sum_{\mu\nu} (M_{\alpha\beta})_{\mu\nu} \lambda_\mu p_\nu$, the angular momentum of collective motion. We repeat here the statement made in part II.3a, that the $x'_{i\alpha}$ and $p'_{i\alpha}$ are not independent variables, and not canonically conjugate. To complete the Hamiltonian, the potential energy has to be written in terms of the ξ_σ and λ_μ :

$$\begin{aligned} V(\dots x_i \dots) &= V(\dots (1+w)x_i' \dots) \\ &= V(\dots x_i' \dots) + \sum_{\alpha\beta} w_{\alpha\beta}(\lambda) \sum_i x'_{i\alpha} \frac{\partial V}{\partial x'_{i\beta}} + \dots \end{aligned}$$

Now again the question comes up to see to which extent an approximate factorization of the wave function appears possible. Beginning this discussion with the consideration of even nuclei with zero angular momentum in their ground states, we are tempted to write:

$$\psi(x_i - X) \simeq \phi(\xi_\sigma) v(\lambda_\mu)$$

and to construct a Hamiltonian averaged over ϕ , which is assumed to be a state with zero intrinsic angular momentum:

$$J'\phi = \left(L' + \frac{1}{2} \sum_i \delta_i \right) \phi \simeq 0$$

For such a state, we have

$$\left\langle \frac{1}{2m} \sum_i p_{i\alpha}^2 + V \right\rangle_\phi = E_0 + \frac{1}{2} C \sum_\mu \lambda_\mu^* \lambda_\mu + \dots$$

The constant C is partly of kinetic, partly of potential origin, but its value can, of course, not be reliably obtained by direct evaluation. It follows that

$$\langle H \rangle_\phi = \frac{1}{2B} \sum_\mu p_\mu^* p_\mu + \frac{C}{2} \sum_\mu \lambda_\mu^* \lambda_\mu \quad 29.$$

with C defined above, and $B^{-1} = \langle 1/m I_0 \rangle_\phi \approx 5/m N R_0^2$ for a homogenous mass distribution over a sphere of Radius R_0 . $\langle H \rangle_\phi$ is a simple oscillator Hamiltonian, with eigenvalues

$$E_N = \hbar\omega \sum_\mu (N_\mu + \frac{1}{2}) \quad \omega = \sqrt{C/B}$$

and N_μ being integers. The z -component of the collective angular momentum $L_{Cz} = i \sum_\mu \mu \lambda_\mu p_\mu$ is diagonal in the same representation and has the eigenvalues $\sum_\mu \mu N_\mu$. We infer that the quanta of collective vibrational excitation (the "surfons") have angular momentum 2 (corresponding to the maximum value of L_{Cz} for a one quantum excitation). This is confirmed by verifying that for any one quantum state $\langle L_{Cz}^2 \rangle = 6\hbar^2$. For higher excited states, there is a degeneracy of the energy levels with respect to L_{Cz} , and the energy eigenstates are not automatically angular momentum eigenstates.

We now take up the question whether such an averaging as carried out above is indeed permissible: (a) As necessary conditions we have clearly first the zero angular momentum in the ground state. Then, in addition, we require the smallness of the collective excitation energy compared with energy of the lowest mode of intrinsic excitation. The experimental material seems to indicate that this condition is never fulfilled; even the lowest collective vibrational excitations are of the order of 1 Mev in medium weight nuclei (26, 51). (b) Under the assumption of the validity of the approximation, B and C may be determined from measured values of $\hbar\omega$ (which is $\propto \sqrt{B/C}$) and of the $E2$ -transition rates, which are $\propto \sqrt{BC}$ (See part III.3b). The fact that the values of B obtained this way are systematically an order of magnitude larger than the value mI_0 sheds considerable doubt on the validity of this approximation.

The obvious refinement of the approximation consists in treating in a more explicit way the dynamic interplay of collective modes and the most easily excitable intrinsic modes. As in the case of rotational levels this may be achieved by dividing the system in core- and extra-nucleons, with the λ_μ describing the collective motion of the core. The core furnishes a λ -dependent potential well for the extra-particles:

$$U(x_r, \lambda) = \left\langle \sum_{\text{core}} V(x_r - x_i) \right\rangle_\phi$$

⁹ Our B differs from Bohr's B_2 (50) by a factor $8\pi/15$, stemming from a difference in scale between our λ_μ and the corresponding α_μ of Bohr.

$$\begin{aligned}
 &= \left\langle \sum_{\text{core}} V(x_r - x_i'(\xi)) \right\rangle_\phi \\
 &\quad + \sum_{\alpha\beta} w_{\alpha\beta}(\lambda) \left\langle \sum_i x'_{i\alpha} \frac{\partial}{\partial x'_{i\beta}} V(x_r - x_i'(\xi)) \right\rangle_\phi + \dots \\
 &\simeq U_0(x_r) + \sum_\mu \lambda_\mu \sum_{\alpha\beta} C_{\alpha\beta}^\mu x_{r\alpha} \frac{\partial U_0}{\partial x_{r\beta}} + \dots
 \end{aligned}$$

The ϕ -averaged Hamiltonian is now

$$\langle H \rangle_\phi = \frac{1}{2B} \sum_\mu p_\mu^* p_\mu + \frac{C}{2} \sum_\mu \lambda_\mu^* \lambda_\mu + \sum_r \left(\frac{p_r^2}{2m} + U(x_r; \lambda) \right) + \sum_{r,s} V_{r,s}. \quad 30.$$

This Hamiltonian has exactly the structure of the model Hamiltonian considered by Bohr (50) and more will be said about it in part III.

4. THE METHOD OF REDUNDANT VARIABLES

a) *Illustration of the method; centre of mass motion.*—In part II it has been shown that if the collective variables are isolated by means of a canonical transformation, none of the remaining intrinsic variables may be identified with particle position coordinates. This is particularly unpleasant in connection with any attempt to describe the intrinsic motion in terms of an "independent particle" picture. The present method is an attempt to combine the advantages of the method of canonical transformations with the advantages of dealing with particle coordinates to describe intrinsic motion. To achieve this, the actual dynamical system is embedded in an enlarged system, whose number of degrees of freedom is larger by the number of collective variables to be introduced. A canonical transformation is then carried out leading to intrinsic variables which are in one-to-one correspondence with the original particle coordinates. A subset of solutions of the enlarged system, satisfying suitable subsidiary conditions, is then equivalent to the solutions of the original system. Various approximation techniques may then be based on the possibility of defining a new zero order Hamiltonian, and wave functions which only approximately satisfy the subsidiary conditions.

As an illustration, we first deal with the centre of mass problem for N particles of equal mass m . This problem has been discussed by Lipkin *et al.* (52), Tamura (53), and Skinner (54). The method consists of replacing the usual transformation:

$$x_{i\alpha} = X_\alpha + x'_{i\alpha}(\xi_\sigma); \quad \sum_i x'_{i\alpha}(\xi_\sigma) = 0; \quad 31a.$$

$$p_{i\alpha} = \frac{1}{N} P_\alpha + p'_{i\alpha}(\pi_\sigma); \quad \sum_i p'_{i\alpha} = 0, \quad 31b.$$

in which neither the $x'_{i\alpha}$ nor the $p'_{i\alpha}$ are independent variables, by a transformation in an augmented system of variables $(x_{i\alpha}, p_{i\alpha})$ and (F_α, G_α) :

$$x_{i\alpha} = X_\alpha + x'_{i\alpha} - \frac{1}{N} \sum_k x'_{k\alpha}; \quad F_\alpha = \frac{1}{N} \sum_k x'_{k\alpha} \quad 32a.$$

and

$$p_{ia} = \frac{1}{N} P_a + p'_{ia} + \frac{1}{N} \sum_k p'_{ka}; \quad G_a = \sum_k p'_{ka} \quad 32b.$$

in Eq. 32 the (x'_{ia}, p'_{ia}) are now independent canonical pairs. We also see that the original transformation corresponds to the restriction $F_\alpha \equiv 0, G_\alpha \equiv 0$. It is interesting to observe the complete symmetry in Eq. 32 between new and old variables. In fact, the inversion of Eq. 32 is obtained simply by the substitution, in Eq. 32, of:

$$x \leftrightarrow x' \quad F \leftrightarrow X \quad p \leftrightarrow p' \quad G \leftrightarrow P$$

The kinetic energy $T = \sum_i p_i^2/2m$ becomes, in terms of the new variables

$$\tilde{T} = \frac{P^2}{2mN} + \frac{\sum p_i'^2}{2m} - \frac{(\sum p_i')^2}{2mN}$$

In an X - F -space representation, the exact eigenfunctions of $H(p_i, x_i)$ are of type $U(F)\psi_n(x_i)$, with an arbitrary function $U(F)$ and ψ_n satisfying $G\psi_n = -i\hbar\partial\psi_n/\partial F = 0$. [We present here only the quantum mechanical methods. A general classical theory of redundant variables has been given by Watanabe (55).] Instead, we are going to use approximate solutions of type $U(F)\psi(x_i, F)$, opening the possibility that

$$\psi(x_i(X, x'_i), F(x'_i)) = \tilde{\psi}(X, x'_i)$$

has a simpler structure, say, may be of independent particle type

$$\tilde{\psi} = f(X) \operatorname{Det} [\varphi_K(x'_i)]$$

The expectation value of the energy depends now on the structure of $U(F)$ and to minimize the error, we may choose

$$|U(F)|^2 = \delta(F),$$

(or even determine $U(F)$ from a variational principle).

The same statements can be made, *mutatis mutandis*, for any representation. In particular, the problem can also be formulated in momentum space, using $\psi(p_i, G)$. Such general aspects of the technique are discussed in a paper by Lipkin (56).

Using momentum space, and trial functions $\psi(p_i, G)$ the expectation value of the kinetic energy T , in the original variables, may be written as:

$$\langle T \rangle = \int dp_i \int dG \delta(G) \psi^*(p_i, G) T \psi(p_i, G)$$

an expression which is easily rewritten in terms of the new variables.

$$\langle T \rangle = \int dP \int dp'_i \delta(\sum p_i') \tilde{\psi}^*(P, p'_i) \tilde{T} \tilde{\psi}(P, p'_i)$$

The structure of \tilde{T} allows to separate off the centre of mass energy in the usual way. The remaining intrinsic kinetic energy is given by

$$\int dp_i' \delta(\sum p_i') \tilde{\psi}^*(p_i') [\sum p_i'^2/2m] \tilde{\psi}(p_i') = \int d\xi \int dx_i' \tilde{\psi}^*(x_i') T_{op} \tilde{\psi}(x_i' + \xi) \quad 33.^{10}$$

The term $-(\sum p_i')^2/2mN$ does not contribute, due to the choice of $U(G)$. This result shows that the method in this form of application gives the same result for the intrinsic energy as the method of part II.2, except that the collective energy $P^2/2mN$ is exactly separated by a coordinate transformation. An exact calculation of the intrinsic energy would have implied the use of a wave function $\tilde{\psi}(p_i')$ satisfying $\sum_i \partial \tilde{\psi} / \partial p_i' = 0$, a condition which cannot be satisfied by an independent particle wave function. We see that the present formalism, despite relaxing the subsidiary condition, gives an improved value for the intrinsic energy, apart from the exact value for the "collective" centre of mass kinetic energy. In this respect, it is seen to be superior to the method of part II.2; in fact, it somehow combines the advantages of the methods of the two previous paragraphs.

It is also seen that a different result is obtained by starting with an X - F -representation and using $|U(F)|^2 = \delta(F)$: The result obtained in that case is

$$\langle T_{\text{intr}} \rangle = \int dx_i' \delta(\sum x_i') \tilde{\psi}^*(x_i') \left[\sum_i p_i'^2/2m - (\sum p_i')^2/2mN \right] \tilde{\psi}(x_i')$$

These alternatives illustrate the flexibility of the method.

b) *Rotational energy*.—The method as illustrated above is easily adapted to the case of collective rotation. [Collective vibrations have been treated with similar methods by Süssmann (58), Marumori *et al.* (59, 60).] One important difference with the previous case, however, remains. The rotational kinetic energy cannot be separated by a transformation of variables based on a purely kinematic argument, and all we are going to get is a result similar to that of part II.3. But we are now in a much better position to carry out additional transformations, aiming at an optimum decoupling of the collective motion, than with the formalism of II.3; in particular, we can now approximate the interaction by a single particle potential and use independent particle wave functions, since the particle coordinates remain independent variables.

In designing the actual transformation, the method applied in part II.4a is copied as closely as possible. An essential point there was the high degree of symmetry between old and new variables, as expressed in the equations

$$x_i - X = x_i' - F, \quad X = \sum_i x_i; \quad F = \sum_i x_i'. \quad 34.$$

X is the centre of mass in x -space, F the centre of mass in x' -space. x_i and F are the "old," x_i' and X the new variables. In analogy to this we introduce two collective rotations, given by the two sets of Euler angles ϵ_s and θ_s .

¹⁰ To assure proper normalization, such an expansion has, of course, to be divided by $\int d\xi \int dx_i' \tilde{\psi}^*(x_i') \tilde{\psi}(x_i' + \xi)$.

ϵ_s is the "redundant" variable, and the transformation is of type

$$(x_{ia}, p_{ia}); \quad (\epsilon_s, G_s) \rightarrow (x'_{ia}, p'_{ia}); \quad (\theta_s, \Pi_s).$$

x'_{ia} and θ_s being the new variables, x'_{ia} the new intrinsic positions, θ_s the Euler angles of the collective rotation, and conjugate to the total angular momentum. $\theta_s = \theta_s(x_{ia})$ and $\epsilon_s = \epsilon_s(x'_{ia})$ are now chosen in such a way as to bring the mass tensors

$$I_{\alpha\beta} = \sum_i x_{ia} x_{i\beta} \quad \text{and} \quad I_{AB} = \sum_i x'_{iA} x'_{iB}$$

to principal axes, respectively

$$R_{PA}(\theta) R_{QB}(\theta) I_{\alpha\beta} = R_{PA}(\epsilon) R_{QB}(\epsilon) I_{AB} = I_P \delta_{PQ} \quad 35.$$

This equation is the analogue of Eq. 34 for the centre of mass case. We have then

$$\begin{aligned} x_{ia} &= R_{PA}(\theta) R_{PA}(\epsilon(x'_{ia})) x'_{ia} \\ \epsilon_s &= \epsilon_s(x'_{ia}) \text{ by Eq. 35} \end{aligned} \quad 36.$$

and the inversion

$$\begin{aligned} x'_{ia} &= R_{PA}(\epsilon) R_{PA}(\theta_s(x'_{ia})) x_{ia} \\ \theta_s &= \theta_s(x_{ia}) \text{ by Eq. 35.} \end{aligned} \quad 37.$$

The expressions for momentum p_{ia} and angular momentum $L_{\alpha\beta}$ are now easily obtained in the new variables, and read:

$$p_{ia} = R_{PA}(\theta) R_{PA}(\epsilon) p'_{ia} + \frac{1}{2} \sum_{P,Q} M_{ia,PQ} (L_{PQ} - L'_{PQ})$$

$$L_{\alpha\beta} = R_{PA}(\theta) R_{QB}(\theta) L_{PQ}$$

L_{PQ} is the angular momentum projected on the principal axes P, Q, R and a linear function of the momenta Π_s conjugate to the θ_s :

$$\Pi_s = \sum_{P<Q} \left(\frac{\partial R_{PA}}{\partial \theta_s} R_{QB} \right) L_{PQ}$$

(analogous to Eq. 19). L' is the intrinsic angular momentum

$$L_{PQ}' = R_{PA}(\epsilon) R_{QB}(\epsilon) L_{AB}' \quad L_{AB}' = \sum_i (x_{iA} p_{iB}' - x_{iB} p_{iA}')$$

Notice that now L' is an ordinary angular momentum, satisfying the usual commutation relations, in contrast to the property of L' in part II.3. $M_{ia,PQ}$ is defined by Eq. 21a. In forming the kinetic energy, the cross terms do not vanish, as they did in part II.3:

$$\tilde{T} = \frac{1}{2m} \sum_{i,A} p_{ia}^2 + \frac{1}{2} \sum_P Q_{PP} (L_P^2 - L'_P)^2 + \frac{1}{2m} \sum_{P,Q} \frac{\{N'_{PQ}, L_{PQ} - L'_{PQ}\}}{I_P - I_Q} \quad 38.$$

with

$$N'_{PQ} = R_{PA} R_{QB} \sum_i (x'_{iA} p'_{iB} + x'_{iB} p'_{iA})$$

and Q_{PP} given by the "hydrodynamic" value of Eq. 23. This result was derived by Lipkin *et al.* (52), Tamura (53) and Nataf (57).

Finally, we give the operator G_s in the new variables:

$$G_s = - \sum_{A < B} \left(\frac{\partial R_{PA}(\epsilon)}{\partial \epsilon_s} R_{PB}(\epsilon) \right) L'_{AB}$$

The result (Eq. 38) is the analogue of Eq. 21, which was obtained without introducing redundant variables. We can simplify, however, the expression for the expectation value of T by a judicious choice of U .

$$| U(G_s) |^2 \rightarrow \prod_i \delta(G_s)$$

It is easily seen, in analogy with Eq. 33 that this corresponds to

$$\langle \tilde{T} \rangle = \int d\Omega_E \int d\Omega_\theta \int \prod_i dx'_i \psi^*(x'_i; \theta_s) \tilde{T} \psi(R(\epsilon)x'_i; \theta_s) \quad 39.$$

$R(E)$ being a rotation of x' -space. In this way again a connection is established with the Peierls-Yoccoz method. Now, the operators L'_{PQ} may be thought of operating on ϵ in Eq. 39 and therefore taken out of the $x'_i - \theta_s$ -integral. They therefore do not contribute to the expectation value of \tilde{T} , which operator may therefore be replaced by

$$\tilde{T}_{\text{eff}} = \sum_i \frac{p_i'^2}{2m} + \frac{1}{2} \sum_P \frac{L_P^2}{Q_{PP}} + \sum_{PQ} \frac{L_{PQ} N'_{PQ}}{m(I_P - I_Q)} \quad 38a.$$

There do not seem to be any developments which go further than this. The programme is fairly evident, though: an additional transformation of the Hamiltonian may separate the collective terms. Such transformations can now easily be formulated since the (x'_i, p'_i) are good canonical pairs. However, the decoupling problem depends on the potential energy too, and its solution therefore requires specific assumptions concerning the interaction. Assuming a single particle potential, this programme should be fairly straightforward.

III. MODELS

1. THE SPHEROIDAL INDEPENDENT PARTICLE MODEL

Although this model is mainly a stepping stone towards more elaborate schemes, we present it here separately, as it has a certain *raison d'être* of its own, distinguished by many characteristic aspects from the shell model.

As mentioned already, we have only rudiments of a really self-consistent calculation of nuclear levels and associated single-particle potentials [Rotenberg (17)]. Already a phenomenological analysis makes clear, however, that (a) the potential well follows the matter distribution quite closely, being at most a fraction of 10^{-13} cm. wider than the latter (17, 61, 62, 63). Neutron- and proton-distributions are almost proportional: the former may have a radius slightly larger than the latter (64, 65, 66, 67). [It has been suggested (71) that in strongly deformed nuclei a separation of protons from neutrons may be responsible for the apparent difficulty of the

Bohr-Mottelson Model with the moment of inertia question. We do not support this idea.] (b) The most favoured shape is the "bathtub" shape, with slanted walls of a width of 2 to 3×10^{-13} cm. (68). (c) The potential is velocity dependent (69). It remains questionable whether this velocity dependence may adequately be described in terms of an effective mass (21, 70) m ; such an attempt leads to $m^* \geq \frac{1}{2}m$. The relevance of this problem in connection with the calculation of moments of inertia is obvious.

The usual approximate determinations of the single particle potential $U(x)$ are based on a parameterization, with subsequent adjustment of parameters to fit the energy:

$$\langle E \rangle = \sum_i \langle T_i \rangle + \frac{1}{2} \sum_i \langle U_i \rangle$$

(the factor $\frac{1}{2}$ being due to the assumed predominance of two body forces), and to give shell closure, etc.

In parameterizing U_i for nonspherical shapes, the condition of "volume preservation" is usually introduced. This is justified by the small compressibility of nuclear matter (62, 72, 73), but should perhaps not be too rigorously enforced for very large deviations from spherical symmetry. This volume preservation allows a minimization of $\langle E \rangle$ with respect to deformation, and therefore, in principle, a calculation of electric quadrupole moments.

We present now a sample of cases that have been investigated and give the most significant results:

a) *Harmonic oscillator without spin-orbit coupling*.—This somewhat academic case has the advantage of being completely transparent, and serves to point out some basic results (74, 75).

With the single particle Hamiltonian

$$H = \frac{\vec{p}^2}{2m} + \frac{1}{2} m [\Omega_1^2 (x^2 + y^2) + \Omega_3^2 z^2] \quad 40.$$

we have the energy levels

$$E_n = \hbar((n_1 + n_2 + 1)\Omega_1 + (n_3 + 1/2)\Omega_3)$$

and $\langle E \rangle = \frac{1}{4} \sum E_n$. Volume preserving deformations may be defined by $\Omega_1^2, \Omega_3 = \Omega_0^2 = \text{const.}$:

$$\Omega_1 \cong \Omega_0(1 + \xi/3) \quad \Omega_3 \cong \Omega_0(1 - 2\xi/3 + \xi^2/3) \quad 41.$$

giving a deformation energy

$$\mathcal{E}(\xi) = 3/4(E(\xi) - E(0))/\hbar\Omega_0 = 1/4[\sum (n_1 + n_2 - 2n_3)\xi + \sum (n_3 + 1/2)\xi^2] \quad 42.$$

In accordance with established custom, we define a deformation parameter β and a r.m.s. radius R_0 through the equations

$$\langle \sum r^2 \rangle = 3/5 A R_0^2, \quad Q = 3/\sqrt{5\pi Z R_0^2 \beta},$$

Q being the electric quadrupole moment. For a nonclosed shell nucleus, for which ξ is determined by the minimum of $\mathcal{E}(\xi)$ (Eq. 42), it follows that

$\beta \approx \xi_{\min}$. If, on the other hand, the occupation numbers satisfy $\sum n_1 = \sum n_2 = \sum n_3$, as for instance in the case of shape oscillations about a spherical equilibrium shape, then $\beta \approx \frac{1}{2}\xi$. In particular this implies that for the harmonic oscillator case, one half of the electric quadrupole moment is due to the deformed filled oscillator shells, the other half due to the extra nucleons (76).

Equation 42 does not account for the preponderance of positive quadrupole moments between closed shells. Instead, the intrinsic moments are positive in the first half of shell filling, negative in the second half. The order of magnitude of the deformations is correct, however.

b) *Harmonic oscillator with spin-orbit term*.—In this model, the potential energy is modified by the addition of a spin-orbit coupling term, $C(\mathbf{l} \cdot \mathbf{s})$, and a further term of type $D\mathbf{l}^2$, whose function is to simulate greater "squareness" of the well [Nilsson (77)]. The corresponding Hamiltonian is diagonalized in an approximation that neglects the off-diagonal elements of the two above mentioned terms between different values of $n = n_1 + n_2 + n_3$ (oscillator shells).

The constants are adjusted separately for protons and neutrons, such as to give the right single particle level structure near closed shells. As a realistic model, it may be tested against experiment.

c) *Square well*.—The infinite well (deformed box) has been considered, with and without $(\mathbf{l} \cdot \mathbf{s})$ coupling, by Moszkowski (78); the finite well without $(\mathbf{l} \cdot \mathbf{s})$ by Uretszky (79) and with $(\mathbf{l} \cdot \mathbf{s})$ by Gallone & Salvetti (80) and by Gottfried (81). The latter's work is the most detailed. His (numerical) calculations are based on an expansion of the deformed potential:

$$U(\vec{r}; \beta) = U_0(r) - \beta Y_{20}(\theta) \left(r \frac{dU_0}{dr} \right) \\ + \frac{1}{2} \beta^2 \left\{ \frac{4}{5\pi} (1 - 2\sqrt{4\pi/5} Y_{20}(\theta)) r \frac{dU_0}{dr} + Y_{20}^2(\theta) \left(r^2 \frac{d^2U_0}{dr^2} - r \frac{dU_0}{dr} \right) \right\}$$

U_0 being an ordinary square well. The spin orbit term is chosen to give a representative level ordering for $\beta=0$; it is found that for large values of β ($\beta \gtrsim 0.3$) the level structure is insensitive to the details of level spacing within a shell. The Hamiltonian is then diagonalized in a finite space of function $|nj\Omega\pm\rangle$. (Ω being the eigenvalue of j_s , the component along the symmetry axis of the well.)

d) *Comparison with experiment*.¹¹—(i) Ground state spins: According to the coupling scheme for strongly deformed nuclei, the ground state spin I_0 is equal to J_s , the projection of the intrinsic angular momentum the nuclear symmetry axis. In the models presented here, J_s is equal to the Ω of the last odd particle. On the basis of this, ground state spins may be read off the energy level diagram as a function of deformation β , the values of β being taken or interpolated from measured values of Q_0 . The agreement with experiment for both Gottfried's and Nilsson's calculation is very good, in the

¹¹ These investigations cover the region $150 < A < 190$.

sense that at the assumed value of β the level giving the expected I_0 value lies actually lowest or is close to the lowest (the exact crossing point of levels being a detail which the model may not reliably supply) (81, 82).

(ii) Quadrupole moments: Gottfried's calculation turns out not to be reliable enough to calculate the equilibrium deformations. On the other hand, Nilsson's level scheme (77) allows to construct a curve $\beta(A)$ for $150 < A < 190$, which agrees well with the experimental data (82, 15), and, in particular, reproduces the steep increase of β above $A = 150$.

(iii) Magnetic moments: Magnetic moments may be calculated under the assumption that the state of the last odd particle determines the g -factor g_0 , and that the g -factor of collective motion has a given value, say $g_c = 0.4$. (See Eq. 3.) Values of g_0 have been calculated on that basis by Gottfried, and are presented, together with the experimental values, in Table II (see under part III.4, Conclusion).

This calculation of g_0 also implies the assumption that there is no further disturbance of the states in the deformed well through the collective rotation of the latter, so that a wave function of the type of Eq. 78 may be used, with $\psi_{\Omega-K}(x)$ being the state of the last odd particle in the deformed well. It follows then that

$$g_0 = g_l + (g_s - g_l) \frac{(\mathbf{s} \cdot \mathbf{L})}{J^2}.$$

The investigations on the Inglis model shed some doubt on the correctness of this approximation: Investigating the moment of inertia problem (part III.2c) one finds that the Coriolis-effect on an unfilled shell amounts to a considerable perturbation, which must make itself felt in the magnetic moments too, affecting the values of both g_c and g_0 . No systematic investigation of this problem has been made yet, however.

2. THE INGLIS (CRANKING) MODEL

a) *Presentation of the model.*—This model consists in a refinement of the previous picture of independent particles in a spheroidal well. The well is assumed to rotate with a constant angular velocity about an axis perpendicular to the axis of symmetry (83). In this way, one simulates, in a semi-classical way, the effect of the precession of the well about the axis of total angular momentum (which is indeed perpendicular to the body-symmetry axis for the rotational level series $K = \Omega = 0$; see section III.3). The energy of the system of A independent particles in the well then assumes a correction term which depends quadratically on the angular velocity ω :

$$E(\omega) = E(0) + \frac{1}{2} \mathfrak{J}_{\text{eff}} \omega^2 + \dots \quad 43.$$

This correction term is interpreted as the classical description of the rotational energy

$$E_{\text{rot}} = \frac{(\mathbf{I})^2}{2 \mathfrak{J}_{\text{eff}}} \quad 44.$$

where, of course, use is made of the relation $\omega = \partial E / \partial \mathbf{I} = \mathbf{I} / \mathfrak{J}_{\text{eff}}$. Assuming a rotation along the x -axis, we have a time dependent potential

$$U(x, y, z; t) = U(x, y'(t), z'(t); 0),$$

y' and z' being the coordinates in the body-fixed system and given by $y' = y \cos \omega t + z \sin \omega t$, $z' = z \cos \omega t - y \sin \omega t$. To have a stationary potential, the Schrödinger equation is written in the body-fixed system, using the relations $\psi(x, y, z; t) = \varphi(x, y', z'; t)$ and

$$i\hbar \frac{\partial \psi}{\partial t} = i\hbar \left(\frac{\partial \varphi}{\partial t} + \frac{\partial \varphi}{\partial y'} \frac{\partial y'}{\partial t} + \frac{\partial \varphi}{\partial z'} \frac{\partial z'}{\partial t} \right) = i\hbar \frac{\partial \varphi}{\partial t} + \omega l_x \varphi.$$

Hence, in the body-fixed system

$$i\hbar \frac{\partial \varphi}{\partial t} = \left(\frac{p^2}{2m} + U(x, y', z') - \omega l_x \right) \varphi = \tilde{H} \varphi \quad 45.$$

The ω -dependence of the eigenvalues E_n of \tilde{H} follows from a straightforward perturbation calculation:

$$E_n(\omega) = E_n^0 - \omega^2 \sum_m \frac{|(m| l_x | n)|^2}{E_m^0 - E_n^0} + \dots \quad 46.$$

(the states φ_n^0 , being eigenstates of $l_{x'}$, give $(n|l_x|n)=0$). E_n is, however, not the energy of the system, which is given by

$$\langle E \rangle_n = E_n(\omega) + \omega \langle l_x \rangle_n = E_n^0 + \omega^2 \sum_m \frac{|(m| l_x | n)|^2}{E_m^0 - E_n^0} \quad 47.$$

From Eq. 43 and 47 we extract an effective moment of inertia

$$\mathfrak{J}_{\text{eff}} = 2 \sum_{n(\text{occ.})} \sum_m \frac{|(m| l_x | n)|^2}{E_m^0 - E_n^0} \quad 48.1$$

This is the basic equation of the model, at least in the original version of strictly independent particles. It is clear from the derivation, that if spin and spin-orbit coupling is taken into account, l_x is simply replaced by j_x in Eq. 48. We emphasize here the fact that a parameter of collective motion, the moment of inertia $\mathfrak{J}_{\text{eff}}$, is calculated on the basis of a strict independent particle picture, in which the only collective feature is the size and shape of the well that contains the particles. Of course, a self-consistent determination of the well parameter is understood here.

b) *Results for noninteracting particles.*—We first apply Eq. 48 to particles in a deformed harmonic oscillator well, Eq. 40, neglecting spin and spin orbit coupling (76, 83, 84).

The operator l_x has matrix-elements within an oscillator shell $n = n_1 + n_2 + n_3$:

$$(n_2 - 1, n_3 + 1 | l_x | n_2 n_3) = (i\hbar/2) \sqrt{n_2(n_3 + 1)} \frac{\Omega_1 + \Omega_3}{\sqrt{\Omega_1 \Omega_3}} \quad 49a.$$

¹² It is interesting to compare this equation with an exact formula for the moment of inertia, derived by Lipkin, de Shalit & Talmi (85).

Due to the deformations of the well, non-zero matrix elements of I_z between shells n and $n \pm 2$ appear, whose value is proportional to the deformation:

$$\langle n_2 + 1, n_3 + 1 | I_z | n_2 n_3 \rangle = (i\hbar/2) \sqrt{(n_2 + 1)(n_3 + 1)} \frac{\Omega_3 - \Omega_1}{\sqrt{\Omega_1 \Omega_3}} \quad 49b.$$

It follows that the effective moment of inertia is given by:

$$\mathfrak{J}_{\text{eff}} = \frac{\hbar}{2} \left(\frac{\Omega_1 + \Omega_3}{\Omega_1 \Omega_3} \right) \left\{ \sum_{\text{occ.}} (n_2 + n_3 + 1) \left(\frac{\Omega_3 - \Omega_1}{\Omega_3 + \Omega_1} \right)^2 + \sum_{\text{occ.}} (n_2 - n_3) \left(\frac{\Omega_3 + \Omega_1}{\Omega_3 - \Omega_1} \right) \right\} \quad 50.$$

To have a reference value, we compare this with the moment of the mass distribution ("rigid-body"-moment):

$$\begin{aligned} \mathfrak{J}_{\text{rig}} &= m \sum \langle y'^2 + z'^2 \rangle \\ &= \frac{\hbar}{2} \left(\frac{\Omega_1 + \Omega_3}{\Omega_1 \Omega_3} \right) \left\{ \sum_{\text{occ.}} (n_2 + n_3 + 1) + \sum_{\text{occ.}} (n_2 - n_3) \left(\frac{\Omega_3 - \Omega_1}{\Omega_3 + \Omega_1} \right) \right\} \end{aligned} \quad 51.$$

We see that it is convenient to split the expression for $\mathfrak{J}_{\text{eff}}$ into two parts, a first part giving the contribution of the filled oscillator shells, and for which therefore $\sum (n_2 - n_3) = 0$, and a second part, giving the contribution of the nucleons occupying unfilled oscillator shells (and being responsible for the deformation). We see that the contribution of the first part is

$$\mathfrak{J}_1 = \left(\frac{\Omega_3 - \Omega_1}{\Omega_3 + \Omega_1} \right)^2 \mathfrak{J}_{\text{rig}} \approx \beta^2 \mathfrak{J}_{\text{rig}} \quad 52.$$

To calculate the second part, we observe that from Eq. 42, it follows that at equilibrium deformation

$$\sum (n_2 - n_3) \approx \left(\frac{\Omega_3 - \Omega_1}{\Omega_3 + \Omega_1} \right) \sum (n_2 + n_3 + 1)$$

so that the contribution \mathfrak{J}_2 of the extra nucleons is

$$\mathfrak{J}_2 \approx \mathfrak{J}_{\text{rig}} \quad 53.$$

The physical reason of this phenomenon is clear. In an unfilled shell, the perturbation ωI_z induces transitions between almost degenerate levels (energy difference $\hbar(\Omega_1 - \Omega_3)$), so that the dimensionless expansion parameter of the perturbation series $\omega/(\Omega_1 - \Omega_3)$ is not so small.¹³ Such transitions are, of course, prohibited for filled shells by the exclusion principle. \mathfrak{J}_1 is therefore due entirely to virtual transitions into the overnext, empty, oscillator shell, with a corresponding energy jump $\hbar(\Omega_1 + \Omega_3)$.

This radically different behaviour of \mathfrak{J}_1 and \mathfrak{J}_2 sheds some light on the question of how a separation should be carried out in the "unified" model between core and extra nucleons. We come back to this in part III.3.

¹³ Clearly, one is not allowed to go to the limit of a spherical potential here; for that eventuality, one has to handle the problem by the methods for degenerate systems; the energy shift is then $\propto \omega^2/(\Omega_1 - \Omega_3)^2 + \omega^2$ (86), so that no rotational spectrum occurs where the expansion is not permissible.

We now discuss the dependence of these results on the simplifying assumptions made to derive the moment of inertia formula: (a) Neglect of spin-orbit coupling; (b) Neglect of distinction between protons and neutrons; (c) Unrealistic well shape; (d) Effective mass effects; and (e) Neglect of residual interactions.

It is quite obvious that a , b , and c , although certainly affecting the results as to detail, do not interfere with the basic mechanism which makes \mathfrak{J}_1 proportional to the square of the deformation, and \mathfrak{J}_2 of the order of the rigid body value, and these results survive therefore in any more realistic model improved according to a , b , and c . The situation is quite different with d . It is still questionable to which extent the effective mass concept may simply be inserted into such a model [Blin-Stoyle (87)]. One is tempted to insert a value of $m^* \approx m/2$ for the effective mass into the above calculations; this would bring down the value of \mathfrak{J}_2 to the order of $\frac{1}{2}\mathfrak{J}_{\text{rigid}}$, agreeing rather well with the maximum observed values of $\mathfrak{J}_{\text{eff}}$ (15, 88). Finally, with regards to point e , it is obvious that processes which establish the value of $\mathfrak{J}_{\text{eff}}$ are very sensitive to any interparticle coupling. To see this, it is sufficient to assume any kind of "pairing energy" which has to be overcome in the virtual transition $n_2 n_3 \rightarrow n_2 \pm 1, n_3 \pm 1$, induced by the Coriolis forces (88). Very roughly, such a coupling has the effect of adding a constant term $\gamma \hbar \Omega_0$ to the small energy denominator, so that

$$\mathfrak{J}_{2\alpha} \sum (n_2 - n_3) \frac{1}{\beta + \gamma}$$

With $\sum (n_2 - n_3) \propto \beta$, the trend of $\mathfrak{J}_2(\beta)$ is now a linear increase with β for $\beta \ll \gamma$, stabilizing towards a value $\approx \mathfrak{J}_{\text{rigid}}$ for $\beta \gg \gamma$. This is indeed roughly the behaviour of $\mathfrak{J}_{\text{eff}}$ borne out by experiments [see (15, 88).] It is clear that a careful study of this effect, along with a critical use of the effective mass concept, opens up the possibility of a better determination of the degree of "independence" of the single particle motion in nuclei.

c) *Relation of Inglis model to exact problem.*—We have presented here the Inglis model as a means of (i) extracting the moments of inertia of rotational levels; (ii) studying the conditions under which rotational levels may be supposed to occur. Clearly the model lends itself to considerable refinement, and appears to be a powerful tool to investigate the connection between collective behaviour and single particle dynamics. It is therefore desirable to have some insight into the relation between the model and the actual nucleus (36, 89). For this purpose, we make use of the transformed particle Hamiltonian (Eq. 24), together with Eq. 23, that is, the "hydrodynamic" value of Q_{AA} . The separation of core and extra nucleons is assumed to be made such as in part *b* of this chapter; the single-particle dynamics should then provide the contribution \mathfrak{J}_2 to the effective moment of inertia, whereas the core should give $\mathfrak{J}_1 \approx \mathfrak{J}_{\text{rigid}} \beta^2$, which is indeed just the value of Q_{11}^{-1} and Q_{22}^{-1} for the axially symmetric (spheroidal) case (Q_{33}^{-1} being zero). In addition, the particular way of dividing the system allows the assumption that

an intrinsic wave function $\phi(\xi)$ of approximately zero angular momentum ($J'\phi(\xi) \approx 0$) may be factored off. Averaging over the intrinsic motion and assuming spheroidal symmetry of the mass distribution, we have:

$$\langle H \rangle_\phi = E_{00} + C\beta^2 + \frac{1}{2\mathfrak{J}_0\beta^2} \left(L_\perp - \sum_r j_{r\perp} \right)^2 + \sum_r \left(\frac{p_r'^2}{2m} + U(x_r'; \beta) \right) + \sum_{r,s} V_{rs}. \quad 54.$$

Notice that $(L_\perp - \sum_r j_{r\perp})$ is a constant of motion in case of spheroidal symmetry, and takes the value zero only.

The connection with the Inglis model rests now upon the following assumptions: (a) The total angular momentum is considered as a classical vector. A quantum mechanical perturbation calculation [Lüders (89)] based on Eq. 54, shows that this approximation implies neglect of the energy $\hbar^2/2\mathfrak{J}_{\text{eff}}$, compared to the level splitting $\Delta E(\beta)$ (e.g., $\hbar(\Omega_3 - \Omega_1)$, for an oscillator potential). The approximation is justified for large deformations β , where the rotational excitation energies are low and L reaches large (classical) values. (b) The coupling between particles is neglected, and $U(x_r'; \beta)$ is representative for the actual potential acting upon the r 'th extra nucleon. This approximation becomes poor if the number of extra particles (that is, particles occupying nonfilled shells) is large; this is a general drawback of this unsymmetric method (and also of the Bohr-Mottelson "unified model"). But for the mere problem of understanding the fundamental connection between Eq. 54 and the Inglis model, we may always assume the number of extra nucleons to be small.

With a and b , we can now use as trial function a determinant of single particle functions, $\varphi_n(x_r)$, giving

$$\begin{aligned} \langle E \rangle &= E_{00} + C\beta^2 + \frac{L_\perp^2}{2\mathfrak{J}_0\beta^2} + \sum_n \left\langle \frac{p^2}{2m} + U(x; \beta) \right\rangle_n \\ &+ \frac{1}{2\mathfrak{J}_0\beta^2} \left\{ \left(\sum_n \langle j_\perp \rangle_n \right)^2 - 2L_\perp \cdot \sum_n \langle j_\perp \rangle_n - \sum_{(\infty)} \sum_{\substack{n \\ (\text{empty})}} \langle j_\perp \rangle_{nm} \langle j_\perp \rangle_{mn} \right\} \end{aligned} \quad 55.$$

Neglecting the very last term, and taking variational derivatives, we obtain the single particle equations:

$$\left(\frac{p^2}{2m} + U(x; \beta) \right) \varphi_n(x) - \left(\frac{L_\perp - \sum_{n'} \langle j_\perp \rangle_{n'}}{\mathfrak{J}_0\beta^2} \right) \cdot j_\perp \varphi_n(x) = E_n \varphi_n(x). \quad 56.$$

This equation clearly has the structure of Eq. 45 of the Inglis model, with

$$\omega_\perp = \left(L_\perp - \sum_{n'} \langle j_\perp \rangle_{n'} \right) / \mathfrak{J}_0\beta^2$$

Now, from the previous discussion it is clear that

$$\sum_n E_n(\omega) = \sum_n E_n(0) - \frac{1}{2} \omega^2 \mathfrak{J}_2$$

and

$$\sum_{n'} \langle j_\perp \rangle_{n'} = \omega_\perp \mathfrak{J}_2$$

and hence

$$\omega_{\perp} = L_{\perp}/(\mathfrak{J}_0\beta^2 + \mathfrak{J}_2)$$

Inserting these results into Eq. 55, it follows that

$$\begin{aligned}\langle E \rangle &= E_{00} + C\beta^2 + \sum_n E_n(\omega) + \left(L_{\perp}^2 + \left(\sum_{n'} \langle j_{\perp} \rangle_{n'} \right)^2 \right) / 2\mathfrak{J}_0\beta^2 \\ &= E_{00} + C\beta^2 + L_{\perp}^2/2(\mathfrak{J}_0\beta^2 + \mathfrak{J}_2)\end{aligned}\quad 57.$$

This clearly shows that a solution of the *eigenvalue* problem of the transformed Hamiltonian, Eq. 24 subject to the approximations stated above, gives a rotational moment of inertia

$$\mathfrak{J}_{\text{eff}} = \mathfrak{J}_0\beta^2 + \mathfrak{J}_2$$

that is, essentially the result of the Inglis model. But one also realizes that the Inglis method is superior to this present calculation, since a higher degree of self-consistency between particle configuration and potential shape is possible, there, due to the symmetric handling of all nucleons, which the present method cannot achieve. The unsymmetric splitting of the system into two parts handled by different methods is always unnatural. The appeal of the method of redundant variables becomes particularly apparent here.

d) *The Inglis model for collective vibrations.*¹⁴—By the same techniques as outlined in part 2a, we can handle the problem of a single particle potential which classically oscillates about a spherical equilibrium shape (90, 91). This, then, is an alternative approach to the problem discussed in part II,3b, where such vibrations are described in terms of the variables λ_{μ} . Let us observe here that by proper combination of modes λ_{μ} we may produce actual vibrations (which go through spherical shapes) and also "tidal waves," which actually are rotations; for these latter, nothing new can be said here, and their "Inglis" treatment has been given in part III,2b. We discuss here the case of a vibration, $\mu=0$: in analogy to Eq. 43 we shall obtain a collective energy

$$E(\lambda) = E(0) + \frac{1}{2}B\lambda^2 + \dots, \quad 58.$$

an expression which defines the inertial parameter B ; for an irrotational flow pattern we should have, according to Eq. 28, $B=mI_0=m\langle \sum x^2 \rangle$. Specializing to the harmonic oscillator case, with frequencies $\Omega_1(t)$ in the x $\Omega_2(t)$ in the z direction, we write

$$\Omega_1(t) = \Omega_0(1 + \sqrt{2/3}\lambda(t))$$

$$\Omega^2(t) = \Omega_0(1 - 2\sqrt{2/3}\lambda(t) + \dots).$$

This normalization makes λ identical with λ_0 of Eq. 26a. Introducing new variables: $x'(t) = (1 + \sqrt{2/3}\lambda(t))^{1/2}x$, etc. and the corresponding momenta p' ,

¹⁴ A method related to the one reported on here has been used by Araujo (92).

and also $\psi(x, y, z; t) = \varphi(x', y', z'; t')$, so that:

$$\frac{\partial \psi}{\partial t} = \frac{\partial \varphi}{\partial t} + \left(\frac{\partial \varphi}{\partial x'} \frac{\partial x'}{\partial t} + \dots \right),$$

we get the Schrödinger equation for φ :

$$i\hbar \frac{\partial \varphi}{\partial t} = H^{(0)}(t)\varphi + \sqrt{1/6}\lambda D\varphi \quad 59.$$

$$H^{(0)}(t) = (1 + \sqrt{2/3}\lambda)[(p_x'^2 + p_y'^2)/2m + 1/2m\Omega_0^2(x'^2 + y'^2)] \\ + (1 - 2\sqrt{2/3}\lambda + \dots)[p_z'^2/2m + 1/2m\Omega_0^2z'^2] \quad 60.$$

$$D = (x'p_z' + y'p_y' - 2z'p_x') \quad 61.$$

It follows then that

$$E_n^{(0)}(t) = \hbar\Omega_1(t)(n_1 + n_2 + 1) + \hbar\Omega_3(t)(n_3 + 1/2)$$

and, by the same argument as used for rotations,

$$B = \frac{1}{3} \sum_{n(\text{occ.})} \frac{|(m| D | n)|^2}{E_m^0 - E_n^0} \quad 62.$$

Now the only nonvanishing matrix-element of D are from n to $n \pm 2$, so that $E_n - E_{n \pm 2} = 2\hbar\Omega_1$ or $2\hbar\Omega_3$. It follows that

$$B = \frac{1}{3} \left(\frac{\hbar}{\Omega_0} \right) \left\{ \sum_{\text{occ.}} (2n_2 + 1) + \frac{1}{2} \sum_{\text{occ.}} (n_1 + n_2 + 1) \right\}$$

$\rightarrow (\hbar/\Omega_0) \sum_{\text{occ.}} (n_1 + \frac{1}{2})$, for a closed shell configuration. This is exactly the required value.

It is clear that the above result does not sensitively depend upon shell closure. However, Mouhasseb (91) has observed that these results are profoundly modified by spin orbit coupling. The small value of B was due to the fact that the operator D had no nonvanishing matrix-elements within an oscillator shell. This is no longer so if an $(l \cdot s)$ -coupling: $-2\kappa(\hbar\Omega_0)(l \cdot s)$ splits the levels of a shell, with the result that nonclosed shells give a contribution of order κ^{-2} . In this way it is again possible for B to exceed the hydrodynamic value mI_0 by a large factor, since κ is $\ll 1$ (0.05 in the case of Nilsson's potential).

As a final remark we observe that the validity of the expansion (Eq. 58), depends on the smallness of λ/Ω_0 . This condition is certainly not fulfilled for closed oscillator shells (90), but becomes more nearly satisfied as the core is "softened" by the addition of nucleons, the more as then λ is reduced by the increase of B .

3. THE "UNIFIED" MODEL OF BOHR-MOTTELSON

a) *Introduction*.—This model is based on the attempt to describe the dynamical interplay between "valence nucleons" and the nuclear "core" (here understood as any essentially spherically symmetric structure with ground state spin $I=0$) in a simple and transparent way. The core is there-

fore replaced first by a continuum, a "liquid drop," and whose lowest modes of excitation are therefore independent of the particle structure. It is now well-known that this is a too drastic assumption; we shall come back to this point again. Specifically, these modes of excitation are assumed to be "phonons," corresponding to an irrotational, incompressible flow pattern about a spherical equilibrium shape. One has then a velocity field satisfying: $\mathbf{v}(x) = -\nabla\chi(x)$; $\nabla^2\chi = 0$. The regular solutions of these equations are the harmonic polynomials; as simplest case we consider

$$\chi(r, \theta, \varphi) = -\frac{1}{2} r^2 \sum_m \dot{\alpha}_m Y_{2m}(\theta, \varphi), \quad 63.$$

corresponding, for small values of α ($\alpha \ll 1$), to a nuclear boundary

$$R(\theta, \varphi) = R_0 \left(1 + \sum_m \alpha_m Y_{2m}(\theta, \varphi) \right) \quad 64.$$

Kinetic energy and angular momentum of the vibrating drop are

$$T = \frac{1}{2} \int d\tau \rho (\nabla \chi)^2 = \frac{1}{2} B_2 \sum_m \dot{\alpha}_m^* \dot{\alpha}_m \quad 65a.$$

$$\vec{L}_e = \int d\tau \rho (r \mathbf{x} \nabla \chi) = iB_2 \sum_{m,m'} \alpha_m^* \dot{\alpha}_{m'} \vec{M}_{m,m'} \quad 65b.$$

with

$$B_2 = \frac{1}{2} \rho_0 R_0^5 = \frac{3}{8\pi} m A R_0^2 \quad 66.$$

and \mathbf{M}_{mm} , the angular momentum matrix-elements defined in part II.3b. The potential energy is of type

$$\frac{1}{2} C_2 \sum_m \alpha_m^* \alpha_m. \quad 67.$$

C_2 may be taken from the empirical surface energy (93, 94), but it is more prudent to keep it as an adjustable parameter. The dynamics of Eq. 65, 66, and 67 has already been discussed in part II.3. In general, then, the nucleus must be divided into a "core," described as above, and extra nucleons. How this division has to be effected is not so clear from the outset. Making use of our experience, we can now say that all nucleons (or holes) in unfilled subshells, thus contributing to the deformation pressure, should be treated as "extra" particles. The core, by this criterion, need not be magic, as closed subshells may be included, as long as they remain fully occupied at the deformation in question.

To describe the coupling of the extra nucleons to the liquid drop it is assumed that shape of the drop closely coincides with shape of the potential for the extra nucleons. This potential is therefore of type

$$U(r, \theta, \varphi) = U_0(r/R(\theta, \varphi)) = U_0(r/R_0) - \left(r \frac{dU_0}{dr} \right) \sum_m \alpha_m Y_{2m}(\theta, \varphi) + \dots \quad 68.$$

The Hamiltonian is then the sum of the liquid drop (oscillator) Hamiltonian, the particle Hamiltonian and a coupling, given by the last term of Eq. 68. The dynamics of this coupled system is relatively simple in two limiting situations: (a) Weak coupling case (nucleus in neighbourhood of closed shells; one or a few extra nucleons). The interactions between drop oscillation and nucleon motion may be described as a perturbation. The amplitude of the 1 phonon component of the ground state wave function is small, and as a consequence, the expectation value of $\langle \alpha \rangle$ (the equilibrium deformation) is small compared to the zero point amplitude of the drop:

$$x = \frac{\langle \alpha \rangle}{\sqrt{\langle \alpha^2 \rangle}} \sim \frac{\left\langle r \frac{dU}{dr} \right\rangle}{\sqrt{\hbar\omega C}} \ll 1 \quad 69.$$

(b) Strong coupling case (medium and heavy nuclei well between major shell closings: $150 < A < 190$ or $A \geq 225$). The combined effects of extra nucleons lead to a value $x \gg 1$, so that we can speak of a nonspherical equilibrium shape. Rotational spectra.

b) *Pure collective excitation*.—For even nuclei in the weak coupling region there is the temptation to throw all nucleons in the core, thus approximating the system by a pure collective oscillator. The resulting pure collective excitations should then be characterized by:

(i) the level spectrum:

$$E_n = (n + 5/2) \cdot \hbar \sqrt{\frac{C}{B}} \quad 70.$$

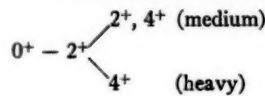
(ii) the angular momenta I_n :

$$I_0 = 0, \quad I_1 = 2, \quad I_2 = 0, 2, 4 \text{ (degenerate)}$$

(iii) the electromagnetic transitions, which are of pure E_2 type, with the selection rules $|\Delta I| \leq 2, \Delta n \pm 1$. This last rule prevents cross-over transitions from the second excited into the ground state. (iv) the absolute transition rates. The first excited state has a reciprocal lifetime.

$$\tau^{-1} = \frac{3}{200\pi} \frac{Z^2}{137} \omega \left(\frac{R_0}{\lambda} \right)^4 \frac{\hbar}{\sqrt{C_2 B_2}} \quad 71.$$

As a possible application of this scheme we consider the medium weight nuclei in the range $22 < N < 90$, and the heavy group $114 \leq N \leq 134$ (centred around the double magic $N=126, Z=82$). Way, *et al.* (26) have pointed out the regularity in the behaviour of the members of this group (except at N or Z magic): (i) The ratio of excitation energies E_2/E_1 is ≈ 2.2 , and E_1 is of order 60 Mev/A (75 Mev/A) for the medium (heavy) members of the group. (ii) The sequence of angular momenta and parities is



(iii) The transitions are predominantly E_2 (51, 95) and strongly enhanced; but the cross-over transition ($E_2 \rightarrow E_0$) not nearly as much as the stop-over ($E_2 \rightarrow E_1$), indicating a relative "forbiddenness" of the former (96) (rule of Kraushaar & Goldhaber). (iv) The transition $E_1 \rightarrow E_0$ has a favoured factor F of order 10 to 40 (95).

The evidence certainly speaks in favour of a degree of truth in the picture. Two observations may be added:

First: Points ii and iii can be taken care of without invoking the collective model at all (96); iii, in particular, by invoking the seniority selection rule. On the other hand, i and iv do not follow naturally from pure shell model considerations.

Second: The numerical values entering i and iv do not fit the simple collective picture either. [For an attempt to interpret the situation through an interpolation between weak and strong coupling description, see Wilets & Jean (97).] Calculations of C_2 and B_2 from experimental data by i and iv give values of B_2 systematically an order of magnitude too large, compared with Eq. 66. The values of C_2 fluctuate about the hydrodynamic value, showing strong correlation with shell closure.

We must conclude from this that the simple collective oscillator is too crude a picture to describe the low-lying levels of the even nuclei in the group considered here. The experimental values of B_2 indicate considerable departure from irrotational flow, indicating that the nucleons in unifilled shells should be described as individuals. It is such a hybrid description (51) which gets to the data with the least amount of complexity.

c) *Weak coupling situation.*—The cases considered here are mainly those for which the usual shell-model picture gives a reasonable approximation. The lowest excited states are definitely particle excitations, and their excitation energy is less than $\hbar\omega$. The weak coupling picture is thus essentially a refinement of the description of these states. The main effects of the coupling to the collective oscillation appear in the modifications of magnetic moments, electric quadrupole moments and lifetimes of excited states. The problem of a single odd nucleon, coupled to the collective modes, has been studied by Foldy & Milford (98), Kerman (99), Ford & Levinson (100), the weak coupling situation in the neighbourhood of Pb^{208} by True (101), and in light nuclei, for the Ca-isotopes, by Levinson & Ford (102).

The most pronounced corrections occur in the quadrupole moments and transition rates. Calling a_0 and a_1 the amplitudes of the zero- and one-phonon components of the wave function, ($a_0^2 + a_1^2 = 1$), we have for the correction to the quadrupole moment

$$Q_{0011} = \pm \frac{6Z}{\sqrt{5\pi}} R_0^2 \sqrt{\frac{\hbar^2/2B_2}{\hbar\omega}} \sqrt{\frac{j(2j-1)}{(j+1)(2j+3)}} |a_1| \quad 72.$$

(+ for hole, - for particle), the important point being linearity in a_1 and proportionality to Z .

The magnetic moment correction is proportional to $|a_1|^2$ and thus considerably less important in the weak coupling approximations, $|a_1|^2 \ll 1$:

$$\mu = \mu_{s.p.} + \frac{|a_1|^2}{2(j+1)} [(g_c - g_{\nu'j})(j(j+1) - j'(j'+1) + 6) + 2(g_{\nu'j} - g_{jj})j(j+1)] \quad 73.$$

(ν', j' being the particle angular momenta in the one phonon component). These corrections are in general much too small to enable the weak surface coupling to account for the observed deviations from the Schmidt Lines [for presentation and discussion of the experimental material, see Blin-Stoyle (103)]. Other mechanisms, for the weak coupling region, in particular configuration mixing induced by the direct internucleon forces, is presumably the main agent for the magnetic moment deviations (104).

Finally, γ -transitions of E_2 type are enhanced considerably even for very weak coupling. Transition probabilities have been discussed by Bohr & Mottelson (16), Ford & Levinson (100), Barker (105). [For experimental data, see (25, 95).]

Odd nuclei are characterized by great fluctuations in the degree of "anomaly" they represent, as measured by magnetic moment deviation, favoured factors in γ -transitions, etc. One is tempted to take this as an indication for a rather complex situation, with the nature of the states mainly determined by the internucleon forces. The fact that collective effects dominate certain γ -transitions and quadrupole moments should not be taken as an indication that dynamically phonon excitation is the essential element of the description.

d) *Strong coupling situation.*—In this case the combined effect of a sufficiently large number of extra nucleons results in a nonspherical equilibrium shape of the drop. It is then more appropriate to express the energy of the collective flow in terms of new variables, namely the orientation of the principal axes of the deformed drop (of ellipsoidal shape) in terms of three Euler angles θ_s , and the deformations β_A , along the three principal axes:

$$R_A = R_0 \left(1 + \sqrt{\frac{5}{4\pi}} \beta_A \right); \quad \beta_A = \beta \cos(\gamma - 2\pi A/3)$$

θ_s , β and γ are the five new independent collective variables. The transformation to these new variables is reminiscent of the techniques of strong coupling field theory, and has been carried out in this fashion by Wentzel (38) and Coester (47). The collective energy (Eq. 65a, 67) becomes

$$H_C = \frac{1}{2} B_2 (\dot{\beta}^2 + \beta^2 \dot{\gamma}^2) + \frac{1}{2} C_2 \beta^2 + \sum_A \frac{L_{C,A}^2}{8B\beta^2 \sin^2 \left(\gamma - \frac{2\pi}{3} A \right)} = H_{\text{vibr.}} + H_{\text{rot.}} \quad 74.$$

$L_{C,A}$ being the projection of the collective angular momentum L_C on the principal axis A .

To H_C has to be added the Hamiltonian of the extra nucleons. If the description of these extra particles is given in the body fixed frame of the liquid drop, we have (see part II for details):

$$H = \text{vibr.} + \sum_{rA} \left(\frac{p_r^2}{2m} + U(x_r; \beta, \gamma) \right) + \sum_A \frac{\left(L_A - \sum_r j_{r,A} \right)^2}{8B\beta^2 \sin^2 \left(\gamma - \frac{2\pi}{3} A \right)} \quad 75.$$

L_A represents now the total angular momentum; it is the same operator on the θ_s as was L_{CA} before, and given by Eq. 19.

The close resemblance between Eq. 75 and 24 is obvious.¹⁶ It must be made clear, however, that Eq. 24 does not provide a justification for 75 and therefore of the model, with its assumption of irrotational in flow. This is true despite the fact that the same zero order moments appear both equations, since

$$m \frac{(I_B - I_C)^2}{I_B + I_C} \simeq 4B_2 \beta^2 \sin^2 \left(\gamma - \frac{2\pi}{3} A \right)$$

These moments have nothing to do with the measured moments as long as the collective rotation is not dynamically decoupled from the intrinsic motion. Now the degree of decoupling is certainly not the same in the two equations. In fact, the assumption of irrotational flow, leading to Eq. 75 can be expressed in Eq. 24 by the condition

$$J_A' \phi(\xi_r, x_{rA}) = 0 \quad 76.$$

an equation which has no reason to hold in general, except perhaps for a magic core. Except for such a case, in which Eq. 76 holds at least approximately, the model does not appear to be justified from general principles.

The solutions of the *eigenvalue* problem of the Hamiltonian (Eq. 75) have been considered by Bohr (50), Bohr & Mottelson (16), Ford (106), Marty (37) and others.

Let us assume here that the system is γ -stable [γ -unstable situations have been considered by Jean & Wilets (97)], and stabilize at $\gamma=0$ (prolate) or $\gamma=\pi$ (oblate), which appears to be the predominant case. We have then cylindrical symmetry, and the operators L_z^2 , L_z , $L_z - \sum_r j_{r,z}$ are constants of the motion, the latter having to be identically zero. In lowest approximation it is then generally assumed that L_z and $\sum_r j_{r,z}$ are separately con-

¹⁶ It is, of course, possible to derive Eq. 75 exactly from the Hamiltonian Eq. 54; in that case, one should keep in mind all the approximations and assumptions that have gone into the derivation of this latter equation, especially the assumption $J' \phi_{\text{intr}} \simeq 0$. In contrast to this, Eq. 24 is an exact equation, and it would be easy there to isolate the collective vibrations too. However, it is not important for the questions to be discussed here.

stants, with eigenvalues K and $\Omega = K$ respectively. In this approximation the rotational energy is decoupled, and has the value

$$\left\langle \frac{1}{8B\beta^2} \right\rangle (I(I+1) - K^2); \quad I \geq K; \quad \Omega = K \neq 1/2. \quad 77.$$

[For the special case $\Omega = K = \frac{1}{2}$, see (15, 16)].

The corresponding zero order wave functions are

$$\Psi^{(0)} = v(\beta, \gamma) (\mathcal{D}_{MK} I^*(\theta_s) \psi_K(x_r) + (-1)^{I-K} \mathcal{D}_{M,-K} I^*(\theta_s) \psi_{-K}(x_r)) \quad 78.$$

with $I = K$ for the ground state. The symmetrization of the wave function, necessary because of the ambiguity of the definition of the body fixed axes, has been discussed in detail by Bohr (50) and by Marty (37). For even nuclei, with ground states $\Omega = K = 0$, Eq. 78 restricts the values of I to 0, 2, 4, . . .

With $\Psi^{(0)}$, electromagnetic moments and transition-probabilities follow in a straightforward way. Calling $\sum j_r \equiv J$, and g_c the g -factor associated with collective motion, one has

$$\begin{aligned} \mathbf{J} &= g_c(\mathbf{L} - \mathbf{J}) + \mathbf{j}_{\text{intr}} \\ \mathbf{j}_{\text{intr}} &= \sum (g_l l + g_s s) \end{aligned}$$

which, in the above approximation, except for $K = \frac{1}{2}$, gives a magnetic moment

$$\mu = (\mathbf{J} \cdot \mathbf{L})/I + 1 = g_c \frac{I}{I+1} + g_\Omega \frac{I^2}{I+1} \quad 79a.$$

g_Ω being defined as

$$\sum (g_l l + g_s s)/I. \quad 79b.$$

The electric quadrupole moment is essentially due to the core deformation. It is given, in the body fixed system, by

$$Q_0 = \frac{3}{\sqrt{5\pi}} Z R_0^2 \langle \beta \cos \gamma \rangle$$

The operator of the spectroscopic quadrupole moment is then

$$Q = P_2(\cos \theta) Q_0$$

and

$$\langle Q \rangle = \langle P_2(\cos \theta) \rangle_{I,M=I} Q_0 = \frac{3K^2 - I(I+1)}{(I+1)(2I+3)} Q_0 \quad 80.$$

Finally, we mention the $E2$ -transition probabilities, which, due to the predominance of the collective contribution, are directly expressible in terms of Q_0

$$B_{E2}(I_i \rightarrow I_f) = \frac{5}{16\pi} I^2 Q_0^2 (I_i 2KO \mid I_f 2I_f K)^2 \quad 81.$$

TABLE I

QUADRUPLE MOMENTS AND MOMENTS OF INERTIA IN THE
REGION $150 < A < 190$ AND $A > 225$

Nucleus	I_0	$ Q_0 $ (barns)*	$3\hbar^2/\mathfrak{J}$ (kev)†	$\beta_B \ddagger$	$\beta_E^2/\beta_B^2 \S$
Sm ¹⁵²		5.7			
Eu ¹⁵³	5/2	7.7	122	0.28	5
Sm ¹⁵⁴		6.7	71		
Gd ¹⁵⁴		6.3	83	0.33	4.6
Gd ¹⁵⁵	3/2	8.0	123	0.30	
Gd ¹⁵⁶		8.8	72		
Gd ¹⁵⁷	3/2	7.7	89	0.41	
Gd ¹⁵⁸		10	66		
Tb ¹⁵⁹	3/2	6.9	79	0.46	
Gd ¹⁶⁰		10	70		
Dy ¹⁶⁰		7.8	76	0.47	
Dy ¹⁶²		8.2	86	0.35	4.8
Dy ¹⁶⁴		8.2	82	0.36	
Er ¹⁶⁴		9.5	73	0.41	
Ho ¹⁶⁵	7/2	7.8	90	0.33	5.4
Tm ¹⁶⁹	1/2	8.9	63		
Yb ¹⁷⁰		7.5	74	0.30	5.6
Lu ¹⁷⁶	7/2	8.2	84		
Hf ¹⁷⁶		7.5	76	0.29	
Hf ¹⁷⁷	7/2	7.5	89		
Hf ¹⁷⁸		8.1	75	0.31	5.5
Hf ¹⁷⁹	9/2	7	91	4.0	
Hf ¹⁸⁰		7.1	66		
Ta ¹⁸¹	7/2	6.8	93	0.27	6.0
W ¹⁸²		7.1	91		
W ¹⁸³	1/2	—	100	0.26	6.5
W ¹⁸⁴		6.5	78		
Re ¹⁸⁵	5/2	5.4	112	0.24	
W ¹⁸⁶		6.5	108		
Os ¹⁸⁶		5.5	124	0.24	
Re ¹⁸⁷	5/2	5.0	137	0.20	6.2
Os ¹⁸⁸		5.1	116		
Th ²³²		10	155	0.18	6.6
U ²³³	5/2	14	52	0.25	3.4
U ²³⁵	7/2	9	35		
N ²³⁷	5/2	9	31		
U ²³⁸		11	28		
Pu ²³⁹	1/2	8.3	44	0.28	3.4
			37		

These data are copied from Ref. 15, except for the last column, which are taken from Ref. 26.

* The values of Q_0 are obtained either from Coulomb-excitation cross sections [Heydenberg & Temmer (25)], or from fast E2-transition probabilities [Sunyar (109)].

B_{E2} being the reduced $E2$ -transition probability (93), and the last factor in Eq. 81 the square of a vector addition coefficient

$$\langle j_1 j_2 m_1 m_2 | j_1 j_2 j m \rangle$$

In assessing the predictions of the strong coupling model, we must clearly distinguish between two classes of statements. There are statements which mainly derive from the mere fact of the existence of a rotational spectrum, without strongly involving other aspects of the dynamics. Such statements are: (a) Ratios of $E2$ -transition probabilities within a rotational band (107), (b) Selection rules, (c) Ratios of transition probabilities to the states of a rotational band in α -decay (31, 108), (d) Relation between Q_0 and B_{E2} .

These statements only invoke the assumptions of the existence of a sufficiently strong equilibrium deformation and the adiabatic slowness of collective rotation, which guarantee the equivalence of the intrinsic structure for all levels of a rotational band. The agreement between observed and predicted values is indeed good. Opposed to these results are "sensitive" statements such as: (a) Moments of inertia, (b) Magnetic dipole moments, (c) Magnetic transistions. Here the basic assumptions of the model enter in a critical way, and even a state which actually diagonalizes the model Hamiltonian (Eq. 75) may not be adequate, for the reasons stated previously.

We conclude this section by giving, in form of tables, some experimental data to illustrate these statements.

4. CONCLUSION

Trying to assess the contribution which the collective point of view has made to our understanding of nuclear dynamics one is impressed by two facts: (a) The essential simplicity of the collective dynamics, which

It is seen that the values of Q_0 for $150 < A < 190$ follow a regular pattern, increasing rapidly to a maximum at $A \approx 160$, then decreasing slowly; there is no marked difference between the even and odd nuclei. This behaviour is explained almost quantitatively by Nielsson's model (part III.1b).

† The values of the moment of inertia \mathfrak{J} are strongly correlated with the value of Q_0 , that is β . Moments of inertia of odd nuclei are systematically larger than those of neighbouring even nuclei, a feature is qualitatively understood on the basis of the Inglis model with residual interaction of the type of a pairing energy.

‡ β_B is the deformation calculated from Q_0 : $Q_0 \approx \sqrt{9/5\pi} Z R_0^3 \beta$; assuming $R_0 = 1.2 A^{1/3} \times 10^{-18}$ cm.

§ β_E^2 is defined by the $\mathfrak{J}_{\text{exp}} = 3B_2\beta_E^2$; $B_2 = 3/8\pi M A R_0^3$ (Eq. 66); β_E is the (fictitious) deformation, which, in connection with the model of irrotational flow, gives the observed moments of inertia. The values of this column illustrate the inadequacy of the hydrodynamic description of the core. In comparison, the rigid body moments are a better approximation.

TABLE II
MAGNETIC MOMENTS IN REGION $150 < A < 190$

Nucleus	Odd part	I_0	μ_{exp}	g_c^*	g_n^*	$g_n^{\text{th}\dagger}$	$\mu^{\text{th}\ddagger}$
Eu ¹⁵³	$Z = 13$	5/2	1.5	0.5	0.6	0.23	0.69
Tb ¹⁵⁹	$Z = 65$	3/2	1.5	0.1	1.6	2.3	2.34
Lu ¹⁷⁵	71	7/2	2.6	0.3	0.9	1.54	4.5
Ta ¹⁸¹	73	7/2	2.1	0.25	0.70	0.42	1.46
Re ¹⁸⁵	75	5/2	3.14	0.5	1.6	1.64	3.22
Re ¹⁸⁷	75	5/2	3.18	0.5	1.6	1.64	3.22
Gd ¹⁵⁵	$N = 91$	3/2	-0.3	0.28	-0.53	-0.34	-0.07
Gd ¹⁵⁷	93	3/2	-0.37	0.27	-0.61	-1.06	-0.71
Hf ¹⁷⁷	105	7/2	0.61	0.21	0.06		
Hf ¹⁷⁹	107	9/2	-0.47	0.2	-0.2		

* These experimental values of g_c and g_n are taken from Eq. 79a for μ , and the expression for the MI -transition-probability, which gives $(g_c - g_n)^2$, [see (15, 25)]. There are two sets of solutions, and we give here the one which agrees better with the theoretical values.

† This is a value calculated by Gottfried, on the basis of Eq. 79b, considering the last odd nucleon only.

‡ This is the theoretical moment on the basis of Eq. 79a, with Gottfried's values for g_n , and $g_c = 0.4$.

gives energy levels, moments, etc., in terms of very few parameters; and the accuracy with which this collective picture reproduces some data. (b) The fact is that we have today only the rudiments of a really unified description of single particle and collective motion. The main point here is to recognize the total inadequacy of the hydrodynamic approximation for the nuclear core, and the promise held out to be able, eventually, to calculate the parameters of the collective picture (deformations, moments of inertia, g -factors) on the basis of the independent particle dynamics.

The main result to be taken from our present insight into the situation is in fact the recognition of the crucial role, which a correct description of the "independent" particle dynamics (including inter-particle coupling) plays for the quantitative understanding of the collective motion.

Although such a synthesis of the collective and the particle aspect of nuclear dynamics is rather easily achieved in words, by simply combining results borrowed from various models, a decent mathematical formulation of the same programme is far from easy. We venture here the opinion that the method of "redundant variables" holds the greatest promise to achieve this goal, but the work is still very much in its beginnings.

ACKNOWLEDGMENTS

The author wishes to acknowledge fellowship grants from the European Organization for Nuclear Research (CERN) and from the John Simon Guggenheim Memorial Foundation, without which this work could not have been written.

LITERATURE CITED

1. Mayer, M. G., *Phys. Rev.*, **75**, 1969 (1949)
2. Haxel, O., Jensen, J. H. D., and Suess, H. E., *Phys. Rev.*, **75**, 1766 (1949)
3. Rainwater, J., *Phys. Rev.*, **79**, 432 (1950)
4. Feshbach, H., Porter, C., and Weisskopf, V. F., *Phys. Rev.*, **90**, 166 (1953)
5. Friedman, F. L., and Weisskopf, V. F., *Niels Bohr and the Development of Physics*, 134-162 (Pauli, W., Ed., Pergamon Press, Ltd., London, England, 195 pp., 1955)
6. *Statistical Aspects of the Nucleus*, Brookhaven National Laboratory Report, BNL 331 (C-21) (1951)
7. Flowers, B. H., *Progr. in Nuclear Phys.*, **2**, 235 (1952)
8. Pryce, M. H. L., *Repts Progr. in Phys.*, **XVII**, 1 (1954)
9. Jensen, J. H. D., *Beta and Gamma Ray Spectroscopy*, pp. 414-432 (K. Siegbahn, Ed., North Holland Publishing Co., Amsterdam, Holland, 959 pp., 1955)
10. Mayer, M. G., and Jensen, J. H. D.: *Elementary Theory of Nuclear Shell Structure* (John Wiley and Sons, New York, N. Y., 284 pp., 1955)
11. Feenberg, E., *Shell Theory of the Nucleus* (Oxford University Press, London, England, 222 pp., 1955)
12. Hill, D. L., and Wheeler, J. A., *Phys. Rev.*, **89**, 1102 (1953)
13. Bohr, A., *Rotational States of Atomic Nuclei*, Doctoral Thesis (Ejnar Munksgaard Forlag, Copenhagen, Denmark, 1954)
14. Bohr, A., and Mottleson, B. R., in *Beta and Gamma Ray Spectroscopy*, 468-493 (K. Siegbahn, Ed., North Holland Publishing Co., Amsterdam, Holland, 959 pp., 1955)
15. Alder, K., Bohr, A., Huus, T., Mottleson, B. R., and Winther, A., *Rev. Mod. Phys.*, **28**, 432 (1956)
16. Bohr, A., and Mottelson, B. R., *Kgl. Danske Videnskab. Selskab, Mat. fys. Medd.*, **27**(16) (1953)
17. Rotenberg, M., *Phys. Rev.*, **100**, 439 (1955)
18. Bethe, H. A., *Phys. Rev.*, **103**, 1353 (1956)
19. Brueckner, K. A., and Levinson, C. A., *Phys. Rev.*, **97**, 1344 (1955)
20. Eden, R. J., and Francis, N. C., *Phys. Rev.*, **97**, 1366 (1955)
21. Bethe, H. A., and Goldstone, J., *Proc. Roy. Soc. (London)*, **A238**, 551 (1957)
22. Brueckner, K. A., Eden, R. J., and Francis, N. C., *Phys. Rev.*, **99**, 76 (1955); **100**, 891 (1955)
23. Bell, J. S., Eden, R. J., and Skyrme, T. H. R., *Nuclear Phys.*, **2**, 586 (1957)
24. Bohr, A., *Phys. Rev.*, **81**, 134 (1951)
25. Heydenburg, N. P., and Temmer, G. M., *Ann. Rev. Nuclear Sci.*, **6**, 77 (1956)
26. Way, K., Kundu, D. N., McGinnis, C. L., and van Lieshout, R., *Ann. Rev. Nuclear Sci.*, **6**, 129 (1956)
27. Davidson, J. P., and Feenberg, E., *Phys. Rev.* **89**, 856 (1953)
28. Bohr, A., and Mottelson, B. R. (Private communication)
29. Bohr, A., in *Proceedings of the International Conference on the Peaceful Uses of Atomic Energy*, Vol. **2**, 151 (United Nations, New York, N. Y., 471 pp., 1956)
30. Wheeler, J. A., in *Niels Bohr and the Development of Physics*, 163-184. (Pauli, W., Ed. Pergamon Press, Ltd., London, England, 195 pp., 1955)
31. Goldin, L. L., Novikova, G. I., and Tretyakov, E. F., *Phys. Rev.* **103**, 1004 (1956)
32. Johansson, S. A. E., *Phys. Rev.*, **105**, 189 (1957)

33. Griffin, J., and Wheeler, J. A. (To be published)
34. Peierls, R. E., and Yoccoz, J. (To be published)
35. Yoccoz, J. (To be published)
36. Villars, F., *Nuclear Phys.*, **3**, 240 (1957)
37. Marty, C., *Nuclear Phys.*, **1**, 85 (1956)
38. Wentzel, G., *Lecture on Strong Coupling Meson Theory*, University of Rochester, 1954 (Unpublished data)
39. Elliott, J. P., and Skyrme, T. H. R., *Proc. Roy. Soc. (London)*, **A232**, 561 (1955)
40. Skyrme, T. H. R. (To be published)
41. Edmonds, A. R., *Angular Momentum in Quantum-Mechanics*, CERN-55-26, Geneva (1955)
42. Redlich, M. G., and Wigner, E. P., *Phys. Rev.*, **95**, 122 (1954)
43. Nataf, R., *Compt. rend.*, **240**, 2510 (1955); **241**, 31 (1955)
44. Tomonaga, S., *Progr. Theor. Phys.*, **13**, 467 (1955)
45. Coester, F., *Nuovo Cimento*, **IV**(10) 1307 (1956)
46. Miyazima, T., and Tamura, T., *Progr. Theor. Phys.*, **15**, 255 (1956)
47. Coester, F., *Phys. Rev.*, **99**, 170 (1955)
48. Nielsen, H. H., *Rev. Mod. Phys.*, **23**, 90 (1951)
49. Kronig, R. de L., *Band Spectra and Molecular Structure* (Cambridge Univ. Press, London, England, 163 pp., 1930)
50. Bohr, A., *Kgl. Danske Videnskab. Selskab Mat. fys. Medd.*, **26** (14) (1952)
51. Scharff-Goldhaber, G., and Weneser, J., *Phys. Rev.*, **98**, 212 (1955)
52. Lipkin, H. J., de Shalit, A., and Talmi, I., *Nuovo Cimento* **2**(10), 773 (1955)
53. Tamura, T., *Nuovo Cimento* **4**(10) 713 (1956)
54. Skinner, R. S., *Can. J. Phys.*, **34**, 901 (1956)
55. Watanabe, Y., *Progr. Theor. Phys.*, **16**, 1 (1956)
56. Lipkin, H. J. (To be published)
57. Nataf, R., *Nuclear Phys.*, **2**, 497 (1957)
58. Süssmann, G., *Z. Physik*, **139**, 543 (1954)
59. Marumori, T., Yukawa, J., and Tanaka, R., *Progr. Theor. Phys.*, **13**, 442 (1955)
60. Marumori, T., and Yamada, E., *Progr. Theor. Phys.*, **13**, 557 (1955)
61. Green, A. E. S., Lee, K., and Buckley, R. J., *Phys. Rev.*, **104**, 1625 (1956)
62. Berg, R. A., and Wilets, L., *Phys. Rev.*, **101**, 201 (1956)
63. Brueckner, K. A., *Phys. Rev.*, **103**, 1124 (1946)
64. Wilets, L., *Phys. Rev.*, **101**, 1805 (1956)
65. Mittelstaedt, P., *Z. Naturforsch.*, **10a**, 379 (1955)
66. Wildermuth, K., *Z. Naturforsch.*, **9a**, 1047 (1954)
67. Swiatecki, W. J., *Phys. Rev.*, **98**, 204 (1955)
68. Ford, K. W., and Hill, D. L., *Ann. Rev. Nuclear Sci.*, **5**, 25 (1955)
69. Weisskopf, V. F. (Privately Circulated Manuscript), Seattle Conference (1956)
70. Brueckner, K. A., and Wada, W., *Phys. Rev.*, **103**, 1008 (1956)
71. Miyatake, O., and Goodman, C., *Phys. Rev.*, **99**, 1040 (1955)
72. Feenberg, E., *Rev. Mod. Phys.*, **19**, 239 (1947)
73. Wilets, L., Hill, D. L., and Ford, K. W., *Phys. Rev.*, **91**, 1488 (1953)
74. Pfirsch, D., *Z. Physik*, **132**, 409 (1952)
75. Gallone, S., and Salvetti, C., *Nuovo Cimento*, **10**(9), 145 (1953)
76. Moszkowski, S. A., *Phys. Rev.*, **103**, 1328 (1956)
77. Nilsson, S. G., *Kgl. Danske Videnskab. Selskab Mat. fys. Medd.*, **29**(16) (1955)
78. Moszkowski, S. A., *Phys. Rev.*, **99**, 803 (1955)

79. Uretzky, J., *Deformed Nuclei and the Finite Square Well* (Doctoral Thesis, Massachusetts Institute of Technology, Cambridge, Mass. 1956)
80. Gallone, S., and Salvetti, C., *Nuovo Cimento*, **8**(9) 970 (1951)
81. Gottfried, K., *Phys. Rev.*, **103**, 1017 (1956)
82. Mottelson, B. R., and Nilsson, S. G., *Phys. Rev.*, **99**, 1615 (1955)
83. Inglis, D. R., *Phys. Rev.*, **96**, 1059 (1954)
84. Inglis, D. R., *Phys. Rev.*, **103**, 1786 (1956)
85. Lipkin, H. J., de Shalit, A., and Talmi, I., *Phys. Rev.*, **103**, 1773, (1956)
86. Valatin, T. J., *Proc. Roy. Soc. (London)*, **A238**, 132 (1956)
87. Blin-Stoyle, R. J., *Nuclear Phys.*, **2**, 169 (1956)
88. Bohr, A., and Mottelson, B., *Kgl. Danske Videnskab. Selskab Mat fys. Medd.*, **30**(1) (1955)
89. Lüders, G., *Z. Naturforsch.*, **11**1, 617 (1956)
90. Inglis, D. R., *Phys. Rev.*, **97**, 701 (1955)
91. Mouhasseb, A., *Compt. Rend.*, **243**, 1289 (1956)
92. Araujo, J. A., *Nuclear Phys.*, **1**, 259 (1956)
93. Blatt, J. M., and Weisskopf, V. F., *Theoretical Nuclear Physics* (John Wiley and Sons, New York, N. Y., 864 pp., 1952)
94. Green, A. E. S., *Phys. Rev.*, **95**, 1006 (1954)
95. de Shalit, A., and Goldhaber M., *Phys. Rev.*, **92**, 1211 (1953)
96. Kraushaar, J. J., and Goldhaber, M., *Phys. Rev.* **89**, 1081 (1953)
97. Wilets, L., and Jean, M., *Compt. Rend. Acad. Sci. (Paris)*, **241**, 1108 (1955); *Phys. Rev.*, **102**, 788 (1956)
98. Foldy, L. L., and Milford, F. J., *Phys. Rev.*, **80**, 751 (1950)
99. Kerman, A., *Phys. Rev.*, **92**, 1176 (1953)
100. Ford, K. W., and Levinson, C. A., *Phys. Rev.*, **100**, 1 (1955)
101. True, W. W., *Phys. Rev.*, **101**, 1342 (1956)
102. Levinson, C., and Ford, K. W., *Phys. Rev.* **100**, 13 (1955)
103. Blin-Stoyle, R. J., *Rev. Mod. Phys.*, **28**, 75 (1956)
104. Arima, A., and Horie, H., *Progr. Theor. Phys.* **12**, 623 (1954)
105. Barker, C. F., *Phil. Mag.*, [8], **1**, 329 (1956)
106. Ford, K. W., *Phys. Rev.*, **90**, 29 (1953)
107. Alaga, G., Alder, K., Bohr, A., and Mottelson, B. R., *Kgl. Danske Videnskab. Selskab Mat. fys Medd.*, **29**(9) (1955)
108. Bohr, A., Fröman, P. O., and Mottelson, B. R., *Kgl. Danske Videnskab. Selskab Mat. fys Medd.*, **29**(10) (1955)
109. Sunyar, A. W., *Phys. Rev.*, **98**, 653 (1955)

NUCLEAR AND NUCLEON SCATTERING OF HIGH-ENERGY ELECTRONS^{1,2}

BY ROBERT HOFSTADTER

Department of Physics, Stanford University, Stanford, California

I. INTRODUCTION

The author recently prepared a review article (1) on high-energy electron scattering and its relation to nuclear structure. In that paper various types of phenomena were discussed, important formulas of scattering theory were given, and experimental results on the sizes of nucleons and nuclei were summarized.

The purpose of the present article is somewhat different, although it, too, will be in the nature of a review and summary. In the first paper the principal results of scattering theory were collected together but not derived. In this paper the intention is threefold: (a) To convey to the reader the fundamental ideas of the important scattering formulas by working out sample derivations. (b) To collect useful results in scattering theory. (c) To bring the experimental and theoretical results up-to-date.

It is almost impossible to keep up with the rapid progress involved in Item (c), and so the present paper makes no claim to be complete.

II. THEORY OF THE SCATTERING PROCESS

A. KINEMATICS

In scattering electrons from massive particles such as nucleons or nuclei, the kinematic relations play a crucial role. For this reason, and because we shall use the kinematic relations in later sections, we wish to present some of the useful results below. The derivation of such purely kinematic results will not be given here, because only the well-known ideas of relativistic dynamics, employing the conservation theorems of energy and momentum, are needed to obtain complete solutions. In fact, for an elastic collision, the energy, momentum, and angular relations are similar to those used in the Compton effect. Since the rest mass of the electron is negligible compared to any nuclear mass, the high-energy incident electron of scattering theory plays the role of the incident γ -ray in the Compton effect and the scattered electron represents the outgoing degraded γ -ray. The struck nucleus is the counterpart of the ejected electron of the Compton effect (2).

Figure 1 shows the essential nature of an elastic collision. The incident

¹ The survey of the literature pertaining to this review was completed in June, 1957.

² The research reported here was supported jointly by the Office of Naval Research and the U. S. Atomic Energy Commission and by the U. S. Air Force, through the Office of Scientific Research of the Air Research and Development Command.

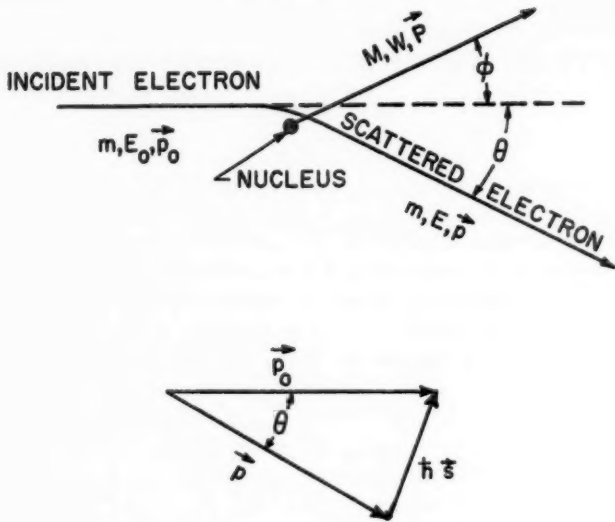


FIG. 1. Electron-scattering diagrams and definitions of symbols.

electron (energy E_0) suffers an energy loss $E_0 - E$ and loses momentum $\hbar s$ in the process, the latter being transferred to the nucleus. If the nucleus, of mass M , was originally at rest, it picks up momentum

$$P = \hbar s = p_0 - p \quad 1.$$

$$E_0 = cp_0; \quad E = cp; \quad E_0 - E = \Delta E \quad 2.$$

with negligible error and thus

$$p = \frac{p_0}{1 + \frac{2E_0}{Mc^2} \sin^2 \theta/2} \quad 3.$$

The kinetic energy (T) of the struck nucleus becomes

$$T = \frac{E_0^2}{Mc^2} \frac{2 \sin^2 \theta/2}{1 + \frac{2E_0}{Mc^2} \sin^2 \theta/2} = \Delta E \quad 4.$$

If the nucleus is nonrelativistic, this expression will also be represented by

$$T = \frac{P^2}{2M} = \frac{\hbar^2 s^2}{2M} \quad 5.$$

Otherwise the relativistic expression for the total energy will apply:

$$W^2 = M^2 c^4 + c^2 P^2 \quad 6.$$

Also

$$\hbar s = \frac{2\vec{p}_0 \sin \theta/2}{\left(1 + \frac{2E_0}{Mc^2} \sin^2 \theta/2\right)^{1/2}} \left[1 + \frac{\frac{E_0^2}{Mc^4} \sin^2 \theta/2}{1 + \frac{2E_0}{Mc^2} \sin^2 \theta/2} \right]^{1/2} \quad 7.$$

and a new four-vector $\hbar q$ is defined such that:

$$q^2 = s^2 - \left(\frac{\Delta E}{\hbar c}\right)^2 = \frac{1}{\hbar^2} |\vec{p}_0 - \vec{p}|^2 - \frac{1}{\hbar^2} (\vec{p}_0 - \vec{p})^2 = 4 \frac{\vec{p}_0 \cdot \vec{p}}{\hbar^2} \sin^2 \theta/2 \quad 8.$$

Other useful results involving q are:

$$\Delta E = \frac{\hbar^2 q^2}{2M} \quad 9.$$

and

$$c^2 P^2 = \frac{\hbar^2 q^2}{2M} (W + Mc^2) \quad 10.$$

The vector q is the four-dimensional momentum-energy transfer and the vector s is its spatial part which is the three-dimensional momentum transfer. The magnitude q is an invariant and the four-vector q is the difference between the four-dimensional momentum-energy vectors (\vec{p}_0, E_0) and (\vec{p}, E) . From Eq. 3 and 8 it follows that

$$|q| = \frac{2 \frac{\vec{p}_0}{\hbar} \sin \theta/2}{\left[1 + \frac{2E_0}{Mc^2} \sin^2 \theta/2\right]^{1/2}} = \frac{2/\lambda \sin \theta/2}{\left[1 + \frac{2E_0}{Mc^2} \sin^2 \theta/2\right]^{1/2}} \quad 11.$$

where λ is the de Broglie wavelength of the electron in the laboratory system. It may be noted that, even for 1-Bev incident electrons scattering against a proton, $|q|$ and $|s|$ differ only by 15 per cent at most when $\theta = \pi$. For nuclei heavier than a proton or for smaller angles, the difference is smaller. It will be seen later that q is the more fundamental quantity of the two, appearing in form factors as an invariant. However, in occasional cases, we may refer to s in partially relativistic calculations, for which the more complete relativistic solution would contain q . In those cases, where the difference between s and q is small, we shall always use q in the final formulas.

For reference, the kinetic energy of the recoiling nucleus, in terms of the angle ϕ in Figure 1, is given by

$$T = E_0 \frac{2 \left(\frac{E_0}{Mc^2}\right) \cos^2 \phi}{\left(1 + \frac{E_0}{Mc^2}\right)^2 - \frac{E_0^2}{Mc^4} \cos^2 \phi} \quad 12.$$

as well as by Eq. 4, which is written in terms of the electron's scattering angle.

B. SCATTERING RESULTS

In this part it will be our aim to set forth three basic methods and the corresponding physical ideas, which appear frequently and are of great utility in understanding the various electron-scattering phenomena. Our program is as follows: In section 1 we shall discuss the underlying concepts which justify the use of electrons in probing the charge density in nucleons and nuclei. In section 4 we shall consider magnetic scattering. In section 12 we shall illustrate the method by which the exact scattering calculations can be carried out, that is, the phase-shift method. We shall also illustrate the various processes with examples taken from experiment and this procedure will permit us to bring the results up-to-date.

1. The first Born approximation for the scattering of an electron without spin from a nucleus without spin.—In order to illustrate the method and physical ideas behind the size determinations, we wish to make some simplifications that may render the physical analysis more transparent. To do this we shall employ the first Born approximation (3), and we shall further assume that the incident electrons do not have spin. We shall show later how the spin may be put back on the incident particle and how more exact methods may be used where needed. Though not exact, the Born approximation supplies a very powerful tool in understanding the physical ideas in the scattering patterns for light nuclei and in giving a qualitative picture of diffraction phenomena for heavier nuclei.

Let us assume that the target nucleus contains Z point-protons, each of charge e , but, like the electron, also without spin. We assign wave functions $\Phi_i (i = 0, 1, 2 \dots)$ to the nucleus containing the coordinates $R_k (k = 1, \dots, Z)$ of all the protons in the nucleus. Φ_0 is the wave function in the ground state. Let r be the electron's position vector. For many purposes it will prove convenient to assume that the target nucleus is very heavy compared to the incident electron. This is true in most cases studied by experiment. However, we shall later also relax this condition.

Now we shall employ one version of the Born approximation given by the first-order time-dependent perturbation theory (4, 5, 6). According to this theory, the transition probability per unit time (w') for an electron to make a jump from its initial state of momentum p_0 (energy E_0) to a final state p (energy E) under the influence of a perturbation, V , is given by:

$$w' = \frac{dw}{dt} = \frac{2\pi}{\hbar} | H |^2 \frac{dn}{dE_f} \quad 13.$$

where H is the matrix element of V , causing the transition. In this equation dn/dE_f is the density of final energy states in the continuum. In order to avoid the infinite densities of the continuum, we shall confine the electron, in a standard manner, to a large cubic box of side L , which we may later allow to approach an infinite size. (As is well-known, it will turn out that the dimensions of the box cancel out and later, in another context, we may assume the box to have a unit side.)

We shall write the perturbing interaction in the form

$$H_1 = eV = e^2 \sum_{k=1}^Z \frac{1}{|\mathbf{r} - \mathbf{R}_k|} \quad 14.$$

which is the usual Coulomb energy of interaction of two point charges. The matrix element H then becomes

$$H = e^2 \int \Phi_f^*(\mathbf{R}_k) \frac{1}{L^{3/2}} \exp(-i/\hbar)(\mathbf{p} \cdot \mathbf{r}) \sum_1^Z \frac{1}{|\mathbf{r} - \mathbf{R}_k|} \Phi_0(\mathbf{R}_k) \frac{1}{L^{3/2}} \cdot \exp(i/\hbar)(\mathbf{p}_0 \cdot \mathbf{r}) d^3 r d^3 R_k \quad 15.$$

The electron's incident and final wave functions were inserted into Eq. 15 as normalized plane waves

$$\psi(\mathbf{r}) = \frac{1}{L^{3/2}} \exp(i/\hbar)(\mathbf{p} \cdot \mathbf{r}) \quad 16.$$

and this step is characteristic of the Born approximation. Now introduce the momentum transfer vector \mathbf{s} , of Figure 1, and H becomes

$$H = \frac{e^2}{L^3} \int \Phi_f^* \Phi_0 \sum_1^Z \frac{1}{|\mathbf{r} - \mathbf{R}_k|} \exp(i\mathbf{s} \cdot \mathbf{r}) d^3 r d^3 R_k \quad 17.$$

When integrating over the electron's coordinates, choose polar coordinates for which the Z axis lies along the direction \mathbf{s} . Furthermore, it is convenient to use a simple shielded potential, V_a ,

$$eV_a(\mathbf{r} - \mathbf{R}_k) = \sum_1^Z \frac{e^2}{|\mathbf{r} - \mathbf{R}_k|} \exp\left(-\frac{|\mathbf{r} - \mathbf{R}_k|}{a}\right) \quad 18.$$

in place of Eq. 14, to take care of shielding by the atomic electron cloud and to make the integration converge. In Eq. 18 a is a parameter of atomic size and is not critical, nor is the shape of the shielding function critical. Thus it is merely necessary to have $a \gg R$, where R is a nuclear dimension. Also place

$$\mathbf{r} = \mathbf{R}_k + (\mathbf{r} - \mathbf{R}_k) \quad 19.$$

and substitute Eq. 18 and 19 into the part of the integral in Eq. 17 having to do with electron coordinates. Thus the integration

$$\varphi(\mathbf{R}) = e \sum_1^Z \int (\exp(i\mathbf{s} \cdot \mathbf{R}_k) (\exp(i\mathbf{s} \cdot (\mathbf{r} - \mathbf{R}_k))) \left(\exp\left(-\frac{|\mathbf{r} - \mathbf{R}_k|}{a}\right) \frac{1}{|\mathbf{r} - \mathbf{R}_k|} \right) d^3 r \quad 20.$$

may be carried out over the electron's coordinates for each separate proton as an origin, and let polar coordinates ρ' , θ' , ϕ' be used where θ' is measured relative to \mathbf{s} . Then $\varphi(\mathbf{R})$ becomes

$$\begin{aligned} \varphi(\mathbf{R}) &= e \sum_1^Z \exp(i\mathbf{s} \cdot \mathbf{R}_k) \int \exp(is\rho' \cos\theta') \frac{\exp(-\rho'/a)}{\rho'} \rho'^2 d\rho' \sin\theta' d\theta' d\phi' \\ &= e \sum_1^Z \exp(i\mathbf{s} \cdot \mathbf{R}_k) \frac{2\pi}{s} \int_0^\infty 2 \left(\exp(-\rho'/a) \sin(s\rho') \right) d\rho' = e \sum_1^Z \exp(i\mathbf{s} \cdot \mathbf{R}_k) \frac{4\pi}{s^2 + 1/a^2} \\ &= \frac{4\pi e}{s^2} \sum_1^Z \exp(i\mathbf{s} \cdot \mathbf{R}_k) \end{aligned} \quad 21.$$

since $a \gg 1/s$ for the interesting scattering events not close to $\theta = 0$. We may then write

$$H = \frac{4\pi e^2}{L^3 s^2} \int_{N.V.} \Phi_f^* \Phi_0 \sum_k^Z \exp is \cdot R_k d^3 R_k = \frac{4\pi e^2}{L^3 s^2} M_{f0} \quad 22.$$

where N.V. stands for integration over the nuclear volume and where

$$M_{f0} = \int_{N.V.} \Phi_f^*(R_k) \Phi_0(R_k) \left(\sum_k^Z \exp is \cdot R_k \right) d^3 R_k \quad 23.$$

$|M_{f0}|$ measures the interference effects between the waves from the various protons. The transition probability w' then becomes

$$w' = \frac{32\pi^2 e^4}{\hbar L^3 s^4} |M_{f0}|^2 \frac{dn}{dE_f} \quad 24.$$

and it is only necessary to evaluate dn/dE_f to obtain the differential cross section for scattering.

If the electrons were free, the density of states would be

$$\left(\frac{dn}{dE_f} \right)_{free} = \frac{p^2 d\Omega L^3}{ch^3} \quad 25.$$

where $d\Omega$ is the elementary solid angle and $p^2 d\Omega d\Omega$ is the momentum contribution to the elementary volume of phase space. c is necessary to transform momentum density to energy density. Since the nuclei are assumed to be massive and to suffer little recoil, like the walls of a box in kinetic theory, we could use Eq. 25 if we wished to. However, it is just as simple, and more convenient for the future, to allow the nuclei to recoil. In this case, Eq. 25 will be changed just as in the recoil of the struck particle in the Compton effect. In this case it is easy to show (7) that

$$\left(\frac{dn}{dE_f} \right) = \frac{p^2 d\Omega L^3}{ch^3} \left(\frac{p}{p_0} \right) \left(\frac{W}{Mc^2} \right) \quad 26.$$

by using the expressions 3 and 6 as in the Compton effect. For our purposes

$$\frac{W}{Mc^2} = 1 + \frac{2 \left(\frac{E_0}{Mc^2} \right)^2 \sin^2 \theta/2}{1 + 2 \left(\frac{E_0}{Mc^2} \right) \sin^2 \theta/2} \cong 1 \quad 27.$$

if the nucleus is massive, and by using 3 we find that

$$\left(\frac{dn}{dE_f} \right) = \frac{p^2 d\Omega L^3}{ch^3} \frac{1}{1 + \frac{2E_0}{Mc^2} \sin^2 \theta/2} \quad 28.$$

We shall see below that when the electron scatters against a relativistic particle, such as a proton, the factor W/Mc^2 of Eq. 26 is cancelled exactly, resulting in a formula like Eq. 28. Eq. 24 becomes therefore

$$w' = \frac{64\pi^4 e^4 d\Omega}{ch^4 L^3 s^4} \frac{p^2}{1 + \frac{2E_0}{Mc^2} \sin^2 \theta/2} |M_{f0}|^2 \quad 29.$$

To obtain the differential scattering cross section, we must divide this transition probability by the probability current in the incident beam, which is c/L^3 . Carrying out this operation and substituting $\hbar = h/2\pi$, we have

$$\frac{d\sigma}{d\Omega} = 4 \left(\frac{e^2}{\hbar c} \right)^2 \frac{p^2}{s^4} \frac{1}{1 + \frac{2E_0}{Mc^2} \sin^2 \theta/2} |M_{f0}|^2 \quad 30.$$

For a target nucleus that is massive and therefore undergoes little recoil, $\Delta E = E_0 - E$ is small, $p = p_0$, etc., and

$$\hbar^2 s^2 = \hbar^2 q^2 = 4p_0^2 \sin^2 \theta/2 = 4p_0^2 \sin^2 \theta/2 \quad 31.$$

by Eq. 8. Hence Eq. 30 becomes finally

$$\frac{d\sigma}{d\Omega} = \left(\frac{e^2}{2E_0} \right)^2 \frac{1}{\sin^4 \theta/2} \frac{1}{1 + \frac{2E_0}{Mc^2} \sin^2 \theta/2} |M_{f0}|^2 \quad 32.$$

This result is educational, but it should not be used for real electrons with spin. However, light bosons would scatter according to this formula. We pass on to a more realistic case.

2. *Scattering of electrons with spin.*—Now let us go to the case of electrons carrying spin. For this we need the Dirac equation (5)

$$(\alpha \cdot p c + \beta mc^2 + eV)\psi = E\psi \quad 33.$$

where the ψ 's are spinor quantities and where α is the current density Dirac operator and β the fourth abbreviated Dirac operator. Thus

$$\alpha = \begin{pmatrix} 0 & \mathbf{d} \\ \mathbf{d}^\dagger & 0 \end{pmatrix}; \quad \beta = \begin{pmatrix} 1 & 0 \\ 0 & -1 \end{pmatrix} \quad 34.$$

and \mathbf{d} represents the usual set of Pauli spin matrix operators:

$$\sigma_x = \begin{pmatrix} 0 & 1 \\ 1 & 0 \end{pmatrix}, \quad \sigma_y = \begin{pmatrix} 0 & -i \\ i & 0 \end{pmatrix}, \quad \sigma_z = \begin{pmatrix} 1 & 0 \\ 0 & -1 \end{pmatrix} \quad 35.$$

eV in Eq. 33 is still given by (14) and the four components of ψ , for plane wave solutions, are abbreviated by the column matrix

$$\psi(r, t) = \begin{bmatrix} \psi_1(r, t) \\ \psi_2(r, t) \\ \psi_3(r, t) \\ \psi_4(r, t) \end{bmatrix} \quad 36.$$

where each ψ can be expressed as

$$\psi_j(r, t) = u_j \exp \frac{i}{\hbar} (\mathbf{p} \cdot \mathbf{r} - Et); \quad j = 1, 2, 3, 4 \quad 37.$$

with similar equations for the ground state $\psi_{0j}(r, t)$.

It is well known in Dirac theory that there are two sets of solutions corresponding to the positive and negative energy states. We shall deal only with the positive energy solutions. Furthermore, among the positive set there are two linearly independent solutions corresponding to two possible spin orientations of the electron. In this case

$$u_1 = -\frac{cp_z}{E + mc^2}, \quad u_2 = -\frac{cp_x + ip_y}{E + mc^2}, \quad u_3 = 1, \quad u_4 = 0$$

and

$$u_1 = -\frac{cp_z - ip_y}{E + mc^2}, \quad u_2 = \frac{cp_x}{E + mc^2}, \quad u_3 = 0, \quad u_4 = 1 \quad 38.$$

or when $mc^2 \ll E$ and $E \approx cp$, as in our case,

$$\begin{aligned} u_1 &= -\frac{p_z}{p}, & u_2 &= -\frac{p_x + ip_y}{p}, & u_3 &= 1, \quad u_4 = 0 \\ u_1 &= -\frac{p_z - ip_y}{p}, & u_2 &= \frac{p_x}{p}, & u_3 &= 0, \quad u_4 = 1 \end{aligned} \quad 39.$$

If each u is multiplied by $1/\sqrt{2}$, the solutions are normalized so that $\psi^* \psi = \sum (\psi_j^* \psi_j) = 1$. The probability density and probability current density are written:

$$\begin{aligned} \psi_j^* \psi_0 &= \text{probability density} \\ -c\psi_j^* \alpha \psi_0 &= \text{probability current density.} \end{aligned} \quad 40.$$

where ψ^* stands for the Hermitian adjoint matrix corresponding to Eq. 36.

When the Dirac plane wave solutions are substituted in the matrix element H , the calculation proceeds exactly as in the spin-less case, except that the four-component character of the electron's wave functions requires that the probability of the transition be proportional to the sum of the four terms:

$$u_f^* u_0 = \sum_i \psi_{fj}^* \psi_{0j} = u_1^* u_{10} + u_2^* u_{20} + u_3^* u_{30} + u_4^* u_{40} \quad 41.$$

in accordance with Eq. 40. The square modulus of the matrix element (23) is then modified by the relativistic considerations so that it contains $|u_f^* u_0|^2$ as a multiplicative factor.

The calculation is then further complicated by the new possibilities for the spins of the ingoing and scattered electrons. If we let I refer to spin-up and II to spin-down, then four transitions are possible thus: $I_f I_0$, $I_f II_0$, $II_f I_0$, $II_f II_0$. However, in a normal scattering experiment, we do not start with a polarized electron beam nor do we examine the spins of the scattered particles. Hence we must carry out an averaging procedure over the initial and final spin orientations. This means that we must evaluate $|u_f^* u_0|^2$ for each of the four combinations, $I_f I_0$, $I_f II_0$, etc., and then take an average over the initial states and a sum over the two final states. This may be done easily with Eq. 38 and 39 by calling them appropriately the initial and final states. Carrying out this algebraic procedure, we obtain for the result:

$$\frac{1}{2EE_0} [m^2 c^4 + EE_0(1 + \cos \theta)] \quad 42.$$

In practice, where $E, E_0 \gg mc^2$ and θ is not extremely close to $\theta = \pi$, this expression is simply $\cos^2 \theta/2$. Thus the cross section corresponding to Eq. 32 now becomes:

$$\frac{d\sigma}{d\Omega} = \left(\frac{e^2}{2E_0}\right)^2 \frac{\cos^2 \theta/2}{\sin^4 \theta/2} \frac{|\Phi_0|^2}{1 + \frac{2E_0}{Mc^2} \sin^2 \theta/2} \quad 43.$$

The more elegant trace methods (4, 8) may also be used and one obtains the same result. Writing the final result in detail, we have

$$\frac{d\sigma}{d\Omega} = \left(\frac{e^2}{2E_0}\right)^2 \frac{\cos^2 \theta/2}{\sin^4 \theta/2} \frac{\left| \int_{N.V.} \Phi_f^*(R_k) \Phi_0(R_k) \sum_1^Z \exp i\mathbf{q} \cdot \mathbf{R}_k d^3 R_k \right|^2}{1 + \frac{2E_0}{Mc^2} \sin^2 \theta/2} \quad 44.$$

where we have replaced s by \mathbf{q} , as explained previously. Now we shall apply this equation.

3. *Elastic scattering*.—For elastic scattering, the conditions are

$$\left. \begin{aligned} \Phi_f &= \Phi_0, & p &= p_0 / \left(1 + \frac{2E_0}{Mc^2} \sin^2 \theta/2 \right) \\ \hbar s &\cong \hbar q = 2p_0 \sin \theta/2 / \left[1 + \frac{2E_0}{Mc^2} \sin^2 \theta/2 \right]^{1/2} \end{aligned} \right\} \quad 45.$$

as given by Eq. 11 and 31. Eq. 44 then takes the form:

$$\frac{d\sigma_{el}}{d\Omega} = \left(\frac{e^2}{2E_0}\right)^2 \frac{\cos^2 \theta/2}{\sin^4 \theta/2} \frac{1}{1 + \frac{2E_0}{Mc^2} \sin^2 \theta/2} \left| \int_{N.V.} |\Phi_0|^2 \sum_1^Z \exp i\mathbf{q} \cdot \mathbf{R}_k d^3 R_k \right|^2 \quad 46.$$

When the nuclear dimensions are small compared to the de Broglie wavelength of the electrons,

$$\mathbf{q} \cdot \mathbf{R}_k \cong 0 \quad 47.$$

and the volume integral is simply the sum of Z charges integrated over the nuclear volume, since $|\Phi_0|^2$ is normalized to unity over the nucleus. The condition given in Eq. 47 means essentially that, for the momentum transfer considered, the nucleus cannot be distinguished from a point of charge Ze . Under such conditions, Eq. 46 may be written

$$\left(\frac{d\sigma_{el}}{d\Omega} \right)_{\text{point}} = \left(\frac{Ze^2}{2E_0} \right)^2 \frac{\cos^2 \theta/2}{\sin^4 \theta/2} \frac{1}{1 + \frac{2E_0}{Mc^2} \sin^2 \theta/2} = \sigma_{NS} \quad 48.$$

where σ_{NS} stands for scattering from a point charge Ze with "no spin."

This simple Born-approximation scattering formula is the justly famous "Mott-scattering formula" and represents the relativistic scattering of Dirac electrons from a massive point nucleus of charge Ze . (The Mott formula is generally written without the center-of-mass correction

$$\frac{1}{1 + \frac{2E_0}{Mc^2} \sin^2 \theta/2},$$

since this term is very close to unity.)

In the event that $q \cdot R$ is not zero, nor small compared to unity, the scattering formula 46 may be written

$$\frac{d\sigma_{el}}{d\Omega} = \left(\frac{e^2}{2E_0} \right)^2 \frac{\cos^2 \theta/2}{\sin^4 \theta/2} \frac{|F(q)|^2}{1 + \frac{2E_0}{Mc^2} \sin^2 \theta/2} \quad 49.$$

where we have introduced the quantity

$$F(q) = \int_{N.V.} |\Phi_0|^2 \sum_{k=1}^Z \exp i q \cdot R_k d^3 R_k \quad 50.$$

$F(q)$ is a type of quantity well known from atomic studies of electron diffraction and x-ray diffraction and is the analog of the so-called "form factor" or "structure factor" of those disciplines. In our work we shall refer to $F(q)$ as the nuclear form factor.

Now in Eq. 50 $|\Phi_0|^2$ contains all the proton-configuration coordinates symmetrically, and so each integral of the sum is like any other. Hence the square modulus of the integral $F(q)$ in Eq. 50 is (9)

$$|F(q)|^2 = Z^2 \left| \int \varphi_0^* \varphi_0 \exp i(q \cdot R) d^3 R \right|^2 \quad 51.$$

since $F(q)$ adds up to Z similar integrals. As in Eq. 51 each of these integrals has an integrand of the form

$$|\varphi_0|^2 = \varphi_0^* \varphi_0 = \int_{N.V.} |\Phi_0|^2 \sum_{k=1}^Z d^3 R_k \quad 52.$$

and $|\varphi_0|^2 d^3 R$ is the probability that there is one proton in $d^3 R$, and all other proton positions are arbitrary. Integration of $|\varphi_0|^2$ over $d^3 R$ will give unity because of the normalization of the wave functions. Thus the effective or "static" nuclear-charge density $\rho_0(R)$, in the ground state of the nucleus, is Ze times expression Eq. 52 or

$$\rho_0(R) = Ze |\varphi_0|^2 \quad 53.$$

and integration of ρ_0 over $d^3 R$ will yield Ze . We may normalize a density, defined slightly differently and called $\rho(R)$, to unity in the sense that

$$\int \rho(R) d^3 R = 1; \quad \rho = \frac{\rho_0}{Ze} \quad 54.$$

instead of to Ze . This is convenient for many calculations. R is then the position vector of a charged volume element in the nucleus measured from its center of mass. We can write

$$F(q) = \int_{N.V.} \rho(R) \exp i q \cdot R d^3 R \quad 55.$$

and Eq. 49 becomes

$$\frac{d\sigma_{el}}{d\Omega} = \left(\frac{Ze^2}{2E_0}\right)^2 \frac{\cos^2 \theta/2}{\sin^4 \theta/2} \frac{|F(q)|^2}{1 + \frac{2E_0}{Mc^2} \sin^2 \theta/2} \quad 56.$$

which is like Eq. 49 except for the factor Z and the new normalized definition of $F(q)$ given in Eq. 55.

From Eq. 48 and 56 we then observe that

$$\left(\frac{\frac{d\sigma_{el}}{d\Omega}}{\frac{d\sigma}{d\Omega}} \right)_{\text{point}} = |F(q)|^2 \quad 57.$$

This amounts to the generally accepted definition of $|F(q)|^2$ as the ratio of the experimental cross section to the point-charge cross section. It may easily be shown by integrating over angle, with $q \approx (2p_0/\hbar)\sin \theta/2$, that Eq. 55 can be reduced to the form

$$F(q) = \frac{4\pi}{q} \int_0^\infty \rho(r) \sin(qr) r dr \quad 58.$$

for a spherically symmetric charge distribution. In future applications of Eq. 58 to high energies it may be necessary to make a small allowance for the center of mass motion.

While Eq. 46 represents elastic scattering, the more general Eq. 44 contains the inelastic scattering formulas in Born approximation. In this case $\Phi_f \neq \Phi_0$ and the so-called transition matrix elements arise from the integral in Eq. 44. We shall return to this problem later.

Many nuclear form-factor results have been given for elastic scattering (1, 9). Figure 2 shows a typical form-factor curve for a charge distribution due to an independent particle shell model of a nucleus for an infinite harmonic well potential. Figure 3 shows the appropriate charge distribution corresponding to $C^{12}(\alpha = 4/3)$ in this shell-model picture, to $O^{16}(\alpha = 2)$, and to other p -shell nuclei. (The abscissa scale is correct only for carbon.) It is typical of many Born-approximation form factors that they show diffraction zeroes such as the one at $x = qa = 4.4$ in Figure 2. (a is the root-mean-square value of the radius of the charge distribution.) On a semi-logarithmic plot, at a true zero, the curve goes to $-\infty$. Experimental data do exhibit minima, as illustrated in Figure 4. In this figure, the experimental points represent electron-scattering results in C^{12} at 420 Mev, obtained by Sobottka & Hofstadter (10), but, of course, the experimental curves do not show true zeroes. The question of minima versus true zeroes has been discussed in some detail (1) and is connected with the fact that the Born approximation is not accurate near diffraction minima and fails also for elements of high atomic number. This problem will be discussed at length in section (12) which is concerned with the exact phase-shift calculations. On the other hand, many charge distributions, such as a Gaussian or an exponential, do not show dif-

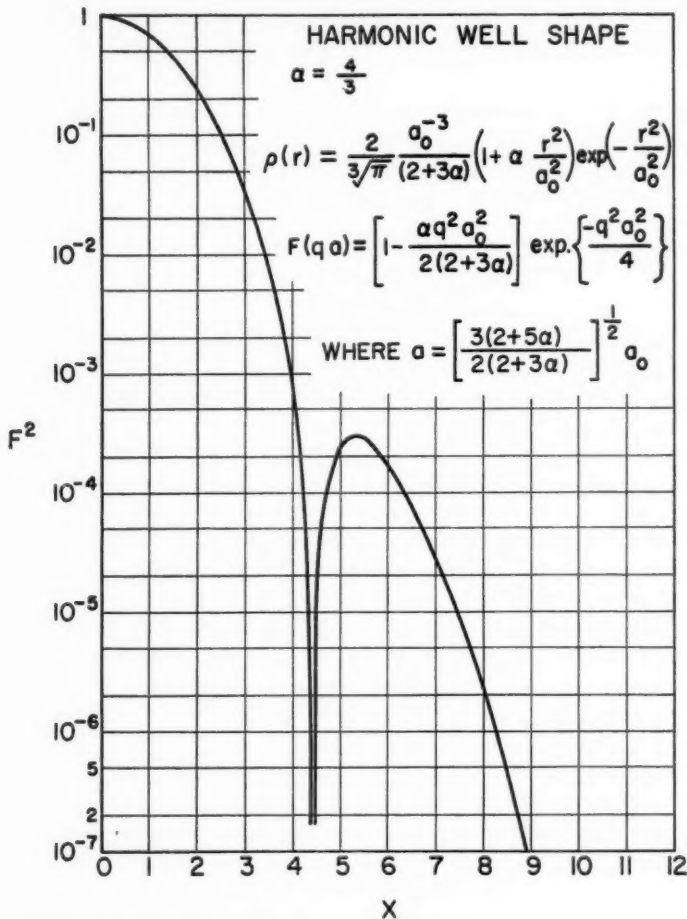


FIG. 2. Born approximation for the absolute square of the form factor associated with the harmonic-well shape in the case, $\alpha = 4/3$, which is appropriate to carbon. $x = qa$.

fraction zeroes, and, for these models, the Born approximation is much more accurate than for models yielding diffraction zeroes, or minima even for nuclei of moderate Z . Figure 4 also shows the Born-approximation results (dotted line) for the same model which gives the exact phase-shift calculations (solid line). Except for the region about the minimum, the Born approximation is surprisingly good, even for this simple model of the carbon nucleus. The exact phase-shift curve in Figure 4 is due to D. G. Ravenhall.

4. *Magnetic scattering of a point.*—At the higher electron energies and at large angles, scattering by the magnetic moment of the target nucleus

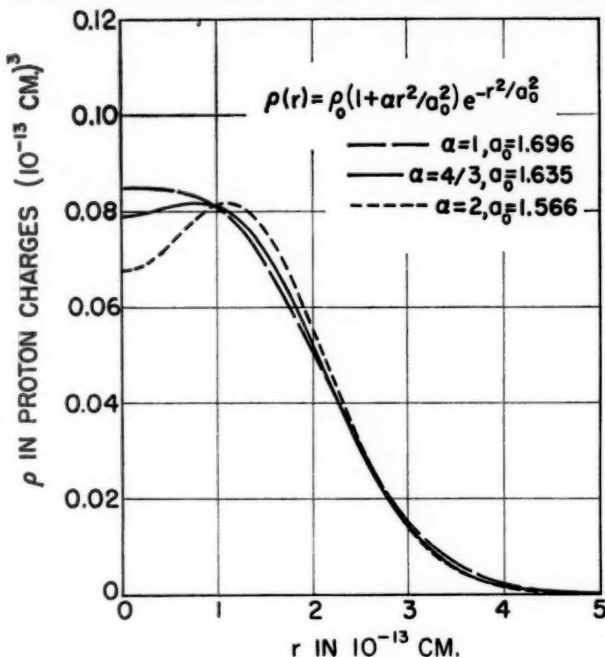


FIG. 3. The charge-density distribution for the harmonic-well nuclear model for three different values of α . The abscissa is correct only for the case of carbon, for which $\alpha=4/3$.

becomes important. We shall try to demonstrate the basic type of analysis involved in this phenomenon by carrying out the calculational details for the case when the target is a proton. We shall consider the fully relativistic treatment for the proton which means that we shall take the proton to be a Dirac particle.

Like the calculations in the preceding sections, this derivation is based on the first Born approximation. There are many equivalent ways of working out a solution, but we shall choose a method involving the Møller potentials (11) because the physical ideas then become rather clear.

We have seen that the transition probability depends on the square modulus of the matrix element H of the perturbing potential, as in Eq. 13. The matrix element is given by Eq. 17, except that we shall now specialize to the case of a single proton, and the summation in Eq. 17 is therefore not required. We shall assume that the box "L" has sides equal to unity, and so it will not be necessary to carry L in the calculations.

Following Møller, we shall first deal with the partially relativistic problem as an example. The integration in Eq. 17 or 20 over the electron's coordinates:

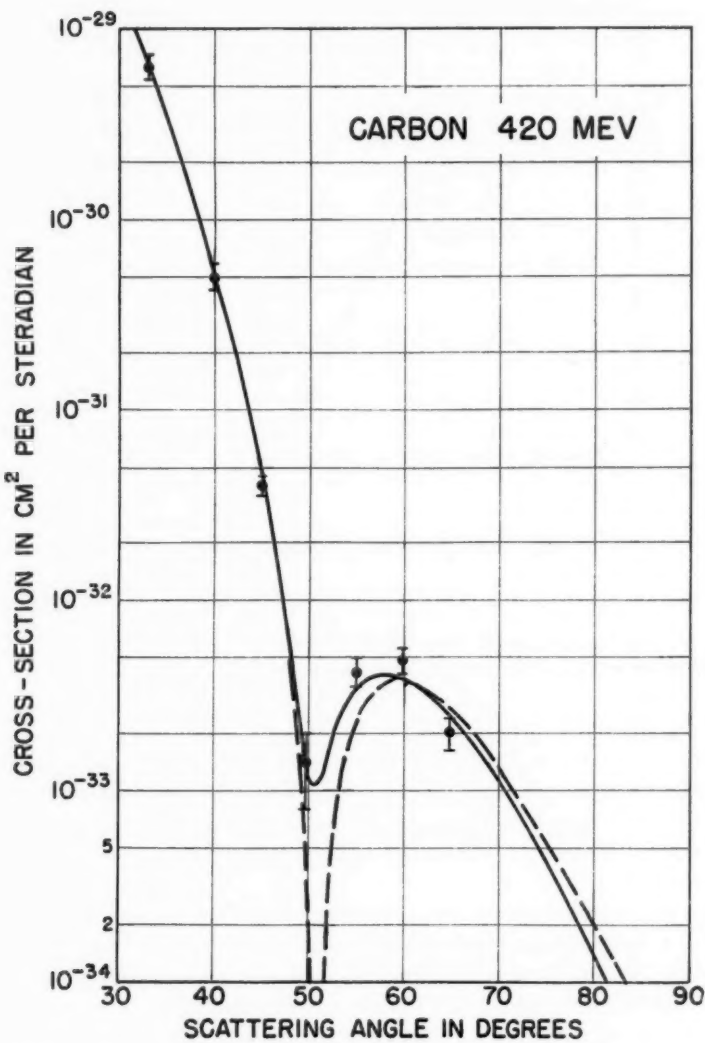


FIG. 4. Recent data in C^{12} observed by Sobottka & Hofstadter (10) at an incident electron energy of 420 Mev. Two theoretical curves are presented for comparison. The dashed curve is the Born approximation for a harmonic-well charge distribution corresponding to Fig. 3 ($\alpha = 4/3$). The solid line is the accurate phase-shift calculation of D. G. Ravenhall, which appears to fit the experimental points rather well.

$$\varphi(\mathbf{R}) = e \int \frac{\exp i/\hbar(\mathbf{p}_0 - \mathbf{p}) \cdot \mathbf{r}}{|\mathbf{R} - \mathbf{r}|} d^3\mathbf{r} = e \int \frac{\exp is \cdot \mathbf{r}}{|\mathbf{R} - \mathbf{r}|} d^3\mathbf{r} \quad 60.$$

yields by the method first given by Bethe (12, 13) (similar to our earlier derivation of equation 21) a scalar potential, $\varphi(\mathbf{R})$, which can be written

$$\varphi(\mathbf{R}) = 4\pi e \frac{\exp is \cdot \mathbf{R}}{|s|^2} = \frac{e\hbar^2}{\pi} \frac{\exp i/\hbar(\mathbf{p}_0 - \mathbf{p}) \cdot \mathbf{R}}{|\mathbf{p}_0 - \mathbf{p}|^2} \quad 61.$$

where \mathbf{R} is the position vector of the proton, and where the scalar potential, $\varphi(\mathbf{R})$, satisfies the Poisson equation

$$\nabla^2\varphi = -4\pi\rho \quad 62.$$

In the latter equation

$$\frac{\rho}{e} = \exp is \cdot \mathbf{R} = \exp i/\hbar(\mathbf{p}_0 - \mathbf{p}) \cdot \mathbf{R} \quad 63.$$

and has been called a "transition-charge density." For the matrix element involving the interaction with a single proton, insertion of the potential φ gives

$$H = \int \Phi_f^*(\mathbf{R}) e\varphi(\mathbf{R}) \Phi_0(\mathbf{R}) d^3\mathbf{R} \quad 64.$$

which is the contraction of H in Eq. 17 to the case of a single proton. We may say that the potential φ corresponds to the transition charge density ρ and acts to make transitions between the states of Φ of the heavy particle.

Now let the electrons satisfy the Dirac Eq. 33 and let their wave functions be represented by Eq. 36 and 37. The solutions corresponding to negative energy states are small and need not be considered. According to the method of Möller, when the treatment is fully relativistic, the transition charge density becomes

$$\rho = -eu_f^* u_0 \exp i \left[s \cdot \mathbf{R} - \frac{1}{\hbar} (E_0 - E)t \right] \quad 65.$$

in analogy with Eq. 63, and the "transition current density" j is given by

$$j = eu_f^* \alpha u_0 \exp i \left[s \cdot \mathbf{R} - \frac{1}{\hbar} (E_0 - E)t \right] \quad 66.$$

where $e\alpha$ is the Dirac current density operator of Eq. 33. The potentials corresponding to Eq. 61 and 62 then satisfy

$$\nabla^2\varphi - \frac{1}{c^2} \frac{\partial^2\varphi}{\partial t^2} = -4\pi\rho \quad 67.$$

$$\nabla^2\mathbf{A} - \frac{1}{c^2} \frac{\partial^2\mathbf{A}}{\partial t^2} = -4\pi \frac{j}{c} \quad 68.$$

where \mathbf{A} is the vector potential corresponding to the current sources j . The latter two equations may be solved as in Eq. 61 and 62 to give

$$\varphi(R) = -4\pi e \frac{u_f^* u_0 \exp i \left[s \cdot R - \frac{1}{\hbar} (E_0 - E)t \right]}{s^2 - \left(\frac{\Delta E}{\hbar c} \right)^2} \quad 69.$$

$$A(R) = -4\pi e \frac{u_f^* \alpha u_0 \exp i \left[s \cdot R - \frac{1}{\hbar} (E_0 - E)t \right]}{s^2 - \left(\frac{\Delta E}{\hbar c} \right)^2} \quad 70.$$

The potentials φ, A of Eq. 69 and 70 are the so-called Møller potentials produced by the passing electron.

The perturbing interaction applied to the proton, when written in terms of these potentials, would be given by

$$e \int [\rho_P \varphi(R) + \alpha_P \cdot A(R)] d^3R \quad 71.$$

where the assumption has been made that the proton obeys the Dirac equation with no anomalous magnetic moment, and where ρ_P and α_P are its corresponding charge and current-density operators, respectively. Then ρ_P must be replaced by the relativistic spinor matrix element

$$e U_f^* U_0 \exp i \left[S_P \cdot r - \frac{1}{\hbar} (W_0 - W)t \right] \quad 72.$$

and the vector α_P by

$$e U_f^* \alpha_P U_0 \exp i \left[S_P \cdot r - \frac{1}{\hbar} (W_0 - W)t \right] \quad 73.$$

where the capital U 's refer to the proton's spin amplitudes, and where the other heavy particle symbols are self-explanatory. Then the scalar product given in Eq. 71 can be written, as shown by Møller,

$$H = -\frac{4\pi e^4}{q^2} \{ (u_f^* u_0)(U_f^* U_0) - (u_f^* \alpha u_0)(U_f^* \alpha_P U_0) \} \quad 74.$$

and exhibits complete symmetry between the electron and the proton. q is given by Eq. 8. In obtaining Eq. 74, the exponential factors are eliminated by well-known methods equivalent to the conservation theorems:

$$\begin{aligned} S_P + s &= P_0 - P + p_0 - p = -P + p_0 - p = 0 \\ W_0 - W + E_0 - E &= 0 \end{aligned} \quad 75.$$

and where $P_0 = 0$ and $W_0 = Mc^2$ represent the proton's initial conditions in the laboratory frame.

The matrix element H , given by Eq. 74, lies at the heart of the electron-proton scattering theory. In recent times it has proved convenient to write the interaction in a completely covariant manner (8, 14), and in this language the matrix element H is given by

$$H = -2\pi i j_\mu^P(P, P_0) \frac{1}{q^2} j_\mu^*(p, p_0) \quad 76.$$

where j_μ^e is the electron's charge-current density, and where

$$q_\mu = P_\mu - P_{\mu_0} = -(p_\mu - p_{\mu_0}) \quad 77.$$

is the recoil four-momentum, and where $1/q^2$ represents the propagation of a virtual photon with four-momentum q_μ between the electron and the proton. Repeated Greek indices indicate the usual summation convention. In covariant notation

$$j_\mu^e(p, p_0) = -ie\bar{u}(p)\gamma_\mu u(p_0) \quad 78.$$

and this density is equivalent to Eq. 65 and 66. The bar over the Dirac spinors will refer to the "adjoint" functions [defined in ref. (8), Eq. 46]. A Dirac proton will have a charge-current density similar to Eq. 78. The γ_μ operators are given in terms of a single vector equation

$$\gamma_\mu = (-i\beta\alpha, \beta) \quad 79.$$

β and α are given in Eq. 34 and 35. The above formalism is very useful in extending the scattering theory to a proton with an anomalous magnetic moment. We shall consider this topic later.

Not let us return to the actual evaluation of the matrix element (74). This calculation may be carried out by methods similar to those used in the evaluation of Eq. 41. However, now the spin transitions are more numerous since the proton has also been assumed to have a spin. Thus combinations such as $(I_L I_H)_f (I_L I_H)_0$; $(I_L I_H)_f (II_L, I_H)_0$, etc., need to be considered, where L stands for the light particle (electron) and H for the proton (heavy particle). Sixteen such combinations can be formed, of which eight are equal pairs. The corresponding scalar products in the bracket of equation 74 are formed and the square modulus found for each combination. The square moduli are then added and an average over initial states and a sum over final states is finally taken. The results before averaging are as follows:

$$\left(\frac{W + Mc^2}{2W}\right)(4 \cos^2 \theta/2) \text{ for the } |(u_f^* u_0)(U_f^* U_0)|^2 \text{ terms} \quad 80.$$

and

$$\left(\frac{W + Mc^2}{2W}\right) \left(\frac{4\Delta E \cos^2 \theta/2}{(W + Mc^2)}\right) (2 \tan^2 \theta/2 + 1) \text{ for the } |(u_f^* \alpha u_0) U_f^* \alpha_p U_0|^2 \text{ terms} \quad 81.$$

and

$$-\left(\frac{W + Mc^2}{2W}\right) \left(\frac{4}{W + Mc^2} \cdot 2\Delta E \cos^2 \theta/2\right) \text{ for the cross terms} \quad 82.$$

When the average over initial spins is taken, one obtains

$$\frac{Mc^2}{W} \cos^2 \theta/2 \left\{ 1 + \frac{\hbar^2 q^2}{4M^2 c^2} \cdot 2 \tan^2 \theta/2 \right\} \quad 83.$$

for the averaged sum. In obtaining this result, use is made of Eq. 9 and 10. The corresponding square of the matrix element H is then $(4\pi)^2 e^4/q^4$ times the result (83) as indicated by Eq. 74. Finally we obtain the cross section through the use of Eq. 3, 8, 13, and 26 and find:

$$\left(\frac{d\sigma}{d\Omega} \right)_d = \left(\frac{e^2}{2E_0} \right)^2 \frac{\cos^2 \theta/2}{\sin^4 \theta/2} \frac{1}{1 + \frac{2E_0}{Mc^2} \sin^2 \theta/2} \left\{ 1 + \frac{\hbar^2 q^2}{4M^2 c^2} (2 \tan^2 \theta/2) \right\} \quad 84.$$

where $(d\sigma/d\Omega)_d$ stands for "Dirac" scattering of an electron against a "Dirac" proton whose magnetic moment would be

$$\mu_d = \frac{e\hbar}{Mc} \quad 85.$$

or one nuclear magneton. Eq. 84 is the prototype of all scattering formulas involving magnetic as well as electric scattering and is therefore a generalization of Eq. 48.

The calculation of $(d\sigma/d\Omega)$ can be simplified by the use of trace methods and projection operators (8), although for some purposes, such as those for which polarization properties are of interest, the method outlined is probably simplest, although tedious.

Now the scattering formula 84 has been calculated for an artificial proton since in reality a physical proton's magnetic moment is 2.79 nuclear magnetons of which 1.0 nuclear magneton (Eq. 85) is the Dirac contribution and the remainder ($K = 1.79$ n.m.) is often called the "Pauli" part of the magnetic moment. The name derives from the fact that Pauli (15) showed that a new term can be added to the Dirac equation, endowing a Dirac particle with an additional magnetic moment, sometimes also called the "anomalous" moment. In the covariant notation, corresponding to Eq. 78 (which is written for an electron without structure), the proton's current density can be generalized to

$$j_\mu^P(P, P_0) = ie\overline{U}(P) \left[\gamma_\mu + \frac{K}{2Mc} \gamma_\mu \gamma_\nu q_\nu \right] U(P_0) \quad 86.$$

in which \overline{U} and U are the usual heavy particle spinor amplitudes and q_ν is the four-component momentum-energy transfer given in Eq. 77. Further calculation, similar to that leading to Eq. 80 to 84, shows that the resulting scattering cross section now contains some additional terms relative to Eq. 84 as follows:

$$\begin{aligned} & \left(\frac{d\sigma}{d\Omega} \right)_R \\ &= \left(\frac{e^2}{2E_0} \right)^2 \frac{\cos^2 \theta/2}{\sin^4 \theta/2} \frac{1}{1 + \frac{2E_0}{Mc^2} \sin^2 \theta/2} \left\{ 1 + \frac{\hbar^2 q^2}{4M^2 c^2} [2(1+K)^2 \tan^2 \theta/2 + K^2] \right\} \quad 87. \end{aligned}$$

and this represents what we may call "Rosenbluth scattering" (16) by a point-charge and point-magnetic moment.

In Figures 5, 6, and 7, we show representative scattering curves in the laboratory system for a point-proton without nuclear spin (Fig. 5), for a "Dirac" point-proton with spin 1/2 and with a Dirac moment (1.0 n.m.) (Fig. 6), and for a point-proton having a real magnetic moment and Rosenbluth scattering ($\mu_P = 1+K = 2.79$ n.m.) (Fig. 7).

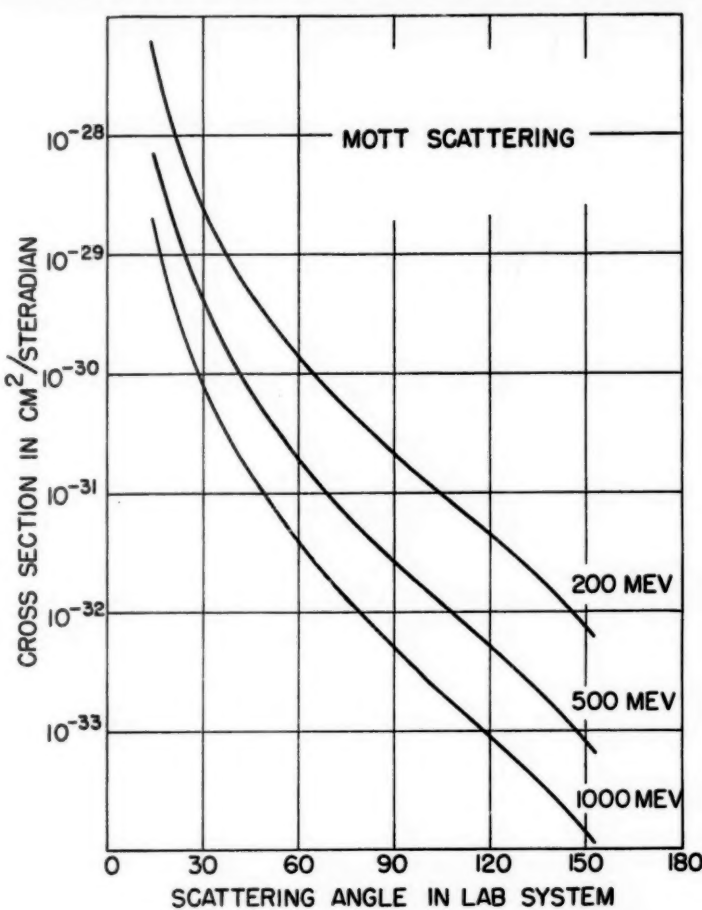


FIG. 5. The Mott-scattering curves for the energies 200, 500, 1000 Mev in the laboratory system. The appropriate cross section is given in Eq. 48 with $Z=1$ and represents electron scattering against a point-proton with zero spin and zero nuclear magnetic moment.

An important feature of magnetic-moment scattering is connected with the $\tan^2 \theta/2$ term since this term becomes dominant at large angles and high energies. The reason the Rosenbluth curves hold up at large angles (Fig. 7) is due to the magnetic-moment term. In principle this fact permits a magnetic-form factor (see below) to be distinguished from a charge-form factor.

5. *Magnetic scattering from a finite nucleon.*—It has been demonstrated experimentally (17, 18, 19) that the physical proton shows deviations from the scattering given by the point proton of Eq. 87. The observed scattering can be accounted for satisfactorily by introducing phenomenological form

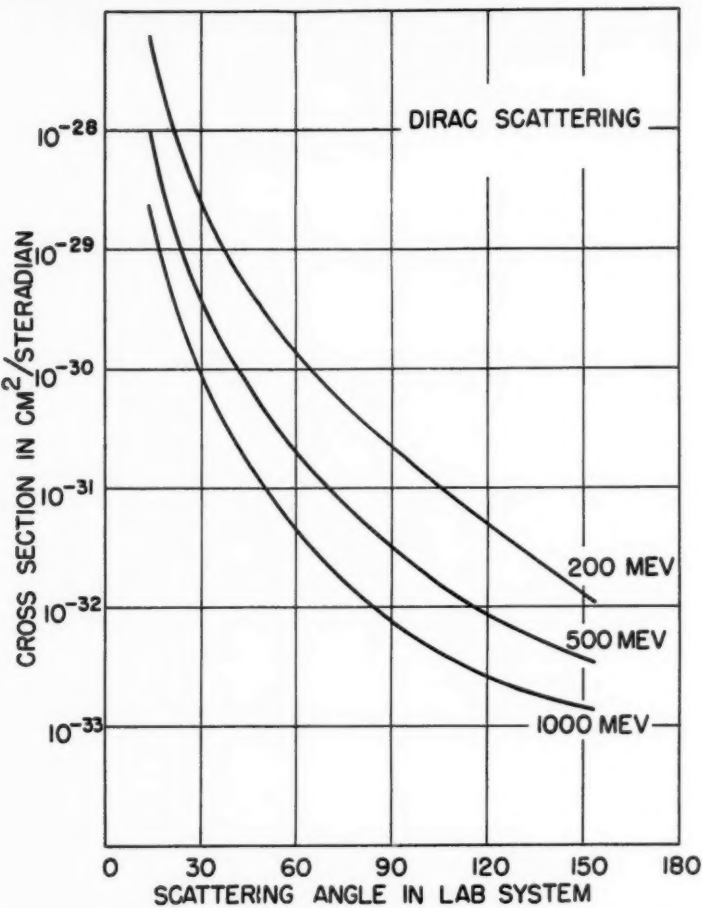


FIG. 6. The "Dirac"-scattering curves for a "Dirac" point-proton with spin $\frac{1}{2} \hbar$ and with a Dirac moment (1.0 nuclear magneton). The appropriate cross section is given by Eq. 87 with $K=0$, or equivalently by Eq. 84.

factors (14, 17), which imply either structure in the proton or a breakdown of electrodynamics at small distances (1, 14). Whichever interpretation applies, it has been shown by Foldy (20) and by Salzman (21) that the most general form of a nucleon's charge-current density must look like:

$$j_\mu^{p,n}(P, P_0) = ie\bar{U}(P) \left(\gamma_\mu F_1^{p,n}(q^2) + \frac{\hbar K^{p,n}}{2Mc} \gamma_\mu \gamma_\nu q_\nu F_2^{p,n}(q^2) \right) U(P). \quad 88.$$

where j_μ^p , etc. applies to a proton and j_μ^n , etc. applies to a neutron. A finite proton would then be described by the phenomenological form factors F_1 and F_2 in Eq. 88. The assumptions behind Eq. 88 are (a) $j_\mu^{p,n}$ must be relativistically covariant, (b) the differential law of current conservation

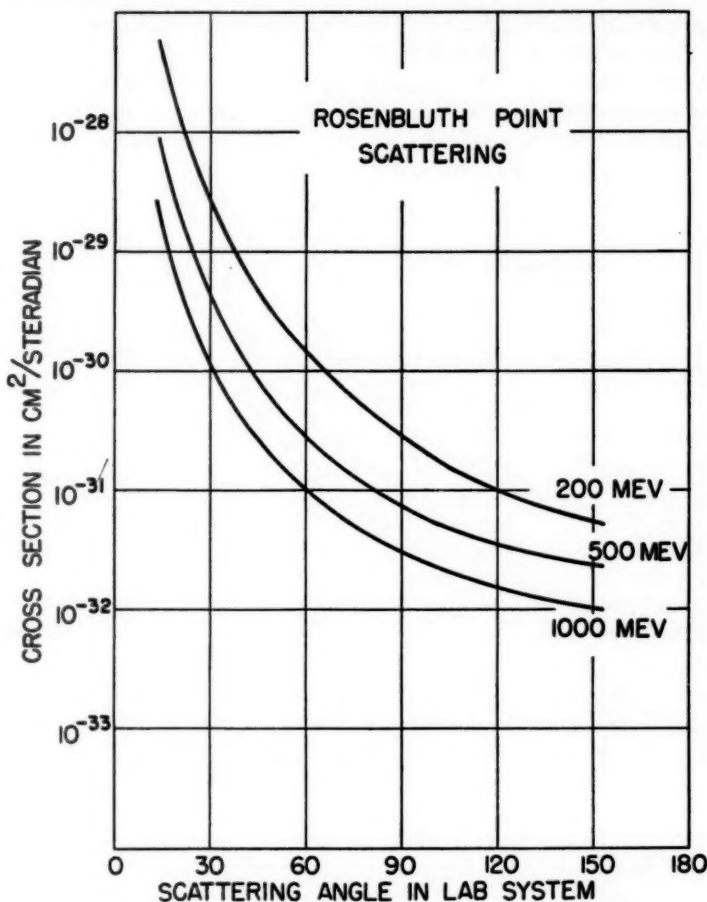


FIG. 7. Rosenbluth-point scattering for point-protons with real values of the nuclear spin and magnetic moment. The appropriate cross section is given by Eq. 87 with $K = 1.79$ nuclear magnetons. ($\mu_p = 2.79$ n.m.)

must hold, and (c) the nucleon behaves according to the Dirac equation [see also ref. (14), footnote 6]. Rosenbluth's calculation (16) had already included form factors of the type given in Eq. 88. In his calculation F_1 and F_2 were obtained from a weak-coupling meson theory.

In Eq. 88 $F_1(q^2)$ clearly should be associated with the proton's charge and Dirac magnetic moment (1.0 n.m.), while $F_2(q^2)$ is to be associated with the Pauli moment (1.79 n.m.). The F_1 and F_2 may be thought of as the relativistic extensions of the form factors of Eq. 50 and 55. For moderate values of the momentum transfer q , this interpretation is quite satisfactory. When the proton or neutron obtains a velocity comparable with c , the simple structural interpretation of F_1 and F_2 may have to be abandoned (14),

although the formulations of $j_{\mu}^{p,n}$ in terms of the phenomenological values of F_1, F_2 , as in Eq. 88, are still valid.

On applying F_1 and F_2 to j_{μ} , it is now clear that Eq. 87 for a point will have a counterpart for finite nucleons. For a physical proton the elastic scattering will have the appearance

$$\frac{d\sigma}{d\Omega} = \left(\frac{e^2}{2E_0}\right)^2 \frac{\cos^2 \theta/2}{\sin^4 \theta/2} \frac{1}{1 + \frac{2E_0}{Mc^2} \sin^2 \theta/2} \cdot \left\{ F_1^2 + \frac{\hbar^2 q^2}{4M^2 c^4} [2(F_1 + KF_2)^2 \tan^2 \theta/2 + K^2 F_2^2] \right\} \quad 89.$$

where F_1 and F_2 are functions of q and the latter is given by Eq. 11.

If now F_1 and F_2 happen to have the same functional form:

$$F_1 = F_2 = F_P \quad 90.$$

then Eq. 89 would have the simple appearance:

$$\frac{d\sigma}{d\Omega} = F_P^2 \times \left(\frac{d\sigma}{d\Omega}\right)_R = F_P^2 \times (\text{scattering by a point}) \quad 91.$$

where $(d\sigma/d\Omega)_R$ is given by Eq. 87.

Now the experiments (1) show that the proton may indeed be described consistently up to an energy of 550 Mev and a laboratory scattering angle of 135° by the choice, $F_1 = F_2 = F_P$, where F_P can be represented, not perfectly uniquely but within certain limits, by a behavior similar to that shown in Figure 8. These results are obtained chiefly from relative data on angular shapes but also from rough absolute measurements (19). In this particular example, the charge distribution in the proton, ρ_P , is given by the exponential

$$\rho_P(r) = \rho_0 e^{-r/a_1} \quad 92.$$

where

$$F_P(qa) = (1 + q^2 a_1^2)^{-1} \quad 93.$$

and where

$$a = \langle r^2 \rangle^{1/2} = a_1 \sqrt{12} \quad 94.$$

in which a is the root-mean-square radius of the charge distribution. This particular charge distribution with $a = 0.80 \times 10^{-13}$ cm. is meant only to be typical of charge distributions which fit the proton within experimental error. Other distributions, such as a gaussian with a slightly smaller rms radius and a hollow exponential (19) with rms 0.78×10^{-13} cm., fit equally well. This is shown in Figure 9, where three typical distributions ($4\pi r^2 \rho$) are shown that provide good fits. A sharply peaked distribution, such as a Yukawa II distribution (1, 19), will not fit, nor will a uniform distribution (not shown). Thus a band of suitable distributions lying near the three satisfactory curves is mapped out. It would be desirable to fix the limits of this region in more detail. Such experiments are now in progress. From the experiments described above, a "best" rms radius of the proton could be ob-

tained and was found to be 0.77×10^{-13} cm. This radius is rather independent of shape and appears to be closely the same for F_1 and F_2 . For further details the original paper (19) may be consulted. R. W. McAllister (109) has recently made an absolute measurement of the electron-proton elastic scattering cross section at 189.6 Mev and 60° and finds that the above radius is in good agreement with the measured cross section. In McAllister's

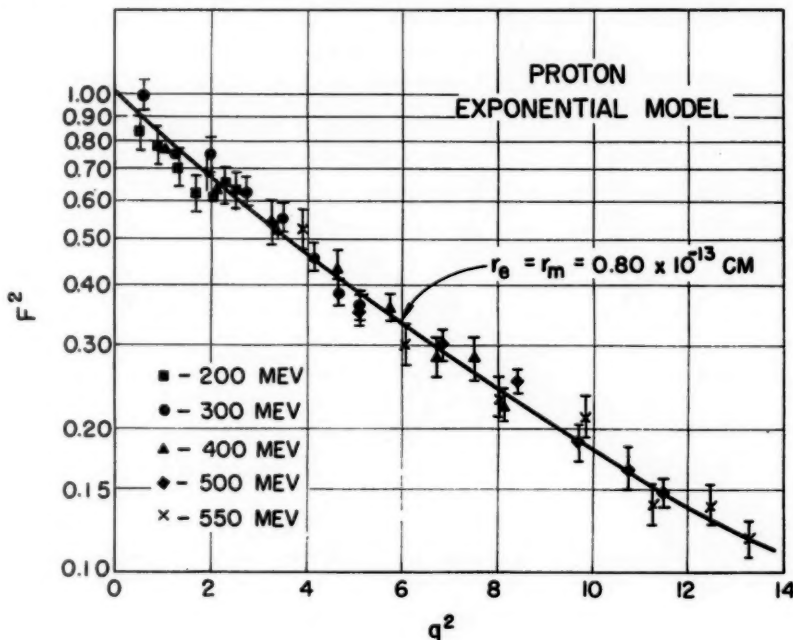


FIG. 8. An example of a model which fits the experimental values of F^2 . This model gives the proton an exponential charge density and an exponential magnetic-moment density with rms radii 0.80×10^{-13} cm. Other close models fit equally well.

work the finite size produces an ~ 17 per cent effect in the cross section. In other recent work of Tautfest & Panofsky (110), the finite size effect is only ~ 3 per cent and is too small to be a test of the size effect.

Clementel & Villi (22) have recently proposed a proton model consisting of a negative δ function for the charge density at the center of the proton together with a Yukawa II (c.f. ref. 1) type positive cloud surrounding the negative core. The fit with experiment is not as good as the best models discussed (19), but is still satisfactory. This proposed model predicts that the electron-proton cross section should have a diffraction zero at 140° for an incident energy of 1.1 Bev. Beyond the zero the cross section increases slowly.

The significance of the findings on the finite size of the proton is not yet clear. There is undoubtedly a correlation of the proton's size with the

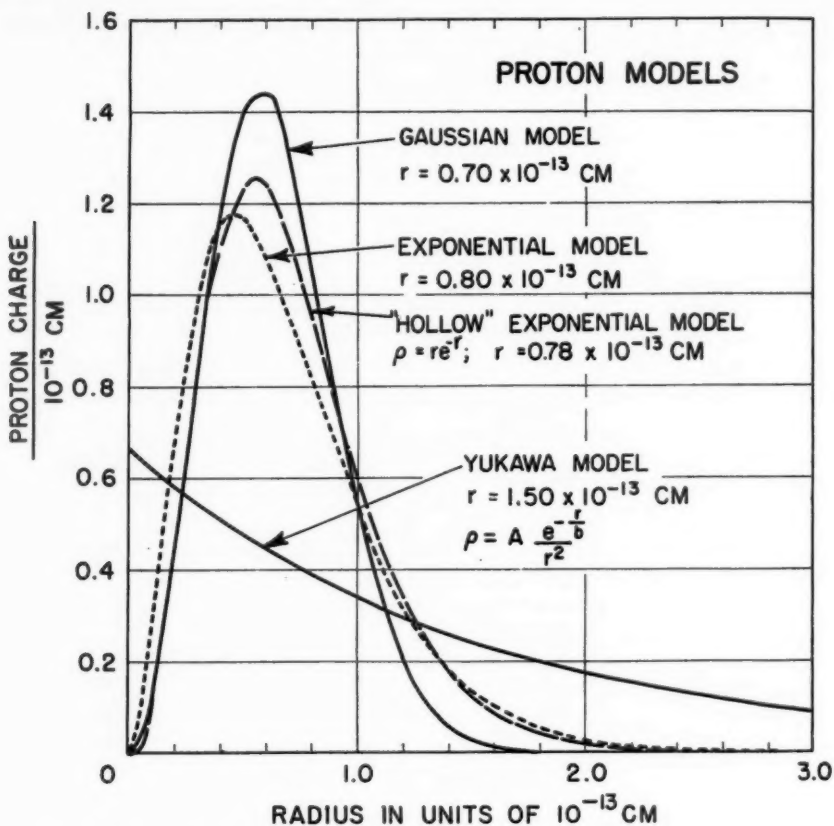


FIG. 9. This graph shows the latitude in the charge and moment distributions allowable in fitting the experiments on the proton (1, 19). The three models: gaussian, exponential, and hollow exponential are equally good. The Yukawa model will not fit, nor will a uniform model (not shown). For the above models, $F_1 = F_2$ for all q values. The ordinate is $4\pi r^3 \rho(r)$.

neutron's mesonic structure (see below), but the investigations are only beginning now, and it is too early to draw definite conclusions. The large size of the proton core is especially difficult to understand. For further comments on the interpretation of proton and neutron structure, see ref. 14 and the papers referred to in that article.

6. *Electron scattering from a deuteron.*—A completely relativistic theory of electron scattering from the deuteron has not appeared in the literature, and for a deuteron composed of finite nucleons such a complete theory can probably not be given at this time. However, certain close approximations can be made. A recent theoretical investigation of electron-deuteron scattering has been presented by Jankus (23). Earlier calculations, applying to lower

energies, were made by several authors (9, 24 to 28) but do not take into account the effects of higher multipoles, which are important for inelastic scattering at large values of the momentum transfer.

As pointed out by Jankus, the matrix elements in electron-deuteron scattering are similar to those involved in the photodisintegration of the deuteron. However, in the photoprocess only real, transverse photons are effective while, in the inelastic-deuteron scattering (electrodisintegration), the main part of the cross section arises from the longitudinal part of the electromagnetic field. Furthermore, it is well known (29) that excitation or disintegration by electrons is quite different from that due to photons. This occurs because in the lowest order processes the photon disappears entirely, that is, it is absorbed. Upon absorption, if it produced a large momentum transfer, it also produced a corresponding large energy change. But in electro-excitation or electro-disintegration processes a large momentum transfer may cause only a small energy transfer. This may be seen, for example, in the excitation of nuclear levels in carbon (30). Thus the photodisintegration results may not easily be applied to the deuteron, e.g., by using the Weizsäcker-Williams method with the matrix elements known from the photoprocesses.

The deuteron will be considered below in a nonrelativistic heavy particle approximation used by Jankus although, of course, in the calculations, the electron will be treated in a fully relativistic manner. Like other computations for low Z elements, the first Born approximation is used in this case also. We employ once again the electron's Møller potentials, Eq. 69 and 70. However, in place of terms for the proton and neutron like those in Eq. 71, the nonrelativistic heavy-particle treatment involves the perturbing interaction:

$$H = e \int \left[\rho_D \varphi - \frac{1}{c} j_D \cdot A - M_D \cdot (\nabla \times A) \right] d^3 R \quad 95.$$

which is perhaps more familiar than Eq. 71. In Eq. 95 the three-dimensional vector M_D is the magnetization density due to the spin-current densities in the deuteron, and j_D is the convection-current density due to the motion of the nucleons within the deuteron. These densities, and also ρ_D , the charge density in the deuteron, compose the perturbation H of Eq. 95.

In Eq. 95 the spin effects (M_D) are separated from those due to the convection-current density (j_D). Although this separation agrees with the more familiar nonrelativistic treatments of electromagnetic interactions, the splitup in Eq. 95 is only an approximation. The degree of approximation can be understood from the physical interpretation of the Dirac equation given by Foldy (20) who shows that "spin-orbit" coupling, the Darwin term and higher order terms, have been dropped in Eq. 95. These terms are of the order (P^2/M^2c^2) and are small compared to the principal term of Eq. 95. At higher energies, however, they must not be neglected. Further, if the exchange currents are neglected and the nucleons are thought of as point

charges and point-magnetic moments, the interaction Eq. 95 becomes

$$H = \sum_{k=1,2} \left\{ e_k \varphi(R_k) + \frac{i}{2} \frac{e_k \hbar}{Mc} [A(R_k) \cdot \nabla_k + \nabla_k \cdot A(R_k)] \right\} - \frac{ie\hbar}{2Mc} \mu_k \delta_k \cdot [\nabla \times A(R_k)] \quad 96.$$

in which R_k is the position coordinate of the k^{th} nucleon, e_k its charge, and μ_k its magnetic moment in terms of a nuclear magneton ($\mu_p = 2.79$, $\mu_n = -1.91$). This expression can be shown to follow from the quantum mechanical operator for current density.

The resulting calculation for elastic scattering is lengthy but straightforward and is carried out in detail in Jankus' thesis (31). The elastic-scattering result is given by the expression

$$\frac{d\sigma}{d\Omega} = \left(\frac{e^2}{2E_0} \right)^2 \frac{\cos^2 \theta/2}{\sin^4 \theta/2} \frac{1}{1 + \frac{E_0}{Mc^2} \sin^2 \theta/2} \cdot G^2 \quad 97.$$

where

$$G^2 = \left[\int_0^\infty (u^2 + w^2) j_0 \left(\frac{1}{2} qr \right) dr \right]^2 + \left[\int_0^\infty 2w(u - 8^{-1/2}w) j_2 \left(\frac{1}{2} qr \right) dr \right]^2 \\ + \frac{2}{3} \frac{\hbar^2 q^2}{4M^2 c^2} [2 \tan^2 \theta/2 + 1] \\ \times \left[\int_0^\infty \left\{ \left[(\mu_p + \mu_n)(u^2 + w^2) - \frac{3}{2} (\mu_p + \mu_n - \frac{1}{2} w^2) \right] j_0 \left(\frac{1}{2} qr \right) \right. \right. \\ \left. \left. + 2^{-1/2}w[(\mu_p + \mu_n)(u + 2^{-1/2}w) + 3 \times 8^{-1/2}w] j_2 \left(\frac{1}{2} qr \right) \right\} dr \right]^2 \quad 98.$$

and where the integral in the second bracket, with j_2 replaced by r^2 , is equal to the quadrupole moment of the deuteron, except for a constant of proportionality. It is to be noted that the coefficient of $E_0/Mc^2 \sin^2 \theta/2$ in Eq. 97 is unity and not two, as in the corresponding center-of-mass term for a proton. This is, of course, because of the doubled mass of the deuteron with respect to that of the proton. The expression for q (Eq. 11) will also be modified in the same way. Although Jankus' result (23) is really expressed in terms of s instead of our q , it is probable that a relativistic generalization would contain q , and so we have made the appropriate changes. In any case, for the present accuracy, the difference is not important.

The result for G^2 may be broken down into three parts. The first bracket gives the scattering from that part of the charge distribution which is spherically symmetric in the deuteron, and the square of the corresponding bracket can be called G_a^2 . The second term is associated with the quadrupole scattering from the deuteron and may be called G_b^2 . The lengthy third term corresponds to the scattering from the magnetic moment of the deuteron and can be recognized by the factor involving $q^2 \tan^2 \theta/2$. The third term will be called G_c^2 . Consequently Eq. 98 can also be expressed in the form

$$G^2 = G_a^2 + G_b^2 + G_c^2 \quad 99.$$

which is suitable for easy reference to the various terms. In Eq. 98

$$j_0(x) = \frac{\sin x}{x} \quad \text{and} \quad j_2(x) = \left(\frac{3}{x^3} - \frac{1}{x} \right) \sin x - \frac{3}{x^3} \cos x \quad 100.$$

and are two spherical Bessel functions [see for example ref. (2), p. 868]. The wave functions for the ground state of the deuteron involve the 3S -state component $u(r)$, and $w(r)$, the 3D -state component, and thus the ground state wave function is generally written (28, 32)

$$\psi_m = (4\pi)^{-1/2} r^{-1} [u(r) + 8^{-1/2} S_{np} w(r)] \chi_m \quad 101.$$

for $m=0$ and ± 1 , where χ_m is the usual triplet-spin function. S_{np} is the tensor operator (32)

$$S_{np} = 3r^{-2} (\boldsymbol{\sigma}_n \cdot \mathbf{r}) (\boldsymbol{\sigma}_p \cdot \mathbf{r}) - (\boldsymbol{\sigma}_n \cdot \boldsymbol{\sigma}_p) \quad 102.$$

and where $1/2 \mathbf{r}$ is the position of the charged proton with respect to the center of mass of the deuteron. $\boldsymbol{\sigma}_n$ and $\boldsymbol{\sigma}_p$ are the Pauli spin-matrix operators for the neutron and proton and are given by Eq. 35.

Since $u(r)$ and $w(r)$ are determined principally from the low-energy theory of the deuteron and depend in large measure on properties outside the range of nuclear forces, Jankus was able to calculate the quadrupole term approximately without assuming a detailed model. The quadrupole term is found to be $8/9(\hbar q/4Mc)^4 Q^2$ for small values of q , where $Q(\hbar/2Mc)^2 = 0.274 \times 10^{-26} \text{ cm}^2$, and is the deuteron's quadrupole moment. For larger values of q , the quadrupole term reaches a maximum value of about 0.002 for a Hulthén potential and about 0.006 for a repulsive-core potential. In either case it remains near these values for $q < 4 \times 10^{13} \text{ cm}^{-1}$. Evidently the quadrupole term is rather small. The magnetic-moment term and the spherically symmetric term are much more important for values of $q < 3 \times 10^{13} \text{ cm}^{-1}$ at low energies.

Jankus (23) shows that, if the quadrupole term is neglected and if other small terms involving w and w^2 are neglected, the expression for eq. 98 may be simplified considerably and becomes

$$G^2 = f_D^2 \left\{ 1 + \frac{2}{3} \frac{\hbar^2 q^2}{4M^2 c^4} (\mu_p + \mu_n)^2 [2 \tan^2 \theta/2 + 1] \right\} \quad 103.$$

where

$$f_D = \int (u^2 + w^2) j_0 \left(\frac{1}{2} qr \right) dr \quad 104.$$

The bracket in Eq. 103 bears a resemblance to the bracket of Eq. 87. The factor $2/3$, in front of the magnetic term in Eq. 103, comes from the spin sums associated with spin 1 in the deuteron. f_D is the spherically symmetric form factor of the deuteron's charge distribution. Because the tensor, or 3D part (w) of the charge distribution, is approximately 4 per cent of the 3S part (u), the w^2 term in Eq. 98 can be neglected with only a small error. In this event the function $u(r)$ determines the main features of the scattering cross section. The function f_D^2 (with w^2 neglected) is plotted in Figure 10, and the graph shows how a repulsive-core potential (curve (c) of the Figure) prevents charge from accumulating at the center of the deuteron, therefore

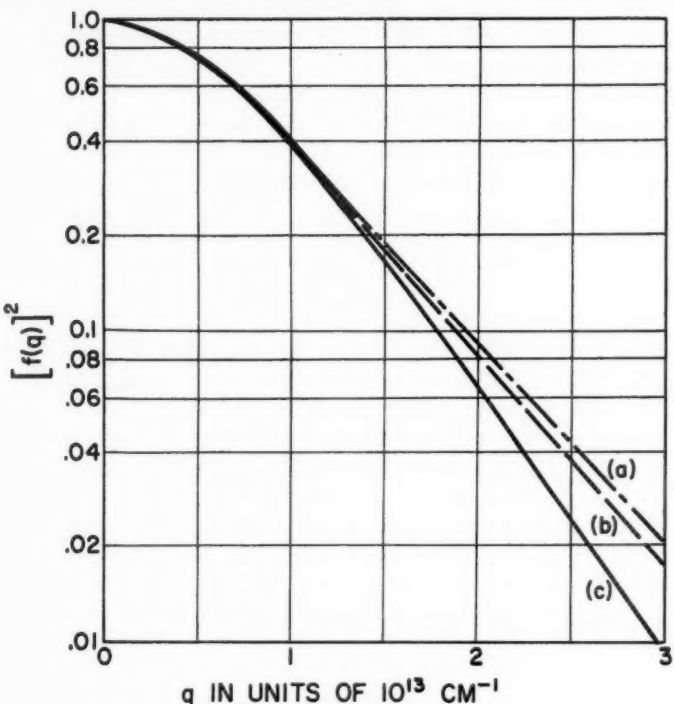


FIG. 10. Three approximate (form factors)² for the deuteron calculated by Jankus (23). Curves (a) and (b) refer to Hulthén distributions with effective range values of 1.77×10^{-13} cm. and 1.88×10^{-13} cm., respectively, while curve (c) refers to a suitable repulsive-core potential.

resulting in less scattering at large angles. This type of behavior is characteristic of all form factors with charge distributions pushed away from the center of a nucleus. Curves (a) and (b) refer to Hulthén distributions for effective ranges of 1.77×10^{-13} cm. and 1.88×10^{-13} cm., respectively.

Figure 11 shows the results of a numerical calculation of form factors made by McIntyre & Dhar (33) with Jankus' formulas (97) and (98) for a typical repulsive-core potential in the deuteron. In this case the w^2 term is retained. The various contributions G_a^2 , G_b^2 , G_c^2 are shown for several different incident electron energies. Since G_b^2 is a function only of q and of the type of interaction (Hulthén, etc.) potential, it has the same appearance at all energies.

The kind of charge distribution which gives the form factors of Figure 11 is illustrated in Figure 12 and has also been calculated by the above authors and independently by Smythe (34). As may be seen from Eq. 101, the sum $u^2 + w^2$ is proportional to the charge in a shell at radius r from the center of mass in the deuteron. The curve for the repulsive-core potential corresponds to Figure 11. Smoother potentials of the Yukawa variety (32), with differing

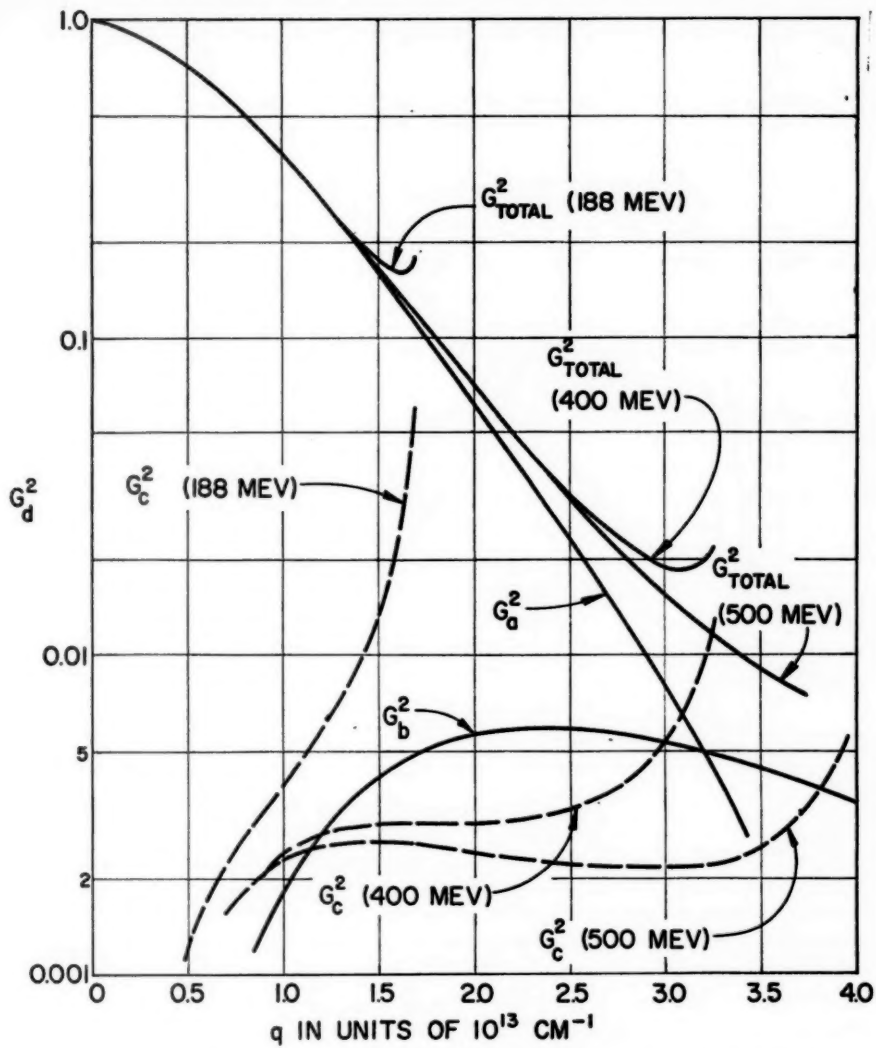


FIG. 11. The calculations of McIntyre & Dhar (33) based on Jankus' Eq. 97 and 98 for a repulsive-core potential in the deuteron. The general appearance is similar to (c) of Fig. 10, except that the quadrupole and magnetic-moment terms are included.

amounts of 3D state contributions, give other charge distributions with more charge at the center of the deuteron. We shall turn later to a comparison with experiment of form factors such as shown in Figure 10 and 11.

A new and interesting theoretical treatment of the problem of elastic scattering from the deuteron has been given by Blankenbecler (35). His analysis is patterned after the corresponding relativistic calculation of

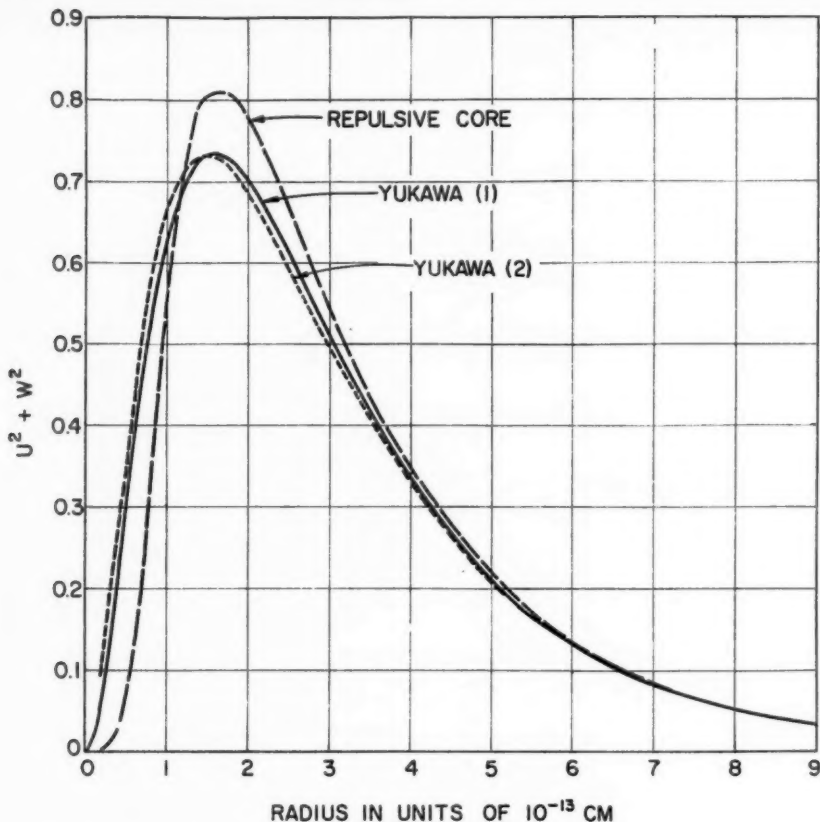


FIG. 12. These curves are proportional to $4\pi r^2 \rho$ for the deuteron and show the differences between the repulsive core and Yukawa type potentials in the deuteron. The small charge densities in the deuteron may be appreciated by referring to Fig. 9, which shows a similar plot in the proton where the radius scale is expanded. The total charge is the same in both cases.

Rosenbluth for electron-proton scattering. Blankenbecler considers the deuteron to be a point particle with spin unity, with a charge e and a magnetic moment $\delta e\hbar/2Mc$ and with a quadrupole moment Q (M is the nucleon mass). This means that in covariant notation the current has three parts:

$$j_\mu(\text{deuteron}) = j_{\mu(\text{charge})} + j_{\mu(\text{mag. mom.})} + j_{\mu(\text{quad. mom.})} \quad 105.$$

He then shows that the electron-deuteron cross section is given by

$$\left(\frac{d\sigma}{d\Omega} \right)_D = \left(\frac{d\sigma}{d\Omega} \right)_{Mott} F^2 = \sigma_{NS} F^2 \quad 106.$$

where σ_{NS} is given by Eq. 48 and

$$F^2 = \left(1 - \frac{(\delta - \frac{1}{2})}{2} \frac{\hbar^2 q^2}{4M^2 c^2} \right)^2 + \frac{2}{3} \delta^2 \frac{\hbar^2 q^2}{4M^2 c^2} \left(2 \tan^2 \theta/2 + 1 \right. \\ \left. + \frac{2E^2}{4(E + Mc^2)^2} \tan^2 \theta/2 \sin^2 \theta/2 \right) + \frac{Q^2}{18} \frac{q^4 \hbar^4}{16M^4 c^4} \quad 107.$$

and where the mass of the deuteron, $2M$, appears in the denominator in the center-of-mass term in σ_{NS} . The various terms in Eq. 107 have the following significance: The first term represents the charge scattering and an interference term between the charge and the "anomalous" magnetic moment. (A "normal" magnetic moment of a spin-one deuteron is $\delta = \frac{1}{2}$.) The first term is analogous to the proton case where the first and last terms of the bracket in Eq. 87 are to be compared with the first bracket of Eq. 107. However, in the latter case, the bracket is squared while in the proton case the bracket appears to the first power. This is due to the higher spin.

The second term in Eq. 107 represents the magnetic-moment scattering and bears a direct resemblance to the magnetic term in Eq. 87, containing $(2K^2 \tan^2 \theta/2)$. However the factor $2/3$ occurs in the deuteron case because of the unit value of spin (see Eq. 103). The $\tan^2 \theta/2 \sin^2 \theta/2$ term in Eq. 107 has little similarity with the cross term involving $2K \tan^2 \theta/2$ in Eq. 87.

The third term containing Q^2 is similar to the quadrupole scattering obtained by Jankus (Eq. 98) and the approximation considered above.

In the spirit of Rosenbluth's calculation, or of the introduction of phenomenological form factors for the proton (1, 14, 17), the constants e , δ , Q may be made functions of q^2 . However the interpretation of these form factors in terms of a physical model of the deuteron is not clear.

7. *Elastic scattering from a deuteron containing finite nucleons.*—The previous section has considered the elastic scattering from a deuteron containing a point proton and a point neutron. The experimental work on the proton (1) shows that it is a spread-out entity and presumably the neutron is spread out also insofar as its meson cloud is concerned. The obvious question may be asked: How do these spread-out particles affect the elastic scattering in the deuteron? Naive considerations would suggest that a folding of the nucleon's charge and moment distributions into the density distributions already given by deuteron theory (section 6), would yield a further spreading of the deuteron. Thus the larger deuteron would scatter less at large angles and high energies than a deuteron containing a point proton and a point neutron. These considerations prove to be correct as we shall see below.

The charge distribution in the deuteron implicit in u and w of Eq. 104 is

$$\rho_D(r) = |\psi_m(r)|^2 \quad 108.$$

where ψ_m is the wave function in the ground state, Eq. 101, and corresponds to a deuteron containing point nucleons. If we make the assumption that the nucleons themselves are not distorted appreciably by the nuclear force in the deuteron and that the heavy particles may be treated nonrelativistically, then the folded charge distribution corresponding to finite nucleons, $\rho_f(r)$, may be represented by

$$\rho_f(r) = \int [\rho_P(|r - r'|) + \rho_N(|r - r'|)] \frac{1}{e} \rho_D(r') d^3r' \quad 109.$$

where ρ_P , ρ_N , and ρ_D are, respectively, the charge density in a finite proton, the charge density in a finite neutron, and the charge density in a deuteron, given by Eq. 108. e In Eq. 109 is the absolute value of the charge of the proton. A folded charge distribution formed from a product of the type of equation 109 may be integrated directly to give a resultant form factor $F_D(q)$ similar to Eq. 55. The resultant $F_D(q)$ is then simply a product of form factors (14, 36)

$$F_D(q) = [F_P(q) + F_N(q)] f_D(q) \quad 110.$$

where f_D is given by Eq. 104 and where $F_P = F_1$ is given by Eq. 90. A typical but not the only form of F_P is shown in Eq. 93. F_N is at present unknown except for indications from experiments on the neutron-electron interaction (37) that $F_N(q) \approx 0$ for small q , since the overall charge on the neutron is zero and since the mean square of the neutron's radius, weighted according to charge, is very small or zero according to those experiments. In principle, it is possible to find $F_N(q)$ if all other quantities in Eq. 110 are known.

It must be noted that only the charge distribution matters in Eq. 110. In actuality, when dealing with the deuteron, the complete expression for the form factor, G , of Eq. 97 and 98 must be used to compare theory with experiment. Fortunately, the quadrupole terms are rather small and this is true also of the magnetic scattering. In the latter case, $\mu_p + \mu_N = 0.857$ n.m., and the magnetic scattering is

$$\sim \frac{2}{3} \times \left(\frac{0.86}{2.79} \right)^2 = 0.063$$

or only about 1/16 as important as in the case of the proton where the magnetic effects are dominant at large angles and high energies. This fortunate circumstance may make it possible to find details of the neutron-proton potential when very accurate elastic-scattering experiments on the deuteron can be performed. In this case, however, it is probable that the quadrupole scattering will need to be known to higher accuracy than it is now known. By the same arguments, it will be difficult to learn about the shape or size of the neutron's magnetic cloud through elastic scattering, because the magnetic term enters only in a minor way into the elastic scattering formulas at presently attainable energies. (The next section will describe how it is possible by another method to determine the shape and size of the magnetic cloud in the neutron.)

Recent experimental work by McIntyre & Dhar (33, 38) on the deuteron shows clearly the effects of the finite size of the proton. Figure 13 provides a comparison of the experimental points showing the ratio of the deuteron's elastic scattering to that from a deuteron with point nucleons. Thus the experimental value of F_D^2 is shown in Figure 13. This is slightly different

from F_D of Eq. 110, because, as explained above, only the charge was taken into account in that equation. However, if f_D of Eq. 110 is taken to be the G of Eq. 98 or its approximation Eq. 104, a direct comparison can be made with the experimental form factor. Then

$$F_{D(\text{exp})} = (F_P + F_N)G \quad 111.$$

In these experiments $F_N \approx 0$ so that

$$F_{D(\text{exp})}^2 = F_P^2 G^2 \quad 112.$$

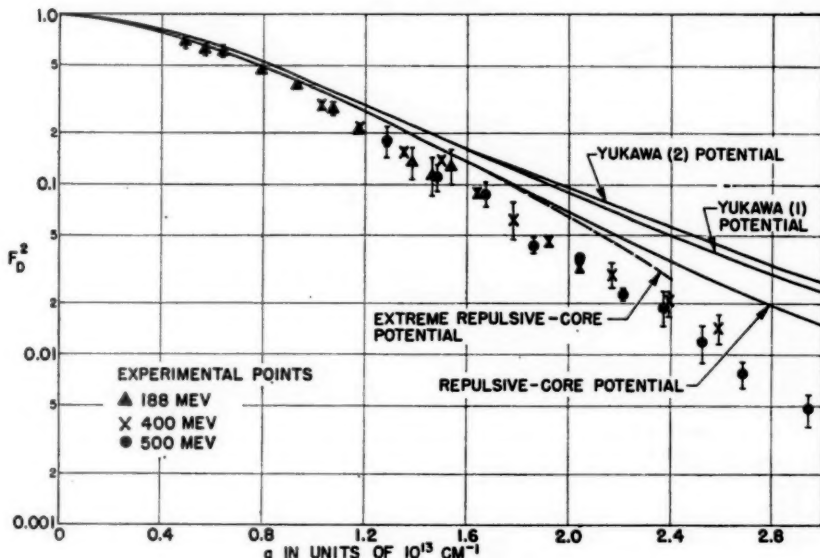


FIG. 13. The experimental value of F_D^2 is compared with theoretical calculations for F_D^2 for a deuteron composed of point nucleons. No allowable stretching of the constants of the theory will permit a good fit with the experiments (33).

and since in Figure 13 F_P^2 has not been allowed for, the experimental curve departs from the scattering expected from a deuteron with a point proton. Neither Yukawa potentials nor a repulsive-core potential, satisfying the parameters found from low-energy studies of the deuteron, are adequate to fit the experimental scattering without the introduction of a finite proton. On the other hand, Figure 14 shows that a repulsive-core deuteron, with a finite proton close to the size found previously (17, 18, 19), will fit the experimental points suitably, and this result confirms those findings. Once again the choice is not unique since an excellent fit is also obtained with a Yukawa potential and the rms proton size 0.78×10^{-13} cm. found by Chambers & Hofstadter (19). The "shape" of the proton was taken to agree with a hollow exponential (re^{-r}) model (ref. 19).

Thus the present conclusion is that the experiments on elastic electron

scattering from the deuteron (33, 38) agree with those on the proton and give essentially the same proton size. This fact may be understood as a verification of the assumption that $F_N \cong 0$, and in this respect it is consistent with the experiments on the neutron-electron interaction (14). On the other hand, the present accuracy of the experiments does not permit conclusions to be drawn about the shape of the neutron-proton potential.

At small angles and lower energies ($\sim 40^\circ$, 192 Mev), the form factors are close to unity and the electron-deuteron scattering (39) shows good agree-

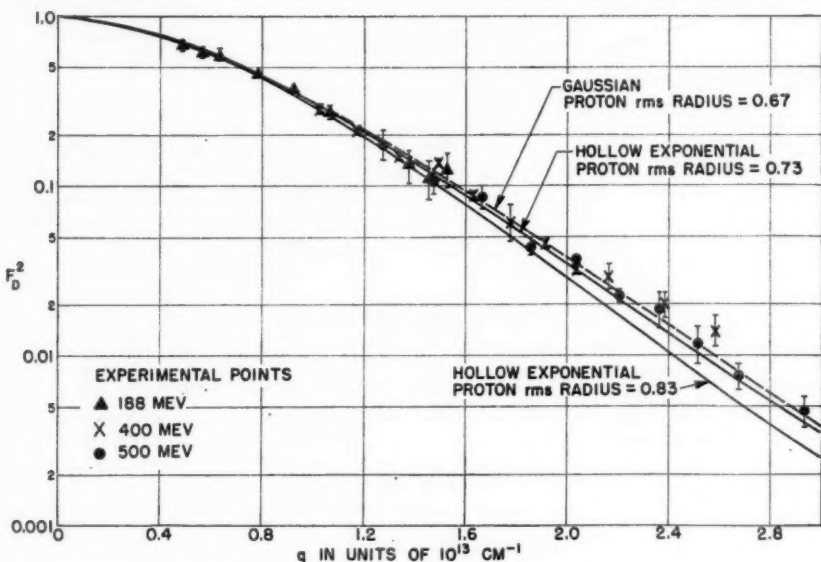


FIG. 14. This plot shows that the experimental values of the deuteron's (form factors)² can be made to agree with the conventional deuteron theory if allowance is made for a finite proton of the type presented in Fig. 9.

ment with the expected behavior for point nucleons and with the usual theory of the deuteron. This is consistent with the corrections for finite size now known.

8. *Inelastic scattering from the deuteron (electrodisintegration).*—In the first of the papers on electron scattering from the deuteron (39), an inelastic continuum was found on the low-energy side of the elastic-scattering peak. The general character of such an inelastic continuum (for complex nuclei) was pointed out by Amaldi *et al.* (40) and later, qualitatively by Feshbach (41). Physically, this type of scattering can be understood qualitatively (1) as elastic scattering of electrons from moving nucleons in a nucleus if the momentum transfer is sufficiently large so that the binding effects in the nucleus can be neglected. This is equivalent to the idea of an electrodisintegration, and an analysis of the cross section can yield the momentum distribu-

tion of nucleons within the nucleus. The experimental realization of such scattering has been illustrated (1) for deuterium and also for helium.

Figure 15, due to Jankus (23), shows the type of inelastic scattering to be expected from the theory for the deuteron at 350 Mev and at 60° in the laboratory system. The elastic cross section, whose size is not indicated in the Figure, is shown at 320.2 Mev. An inelastic cross section in the deuteron arises from terms such as

$$\begin{aligned} \left(\frac{d\sigma}{d\Omega} \right)_{in} = & (4\pi)^{-3} \left(\frac{e^2}{E_0} \right)^2 \frac{1}{\sin^4 \theta/2} k d\Omega_k \\ & \times \left| \left\langle \text{fin} \left[a_0 - i \nabla \cdot a + \frac{1}{2} i \frac{\hbar}{Mc} \mu_p \delta_p \cdot (q \times a) \right] \exp \frac{1}{2} iq \cdot r \right. \right. \\ & \left. \left. + \frac{1}{2} i \frac{\hbar}{Mc} \mu_n \delta_n \cdot (q \times a) \exp -\frac{1}{2} iq \cdot r \right| \text{init} \right\rangle \right| \quad 113. \end{aligned}$$

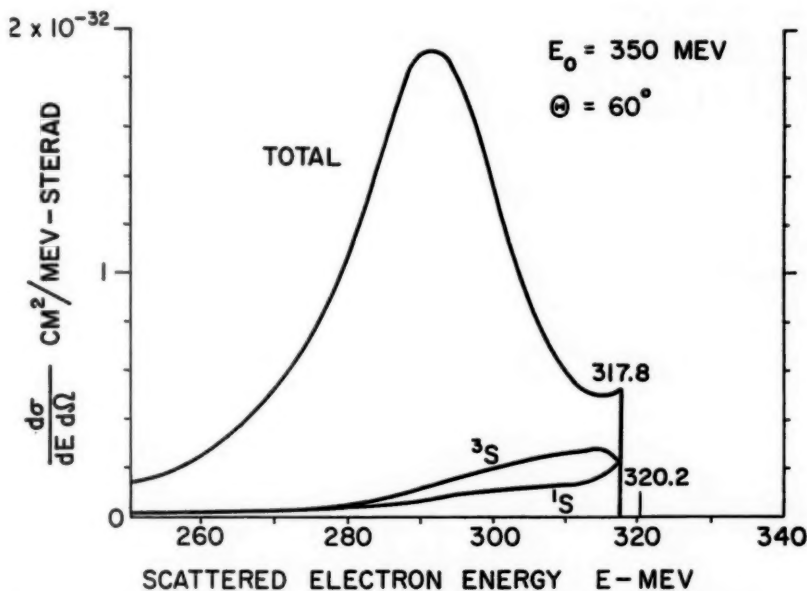


FIG. 15. A typical plot of the inelastic continuum in the deuteron obtained from the Jankus theory (23). The 3S and 1S contributions are also shown.

where k represents the final momentum of the proton with respect to the center of mass of the recoil deuteron, and where a and a_0 are the matrix elements of the Dirac α and β operators. $d\Omega_k$ is the relevant proton solid angle and p refers to the momentum of the scattered electron. The above expression has been obtained by Jankus from Eq. 96.

The general evaluation of Eq. 113 is quite complex but, when completed, does provide the continuous energy spectrum of electrons scattered into

any energy interval at a given angle. As shown experimentally at 500 Mev, 135° (42), the distribution has a rather narrow width at half-maximum (~ 44 Mev). The same behavior is also apparent from theory in Figure 15, due to Jankus. At 350 Mev and 60° , the width is about 23 Mev. (The change in width with incident energy is easily seen to be consistent with relativistic kinematics.) Thus, as a crude approximation, the momentum transfer, q , does not vary very much over the important region in the inelastic peak where the cross section accumulates most of its value. The rough approximation can then be made that q is constant and may be taken out of the integral (over $d\Omega$) involving the differential cross section Eq. 113. Using the closure property of the deuteron's final wave functions, a total cross section at a given angle can be found. Then the elastic cross section, given approximately by Eq. 97 and 103, may be subtracted from the total cross section just found and the difference yields the inelastic cross section at a given angle. This procedure led Jankus to an important approximate formula³ for large q , giving the total inelastic cross section of the deuteron at a given angle:

$$\begin{aligned} \left(\frac{d\sigma}{d\Omega} \right)_{in} &= \left(\frac{e^2}{2E_0} \right)^2 \frac{\cos^2 \theta/2}{\sin^4 \theta/2} \frac{1}{1 + \frac{2E_0}{Mc^2} \sin^2 \theta/2} \\ &\times \left\{ (1 - f_D^2) + \frac{\hbar^2 q^2}{4M^2 c^2} [2(\mu_P^2 + \mu_N^2 - 3f_D^2) \tan^2 \theta/2 + \mu_P^2 + \mu_N^2 - 3f_D^2] \right\} \end{aligned} \quad 114.$$

which can be used only when $q > \alpha$, where $1/\alpha$ is the usual size of the deuteron [$(1/\alpha) \approx 4 \times 10^{-13}$ cm]. Examination of Eq. 114 shows that for larger values of q , that is, where f_D is small,

$$\begin{aligned} \left(\frac{d\sigma}{d\Omega} \right)_{in} &= \left(\frac{e^2}{2E_0} \right)^2 \frac{\cos^2 \theta/2}{\sin^4 \theta/2} \frac{1}{1 + \frac{2E_0}{Mc^2} \sin^2 \theta/2} \\ &\times \left\{ 1 + \frac{\hbar^2 q^2}{4M^2 c^2} [2(\mu_P^2 + \mu_N^2) \tan^2 \theta/2 + \mu_P^2 + \mu_N^2] \right\} \end{aligned} \quad 115.$$

and this is approximately the same, for point nucleons, as

$$\left(\frac{d\sigma}{d\Omega} \right)_{in} = \left(\frac{d\sigma}{d\Omega} \right)_P + \left(\frac{d\sigma}{d\Omega} \right)_N \quad 116.$$

Now the theory of Jankus makes certain nonrelativistic approximations referred to previously. Blankenbecler (43) has avoided making some of these assumptions and arrives at an expression identical with Eq. 116 except for small correction terms of the order of a few per cent.

Further details on the shape of the inelastic spectrum of electrons scattered against deuterium must be left to the original paper of Jankus, since

³ Jankus' (31) result for inelastic scattering, given in his Eq. 7, contains the factor $[1 + (E_0/Mc^2)]^{-1}$ instead of $[1 + (2E_0/Mc^2)]^{-1}$. Although the former factor is correct for elastic scattering, it is not correct for inelastic scattering. [The correct result was given in ref. 1, Eq. 59 and has been proved by Blankenbecler (43)].

the computations are quite intricate. However, we should not fail to note in passing that the interaction between the neutron and proton in the final state must be taken into account. This has been done approximately by Jankus for a Yukawa potential. He shows that there is an effect of the order of 10 per cent on the shape of the inelastic continuum of Figure 15. The change in the total cross section at a given angle appears to cancel out, at least approximately, although the spectrum suffers slight changes. Thus it may be expected that the effect of the interaction on equation 116 will be small. It would be interesting to carry out a similar calculation for a repulsive-core potential where the effect might be larger. To the author's knowledge this calculation has not been made.

9. *The neutron.*—Inelastic electron scattering from the deuteron is extremely interesting from the viewpoint of determining the neutron's structure. It was previously suggested (1) that by examining the inelastic scattering in the deuteron at large values of the momentum transfer, it might be possible to separate the scattering effects of the neutron and proton and thus to measure the form factor of the neutron. The basic equation 116 would permit a determination of the neutron's cross section by a subtractive method

$$\sigma_N = \sigma_{in}^D - \sigma_P$$

117.

in which it would be necessary to know the proton's cross section. For convenience we have replaced the differential cross-section symbols by the corresponding σ 's. These σ 's are integrals over the spectrum of the inelastic-deuteron peak and the proton's elastic peak at a given angle.

Now Eq. 117 or 116 have been worked out for point nucleons, and it might be expected that finite-nucleon size could have a very large effect on the magnitude of the scattering cross sections. We have already seen in section 7 how the elastic scattering is modified by the effect of finite-proton size. If the scattering from proton and neutron are independent and incoherent as suggested by Eq. 117, our crude expectation would be that the point-nucleon cross sections would be multiplied by their respective (form factors)² when the nucleons are permitted to have finite dimensions. Our assumptions would involve the notions: (a) that the nucleons are not distorted by the presence of each other, (b) that exchange effects are small, and (c) that polarizability effects between the electron and the nucleons' mesonic clouds are also small. With respect to (a), nothing is now known of such effects. In case (b), Jankus suggests that exchange effects are small (23). For (c), Drell & Ruderman (44) show that below 500 Mev electron-induced polarization in the proton is small, corresponding to a 0.5 per cent effect at 400 Mev and 90° scattering.

Consequently, it appears reasonable to assume that mesonic effects will not influence the interpretation of Eq. 117 in an important manner when it is applied to nucleons of finite dimensions. Blankenbecler (35) has considered the modifications of Eq. 117 required by a relativistic treatment of the sum rule from which Eq. 117 was derived and includes the effect of finite size

of the nucleons. Thus his treatment considers the variation of q over the energy spectrum of the inelastic continuum and the variation of the free nucleons' form factors over the same region. Mesonic corrections due to the exchange of charged mesons or other corrections discussed above are not included in his work.

Blankenbecler's result is given below:

$$\sigma_{in}^D = A [\sigma_P^F + \sigma_N^F]_{p_f - \bar{p}_f + B/A - \epsilon} \quad 118.$$

where

$$A = 1 + 0.847\langle p^2 \rangle = 1.017$$

$$B = 0.574\langle p^2 \rangle = 0.0115. \quad 119.$$

A and B are correct up to $\langle p^2 \rangle \rightarrow (v^2/c^2)$ but not including $\langle p^4 \rangle \rightarrow (v^4/c^4)$ at angle of 135° and incident energy of 470 Mev, and a value of $\langle p^2 \rangle = 0.02$. The mean-square value of the momentum spread is $\langle p^2 \rangle = 0.04$ for a repulsive core and 0.015 for a Hulthen potential, p is measured in units of the rest energy of a nucleon and thus B corresponds to about 10 Mev when $\langle p^2 \rangle$ corresponds to about 19 Mev. The value of the bracket in equation 118 is to be found at a final scattered energy corresponding to the free proton-recoil energy (\bar{p}_f) plus approximately 10 Mev (B/A) minus the binding energy of the deuteron ($\epsilon = 2.2$ Mev). The superscript F stands for the free proton and free neutron cross sections including the effects of their form factors. The final state attraction is taken into account and influences the value and sign of B . Eq. 118 allows for the fact that the deuteron is a bound structure and hence the electron scatters at an effectively different mean energy from the incident energy. The variation of the form factors of the nucleons over the momentum spectrum of the moving nucleons is also included in this equation. It is as if the electron were scattering against nucleons sometimes moving with momentum components along its direction and sometimes against its direction. When the terms of Eq. 118 are evaluated, the result is that $\sigma_{in}^D = \sigma_p^F + \sigma_N^F$ with an error of less than 8 per cent for the stated conditions. The sign of the correction is positive so that the resulting σ_{in}^D is 8 per cent greater than would correspond to Eq. 117 when applied to nucleons of finite size.

Figure 16 shows an experimental realization of the inelastic scattering in the deuteron and represents recent data obtained by Yearian & Hofstadter (45). The data were obtained at 135° at an incident energy of 500 Mev and were found by direct comparison between a liquid-deuterium target and a liquid-hydrogen target. In this figure one sees the slight shift (C) to lower energies of the maximum of the inelastic spectrum compared to the electron-proton peak (A). At low-energy settings (D) (~ 139 Mev) one observes the scattering of electrons which have produced mesons in the deuteron. The bremsstrahlung tail of the free-proton peak is also clearly shown at (B).

In order to subtract the deuteron and proton cross sections, it is necessary to find the area under each peak. In this calculation a correction must be made for the radiative effect, that is, for electrons not counted because

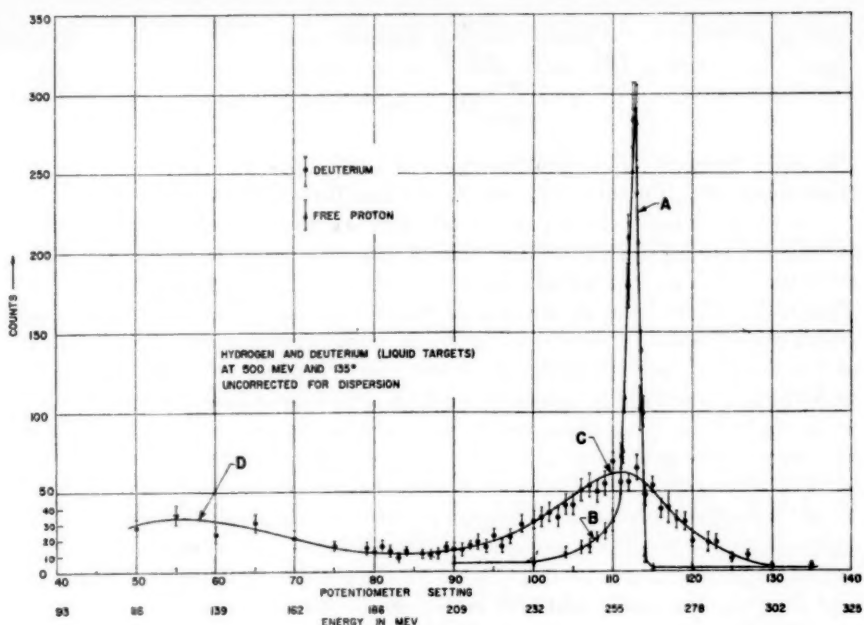


FIG. 16. The experimental comparison of the scattering from the moving proton and neutron in the deuteron (C) and the scattering associated with free protons (A). The data are taken from Yearian and Hofstadter (45). At (D) there is a peak belonging to electrons which have been scattered after producing pions in deuterium. From the scattering data in this figure, the magnetic form factor of the neutron can be obtained. It is found to be larger than that of a proton for a similar momentum transfer.

they radiated high-energy photons and appeared at very low final energies. This correction may be evaluated using the Schwinger formula straggling, etc. (1). Furthermore, the usual $(1/E)$ instrumental correction corresponding to the use of constant-width energy slit must be made. When these corrections are applied, the resulting ratio, σ_N/σ_P , comes out to be 1.0 ± 0.20 .

Except for Blankenbecler's correction, the actual calculation of a neutron form factor may be made with the help of Eq. 89. When applied to a neutron, for which we may take $F_1 = 0$, at least approximately, we obtain

$$\sigma_N = \sigma_{NS} F_{2N}^2 K_N^{-2} \frac{\hbar^2 q^2}{4M_e^2 c^2} \{2 \tan^2 \theta/2 + 1\} \quad 120.$$

whereas, from the result of Chambers & Hofstadter (19), Eq. 90, $F_1 = F_2 = F_P$, holds and thus

$$\sigma_P = \sigma_{NS} F_P^2 \left\{ 1 + \frac{\hbar^2 q^2}{4M_e^2 c^2} [2(1 + K_P)^2 \tan \theta/2 + K_P^2] \right\} \quad 121.$$

Then

$$\frac{\sigma_N}{\sigma_P} = \frac{F_{2N}^2}{F_P^2} \frac{\frac{K_N^2 \hbar^2 q^2}{4M^2 c^2} [2 \tan^2 \theta/2 + 1]}{1 + \frac{\hbar^2 q^2}{4M^2 c^2} [2(1 + K_P)^2 \tan^2 \theta/2 + K_P^2]} \quad 122.$$

The ratio depends on incident energy and angle since q depends on both of these quantities. Further, F_{2N} and F_P are functions of q .

As we have seen, the experimental ratio, σ_N/σ_P , is in the neighborhood of unity. Placing the right-hand side of Eq. 122 equal to unity, we may solve for F_{2N}^2/F_P^2 . The solution is found to be approximately $F_{2N}^2/F_P^2 = 2.2$. This ratio differs from σ_N/σ_P not so much because of the proton charge, which makes a small contribution at these momentum transfers, but because of the differing magnetic moments of neutron and proton. Now it is possible to find F_{2N}^2 , since F_P^2 is known to be 0.15. The approximate value is found to be $F_{2N}^2 = 0.33$. From these results we find that F_N and F_P are unequal for virtually the same value of q . Thus, if it can be assumed that mesonic effects involve only small correction and if Blankenbecler's expansion is rapidly convergent, the dimensions and magnetic structure of the neutron are somewhat different from those of the proton. This would mean that a failure of electrodynamics cannot be wholly responsible for the size effects found in the proton and neutron, and this would be a major conclusion from the experiments on the size of nucleons (1, 17, 18, 19, 45). On the other hand, if the corrections in the Blankenbecler expansion are positive and not negligible, the form factors of neutron and proton can be the same. It should be emphasized that a complete form-factor curve must be obtained in order to be certain about these facts; *i.e.*, the consistency of the results at different values of q must be examined. Such a program is now in progress, but it is too early to give a definite answer to the problem. Thus, although the experiments are definite, the precise neutron structure question now awaits a more detailed calculation for the nuclear two-body problem. Even though there are some theoretical uncertainties, the observed cross sections definitely rule out a point magnetic moment for the neutron and the neutron size is crudely the same as that of the proton. Taking the data at face value, the neutron's rms magnetic radius is $(0.61 \pm 0.10) \times 10^{-18}$ cm.

One bit of experimental evidence that indicates that mesonic effects are not important may be obtained from the shape of the inelastic deuteron peaks at different mean values of q , such as those obtained at 75° , 90° , 105° , 120° , and 135° at 500 Mev. It is found (45) that all the peaks have essentially the same shape and half-width. If mesonic effects are important, it might be expected that the shapes would vary, particularly for such q 's that the isobaric state of the nucleon is excited. There appears to be no large effect of this kind.

Simple relativistic calculations for a collision between an electron and nucleons in motion have been made by the author. These show that, at a given energy at large angles, the scattered electrons resulting from electro-

disintegration of the deuteron will preserve an almost constant value for the half-width of the inelastic-energy spectrum. The experiments show just this behavior between 75° and 135° at 500 Mev, and thus it appears unlikely that mesonic effects will influence the validity of Eq. 116 to a large extent.

10. *The alpha particle.*—No new electron-scattering experiments on the alpha particle have been carried out beyond those reported (1). The experiments at 188 Mev (46) and at 400 Mev (47) are consistent with each other and show that the charge distribution is close to gaussian with a root-mean-square radius of 1.61×10^{-13} cm. It was pointed out by McAllister & Hofstadter (46) and also by Rustgi & Levinger (48) that the finite size of the proton should be allowed for in discussions of the "radius" of the alpha particle. Thus the root-mean-square radius (R), appropriate to an alpha particle containing point-nucleons, is close to 1.41×10^{-13} cm, as shown by the equation

$$R^2 = R_{ex}^2 - a_p^2; \quad a_p = 0.77 \quad 123.$$

where the radii are measured in units of 10^{-13} cm and R_{ex} is the experimental value of the radius, rather than equal to the experimental value, $R_{ex} = 1.61 \times 10^{-13}$ cm. The value, $R = 1.41 \times 10^{-13}$ cm, is in quite good agreement with the radius, 1.44×10^{-13} cm, obtained by Rustgi & Levinger (48) from an analysis of photodisintegration data on the alpha particle.

Foldy (49) has recently demonstrated for light nuclei that under very general assumptions the integrated electric-dipole photodisintegration cross section

$$\sigma_b = \int_0^\infty \frac{\sigma(E)}{E} dE \quad 124.$$

summed for photons of all energies E , may be written in the form originally discovered by Levinger & Bethe (50)

$$\sigma_b = \frac{4\pi^2}{3} \left(\frac{e^2}{\hbar c} \right)^2 \frac{ZN}{A-1} R^2 \quad 125.$$

in which N is the neutron number, Z the atomic number, A the mass number of the nucleus, and R^2 the mean-square-radius of the nucleus in its ground state. This radius refers to a nucleus composed of point-nucleons. Replacing R^2 according to Eq. 123, we may write

$$\sigma_b = \frac{4\pi^2}{3} \left(\frac{e^2}{\hbar c} \right)^2 \frac{ZN}{A-1} (R_{ex}^2 - a_p^2) \quad 126.$$

Both Rustgi & Levinger, and Foldy, find that the photodisintegration-data for helium yield $\sigma_b \approx 2.5$ to 2.7 millibarns while the expression (126) gives $\sigma_b = 2.53$ millibarns for $R_{ex} = 1.61 \times 10^{-13}$ cm. and $a_p = 0.77 \times 10^{-13}$ cm. Thus the agreement between the electron-scattering radius and the photodisintegration radius is quite satisfactory.

A similar analysis has been applied to the deuteron by the above authors (48, 49). If one allows for the finite size of the proton in the deuteron, the agreement with photodisintegration-data is also quite good.

11. *Nuclei of the first p-shell.*—In this section we shall treat nuclei of the first *p*-shell, i.e., those lying between lithium and oxygen, including carbon. The elastic scattering of C¹² has been investigated extensively both in experiment (51, 52) and in theory (53 to 56). The experiments of Fregeau and Hofstadter (51) and Fregeau (52) have been shown to be consistent with several alternative nuclear models whose broad features lie in between a uniform-charge distribution and a gaussian. The independent-particle shell model of a nucleus with an infinite harmonic well provides just such nuclear charge distributions. Fitting procedures (52, 53) show that this particular model reproduces the experimental results in carbon remarkably well. Because of this success in carbon, it is likely that the same model will generate charge distributions agreeing with experimental data for other members of the *p*-shell. For this reason we shall use this model as a spring board or as a first guess for finding the real charge distributions of such nuclei.

It has been shown by many investigators (40, 53, 54, 55, 56, 57, 58) that, for nuclei with incomplete 1 *p*-shells, the charge distribution may be expressed as

$$\rho(r) = \frac{2}{\pi^{3/2}} \frac{1}{a_0^3(2+3\alpha)} \left(1 + \alpha \frac{r^2}{a_0^2}\right) \exp - (r^2/a_0^2) \quad 127.$$

where the root-mean-square radius (*a*) of the charge distribution is given by

$$a = a_0 \sqrt{\frac{3(2+5\alpha)}{2(2+3\alpha)}} = ka_0 \quad 128.$$

and where the form factor is

$$F(qa) = \left[1 - \left(\frac{\alpha q^2 a_0^2}{2(2+3\alpha)}\right)\right] \exp - (q^2 a_0^2 / 4) \quad 129.$$

In these expressions

$$a_0 = \left(\frac{\hbar^2}{M\epsilon}\right)^{1/2} \quad 130.$$

where ϵ is the equidistant-energy interval between the successive levels of the harmonic oscillator, and a_0 is related to the curvature of the well. M is the usual mass of a proton. Using appropriate harmonic-well wave functions (40, 58, 59), one easily finds that

$$\alpha = \frac{1}{3}(Z - 2) \quad 131.$$

where Z is the atomic number of the *p*-shell nucleus. For example, $\alpha = 4/3$ for C¹² and Figure 3 shows typical harmonic-well charge distributions for B, C, and O. Now we shall turn to some specific cases. However, before we discuss the *p*-shell nuclei, we note that for the preceding *s*-shell, the helium nucleus is the special case where $Z = 2$.

(a) Helium. It is to be noted that for this nucleus one obtains $\alpha = 0$, and the shell model gives a pure Gaussian, as found by experiment (section 10).

For helium the experimental rms radius, $a = 1.61 \times 10^{-13}$ cm., yields, according to expression (128), $a = 1.223 a_0$ or $a_0(\text{He}) = 1.31 \times 10^{-13}$ cm. If corrected for the finite size of the proton, a corresponding value of a_0 , called a'_0 , would equal 1.15×10^{-13} cm., since $a = 1.41 \times 10^{-13}$ cm. in this case.

(b) Lithium. Li^6 belongs to a $(1s)^2(1p)^1$ proton configuration. For this nucleus, $Z = 3$ gives $\alpha = 1/3$. Now, Streib's (1) preliminary value of the rms radius for Li^6 was given as 2.78×10^{-13} cm, and the model used was a modified exponential [model XII (1)]. Further independent studies by Streib and the author show that other models with smaller rms radii also fit the data as well. A gaussian, with rms radius 2.37×10^{-13} cm and a uniform charge distribution with rms radius 2.10×10^{-13} cm, will provide satisfactory fits. If a harmonic-well p -shell type model is used, a is found to be about 2.44×10^{-13} cm and $a_0 = 1.80 \times 10^{-13}$ cm. Unfortunately there are no data at lower or higher energies, or absolute values of the cross section, to fix which of these models is correct. Higher energy experiments to settle these questions are now in progress. Thus, at present, it is not possible to decide between the larger and smaller sizes. However, as we shall see, the evidence from nearby nuclei probably favors the smaller size. Of course, with precise data, it is possible to decide between the shapes and sizes unequivocally. (Newer data at 420 Mev taken by G. Burleson and the author support the smaller size and give a in the neighborhood of 2.1×10^{-13} cm.)

(c) Beryllium. This nucleus has the proton configuration $(1s)^2(1p)^2$. The early data of Hofstadter *et al.* (60) at 125 Mev were analyzed by these authors and yielded best fits for the rms radius of uniform and gaussian models of 1.90×10^{-13} cm and 1.96×10^{-13} cm, respectively. However, the early data were corrected for the "anomalous" width of the elastic profiles. [See Fig. 6 and 10 of ref. (60).] This width at large angles was later shown to be due to the partial inclusion in the elastic profile of the first inelastic peak (61). By using the original data, instead of the "corrected" data, of Figure 10 (60), one easily finds that the rms radii for the uniform and gaussian models are 2.17 and 2.28×10^{-13} cm, respectively. The independent data at 190 Mev (61) can also be analyzed and the results in this case are found to give corresponding values of 1.99 and 2.39×10^{-13} cm for the uniform and gaussian models, respectively.

The harmonic-shell charge distribution Eq. 127 with $\alpha = 2/3$ ($Z = 4$) may also be fitted to the two angular distributions at 125 Mev and 190 Mev (60, 61) and yields, since $a = \sqrt{2}a_0$ for $Z = 4$, the value $a = 2.2 \times 10^{-13}$ cm or $a_0 = 1.56 \times 10^{-13}$ cm. It is to be noted that the energy 125 Mev is low enough so that there is little effect on the rms size because of a choice of different models. Thus the rms size is uniquely found to be $2.2 \pm 0.2 \times 10^{-13}$ cm. All the above results are consistent with this value. The preliminary data of Streib (62) are also in agreement with the above conclusions. Gatha *et al.* (63) and Tassie (59) have analyzed the Be scattering data of references 60 and 61 and find agreement with the above conclusions within the experimental error.

(d) Carbon. The details of obtaining the best fit between experiment and

theory for this $(1s)^2(1p)^4$ proton configuration will be found in the original papers and have been discussed (1). In this section we shall merely point out that a harmonic-well model (Eq. 127) with $\alpha=4/3$ fits the elastic-scattering data extremely well. It is not possible to distinguish convincingly between $\alpha=4/3$ and other close values such as $\alpha=1$ and $\alpha=2$, provided that appropriate choices of a are also made. However, $\alpha=4/3$ gave the best fit of all models tried.

Now in the case of C^{12} there are new data at higher energy to compare with the predictions of the older models. In Figure 4 we have already shown the new data of Sobottka & Hofstadter (10). The data can be analyzed by the Born approximation shown as a dashed line in Figure 4. However, the minimum is not properly reproduced, as expected. The solid line in Figure 4 represents the results of the accurate phase-shift method to be discussed in section 12. The exact calculation shown in the figure has been made by D. G. Ravenhall for the model of eq. 127 with $\alpha=4/3$ and $a=2.40 \times 10^{-13}$ cm. or equivalently $a_0=1.64 \times 10^{-13}$ cm. These are essentially the same parameters which are used to fit the low-energy data (187 Mev) (51, 52). The fit is seen to be very good, and the position and depth of the minimum are reproduced within experimental error. Since the low-energy analysis did not have the advantage of working with the diffraction minimum of Figure 4, the good fit must be counted as a strong justification for the method and confirms many of the assumptions which have gone into the theory. In particular, the static model of the charge distribution in the nucleus appears to be quite faithful, and dispersion corrections to this model must be very small.

It should be mentioned that when the proton size is allowed for, the parameter of the best fit, such as $a_0=1.64$, will be changed slightly, but the phenomenological shell-type charge distribution given by Eq. 127 still describes the experimental scattering. Folding-in of the proton charge distribution will multiply the form factor of Eq. 129 by $\exp(-q^2 a_0^2(p)/4)$, thus giving

$$F(qa) = \left[1 - \frac{\alpha q^2 a_0^2}{2(2+3\alpha)} \right] \exp \left[-\frac{q^2}{4} (a_0^2 + a_0^2(P)) \right] \quad 132.$$

where

$$a_0(P) = \frac{0.72}{1.224} \times 10^{-13} \text{ cm.} = 0.59 \times 10^{-13} \text{ cm.}$$

if a gaussian model with $a=0.72 \times 10^{-13}$ cm. is chosen for the proton.

(e) Oxygen. The same type of shell-model calculation can be applied to O^{16} , where shell theory predicts a value $\alpha=2$, since O^{16} is expected to have the proton configuration $(1s)^2(1p)^6$. The Born-approximation form factor for this case is quite similar to the curve shown in Figure 2 for $\alpha=4/3$, except that the $O^{16}(\alpha=2)$ minimum occurs at a value of $x=qa=4.24$ instead of 4.42 for C^{12} ($\alpha=4/3$). The maximum near $x=5.3$ is also slightly higher for $\alpha=2$ than for $\alpha=4/3$. Figure 17 shows new experimental data in O^{16} of Ehrenberg, Meyer-Berkhout, and the author (64), obtained at 420 Mev with the

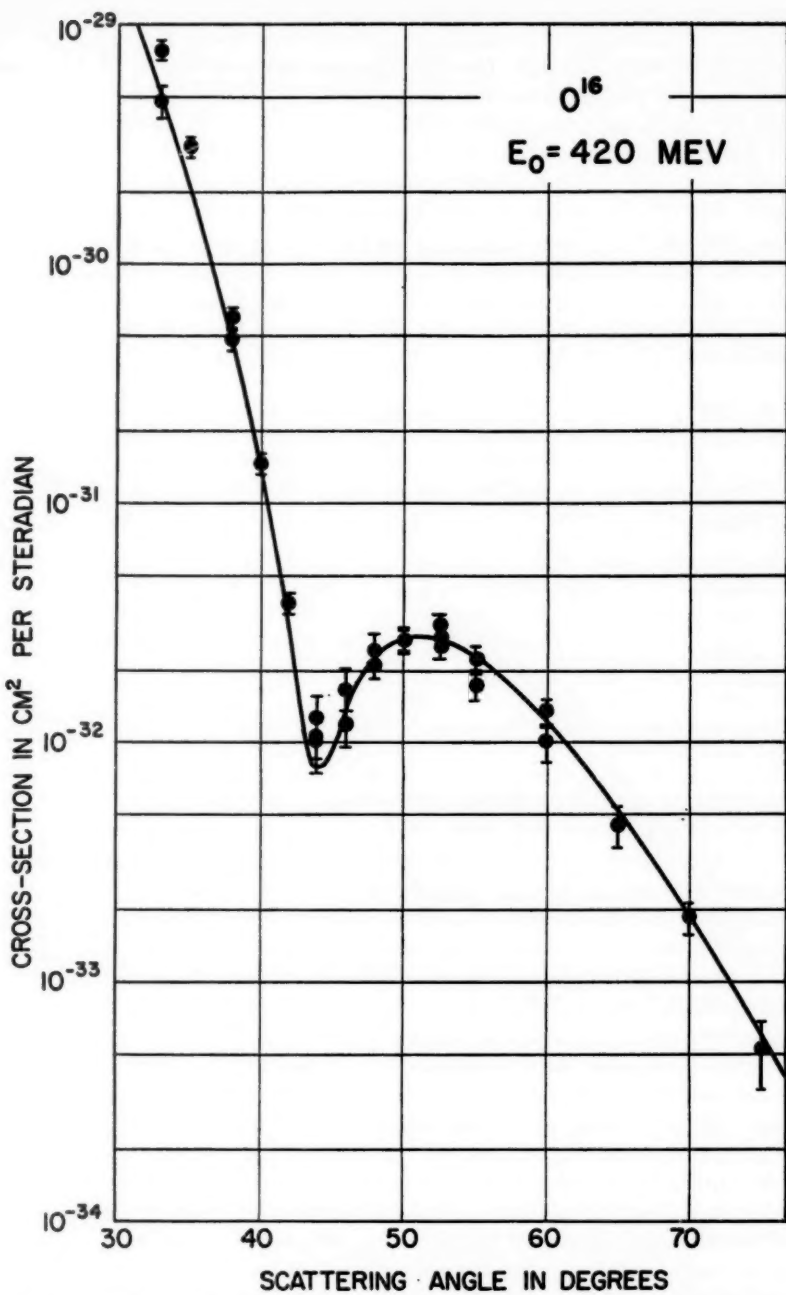


FIG. 17. New experimental data of Ehrenberg *et al.* (64) obtained at 420 Mev for the O^{16} nucleus. The figure also shows the exact calculations of D. G. Ravenhall for the harmonic-well model for which $\alpha=2.0$ and $a_0=1.75\times 10^{-13} \text{ cm}$.

Stanford 36" spectrometer. The minimum occurs near 43.7° and when used with the Born-approximation form factor, Eq. 129, gives a value of $a = 2.64 \times 10^{-13}$ cm. or $a_0 = 1.77 \times 10^{-13}$ cm. Again, if a correction is made for the finite size of the proton, the value of a_0 would be slightly smaller for a given value of a . Figure 17 shows also the exact phase-shift calculation of D. G. Ravenhall for the harmonic-well model ($\alpha = 2$) and the parameter $a_0 = 1.75 \times 10^{-13}$ cm. As in the case of carbon, the fit is very good.

Summary.—We may summarize the above results for a_0 in Table I. No correction has been applied for a finite proton size in the table.

Thus, except for the Li⁶ result, which is questionable, there is a slight tendency for ϵ to decrease as the p -shell is filled in. We must await more

TABLE I
PARAMETERS FOR p -SHELL NUCLEI

Nucleus	Proton Configuration	$a(10^{-13}\text{cm.})$	$a_0(10^{-13}\text{cm.})$	$\epsilon(\text{Mev})$
He ⁴	(1s) ²	1.61	1.31	18.7
Li ⁶	(1s) ² (1p) ¹	2.44(?)	1.80(?)	9.9(?)
Be ⁹	(1s ²)(1p) ²	2.2	1.56	13.3
C ¹²	(1s ²)(1p ⁴)	2.40	1.64	12.0
O ¹⁶	(1s ²)(1p ⁶)	2.64	1.77	10.3

accurate data to substantiate these results but the tendency already seems clear. The newer data on Li⁶ ($a = 2.1$) confirms the tendency.

12. Heavier nuclei: The phase-shift calculations for elastic scattering

(a) Lower energies.—We have seen in section II, B, 3 that the experimental results for nuclei heavier than the proton or deuteron, such as C¹², could not be analyzed precisely by the Born approximation because of inaccuracy near the diffraction features of the scattering pattern. On the other hand, the Born approximation is quite good for C¹² and for other light nuclei in regions more remote from the diffraction zeroes, and it has been useful in describing the coarse features of electron scattering even for nuclei as heavy as copper ($Z = 29$). The same kind of relationship exists also for the point-nuclear-model, and it was recognized early by Bartlett & Watson (65) and by Feshbach (66) that the accurate calculations for high Z differed widely from the Born results. Nowadays the model of a point-nucleus of high-atomic number is of more-or-less academic interest in its own right, but because of its relevance to low-energy scattering (0–10 Mev) and also because the more exact methods make phase-shift comparisons with the point-charge wave functions, the point-charge calculations have considerable value.

For low values of Z , McKinley & Feshbach (67) have carried out an evaluation of the conditionally convergent, infinite series of Mott (67a) and have derived a scattering formula for cases when $Z/137$ is not large and when

$$\beta = \frac{v}{c} \cong 1 \quad 133.$$

This formula applies with relatively small errors for nuclei up to values of $\alpha \cong 0.2$ where

$$\alpha = \frac{Ze^2}{\hbar c} = \frac{Z}{137} \quad 134.$$

thus up to about copper. The McKinley-Feshbach formula for elastic scattering may be represented in closed form as

$$\left(\frac{d\sigma}{d\Omega} \right)_F = \left(\frac{Ze^2}{2E_0} \right)^2 \frac{\cos^2 \theta/2}{\sin^4 \theta/2} \left[1 + \frac{\pi Z}{137} \frac{(\sin \theta/2)(1 - \sin \theta/2)}{\cos^2 \theta/2} \right] \quad 135.$$

where the center-of-mass correction has been omitted since it is so very small.

However, this formula fails for higher values of Z and an accurate closed formula for such scattering is unknown. [For a closed-formula approximation, see ref. (131).] McKinley & Feshbach also developed an expansion which yields the scattering up to terms in α^4 , but these results must be expressed numerically (67). R. M. Curr (68) has extended these calculations to energies greater than 0.5 Mev ($\alpha \cong 1$) up to and including terms in α^8 . Thus, for $Z \cong 82$ ($\alpha = 0.6$), the error of these solutions is less than 1 per cent. The power series of Curr, which is expressed as a ratio

$$R = \frac{\sigma}{\sigma_R} \quad 136.$$

of σ to the Rutherford cross section,

$$\sigma_R = \left(\frac{Ze^2}{2mv^2} \right)^2 (1 - \beta^2) \csc^4 \theta/2 \quad 137.$$

is given in the form of a single power series. Curr compares his approximation with an exact calculation of Yadav (69) for uranium. The results are shown in Figure 18. Thus we may say that for energies > 0.5 Mev, the point-charge scattering problem for unpolarized electrons has been solved to a high degree of accuracy for all elements. Tables of the desired scattering cross sections are to be found in Curr's paper. (See also footnote on p. 201 of ref. 73).

The question of experimental verification of the low-energy electron scattering theory is a long and involved one. Recent work, in which references to the early papers are given, has been reported by Chapman *et al.* at 0.4–0.5 Mev (70), Brown *et al.* at 0.4–0.5 Mev (71), Bayard & Yntema at about 1 Mev (72), and Damodaran & Curr (73). The new results in Al, Au, and U are in quite good agreement with Curr's theoretical work, and there seems to be little doubt that the Curr theory gives a correct representation of all the experiments. The early work by Van de Graaff *et al.* (74, 75) also gave excellent agreement with theory. [See Figure 5 of ref. (67).] A review of these and other pertinent electron-scattering results up to 1955 has been given by Urban (76).

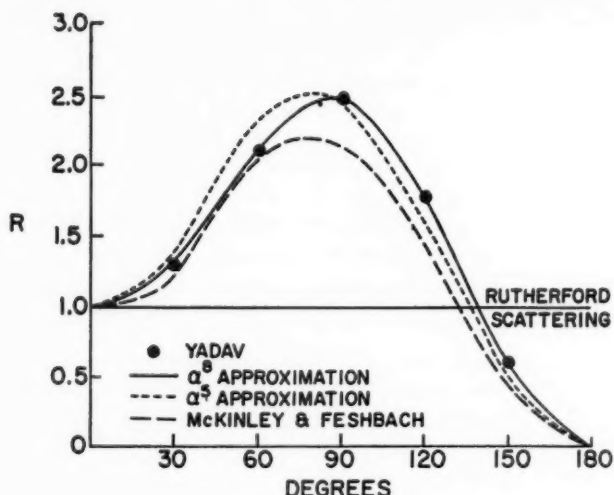


FIG. 18. Comparison of the results of the Curr approximation (68) with the exact calculations of Yadav (69) for point-uranium nuclei. The results of the McKinley-Feshbach calculation are also shown. The value of R is given in Eq. 136.

At energies even lower than those discussed above, exact calculations have been made by Doggett & Spencer (77) and by Sherman (78). The latter work also presents data on polarization. Doggett & Spencer's calculation covers the energy range (0.05 to 10 Mev) and provides positron-scattering results as well as electron-scattering data.

For the heavier nuclei of finite size, the phase-shift methods must be employed (79, 80). Elton (81) and Parzen (82) appear to have been the first investigators to look into the effects of finite nuclear size on the exact phase-shift scattering formulas, although, as is well known, the Born approximation was first applied to problems of finite nuclei by Guth (83) and independently by Rose (26). Elton was successful in finding such effects at electron energies in the neighborhood of 20 Mev for gold nuclei, and offered an explanation of the experimental results at 15.7 Mev of Lyman *et al.* (84) in terms of uniform and spherical-shell charge distributions with radii $R = 1.41 \times A^{1/3} \times 10^{-13}$ cm. Elton showed also that only the zero-order phase shift was important for the calculations at an energy of 20 Mev, unless very high experimental accuracy could be obtained.

Acheson (85) and Feshbach (86) made further developments along these lines for various values of Z at energies between 15 and 40 Mev. Acheson showed that at such energies the rest mass of the electron could be ignored in the basic differential equations, and the resulting calculations could be greatly simplified. All succeeding authors employ this approximation. Acheson and Feshbach demonstrated further that the phase shifts at high energies essentially depend only on a product of the incident electron energy and a radial parameter of the nucleus and not separately on these quantities.

The scattering depends also, to be sure, on the nuclear charge Z . At energies for which the energy-radius product is small compared with unity, Feshbach showed that the zero-order phase shift involves only the volume integral over the nucleus of the deviation of the electrostatic potential from that of a point charge. This kind of result led to the term "model independence" of the nuclear charge distribution (87, 88) in connection with low-energy (20 Mev for heavy nuclei) electron scattering experiments. For such energies, the scattering cross section is essentially the same for two different models whose mean-square radii are chosen to be equal. An exact statement of this result is given in Eq. 26 of Feshbach's article (86) in terms of the electrostatic potentials of the respective charge distributions. Further work on Feshbach's low-energy theorem will be found in an investigation by Bodmer (89).

On the other hand, Elton (87) and Bodmer (89) show already that at ~ 40 Mev for heavy nuclei model independence begins to break down. Again, Glassgold (90) has made exact phase shift calculations with various models to test the idea of model independence at higher energies, and finds, in agreement with Elton and Bodmer, that at 30 to 45 Mev for heavy nuclei, shell and uniform distributions give different scattering cross sections at large angles. Thus the idea of model independence has limited applicability and only in those cases for which not more than one or two phase shifts are important for the calculation of the cross sections, or essentially where $R < \lambda$. R is the "radius" and λ is the reduced de Broglie wavelength of the incident electrons.

There appears to be a fair amount of confusion in the literature regarding model independence at higher energies. For example, it has been stated (91) that if the scattering experiments "are used to derive as detailed a picture as possible of the density distribution, the electron energy ought not to be taken too large," and therefore it is suggested that the greatest sensitivity should be obtained at about 70 Mev. The basis of the statement is attributed to work of Fowler (92) and Reignier (93, 94). However, it must be pointed out that Fowler's work considers only s , p , and d phase shifts. Of these, the d phase-shift correction is made model independent by a proper choice of the ratio of sizes of shell and uniform charge-density models. Actually, however, the s phase shift is observed to be "model dependent" and no calculation is presented for the p phase shift. Reignier's work also shows that all phase shifts cannot be simultaneously made model independent by a proper choice of radii. In fact, as we shall now see, and this seems to be not properly appreciated by many authors, the exact phase shift methods at the higher energies ($E > 100$ Mev) demonstrate unequivocally that the higher phase shifts are very important and must not be neglected. Even the smallest differences in phase shifts make very appreciable changes in cross section because of a very delicate cancellation which takes place in the sum of the partial wave contributions at the larger scattering angles. In the next sections we shall deal with the exact method at high energies and shall illustrate this very great sensitivity to small variation in phase shift (116).

(b) Higher energies. At higher energies nuclei no longer appear as points and their various shapes and sizes may be delineated by the methods of electron scattering. Several independent calculations have been carried out with the Dirac electron theory for nuclei of finite size at higher energies ($E > 100$ Mev) by the exact phase-shift methods. Among these, we may enumerate the works of Yennie, Ravenhall & Wilson (95, 96), Brenner, Brown & Elton (97), Ravenhall & Yennie (98), Brown & Elton (99), Hill & Freeman & Ford (100), Hahn, Ravenhall & Hofstadter (101). Most of these calculations are not different in principle. Some differ in computational details, others differ because they are applied to different nuclear models. Furthermore, all methods are similar to those developed by Elton (81) and Parzen (82) for the lower energies. The newer calculations require the use of more numerous phase shifts.

Many of the recent calculations are similar to those of Yennie *et al.* (96) and since that paper gives a straightforward account of the general method, we choose below to follow their outline of theory. We shall omit computational details but shall retain enough of the method to permit a basic understanding of the mode of calculation required for finite nuclei at high energies.

Before we study the method itself, a few remarks about its limitations should be stated. The finite nucleus will be treated in the elastic-scattering approximation in which granular structure is ignored. Instead, the nuclear charge distribution will be represented by a smoothed static potential. Furthermore, we shall restrict the calculations to cases where the density distribution is known to be spherically symmetric, or nearly so. In the literature, as far as the author knows, there is no evidence that the outlined method of approach is not satisfactory for elastic scattering at the energies under consideration, say less than 500 Mev.

Effects of granularity do appear in the inelastic-scattering continua observed from all nuclei at high energies, and can thus indirectly affect the elastic scattering. [See section 8 and refs. (1), (40), and (41).] An estimate of the effect of the totality of all kinds of (nonradiative) inelastic processes on the magnitude of the elastic-scattering process has been carried out by Valk (102), according to a phenomenological first Born-approximation theory. Valk's theory describes the inelastic processes by the addition of an imaginary term to the interaction Hamiltonian responsible for elastic scattering and is thus similar in approach to nuclear-reaction theory. The theory is applied to electron-proton and electron-deuteron elastic scattering. Up to reasonably high energies and large angles (450 Mev, 120°), the corrections are less than a few per cent and practically zero for the proton. Ravenhall (103) has estimated that for heavier nuclei the corrections still remain small.

The effects of granularity are related to correlations in the nucleons' coordinates and these in turn are related to "dispersion effects." Thus a limitation of the method is that dispersion scattering is not included. The dispersion process refers to a double interaction in which a nucleus may be raised virtually to an excited state by the incident electron. The nucleus, during a subsequent transition and scattering process, returns the excitation

to the electron. Thereby the nucleus is returned to its ground state. Since the process involves two steps, it may understandably be smaller than the direct interaction of the electron with the ground state of the nucleus. With the Born approximation, Schiff (104) and Valk & Malenka (105) have shown that the contribution of dispersion scattering, due to virtual excitation, is only of the order of 1/137 of the usual elastic scattering from the ground state. No experimental test of this conclusion is as yet available. (For a further discussion of correlation effects, see section 15.)

The radiative correction of Schwinger (106) and Suura (107) will only be mentioned briefly at this point, because the correction itself is small for relative measurements. When absolute cross sections are to be compared with theory, the correction must be included and is of the order of 10 to 20 per cent. A discussion of the radiative correction has been given in reference 1,⁴ and since the theory of the radiative process will not be entered into in this review, it appears wiser to omit further discussion of the theory.

Reference should be made however to a recent suggestion by Lomon (108) for a test of the radiative correction at high energies, and to recent articles by McAllister (109) and Tautfest & Panofsky (110), who have shown that there is no outstanding violation of the Schwinger-Suura result. However, these recent results do not furnish a sensitive test of the theory of the radiative corrections.

Subject to the limitations and corrections just described, the representation of Yennie *et al.* (96) of the Dirac electron-finite-nucleus scattering theory will be treated below. As pointed out by Acheson (85), the rest-mass of the electron may be eliminated from the basic equations of high energy electron scattering theory without introducing relative errors greater than $(mc^2/E_0)^2$, which is exceedingly small. The elimination of the mass-term results in a great simplification of the theory, and the Dirac Eq. 33 can be written

$$(\alpha \cdot pc + W)\psi = E\psi \quad 138.$$

where

$$W = eV \quad 139.$$

and is the electrostatic potential energy of the smoothed density distribution. It proves advisable to choose a representation for the Dirac matrices which is slightly different from the one given by Eq. 34:

$$\alpha_1 = \begin{bmatrix} 0 & 1 & 0 & 0 \\ 1 & 0 & 0 & 0 \\ 0 & 0 & 0 & -1 \\ 0 & 0 & -1 & 0 \end{bmatrix}; \quad \alpha_2 = \begin{bmatrix} 0 & -i & 0 & 0 \\ i & 0 & 0 & 0 \\ 0 & 0 & 0 & i \\ 0 & 0 & -i & 0 \end{bmatrix}; \quad \alpha_3 = \begin{bmatrix} 1 & 0 & 0 & 0 \\ 0 & -1 & 0 & 0 \\ 0 & 0 & -1 & 0 \\ 0 & 0 & 0 & 1 \end{bmatrix}; \quad 140.$$

$$\beta = \begin{bmatrix} 0 & 0 & 1 & 0 \\ 0 & 0 & 0 & 1 \\ 1 & 0 & 0 & 0 \\ 0 & 1 & 0 & 0 \end{bmatrix}.$$

⁴ Typographical errors were made in equation 31 (1). The fraction $\frac{17}{13}$ should be replaced by $\frac{17}{2}$, and the capital M should be replaced by small m.

This set of matrix operators may be represented more conveniently as

$$\alpha_i = \rho_i \sigma_i \quad \beta = \rho_1 \quad 141.$$

in terms of Dirac's nomenclature (111). The Dirac matrices $\sigma_1, \sigma_2, \sigma_3$ may be identified with (4×4) matrices in which the Pauli (2×2) matrices $\sigma_x, \sigma_y, \sigma_z$ of Eq. 35 are repeated along the diagonals (111). The representation in Eq. 141 is especially useful for working with the double set of two-component wave functions,

$$\begin{pmatrix} \phi_1 \\ \phi_2 \end{pmatrix}, \quad \begin{pmatrix} \chi_1 \\ \chi_2 \end{pmatrix},$$

thus

$$(\delta \cdot \mathbf{p}c + W - E) \begin{pmatrix} \phi_1 \\ \phi_2 \end{pmatrix} = 0 \quad 142.$$

$$(-\delta \cdot \mathbf{p}c + W - E) \begin{pmatrix} \chi_1 \\ \chi_2 \end{pmatrix} = 0 \quad 143.$$

where δ refers to the Pauli matrices of Eq. 35. This is clear since β may be neglected in Eq. 33, because of the small electron rest mass, and then the α matrices break down into the smaller Pauli matrices.

When the potential is removed, thus for free waves,

$$\begin{pmatrix} \phi_1 \\ \phi_2 \end{pmatrix} = \begin{pmatrix} u_1 \\ u_2 \end{pmatrix} \exp i\mathbf{k} \cdot \mathbf{r}; \quad \begin{pmatrix} \chi_1 \\ \chi_2 \end{pmatrix} = \begin{pmatrix} v_1 \\ v_2 \end{pmatrix} \exp i\mathbf{k} \cdot \mathbf{r} \quad 144.$$

where

$$\mathbf{k} = \frac{\mathbf{k}_0}{\lambda} \quad 145.$$

and \mathbf{k}_0 is a unit vector in the direction of the incident wave (polar angles θ, φ). The solutions for ϕ and χ may then be found by substitution in Eq. 142 and 143 and are

$$\begin{pmatrix} \phi_1 \\ \phi_2 \end{pmatrix} = \begin{pmatrix} \cos \theta/2 \\ \sin \theta/2 e^{i\varphi} \end{pmatrix} \quad 146.$$

$$\begin{pmatrix} \chi_1 \\ \chi_2 \end{pmatrix} = \begin{pmatrix} -\sin \theta/2 e^{-i\varphi} \\ \cos \theta/2 \end{pmatrix} \quad 147.$$

The solutions ϕ, χ correspond to the two spin states of the electron relative to the direction of the electron's momentum. In the first state the spin vector may be thought of qualitatively as precessing tightly about the incident momentum vector with a positive component along that direction, and in the second state the component will be negative along \mathbf{k}_0 . The solutions corresponding to Eq. 146 and 147 may be written equivalently as

$$\phi = \begin{pmatrix} 1 \\ \tan \theta/2 e^{i\varphi} \end{pmatrix} \quad 148.$$

$$\chi = \begin{pmatrix} -\tan \theta/2 e^{-i\varphi} \\ 1 \end{pmatrix} \quad 149.$$

where the normalization factor is modified by dividing by $\cos \theta/2$. Now, when the potential energy W is put back into the Dirac equation, the asymptotic form of the solutions will have to resemble the free wave situation, Eq. 148 and 149, except for the radial spreading factor $r^{-1}e^{ikr}$ and angular factors f_1, f_2 which determine the angular distribution of scattered electrons. Putting $\theta=0$ for the incident state vector (first term in Eq. 150 and 151), we may write for the complete asymptotic wave functions

$$\phi \rightarrow \begin{pmatrix} 1 \\ 0 \end{pmatrix} e^{ikz} + r^{-1}f_1(\theta, \varphi) \begin{pmatrix} 1 \\ \tan \theta/2 e^{i\varphi} \end{pmatrix} e^{ikr} \quad 150.$$

$$\chi = \begin{pmatrix} 1 \\ 0 \end{pmatrix} e^{ikz} + r^{-1}f_2(\theta, \varphi) \begin{pmatrix} -\tan \theta/2 e^{i\varphi} \\ 1 \end{pmatrix} e^{ikr} \quad 151.$$

where the direction of the original beam lies along the z axis. It may be shown (96) that at the high energy in this problem there is nothing physical to distinguish between the scattering of the two spin states for a spherically symmetric potential. Hence in the scattering problem only the first wave, ϕ , needs to be considered. χ adds nothing new.

The phase-shift method now proceeds to decompose the solutions ϕ of the scattering Eq. 142 into a set of partial waves which are simultaneous eigenfunctions of the total angular momentum operator (squared), J^2 , and its z -component, J_z . The operator J can be written as

$$J = \mathbf{r} \times \mathbf{p} + \frac{1}{2}\hbar\mathbf{\sigma} \quad 152.$$

and the z component

$$J_z = xp_y - yp_x + \frac{\hbar}{2}\sigma_z = \frac{\hbar}{i} \left(x \frac{\partial}{\partial_y} - y \frac{\partial}{\partial_x} \right) + \frac{\hbar}{2}\sigma_z \quad 153.$$

The eigenvalues of J^2 and J_z are $j(j+1)\hbar^2$ and $m\hbar$ according to the well-known behavior:

$$J^2\phi_{jm} = j(j+1)\hbar^2\phi_{jm}; \quad J_z\phi_{jm} = m\hbar\phi_{jm} \quad 154.$$

where the wave function ϕ is now broken down into its partial waves ϕ_{jm}

$$\phi = \sum a_{jm}\phi_{jm} \quad 155.$$

For the incident plane wave, that is, the first term in equation 150, $m=+\frac{1}{2}$, and since we shall consider only one spin orientation, the only states of concern are those designated as $\phi_{j,1/2}$. It may be noticed that the decomposition of Eq. 155 into states of given j is a bit unlike the usual treatment (13). In Eq. 155, states of a given $\phi_{j,1/2}$ do not have a definite parity. On the other hand, the usual decomposition into states of given orbital-angular momentum gives them a definite parity.

The scattered angular-wave-parts of the complete wave functions (of which Eq. 150 and 151 are the asymptotic forms) are

$$\chi_j^{(1)} = \begin{pmatrix} (j + \frac{1}{2})P_{j-1/2}(\cos \theta) \\ -P_{j-1/2}^1(\cos \theta)e^{i\varphi} \end{pmatrix} \quad 156.$$

$$\chi_j^{(2)} = \begin{pmatrix} (j + \frac{1}{2})P_{j+1/2}(\cos \theta) \\ P_{j+1/2}^1(\cos \theta)e^{i\varphi} \end{pmatrix} \quad 157.$$

where $\chi^{(1)}$ and $\chi^{(2)}$ are not to be confused with the χ of Eq. 143, corresponding to the second spin state. Two sets of Legendre functions $P_{j-1/2}$ and $P_{j+1/2}$ are now required, corresponding to the fact that two values of the orbital-angular momentum are associated with a given value of j . One has even and the other had odd parity. The associated Legendre functions $P_{j-1/2}^l$ or $P_{j+1/2}^l$ are to be found in many sources [p. 127 of ref. (112)]. The partial wave functions $\chi_j^{(1)}$ and $\chi_j^{(2)}$ are essentially like those found originally by Darwin (113), but the notation is not the same. [The difference in notation is explained in detail in Appendix 1 of ref. (96).]

The partial wave, now containing the radial behavior as well as the angular part of Eq. 156 and 157, becomes

$$\phi_{j,1/2} = r^{-1}(G_j(r)\chi_j^{(1)} + iF_j(r)\chi_j^{(2)}) \quad 158.$$

which is really a double equation, corresponding to the two rows of each of Eq. 156 and 157. F_j and G_j are the radial wave functions satisfying the Dirac equation and both F_j and G_j will depend on the exact nature of the potential V and hence on the assumed distribution of charge density in the nuclear model. The equations for F and G , corresponding to the Darwin treatment [see ref. (13), p. 75], can be obtained as shown in reference 96, by the use of appropriate simplifications, in the following form.

$$\frac{dG_j}{dr} - \frac{(j+\frac{1}{2})}{r} G_j + \frac{(E-W)}{\hbar c} F_j = 0 \quad 159.$$

$$\frac{dF_j}{dr} + \frac{(j+\frac{1}{2})}{r} F_j - \frac{(E-W)}{\hbar c} G_j = 0 \quad 160.$$

It is necessary to solve this pair of coupled equations, from which one can obtain a single second-order differential equation. It may easily be seen that the substitutions

$$x = kr \quad 161.$$

$$w = \frac{W}{E} \quad 162.$$

make the Eq. 159 and 160 dimensionless, in which case we obtain

$$\frac{dG_j}{dx} - \frac{(j+\frac{1}{2})}{x} G_j + (1-w)F_j = 0 \quad 163.$$

$$\frac{dF_j}{dx} + \frac{(j+\frac{1}{2})}{x} F_j - (1-w)G_j = 0 \quad 164.$$

In practice, w is generally a small quantity, though we shall not require w to be small in the following treatment.

It is well known [ref. (13), p. 78] that the long-range character (r^{-1}) of the Coulomb interaction distorts the waves far from the charge center into a form like Eq. 150 and 151, but containing an extra $\ln r$ term in the exponent of the exponential term. This additional radial dependence does not introduce any real difficulties into the problem, but it proves useful to illustrate first the phase-shift method with a simpler example not containing the additional radial term. Later we shall come back to the Coulomb case. With

any non-Coulomb field, which falls to zero faster than r^{-1} outside a certain finite range, the wave function ϕ will have the asymptotic form

$$\phi_{\text{incident}} + \phi_{\text{scattered}} = \phi \cong \begin{pmatrix} 1 \\ 0 \end{pmatrix} e^{ix \cos \theta} + x^{-1} k f(\theta) \begin{bmatrix} 1 \\ \tan \frac{\theta}{2} e^{i\varphi} \end{bmatrix} e^{ix} \quad 165.$$

which is Eq. 150 together with the substitution of Eq. 161. Now the differential scattering cross section employs Eq. 41, although we have now reduced the problem from four components to the two components of Eq. 165 by our previous elimination of the second spin state. As we have seen, this second state gives the same results as the spin state we are using. The incident beam is normalized to unity, according to the first term in Eq. 165 so that the cross section for the scattered wave is obtained from the two components of the second term and is

$$\frac{d\sigma}{d\Omega} = \frac{x^2}{k^2} |x^{-1} k f(\theta)|^2 (1 + \tan^2 \theta/2) = \sec^2 \theta/2 |f(\theta)|^2 \quad 166.$$

The usual method of finding $f(\theta)$ depends on a comparison of the wave function ϕ of Eq. 165 with the expansion of the incident plane wave into partial waves in a well-known manner (ref. 13, p. 22), thus

$$\phi_{\text{incident}} = \sum_{j=1/2=0}^{\infty} \left(\frac{\pi}{2x} \right)^{1/2} i^{j-1/2} \{ J_j \chi_j^{(1)} + i J_{j+1} \chi_j^{(2)} \} \quad 167.$$

corresponding to the functions of Eq. 156 and 157. The J_j are the ordinary Bessel functions (114) and are related to the spherical Bessel functions (Eq. 100) through the relation

$$j_l(x) = \sqrt{\frac{\pi}{2x}} J_{l+1/2}(x) \quad 168.$$

The expression for the incident wave is more commonly written as an expansion in terms of waves of a single parity instead of terms of mixed parity as in Eq. 167. With some algebraic manipulations, the form of Eq. 167 may be shown to be equivalent to the more common expansion (ref. 13, p. 22).

The complete wave, $\phi_{\text{incident}} + \phi_{\text{scattered}}$, is also expanded into a series of eigenfunctions

$$\phi = \sum_{j=1/2=0}^{\infty} x^{-1} i^{j-1/2} e^{i\eta_j} [G_j \chi_j^{(1)} + i F_j \chi_j^{(2)}] \quad 169.$$

and must be identical with ϕ of Eq. 165. Thus the expression in Eq. 167 is really a part of ϕ in Eq. 169. The $e^{i\eta_j}$ are introduced as arbitrary coefficients of expansion which are to be chosen to satisfy the particular conditions of the scattering problem. It will be seen that the η_j introduced here are the all-important phase shifts.

In Eq. 163 and 164, when $x \rightarrow \infty$, the asymptotic solutions for G and F are easily found to satisfy

$$\frac{d^2G_j}{dx^2} + G_j = 0; \quad \frac{d^2F_j}{dx^2} + F_j = 0 \quad 170.$$

since $w \rightarrow 0$ and the $1/x$ term approaches zero as $x \rightarrow \infty$. Consequently G_j and F_j are harmonic functions at ∞ . Asymptotically, therefore,

$$G_j \rightarrow \sin(x - \frac{1}{2}(j - \frac{1}{2})\pi + K_j) \quad 171.$$

and there is a similar equation for F_j . The phase K_j , which is a constant of integration, is written in the form of Eq. 171 so that G_j may be compared with the asymptotic behavior of Eq. 167, which is determined by (ref. 2, p. 868).

$$J_j(x) \rightarrow \left(\frac{2}{\pi x}\right)^{1/2} \sin(x - \frac{1}{2}(j - \frac{1}{2})\pi) \quad 172.$$

By substitution of Eq. 171 into Eq. 169 and Eq. 172 into Eq. 167 and subsequent comparison, it is easily seen that

$$K_j \equiv \eta_j \quad 173.$$

and thus the phases K_j are identical with the η_j originally introduced as arbitrary coefficients.

Now by equating Eq. 169 to Eq. 165 with the substitution for the incident wave equation 167 and by placing the coefficients of the e^{ikr} terms equal to each other, we obtain

$$f(\theta) = \frac{1}{2ik} \sum (e^{2i\eta_j} - 1)(j + \frac{1}{2})(P_{j-1/2} + P_{j+1/2}) \quad 174.$$

$$= \frac{1}{2ik} \sum e^{2i\eta_j}(j + \frac{1}{2})(P_{j-1/2} + P_{j+1/2}) \quad 175.$$

where the second part of the first parenthesis of the summation of Eq. 174 yields zero (96) except in the forward direction ($\theta = 0$), where we shall not use $f(\theta)$ anyway.

With $d\sigma/d\Omega$, given by Eq. 166 and the expression 175 just derived for $f(\theta)$, we are enabled to find the differential scattering cross section. However, now we see that it is necessary to find the series of values η_j . This is the main part and the most difficult part of the scattering problem and can only be done by solving Eq. 163 and 164 in a suitable manner, so that the solution for G_j joins on smoothly with the asymptotic value it must have in Eq. 171. However, G_j of Eq. 171 is the non-Coulombic solution for potentials w that vanish quickly enough with increasing r . Now the Coulomb functions do not vanish so quickly and therefore we must make a modification in the asymptotic behavior of G_j . In the Coulomb case [ref. (13), p. 78],

$$G_j(x) \rightarrow \sin[x + \gamma \ln 2x - \frac{1}{2}(j - \frac{1}{2})\pi + \eta_j] \quad 176.$$

where

$$w = -\frac{Ze^2}{\hbar c} x^{-1} = -\gamma x^{-1} \quad 177.$$

and where

$$\phi_{\text{scatt}} = x^{-1} k f(\theta) \left[\tan \frac{\theta}{2} e^{i\varphi} \right] \exp i(x + \gamma \ln 2x) \quad 178.$$

It may be shown, by a procedure like that used in the non-Coulomb case, that $f(\theta)$ is given once again exactly by the expression 175.

As we have stated, the difficult part of the problem is to integrate the differential equations 163 and 164 for the potential V provided by the nuclear-density distribution. This can be done in terms of well-known functions for the point-charge case, i.e., the pure Coulomb field. The solution for G in this case is a hypergeometric function [Ref. (13), p. 79]. For finite nuclear-density distributions, $\rho(x)$, the solutions are not expressible in simple form, except in the case of a shell distribution where the solutions are spherical Bessel functions (90). In any case, it is necessary to fit the regular solutions of the radial Eq. 163 and 164 inside the nucleus to the regular and irregular solutions of these equations outside the nucleus. Only the regular types of solutions arise in the pure Coulomb case because the solutions must not go to infinity at the origin. However, outside a finite nucleus, the behavior at $r=0$ is no longer of interest, and an independent set of irregular solutions does exist. Further, outside the nucleus the potential again becomes Coulombic. For the outside regions, therefore, the radial functions are a linear combination of regular and irregular point-charge or Coulomb functions and may be written

$$C_j G_j^+(x) + D_j G_j^-(x) \quad 179.$$

and

$$C_j F_j^+(x) + D_j F_j^-(x) \quad 180.$$

where the C_j and D_j are constants of integration. The + sign stands for a regular function and the - sign for an irregular one. Now the requirements of continuity of charge and current specify that the regular functions F_j and G_j inside the nucleus, corresponding to the solutions of Eq. 163 and 164 for the density ρ , must match the functions 179 and 180 at a radius outside the nucleus, where $\rho=0$. If we call this radius

$$x_0 = kr_0 \quad 181.$$

the so-called "fitting-on radius," we must have

$$G_j(x_0) = C_j G_j^+(x_0) + D_j G_j^-(x_0) \quad 182.$$

$$F_j(x_0) = C_j F_j^+(x_0) + D_j F_j^-(x_0) \quad 183.$$

Putting in asymptotic forms of these functions, which must also satisfy the same relation, we have (see Eq. 176)

$$G_j = \sin [x + \gamma \ln 2x - \frac{1}{2}(j - \frac{1}{2})\pi + \eta_j] = C_j \sin [x + \gamma \ln 2x - \frac{1}{2}(j - \frac{1}{2})\pi + \eta_j^{e+}] \\ + D_j \sin [x + \gamma \ln 2x - \frac{1}{2}(j - \frac{1}{2})\pi + \eta_j^{e-}] \quad 184.$$

where η_j^{c+} stands for a pure Coulomb (point-charge) regular phase shift, etc. If we make the simplifications

$$\delta_j = \eta_j - \eta_j^{c+} \quad 185.$$

$$\epsilon_j = \eta_j^{c-} - \eta_j^{c+} \quad 186.$$

the trigonometric formula for the sum of two angles, when applied to Eq. 184, gives directly

$$\tan \delta_j = \frac{\sin \epsilon_j}{\frac{C_j}{D_j} + \cos \epsilon_j} \quad 187.$$

and this simple formula was given by Elton (81) and Parzen (82). Now C_j/D_j is immediately obtained from Eq. 182 and 183

$$\frac{C_j}{D_j} = - \left[\frac{G_j^- - \left(\frac{G_j}{F_j} \right) F_j^-}{G_j^+ - \left(\frac{G_j}{F_j} \right) F_j^+} \right]_{x=x_0} \quad 188.$$

evaluated at $x=x_0$.

Thus, aside from the Coulomb values of G_j^- , G_j^+ , F_j^- , F_j^+ , which are all known, the ratio C_j/D_j depends simply on the value of $(G_j/F_j)_{x=x_0}$ for the charge distribution ρ . Finally, the relative phase shifts δ_j depend only on (C_j/D_j) and other known values of ϵ_j .

The actual values of the Coulomb phase shifts η_j^{c+} and ϵ_j are given by Mott & Massey [ref. (13), p. 79]

$$\exp 2i\eta_j^{c+} = \frac{\sigma_j - i\gamma}{j + \frac{1}{2}} \frac{\Gamma(\sigma_j - i\gamma)}{\Gamma(\sigma_j + i\gamma)} \exp \pi i(j + \frac{1}{2} - \sigma_j) \quad 189.$$

and

$$\exp ie_j = \frac{1 - i \tan \pi(i + \frac{1}{2} - \rho_j) \coth \pi\gamma}{|1 - i \tan \pi(j + \frac{1}{2} - \rho_j) \coth \pi\gamma|} \exp -\pi i(j + \frac{1}{2} - \sigma_j) \quad 190.$$

where

$$\sigma_j = [(j + \frac{1}{2})^2 - \gamma^2]^{1/2} \quad 191.$$

The point-charge quantities and phase shifts needed above may be found in a report of Glassgold & Mack (115), but it is usually necessary to calculate these quite accurately in any practical case. Sample values of the phase shifts η_j^{c+} , ϵ_j , δ_j , are given in Yennie *et al.* (96) for gold. We have reproduced their values in our Table II. In this table, $\delta_j^{(1)}$ refers to a uniform charge distribution ($kR=4.0$) and $\delta_j^{(2)}$ to a gaussian, $b=2.12$ in Yennie's notation. It can be seen that the phase shifts increase slowly (numerically) as j increases.

The angular distributions, which are the ultimate objectives of the scattering problem, still need to be evaluated from Eq. 175, and this is a difficult problem because of the high accuracies needed. Yennie *et al.* (96) have

TABLE II
PHASE SHIFTS FOR GOLD

j	η_j^e	ϵ_j	$\delta_j^{(1)}$	$\delta_j^{(2)}$
1/2	0.40736	-1.17386	-0.85820	-0.71689
3/2	-0.23797	-0.54728	-0.27143	-0.18795
5/2	-0.53303	-0.36074	-0.07633	-0.04846
7/2	-0.72659	-0.26951	-0.01494	-0.01064
9/2	-0.87098	-0.21523	-0.00199	-0.00199
11/2	-0.98623	-0.17918	-0.00017	-0.00030
13/2	-1.08218	-0.15350	-0.00001	-0.00004
15/2	-1.16438	-0.13426	-0.00000	-0.00000
17/2	-1.23628	-0.11931	-0.00000	-0.00000

been most successful in developing a method of quickly summing the series for $f(\theta)$, Eq. 175. In older calculations the series converged very slowly, but Yennie *et al.* improved the evaluation of the sum considerably by introducing the method of their so-called "reduced" series. These series are formed by multiplying $f(\theta)$ by powers of $(1 - \cos \theta)$. The reduced series converge rapidly and so $f(\theta)$ can be found quickly by dividing the reduced sum by the proper power of $(1 - \cos \theta)$. This step was of great practical importance in finding exact values of the scattering cross section, particularly those due to the partial waves of large j value.

It should be pointed out that as j increases η_j and $\eta_j e^+$ do not approach zero but approach closer and closer together. This may be seen very clearly in Figure 19 taken from a recent paper of Ravenhall & Yennie (116). Thus δ_j , which is the phase difference, must be known very accurately, especially for the scattering behavior at large scattering angles. Hence, although two charge distributions have very similar sets of η_j , they may yet correspond to quite different differential cross sections as a function of scattering angle.

This fact is shown clearly by Ravenhall & Yennie (116) in Figure 20; where the large-angle scattering cross section is shown for four different nuclear models shown in the inset. The phase shifts for all the models lie in a region around the lowest curve of Figure 19 and are indistinguishable on a plot of this size. Nevertheless the very slight differences in phase shifts between these models are responsible for the vast changes occurring in the summation of the Legendre series and in the corresponding cross sections of Figure 20. If the quantity δ_j , of Eq. 185, is plotted on semi-logarithmic paper, the differences between the models show up quite clearly. All δ_j curves and cross-section curves merge together at small values of q or at small angles where the nucleus appears effectively as a point.

From the above discussion we see that "model independence" cannot rest upon a similarity in phases η_j but must take into account their very slight differences for high j , and this in fact leads to the breakdown of "model

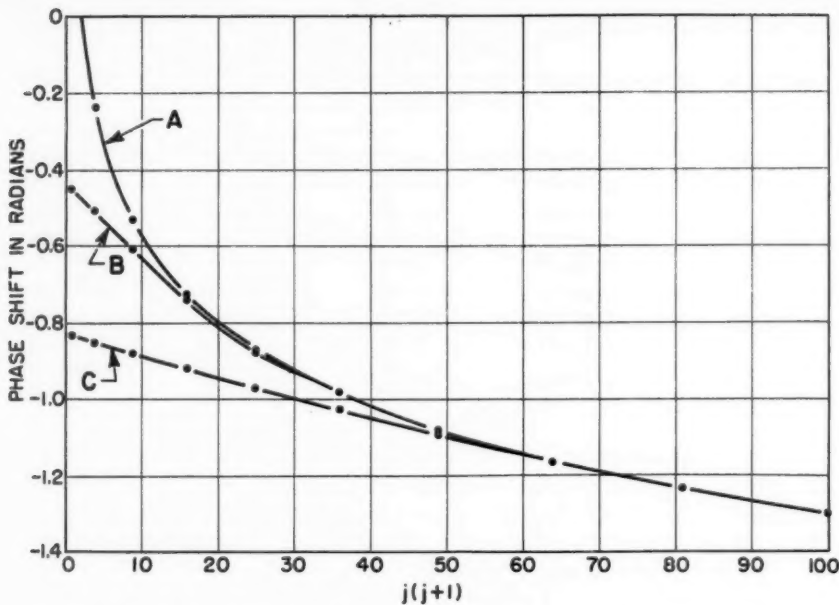


FIG. 19. Various phase shifts for gold are shown in this figure, drawn from the calculations of Ravenhall and Yennie (116). Curve A shows the regular Coulomb-phase shift. Curve B shows the phase shift, η_j , due to a uniform charge distribution in gold for which $kR = 4.0$. Curve C shows η_j for a uniform model of gold at $kR = 8$. Curve C is actually composed of four different curves which cannot be distinguished from each other on a plot of this size. The four curves are associated with (a) a uniform model of gold, (b) a Fermi 2-parameter best fit at 236 Mev in gold (see equation 192 below), (c) a Fermi 3-parameter model of gold at 236 Mev (see reference 101, Eq. 8), and (d) a shell distribution for which $kR = 5.6$. The different charge distributions are shown in the inset of Fig. 20.

independence" at high energies. This point, established by Yennie & Ravenhall (116), does not appear to be adequately appreciated in recent literature.

We have now sketched the main method of Yennie *et al.*, and Elton, etc. in finding exact scattering patterns for high Z and high energies. No computational details will be discussed at this point, since the numerical methods employed have been very well described in the respective papers.

Various approximation methods have been discussed in the literature, but it is not certain at the moment that an approximate calculation involves less computation than the more exact methods. Furthermore it is probable that an approximation is less reliable than an exact calculation particularly when small differences are important.

It would be valuable to see exact calculations made for nuclear models of various shapes and sizes so that an interpolation between such models can be used to fit experimental cross sections for which suitable nuclear models

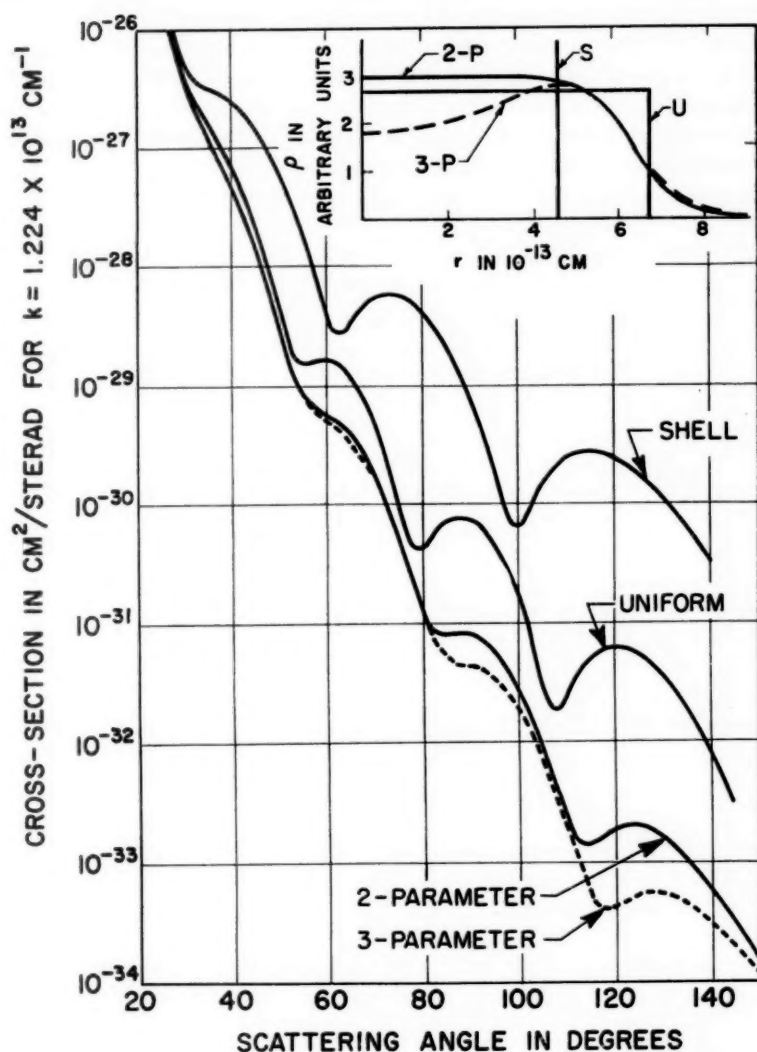


FIG. 20. The angular distributions in gold for the four different nuclear models shown in the inset. The electron energy is approximately 236 Mev. The corresponding phase shifts are given in (C) of Fig. 19. The curves of Fig. 19 and 20 demonstrate the breakdown of the idea of "model independence." This figure is taken from a forthcoming publication of Ravenhall & Yennie (116).

are not yet known. There are a few such models in the literature (96 to 101) but no systematic attempt in this direction has yet been made.

13. *Results for heavier nuclei.* Some of the principal results for heavier nuclei have already been described in reference 1, and we shall try to avoid repeating those except for brief mention of the more important features. Before discussing actual nuclear models, we shall show briefly the kind of results predicted by the phase-shift calculations.

Figure 21 shows the cross sections obtained by Yennie *et al.* (96) for

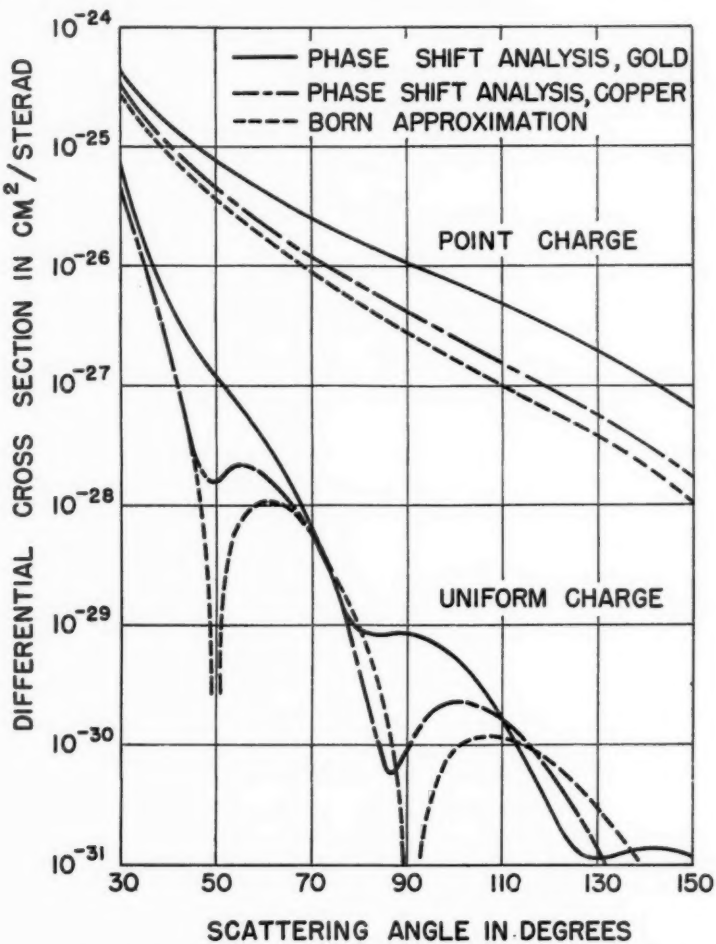


FIG. 21. This figure shows the results of exact phase-shift calculations for the point-charge and the uniform-charge models of gold at a value of $kR=5.4$ (approximately 155 Mev). The Fig. also shows similar curves for copper at about 230 Mev. Comparisons with the Born approximation are also given.

uniform charge distributions in copper and gold, as well as the point-charge cross sections given by the exact theory. Also shown for comparison are the Born-approximation results. The Born approximation is not accurate for copper and is particularly bad at the diffraction minima, as has been pointed out previously. Of particular interest is the manner in which the exact theory washes out the clear diffraction features of the Born approximation. Even so, the uniform charge distribution shows relatively prominent diffraction dips compared with smoother charge distributions.

Figure 22 shows the relative behavior of a gaussian-charge distribution given by exact calculation (96) and by the Born approximation both for

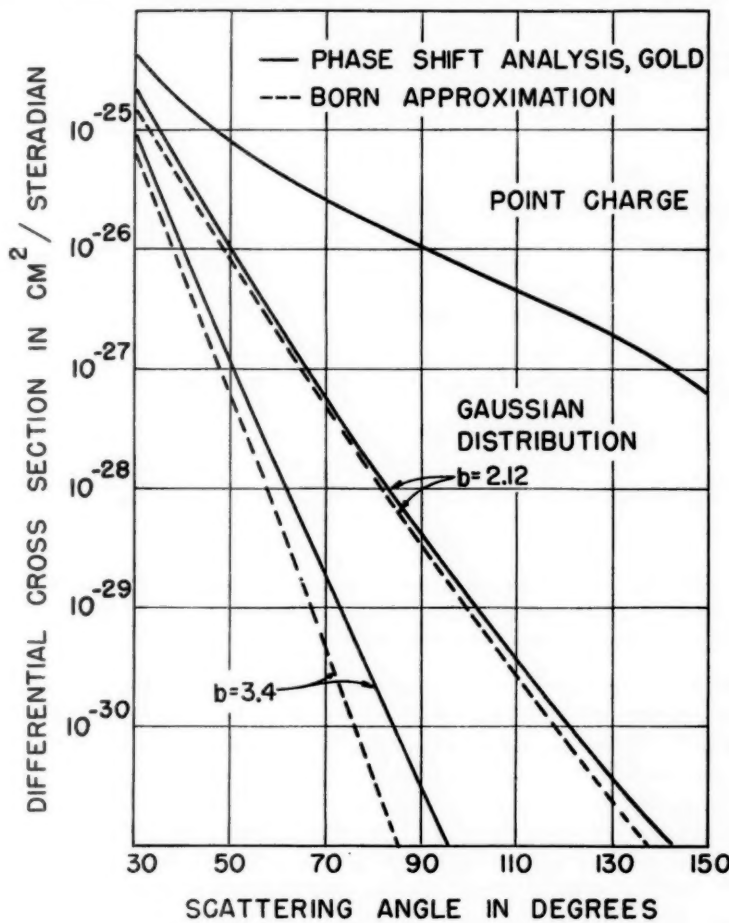


FIG. 22. Angular distributions in gold at an energy of about 155 Mev for two gaussian-charge distributions straddling the real distribution in gold. [The values of b are defined in ref. (96).] Born-approximation results are also indicated.

gold ($Z = 79$). It is apparent that for low Z , say even copper ($Z = 29$), the Born approximation would be excellent. This behavior appears to be true for relatively feature-less charge distributions. For those with sharp edges or "skin thicknesses," the approximations are not as good. In actuality the models that seem to fit the general trend of real nuclei fairly well are neither gaussian nor uniform and have been found by Hahn *et al.* (101) as shown in Figure 23. The accuracy obtained in these experiments does not make it

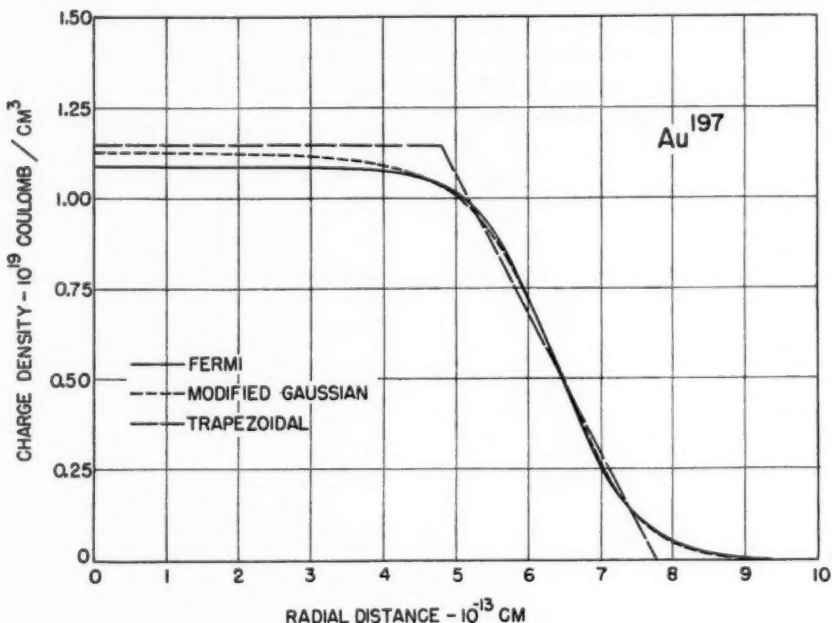


FIG. 23. The models which fit the experimental data for the medium and heavy nuclei (101). A typical set is shown for gold. Present accuracy in the experiments does not permit one to distinguish between the three types.

possible to tell the difference between these very close and alternative models. Newer experiments at higher energies now show signs of distinguishing between such models. However, even the older data definitely show that gaussian, exponential, uniform, etc. models are not like real nuclei and many possible nuclear models are definitely excluded by these experiments.

The types of models shown in Figure 23 appear to provide a fairly good characterization of the spherical nuclei investigated between $Z = 20$ and $Z = 83$. The charge densities of these nuclei are shown in Figure 24, where the "Fermi" model has been selected for general use from among the three types of Figure 23. The Fermi model has the analytic form

$$\rho(r) = \frac{\rho_1}{\exp [(r - c)/z_1] + 1} \quad 192.$$

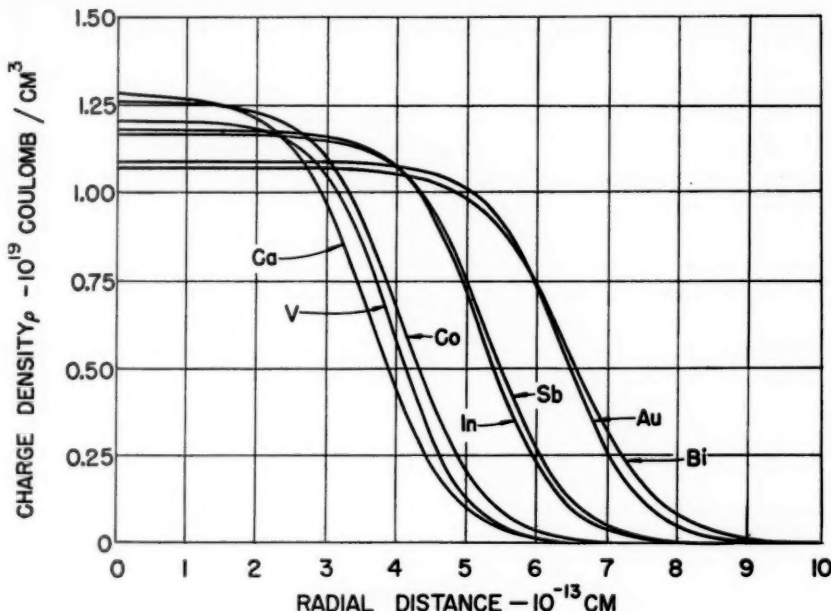


FIG. 24. The Fermi distribution for various nuclei (101). Note the tendency of the central charge density to diminish as A is increased.

and Figure 25 illustrates its shape and relevant parameters.

According to these ideas a model for the nuclei which have been investigated can be represented by a two-parameter family having a "half-density" radius of

$$c = 1.07A^{1/3} \times 10^{-13} \text{ cm.} \quad 193.$$

and a skin thickness

$$t = 2.4 \times 10^{-13} \text{ cm.} = 4.4c_1 \quad 194.$$

where t is measured between the 90 per cent and 10 per cent points, as shown in Figure 25. While this representation appears to give a satisfactory picture of most nuclei, newer experiments now in progress at 420 Mev are seeking finer details and possibly a third parameter to add to the two of Eq. 193 and 194. The Fermi type model, the trapezoidal model, and other similar models have the same values of the constants in Eq. 193 and 194 and are dealt with analytically by Hahn, Ravenhall & Hofstadter (101).

On the other hand, if the rules in Eq. 193 and 194 were to apply to still lighter nuclei such as Be⁹, C¹², O¹⁶, Mg²⁴, etc., the model would imply that these nuclei were "almost all surface." Experiments to test this point have been analyzed by various authors (36, 51, 52, 53). The model which follows the rules of Eq. 193 and 194, does not, of course, fit the light nuclei precisely, but the correspondence is surprisingly good as we shall see below.

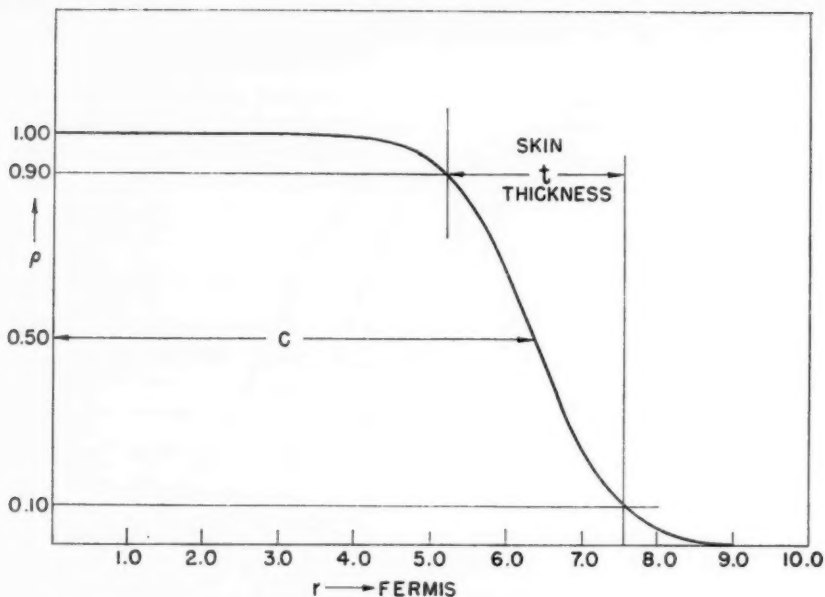


FIG. 25. Shape and parameters of the Fermi model as typified by the charge distribution in the gold nucleus.

Figure 3 shows the model ($\alpha=4/3$) and dimensions which seems to fit C^{12} in a very satisfactory manner. The shape ($\alpha=2$) fits O^{16} quite well, although the dimensions of length in the curve of Figure 3 are not appropriate to this nucleus. It can be seen that the "surface" forms a good part of these nuclei. For C^{12} and O^{16} the skin thicknesses are both approximately 1.90×10^{-13} cm. and represent about 73 to 83 per cent of the distance to the half-density points.

The nuclei Mg^{24} , Si^{28} , S^{32} , Sr^{88} have been investigated by Helm (36) who has analyzed the experimental data with the Born approximation using folded charge distributions. A uniform distribution, smeared at the edge by a gaussian, is called by Helm a gU charge distribution. A uniform distribution, smeared likewise by a second narrower uniform distribution, results in a uU charge distribution. These charge distributions are shown in Figure 26, and the values of c and t are listed below in Table IV. Also included in Figure 26 are representations of C^{12} and Ca^{40} according to these models. [The C^{12} and Ca^{40} charge distributions are observed to be in excellent agreement with those obtained in references (51), (52), and (101).] A correction factor, taking into account the change of dimensions arising from failure of the Born approximation (6 per cent for Sr), is included in the parameters of Figure 26. The above set of nuclei, with the exceptions of C^{12} and Ca^{40} , have not yet been analyzed by the exact phase-shift methods, but it is clear that the c and t values lies close to the values of Eq. 193 and 194.

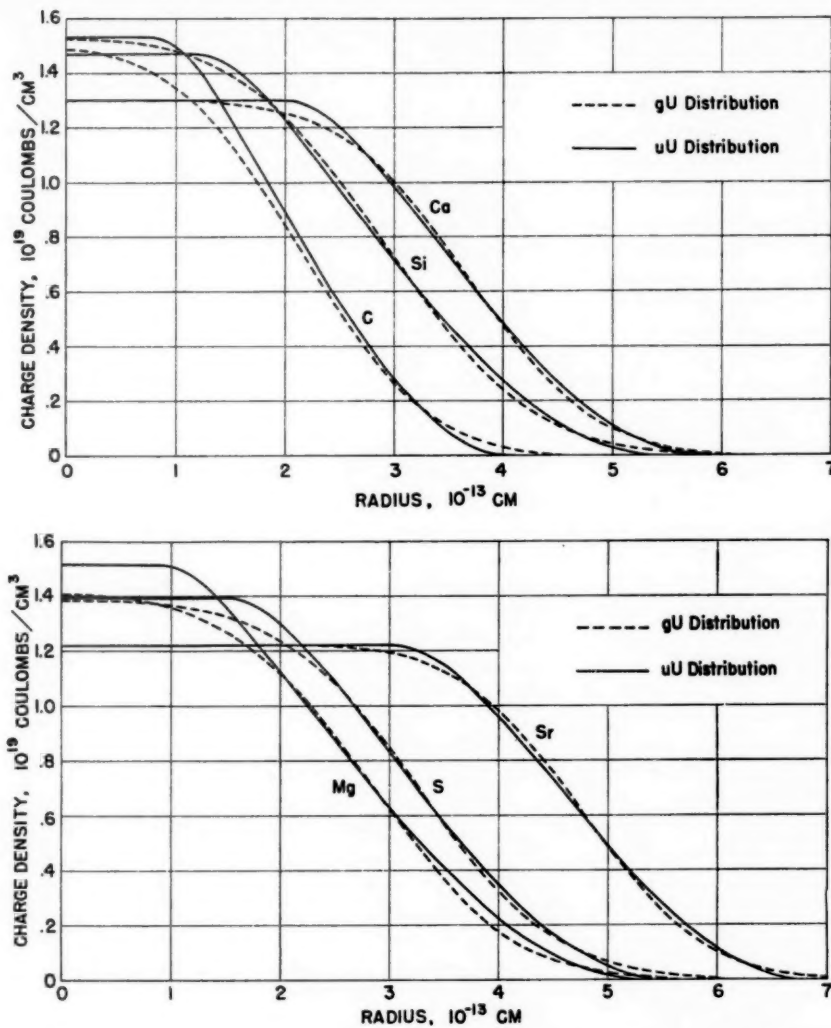


FIG. 26. Corrected Born-approximation deductions of the gU charge distribution in Mg^{24} , Si^{32} , S^{32} , and Sr^{88} , according to Helm (36). gU curves for C^{12} , and Ca^{40} are shown for comparison. The results for C^{12} and Ca^{40} on this model agree well with other more exact analyses of these distributions.

14. *Neighboring nuclei.* In this section we shall comment briefly on a new method of measuring small variations in the charge distributions of neighboring nuclei (117). It is desired to find out how the parameters c and t of Eq. 193 and 194 behave when the construction of a nucleus is varied slightly, e.g., as in proceeding from $_{28}Ni^{58}$ to $_{28}Ni^{60}$. In this case the number of neutrons is increased by two without any change in the number of protons.

The method is based on measuring ratios of elastic scattering from the two nuclei at the same angles. Experimentally, ratios of cross section can be found more accurately than individual cross sections. Furthermore, theory shows that the ratio of cross sections (R) depends only slightly on the exact analytical form of the charge distribution, so that changes in the parameters c and t may be found without knowing the precise type of nuclear model. Of course, the model employed in the calculation must be approximately of the right type for the nuclear pair under consideration. This is guaranteed by fitting the experimental angular distribution of either nucleus with a model

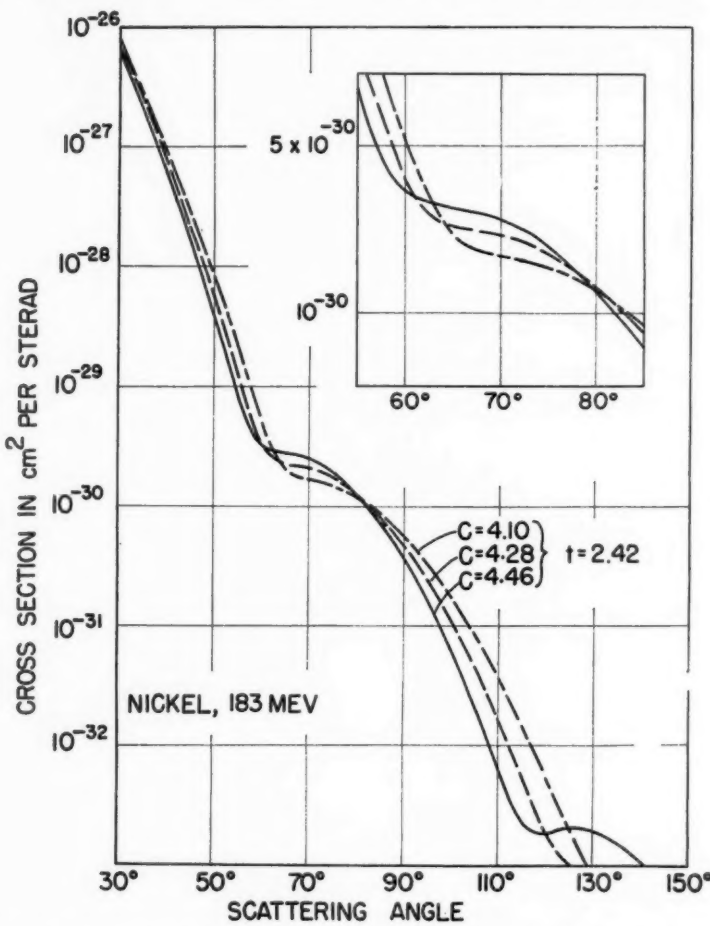


FIG. 27. The calculated behavior of the angular distribution in Ni at 183 Mev, when the c -value is varied from $4.10 \times 10^{-13} \text{ cm.}$ to $4.46 \times 10^{-13} \text{ cm.}$, and the skin thickness is left unchanged. The calculations are exact (117). The inset shows the crossover region in greater detail.

which gives by exact phase-shift methods the smallest least squares fitting errors. The Fermi model, Eq. 192, is satisfactory for this purpose and has been used in practice (117).

Figure 27 illustrates how the elastic cross section in nickel changes for the Fermi shape when the surface-thickness parameter, t , is unchanged but when the radius parameter c is varied by a small amount. The values of c which are used vary from 4.10×10^{-13} cm. to 4.46×10^{-13} cm. The inset in the

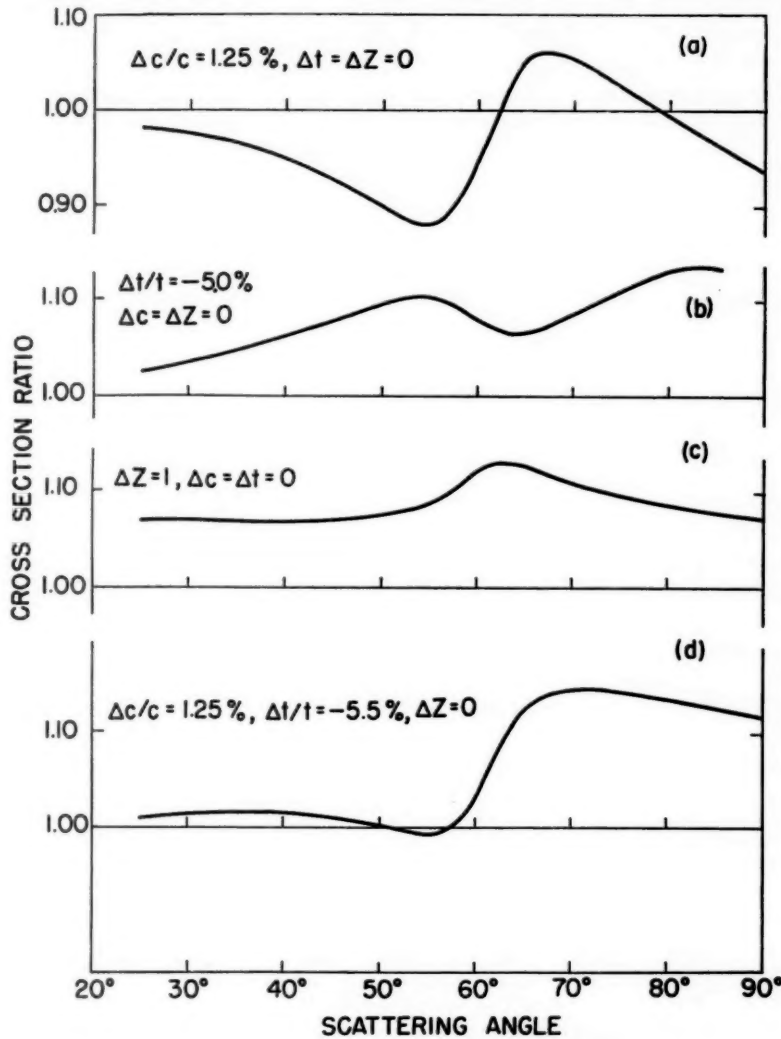


FIG. 28. The corresponding ratios of cross sections for the indicated changes in c , t , and Z . The ratios are calculated for the Fermi model.

figure shows that there are two crossover regions near 63° and 80° in between which the ratio of cross sections undergoes wide variations. Immediately outside this region the curves also depart from each other rather strikingly. Figure 28 shows the ratio for some particular changes in c , t , and Z . It can be seen that certain characteristic trends are associated with the changes in Δc , Δt , and ΔZ . The absolute value of the ratio at small angles is

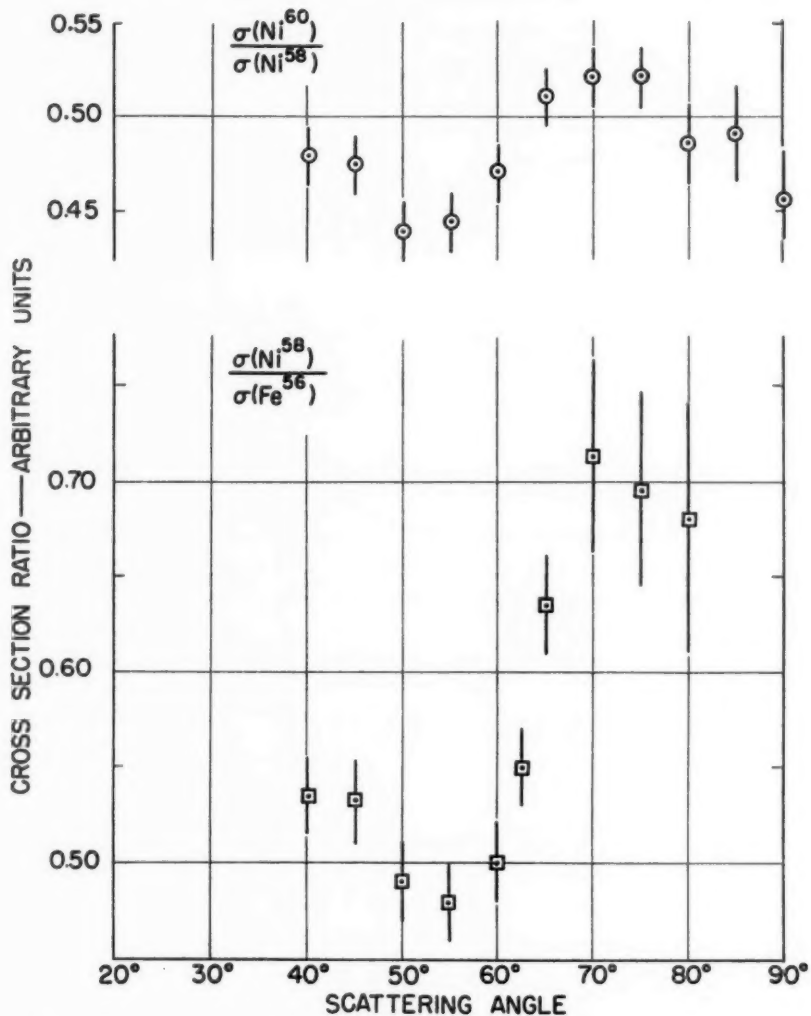


FIG. 29. The experimentally observed ratios in the pair of nickel nuclei (Ni^{60} , Ni^{58}) and in the combination (Ni^{58} , Fe^{56}). The ordinate is given in an arbitrary scale for the respective ratios.

also quite important. From curve (a) it appears that a change of $\Delta c/c$ by 1.25 per cent results in about a 20 per cent change of the cross-section ratio, and therefore the method can measure quite small differences in size. As curve (b) shows, the behavior of the ratio is also sensitive to small changes in t : a 5 per cent change in t is equivalent to a distance of about 1.3×10^{-14} cm.

The experimental cross sections at 183 Mev are illustrated for several isotopes in Figure 29 and show patterns similar to the curves of Figure 28. Unfortunately due to monitoring difficulties in the experiments the absolute value of the ratio was not obtained and this fact prevents complete identification of the changes taking place. For example, it is not possible to distinguish between curves (a) and (d) of Figure 28 within experimental error, since the absolute value of the ratio is unknown.

In spite of this temporary deficiency of the experimental data, it is possible to say that the charge distributions in the members of the pairs Ni⁵⁸, Ni⁶⁰, and Fe⁵⁶, Ni⁵⁸ are different. Thus two extra neutrons in Ni⁶⁰ affect the closed-shell proton structure in nickel. It is also possible to say that a change of the mass number introduces a change of c by a factor of approximately $[(A+2)/A]^{1/3} \approx 1.01$ for a constant surface thickness t . However, it is not possible to exclude a 10 per cent change in t . Better data will rectify this situation.

Incidental information from this experiment yields the "best fit" for the Fermi model of the Ni⁵⁸ isotope. The parameters of this fit are $c = 4.28 \times 10^{-13}$ cm., $t = 2.49 \times 10^{-13}$ cm., or $z^2 = 0.56 \times 10^{-13}$ cm.

15. *Assorted topics.* It is not possible to do justice in this article to many interesting subjects related to electron scattering. We may mention a few: inelastic scattering from discrete nuclear levels, polarization studies on non-spherical nuclei, positron scattering, correlation effects, radiative effects, electron scattering with meson production, etc. We have not been able to discuss such topics in detail in previous sections, and we shall not attempt to do so in this section. It seems worth while, however, to mention a few recent studies and to show where the problems in these fields lie. Perhaps these subjects may be treated at a later time in more detail.

(a) Inelastic level scattering. This interesting topic has been considered briefly (1) from an experimental standpoint. Theoretical papers dealing with level scattering have been written, for example, by Amaldi *et al.* (40, 118), Schiff (119), Sherman & Ravenhall (120), Ferrell & Vischer (55), Morpurgo (54), Tassie (59, 121), etc. The theoretical material is therefore well developed and it would be desirable to have complementary inelastic-electron scattering data from discrete nuclear levels.

We have briefly discussed electrodisintegration and the inelastic continuum in this article and elsewhere (1). It is interesting to see that Amaldi *et al.* (40) have indicated how the level scattering yields a behavior very suggestive of the inelastic continuum. The model chosen was the independent-particle type with an infinite harmonic-well potential. Amaldi's

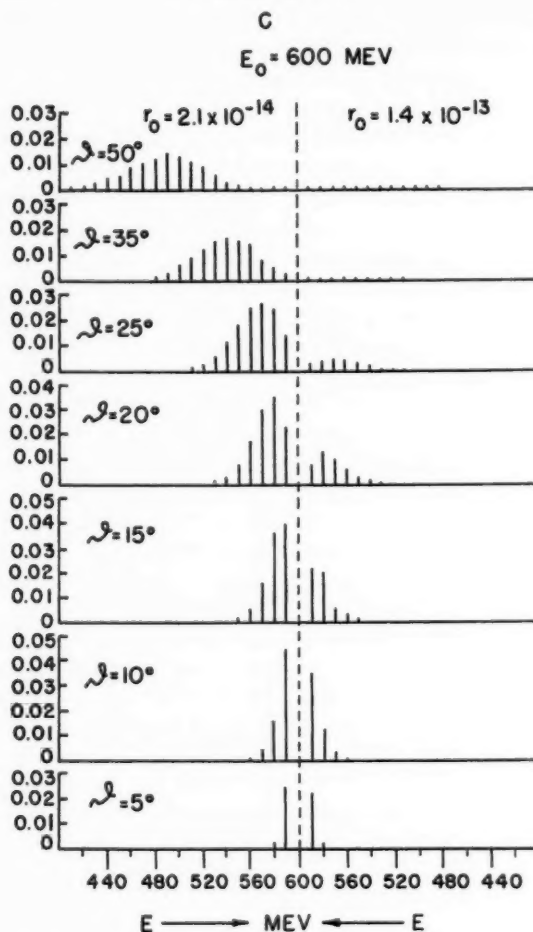


FIG. 30. Predictions of Amaldi *et al.* (40) for inelastic scattering at various angles in carbon at 600 Mev. The calculations are based on the Born approximation. r_0 in the figure refers to the proton size. The effects on the inelastic spectrum are shown to the left and right of center.

results are shown for carbon in Figure 30 for an incident energy of 600 Mev. As the angle of scattering is increased, the peak of the distribution of level scattering moves to lower energies in just the way the inelastic continuum behaves in helium or carbon (1).

Particular attempts at finding the quantum numbers of levels from observed transitions have been made (36, 51, 52, 54, 55, 119, 120, 121) and by Ravenhall (122). Not only do the data supply information about multipolarities of the transitions, but also the values of the transition matrix

elements emerge rather directly from an interpretation of the experiments with the help of equations similar to (44).

In cases where the scattering from nuclear levels cannot be resolved from the elastic scattering, some information about the levels may still be obtained. An example of this occurs for Ta¹⁸¹, where an analysis of experiments by Hahn *et al.* (101, 128) has been made by Downs *et al.* (126, 127) with a modified Born-approximation method. In this way it has been possible to estimate the distortion parameter in Ta¹⁸¹ which is found to be in good agreement with the spectroscopic and Coulomb-excitation values.

(b) Polarization studies. Interesting papers related to polarization phenomena have been written by Ferroni & Fubini (123), Newton (124), and Bernardini, Brovotto, & Ferroni (125). The last article contains references to other work in this field. Ferroni *et al.* (123) and Bernardini (125) carry out Born-approximation calculations for high-energy electrons scattered against polarized nuclei and consider Ta¹⁸¹ as a special case. The predicted azimuthal anisotropy in the cross section is shown to vary from 130 per cent to 50 per cent, depending on the nuclear model of Ta. While the Born approximation cannot be expected to be accurate for such a heavy nucleus, it is likely that the results are qualitatively correct. Therefore it appears desirable to attempt experiments of this type. Unfortunately the experiments are difficult mainly because, if a metallic target is to be used, the primary electron beam develops considerable heat in the target, and the required low temperature of the target cannot be maintained. Probably the Overhauser effect offers a reasonably practical method of obtaining the polarized target nuclei (125). The paper of Newton (124) considers double-electron scattering against lined-up magnetic moments of target nuclei, but these experiments presently appear to be difficult because of intensity reasons.

A simple use of a polarized target has been suggested by Downs *et al.* (127). They point out that the scattered waves from the spherically symmetric part of the charge distribution can interfere with those arising from the quadrupole distortion. The resulting diffraction structure, which will alter with the direction of polarization, should on analysis yield considerably more information about the radial charge distribution in these nuclei than has been obtainable hitherto.

Nonspherical nuclei may also be studied by direct-electron scattering experiments, without the necessity of employing polarization techniques (101, 126, 127, 128), but clearly polarization effects would add greatly to the amount of information that could be extracted from experiments on oriented nuclei.

(c) Positron scattering. In the first Born approximation, elastic scattering of positrons is identical with the corresponding scattering of electrons. The second Born approximation introduces relative differences in the cross sections of the order of $2\pi Z/137$ per cent, as may be seen from Eq. 135.

The calculations for point nuclei of higher atomic number have been

evaluated by Massey (129), Feshbach (66), Yadav (130), Curr (68), Doggett & Spencer (77), and Parzen & Wainright (131). The experimental situation on point scattering of positrons has recently been summarized by Allen *et al.* (132) along with results of new experiments by this group at 9.8 Mev in xenon. Within the accuracy of the experiments, the recent results are in reasonable agreement with theory.

The difference between positron and electron scattering for point nuclei was shown by Massey to be due to a spin-orbit effect, and this effect acts to reduce the scattering cross section relative to that for electrons. Figure 31 shows the ratio of positron to electron cross sections calculated by Feshbach (66) for point nuclei for various angles as a function of the atomic number when $\beta = v/c \approx 1$.

Positron scattering from nuclei of finite size has been investigated by Elton & Parker (133). These authors used the exact phase-shift method up to energies of 20 to 30 Mev for the gold nucleus. For a model with a delta function at the surface (shell distribution) and the kR values used in the calculation, the presently accepted size of gold would imply an energy of 30.5 Mev. Although the shell distribution is not appropriate to a real gold nucleus, the typical effects of the finite size upon positron scattering may be observed in Table III, which is taken from the work of Elton & Parker (133).

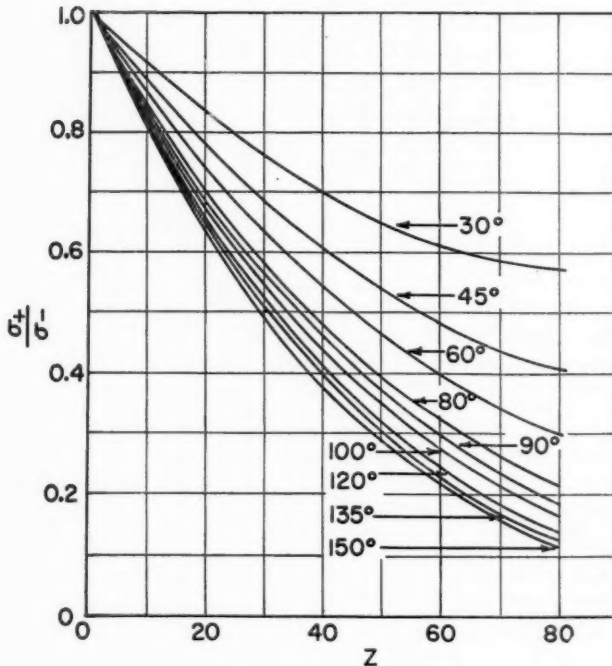


FIG. 31. The ratio of positron to electron-scattering cross sections calculated for point charges by Feshbach (66).

TABLE III

ELECTRON AND POSITRON CROSS SECTIONS FOR POINT GOLD NUCLEUS
AND AN EXTENDED GOLD NUCLEUS

θ (deg.)	15	30	45	60	80	90	100	120	135	150	
Electrons	$k^2 I_A$	323	25.6	6.49	2.54	0.945	0.638	0.412	0.186	0.0897	0.0377
	$k^2 I_C$	331	24.7	5.02	1.45	0.330	0.178	0.090	0.031	0.0123	0.0052
Positrons	$k^2 I_A$	265	14.4	2.59	0.75	0.204	0.117	0.069	0.025	0.0110	0.0044
	$k^2 I_C$	265	14.2	2.47	0.68	0.172	0.095	0.054	0.018	0.0075	0.0029

In the table quantities proportional to the differential cross sections for points are labeled $k^2 I_A$ and those for finite nuclei $k^2 I_C$. It can be seen that the positron-point nucleus cross section is smaller than the electron-point nucleus value by rather considerable factors at the large angles (3 to 8), while the corresponding cross sections for a finite nucleus are less by factors only about 2. Thus the effect of the finite size is to increase the positron scattering in relation to that of the electrons. At higher energies the positron scattering will exceed that from electrons.

This behavior may be understood since the positron-nucleus Coulomb force is repulsive while the electron-nuclear force is attractive. Hence the electron waves, as measured by their probability amplitude, will tend to penetrate the nucleus to a greater extent than the positron waves, and the interference effects, which give rise to the form factors, are correspondingly greater for electrons than for positrons. Thus the cross sections for electrons are reduced greatly by the form factors while the positron form factors are not reduced so effectively.

New experimental information on positron scattering at high energies (50 to 170 Mev) has recently been made available by Miller & Robinson (134). In an ingenious experiment bremsstrahlung x-rays from a betatron were allowed to fall on a target foil. Electrons and positrons from the target were analyzed by a spectrometer magnet placed at various angles between 21° and 74° from the incident x-ray beam. By separating linear and quadratic yields from Pb targets of various thicknesses, the results could be analyzed in terms of (a) the scattering of electrons and positrons produced as pairs at zero degrees and (b) the direct large-angle pair production of electrons and positrons. For checking the experimental technique, previous electron-scattering results in the same energy range could be used. The results appear to confirm the predictions of Elton & Parker (133) and point to a new method of studying positron scattering by finite nuclei.

(d) Correlation effects in nuclear matter. This interesting subject has received considerable attention recently (9, 104, 105, 135, 136, 137, 138) and is related to the variations of local charge density in the neighborhood of a particular proton in a nucleus. The correlation effects are produced by the operation of the specifically nuclear and coulomb forces between nucleons and the intervention of the Pauli principle. In the first Born approximation,

the correlations do not introduce any modifications in the elastic scattering of high-energy electrons (9, 135). In the same approximation, the sum over all possible inelastic transitions yields more information about correlations than a study of particular transitions to discrete nuclear levels (9, 135, 138). Schiff (138) has recently shown that the same behavior is obtained for all orders in the Born-approximation sum and is not merely a characteristic of the first and second Born approximations.

The qualitative way in which correlation effects may be expected to appear in experiment has been worked out by Smith (9) in the first-order Born approximation. As an extreme example he considers that heavy nuclei are built in the form of crystals with a regular lattice structure. The nucleons are permitted to be smeared about their regular lattice positions in a manner reminiscent of thermal motion, just as atoms in crystals are known to behave. Thus there are two parameters in the theory: one related to the side of the basic cell in the lattice and the second associated with the freedom or amplitude of motion about the occupation points.

The inelastic-scattering cross sections are summed by Smith (9) over an energy region (~ 15 to 30) Mev from the elastic-scattering peak and thus include essentially all the important transitions to the discrete levels. At the same time, the mean-energy change of the electron (~ 18 Mev) is still small compared with the energy of the incident or scattered electron (~ 200 Mev), and the value of q (momentum transfer of Eq. 11) may be assumed to be roughly constant at a given angle θ . The closure operation then permits Smith to evaluate the sum of the inelastic-scattering cross sections to the discrete levels and to evaluate an effective "form factor for summed inelastic scattering."

As is usual in such calculations, the "two-particle density" function is an important element in the analysis and is an example of the type of information which can be extracted from the experiments. The two-particle density characterizes the correlation in position of pairs of protons, while the single-particle density (Eq. 53) is the usual charge density $\rho(\mathbf{R})$ involved in elastic scattering. In theories of correlations effects, the two-particle density is a function integrated over all proton coordinates, except the two of a pair, and the single-particle density is integrated over all proton coordinates except one (9, 137).

With the crystal model of a Pb nucleus, Smith evaluates the inelastic form factor (F) referred to above, and finds that, at large q , F^2 has maxima and minima greater and less than unity. Thus there is a modulation of point-charge inelastic scattering with a factor greater and less than unity and it is this type of pattern that would be looked for if nuclei were really expected to have a crystalline structure. Of course, any other type of correlation or short range order would give a qualitatively similar modulation of the inelastic-scattering cross section. The sharpest interference patterns naturally result from the most definite or regular correlation effects (less equivalent "thermal" motion). In Smith's work the interference maxima or minima

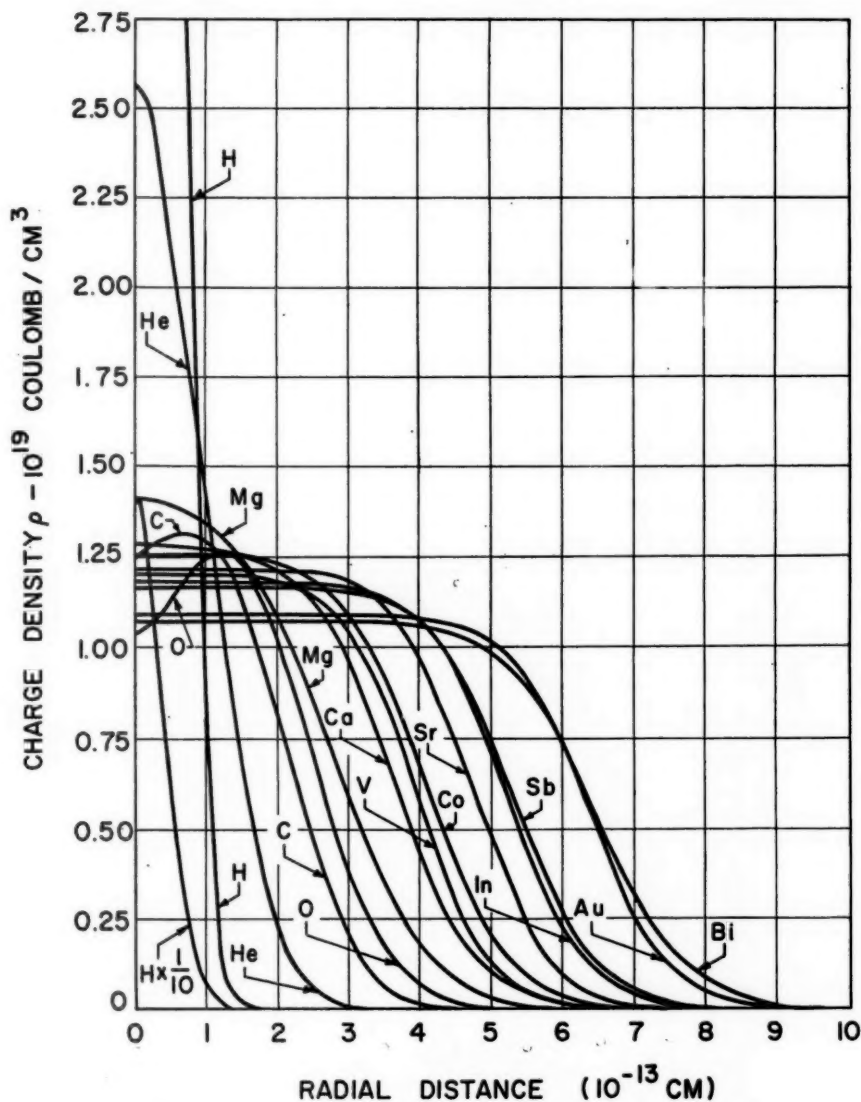


FIG. 32. This figure represents a summary of the charge distributions found for various nuclei by electron-scattering methods.

TABLE IV*
SUMMARY OF NUCLEAR SIZE PARAMETERS

Nucleus (1)	Type of charge distribution (2)	rms radius (3)	Radius of equivalent uniform model R_u (4)	$r_0 = \frac{R_u}{A^{1/3}}$ (5)	Skin-thickness t (6)	Half-density Radius c (7)	$r_1 = \frac{c}{A^{1/3}}$ (8)	$\rho_a \dagger$ (9)	$A^{1/3}$ (10)	Ref. No. (11)
$^1\text{H}^1$	Gaussian Exponential Hollow exponential	0.72 0.80 0.78	0.77 ± 0.10	$1.00 \ddagger$ —	1.00 —	— —	— —	0.239 —	1.00 —	$17, 18, 19$
$^1\text{D}^2$	Deuteron wave-function plus proton	$2.11 \pm .05$	$2.73 \S$	2.16	—	—	—	0.0116	1.26	$33, 38$
$^3\text{He}^4$ $^3\text{Li}^8 \S\S$	Gaussian Gaussian Uniform Modified exponential	1.61 2.37 2.10 2.78	2.08 $2.84(?) \#$ 1.56 —	1.31 — —	— — —	— — —	— — —	0.053 $0.03(?)$ —	1.59 1.82 —	18 62 (see text)
$^3\text{Li}^7$	Harmonic-well $\alpha = 1/3$ Approximately same as $^3\text{Li}^8$	2.44 $2.20(?)$	— $2.84(?)$	1.49 —	— —	— —	— —	$0.03(?)$	1.91 62 (see text)	$60, 61, 62$
$^4\text{Be}^9$	Harmonic-well $\alpha = 2/3$	2.2 ± 0.2 2.37	2.84 3.04	1.37 1.33	— —	— —	— —	0.04	2.08	$60, 61, 62$
$^6\text{C}^{12}$	Harmonic-well $\alpha = 4/3$	2.64	3.41	1.35	1.9	2.3	1.00	0.051	2.29	$10, 51, 52,$ 53
$^8\text{O}^{16}$	Harmonic-well $\alpha = 2.0$					2.6	1.03	0.049	2.52	64

$^{13}\text{Mg}^{34}$	2.98	3.84	1.33	2.6	2.93	0.99	0.051	2.89	36	
$^{14}\text{Si}^{36}$	3.04	3.92	1.29	2.8	2.95	0.97	0.056	3.04	36	
$^{14}\text{S}^{32}$	3.19	4.12	1.30	2.6	3.26	1.03	0.055	3.17	36	
$^{20}\text{Ca}^{40}$	3.52	4.54	1.32	2.5	3.64	1.06	0.052	3.42	101	
Fermi	3.59	4.63	1.25	2.2	3.98	1.07	0.055	3.71	101	
$^{21}\text{V}^{31}$	3.59	4.83	1.27	2.5	4.09	1.05	0.054**	3.90	101	
Fermi	3.83	4.94	1.31	2.49	4.28	1.10	0.052	3.87	117	
$^{21}\text{Co}^{59}$	3.93	5.09	1.20	2.3	4.80	1.08	0.060	4.45	36	
Fermi	4.14	5.34	1.19	2.3	5.24	1.08	0.060	4.86	101	
$^{20}\text{In}^{65}$	4.50	5.80	1.20	2.5	5.32	1.07	0.058	4.96	101	
Fermi	4.63	5.97	1.25	2.8	~6.45	~1.14	0.049	5.66	126, 127,	
$^{21}\text{Ta}^{181}$	5.50	~7.10††	~1.25	~2.8					128,	
Fermi plus quadrupole										
$^{75}\text{Au}^{197}$	5.32	6.87	1.180	2.32	6.38	1.096	0.0585	5.82	101	
$^{82}\text{Pb}^{208}$	$n=10; s=0$	~5.42	7.0	~2.3	~6.5	~1.09	0.057	5.93	100	
$^{81}\text{Bi}^{209}$	Fermi	5.52	7.13	1.20	2.7	6.47	1.09	0.0548	5.935	101

* All distances in the table are quoted in units of 10^{-11} cm.

† The units of ρ_u are proton charges per 10^{-38} cubic centimeter. ρ_u is derived from the expression $3Ze/4\pi R_u^3$ and R_u is given by Eq. 197.

‡ The magnetic distribution is similar to the charge distribution. The circumstance that $R = 1.00$ is purely accidental.

§ This radius is different from that given elsewhere (ref. 1, Table VI), because the proton size is specifically included in this listing, whereas the R of Eq. 123 was quoted in the older reference. The charge distribution is given by the deuteron wave function modified by the folding-in of a finite proton's charge distribution.

|| These values are at present uncertain.

¶ These values are at present uncertain.

** A numerical error appeared in the corresponding item of Table VI of ref. 1.

†† The radial distances should be considered "effective" radii in view of quadrupole distortions.

† The model of Hill *et al.* is similar to the Fermi model.

§§ Newer data at 420 Mev taken by G. Burleson and the author support the smaller size in the neighborhood of $a = 2.1 \times 10^{-11}$ for the rms radius.

appear at large values of $x = qr_1$, where r_1 is a parameter which measures the lattice spacing. It is therefore necessary to go to high values of q to make the interference features experimentally observable. This is a reasonable result if one remembers that, in elastic scattering, diffraction features associated with small separations also require large q values.

Smith (9) also considers the effect of the Pauli principle on correlations by imagining the Z protons to be limited to a cubic box of side L . F^2 is found to increase from zero to unity in a gradual way when $x = qr_1$ varies from zero to ~ 3.0 . r_1 in this case is the radius of a spherical volume containing one nucleon, thus

$$L^3 = \frac{4\pi}{3} Ar_1^3 \quad 195.$$

There is also a slight dependence of F^2 on R_{12} , where R_{12} is the upper limit for inter-particle distances in the nucleus. In the main, the effect of the Pauli principle is to repress inelastic scattering until q reaches a certain value where the recoil momentum given to the struck nucleon is large enough to eject it from the Fermi sea.

Unfortunately no experiments are available to test these ideas at present, although it is possible that the inelastic results in carbon (51, 52) might be analyzed in this connection. Considering the well-developed theoretical background for correlation effects in nuclear theory, as well as in atomic theory (139, 140, 141), it is to be hoped that electron-scattering experiments will be carried out soon to test the theory and to look for such effects in nuclei.

(e) Radiative effects. Very little experimental work on this topic has been carried out to date. For that reason we shall not discuss radiative effects in this article, and again particularly because the theory appears to be rather complex. It may be worth while to collect herewith some references to recent work in this field, e.g. (106 to 110, 142 to 145).

(f) Electron scattering with meson production. Figure 16 shows a low-energy scattering peak, labeled D , which results from electrons which have produced π -mesons of various kinds in deuterium (45). It can be seen that, apart from the intrinsic interest in this phenomenon, it is necessary to know the shape of the peak because of its possible contribution to the tail of the inelastic continuum at C in the figure. Even more so, as one goes to heavier nuclei, such as Li, Be, or C, the meson-producing scattered electrons grow in number (146) and the analogous peak D becomes comparable to peak C . A recent theoretical account of this process in electron-proton collisions has been given by Dalitz & Yennie (147). Related cross sections for production of mesons of definite energy and direction have been reported experimentally by Panofsky *et al.* (148).

16. *Summary of results.* A portion of the information presented in this paper can be summarized with the help of a graph and a table. Figure 32 shows a representation of the charge densities for typical nuclei investigated

by electron-scattering methods. Table IV presents the data pertaining to density distributions and the parameters appropriate to the various nuclei. Certain tendencies in the data stand out quite strikingly: (a) Our first observation is that the average-central charge density decreases as the nuclear charge is increased. The maximum-central density is reached in the proton. Next to the proton the alpha particle has the highest central density, and it is worth noticing that the charge density is extraordinarily high in this nucleus—roughly speaking about twice as high as in most heavier nuclei. (b) Except for extremely light nuclei such as He and Li, a reasonable representation of the charge density in all the remaining nuclei can be given by a two-parameter family of curves with half-density radius c and skin thickness t , corresponding to the constants of Eq. 193 and 194. " t " is thus a constant for all nuclei and it is as if the heavier nuclei could be manufactured from the light nuclei simply by stuffing nucleons in the central regions and pushing the constant skin outwards. Even lighter nuclei seem to subscribe to this plan. It is highly likely that, when additional parameters of the nuclear-charge distributions become known, variations from the prescription will be found, but it appears unlikely that the differences will be marked. (c) Associated with the description of c and t given above, the charge distributions of heavier nuclei are characterized by sizes smaller than those provided by older methods which depend on nuclear interactions rather than electromagnetic processes. Indeed it has not been necessary to refer to the "radius" of a nucleus in this paper, because it is apparent that the whole shape must be specified rather than a single parameter. It has been pointed out previously (1) that if one wishes to choose a single parameter representing nuclear "size," such as the "equivalent uniform-charge radius, R_u ,"

$$R_u = r_0 A^{1/3} \quad 196.$$

and where

$$a_u = \left(\frac{3}{5} \right)^{1/2} R_u \quad 197.$$

is the root-mean-square radius, then it follows that

$$r_0 = \left(\frac{5}{3} \right) a_u A^{-1/3} \quad 198.$$

is no longer a constant, as in older models, but is a variable. The value of r_0 , consistent with electron-scattering data, ranges from about 1.18×10^{-13} cm. to 1.30 to 1.40×10^{-13} cm. for light nuclei. A recent redetermination of mirror-nuclei radii (149, 150) appears to be in excellent agreement with this conclusion. Only one size parameter, of course, is obtained in the mirror-nuclei method. Another recent investigation (151) which is in agreement with the electron-scattering data has been concerned with measurements of the diffraction and absorption cross sections of nuclei for negative pions of high kinetic energies (0.6–1.4 Bev). The data are found to be consistent with "radii" taken from electron-scattering results, provided one allows for a

range of the pion-nuclear force of 1.0×10^{-13} cm. This is a reasonable value. Moreover, it is found that a uniform distribution of charge in nuclei is not consistent with the pion experiments, which is again in agreement with electron-scattering experiments (4). Finally, the size and shape found for the distribution of charge and magnetic moment in the proton and neutron appear to be difficult to understand with current field-theory, since the nucleon core appears unreasonably large. The apparent lack of charge independence in the mesonic clouds is also somewhat puzzling, though, of course, the neutron and proton are dissimilar in the values of their static moments. It is hoped that the forthcoming years will witness a clarification of the present "anomalies."

ACKNOWLEDGMENTS

The author wishes to thank Drs. D. G. Ravenhall and D. R. Yennie for their kind and generous assistance in discussions of the theoretical material. He is also greatly indebted to Drs. U. Meyer-Berkhout and L. I. Schiff for their critical reading of the manuscript. For making available results in advance of publication, the author makes acknowledgment with thanks to: R. Blankenbecler, R. Cool, H. Ehrenberg, J. A. McIntyre, U. Meyer-Berkhout, R. C. Miller, D. G. Ravenhall, L. Rosenfeld, C. S. Robinson, L. I. Schiff, S. Sobottka, J. F. Streib, M. R. Yearian, and D. R. Yennie. For technical help with the manuscript, the author wishes to express his thanks to F. Adams, F. Bunker, J. E. Gill, R. Keith, E. McWhinney, E. Searby, and N. Vettini.

NUCLEAR AND NUCLEON SCATTERING OF ELECTRONS 313
LITERATURE CITED

1. Hofstadter, R., *Rev. Modern Phys.*, **28**, 214 (1956)
2. Evans, R. D., *The Atomic Nucleus* (McGraw-Hill Book Co., Inc., New York, N. Y., 972 pp., 1955)
3. Born, M., *Z. Physik*, **38**, 803 (1926)
4. Heitler, W., *The Quantum Theory of Radiation*, 3rd ed., Chap. 4 (Oxford University Press, Oxford, England, 430 pp., 1954)
5. Schiff, L. I., *Quantum Mechanics*, 2nd ed. (McGraw-Hill Book Co., Inc., New York, N. Y., 417 pp., 1955)
6. Dalitz, R. H., *Proc. Roy. Soc. (London)*, **206A**, 509 (1951)
7. Heitler, W., *The Quantum Theory of Radiation*, 3rd ed., 214 (Oxford University Press, Oxford, England, 430 pp., 1954)
8. Schweber, S. S., Bethe, H. A., and de Hoffmann, F., *Mesons and Fields*, 1, (Row, Peterson, and Co., Evanston, Ill., 449 pp., 1955)
9. Smith, J. H., *Phys. Rev.*, **95**, 271 (1954)
10. Sobottka, S., & Hofstadter, R. (To be published)
11. Møller, C., *Z. Physik*, **70**, 786 (1931)
12. Bethe, H. A., *Ann. Physik*, **5**, 325 (1930)
13. Mott, N. F., and Massey, H. S. W., *The Theory of Atomic Collisions*, 2nd ed., (Oxford University Press, Oxford, England, 388 pp., 1949)
14. Yennie, D. R., Lévy, M. M., and Ravenhall, D. G., *Rev. Modern Phys.*, **29**, 144 (1957)
15. Pauli, W., *Rev. Modern Phys.*, **13**, 203 (1941)
16. Rosenbluth, M. N., *Phys. Rev.*, **79**, 615 (1950)
17. Hofstadter, R., and McAllister, R. W., *Phys. Rev.*, **98**, 217 (1955)
18. McAllister, R. W., and Hofstadter, R., *Phys. Rev.*, **102**, 851 (1956)
19. Chambers, E. E., and Hofstadter, R., *Phys. Rev.*, **105**, 1454 (1956)
20. Foldy, L. L., *Phys. Rev.*, **87**, 688 (1952)
21. Salzman, G., *Phys. Rev.*, **99**, 973 (1955)
22. Clementel, E., and Villi, C., *Nuovo Cimento*, **10**, 1207 (1956)
23. Jankus, V. Z., *Phys. Rev.*, **102**, 1586 (1956)
24. Bethe, H. A., and Peierls, R., *Proc. Roy. Soc. (London)*, **148A**, 146 (1935)
25. Peters, B., and Richman, C., *Phys. Rev.*, **59**, 804 (1941)
26. Rose, M. E., *Phys. Rev.*, **73**, 282 (1948)
27. Thie, J. A., Mullin, C. J., and Guth, E., *Phys. Rev.*, **87**, 962 (1952)
28. Schiff, L. I., *Phys. Rev.*, **92**, 988 (1953)
29. Schiff, L. I., *Science*, **121**, 881 (1955)
30. Hofstadter, R., *Rev. Modern Phys.*, **28**, 214 (1956)
31. Jankus, V. Z., *Theoretical Aspects of Electron-Deuteron Scattering* (Doctoral Thesis, Stanford Univ., Stanford, Calif., 1956)
32. Blatt, J. M., and Weisskopf, V. F., *Theoretical Nuclear Physics* (John Wiley and Sons, Inc., New York, N. Y., 864 pp., 1952)
33. McIntyre, J. A., and Dhar, S., *Phys. Rev.*, **106**, 1074 (1957)
34. Smythe, W. R., "Recoil Protons from Meson Photoproduction in Hydrogen and Deuterium" (Doctoral Thesis, California Inst. of Technology, Pasadena, Calif., 1957)
35. Blankenbecler, R. (To be published)
36. Helm, R. H., *Phys. Rev.*, **104**, 1466, 1468, 1469 (1956)

37. Yennie, D. R., Lévy, M. M., and Ravenhall, D. G., *Rev. Modern Phys.*, **29**, 144, 146 (1957)
38. McIntyre, J. A., *Phys. Rev.*, **103**, 1464 (1956)
39. McIntyre, J. A., and Hofstadter, R., *Phys. Rev.*, **98**, 158 (1955)
40. Amaldi, E., Fidecaro, G., and Mariani, F., *Nuovo cimento*, **7**, 553 (1950)
41. Feshbach, H., *Symposium on Electron Physics* (National Bureau of Standards, Washington, D. C., Oct., 1951)
42. Hofstadter, R., *Rev. Modern Phys.*, **28**, 214 (1956)
43. Blankenbecler, R. (Private communication)
44. Drell, S. D., and Ruderman, M. A., *Phys. Rev.*, **106**, 561 (1957)
45. Yearian, M. R., and Hofstadter, R. (To be published)
46. McAllister, R. W., and Hofstadter, R., *Phys. Rev.*, **102**, 851 (1956)
47. Hofstadter, R., *Rev. Modern Phys.*, **28**, 214 (See Section Ve) (1956)
48. Rustgi, M. L., and Levinger, J. S., *Phys. Rev.*, **106**, 530 (1957)
49. Foldy, L. L. (To be published)
50. Levinger, J. S., and Bethe, H. A., *Phys. Rev.*, **78**, 115 (1950)
51. Fregeau, J. H., and Hofstadter, R., *Phys. Rev.*, **99**, 1503 (1955)
52. Fregeau, J. H., *Phys. Rev.*, **104**, 225 (1956)
53. Ravenhall, D. G. (Private communication)
54. Morpurgo, G., *Nuovo cimento*, **3**, 430 (1956)
55. Ferrell, R. A., and Visscher, W. M., *Phys. Rev.*, **104**, 475 (1956)
56. Tassie, L. J., *Australian J. Phys.*, **9**, 400 (1956)
57. Gatto, R., *Nuovo cimento*, **10**, 1559 (1953)
58. Feenberg, E., *Shell Theory of the Nucleus*, 20, 21 (Princeton University Press, Princeton, N. J., 211 pp., 1955)
59. Tassie, L. J., *Proc. Phys. Soc. (London)*, **69A**, 205 (1956)
60. Hofstadter, R., Fechter, H. R., and McIntyre, J. A., *Phys. Rev.*, **92**, 978 (1953)
61. McIntyre, J. A., Hahn, B., and Hofstadter, R., *Phys. Rev.*, **94**, 1084 (1954)
62. Streib, J. F., *Phys. Rev.*, **100**, 1797 (1955)
63. Gatha, K. M., Patel, N. J., and Patel, R. F., *Proc. Phys. Soc. (London)*, **67A**, 1111 (1954)
64. Ehrenberg, H., Meyer-Berkhout, U., and Hofstadter, R. (To be published)
65. Bartlett, J. H., and Watson, R. E., *Proc. Am. Acad. Arts Sci.*, **74**, 53 (1940)
66. Feshbach, H., *Phys. Rev.*, **88**, 295 (1952)
67. McKinley, W. A., Jr., and Feshbach, H., *Phys. Rev.*, **74**, 1759 (1948)
- 67a. Mott, N. F., *Proc. Roy. Soc. (London)*, **124A**, 425 (1929); Mott, N. F., *Proc. Roy. Soc. (London)*, **135A**, 429 (1932)
68. Curr, R. M., *Proc. Phys. Soc. (London)*, **68A**, 156 (1956)
69. Yadav, H. N., *Proc. Phys. Soc. (London)*, **68A**, 348 (1955)
70. Chapman, K. R., Matsukawa, E., Rose, P. H., and Stewardson, E. A., *Proc. Phys. Soc. (London)*, **68A**, 928 (1955)
71. Brown, B., Matsukawa, E., and Stewardson, E. A., *Proc. Phys. Soc. (London)*, **69A**, 496 (1956)
72. Bayard, R. T., and Yntema, J. L., *Phys. Rev.*, **97**, 372 (1955)
73. Damodaran, K. K., and Curr, R. M., *Proc. Phys. Soc. (London)*, **69A**, 196 (1956)
74. Van de Graaff, R. J., Buechner, W. W., and Feshbach, H., *Phys. Rev.*, **69**, 452 (1946)
75. Buechner, W. W., Van de Graaff, R. J., Sperduto, A., Burrill, E. A., and Feshbach, H., *Phys. Rev.*, **72**, 678 (1947)

76. Urban, P., *Fortschr. Physik*, **III** (1) (1955)
77. Doggett, J. A., and Spencer, L. V., *Phys. Rev.*, **103**, 1597 (1956)
78. Sherman, N., *Phys. Rev.*, **103**, 1601 (1956)
79. Faxén, H., and Holtsmark, J., *Z. Physik*, **45**, 307 (1927)
80. Rayleigh, Lord B., *Theory of Sound* (Dover Publications, New York, N. Y., 504 pp., 1945)
81. Elton, L. R. B., *Proc. Phys. Soc. (London)*, **63A**, 1115 (1950); *Phys. Rev.*, **79**, 412 (1950)
82. Parzen, G., *Phys. Rev.*, **80**, 355 (1950)
83. Guth, E., *Wien. Anz. Akad. Wiss.*, **24**, 299 (1934)
84. Lyman, E. M., Hanson, A. O., and Scott, M. B., *Phys. Rev.*, **79**, 228 (1950)
85. Acheson, L. K., Jr., *Phys. Rev.*, **82**, 488 (1951)
86. Feshbach, H., *Phys. Rev.*, **84**, 1206 (1951)
87. Elton, L. R. B., *Proc. Phys. Soc. (London)*, **66A**, 806 (1953)
88. Bitter, F., and Feshbach, H., *Phys. Rev.*, **92**, 837 (1953)
89. Bodmer, A. R., *Proc. Phys. Soc. (London)*, **66A**, 1041 (1953)
90. Glassgold, A. E., *Phys. Rev.*, **98**, 1360 (1955)
91. Rosenfeld, L., *Nuclear Physics*, **2**, 450 (1956)
92. Fowler, G. N., *Proc. Phys. Soc. (London)*, **68A**, 559 (1955)
93. Reignier, J., *Bull. Acad. Roy. Belg. Cl. Sc.*, **41**, 151 (1955)
94. Reignier, J., *Nuclear Physics*, **3**, 340 (1957)
95. Yennie, D. R., Wilson, R. N., and Ravenhall, D. G., *Phys. Rev.*, **92**, 1325 (1953)
96. Yennie, D. R., Ravenhall, D. G., and Wilson, R. N., *Phys. Rev.*, **95**, 500 (1954)
97. Brenner, S., Brown, G. E., and Elton, L. R. B., *Phil. Mag.* (7), **45**, 524 (1954)
98. Ravenhall, D. G., and Yennie, D. R., *Phys. Rev.*, **96**, 239 (1954)
99. Brown, G. E., and Elton, L. R. B., *Phil. Mag.*, (7), **46**, 154 (1955)
100. Ford, K. W., and Hill, D. L., *Ann. Rev. Nuclear Sci.*, **5**, 25 (1955)
101. Hahn, B., Ravenhall, D. G., and Hofstadter, R., *Phys. Rev.*, **101**, 1131 (1956)
102. Valk, H. S., *Nuovo cimento* (To be published)
103. Ravenhall, D. G. (Private communication)
104. Schiff, L. I., *Phys. Rev.*, **98**, 756 (1955)
105. Valk, H. S., and Malenka, B. J., *Phys. Rev.*, **104**, 800 (1956)
106. Schwinger, J., *Phys. Rev.*, **75**, 898 (1949)
107. Suura, H., *Phys. Rev.*, **99**, 1020 (1955)
108. Lomon, E. L., *Nuclear Physics*, **1**, 101 (1956)
109. McAllister, R. W., *Phys. Rev.*, **104**, 1494 (1956)
110. Tautfest, G. W., and Panofsky, W. K. H., *Phys. Rev.*, **105**, 1356 (1957)
111. Dirac, P. A. M., *Proc. Roy. Soc. (London)*, **117A**, 610 (1928); *The Principles of Quantum Mechanics*, Chap. 11, 256 (Oxford Univ. Press, Oxford, England, 311 pp., 1947)
112. Pauling, L., and Wilson, E. B., *Introduction to Quantum Mechanics* (McGraw-Hill Book Co., Inc., New York, N. Y., 468 pp., 1935)
113. Darwin, C. G., *Proc. Roy. Soc. (London)*, **118A**, 654 (1928)
114. Watson, G. N., *Theory of Bessel Functions* (Macmillan Co., New York, N. Y., 804 pp., 1948)
115. Glassgold, A. E., and Mack, E. W., *Mass. Inst. Technol. Research Lab. for Nuclear Sci. and Eng., Tech. Rept.*, **65** (Aug. 31, 1954)
116. Ravenhall, D. G., and Yennie, D. R. (To be published)
117. Hahn, B., Hofstadter, R., and Ravenhall, D. G., *Phys. Rev.*, **105**, 1353 (1957)
118. Amaldi, E., Fidecaro, G., and Mariani, J., *Nuovo cimento*, **7**, 757 (1950)

119. Schiff, L. I., *Phys. Rev.*, **96**, 765 (1954); *Phys. Rev.*, **98**, 1281 (1955)
120. Sherman, B. F., and Ravenhall, D. G., *Phys. Rev.*, **103**, 949 (1956)
121. Tassie, L. J., *Australian J. Phys.*, **9**, 407 (1956)
122. Ravenhall, D. G. (Private communication)
123. Ferroni, S., and Fubini, S., *Nuovo cimento*, **1**, 263 (1955)
124. Newton, R. G., *Phys. Rev.*, **103**, 385 (1956)
125. Bernardini, M., Brovetto, P., and Ferroni, S., *Nuovo cimento*, **5**, 1292 (1957)
126. Downs, B. W., *A Study of Electric Quadrupole and Proton Correlation Effects in the Scattering of High-Energy Electrons by Heavy Nuclei* (Doctoral thesis, Stanford Univ., Stanford, Calif., 1955)
127. Downs, B. W., Ravenhall, D. G., and Yennie, D. R., *Phys. Rev.*, **98**, 277A (1955); Yennie, D. R., Ravenhall, D. G., and Downs, B. W., *Phys. Rev.*, **98**, 277A (1955); *Phys. Rev.*, **106**, 1285 (1957)
128. Hahn, B., and Hofstadter, R., *Phys. Rev.*, **98**, 278A (1955)
129. Massey, H. S. W., *Proc. Roy. Soc. (London)*, **181A**, 14 (1942)
130. Yadav, H. N., *Proc. Phys. Soc. (London)*, **65A**, 672 (1952)
131. Parzen, G., and Wainright, T., *Phys. Rev.*, **98**, 188 (1954)
132. Allen, K. R., Finlay, E. A., Lipsicas, M., Major, D., and Phillips, K., *Proc. Phys. Soc. (London)*, **70**, 355 (1957)
133. Elton, L. R. B., and Parker, K., *Proc. Phys. Soc. (London)*, **66**, 428 (1953)
134. Miller, R. C., and Robinson, C. S., *Ann. Phys.* (To be published)
135. Gatto, R., *Nuovo cimento*, **2**, 669 (1955)
136. Downs, B. W., *Phys. Rev.*, **101**, 820 (1956)
137. Lewis, R. R., *Phys. Rev.*, **102**, 544 (1956)
138. Schiff, L. I., *Nuovo cimento*, **5**, 1223 (1957)
139. Van Hove, L., *Phys. Rev.*, **95**, 249 (1954)
140. Waller, I., *Z. Physik*, **51**, 213 (1928)
141. Waller, I., and Hartree, D. R., *Proc. Roy. Soc. (London)*, **124A**, 119 (1929)
142. Elton, L. R. B., and Robertson, H. H., *Proc. Phys. Soc. (London)*, **65A**, 145 (1952)
143. Schiff, L. I., *Phys. Rev.*, **87**, 750 (1952)
144. Redhead, M. L. G., *Proc. Roy. Soc. (London)*, **220A**, 219 (1953)
145. Biel, S. J., and Burhop, E. H. S., *Proc. Phys. Soc. (London)*, **68A**, 165 (1955)
146. Bumiller, F., Ehrenberg, H., Hofstadter, R., and Meyer-Berkhout, U., *Proc. 7th Ann. Rochester Conf.* (1957)
147. Dalitz, R. H., and Yennie, D. R., *Phys. Rev.*, **105**, 1598 (1957)
148. Panofsky, W. K. H., Woodward, W. W., and Yodh, G. B., *Phys. Rev.*, **102**, 1392 (1956)
149. Kofoed-Hansen, O., *Nuclear Physics*, **2**, 441 (1956)
150. Cooper, L. N., *Nuovo cimento*, (Suppl. to Vol. IV), **3**, 1125 (1956)
151. Cronin, J. W., Cool, R., and Abashian, A. (To be published)

COLLISIONS OF ≤ 1 BEV PARTICLES (EXCLUDING ELECTRONS AND PHOTONS) WITH NUCLEI¹

BY S. J. LINDENBAUM

Brookhaven National Laboratory, Long Island, N. Y.

INTRODUCTION

In the past several years a great deal of progress has been made in experimentally determining the properties of the collisions of particles exhibiting strong nuclear interactions both with each other and with nuclei. Pions² and nucleons have been most extensively studied. Their relatively long lifetime and abundant production at various accelerators have provided beams of these particles of sufficient intensity for detailed observation of the interactions resulting from their collisions with nucleons and nuclei.

The greatest theoretical attack has been made on pion-nucleon interactions. It has been particularly encouraging that most of the dominant features of the lower energy interactions (pions of kinetic energy < 250 Mev) have been satisfactorily explained by one resonant state of isotopic spin (T) and angular momentum (J) equal to $3/2$, with a resonant energy of ~ 190 Mev (kinetic—L.S.) and the considerable peak cross-section of about 200 mb (millibarns) near the resonance.

The higher energy pion-nucleon interactions (500 Mev to ≥ 1 Bev) are less understood; however, one dominant feature is that the $T = \frac{1}{2}$ cross-section has a peak of ~ 60 (mb) at about 1 Bev while the $T = 3/2$ cross-section is generally much smaller in this region. However, it has a rise from a minimum of ~ 15 mb near 650 Mev to a peak of ~ 40 mb near 1.3 Bev.

The concept of charge independence or conservation of isotopic spin in strong nuclear interactions has been successfully applied in analyzing the data, and has not been contradicted in any experiment performed to date. Elastic nucleon-nucleon collisions below 500 Mev are still only partially understood; however, the behavior of the cross-sections experimentally is quite well known. Above 500 Mev, pion production becomes important and the properties of the pion-nucleon interaction seem to play a predominant role in this. The total p - p and n - p cross-sections and the elastic and inelastic parts of the p - p cross-section have been fairly well determined. The elastic

¹ The general survey of literature pertaining to this review was completed in December, 1956. However, some particularly relevant later publications previously available privately to the author have been referred to.

² The term pion for the π -meson has been extensively employed lately and will be used freely throughout this article. Energies cited will be kinetic energy in the lab system unless otherwise specified.

cross-section at these higher energies can be generally explained as a diffraction cross-section accompanying the inelastic meson production.

The interactions of nucleons with nuclei (kinetic energy ≥ 50 Mev) is generally consistent with the optical model, and the inelastic parts thereof can be explained in terms of primary nucleon-nucleon encounters in the nucleus which are followed by a nucleonic cascade of the nucleons and produced pions, and finally by an evaporation process.

The interactions of pions with nuclei are generally consistent with primary pion encounters with one or a pair of nucleons in nuclear matter followed by nucleonic cascade initiated by the products which often includes absorption of the pion and finally an evaporation process.

The treatment in this article will be confined exclusively to those particles produced prolifically in collisions of $\lesssim 1$ Bev nucleons with nuclei, namely nucleons and pions. The major emphasis will be placed on those interactions of pions and nucleons with nucleons and nuclei, which are important for incident energy of $\lesssim 1$ Bev. However, the treatment will be extended to higher energies in cases such as pion production and pion interactions, where the physical phenomenon is either essentially clarified thereby, or relevant individual investigations considered have extended to higher energies.

The cross-section for the production of strange particles is less than ~ 3 per cent of the inelastic cross-section in all collisions considered here. Strange particle production and interactions will be reviewed in this volume by Gell-Mann & Rosenfeld in an article entitled "Hyperons and Heavy Mesons (Systematics and Decay)" (cf. p. 407). Therefore these subjects will not be considered here.

It is clear that all relevant topics in pion and nucleon collisions cannot be fully treated in this review and that some will have to be omitted or mentioned briefly.

COLLISIONS OF POSITIVE AND NEGATIVE PIONS WITH HYDROGEN

The scattering of π^\pm mesons by hydrogen.—Since the previous review by Gell-Mann & Watson (1) three years ago, the available data on the total and differential cross-section of $\pi^\pm + p$ have increased markedly both in the number of measurements and the accuracy thereof. Figure 1 shows a compilation of the latest and most accurate available data on the $\pi^+ + p$ total cross-section for incident pion energies of 125 to 250 Mev. The $\pi^+ + p$ scattering for this energy region has received a great deal of attention lately, since it involves a pure isotopic spin $3/2$ state, and hence is best suited for determining whether there is, as now generally believed, a resonance in the state of isotopic spin and angular momentum $3/2$ at a pion kinetic energy of ~ 190 Mev. The most extensive investigations have been made by Ashkin *et al.* (2), Lindenbaum & Yuan (3, 4), and Mukhin *et al.* (5, 6). The absolute accuracy of the behavior of these total cross-sections as a function of energy is now generally known within ± 5 per cent, and the relative value of the

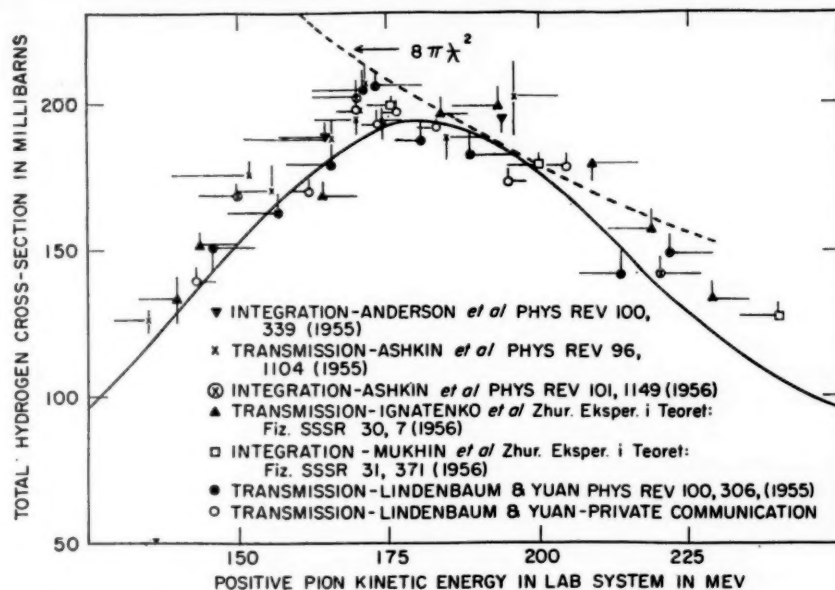


FIG. 1. A plot of the latest and most accurate $\pi^+ + p$ total cross-section data in the energy region 125 to 250 Mev. The solid line represents the contribution of α_{33} alone, taken from Fig. 2 (2 to 6, 10, 11).

$\pi^+ + p$ total cross-section curve around the resonance peak has now been determined to approximately ± 2 per cent in a recent experiment (4).

The $8\pi\chi^2$ curve shows the contribution to the $\pi^+ + p$ total cross-section at the resonance energy, due to a P -wave resonance in the state of isotopic spin (T) and angular momentum (J) equal to $3/2$. It is clear that within the errors the total $\pi^+ + p$ cross-section curve appears to be either tangent to or larger than the $8\pi\chi^2$ line in the region of 180 to 200 Mev. Hence these data are consistent with a resonance in the $T = J = 3/2$ state in this energy region.

The Chew-Low equation.—Chew & Low (7b) recently investigated an exact equation deduced by Low (7a) for pion-nucleon interactions which included the pion cloud effects in the nuclear wave function and obtained as an approximate solution for the scattering in the symmetric pseudoscalar meson theory in the one meson approximation:

$$\frac{\eta^3}{\omega_t^*} \cot \alpha_{33} = \frac{3}{4} (\beta^2)^{-1} F(\omega_t^*) \quad 1.$$

Where η is the c.m.s. pion momentum in units of $m_\pi c$; ω_t^* is the total c.m.s. energy of the pion plus the nucleon kinetic energy³ in units of $m_\pi c^2$; m_π is the pion rest mass; c is the velocity of light; α_{33} is the phase shift in the $T = J = 3/2$

³ The inclusion of the recoil nucleon kinetic energy in the total c.m.s. energy (ω_t^*) is an attempt to take into account approximately the nucleon recoil effects.

state; f^2 is the renormalized unrenormalized coupling constant; and $F(\omega_i^*)$ is of the form $1 - \omega_i^* r_a(\omega_i^*)$ with $r_a(\omega_i^*)$ almost a constant for small ω_i^* . This allows a determination of f^2 by extrapolation as will be explained later.

Serber & Lee (c.f. p. 457 of ref. 9) have found that the exact solution of the Chew-Low equation for charged and neutral scalar meson theories in the one meson approximation is:

$$\frac{\eta^2}{\omega_i^*} \cot \alpha_{33} - \frac{1}{\omega_i^*} = \frac{3}{4} (f^2)^{-1} F(\omega_i^*) \quad 2.$$

An analysis of the effective range approximation, the experimental data, and other reasons led Chew and Low to originally assume that $F(\omega_i^*) = 1 - (\omega_i^*/\omega_0^*)$ where ω_0^* is the resonance energy. One should note that the cut-off model (7b) predicts a low energy resonance in the $T=J=3/2$ state for the observed values of the coupling constant, provided that the cut-off energy ω_{\max} is large enough. The resonance energy (ω_0) depends on f^2 and ω_{\max} , and therefore ω_0 can replace ω_{\max} as a parameter in the theory. It has been shown (3) that this particular choice (Eq. 2) for $F(\omega_i^*)$ results in a variation of the $\pi^+ + p$ total cross-section generally similar to the one obtained by Brueckner (8), when he fitted a one-level Breit-Wigner resonance formula to the observed energy variation of the $\pi^+ + p$ total cross-section assuming the $T=J=3/2$ state resonates.

It is also clear that with $F(\omega_i^*) = 1 - (\omega_i^*/\omega_0^*)$, if the left hand side of Eqs. 1 or 2 is plotted as an ordinate, versus ω_i^* as an abscissa, a straight line is predicted by the theory which determines the resonance energy at the point where $\cot \alpha_{33} = 0$. This is the point where the ordinate is 0 or $-(1/\omega_i^*)$, for the Chew-Low plot or Serber-Lee plot, respectively. The coupling constant f^2 is also obtained by extrapolating the line to determine the y intercept at $\omega_i^* = 0$.⁴

The Serber-Lee plot is shown in Figure 2. The values of α_{33} were obtained from the best values of the phase shift analysis of the differential scattering and charge exchange cross-section of pion-nucleon scattering. These experiments will be discussed later.

It is clear from Figure 2 that the data can be fitted by one straight line below resonance and another straight line of considerably different slope above resonance. This change in slope exists also for the Chew-Low plot (not shown) as well as for the Serber-Lee plot and has been previously suggested (3).

The resonance energy is defined as that energy where α_{33} passes through 90° or equivalently where the ordinate of the Serber-Lee plot equals $-(1/\omega_i^*)$. Due to the change in slope of the Serber-Lee plot near resonance,

⁴ Chew & Low (7b) point out that the change in f^2 due to the inclusion the $-(1/\omega_i^*)$ term in the ordinate of the plot may be of the same order of magnitude as the second order correction and the errors in the experimental data.

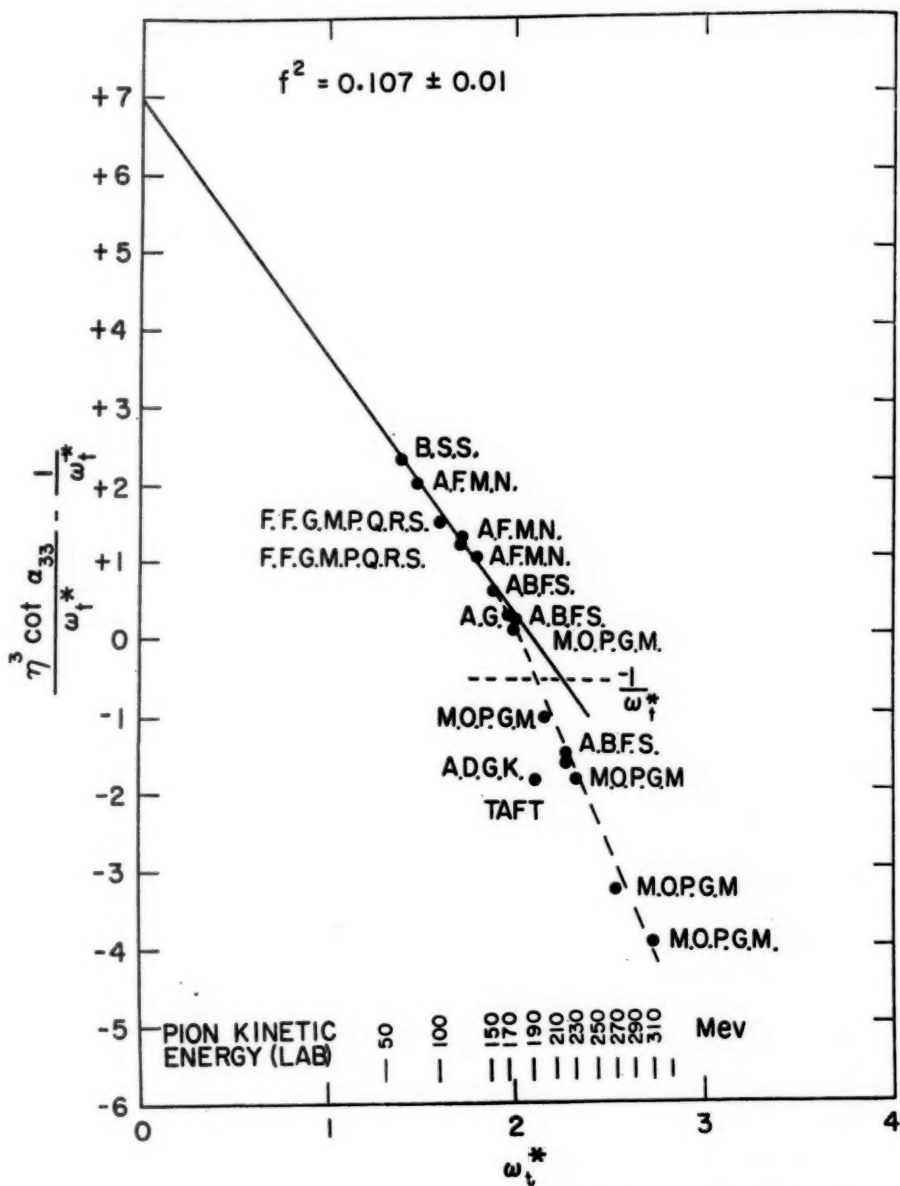


FIG. 2. A Serber-Lee plot—see text on original Chew-Low plot which is similar except for lack of $-(1/\omega_t^*)$ term in the ordinate. Initials of author's last names are used for identification of points (6, 10, 11, 12, 16, 17, 27).

the intersection of the plot with the $-(1/\omega_t^*)$ curve is uncertain. However the best guess for which the rate of change in slope is not too rapid, is that the intersection of the broken line (solution above resonance) with the $-(1/\omega_t^*)$ curve is the resonant point. A reasonable estimate from Figure 2 is that the resonant energy is 190_{-10}^{+20} Mev, where the estimation of errors is somewhat arbitrary and uncertain.

The fact that the Serber-Lee or Chew-Low plots are not unique straight lines is not surprising, since $F(\omega_t^*)$ was more or less arbitrarily chosen and its form can only be even approximately justified near $\omega_t^* = 1$. One might also note that the resonance energy is approximately at the threshold for producing an additional pion; hence two meson states may begin to contribute appreciably. Furthermore, Castillejo *et al.* (9) have investigated the Chew-Low equation for charged and neutral scalar meson theories treated in the one meson approximation. They demonstrated that the Chew-Low equation does not have a unique solution, and indeed does not contain more information or restrictions than a generalized dispersion formula of the Wigner-Eisenbud type. It is not at present known whether this also holds true for pseudoscalar meson theory when all higher approximations are included, however, there is certainly no reason to assume that a unique and more restrictive solution exists for the pseudoscalar case. It was previously pointed out (3), that the particular solutions chosen by Chew & Low and Serber & Lee have properties generally similar to a P-wave Breit-Wigner one-level resonance formula plotted in a linear form, and hence represent convenient ways to analyze the data. Furthermore, Chew & Low point out that their solution may possibly be the only one of physical interest.⁵

The coupling constant deduced from Figure 2 is $f^2 = 0.107 \pm 0.01$. This value will be compared to others obtained by different methods in a subsequent section.

The contribution to the $\pi^+ + p$ total cross-section as a function of energy by the α_{33} phase shift variation is shown in Figure 1 and also Figure 3 where the solid line $\pi^+ + p$ curve has been computed this way until 650 Mev. The variation of α_{33} with energy was taken from the Serber-Lee plot (Fig. 2) by following the solid line to ~ 170 Mev and the broken line thereafter. As one can see, the observed $\pi^+ + p$ total cross-section can be represented very well, to within a few per cent, by the contribution of α_{33} alone to energies well beyond the highest energy (307 Mev), for which α_{33} has been well determined. This curve has a peak in the laboratory system at a pion kinetic energy ~ 180 Mev, and is consistent with a resonance in the $T=J=3/2$ state at ~ 190 Mev.

⁵ Chew & Low (7b) point out that their solution is the only one which is an analytic continuation of the perturbation theory power series solution. Hence they argue if one assumes that the original field theoretic problem has a unique solution which is an analytic continuation of the power series then their solution is the only one of physical interest.

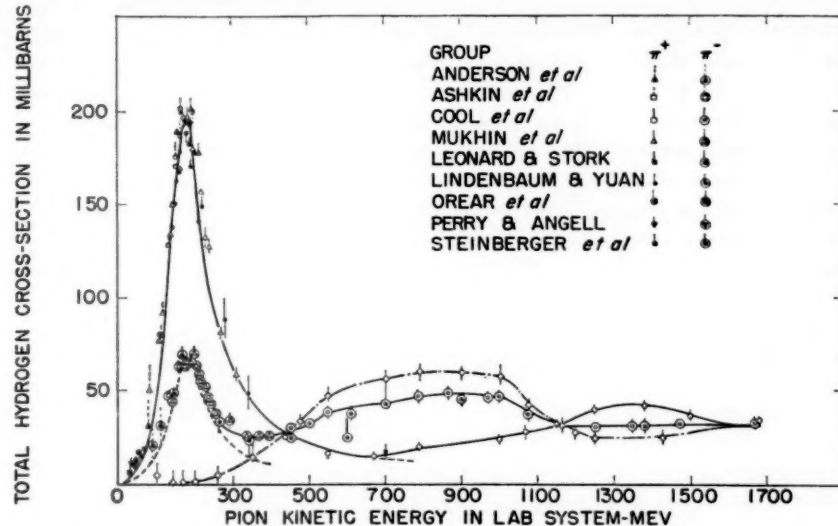


FIG. 3. A plot of $\pi^\pm + p$ total cross-sections as a function of energy, using in general significantly more accurate data when a choice exists. The contribution of α_{33} alone to the cross-section is shown for $\pi^+ + p$ by the solid line below ~ 650 Mev and the broken line thereafter; for $\pi^- + p$ by the broken line. The following are empirical curves: the solid line for $\pi^+ + p$ beyond ~ 650 Mev; the solid line for $\pi^- + p$; the dash-dot curve through the open diamond points was obtained for the $T = \frac{1}{2}$ cross-section by the standard subtraction method (2 to 6, 10, 11, 12, 15, 22, 25 to 28).

The phase shifts of the other S and P states namely α_3 and α_{31} which accompany the α_{33} resonance-solution are quite small and contribute ≤ 5 per cent to the $\pi^+ + p$ total cross-section. These will be discussed in a later section. The contributions to the $\pi^- + p$ total cross-section as a function of energy by the α_{33} phase shift is shown in Figure 3 by the dashed line near the $\pi^- + p$ points. It is clear that up to ~ 200 Mev the total $\pi^- + p$ cross-section curve can be represented well, to within a few per cent, by the contribution of α_{33} alone.

One should note here that the extrapolation beyond 307 Mev of the line in the Serber-Lee plot which fits the data above resonance, is at best a questionable procedure since there are no accurate measurements of α_{33} beyond this energy. The apparent agreement of the $\pi^+ + p$ total cross-section with this extrapolation to beyond 600 Mev may well be purely accidental. It will be pointed out later that even at 307 Mev there is some evidence that suggests an appreciable D-wave contribution which could of course become large at the higher energies.

Phase shifts.—The angular distribution of positive and negative pions incident on hydrogen which are direct and charge exchange scattered have

been extensively studied recently. The most extensive investigations have been performed by Ashkin *et al.* (10) for $\pi^\pm + p$ at 150, 170 and 220 Mev, Mukhin *et al.* (6) for $\pi^+ + p$ at 176, 200, 240, 270 and 307 Mev,⁶ and Anderson *et al.* (11) for $\pi^\pm + p$ at 165 and $\pi^+ + p$ at 189 Mev. These results have been subjected to the S and P wave phase shift analysis first introduced by Fermi and his co-workers (12) which assumes charge independence and involves the six phase shifts α_3 , α_{31} , α_{33} , α_1 , α_{11} , and α_{13} . The first index equals twice the isotopic spin and the second equals twice the angular momentum. Although several possible solutions can be found to the data (13, 14), the one generally accepted as most likely to be physically significant and most compatible with all experimental observations is the Bethe-DeHoffman *et al.* (13a, 14) solution for the so-called Fermi phase shifts. In this solution α_{33} passes through resonance at about 195 Mev, and all others are small below 200 Mev.

A compilation of α_{33} phase shifts of this type are shown in Figure 2 in the form of the Serber-Lee plot. The sign of α_{33} has been determined by Orear (15), Ferrari *et al.* (16), and Taft (17) who observed the interference of $\pi^+ + p$ nuclear scattering with the Coulomb scattering. This also determines the absolute sign of other phase shifts in a particular phase shift analysis. The values of α_3 appear to be consistent with the Orear proposal (18) $\alpha_3 = -0.11\eta$ until 200 Mev. Above 200 Mev α_3 seems to increase more rapidly with increasing η than the foregoing if only an S-P analysis is considered (6). However, under an S-P-D analysis (6) the foregoing prescription still seems to hold with small amounts of D wave predicted, namely:

$$\delta_{33} = +0.20\eta^5 \quad \text{and} \quad \delta_{33} = -0.21\eta^5$$

These D wave formulae correspond to less than $\sim 10^\circ$ D-wave at 307 Mev, which is the highest energy analyzed.

The behavior of α_1 is less well known. However, the Orear prescription (18) of $\alpha_1 = 0.16\eta$ still seems consistent with the data.

The behavior of α_{31} is still uncertain. However, the analyses of recent $\pi^+ + p$ differential cross-section experiments by Ferrari *et al.* (16) between 70 and 130 Mev and Mukhin *et al.* (6) between 176 and 307 Mev, make it appear likely that it is small and negative with a value of $\lesssim 10^\circ$ for energies below 307 Mev. The values of α_{13} and α_{11} are both small and essentially undetermined even by the latest analyses.

The other set of phase shifts which is of most interest is the Yang set (19) which is related to the Fermi or Bethe-deHoffmann set by the following equations:

$$\alpha_{33} - \alpha_{31} = -(\alpha'_{33} - \alpha'_{31}) \quad 3.$$

$$2e^{2i\alpha_{33}} + e^{2i\alpha_{31}} = 2e^{2i\alpha'_{33}} + e^{2i\alpha'_{31}} \quad 4.$$

⁶ Some work of lower statistical accuracies on positive pion scattering by hydrogen at 260, 300, and 400 Mev observed in hydrogen diffusion chambers has been reported by Margulies (89).

The Yang set has been found by Bethe & DeHoffman (13a, 14) to show three resonances ($\alpha_{31} = 90^\circ$ and 270° ; $\alpha_{33} = 90^\circ$) by the time the α_{33} of the Fermi solution has reached only 120° . This is considered to be a less likely physical behavior.

Another ambiguity in the phase shifts has been pointed out by Minami (20a), however, for several reasons [see p. 75 of ref. (14)] this solution is considered to be unlikely.

A recent application of causality using spin-flip amplitudes (21) supports the Fermi set and tends to reject the Yang set. An earlier different application of causality using non-flip amplitudes (22) could not rule out the Yang set.

Fermi pointed out that the polarization (23) of the recoil nucleon in meson-nucleon scattering is quite different for the Fermi and Yang phase shifts. Several experiments (24) are now in progress which are attempting to observe the polarization and so distinguish between the two sets on a direct absolute basis.

Hayakawa *et al.* (20b) have shown that the Minami ambiguity can also be settled by observing the polarization of the recoil nucleon.

Total $\pi^\pm + p$ cross-sections.—The total cross-section (2 to 6, 10 to 12, 15 to 18, 22, 25 to 28) of $\pi^\pm + p$ as a function of pion kinetic energy are plotted in Figure 3 (also see Fig. 1). The higher energy points have been mainly investigated by Cool, Piccioni & Clark (25). The assumption of charge independence, or, equivalently, conservation of isotopic spin, has been made in obtaining the total cross-sections for the two isotopic spin states $T = \frac{1}{2}$ and $T = 3/2$ which are involved in these interactions. The relations used are:

$$\sigma(\pi^+ + p) = \sigma(T = 3/2) \quad 5.$$

$$\sigma(\pi^- + p) = \frac{1}{3}\sigma(T = 3/2) + 2/3\sigma(T = \frac{1}{2}) \quad 6.$$

Since within the errors the $T = \frac{1}{2}$ cross-section is zero below 200 Mev it is implied that the low energy $\pi^- + p$ cross-section is probably mainly due to the previously noted resonance in the $T = J = 3/2$ state. In fact, the dashed line curve shows the total cross-section contribution computed from the α_{33} phase shift. The fit to the observed total cross-section is reasonably good to within a few per cent below 200 Mev. However the $T = \frac{1}{2}$ cross-section rises steeply above 200 Mev and reaches a peak at about 1.0 Bev. This phenomenon has been subjected to many investigations. One early proposal due to Dyson (29), Takeda (30), and Piccioni⁷ (25) was that the 1.0 Bev peak is due to a resonance in the interaction of the incident pion with a pion in the nucleon cloud. This possibility has been investigated by several groups recently and does not appear to be consistent with the experimental data. One major difficulty is that the expected internal momentum distribution of the pion in the cloud would spread even a sharp resonance by

⁷ A resonance corresponding to $J = 5/2$ has also been found to be compatible with the data by this group.

± 1 Bev/c (25) which would wash out the peaked behavior observed in the cross-section. Another difficulty is that an investigation of the inelastic pion production by negative pions of ~ 1 Bev energy incident on hydrogen, Walker *et al.* (31) conclude that the experimental evidence does not support this model.

One recent approach (32) has been to associate the rise in the $T=\frac{1}{2}$ cross-section with the formation of the already known nucleon isobar with $T=J=3/2$ followed by its subsequent decay via pion emission. This approach appears promising in explaining the general behavior of the total cross-sections and also the characteristics (32, 33) of the inelastic pions.

The treatment of the production of pions by pions incident on nucleons via the Chew-Low formalism (34) has also been considered recently.

Causality and dispersion relations.—The Kramers-Kronig dispersion relation for light was derived from the condition that the scattered wave amplitude should be zero until the incident wave reached the scatterer, and that signals cannot propagate faster than the velocity of light. Such causality relations which relate the real part of the forward scattering amplitude to an integral over the imaginary part have recently been developed for pion-nucleon scattering by Karplus & Rudeman (35) for the scattering of neutral pions, and later by Goldberger and co-workers (36) for charged pion scattering. Anderson *et al.* (22) have found that they can be used successfully in deducing the forward scattering amplitude for $\pi-p$ scattering via integrals over the total cross-sections.

Dispersion relations for scattering at all angles have recently been proposed by several groups (21, 37). In regard to the validity of these relationships one might note that until recently the best support for them was that for pseudoscalar couplings, these hold in all orders of perturbation theory.

Recently, Symanzik (37) has proved these relations for the forward direction and for infinitesimal angles under certain conditions. Bogoliubov (38) has proved them for any finite angle.

They have been applied to reject some of the many phase shift solutions of $\pi^+ - p$ scattering (22) and in fact in a recent application (21), appear to discriminate against the Yang set and support the Fermi set. The spin-flip amplitudes were used, which in effect is equivalent to performing a theoretical polarization experiment.

As pointed out by Goldberger and co-workers (36) with certain assumptions one can get equations similar to Low's integral equations for the phase shifts.

The dispersion relations depend only on microscopic causality, Lorentz invariance, and several general relations for local field theories. Therefore they represent a general equivalent for the usual concepts of conventional local field theory.

Coupling constant.—The renormalized, unratinalized coupling constant f^2 deduced from the Serber-Lee plot in Figure 2 is $f^2 = 0.107 \pm 0.01$. If a Chew-

Low plot (not shown) had been used one would have obtained $f^2 = 0.96 \pm 0.01$ or about a 10 per cent smaller number.⁸ The experimental errors are at present larger than the difference in the two methods. A straight line extrapolation for a coupling constant determination from a nonspin-flip dispersion relation has been used by Haber-Schaim (39) who obtained $f^2 = 0.082 \pm 0.015$. This dispersion relation is rapidly convergent and probably represents the most accurate extrapolation that can be made at this time. Bernardini and co-workers (40a) have obtained from their experiments on photoproduction, a zero point determination of the coupling constant $f^2 = 0.067 \pm 0.003$. The Bernardini value is not inconsistent with the Haber-Schaim value based on dispersion theory within the errors. It has been pointed out by Puppi & Stanghellini (41a) that the significantly lower results of the Bernardini and Haber-Schaim coupling constant determinations from those previously obtained for the Serber-Lee or Chew-Low plots may be due to the fact that the Serber-Lee and Chew-Low plots consider scattering in the $T = J = 3/2$ state while both the photoproduction and dispersion theory [Haber-Schaim] determinations involve the $T = \frac{1}{2}$ state also. Puppi (41b) finds that the predicted coupling constant based on applying causality to $\pi^- + p$ scattering only is much smaller. A recent determination by Davidon & Goldberger (21b) of f^2 using spin flip-amplitudes from dispersion theory which depend on α_{33} and α_{31} has yielded $f^2 \approx 0.1$ for the Fermi set. Hence, it appears that determinations of f^2 which involve pure $T = 3/2$ states seem to yield higher values than those which involve $T = \frac{1}{2}$ states as well. Errors in the evaluation of the various extrapolation procedures, or electromagnetic effects (41c, 41d, 41e) do not appear to be large enough to account for the discrepancies. If the experimental results are correct, either charge independence or more likely microscopic causality appear to be violated. However, an underestimation of electromagnetic effects or an incorrect evaluation of the dispersion integrals at high energies may possibly be the explanation (41b, 41c, 41d, 41e).

COLLISIONS OF POSITIVE AND NEGATIVE PIONS WITH HEAVIER NUCLEI

Cross-sections.—The total cross-sections of deuterium for negative pions has been recently measured with counter techniques from 128 to 400 Mev (2, 42) and 0.8 to 1.9 Bev (25). One can represent the deuterium cross-section by the sum of the individual pion-nucleon cross-sections plus a correction term as follows:

$$\sigma(\pi^- + D) = \sigma(\pi^- + n) + \sigma(\pi^- + p) + \Delta \quad 7.$$

If it is then assumed by the principle of charge symmetry that $\sigma(\pi^- + n) = \sigma(\pi^+ + p)$, one finds from these experiments that Δ is negative and of the order of 15 per cent or less of $\sigma(\pi^- + D)$. Both its sign and magnitude can be

⁸ A value of $f^2 \approx 0.010$ has also been obtained from Low's equations by Cini & Fubini (90).

reasonably explained by interference (43) and shadow (44) effects. This supports the principle of charge symmetry.

Some measurements have also been made for $\sigma(\pi^+ + D)$ at 120 to 180, 550 and 740 Mev (2, 25). In all cases it was found that within the errors $\sigma(\pi^+ + D) = \sigma(\pi^- + D)$ which strongly supports the principle of charge symmetry. Rogers & Lederman (45a) have investigated the scattering of 85 Mev positive pions in a deuterium filled diffusion chamber, and also find results consistent with the sum of the free nucleon scattering cross-section when interference effects (45b) are taken into account.

The total cross-sections of Be, C, and O and the inelastic collision cross-sections of Be, C, Cu, and Pb for 140 to 400 Mev π^- mesons have been measured with counter techniques by Ignatenko *et al.* (46). For the light nuclei both the total and the inelastic cross-sections follow the general energy behavior of the pion-hydrogen total cross-sections (see Fig. 3); however, the region near the peak cross-section relative to the tails is smaller and broader. The total and inelastic cross-sections are relatively constant in the energy interval of 140 to 250 Mev but drop fairly rapidly thereafter. For the heavier nuclei the energy variation of the cross-sections is smaller, as one would expect, which is attributable to the increasing importance of the shadowing of nucleons by others. The shadowing effects also qualitatively explain the previously noted behavior of the cross-sections of light nuclei.

In general, the behavior of the total and inelastic cross-sections of Be, C O, Cu, and Pb for negative pions in the energy range 140 to 400 Mev has been found by these authors to be consistent with the predictions of the optical model (47, 48) with a nuclear radius of $1.42A^{1/3} \times 10^{-13}$ cm. The observed results were not sensitive to the effects of the Pauli Exclusion Principle for incident pion energy ≥ 150 Mev.

Total cross-sections for Be, C, Al, Ca, and the inelastic cross-sections of Be, C, Al, Ca, Cu, Sn, and Pb for 970 Mev π^- have been determined by Abashian *et al.* (49). These authors find their results are consistent with the optical model when it is modified by using the shape of the nucleus deduced by Hofstadter and co-workers (50) and a radius about 5 per cent larger than the electromagnetic radius. Williams (51) has analyzed the elastic and inelastic cross-sections of emulsion nuclei for 1.5 Bev negative pions and finds an approximate agreement with the optical model for a tapered nucleus (50, 51). Some general comments in regard to the different nuclear radii and density distributions used by various authors will be made in the last section of the paper in connection with an analysis of the optical model for nucleon-nucleon collisions.

Elastic and inelastic scattering.—Differential elastic scattering of 80 Mev positive and negative pions has been investigated by Pevsner *et al.* (52) for Al and by Williams *et al.* (53) for Li and Cu. The differential elastic scattering cross-sections of Cu and Al drop rapidly from values of $\sim 1,000$ mb per steradian at $\theta \sim 15^\circ$ to values of $10 \geq$ mb per ster. at $\theta \geq 5^\circ$. For Cu and Al the

experimental results were in reasonable agreement in the forward hemisphere with the predictions of an exact optical model phase shift calculation (52, 53) using a complex attractive square well potential for $r \leq 1.4A^{1/3} \times 10^{-13}$ cm. and the Coulomb potential for $r > 1.4A^{1/3} \times 10^{-13}$ cm. The calculations were performed by actually solving the Klein-Gordon equation for the angular momentum states which contribute appreciably, using a square well with suitable boundary conditions which include matching external Coulomb wave functions. The optical model predictions beyond the first diffraction minimum departed progressively with angle from the experimental results. In particular, the experimental results indicated too large a cross-section in the backward direction and did not show the well defined subsequent minima and maxima present in the theoretical diffraction pattern results.

These authors felt that at the larger angles inelastic transitions accepted within the experimental energy resolution, the width of the angular resolution and the possible effects of a tapered edge nucleus could probably account for the observed discrepancies. In a continuation of this work [see note added in proof, (53b); (54)] with a new detection method which greatly increased discrimination against inelastic events, reasonable indications of diffraction patterns were found, and a general behavior in agreement with the predictions of the optical model was observed. The remaining discrepancies with the theoretical predictions can probably be attributed to the effects previously mentioned above.

All experiments show a characteristic interference of the nuclear and Coulomb scattering which is destructive for π^+ and constructive for π^- implying a positive sign for the α_{33} phase shift. Several modified Born approximation calculations (52, 53) in which coherent additions of π -nucleon scattering from individual nucleons are multiplied by suitable form factors and attenuation factors were also performed, and the results agree reasonably well with the experimental behavior for the forward angles. The complex nuclear potential was included in the energy term in the Klein-Gordon equation as the fourth component of a four-vector. The potential which fits the results for Al and Cu reasonably well is approximately a uniform well with a real part ~ 30 Mev deep and an absorptive imaginary part ~ 20 Mev. One should note that the theoretical results are not very sensitive to small variations of these values.

In the case of pion-lithium (53) elastic scattering the Born approximation calculation was in reasonable agreement with the experimental data at all angles, and it appears to be a much more suitable treatment than the optical model for the case of very light nuclei at low pion energies. It is obvious that the usual optical model approximation of a uniform complex potential within a definite radius would improve for large nuclei and higher energy pions with a correspondingly smaller deBroglie wave length.

The elastic and inelastic scattering of pions in the energy range 230 to 330 Mev have been investigated recently by Dzhelepov *et al.* (55) in carbon

and Pb plates in a Wilson chamber; by Kozodaev and his associates (56) in a helium diffusion chamber, and by Mitin & Grigoriev (57) in photographic plates. These experiments have also been treated in a review by Ignatenko (58). The predictions for the elastic scattering of pions in carbon and helium have been computed for the optical model and are consistent with the experimental results. These results are only significant for scattering angles less than 50° due to the limited statistics, and the fact that the elastic scattering cross-section drops rapidly with increasing angle.

One of the most significant features of the inelastic pion scattering is the large loss of pion energy which is ~ 150 - 220 Mev on the average. This is interpreted (58) as evidence for several collisions of the incident pion with individual nucleons in the nucleus. This would be expected especially for emulsion and Pb nuclei considering the short mean free path in nuclear matter of pions in this energy range. Further support for this hypothesis of several individual pion-nucleon collisions is the observed changes in the angular distribution of inelastically scattered pions both with angle and also increasing atomic weight. The angular distribution in carbon is similar to that expected for the scattering of negative pions on free nucleons. The results in emulsion and Pb are quite different, however, in the backward direction similarity to the scattering by free nucleons is greatest, and conversely in the forward direction the changes are greatest. This can be explained by the fact that the pion mean free path in nuclear matter is very small at these energies so that the first interactions would take place near the surface. Hence a backward scattered pion has more chance of escaping without a second scattering, whereas those emerging in the forward direction would have in general had to interact several times. The observed relations of the energy loss of pions to the scattering angle have been compared to the calculated relations for single collisions. This comparison implies that multiple collisions are common for the forward angles and become less important for the backward ones, which is consistent with the previous conclusions.

The interaction of 750 Mev π^- -mesons with emulsion nuclei have been investigated by Blau & Oliver (59a). They find that inelastic meson scattering with the production of a second meson by the incident one is an important process which is estimated from the observed cases to occur ~ 40 per cent of the time at 750 Mev and was previously estimated to occur ~ 10 per cent of the time at 500 Mev (59b). The mean prong number of the stars without escaping mesons is \sim four at both energies and \leq three for stars containing an outgoing meson. These observations are also consistent with several collisions of the incident meson with final absorption of it by the nucleus accounting for ~ 40 per cent of the cases at 750 Mev. The stars in general do not exhibit the characteristic forward nucleon cascade of grey tracks seen in nucleon induced stars produced by fast nucleons.

Approximately 7 per cent of the stars (at 750 Mev) of more than five prongs exhibited fragments ($Z \geq 3$) compared to a frequency of less than 1 per cent for stars induced by nucleons of 200 to 400 Mev for which meson

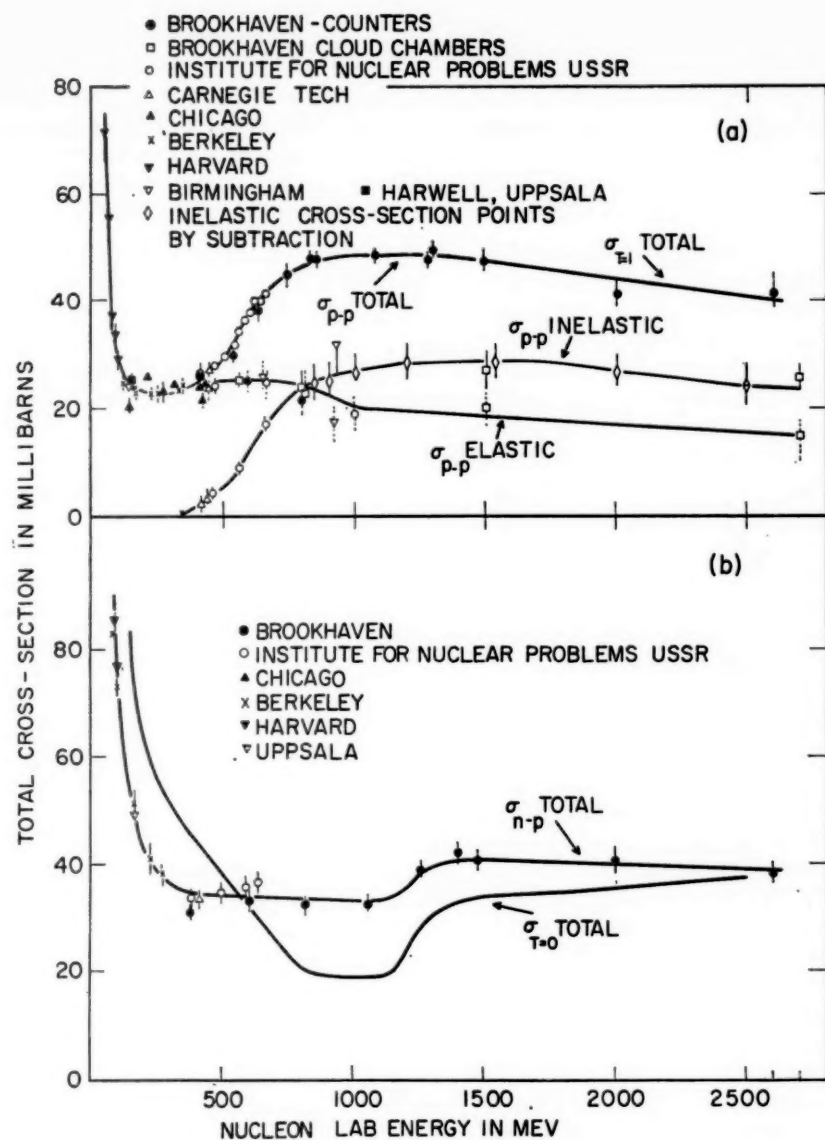


FIG. 4a. The $p\text{-}p$ total, the elastic, and the inelastic cross-section as a function of energy. All curves shown are empirical. The open diamond points have been obtained by a subtraction of the elastic cross-section curve from the total cross-section curve and estimated errors are attached. In the region beyond 300 to 400 Mev, the errors on elastic points have been made by broken lines so that they may be distinguished from inelastic or total cross-sections. Since $p\text{-}p$ contains only the $T=1$ state the cross-sections are equal to the corresponding ones for the $T=1$ state (61 to 65).

FIG. 4b. The total $n\text{-}p$ cross-section is shown as a function of energy. The $T=0$ total cross-section deduced from the total $p\text{-}p$ and total $n\text{-}p$ (see text) is also shown. All curves are empirical (61, 67, 68).

production is infrequent. Furthermore, mesonless stars were relatively rich in fragments implying strongly that meson absorption is responsible for fragment emission.

COLLISIONS OF NUCLEONS WITH HYDROGEN AND DEUTERIUM

p-p collisions.—The behavior of the $p-p$ cross-section as a function of energy has previously been fairly thoroughly investigated from low energies to about 400 Mev by various groups using the several F. M. cyclotrons available in this energy range for some time.

The total $p-p$ cross-section [see Fig. 4a] is approximately constant from 150 to 350 Mev, and the angular distribution is more or less isotropic outside the region of coulomb interference at small angles.

The theoretical explanation of these characteristics is not completely clear, however, considerable progress (60) has been made recently in fitting both $p-p$ cross-sections and polarization experiments.

Recently, the new higher energy machines at Brookhaven, 3 Bev, (61, 62); U.S.S.R. Institute for Nuclear Problems, 660 Mev (63); and Birmingham, 1.0 Bev (64) have been used by several groups to extend the measurements of total, elastic, and inelastic cross-sections to beyond 2.0 Bev.

Figure 4a shows the latest compilation of $p-p$ cross-sections including these higher energy points (61 to 64) and also some lower energy work⁹ (65). The most extensive investigations have been made by Meshcheriakov, Dzhelepov, and co-workers (63), Chen *et al.* (61), Shutt and co-workers (62), Smith *et al.* (61a), Batson *et al.* (64a) and Hughes *et al.* (64b). The total and elastic cross-section measurements have been mostly made directly, however, inelastic cross-sections have been determined both directly and also by subtraction of the elastic from the total cross-sections.

The most striking feature in the new results is the rapid increase of the inelastic cross-section from near zero at 350 Mev to about 25 mb at 800 Mev and its more or less constant value (25 to 30 mb) at higher energies. The elastic cross-section on the other hand remains fairly constant (~ 25 mb) from 350 to 800 Mev and decreases slowly thereafter to about 15 mb at 2.6 Bev. Due to the relative constancy in the elastic cross-section the total cross-section, which is the sum of elastic and inelastic, essentially shows the same sharp rise of about 25 mb as the inelastic cross-section does between 350 and 800 Mev followed by a more or less constant cross-section thereafter. The rise in the inelastic cross-section from 350 to 800 Mev has been found experimentally (62, 64) to be composed almost entirely of single pion production below 1.0 Bev incident proton energy.

The differential elastic scattering cross-section above 400 Mev (61, 62, 63) has shown a rapid change from the former (≤ 350 Mev) isotropy to an

⁹ See the table on pp. 222 to 223 of Chen *et al.* (61) for a recent summary used which includes references to the older low energy work.

increasingly forward peaked distribution which at ≥ 0.7 –1.0 Bev is in general characteristic of the expected diffraction pattern (61 to 64, 66) accompanying the inelastic absorption of the incident wave.

n-p and p-d collisions.—The behavior of the $n-p$, total cross-section as a function of energy, is shown in Figure 4b. Although a few points (67, 68) beyond 400 Mev have been obtained directly, most of the higher energy data (61) has been determined by the difference between $p-d$ and $p-p$ to which is added a correction (positive throughout) for interference effects which correspond to ≤ 20 per cent of the $n-p$ cross-section. The error on this correction is probably a small fraction of it, due to the fact that the observed differences between several points of $n-p$ measured directly and the indirect method described are small.

Assuming charge independence, a separation of the $p-p$ and $n-p$ total cross-sections has been made into the two isotopic spin states involved, ($T=0$ and $T=1$) according to the well known relations:

$$\sigma_{T=1} = \sigma_{p-p} \quad 8.$$

$$\sigma_{T=0} = 2\sigma_{n-p} - \sigma_{p-p} \quad 9.$$

The results are shown in Figures 4a and 4b. The total $T=0$ cross-section ($\sigma_{T=0}$) continues to follow its lower energy behavior and continuously decreases in the region of 400 to 800 Mev, and then levels off at a minimum value to beyond 1 Bev, after which it increases rapidly from ~ 1.1 Bev to ~ 1.5 Bev and only slowly thereafter. Hence it appears that in the region of 400 to 800 Mev while single pion production is rapidly increasing in the $T=1$ state, which is accompanied by the sudden rise in $\sigma_{T=1}$, this does not appear to occur in the $T=0$ state. Dzhelepov *et al.* (67) have deduced a value for the inelastic cross-section in the $T=0$ state of 9 ± 4 mb at 580 Mev by subtraction methods. The large errors and uncertainty in the cross-sections used in the subtraction method make it difficult to decide that the real value is different from zero within all possible errors.¹⁰ On the other hand, double pion production is known (62, 69) to set in rapidly in the $T=1$ state between 1.0 and 1.5 Bev while in this energy range the $T=0$ state shows a sharp rise of ~ 17 mb similar to that shown by the $T=1$ state in the region of 400 to 800 Mev. This is observed experimentally (70) to be accompanied by a much larger ratio of double to single pion production in $n-p$ collisions than in $p-p$. Hence, it is implied that only double pion production can occur in the $T=0$ state while both single and double pion production can occur in the $T=1$ state. This is additional support for the assumption to be discussed later that pion production proceeds through excitation of a nucleon to the resonant $T=J=3/2$ (isobaric) state observed in the pion-nucleon scattering. For this case, zero, one or two, $T=J=3/2$ nucleon isobars for elastic scatter-

¹⁰ A. P. Batson, B. Culwick, and L. Riddiford have recently determined that the inelastic cross-section in the $T=0$ state is zero within the errors at 950 Mev (91).

ing, single, or double pion production respectively can be formed in a $T=1$ state. However, either zero or two $T=J=3/2$ nucleon isobars for elastic scattering or double pion production respectively can be formed in a $T=0$ state.

The fact that in the $T=1$ state neither the total nor the inelastic cross-section increases much further when double production sets in can be explained by assuming that a saturation of the inelastic cross-section has already occurred with single pion production and this cross-section ~ 27 mb corresponds to the size of the region in which inelastic interactions occur.

One should remark here that neither charge symmetry or charge independence have been found to be violated by any of the experiments performed to date.

PION PRODUCTION

In $p-p$ and $n-p$ nucleon-nucleon collisions producing a single pion all of the reactions consistent with charge conservation have been previously observed (1, 71), and are listed below:

(a)	$p + p$	$p + n + \pi^+$	(e)	$p + n$	$p + p + \pi^-$
(b)	$p + p$	$p + p + \pi^0$	(f)	$p + n$	$p + n + \pi^0$
(c)	$p + p$	$D + \pi^+$	(g)	$p + n$	$D + \pi^0$
(d)	$p + n$	$2n + \pi^+$			

The corresponding $n-n$ reactions are related to (a), (b), and (c) by the principle of charge symmetry.

Reactions (c) and (g) dominate pion production near threshold (~ 300 to 400 Mev). However, as the energy increases, the cross-section for (c) increases rapidly to a peak reported value (72) of 3.1 ± 0.2 mb at 660 Mev and drops rapidly thereafter to a value of ~ 0.5 mb beyond 800 Mev (62, 64). Reaction (g) is not as well determined experimentally but the general behavior is probably the same. These two reactions have been adequately explained (71, 73) as a consequence of the large final state interaction of the two slow nucleons in the deuteron state when mesons are produced near threshold. Hence they rapidly become less important with increasing energy. The same is obviously true for the inverse reaction to (c) which is pion absorption in deuterium leading to a two nucleon final state. Several well known phenomenological treatments of pion production which make use of charge independence, a consideration of the properties of the nucleon-nucleon final states including interactions, and various assumptions about matrix elements for meson production have been described elsewhere (1, 71, 73) and will not be considered here. One might generally remark that these methods are most suitable near the pion threshold where they were originally applied, and their usefulness decreases rapidly with increasing energy.

Many investigations of reactions (a) and (b) and the corresponding unbound reactions for double pion production have been performed recently

in the energy range beyond 400 Mev. Pion production in p - p collisions has been observed with hydrogen filled chambers (62, 64, 74) at 380, 650, 800 Mev, 1.5 and 2.75 Bev, with counters (69, 72) from 440 to 660 Mev, 1.0 and 2.3 Bev, and with emulsions (64, 72) at 660 and 925 Mev.

The total pion production cross-section is given as a function of energy by the inelastic p - p cross-section curve in Fig. 4a. The rapid increase below 1.0 Bev is due to single pion production since double production is small below 1.0 Bev. Beyond 1 Bev double pion production increases rapidly until ~ 2 Bev with only small increases thereafter (62, 69). The ratio of cases of double production to single production changes from $\lesssim 1:20$ at 0.8–1.0 Bev to $\sim 1:3$ at 1.5 Bev to $\sim 1-1.5:1$ in the range 2.0 to 2.7 Bev¹¹ (62, 69).

A remarkable general similarity of the energy spectra of the pions¹² (see Fig. 5) in the nucleon-nucleon c.m.s. is exhibited by all of the experiments in the energy range of 0.8 to 2.3 Bev (62, 64, 69). All c.m.s. pion energy spectra show a peak at ~ 100 to 200 Mev and a general similarity to the $\pi^+ + p$ total cross-section (see Fig. 3) in the energy range (0 to 500 Mev). The peak in the $\pi^+ + p$ total cross-section at ~ 180 Mev in the lab system corresponds to a peak at ~ 120 Mev in the c.m.s. Of course the high energy cut-off and the width of the peak in the pion energy spectra both increase with energy. At the higher energies ~ 2.0 Bev the single pion energy spectrum is broader than the double pion energy spectrum which is closer in appearance to the $\pi^+ + p$ total cross-section curve. This general similarity in the pion energy spectra extends down to 660 Mev if one does not include the effects of the deuteron formation which adds a high energy peak to the spectrum. The similarity at 660 Mev (72) is particularly noticeable at wide angles (46°) in the lab system since the deuterons and their associated π^+ are peaked near the beam direction. This angle (46° lab) corresponds for the pions to $\sim 77 - 90^\circ$ in the c.m.s.

The energy spectra predicted by the Fermi statistical theory (92) for each multiplicity are completely determined and independent of the volume. Comparisons of the Fermi spectra for the individual multiplicities and also appropriately combined with the observed experimental multiplicities to obtain predictions for the total pion spectrum have been made (62, 64, 69, 75). Except in special cases, where the agreement appears accidental (75), the Fermi theory disagrees badly with experiment mainly because there are too many high energy pions and too few low energy pions.

¹¹ Triple pion production is observed at 2.7 Bev to occur in ~ 15 per cent of all inelastic interactions.

¹² Most of the detailed investigations have been made for π^+ which accounts for ~ 80 per cent of the single pion cross-section and is easy to measure experimentally. The energy spectra of π^0 are obviously more difficult to obtain, but where checked (72) exhibit this general similarity. The production of π^- in p - p collisions only occurs in double production and to date only fragmentary information exists which is generally consistent with the foregoing.

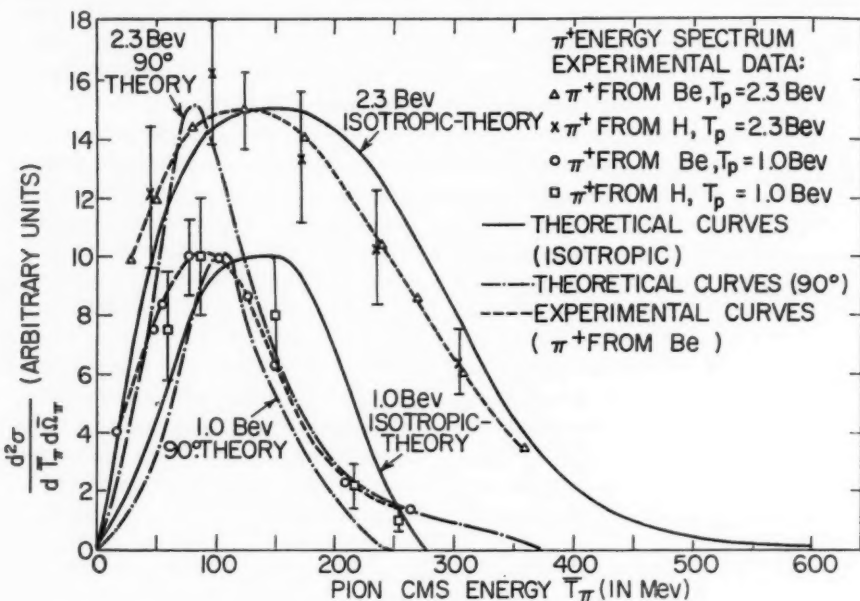


FIG. 5. The π^+ energy spectra from $p\bar{p}$ and p -Be collisions at $T_p = 1.0$ and 2.3 Bev (69) are given and compared to calculations (75) based on an isobaric nucleon model (discussed in text). Results for isotropic, and only forward and backward, emission of isobars in the c.m.s. observed at $\sim 90^\circ$ [labelled 90° theory] are shown. The experimental data corresponds to pion emission angles in the c.m.s. of ~ 60 to 75° at 1.0 Bev and $\sim 73^\circ$ to 105° at 2.3 Bev. An analysis of the cloud-chamber experiments (62) indicates isotropic pion emission at 2.3 Bev and a considerable amount of forward-backward peaking at 1.0 Bev which therefore implies reasonably good agreement of the calculations with the data. The cloud chamber data (not shown), although of considerably lower statistical accuracy and momentum resolution, are in general agreement with the counter data.

The general qualitative features of the experimental pion energy or momentum spectra have been explained by the hypothesis that both single and double pion production proceeds through excitation of one or both nucleons respectively to the isobaric state of $T = J = 3/2$ (69, 70, 75) previously observed in the $\pi^+ + p$ scattering resonance at ~ 190 Mev. Quantitative agreement with the experimental π -meson energy spectra in $p\bar{p}$ collisions has been obtained at energies of 0.8 Bev, 1.0 Bev, 1.5 Bev, and 2.3 Bev with an isobaric nucleon model by Lindenbaum & Sternheimer (75). [See Fig. 5 for 1.0 and 2.3 Bev π^+ spectra.] The relative probability for isobar formation and subsequent decay with a variable total energy in the isobar rest system was phenomenologically related to the total $\pi^+ + p$ scattering cross-section.

Another difficulty with the Fermi theory is the inability to explain the

sudden increase of double pion production beyond 1 Bev with a volume corresponding to the Compton wave length of a pion (62, 69, 75). The experimental inelastic cross-section actually corresponds to a black sphere much smaller than this, which would make the disagreement even more marked. On the other hand, the isobaric nucleon model (75) predicts the correct general behavior for the double pion production. The observed branching ratios of various charge states (62, 75, 76), Q value distributions between pions and nucleons, and the angular correlation between pions and nucleons (62) are also in reasonable agreement with the predictions.

Investigations of $n-p$ pion production in hydrogen filled chambers (70) for effective incident energies of ~ 1.1 and 1.7 Bev have revealed many of the general features of pion production found in $p-p$ collisions. However one notable exception is the considerable increase in double relative to single production. This is also in qualitative agreement with the predictions of the isobaric nucleon model since as previously pointed out, only double pion production can occur in a $T=0$ state since one $T=3/2$ isobar cannot be combined with a $T=\frac{1}{2}$ recoil nucleon to form a $T=0$ state. A quantitative agreement has also been obtained (75). The energy spectra of π^+ and π^0 mesons and the π^+/π^0 ratio for mesons produced in $p-p$ collisions at 556 and 667 Mev also appears to be consistent with the formation of a nucleon isobar (72).

A modification of the Fermi statistical theory by Kovacs (77) to include relative enhancement of those final states for which the pion nucleon interaction is large, has yielded reasonable predictions for the branching ratios of various charge states and the behavior of the pion multiplicity as a function of energy (62, 70).

Lepore & Neumann (93) have developed a relativistic phase space theory which conserves the relativistic center of energy and thus reduces the volume of phase space accessible to high energy pions. This effect tends to modify the energy spectra in the right direction but, of course, will not provide the many clear-cut characteristics of the $T=J=3/2$ state that seems to pervade the data at these energies.

Belanki & Nikishov (78) have found that inclusion of isobars in the statistical theory yields reasonable agreement for various charge state ratios and the behavior of the multiplicity with energy.

One should note that the experiments on pion production in nucleon-nucleon collisions have established the dominant features of the interactions; however, the details are not definitely determined. For example, 50 to 100 events are involved in many of the experimental pion spectra obtained by cloud chambers. The counter experiments on the other hand provide more accurate energy spectra but are less complete in that all the details of an individual event are not measured together. One should keep the foregoing in mind relative to the experimental agreements with theories, which while encouraging in general features do not necessarily imply agreement in the finer details.

Charged pion production in beryllium has been studied with counter

techniques at 660 Mev (72), 1.0 Bev and 2.3 Bev (69) and at 2.2 Bev with emulsions (79). Carbon has been studied at 660 Mev (72). The observed pion spectra and other general properties of these reactions are very similar to those observed in $p-p$ (see Fig. 5) and $n-p$ collisions. This is true at 660 Mev only if the unbound reaction (without deuteron formation) is considered.

As a matter of fact, originally the p -Be pion spectra (69) at 1.0 and 2.3 Bev were successfully analyzed on the assumption that essentially free nucleon-nucleon collisions occur without important changes in properties due to subsequent interaction.

One should note here that the energy spectra of π^+ produced in Be at wide angles in the c.m. system are generally similar at 660 Mev, 1.0 and 2.3 Bev. The π^- energy spectra also have the same general properties.

The average mean free path for pions near the resonance energy is $\sim 10^{-13}$ cm., however, on both sides of this peak it increases very rapidly so that the average mean free path is probably $2-3 \times 10^{-13}$ cm. for the observed pion spectra in the incident nucleon energy range of 0.6 to 3.0 Bev.

In even the lightest nuclei this average mean free path is of the order of a radius ($\sim 3 \times 10^{-13}$ cm. for Be). However, since many of the nucleons are near the surface a fair share of the pions can escape with zero or perhaps one collision following production.

In the heavier nuclei $A \sim 100-200$ the radius is $\sim 6-9 \times 10^{-13}$ cm. and hence many free paths. As previously noted, single pion production increases rapidly beyond 400 Mev to the order of half the total $p-p$ cross-section ($T=1$) above 800 Mev and double pion production becomes large in both the $T=1$ and the $T=0$ states above $\sim 1.2-1.5$ Bev.

The combination of a large mean pion production per nuclear interaction (estimated to be ~ 0.8 at 1.0 Bev and ~ 1.5 at 2.0 Bev) coupled with the short mean free path of the low energy pions produced in heavy nuclei, obviously implies a series of additional scatterings of these pions. In many cases their eventual absorption either directly or after slowing down to < 150 Mev where the two-nucleon absorption becomes large is also to be expected. Hence a mechanism for increasingly large transfers of excitation energy to a nucleus is present as the incident nucleon energy increases above the pion production threshold. This is in contrast to the more or less constant low average values of the excitation energy (~ 50 Mev) transferred to the nucleus by the nucleonic cascades resulting from elastic collisions below 400 Mev (80). This general mechanism for large excitation energy transfers to nuclei has been previously postulated by Friedlander and co-workers (81) and then by Lock *et al.* (82) to explain their experiments.

The hypothesis of the interaction of incident nucleons of 100 to 400 Mev with nucleons of heavy nuclei, as if they were free except for the Pauli Exclusion Principle effects, has been successful in explaining the experimental results for Ag-Br nuclei in emulsions (80). The struck nucleons together with

the incident ones are considered to interact in the same manner until they either reach the edge of the nucleus with an energy greater than the effective potential and escape or else lose sufficient energy to drop below the nuclear potential barrier and be captured.

The thermal excitation transferred to the nucleus in this model is due to both captured nucleons and the excitation due to holes left in the energy momentum distribution. Subsequent boiling off or evaporation of nucleons and some heavier particles is the end result. This thermal excitation is reasonably constant and is of the order of 50 Mev for incident nucleon energies from 90 to 400 Mev (80). Considering elastic nucleon-nucleon scattering collisions only the estimated average contribution to thermal excitation by a 1 Bev nucleon is ~ 70 Mev (80, 82). If on the other hand at 1.0 Bev approximately $\frac{1}{3}$ of the time one pion of mean total energy ~ 300 Mev is produced and absorbed in a heavy nucleus, an additional excitation energy ~ 100 Mev average is contributed to give a total average excitation of ~ 150 Mev. At 2.0 to 3.0 Bev, due to the increase in double and plural production, one might expect perhaps twice this additional excitation corresponding to a total average excitation energy of perhaps 250 Mev. Obviously the statistical fluctuations will allow a wide distribution of thermal energies with a large fraction of the incident energy transferred to thermal excitation in some cases. This thermal excitation may never approach the simple concept of a uniform equilibrium temperature but may rather be characterized by a random distribution of local hot spots with local disintegration before equilibrium is established.

CHARACTERISTICS OF THE INELASTIC INTERACTIONS OF NUCLEONS WITH NUCLEI

The nuclear interactions of 600 Mev and 950 Mev protons with the nuclei of G-5 emulsion have been studied by Lock *et al.* (82, 83a). In general they find that π -meson production greatly affects the characteristics of the interactions at 950 Mev and has some effect even at 600 Mev.

The prong distribution of stars at 600 Mev is similar to that at 400 Mev except for a slight increase in large prong numbers. At 950 Mev there is a great increase in stars with ≥ 6 prongs (by a factor of 3) and a corresponding decrease in the smaller stars. This behavior has been qualitatively explained by the large increase in single pion production at 950 Mev.

Some crude estimates of the development of the nucleonic cascade in the heavy emulsion nuclei (Ag-Br) including meson production and reabsorption were made by these authors and compared to stars in Ag-Br. They find that the mean prong number of grey plus shower tracks (protons > 30 Mev) and black tracks (protons < 30 Mev) can be approximately explained. An average thermal excitation of 70 Mev was taken for 40 per cent of the cases in which meson production is assumed not to occur and 25 per cent of the cases for which meson production does occur but the meson escapes. In approxi-

mately 35 per cent of the cases it was assumed that a meson was created and reabsorbed resulting in an average thermal excitation of 210 Mev. This procedure gives a mean thermal excitation of ~ 120 Mev for all interactions.

The black protons seem to be more isotropic than at lower energies and follow an evaporation spectrum calculated for the estimated mean thermal excitation. The process of meson production and absorption seems to have washed out some of the forward peaked behavior and lowered the mean energy of the black knock-on protons observed at lower energies (80). However, there is still reason to believe from the cascade calculations that ~ 20 per cent of black protons are still of knock-on origin.

There is some evidence that α -particles are forward-peaked in angle and it is concluded that some are also ejected in the cascade from heavy nuclei at 950 Mev. This latter process may well be connected with meson absorption as it was previously noted, that in pion induced stars fragment emission is enhanced.

McKeaque (83b) (cf. also ref 82b), has separated the disintegrations predominantly induced in light nuclei of the G-5 emulsion by 950 Mev protons. A discussion of the method is presented in the papers. The general characteristics of the stars in light and heavy nuclei are remarkably similar in regard to mean prong numbers of total, shower, grey, and black prongs. However, the prong distribution in light nuclei is peaked at about five and is small or zero above 8 prongs, while in heavy nuclei the prong distribution is peaked at about one or two and extends to ~ 15 prongs. The black protons and α -particle spectra both have a peak at ~ 4 Mev for light nuclei corresponding to peaks at ~ 7 and ~ 11 Mev respectively for heavy nuclei.

These characteristics are consistent with the interpretation that in light nuclei smaller cascades are developed followed by a thermal evaporation or break-up of the nucleus into several very low energy protons, alphas, and other fragments. In the heavier nuclei, on the other hand, more extensive cascades are developed with a more complete sharing of the incident proton energy among a greater number of particles, and a resultant larger thermal excitation. Therefore the sharper distinction in energy found in light nuclei between the knock-ons and the particles due to evaporation or break-up of the residual nucleus is reduced in the case of heavy nuclei. The differences in prong distribution also reflect the effect of a more extensive cascade in the heavier nuclei.

Some evidence is also present in this analysis for the possible interaction of the incident proton with sub groups (mainly α) of the light nucleus, in this and other experiments, quoted in (83), at lower energies.

Another approach to the study of inelastic interactions of high energy protons with nuclei is the radio chemical method for determining the distribution of residual nuclei resulting from bombardment of a heavy nucleus. The products resulting from bombardment of bismuth with protons of 340 Mev [Biller (84a)], 480 Mev [Vinogradov *et al.* (84b)] and 660 Mev [Murin

et al. (84c)] fall into two distinct mass regions: the so-called spallation region and the fission region. The spallation region refers to products with a mass number generally smaller than that of the target by less than 40 mass units and has a rapidly decreasing cross-section with decreasing A . The fission region has a peak at $A \sim 90$ to 95 and is characterized by a region of very low yield above $A \sim 140$ situated between the fission and spallation regions. The ratio of bismuth fission to total inelastic cross-sections increases monotonically from 0.06 at 100 Mev to 0.13 at 340 Mev and more slowly thereafter to 450 Mev (84).

Friedlander and his co-workers (81) found that for 2.2 Bev protons incident on bismuth and Pb, the valley between fission and spallation observed at lower energies disappeared. The formation cross-section for nuclides in the mass range ~ 130 to 180 had increased by a factor of 4 from 480 Mev to 660 Mev (81, 84), but increased by two orders of magnitude when the proton energy was raised to 2 Bev.

A detailed study of the energy dependence of formation cross-sections of about 30 nuclides of $A \leq 140$ formed by the interaction of lead with protons in the energy range 0.6 to 3.0 Bev has been reported, and thoroughly analyzed by Friedlander *et al.* (81). They find that the average energy transfer to the nucleus appears to change from the order 50 to 100 Mev at 400 Mev bombardment to \sim several hundred Mev for 3.0 Bev incident protons with an appreciable probability for energy transfers ≥ 1 Bev. Their data clearly support their hypothesis that meson production is the vehicle for the greatly increased energy transfer above 400 Mev. Although the pion production cross-section increases only slowly beyond 1 Bev where single pion production seems to saturate, increases in the energy transfer seem to occur until 3.0 Bev. This is probably due to the increasing multiplicity of pion production and even the effects of plural production may be significant at 3.0 Bev. The increased probability of large energy transfers actually is expected to lead to a broad distribution of energy transfers from quite small to large values due to the large statistical fluctuations in the cascade mechanism.

At 3.0 Bev bombarding energy, spallation events involving 60 or 70 nucleons or their equivalent are found to be quite prevalent. The fission cross-section seems to decrease by a factor of ~ 3 from 700 Mev to 3.0 Bev due to increasingly important competition from spallation and fragmentation.

The latter process was postulated (81) to account for product yields of $10 < A < 40$, and is pictured as a local rapid break-up or as a fast fragmentation of a small area of the nucleus, which has been highly heated locally by pion absorption or other effects. This is of course a different process than spallation which is thought to involve a thermal evaporation from the nucleus as a whole.

Actually it is questionable whether true spallation ever occurs at these high energies. One can seriously question the concept of an equilibrium

temperature in a greatly disrupted nucleus from which many nucleons have been ejected as knock-ons and which has absorbed an excitation comparable in many cases with its binding energy. Perhaps a more logical concept is that fragmentation occurs almost everywhere in the nucleus, but that in those areas where by chance or a sufficient thermal exchange with neighboring nucleons, or other local emission processes, the local temperature does not differ too much from the average temperature, the evaporated products can be considered as equivalent in properties to those which would correspond to a uniform average nuclear temperature. On the other hand, wherever there are large fluctuations in nuclear temperature, it is more fruitful to treat the particles emitted as originating from local hot or cold spots and so call them products of fragmentation. The connection between fragment emission and pion absorption has been previously observed in both pion induced stars and proton induced stars with associated meson production and absorption.

An extensive series of nuclear cascade calculations have been recently carried out at the Maniac Electronic Computer (85).

Previous Monte Carlo calculations (80) have been extended into the Bev region as well as improved statistically at lower energies. A three dimensional geometry was used and a cascade of nucleon-nucleon collisions including pion production and reabsorption were considered. The number, kind, energy, and the direction of the emitted particles in each cascade and the nature and state of the excitations of the residual nucleus were tabulated.

Incident energies ranging from 46 to 1,830 Mev for nucleons, and 0 to 1,500 Mev for pions were considered for various target nuclei which include Al, Cu, Ru, Ca, Bi, and U. About 1,000 cascades were computed for each interaction.

Some preliminary comparisons of the theoretical results with radio chemical and other data have been made and seem to yield a general agreement. The final compilation of these results and a systematic comparison with experimental data now available and also future data of sufficient accuracy for a detailed comparison should provide a critical test of the nucleonic cascade mechanism. One of the features which could still be considerably improved in this computation is the energy spectra assumed for the pion, which was based on an equal momentum for all particles in the c.m.s.

TOTAL, ELASTIC, AND INELASTIC CROSS-SECTIONS OF NUCLEI FOR NUCLEONS

The inelastic and total cross-sections of various nuclei ranging from Be to Pb for protons and neutrons of various energies in the range 50 Mev to 1.4 Bev have been determined and analyzed (86, 87, 88, 51, 68). The basic optical model proposed by Fernbach, Serber & Taylor (47b) seems to still give a reasonable fit to the general features of the experimental data.

The simplest approximation to the optical model solution which was

originally used (47) is the assumption of a spherical complex well with a complex potential inside a radius R and no nuclear potential outside except the Coulomb field. The imaginary (absorptive) part of the potential is determined by the free nucleon-nucleon interaction cross-sections suitably modified by the Pauli Exclusion Principle and also the density of nuclear matter which in turn depends upon the radius assumed. The real part of the potential is generally adjusted to fit the data.

The results are usually expressed in terms of the three parameters, K the absorption coefficient in nuclear matter, k_1 the change in wave number upon entering the nucleus, and R the radius of the well. Refraction and reflection were neglected in the original simple treatment which was solved in analogy to the optical case for a uniform nuclear density. The inelastic cross-section depends only on K and R , and is experimentally the easiest to measure.

This simple picture seems to work at any one energy for the heavier elements but generally tends to require a radius $R = r_0 A^{1/3}$ which involves higher values of r_0 for the light nuclei, but reasonably constant values for r_0 seem to suffice for the medium weight and heavy nuclei. The form $R = (b + aA^{1/3})$ fits the data for various nuclei better at any one energy but different values of a and b are required at various energies (87).

Furthermore the lower energy results (< 100 to 200 Mev) seem to require for a spherical well radius $R \sim 1.4 - 1.5 A^{1/3} \times 10^{-13}$ cm. for medium weight and heavy nuclei while the higher energy data (300 Mev to 1.4 Bev) seem to require $R \sim 1.2 - 1.3 A^{1/3} \times 10^{-13}$ cm.

Several authors (51, 87) have attempted to improve the approximations involved in the optical model. A tapered nuclear edge which in effect is similar to the Hofstadter nucleon density distribution, reflection, and refraction at the nuclear surface, exact phase shift calculations, and other techniques have been used to attempt to obtain agreement with a nuclear radius which varies like $A^{1/3}$ in a consistent manner and is not too dependent on the incident energy. These procedures, notably the tapered edge, improve the situation considerably but it is not yet clear that all discrepancies can be removed. However, one might note that the sensitivity to the tails of the nuclear distribution obviously depends upon the cross-section of the incident particles for nucleons in the nucleus. A high cross-section increases the effects of the outermost regions of the nuclear distribution. Furthermore, there is an effective range of potential due to the finite size of the interaction range of the incident particle. Therefore it is not at all surprising that for incident particles with a high cross-section (lower energy nucleons) a relatively larger radius is required, and that these effects are magnified for the lighter nuclei. Similar effects have been previously observed in pion-nucleus interactions, where larger radii are required in the energy region where the pion-nucleon cross-sections are large.

The differential elastic scattering cross-section predicted by the optical model also seems to be in reasonable agreement where checked for smaller

angles than the first minimum (88). At and beyond the first minimum the details of the predicted diffraction pattern are quite sensitive to the nuclear density shape, the experimental angular, and elastic energy resolution, and also the dependence of the real potential on spin orbit coupling. However, for medium weight and heavy nuclei diffraction patterns in reasonable agreement with predictions have been observed (88). For the lightest nuclei, agreement is poor but the basic validity of the optical model approximation is more questionable and in fact difficulties in fitting the inelastic cross-section in light nuclei have been previously mentioned.

In the lightest nuclei the coherent elastic scattering cannot be expected to fit the optical model approximation, and indeed should to a certain extent exhibit the characteristics of the Born approximation estimate of the scattering from individual nucleons suitably modified by attenuation and form factors, as previously noted for elastic scattering of pions from light nuclei.

The analyses do not in general accurately determine k_1 ; however, it appears that k_1 probably is different from zero even near 1 Bev and corresponds to a real potential depth of ~ 10 to 50 Mev where the latter value is the upper limit at 870 Mev (88).

There have been some indications from comparisons of neutron and proton results at low energies (87) that the distribution of neutrons in the nucleus has an effectively larger radius than the proton distribution. This interpretation is open to question at present and does not seem to be consistent with recent inelastic cross-section measurements of Pb for charged pions (49).

LITERATURE CITED

1. Gell-Mann, M., and Watson, K. M., *Ann. Rev. Nuclear Sci.*, **4**, 219 (1954)
2. Ashkin, J., Blaser, J. P., Feiner, F., Gorman, J. G., and Stern, M. O., *Phys. Rev.*, **96**, 1104 (1954)
3. Lindenbaum, S. J., and Yuan, L. C. L., *Phys. Rev.*, **100**, 306 (1955)
4. Lindenbaum, S. J., and Yuan, L. C. L. (Private communication)
5. Ignatenko, A. E., Mukhin, A. I., Ozerov, E. B., and Pontekorvo, B. M., *Zhur. Eksp. i Teoret. Fiz.*, **30**, 7 (1956)
6. Mukhin, A. I., Ozerov, E. B., and Pontekorvo, B. M., *Zhur. Eksp. i Teoret. Fiz.*, **31**, 371 (1956)
7. (a) Low, F. E., *Phys. Rev.*, **97**, (1955); (b) Chew, G. F., and Low, F. E., *Phys. Rev.*, **101**, 1570 (1956); (Private communication)
8. Brueckner, K. A., *Phys. Rev.*, **86**, 106 (1952)
9. Castillejo, L., Dalitz, R. H., and Dyson, F. J., *Phys. Rev.*, **101**, 453 (1956)
10. Ashkin, J., Blaser, J. P., Feiner, F., and Stern, M. O., *Phys. Rev.*, **101**, 1149 (1956); *Phys. Rev.*, **105**, 724 (1957)
11. (a) Anderson, H. L., and Glicksman, M., *Phys. Rev.*, **100**, 268 (1955); (b) Anderson, H. L., Davidon, W. C., Glicksman, M., and Kruse, U. E., *Phys. Rev.*, **100**, 279 (1955)
12. Anderson, H. L., Fermi, E., Martin, R., and Nagle, D. E., *Phys. Rev.*, **91**, 155 (1953)
13. (a) de Hoffmann, F., Metropolis, N., Alei, E. F., and Bethe, H. A., *Phys. Rev.*, **95**, 1586 (1954); (b) Anderson, H. L., and Metropolis, N., *Proc. 6th Ann. Rochester Conf on High Energy Physics*, Chap. 1, 19 (Interscience Publisher Inc., New York, N. Y., 1956)
14. Bethe, H. A., and de Hoffmann, F., *Mesons and Fields*, **2**, (Row Peterson and Company, 446 pp., White Plains, N. Y. 1955)
15. Orear, J., Jr., *Phys. Rev.*, **96**, 1417 (1954)
16. Ferrari, G., Ferretti, L., Gessaroli, R., Manaresi, E., Puppi, G., Quarenii, G., Ranzi, A., and Stanghellini, A., *CERN Symposium Proc. (Geneva)*, **V2**, p. 230 (1956)
17. Taft, H., *Phys. Rev.*, **101**, 1116 (1956)
18. (a) Orear, J., *Phys.*, **96**, 176 (1954) (b) *Phys. Rev.*, **100**, 288 (1955)
19. Yang, C. N., (Private communication to E. Fermi)
20. (a) Minami, S., *Progr. Theoret. Phys.*, **11**, 213 (1954); (b) Hayakawa, S., Kawaguchi, M., and Minami, S., *Prog. Theoret. Phys.*, **11**, 332 (1954)
21. (a) Salam, A., *CERN Symposium Proc. (Geneva)*, **V2**, p. 179 (1956); (b) Davidon, W. C. and Goldberger, M. L., *Phys. Rev.*, **104**, 1119 (1956); (c) Capps, R. N., and Takeda, G., *Phys. Rev.*, **103**, 1877 (1956); (d) Goldberger, M. L., *6th Ann. Rochester Conf. on High Energy Physics*, Chap. 1, 1 (Interscience Publisher, New York, N. Y., 1956)
22. Anderson, H. L., Davidon, W. C., Kruse, U. E., *Phys. Rev.*, **100**, 339 (1955)
23. Fermi, E., *Phys. Rev.*, **91**, 947 (1953)
24. (a) Ashkin, J. (Private communication); (b) Feld, B. T., (Private communication)
25. Cool, R., Piccioni, O., and Clark D., *Phys. Rev.*, **103**, 1082 (1956)
26. Leonard, S. J., and Stork, D. H., *Phys. Rev.*, **93**, 568 (1954)
27. Bodansky, D., Sachs, A., and Steinberger, J., *Phys. Rev.*, **93**, 1367 (1954)
28. Perry, J. P., and Angell, C. E., *Phys. Rev.*, **91**, 1289 (1953)
29. Dyson, F. J., *Phys. Rev.*, **99**, 1037 (1955)

30. Takeda, G., *Phys. Rev.*, **100**, 440 (1955)
31. Walker, W. D., Hushfar, F., Shephard, W. D., *Phys. Rev.*, **104**, 526 (1956)
32. Lindenbaum, S. J., and Sternheimer, R. M., *Phys. Rev.* (In press)
33. Crew, J. E., Hill, R. D., and Lavatelli L., *Phys. Rev.* (In press)
34. (a) Barshay, S., *Phys. Rev.*, **103**, 1102 (1956); (b) Franklin, J., *Phys. Rev.*, **105**, 1101 (1957)
35. Karplus, R., and Ruderman, M. A., *Phys. Rev.*, **98**, 771 (1955)
36. (a) Goldberger, M. L., *Phys. Rev.*, **99**, 979; (b) Goldberger, M. L., Miyazawa, H., and Oehme, R., *Phys. Rev.*, **99**, 986 (1955)
37. Symanzik, K., *Phys. Rev.*, **105**, 743 (1957)
38. Bogoliubov, N. N., (Paper presented at the Intern. Conf. on Theoret. Phys. Seattle, Wash. (1956))
39. Haber-Schaim, U., *Phys. Rev.*, **104**, 1113 (1956)
40. (a) Bernardini, G., and Goldwasser, E. L., *Phys. Rev.*, **95**, 857 (1954); (b) Beneventano, M., Stoppini, G., Tau, L., and Bernardini, G., *CERN Symposium Proc. (Geneva)*, **V2**, p. 259 (1956)
41. (a) Puppi, G., and Stanghellini, A., *CERN Symposium Proc. (Geneva)*, **V2**, 182, (b) Puppi, G., (Private communication) (c) Chew, G. F., Private communication (d) Goldberger, M. L., (Private communication) (e) Agodi, A., Cini, M., Vitale, B., (Private communication).
42. Ignatenko, A. E., Mukhin, A. I., Ozerov, E. B., and Pontekorvo, B. M., *Doklady Akad. Nauk. S.S.R.*, **103**, 209 (1955)
43. (a) Brueckner, K. A., *Phys. Rev.*, **89**, 834 (1953); (b) *Phys. Rev.*, **90**, 715 (1953); Tamm, I. E., Gol'dfand, I. A., Zharkov, G. F., Poriskoiia, L. V., and Feinberg, V. I., *Conf. on Quantum Electrodynamics and the Theory of Elementary Particles, U.S.S.R.* March 31, (1955)
44. Glauber, R. J., *Phys. Rev.*, **100**, 242 (1955)
45. (a) Rogers, K. C., and Lederman, L. M., *Phys. Rev.*, **105**, (1957); (b) Rockmore, R., *Phys. Rev.*, **105**, 256 (1957)
46. Ignatenko, A. E., Mukhin, A. I., Ozerov, E. B., and Pontekorvo, B. M., *Doklady Akad. Nauk. S.S.R.*, **103**, 395 (1955); *Rept. Inst. of Nuclear Problems, U.S.S.R. Acad. Sci., Moscow* (1955)
47. (a) Serber, R., *Phys. Rev.*, **72**, 1114 (1947); (b) Fernbach, S., Serber, R., and Taylor, T. B., *Phys. Rev.*, **75**, 1382 (1949)
48. Sternheimer, R. M., *Phys. Rev.*, **101**, 384 (1956)
49. Abashian, A., Cool, R., and Cronin, J., *Bull. Am. Phys. Soc.*, [II], **1**, 350 (1956); *Phys. Rev.*, **104**, 855 (1956)
50. Hahn, B., Ravenhall, D. G., and Hofstadter, B., *Phys. Rev.*, **101**, 1131 (1956)
51. Williams, R. W., *CERN Symposium Proc. (Geneva)*, **V2**, 182 (1956); *Phys. Rev.*, **99**, 1387 (1955)
52. (a) Pevsner, A., Rainwater, J., Williams, R. E., and Lindenbaum, S. J., *Phys. Rev.*, **100**, 1419 (1955); (b) Pevsner, A., and Rainwater, J., *Phys. Rev.*, **100**, 1431 (1955)
53. (a) Williams, R. E., Rainwater, J., and Pevsner, A., *Phys. Rev.*, **101**, 412 (1956); (b) Williams, R. E., Baker, W. F., and Rainwater, J., *Phys. Rev.*, **104**, 1695 (1956)
54. Baker, W. F., *Scattering of 80 Mev n Mesons by Complex Nuclei* (Doctoral Thesis, Columbia University, New York, N. Y., March 1957)
55. Dzhelepov, V. P., Ivanov, V. G., Kozodaev, M. S., Osipenkov, V. T., Petrov, N. I., and Rusakov, V. A., *Rept. Inst. of Nuclear Problems, U. S.S.R. Acad. Sci., Moscow* (1955)

56. Kozodaev, M. S., Sulaiev, R. M., Filippov, A. I., and Scherbakov, I. A., *RINP*, (USSR) (1955)
57. Mitin, N. A., and Grigoriev, E. L., *Doklady Akad. Nauk. S.S.R.*, **103**, 210 (1955)
58. Ignatenko, A. E., *CERN Symposium Proc. (Geneva)*, **V2**, 313 (1956)
59. (a) Blau, M., and Oliver, A. R., *Phys. Rev.*, **102**, 489 (1956); (b) Blau, M., and Caulton, M., *Phys. Rev.*, **96**, 150 (1954)
60. (a) Feldman, D., *Proc. of 6th Ann. Rochester Conf. on High Energy Physics* Chap. 1, 1 (Interscience Publisher, New York, N. Y., (1956); (b) Wolfenstein, L., *Ann. Rev. Nuclear Sci.*, **6**, 43 (1957); (c) Signell, P. S., and Marshak, R. E., *Phys. Rev.* (In press); (d) Gammel, J. L., and Thaler, R. M., *Phys. Rev.* (In press)
61. (a) Smith, L. W., McReynolds, A. W., and Snow, G., *Phys. Rev.*, **97**, 1186 (1955); (b) Chen, F. F., Leavitt, C., and Shapiro, A. M., *Phys. Rev.*, **103**, 211 (1956)
62. Fowler, W. B. *et al.*, *Phys. Rev.*, **103**, 1472, 1479, 1484, 1489, (1956)
63. (a) Meshcheriakov, M. G., Neganov, B. S., Soroko, L. M., Vzorov, I. K., *Doklady Akad. Nauk. S.S.R.*, **99**, 959 (1954); (b) Dzhelepov, V. P., Moskolov, V. I., Medved., S. V., *Doklady Akad. Nauk. S.S.R.*, **104**, 380 (1955); (c) Meshcheriakov, M. G., Bogochev, N. P., Leskin, G. A., Neganov, B. S., and Piskarev, E. V., *CERN Symposium Proc. (Geneva)*, **V2**, p. 125 (1956)
64. (a) Batson, A. P., Culwick, B., Riddiford, L., and Walker, J., *CERN Symposium Proc. (Geneva)*, **V2** p. 340 (1956); (b) Hughes, I. S., March, P. V., Muirhead, H., and Lock, W. O., *CERN Symposium Proc. (Geneva)*, **V2**, 344 (1956)
65. (a) Sutton, R. B., Fields, T. H., Fox J. G., Kane, J. A., Mott, W. E., and Stallwood, R. A., *Phys. Rev.*, **97**, 783 (1955); (b) Marshall, J., Marshall, L., and Nedzel, V. A., *Phys. Rev.*, **98**, 1513 (1955); (c) Kruse, U. E., Teem, J. M., and Ramsey, N. F., *Phys. Rev.*, **101**, 1079 (1956)
66. (a) Serber, R., and Rarita, W., *Phys. Rev.*, **99**, 629(A) (1955); (b) Rarita, W., *Phys. Rev.*, **104**, 221 (1956)
67. Dzhelepov, V. P., Golovin, B. M., Kazarinov, I. M., and Semenov, M. M., *CERN Symposium Proc. (Geneva)*, **V2**, 115 (1956)
68. Coor, T., Hill, D. A., Hornyak, W., Smith, L., and Snow, G., *Phys. Rev.*, **98**, 1369 (1955)
69. Yuan, L. C. L., and Lindenbaum, S. J., *Phys. Rev.*, **103**, 404 (1956); *Phys. Rev.*, **93**, (1954)
70. (a) Fowler, E., Shutt, R. P., Thorndike, A. M., and Whittemore, W. L., *Phys. Rev.*, **95**, 1026 (1954); (b) Wallenmeyer, W. A., *Phys. Rev.*, **105**, 1058 (1957)
71. (a) Rosenfeld, A. H., *Phys. Rev.*, **96**, 139 (1954); (b) Merrison, A. W., *CERN Symposium Proc. (Geneva)*, **V2**, 239 (1956)
72. (a) Meshcheriakov, M. G., Neganov, B. S., *Doklady Akad. Nauk. S.S.R.*, **100**, 677 (1955); (b) Meshcheriakov, M. G., Zrelov, V. P., Neganov, B. S., Vzorov, I. K., and Shabudin, A. F., *CERN Symposium Proc. (Geneva)*, **V2**, 347, 353, 357, (1956); (c) Mesh Kovshki, A. G., Pligin, Iu. S., Shalomov, Ia. Ia., and Shebanov, V. A., *CERN Symposium Proc. (Geneva)*, **V2**, p. 362 (1956); (d) Sidorov, V. M., *CERN Symposium Proc. (Geneva)* **V2**, 366 (1956); (e) Baiukov, Iu. D., Kozodaev, M. S., and Tiapkin, A. A., *CERN Symposium Proc. (Geneva)*, **V2**, p. 398 (1956)
73. (a) Brueckner, K. A., *Phys. Rev.*, **82**, 598 (1951); (b) Watson, K. M., and Brueckner, K. A., *Phys. Rev.* **83**, 1 (1951)

74. Alston, M. H., Crewe, A. V., Evans, W. H., and Von Gierke, G., *CERN Symposium Proc. (Geneva)*, **V2**, 334 (1956)
75. Lindenbaum, S. J., Sternheimer, R. M., *Phys. Rev.*, **105**, 1874 (1957)
76. (a) Peaslee, D. C., *Phys. Rev.*, **94**, 1085 (1954); (b) *Phys. Rev.*, **95**, 1580 (1954)
77. Kovacs, J. S., *Phys. Rev.*, **101**, 397 (1956)
78. Belenki, S. Z., and Nikishov, A. I., *Zhur. Eksp. i Teoret. Fiz.*, **28**, 744 (1955)
79. Preston, W. M., *Proc. 6th Ann. Rochester Conf.*, Sec. IV-47 (1956)
80. (a) Bernardini, G., Booth, E. T., and Lindenbaum, S. J., *Phys. Rev.*, **83**, 669 (1951); (b) *Phys. Rev.*, **88**, 1017 (1952); (c) Morrison, G. C., Muirhead, H., and Rosser, W. G. V., *Phil. Mag.*, **44**, 1326 (1953); (d) Goldberger, M. L., *Phys. Rev.*, **74**, 1269 (1948); (e) McManus, H., Sharp, W. T., and Gell-Mann, H., *Bull. Am. Phys. Soc.*, **28**, 20 (1953)
81. Wolfgang, R., Baker, E. W., Caretto, A. A., Cumming, J. B., Friedlander, G., and Hudis, J., *Phys. Rev.*, **103**, 394 (1956)
82. (a) Lock, W. O., March, P. V., Muirhead, H., and Rosser, W. G. V., *Proc. Roy. Soc. (London) A*, **230**, 215 (1955); Lock, W. O., March, P. V., and McKeaque, R., *Proc. Roy. Soc. (London) A*, **231**, 368
83. (a) Lock, W. O., and March, P. V., *Proc. Roy. Soc. (London) A*, **230**, 223 (1955); (b) McKeaque, *Proc. Roy. Soc. (London) A*, **236**, 104 (1956)
84. (a) Biller, W. F., *Univ. Calif. Radiation Lab. UCRL Report 2067* (unpublished); (b) Vinogradov, A. P., Alimarin, I. P., Baranov, V. I., Lovrakhina, A. P., Baranova, T. V., Povlotskaya, F. I., Bragina, T. V., and Yakovlev, Yu. V., *Conf. Acad. Sci. U.S.S.R. Peaceful Uses of Atomic Energy, Moscow 1955, Session Div. Chem. Sci.*, 97; (c) Murin, A. N., Preobrazhensky, B. K., Yutlandov, I. A., and Yokimov, M. A., *Conf. Acad. Sci. U.S.S.R., Peaceful Uses of Atomic Energy, Moscow 1955, Session Div. of Chem. Sci.*, 160; (d) Steiner, N. M., and Jungerman, J. A., *Phys. Rev.*, **101**, 807 (1956)
85. Bivins, R., Metropolis, N., Storm, M., Turkevich, A., Miller, J. M., and Friedlander, G., *Bull. Am. Phys. Soc. [II]*, **2**, 63 (1957)
86. (a) Nedzel, V. A., *Phys. Rev.*, **94**, 174 (1954) (b) Taylor, T. B., *Phys. Rev.*, **92**, 831 (1953)
87. Voss, R. G. P., and Wilson, R., *Proc. Roy. Soc. (London) A.*, **236**, 41 (1956); Woods, R. D., and Saxon, D., *Phys. Rev.*, **95**, 1279 (1954)
88. (a) Chen, F. F., Leavitt, C., Shapiro, A. M., *Phys. Rev.*, **99**, 857 (1955); (b) Richardson, R. E., Ball, W. P., Leith, C. E., Jr., and Moyer, B. J., *Phys. Rev.*, **86**, 29 (1952)
89. Margulies, R. S., *Bull. Am. Phys. Soc.*, **30**, 28 (1955)
90. Cini, M., and Fubini, S., *CERN Symposium Proc. (Geneva)*, **V2**, 171 (1956)
91. Batson, A. P., Culwick, B., and Piddiford, L. (Private communication)
92. Fermi, E., *Progr. Theoret. Phys. (Japan)*, **5**, 570 (1950); *Phys. Rev.*, **92**, 452 (1953); **93**, 1435 (1954)
93. Lepore, J. V., and Neumann, M., *Phys. Rev.*, **98**, 1484 (1955)

THE MEASUREMENT OF THE NUCLEAR SPINS AND STATIC MOMENTS OF RADIOACTIVE ISOTOPES¹

By W. A. NIERNBERG

Department of Physics, University of California, Berkeley, California

INTRODUCTION

During the past several years great advances have been made in the measurement of the spins and the static moments of the radioactive nuclei.²

These achievements can be measured by the large number of nuclei treated, the reduction in the number of atoms required to make a measurement (1) (now in the neighborhood of 10^{10} atoms), and the lower limit of the half-life required (1) (half-lives of the order of one half hour have been successfully handled). This last comment should not be confused with the very successful work (2) on the nuclear *g*-factors of intermediate states of half-lives $\sim 10^{-7}$ sec which is in an entirely different range.

In addition, as it is now possible to treat alpha and proton induced activities (3) as easily as neutron activated materials, reliable information has been obtained on the neutron-deficient isotopes. This last is important in the theory of nuclear structure because several examples now exist of measured sets of isotopes of the order of ten in a set that differ by essentially one neutron number per isotope. Table I is such an arrangement of experimental results for the Rb and Cs isotopes. The Cs isotopes, for example, start at a magic number of neutrons and decrease to a number ten deficient from the magic number. The clearly anomalous results of $I = \frac{1}{2}$ for Cs¹²⁷ and Cs¹²⁹ give rise to interesting speculations (4). We are no longer restricted to the essentially one-dimensional line of stable nuclei of the Segre diagram, but can now cover the entire three-dimensional region of radio-nuclides and their isomers.

The advances in technique that have facilitated this progress have been many. It is the purpose of this article to review them, put them in perspective, and compare them as to suitability from the viewpoint of number of atoms needed, half-life, range of spin values possible, and other required

¹ The survey of literature pertaining to this review was completed in August (1957).

² The question of what is a "radioactive nucleus" is clearly of technical interest only. Since a nuclear frequency or "frequency of revolution" \sim of 10^{+22} sec.⁻¹ frequency, for any half-life longer than 10^{-20} sec. or so, the nuclear spin must be considered a good quantum number. This brings to mind the story of a paper read by Zacharias describing his now classic experiment on K⁴⁰ in which he emphasized that this was the first spin of a radioactive nucleus that had been measured. However, Millman was in the audience and pointed out that Rb⁸⁷ was the first such nuclear spin measured, but "we didn't know that it was radioactive when we measured it!"

TABLE I
SPINS AND MOMENTS OF THE CESIUM ISOTOPES

Cs	T _{1/2}	I	μ (n.m.)	Rb	T _{1/2}	I	μ (n.m.)
127	6.2 hr	1/2	+1.41 ± .04	81	4.7 hr	3/2	+2.05 ± .02
129	31 hr	1/2	+1.47 ± .04	81m	31.5 min	9/2	—
130	30 min	1	±1.5 ± .3	82	6.3 hr	5	+1.50 ± .02
131	9.7 day	5/2	+3.48 ± .04	83	83 day	5/2	+1.42 ± .02
132	6.2 day	2	+2.22 ± .02	84	33 day	2	-1.32 ± .02
133	stable	7/2	+2.58	85	stable	5/2	+1.35
134	2.3 yr	4	+2.95 ± .01	86	18.6 day	2	-1.67 ± .40
134m	3.1 hr	8	+1.10 ± .01	87	stable	3/2	+2.75
135	2.0 × 10 ⁶ yr	7/2	+2.74				
137	30 yr	7/2	+2.85				

The magnetic moments μ are given to three significant figures only. The sign of the moment is explicitly shown if known.

properties. Perhaps the most significant advances from the viewpoint of actual results have been in the field of atomic beams. In this case it is not a question of fundamental principle that is involved. The method is the use of space quantization and the Breit-Rabi formula (5) coupled with the atomic resonance method (6) and the "flop-in" technique first used by Zacharias (7) in the K⁴⁰ experiments. It was this latter experiment that served as a general model of technique to be employed by many in low background experiments involving small numbers of atoms. Historically this experiment was one of the first cleanly to resolve a major difficulty of β theory and emphasize the necessity for reliable spin determinations. Thus, while the six-pole focussing apparatus of Hamilton (8) and the Princeton group marked a significant advance in intensity (solid angle), the fundamental principles of application of the Breit-Rabi formula to obtain the spins and moments of the nuclei remain the same. The actual improvements have come about from the radioactive nature of the atoms of the beam itself. The beam detection (always a problem) is solved by collecting samples on appropriate surfaces and counting. Thus the advantages of particle detectors are utilized to give a greatly enhanced signal-to-noise ratio in terms of numbers of atoms. The pioneer results were obtained by Bellamy & Smith (9), and others soon appeared by Lemonick & Pipkin (10), Gilbert & Cohen (11), Goodman & Wexler (12), and Hobson *et al.* (13). (Parenthetically it should be noted that the last method, employed to measure the spin of Rb⁸¹, is the "zero-moment" (14) method, also based on the Breit-Rabi diagram. The method is poor in intensity and will not be further discussed.) The isotopes measured (9 to 12) were primarily reactor-produced and hence were made in relatively large abundance, $\sim 10^{17}$ or more atoms. In fact, in some of these experiments the specific radioactivity was not employed in detection but rather the conven-

tional hot-tungsten wire and mass spectrometer (15). For reasons that will be considered in the detailed discussion of the atomic beams method, the inevitable carrier restricts the specific activity and thus prevents the efficient use of the isotope produced by the pile if the half-life is of the order of a day or less. The last step that resulted in the largest decrease in number of atoms needed to make a measurement ($\sim 10^{10}$ atoms) came in the use of the neutron-deficient isotopes from the cyclotron. While the total activity is less, the specific activity is greater (in fact, in principle, controlled by the experimenter), and more isotopes (up to as many as six in the case of Cs) are available for research with present techniques. Another general comment is that the tracer technique here described has in a sense solved the universal detector problem of atomic beams.

The next most useful method is that of paramagnetic resonance in crystals. This method has been very successfully employed in the measurement of spins of the iron group, rare earths and actinides by the group in Oxford associated with Bleaney (16, 17), the group in Berkeley associated with Jeffries (18), and the group in Chicago associated with Hutchison (19). The theoretical basis of this work is the Hamiltonian of Abragam & Pryce (20). For those readers familiar with the Breit-Rabi Hamiltonian and diagram for the free atom (which will be reviewed briefly below) it is a useful simplification to understand the Abragam-Pryce Hamiltonian as an extension of the Breit-Rabi Hamiltonian to the paramagnetic ion in the crystal. The ion is considered as free (except for the very weak nearest neighbor effects responsible for the relaxation processes) in the nonspherically symmetric strong field of the crystal as a whole. This field serves to decouple the hyperfine structure and liquid He temperatures often employed serve to populate the levels differentially. The resonances are observed as microwave absorptions and are swept by varying an external field at fixed oscillator frequency. This method suffers from the relatively large amount of material required ($\sim 10^{15}$ atoms) and long half-lives needed because of the slow process of crystal growth. However, it is useful because it has treated those isotopes which, because of their refractory nature, have been difficult, but not impossible, to handle as a beam (21).

The next class of methods responsible for some nuclear information are those based on paramagnetic resonances in gases and solids where special techniques have been proposed and achieved for sharpening the observed resonances. The idea of employing a magnetically neutral buffer gas such as He to separate the paramagnetic atoms of interest was first proposed by Kastler (22) and employed by Dicke (23) and Sagalyn (24), using polarized resonance radiation and rf oscillator to measure the atomic quadrupole interaction in the Na^{23} atom. Here also the net effect of the buffer gas is to permit an atomic approximation allowing the use of the Breit-Rabi Hamiltonian with a high degree of rigor. This method has been employed by Beringer (25) to study the fine structure of O^{16} . Judging from these results, it would appear entirely feasible to measure spins with a total num-

ber of 10^{13} atoms or less. This is very encouraging and the method may be particularly appealing for the measurement of hyperfine structure anomalies (26), discussed below. A method closely related in principle, although not in practice, is the double resonance method in solids introduced by Feher (27). In the semiconductor silicon, P and As are "acceptor" atoms. Applying the general concepts of the Abragam-Pryce formalism, the dilute P or As atoms appear as isolated atoms in the solid. The Breit-Rabi formula again appears as the controlling equation to a high degree of approximation with the difference that the free electrons have the effect of a dielectric constant that reduces the Coulomb potential of the valence electron and therefore reduces the hyperfine structure constant by about one order of magnitude. The double resonance method has been so powerful that Feher has measured the hyperfine structure anomalies with a precision that is on a par with that obtained in atomic beams. Li has also been successfully diffused into the Si lattice and its lines observed to the same resolution. The method is capable of research on 10^{13} atoms at the present time and undoubtedly can be pushed to a much smaller number of atoms. The principal limitation is the number of elements that can be used as acceptors or can be diffused into the Si.

A closely related class of methods that have just begun to give results are those that employ the general techniques of nuclear orientation by application of very low temperatures (28, 29, 30). Then there is a general class of methods stimulated by Overhauser's suggestion (31) which uses rf saturation techniques and a technique first suggested by Abragam (32, 33) for attaining nuclear polarization in solids at liquid helium temperatures by variation of the applied magnetic field from the Paschen-Back to the weak Zeeman region of the Breit-Rabi diagram and back to the strong field. In this latter technique no radiofrequency is required, since the state mixing is at zero field and due presumably to the very weak dipolar fields of the solids. The method of nuclear orientation by very low temperatures is probably not of very general application because of the large quantity of low temperature equipment required and the difficulty of employing the nuclear detectors to make a definite spin assignment. The Abragam technique suffers from the same difficulty as Feher's double resonance technique in that it would appear that the number of isotopes that can be studied is strictly limited. A modification of Overhauser's method applied to paramagnetic resonance has been successfully applied by Jeffries (34) to demonstrate the spin of Co^{60} . It combines the best features of paramagnetic resonance and particle detection and may prove to be a powerful tool. The spin degeneracy is demonstrated explicitly. However, again the crystal-growing time will set a lower limit to the observable half-life of a few hours.

The methods noted above have been emphasized because of their novelty. However, progress in the improvement of spectroscopic resolution has been great and figures of 5 to 15 Mc/sec. have been quoted. In this connection, the work of Manning, Fred & Tomkins (35), Jackson (36), Conway (37), and

Jenkins (38), must be cited. This research has centered mainly on the rare earths and transuranics, which have been technically difficult by other methods, and many results have been obtained. Now, however, that atomic beams (39) of Pu and Am have been obtained and resonances observed, many of the rare isotopes of the transuranics will undoubtedly be amenable to treatment. Microwave molecular resonance in gases will continue to supply measurements. A most recent example is the spin and quadrupole moment of I¹²⁵ measured by Townes' group (40).

This account would not be complete without some mention of the method of optical excitation as applied to atomic beams. One of the limitations of the beams method is that it can only work with the atomic ground state. The highest nuclear moment observable in an atom is equal to $2I$ or $2J$, whichever is smaller, where I is the nuclear spin and J is the atomic angular momentum. If $J=0$ no moments are observable, if $J=\frac{1}{2}$ only the magnetic moment is observable but not the quadrupole moment, and so on. These restrictions apply to some of the most important elements under investigation. Rabi (41) and his group and Kusch (42) and his group have succeeded in using optical excitation in the alkalis and Tl respectively to obtain the atomic states of higher J and thereby see the quadrupole interactions. The nuclear information so obtained is important but the technical problem of applying the method to trace quantities appears to be too formidable at the present time.

THE FERMI-SEGRÈ FORMULA AND THE BREIT-RABI DIAGRAM

There are many derivations of the Fermi-Segrè formula (15) and the reader is referred to the original paper by Fermi (43) for the hyperfine structure of a hydrogen-like atom. In this calculation, Fermi used the Dirac equations of motion for the electron but, as will be seen, this point is not essential. The complete hyperfine structure interaction of a nucleus with its atom of interest here may be defined as the nonspherical nuclear-extraneous electronic interaction. This interaction can only be measured by observing the energy required to change the relative orientation of the nuclear spin and the electronic angular momentum. This definition excludes the absolute shift in energy due to that part of the interaction which comes from the finite size of the nucleus and is not orientation-dependent. This contribution is responsible for the classical spectroscopic isotope shift. For a complete and unambiguous account of the hyperfine structure terms, the reader is referred to the excellent paper by Schwartz (44), where the nuclear moments are defined in general and explicit expressions for the matrix elements of the interactions are given. [See also Kramers (45), Casimir (46), and Schwinger (47).]

In most of the research now being undertaken, the principal terms in the interaction Hamiltonian are the magnetic dipole and the electric quadrupole term. The treatment of these terms will be briefly reviewed here (although

they are mathematically more rigorously treated in the given references) because there are physical ideas that have been overlooked and there are points of view that need additional emphasis in the light of modern work. The dipolar term is the result of the interaction of the nuclear magnetic moment with the electrons in the atom. For that part of the electronic wave function which is nonspherically symmetric, the treatment is straightforward and will not be repeated here. This follows from the fact that an electron of orbital angular momentum l has a density of r^{2l} at the origin. Since the measurable interesting effects (and difficulties of interpretation) occur for the region of overlap of the electron and nuclear charge densities, only s -wave electronic functions will be considered. We therefore consider an atom in a spherically symmetric state (of $\psi^*\psi$), of electronic angular momentum J and nuclear angular momentum I , where I and J will be considered good quantum numbers throughout. This assumption is valid if the hyperfine structure energy is small compared to the atomic term differences and allows the use of lowest order perturbation theory. The diagonal matrix elements of the electronic and nuclear angular momenta can be written as

$$\begin{aligned}\mathbf{\mu}_I &= g_I \mu_0 I, \\ \mathbf{\mu}_J &= g_J \mu_0 J.\end{aligned} \quad 1.$$

g_I and g_J are the appropriate Landé g -factors and, since μ_0 is the Bohr magneton, $g_I \ll g_J$ and, in fact, $g_I \sim (1/2000)g_J$. The vector potential of the nucleus, assumed to be a point dipole, is

$$\mathbf{A}_I = -\mathbf{\mu}_I \times \nabla \frac{1}{r} = -g_I \mu_0 I \times \nabla \frac{1}{r}, \quad 2.$$

where the nucleus is at the origin and the electron is at \mathbf{r} . Taking the curl of \mathbf{A} to get the magnetic field and then the negative cosine product of the electron moment with the field, we obtain the Hamiltonian

$$\mathcal{H} = g_I g_J \mu_0^2 \mathbf{J} \cdot \nabla \times \left(\mathbf{I} \times \nabla \frac{1}{r} \right), \quad 3.$$

and this expands to

$$\mathcal{H} = g_I g_J \mu_0^2 \mathbf{J} \cdot \nabla^2 \frac{1}{r} - g_I g_J \mu_0^2 (\mathbf{J} \cdot \nabla) (\mathbf{I} \cdot \nabla) \frac{1}{r}. \quad 4.$$

Now the first term is spherically symmetric and $\nabla^2 1/r = -4\pi\delta(\mathbf{r})$, where $\delta(\mathbf{r})$ is the Dirac delta-function. The second term splits into a spherically symmetric part equal to $-\frac{1}{3}g_I g_J \mu_0^2 \mathbf{J} \cdot \nabla^2 1/r$ and a pure angular dependent term. It is interesting to note that for a non- s -wave function this last part gives a contribution while the $\nabla^2 1/r$, or "contact terms" vanish, whereas for an s -wave function the angular part vanishes and the $\nabla^2 1/r$ terms yield the only contribution. For an s -wave function, therefore,

$$\mathcal{H} = -\frac{8\pi}{3} g_I g_J \mu_0^2 \mathbf{J} \cdot \nabla \delta(\mathbf{r}), \quad 5.$$

and averaging over the electronic state we have the Fermi result

$$W = -\frac{8\pi}{3} g_I g_J \mu_0^2 |\psi(0)|^2 \mathbf{I} \cdot \mathbf{J}, \quad 6.$$

$$W = a \mathbf{I} \cdot \mathbf{J},$$

and, since $g_J < 0$, $a > 0$ for a positive nuclear moment $g_I > 0$, and the hyperfine structure is normal. By normal is meant that the level of largest F , where $\mathbf{F} = \mathbf{I} + \mathbf{J}$, lies highest. As a result of this calculation, the physical interpretation of the hyperfine structure interaction in s -states becomes clear. Fig. 1a is a picture of what is happening. The nucleus is idealized as a small, uniform sphere of electricity which is rotating. From elementary considerations, if the sphere is to appear externally as a magnetic dipole of strength $\mathbf{y}_I = g_I \mu_0 \mathbf{I}$, it will have a uniform internal field given as $8\pi/3$ times the magnetization. The magnetization is the dipole moment divided by the volume of the sphere, V , so the uniform magnetic field inside the nucleus is

$$\mathbf{B} = \frac{8\pi}{3} \frac{g_I \mu_0 \mathbf{I}}{V}. \quad 7.$$

The interaction energy is the average of the negative scalar product of the nuclear magnetic field and the electron magnetic moment. That part of the interaction which is outside the sphere averages to zero for a spherically symmetric electron distribution. (This part corresponds to the angular dependent part of Eq. 4.) That part of the interaction which lies inside the

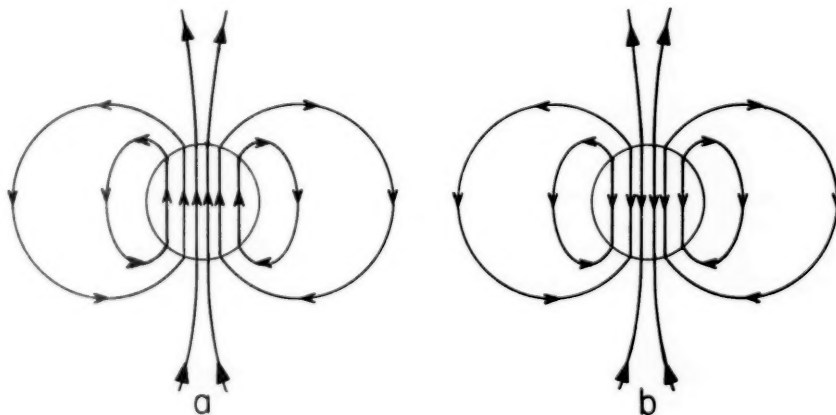


FIG. 1. Schematic diagram of magnetic lines of force for a nucleus. Figure 1a represents the field as derived from a vector potential, Figure 1b represents the field as derived from a scalar potential.

sphere makes the only contribution and it occurs with a probability which is equal to the square of the electronic wave function at the nucleus (assumed to have negligible variation over the nuclear radius) times the volume of the interacting region V . Putting the factors together we have

$$\mathfrak{J}C = -\frac{8\pi}{3} g_I g_J \mu_0^2 \frac{\mathbf{I} \cdot \mathbf{J}}{V} \cdot V \cdot |\psi(0)|^2, \quad 8.$$

which is the same result as Eq. 6. An altogether different approach, and one that is very illuminating, is to derive the magnetic field of the nucleus from a scalar potential χ . In that case we may write

$$\chi = -\psi_I \cdot \nabla \frac{1}{r}, \quad 9.$$

and

$$\mathbf{B} = \nabla \left(\psi_I \cdot \nabla \frac{1}{r} \right). \quad 10.$$

It follows, from similar arguments to those already used for a spherically symmetric state, that

$$\mathfrak{J}C = \frac{4\pi}{3} g_I g_J \mu_0^2 \mathbf{I} \cdot \mathbf{J} \delta(r). \quad 11.$$

This result is exactly one-half the result of Eq. 8 and is opposite in sign. To interpret this result we refer to Figure 1b. The use of a scalar potential throughout implies that the source of the magnetism in the nucleus is a kind of spherical bar magnet so constructed that the external field is that of a dipole of strength $g_I \mu_0 \mathbf{I}$. In such a case the magnetic field that exists in the nucleus and is used to obtain Eq. 11 must be \mathbf{H} , which goes from the nuclear north pole to the nuclear south pole, and therefore is opposite to the corresponding field of Figure 1a. This gives the sign reversal. The factor 2 appears from the well known fact that $\mathbf{H} = -(4\pi/3)\mathbf{M}$, where \mathbf{M} is the magnetization, for this situation, instead of $\mathbf{B} = 8\pi/3\mathbf{M}$ that arose from the consideration of the nucleus as a spinning charge. The experimental observations (48, 49) agree with Eq. 6, so even rough agreement is enough to fix the source of nuclear magnetism and the very close agreement in the case of the hydrogen atom demonstrates the faithfulness of the picture. The remark is often made that it is necessary to use the Dirac equation of the electron to obtain the right answer. This is not correct, as the above analysis shows. Rather, the confusion stems from a more routine problem in magnetism, namely the difference between \mathbf{B} and \mathbf{H} . This point was clearly understood by Bloch (50) at an early date.

The possible total angular momenta of the system are $\mathbf{F} = \mathbf{I} + \mathbf{J}$, where F assumes the values $I+J, I+J-1, \dots, |I-J|$. The differences in energy of adjacent hyperfine levels are now usually reported³ in units of Mc./sec.

³ In cryogenic work it has become customary to report these differences in K°.

and they range from 10 Mc./sec. to over 20,000 Mc./sec. If $J = \frac{1}{2}$, the two values of F are $I + \frac{1}{2}$ and $I - \frac{1}{2}$, and the one frequency difference is

$$\hbar\Delta\nu = a\left(I + \frac{1}{2}\right) = -\frac{4\pi}{3}g_I g_J \mu_0^2 |\psi(0)|^2 (2I + 1). \quad 12.$$

If two isotopes are compared, to a very good approximation, it is expected that

$$\frac{\Delta\nu_1}{\Delta\nu_2} = \frac{g_{I_1}(2I_1 + 1)}{g_{I_2}(2I_2 + 1)}. \quad 13.$$

The $\Delta\nu$'s can be measured to almost any precision desired by atomic beams or some related method, and the ratio of the g_I 's is usually known from nuclear resonance work or lacking that, from very high resolution experiments in atomic beams (51, 52). The extent to which Eq. 13 does not hold is considered to be a measure of the failure of the approximations in the derivation of the Fermi formula, Eq. 12. Among the approximations made is the assumption that the magnetization is uniformly distributed over the nucleus. Bohr & Weisskopf (53) have formed theories covering this point and now the hyperfine structure anomalies (as deviations from Eq. 13 are called) can be used as experimental data in discussing nuclear structure in the same manner as are the magnetic moments and the quadrupole moments. The effects run as high as 0.5 per cent in s -states, but even so it has not yet been possible to measure more than isolated pairs of nuclei, with the exception of the Cs isotopes of which Stroke *et al.* (54, 55) have reported on Cs^{133} , Cs^{134} , Cs^{135} and Cs^{137} . Now that quite a few other Cs isotopes (1, 56) are available for research, it is hoped that more progress will be made in applying the results of hyperfine structure anomaly research to nuclear theory. So far, the agreement with theory has not been uniformly consistent.

Besides the magnetic dipole moment interaction, there are higher moment terms. In the absence of external fields and therefore due to the spherical symmetry requirement, the diagonal Hamiltonian in orientation dependent terms must appear as a power series in $(\mathbf{I} \cdot \mathbf{J})^n$.

$$\mathcal{H} = a_0(\mathbf{I} \cdot \mathbf{J}) + a_1(\mathbf{I} \cdot \mathbf{J})^2 + \dots \quad 14.$$

In the classical case, this would be an infinite power series in $\cos^n \Theta$, where Θ is the angle between \mathbf{I} and \mathbf{J} . In the quantum mechanical situation, the series must terminate at a power $n = 2I$ or $2J$, whichever is smaller. The reason can be understood in terms of the indicial equation for $\mathbf{I} \cdot \mathbf{J}$ itself (57). According to the fundamental Hamilton-Cayley theorem on matrices, $\mathbf{I} \cdot \mathbf{J}$ must identically satisfy its own indicial equation. Due to the rotational invariance, m_F , the quantum number of F_z , is a good quantum number. The matrix of $\mathbf{I} \cdot \mathbf{J}$, therefore, breaks up into submatrices along the diagonal labeled by a given m_F . The largest dimension of any of these submatrices can only be $2I+1$ or $2J+1$, whichever is smaller. It follows that the Hamilton-Cayley equation for $\mathbf{I} \cdot \mathbf{J}$ is of degree either $2I+1$ or $2J+1$. Assume, for argument's sake, that $J \leq I$, then the $(2J+1)$ th power of $\mathbf{I} \cdot \mathbf{J}$ must be identi-

cally equal to a linear combination of lower powers of $I \cdot J$. The coefficients are functions of I and J only, and it is this identity that terminates the series Eq. 14. The series of Eq. 14 is not particularly useful because, except for the coefficient a_{2I} , the coefficients a_n are not directly related to the nuclear moments as usually defined (44), but rather are linear combinations of these moments. A simple way of deriving the hyperfine energy level spacing is included that shows the origin of the characteristic deviations from the interval rule in what may seem to some to be a physically more satisfying picture (58). What is wanted, in general, are the eigenvalues of the classical operator given by the expression

$$\mathcal{H} = \sum a_l P^l(\cos \Theta_{IJ}), \quad 15.$$

and the coefficient a_l will be the l th pole interaction term. Unfortunately the discussion is not as neat as it might be because the cosine and quadrupole terms have already been defined into general usage in a manner not quite consistent with Eq. 15. The general procedure is to apply the addition theorem

$$\begin{aligned} P^l(\cos \Theta_{IJ}) &= P^l(\cos \theta_I) P^l(\cos \theta_J) \\ &+ \sum \frac{(l - |m|)!}{(l + |m|)!} P_l^m(\cos \theta_I) P_l^m(\cos \theta_J) e^{im(\phi_I - \phi_J)}. \end{aligned} \quad 16.$$

θ_I, ϕ_I and θ_J, ϕ_J are the polar angles of I and J respectively. The matrix elements of the operator $P^l(\cos \Theta_{IJ})$ are taken in this form and in the Paschen-Back representation, where m_I and m_J are good quantum numbers. The term $P^l(\cos \theta_I) P^l(\cos \theta_J)$ contributes diagonal (in m_I and m_J) matrix elements only, whereas the other terms contribute elements off the diagonal. The problem is spherically symmetric and a Slater procedure on the diagonal elements gives the eigenvalues. Furthermore, the diagonal matrix elements are easily obtained as can be seen from the following example where the octupole moment is treated.

$$r^3 P^3(\cos \theta) = \frac{5}{2} z^3 - \frac{3}{2} z(x^2 + y^2 + z^2). \quad 17.$$

Normally a direct substitution of $I_z = z$, $I_x = x$, $I_y = y$ will suffice to give the matrix elements of this operator. Caution must be exercised, because the result in this form will not be Hermitian in general; therefore the correct form for Eq. 17 is

$$r^3 P^3(\cos \theta) = \frac{5}{2} z^3 - \frac{1}{2} (zx^2 + xzx + x^2z + zy^2 + zyz + yz^2 + z^3). \quad 18.$$

If the substitution of $I_z = z$, $I_x = x$, $I_y = y$ is now made to obtain the diagonal matrix elements, one obtains, in agreement with Casimir (46),

$$\langle m_J | r^3 P^3(\cos \theta) | m_J \rangle = \frac{5}{2} m_J^3 - \left[\frac{3}{2} J(J+1) - \frac{1}{2} \right] m_J. \quad 19.$$

A similar equation holds for m_I , so the diagonal matrix element of the octupole interaction must be of the form

$$\langle m_I m_J | \Theta | m_I m_J \rangle = \frac{C_I C_J \{5m_J^3 - [3J(J+1) - 1]m_J\} \{5m_I^3 - [3I(I+1) - 1]m_I\}}{4J(J-1)(2J-1) I(I-1)(2I-1)}. \quad 20.$$

The usual convention has been followed of introducing a factor, function of I and J , which makes the coefficient of $C_I C_J$ unity when $m_I = I$ and $m_J = J$. Thus when ultimately the quantity C_I , for example, is calculated from the current distribution in the nucleus to give the octupole moment, this octupole moment will be defined for the nuclear state $m_I = I$, as is customary. The eigenvalues of the matrix can be calculated by using the diagonal matrix elements of Eq. 20. Thus when $m = I + J$, $m_I = I$ and $m_J = J$, there are no elements connecting this state to any other, and the corresponding diagonal matrix element is an eigenvalue of Θ corresponding to $F = I + J$ and it is $[2(I+J)+1]$ -fold degenerate. When $m = I + J - 1$, there is a two by two matrix to be treated. However, one of the two eigenvalues has already been found and the spur of the 2×2 matrix minus that of the 1×1 matrix is the eigenvalue of Θ belonging to $F = I + J - 1$. If the spur of the submatrix belonging to $m = J + I - i$ be denoted by S_i , then the rule is

$$W_{J+I-i} = S_i - S_{i-1}. \quad 21.$$

This terminates when $i = I$, if $I \leq J$. Interactions with the same symmetry as magnetic octupole interactions have been observed for I and Ga (59, 60). The results are difficult to interpret because the interaction is small and there are effects due to off-diagonal dipole and quadrupole interactions that have the same effect and magnitude (44). So far, the octupole moments measured are too few and too uncertain to be genuinely useful in nuclear theory.

In the absence of an external field, the hyperfine terms are equal to the values of Eq. 21 when $(I \cdot J)$ is replaced by $\frac{1}{2}[F(F+1) - I(I+1) - J(J+1)]$. Each F level is $(2F+1)$ degenerate and, if a weak magnetic field is applied, they split linearly with H (except for $m=0$ states which go quadratically). A weak magnetic field is one for which $g_F \mu_0 H$ is numerically much smaller than the difference between adjacent hyperfine terms. This is the Zeeman region and the Landé g factor is

$$g_F = g_J \frac{F(F+1) - I(I+1) + J(J+1)}{2F(F+1)} + g_I \frac{F(F+1) + I(I+1) - J(J+1)}{2F(F+1)}. \quad 22.$$

The energy of a given level is approximately

$$W_{F,m} = W_F + g_F \mu_0 H m, \quad 23.$$

and, since the selection rules are $\Delta F = 0, \pm 1$; $\Delta m = 0, \pm 1$, the frequencies that vanish with the field are

$$\nu_F = g_F \mu_0 H / \hbar, \quad 24.$$

equal for a given g_F . It is very important to note that, since $g_I \sim 1/2000$, g_F may, to a very good approximation, be written as

$$g_F \approx g_J \frac{F(F+1) - I(I+1) + J(J+1)}{2F(F+1)}. \quad 25.$$

As another useful example, consider $J = \frac{1}{2}$ and $F = I + \frac{1}{2}$, then

$$g_F \cong g_J \frac{1}{2I+1}. \quad 26.$$

Notice that from Eqs. 24, 25, and 26, the resonant frequency of the system depends on g_J , an atomic factor presumably well known or easily determined, and on no nuclear factor other than the spin which is a discrete quantity. This point plays a decisive role in the atomic beams method of determining spin. The physical picture is the following. By virtue of the tight hyperfine coupling, which a weak magnetic field cannot affect, the inertia of the system to an applied torque is increased because the angular momenta of the electron and nucleus are combined. The magnetic moment of the system remains virtually the same because of the vanishingly small nuclear moment. Therefore an applied field will exercise the same torque as to the electron alone, but the entire system will precess more slowly due to the greater spin. This is the origin of the factor $(2I+1)^{-1}$ in Eq. 26. As the field is increased, quadratic terms in H appear. At a field where $|\mu_0 g_J H / h| \ll \Delta\nu$ (this is a field ~ 100 to 10,000 gauss) the two angular momenta are decoupled and the Paschen-Back approximation is valid. In this approximation m_J and m_I are treated as good quantum numbers, the external field interactions are diagonal and the averages of the cosine couplings are the first order perturbations. The appropriate formula is

$$W_{m_I, m_J} = -g_J m_J \mu_0 H - g_I m_I \mu_0 I + am_I m_J + \frac{b}{4I(2I-1)J(2J-1)} [3m_I^2 - I(I+1)][3m_J^2 - J(J+1)] + \dots, \quad 27.$$

where b is now the accepted definition of the quadrupole interaction constant in atomic hyperfine work (61). These two approximations (Eqs. 26 and 27) plus the rule that levels of the same m_F never cross are sufficient to sketch out the energy level diagrams as a function of the field. Fig. 2a is a diagram for $j = \frac{1}{2}$, $I = \frac{1}{2}$, and Fig. 2b is a diagram for $J = \frac{1}{2}$, $I = \frac{1}{2}$. In the very special but important case where $J = \frac{1}{2}$, the secular equation is quadratic and therefore expressible in terms of a simple expression which goes by the name of the Breit-Rabi formula. There is no quadrupole term and

$$W_m = -\frac{\hbar\Delta\nu}{2(2I+1)} - g_I \mu_0 H m \pm \frac{\hbar\Delta\nu}{2} \left(1 + \frac{4mx}{2I+1} + x^2\right)^{1/2} \quad 28.$$

$$x = -(g_J - g_I)\mu_0 H / \hbar\Delta\nu,$$

for the Hamiltonian

$$\mathcal{H} = -\mu_0 g_I \mathbf{I} \cdot \mathbf{H} - \mu_0 g_J \mathbf{J} \cdot \mathbf{H} + \frac{\hbar\Delta\nu}{I + \frac{1}{2}} \mathbf{I} \cdot \mathbf{J}.$$

The positive square root goes to the $F = I + \frac{1}{2}$ level in the limit of $H \rightarrow 0$. Notice that the levels $m = \pm(I + \frac{1}{2})$ are linear functions of the field. These levels are exceptional in that they are simultaneous eigenstates of F_z , I_z , J_z for all values of H . Note also that the level $m = -I - \frac{1}{2}$ "crosses the diagram"

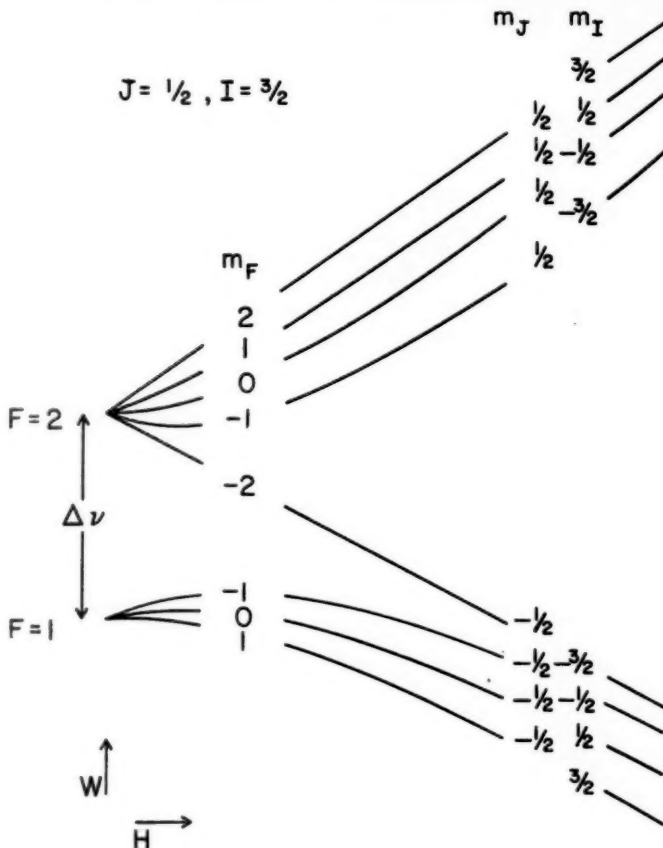


FIG. 2a. The hyperfine energy levels versus magnetic field for $J=\frac{1}{2}$, $I=3/2$. The abscissa is proportional to $g_I\mu_0H/\Delta\nu$. This is the situation for the electronic ground state of the alkalis, Au, Ag, Cu, Tl, Th, Ga, etc., with appropriate values of I .

to change the statistically unequal states $F=I \pm \frac{1}{2}$, to the statistically equal states $m_J = \pm \frac{1}{2}$. The order of the states in the Paschen-Back region is significant. At fields $\sim 10,000$ gauss it is usually determined by the hyperfine structure interaction. However, for fields between 10^5 and 10^6 gauss, the direct nuclear terms $-g_I m_I \mu_0 H$ of Eq. 27 become comparable to $a m_I m_J$, and at higher fields the levels cross and are rearranged. The other case directly solvable by a simple formula is that corresponding to $I=\frac{1}{2}$ and J arbitrary. An example of this is Pu^{239} , where the $J=1$ level has been studied (39). Figure 2c is the Breit-Rabi diagram for Pu^{239} . The appropriate equation is Eq. 28 with I and J interchanged.

The formula of Eq. 28 has been proved to hold to five or six significant figures for the alkalis, Ga, In, and for the halogens by many workers.

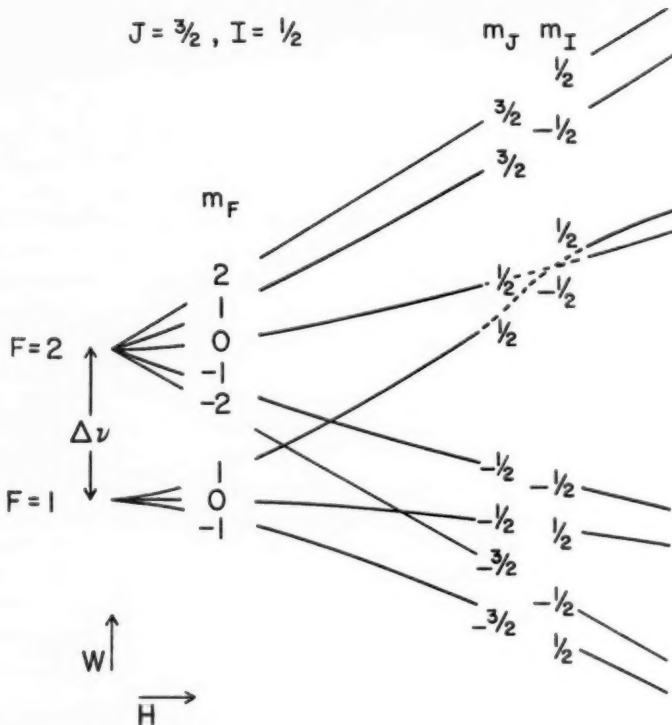


FIG. 2b. The hyperfine energy levels versus magnetic field for $J=3/2$, $I=\frac{1}{2}$. The abscissa is proportional to $g_J\mu_0H/\Delta\nu$. This is the situation for the electronic ground state of the halogens, Bi, and the metastable states of Tl, In, and Ga for appropriate values of I . If $I > \frac{1}{2}$, there can be as many as three hyperfine intervals in zero field.

Its great validity has been of primary importance in such experiments as that of Nafe & Nelson (48), and Kusch and his coworkers (49, 62) on the anomalous spin magnetic moment of the electron. An especially good example is the work of Stroke *et al.*, previously cited (54), on the direct determination of the hfs anomalies of the Cs isotopes, where the g_I of Cs¹³⁴, Cs¹³⁵, and Cs¹³⁷ were determined directly in strong fields due principally to the small term $-g_I m_I \mu_0 H$ in Eq. 27. It is interesting to note that the perturbing effect of another configuration in the case of the $^2S_{1/2}$ level in the alkalis is very small (63), and Clendenin (64) has shown that the lowest order effect of a $^2P_{3/2}$ state on a $^2P_{1/2}$ state is a very slight modification of g_I and a in Eq. 28 by an amount proportional to the ratio of the hyperfine structure constant to the fine structure constant. This is due to the Zeeman mixing of the $^2P_{3/2}$ and $^2P_{1/2}$ states, but in any event it does not change the functional form of Eq. 28.

$$J=1, I=\frac{1}{2}$$

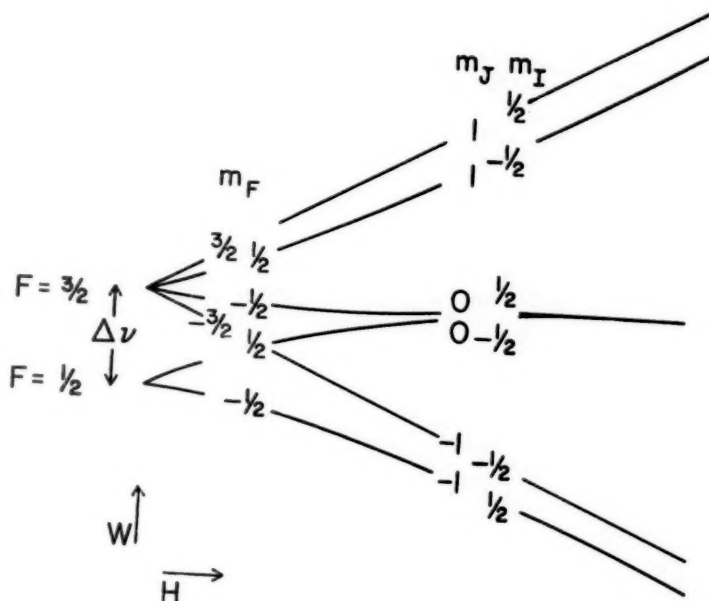


FIG. 2c. The hyperfine energy levels versus magnetic field for $J=1, I=\frac{1}{2}$. The abscissa is proportional to $g_J\mu_0H/\Delta\nu$. The state $F=3/2, m_F=-\frac{1}{2}$, has a negligible moment in strong fields, thus requiring a modification of the Zacharias "flop-in" technique.

MEASUREMENT OF SPINS AND MOMENTS OF SHORT-LIVED RADIO-ISOTOPES BY METHOD OF ATOMIC BEAMS

The general method of atomic beams for the measurement of the spins and moments of rare isotopes was first introduced by Zacharias (7) in the K^{40} experiments. The following is a detailed description of the method developed by the authors cited in the previous section, with the additional modifications imposed by the small number of radioactive atoms generally available from a cyclotron bombardment. Figure 3 is a schematic of a typical apparatus designed for this work (3). The A and B magnetic fields are strongly inhomogeneous magnetic fields with both the field and the inhomogeneity in the same direction. The C field is a uniform field supplying the magnetic field H of Eq. 28 in which the transitions are induced by a small additional rf field. The B field is about 50 cm. long and a clearance is supplied between the pole tips, which are circular arcs in cross section, so that an average atom of Na in a thermal beam is deflected about 0.1 in. in going

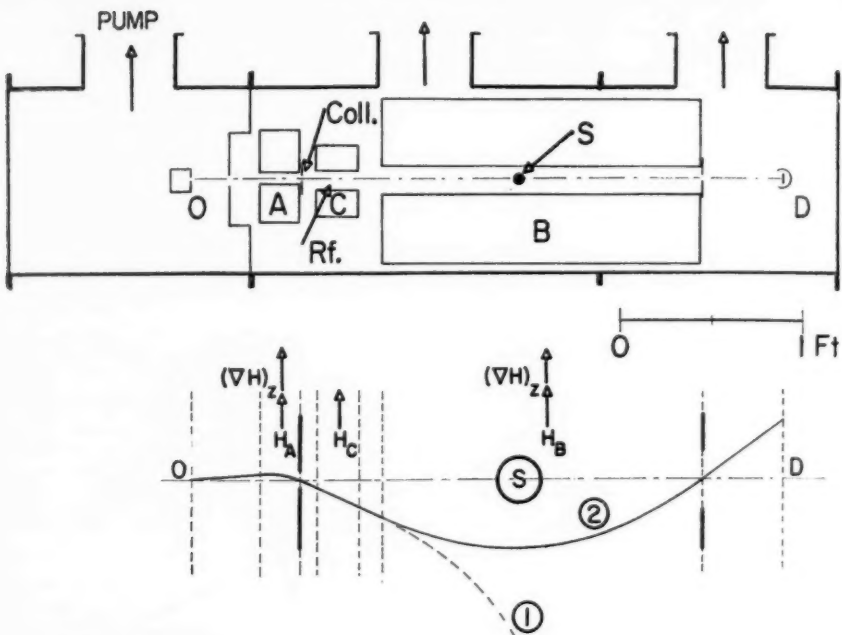
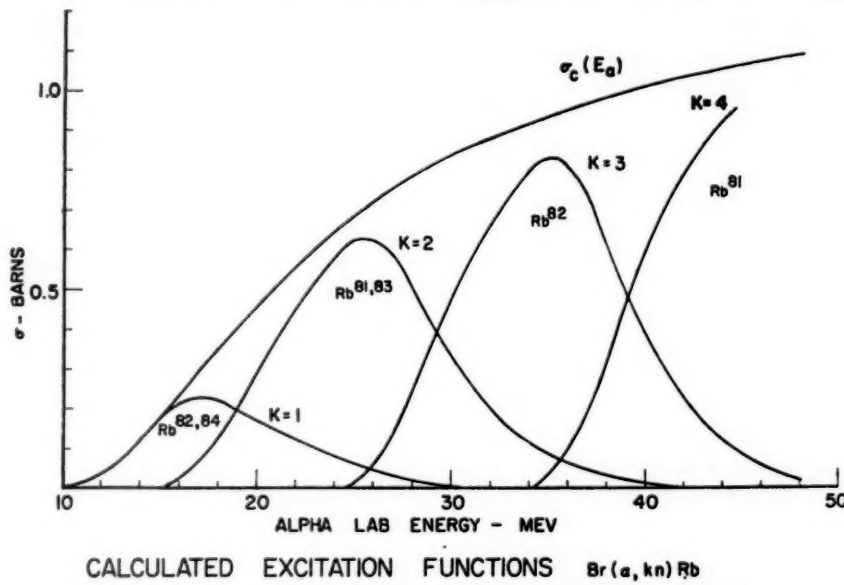


FIG. 3. Schematic of an atomic beam apparatus. O is the source, Coll. is the collimator, and D the detector. A and B are the inhomogeneous deflecting fields. C is the uniform field in which the resonance takes place. S is the stop wire.

through the apparatus. The A and B fields at the position of the beam are about 6000 gauss and the inhomogeneity in the B field,

$$\frac{1}{H} \frac{dH}{dy},$$

is about 1 cm.^{-1} . The apparatus is unconventional in that the A field is of negligible length compared to the B field. This tapering gives nearly a factor 4 improvement in intensity. This comes about because, in reducing the length of the A field, the angle through which the particle path is swung remains the same, since the gap between the magnets is decreased. The net effect is an increase in the solid angle seen by the detector. Typically, the improvement is a factor of 3 in transmission and, where the detection is statistically limited, this means a factor of 3 reduction in the counting time. In normal operation, this apparatus will deflect about 95 per cent of an atomic beam when the atom is in a $^2S_{1/2}$ state and the hyperfine structure is decoupled. The remainder is prevented from reaching the detector by an obstacle called a "stop wire" which blocks the geometric line of sight that exists between the source slits, the collimator slits and the detector slits. The path numbered 1 in the diagram is that of an atom moving with thermal velocity in the field

FIG. 4. (α, kn) excitation function for the production of Rb from Br.

gradients. Its curvature is in one direction and it does not reach the detector. Reference to Figure 3 shows that there are two levels, $F = I + \frac{1}{2}$, $m_F = -I - \frac{1}{2}$ and $m_F = -I + \frac{1}{2}$, which have the very special property that, when Paschen-Backed, they have essentially equal and opposite slopes to within a few per cent. Since the selection rule in weak C fields for rf induced transitions is $\Delta m_F = \pm 1$ for $\Delta F = 0$, a transition between these levels is possible. The equality of the absolute values of the slopes, $\partial W / \partial H$, means the equality of the forces (but reversed in sign) for the two levels

$$\left(f_z = - \frac{\partial W}{\partial H} \frac{\partial H}{\partial x} \right),$$

and therefore the curvature of the path reverses as for the one labeled 2.

At resonance, a signal can be observed at the exit slit if there is an appropriate detector for the beam. Therefore the method is positive in that no signal is observed unless there is a resonance. The important point to note is that it is not critical that the two slopes be exactly equal. A matching of the focusing forces to about 10 per cent is reasonable and does not affect the transmission to an extreme. It is also necessary to have a sufficiently reliable pre-estimate of the hyperfine structure such that it be reasonable to expect the decoupling of I and J that is necessary for operation. Under attainable experimental conditions, hyperfine structures up to about 20,000 Mc./sec. can be dealt with this way. This method is not unique and several variations can be employed. Where J is integral (Fig. 2c), there is no corresponding

transition because of the states $m_J = 0$ in strong fields. This problem has been solved and resonance observed in Pu^{239} by considering transitions equivalent to $F = \frac{1}{2}$, $\Delta m_F = -\frac{1}{2} \leftrightarrow -\frac{1}{2}$, and by putting the oven off-axis.

As an example of the special techniques required to apply this method to short-lived radioisotopes, it is instructive to consider the problem of the isotopes of rubidium, Rb^{81} , Rb^{82} , Rb^{83} , and Rb^{84} . Of these, the members of the first pair have half-lives of 4.7 and 6.3 hr. respectively, the second pair have half-lives of 33.0 days and 80 days respectively. In an alpha bombardment of Br^{79} and Br^{81} (about equal in natural abundance) at about 45 Mev, all four isotopes are produced. The first difficulty is identification. Once this is solved, the technique is rewarding in that all four spins are observed in one experimental run. Figure 4 shows the production cross section of the Rb isotopes by (α, kn) reactions, where $k = 1, 2, 3$, or 4. In a four-hour bombardment, about 10^{13} atoms of each isotope can be produced in BaBr_2 powder. This requires about 25 milliamperes of beam. The problem of cooling the powder to prevent evaporation is solved by packing the powder into ribbed channels on a water-cooled aluminum plate and covering it with a .001" aluminum foil backed by an open grid whose ribs are perpendicular to the set of ribs in the plate. Bombardments up to 50 m. amp. have been safely handled this way without seriously volatilizing the powder. The reasons for the choice of BaBr_2 is complicated and peculiar to the technique of atomic beams. At first sight, RbBr would seem far simpler. After bombardment, it is just necessary to put the RbBr containing trace amounts of radioactive rubidium into the oven and heat it in contact with calcium metal. This is a common method of producing an alkali beam. The stable rubidium is easily detected by the standard method of allowing it to impinge on a hot tungsten wire. The atoms are ionized, collected, and measured by means of a suitable electrometer. Thus it can serve both to calibrate the magnetic field and to monitor the radioactive beam. The difficulty is that several grams of carrier is the minimum amount that is involved. In practice, the effusion rate is limited by the "Knudsen" condition that the mean free path of the atoms in the oven be greater than the slit width for a tolerable beam. This implies an interval of about four days to empty the oven. Hence most of the unknown isotope decays in the oven if it is of short half-life. [This remains a fundamental obstacle in (n, γ) reactions.] The difficulty is avoided by the use of BaBr_2 and an involved chemistry that precipitates out the Ba. The chemistry is preceded by the addition of controlled amounts of carrier RbBr (~ 10 mg.) and followed by a differential sublimation of the $(\text{NH}_4)_2\text{CO}_3$ which remains after the precipitation of the Ba as BaCO_3 . The beam is produced from the RbBr in a conventional way. The second difficulty that has to be solved is the collection of the beam. The first method employed was again the ionization of the beam by means of a hot tungsten ribbon (9), but then a voltage was employed to collect the ions on a standard metal surface (brass) which can be inserted through a vacuum lock. The collected sample was assayed on a counter. It was soon found that this method was only a few per cent efficient. Furthermore, most obvious metal surfaces,

such as brass, were not much more than 20 per cent reproducible for the collection of neutral atoms. By a clever guess, Huffman (65) suggested the use of sulfur-coated collectors. These worked with close to full efficiency for K, Cs, Rb, Cu, Ag, Ga, and Tl. They did not work for iodine, but silver-plated surfaces did. It is clear that the collection problem will continue to be a problem in special cases. Other workers have used liquid air cooled surfaces with considerable success. The collection process is only one part of the detection problem; the other is the radioactive counting. The maximum intensity of a transition is $1/(2I+1)$ of the total beam, since two states out of $2(2I+1)$ states are involved. The transmission of a conventional apparatus is 10^{-5} and perhaps 50 samples have to be collected in the course of a run. This comes to about 10 disintegrations per minute on a resonance. Conventional low background counting is about 5 per cent efficient, and considerable research has been undertaken to determine the most suitable counting technique. Again the special property of an atomic beam was used. A beam has an area .1 in. \times .5 in. at the exit slit. A NaI crystal of dimensions just slightly larger than the exit slit was cleaved to about 1 mm. in thickness. Since most of the isotopes considered decay by K-capture and the K x-ray is completely absorbed by the thin crystal, the counter is very efficient. The small crystal volume cuts the background counting rate to very low values with two-in. lead shielding around the counter and the carefully selected photomultiplier. The background is further reduced by using a discriminating window in the circuit. Typical background counting rates are 1.2 counts per min. for 8 kev K x-rays, 0.6 for 12 kev, 0.35 for 30 kev and back to one count per min. for 80 kev. It is believed that the principal source of this background is the cosmic ray μ -meson. The efficiency is high and is presumably only limited by the Auger effect. This is important only for low Z , and there are relatively few isotopes of interest in this region. Because of their small area, these counters have proved to be surprisingly efficient for Tl²⁰⁴ and K⁴³ β 's with backgrounds of the order of five counts per minute.

An average Rb chemistry takes about two hours, which is only a fraction of the half-life of Rb⁸¹. The beam can be produced by heating the oven with tantalum coils, which generally takes about one-half hour. During the entire run, the carrier beam is monitored by the tungsten detector, and all results are normalized to these readings. After the beam is stabilized, the first step is the location of the stable Rb⁸⁵ ($I = \frac{5}{2}$) and Rb⁸⁷ ($I = \frac{3}{2}$) resonances by varying the frequency of the rf oscillator. The C field is then adjusted to bring one of these resonances to some value in the Zeeman region, which a priori seems to be reasonable in view of some assumed hyperfine $\Delta\nu$ for the unknown. The frequency of the transition is

$$\nu \approx \nu_\infty + \frac{2I\nu^2}{\Delta\nu}, \quad 29.$$

where ν_∞ is the frequency for the unknown spin if the $\Delta\nu$ were infinite. There is a similar shift for the calibrating isotope. If, for example, $\Delta\nu \sim 2000$ Mc./sec. and $I = \frac{3}{2}$ at 5 Mc./sec., the shift is .04 Mc./sec., which is small compared

TABLE II
RESONANT FREQUENCY FOR SPIN I
Assume $I_0 = 5/2$ resonance at 10 Mc./sec.

$$\nu = \frac{2I_0 + 1}{2I + 1} \nu_0 = \frac{60}{2I + 1} \text{ Mc./sec.}$$

I	ν	I	ν
1/2	30.00	0	60.00
3/2	15.00	1	20.00
5/2	10.00	2	12.00
7/2	7.50	3	8.57
9/2	6.00	4	6.67
11/2	5.00	5	5.45
13/2	4.29	6	4.62

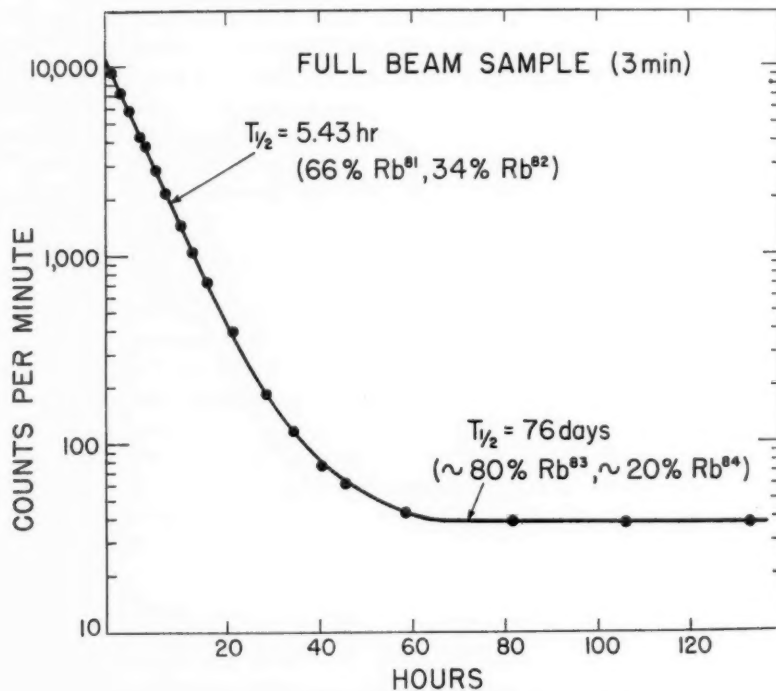


FIG. 5. The radioactive decay of a collected beam of radio-rubidium.

to a line width of .20 Mc./sec. The resonant frequency for the unknown resonance is related to that for the known (labeled by a zero index) by the following relation

$$\nu \approx \frac{2I_0 + 1}{2I + 1} \nu_0. \quad 30.$$

Table II gives typical search frequencies for a calibrating frequency of 10 Mc./sec. and $I_0 = \frac{5}{2}$. If a high spin is indicated, the separation between spins may become too small and a higher field or better resolution is indi-

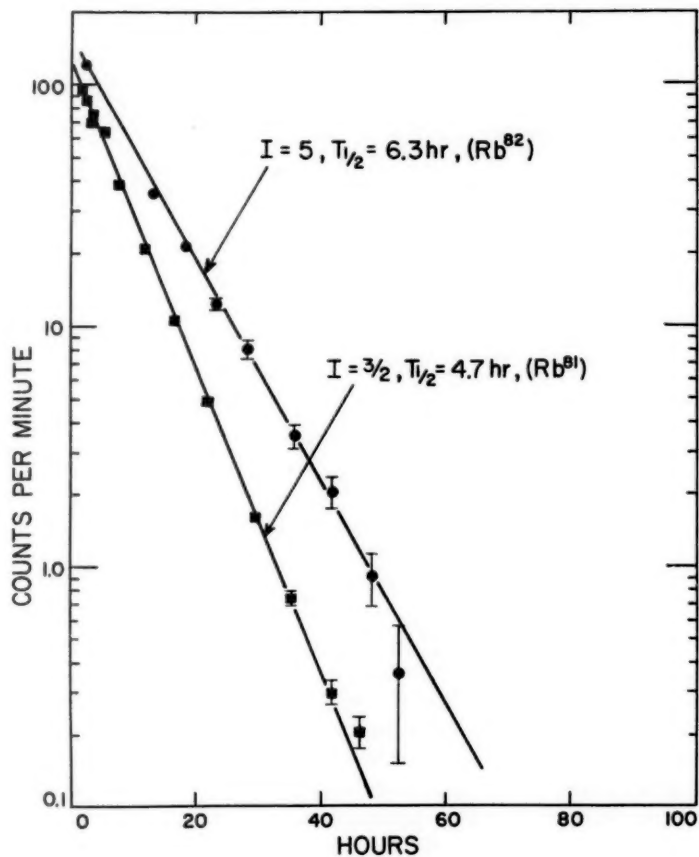


FIG. 6. The radioactive decay of two resonance peak beam samples collected for about five minutes each. The resonances were taken at frequencies corresponding to $I=5$ and $3/2$ respectively. Beside the fact that these were the only spin settings that yielded appreciable counting rates, the difference in half-lives between the two resonances themselves and the full beam of Figure 6 is very strong evidence for the interpretation indicated.

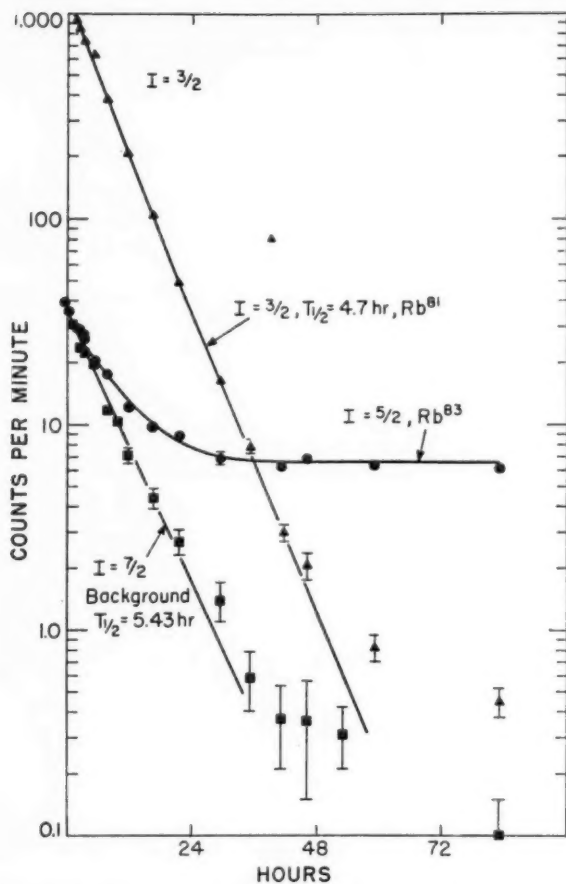


FIG. 7. Comparison of the decay of $I=3/2$, $5/2$, and $7/2$ samples. These exposures were taken for about thirty minutes each.

cated. Since resolutions to 10 kc./sec. have been achieved, there is in practice no reasonable limit to the value of the unknown spin. The largest spin measured to date (11, 12) is $I=8$ for metastable Cs^{134} . In the problem at hand, only two resonances are expected within a few hours after bombardment, one for half-integral spin (Rb^{81}), and one for integral spin (Rb^{82}). By setting the frequency for appropriate spin values and collecting the beam for about five minutes, two buttons show counting rates considerably above the rest. Figures 5 and 6 show the first results. Figure 5 is the decay curve of a sample collected for three minutes with the stop wire removed and the magnetic fields off. As expected, the decay has a short component of 5.4 hr. half-life and a long component of 76 days half-life. The short half-life indicates a fraction (by counting) of Rb^{81} of 66 per cent and of Rb^{82} of 33

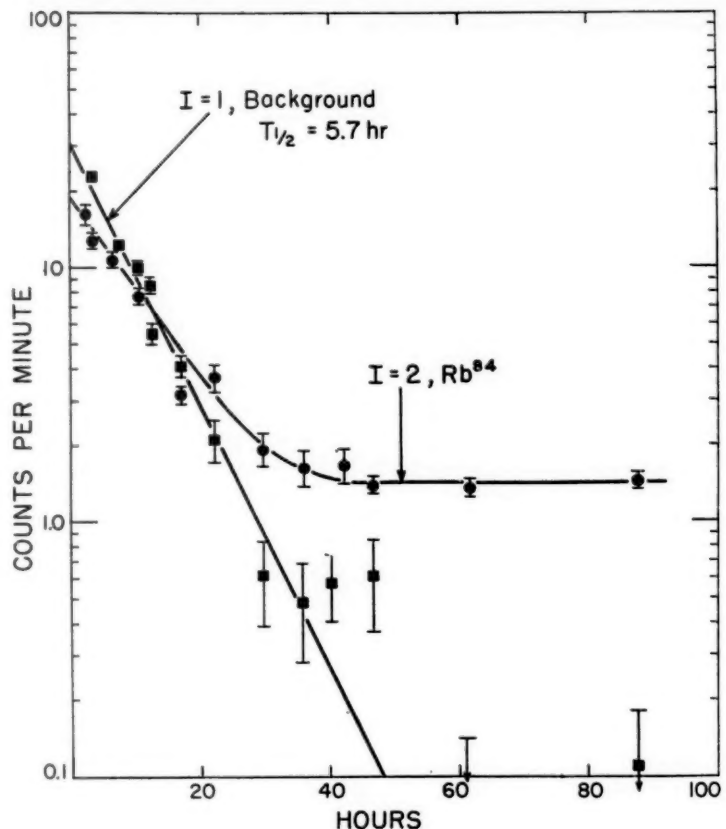


FIG. 8. Comparison of the decay of $I=1$ and 2 samples. These exposures were taken for about thirty minutes each.

per cent. Figure 6 shows the decay curves of the activities of the $I=\frac{1}{2}$ and the $I=5$ samples. They decay at the established rates for Rb^{81} and Rb^{82} respectively and quite different rates from that of the main beam in Figure 5. The isotope separation is clear. There is no doubt as to the spin assignments and they have been further verified by observations at several other fields. After several days, the two short components decay completely. At this point the same sample buttons can be recounted to locate the resonances of Rb^{83} and Rb^{84} . Again the one is half-integral spin, the other integral. Figure 7 compares the decays of three buttons corresponding to $I=\frac{3}{2}$, $\frac{5}{2}$, and $\frac{7}{2}$ respectively. Initially the $I=\frac{3}{2}$ sample dominates by several orders of magnitude as expected from the results for Rb^{81} . After several days, however, it disappears into background along with the $I=\frac{7}{2}$ button and only the $I=\frac{5}{2}$ is left with a significant counting rate of the order of six counts per minute. $I=\frac{5}{2}$ is therefore assigned to Rb^{83} . Similarly Figure 8 is the com-

parison of the integral spins, $I=1$ and $I=2$, and again only the $I=2$ is left with the residual of about 0.5 cpm. This low rate is due to the poor relative production of Rb⁸⁴ (which is assigned the $I=2$) by the (α , n) reaction on Br⁸¹. The decay of the two spin samples is observed (Fig. 9) for a long enough period to establish acceptable values for the half-lives. The observed half-lives are in reasonable agreement with the reported values (67). The measured half-life of the Rb⁸⁴ is relatively poor, being about 20 per cent too high. This is primarily due to background contamination from the Rb⁸³ in the beam. A word must be said about this background and its causes, because it is one of the principal limitations of this technique. In principle, unless there is a resonant transition, no atom can reach the detector. However, it is possible to contaminate the detector by beam scattering from the residual gas in the apparatus. It also happens that, due to abrupt magnetic transitions in going from the A field to the C field and back to the B field, the atom will have a small probability of undergoing nonadiabatic transitions of the type first discussed by Majorana (68). This effect can be reduced by tapering the fields at the ends, but this increases the length of the apparatus with a consequent loss in transmission. There are other such effects and the sum

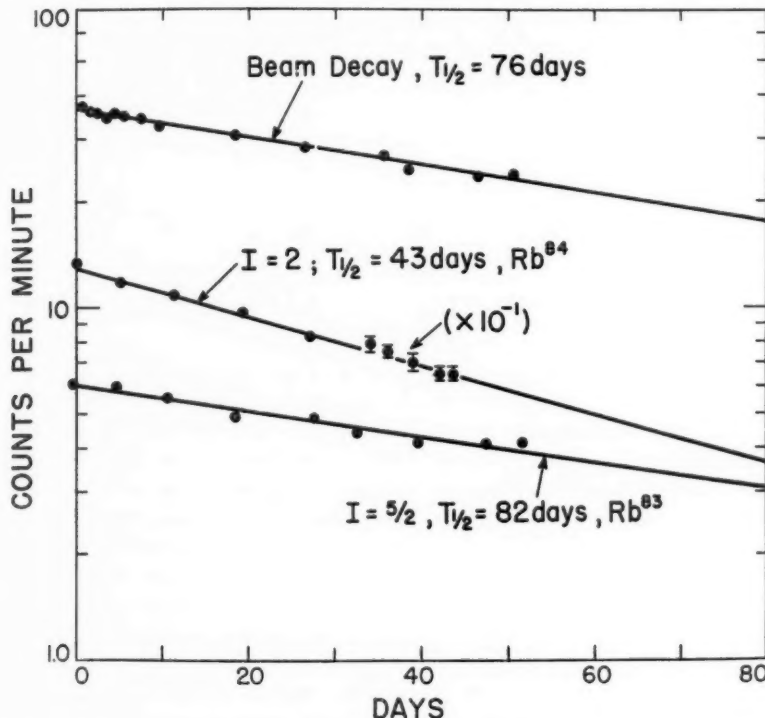


FIG. 9. The decay of the long-lived resonances of Rb⁸³ and Rb⁸⁴ versus the full beam.

total is a background not greater than about 0.1 per cent of the total beam. Typically, an $I = \frac{3}{2}$ should have a resonance intensity of about 25 per cent of the total beam. In practice, it is about 10 to 15 per cent. This is considerably above the background. However, if a second isotope is present to 10 per cent (by activity) of the first and has a spin $I = \frac{9}{2}$, its resonance is about 0.4 per cent of the beam and starts to compete with the background. The results of all the measurements can be summarized in a single diagram, Figure 10, in which the observed resonances for a number of runs are plotted against some arbitrary frequency scale corresponding to $1/(2I+1)$. Each isotope is shown with its resonance normalized by its estimated fraction in the beam. The circular points are the short half-lives extrapolated to the time the sample left the cyclotron, and the square points are the long half-lives. Resonances are observed only for $I = \frac{3}{2}, \frac{5}{2}, 2$ and $\frac{5}{2}$ and for no other spins. The intensities of the resonances vary roughly as $1/(2I+1)$. Furthermore, an estimate can be made of the total intensity expected. This is a combination of the production cross sections, the counter efficiency, the

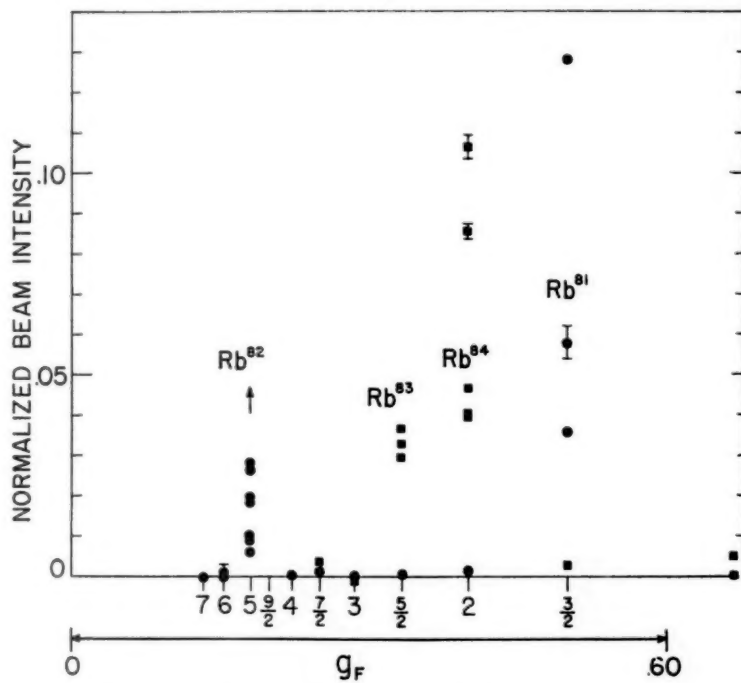


FIG. 10. The normalized Rb resonances. The circled points represent the short-lived components extrapolated to the time the sample was removed from the cyclotron. The square points are the long-lived components. Notice that the resonances are roughly proportional to $(2I+1)^{-1}$.

Auger effect, the competing processes from what is known of the decay schemes, and the effect of the daughter, if any. The observed intensities agree to about a factor of two, which is as good as can be expected.

The specific discussion of the spin measurements of the four Rb isotopes has been used to illustrate the various problems that have to be met in the research. The usefulness of the isotope separation property can be demonstrated in another kind of problem; that of measuring spins of half-lives of less than one hour. Because of the short half-life and large expected value of I for Rb^{81m} ($T_{1/2} = 30$ m), the background in an experiment can be expected to be high. The fast decay of the Rb^{81m} sample can serve to identify it in the resonance. Figure 11 is a typical decay of an $I = \frac{9}{2}$ sample. The fast component is enriched in this sample compared to the control samples. The absolute counting rates are not as useful in this kind of research as the decay rates. It should be of interest to note that this is perhaps the only available method of physically separating an isomeric state. Figure 12 is an example of the resonance of 30 min Cs^{130} . It is experimentally cleaner because of the low spin value. Other difficulties may arise, as in the case of Cs^{127} and Cs^{129} where only one resonance, many times background, was observed, corresponding to $I = \frac{1}{2}$. A careful comparison was made of the decay of the full beam and the resonance sample, and they turned out to be identical, showing

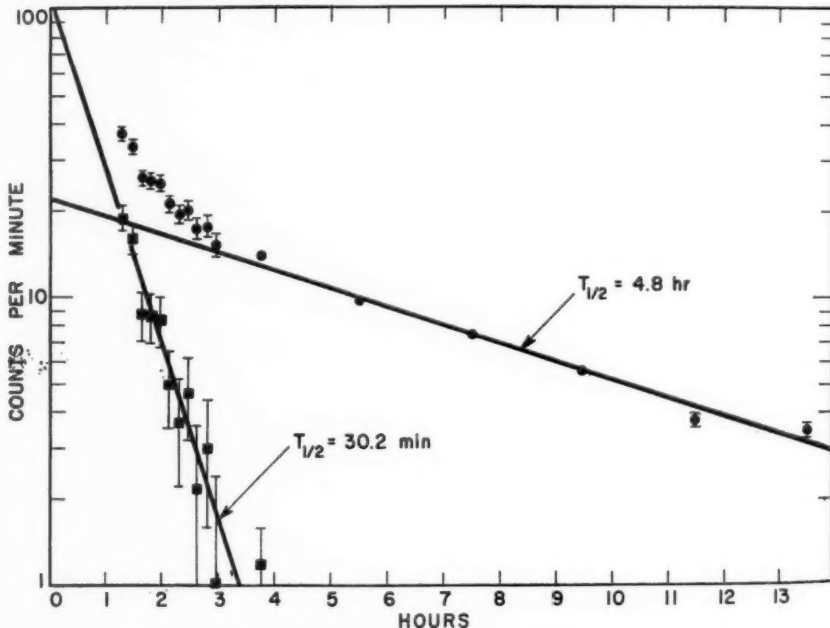


FIG. 11. The decay of an $I = 9/2$ resonance ascribed to Rb^{81m} (30 min.). The identification is primarily on the observed isotope enrichment from the decay curve.

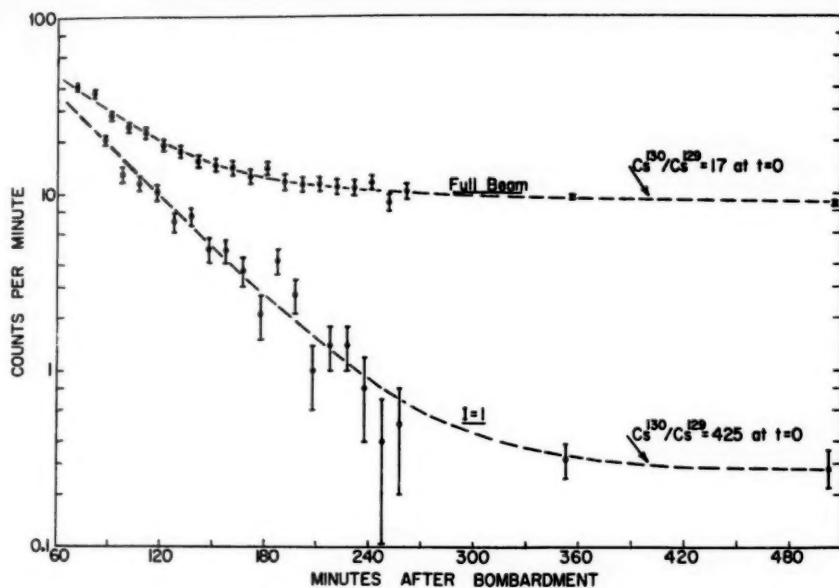


FIG. 12. This is the Cs^{130} (30 min.) resonance decay. This is to be compared to Figure 11. The result is much sharper because of the lower spin value.

no isotope separation. To confirm this, a thin sample of BaI_2 was bombarded to enhance the ratio of Cs^{127} and Cs^{129} with the same results. It was concluded that $I=\frac{1}{2}$. (Increasing the magnetic field to split the resonance was only partially successful. At the highest frequency available, the line was broadened. A differential decay analysis was needed to show a split corresponding to a 4 per cent difference in hyperfine structure.) This technique, employing thin targets or absorbers to alter the isotopic ratio, is particularly useful where background is troublesome. Another method of achieving the same result is the use of (p, n) reactions. The (p, n) reaction (69) on Kr is useful to improve the Rb^{84} to Rb^{83} ratio and incidentally to give an independent check of the Rb^{84} spin. The (p, n) reaction (70) on Xe is used to verify the spins of Cs^{127} and Cs^{129} ($I=\frac{1}{2}$) and also yields the spin of Cs^{132} ($I=2$). The gas bombardment turns out to be the most efficient means of producing the radioisotopes because of the good heat transfer properties and the lack of diluting target nuclei. There is no chemistry. The chamber is washed with a solution of an appropriate carrier salt. In this respect, a variety of processes involving the extraction of radioisotope has been employed. The simplest (71) is the case of Cu^{61} (3.3 hr., $I=\frac{3}{2}$), where the target Co is precut and loaded directly into an oven. This gives a fairly steady beam on heating. This method (72) works for Ag^{105} (40d, $I=\frac{1}{2}$), which is made by (α, kn) on Rh, but the beam is decidedly unstable. For

the Tl isotopes (73), a predistillation process is employed to transfer the Tl from the gold target to the oven. Perhaps the most difficult chemistry has been the extraction of Ga from Cu by an electroplating process. As an example of a technique gone wrong, an attempt to distill I from Sb apparently yielded some antimonyiodine complex, which proved too difficult to handle in a discharge. However, Lipworth (74) has shown that with a conventional iodine generator and a discharge source chamber, an atomic beam of radioiodine can be produced.

After the spin, the hyperfine structure constant is of most interest. The problem is no longer one of looking at discrete frequencies, but rather searchlike in nature and a routine has to be developed that will reduce the search to a minimum in view of the limited amount of isotope and the short half-lives often involved. The procedure is generally to go to a value of the magnetic field, where the Zacharias transition is no longer linear with the field. The larger the deviation from linearity at a given field, the smaller the $\Delta\nu$. To minimize the search required, however, a special procedure is employed. For example, suppose that the isotope has a known spin of $\frac{1}{2}$ and a hyperfine structure that is not less than 1000 Mc./sec. Eq. 29 then indicates that at a resonant frequency of 20 Mc./sec. the departure from the Zeeman line is no more than 1.2 Mc./sec. This region of frequency can be covered in six steps if the line width is 0.2 Mc./sec. One sample will show a counting rate and this will constitute a measurement of $\Delta\nu$ to say 20 per cent, for example, 5000 ± 1000 Mc./sec. This process can be continued by increasing the field in steps that enable the uncertainty in $\Delta\nu$ to be covered by taking five to ten samples. At this rate the $\Delta\nu$ can be obtained to better than 5 per cent with the use of only twenty to thirty experimental points. At the highest convenient field, the remaining sample is used to determine a complete resonance curve. Figure 13 is an example of a typical resonance. The drawn curve is an example of a least squares fit of a resonance curve by a method due to H. B. Silsbee (75) using the I.B.M. 650. The statistical error in the central frequency due to counting is usually much less than the errors due to poor line shape and fluctuations in the beam intensity. A useful algebraic form (76) for $\Delta\nu$, as calculated from the frequency of the "flop-in" transition and the magnetic field, is

$$\Delta\nu = \frac{(\nu + \mu_0 g_I H/h)(-\mu_0 g_J H/h - \nu)}{\nu + \mu_0 g_J H/[h(2I+1)] + 2I\mu_0 g_I H/[h(2I+1)]} . \quad 31.$$

There is an uncertainty in the application of Eq. 31 because the sign of g_J is unknown *a priori*. There is no simple experimental method of determining the sign of a (Eq. 6) (or what is the same, g_J) for $^2S_{1/2}$ states. If $a < 0$, the levels $F=I+\frac{1}{2}$ and $F=I-\frac{1}{2}$ of Figure 2a are inverted. Figure 2a is rotated 180° about a line parallel to the x axis. No system of stops or slits can differentiate these cases unless the apparatus is set at intermediate field values. This is a very uncertain procedure and fraught with certain dangers. In addition, the low field values required decrease the transmission of the apparatus consider-

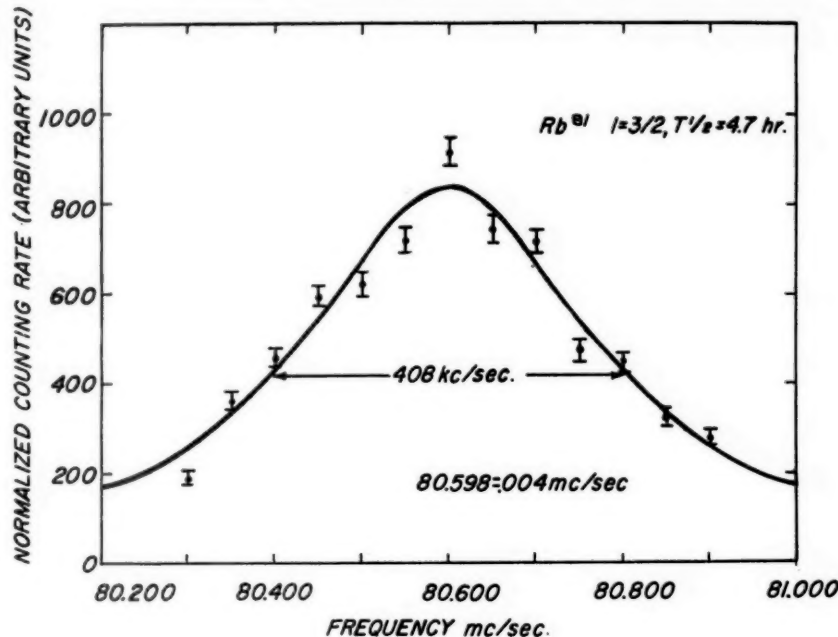


FIG. 13. A typical resonance curve obtained by counting. The observed fit is a least mean square fit. The standard deviation in the center frequency is due to the counting statistics and is less than the error due to the line shape distortion and fluctuating beam intensity. This is the more usual problem in atomic beams and thus the intensity problem can be said to be "solved" for such situations as these.

ably. There is one standard method of determining the sign of g_I . An examination of Eq. 31 for $\Delta\nu$ shows the denominator to be

$$\nu - \frac{|g_I| \mu_0 H}{h(2I+1)} + \frac{2Ig_I\mu_0 H}{h(2I+1)},$$

where ν is the observed resonance frequency. In the limit $H \rightarrow 0$, the difference

$$\nu - \frac{|g_I|}{h(2I+1)} \mu_0 H$$

behaves like H^2 (Eq. 29), and the term $g_I\mu_0 H 2I/h(2I+1)$ has an increasingly greater effect. g_I is approximated sufficiently well by Eq. 13, but if its sign is incorrectly chosen, an incorrect value of $\Delta\nu$ will result which will deviate more and more as $H \rightarrow 0$. As H increases, this term is of decreasing importance, and finally the two values of $\Delta\nu$, $\Delta\nu^+$ and $\Delta\nu^-$, calculated on the basis of either sign of moment, level off to constant, although different, values. Therefore a measurement of $\Delta\nu$ at a very low field (which gives an

intrinsically poor absolute result) combined with a measurement at as high a field as is necessary to give a reasonably accurate value of $\Delta\nu$, is sufficient to determine the sign of a (and therefore g_I). The success of this method depends on the absolute value of $\Delta\nu$, g_I , and the line width. For example, if the line width is ~ 0.2 Mc./sec., a lower limit to the $\Delta\nu$ is about 2000 Mc./sec. Figure 14 is a plot of the results of such calculations for Rb⁸¹. $\Delta\nu$ is 5100 Mc./sec., as shown by the constant value of $\Delta\nu^+$ versus field. The $\Delta\nu^-$

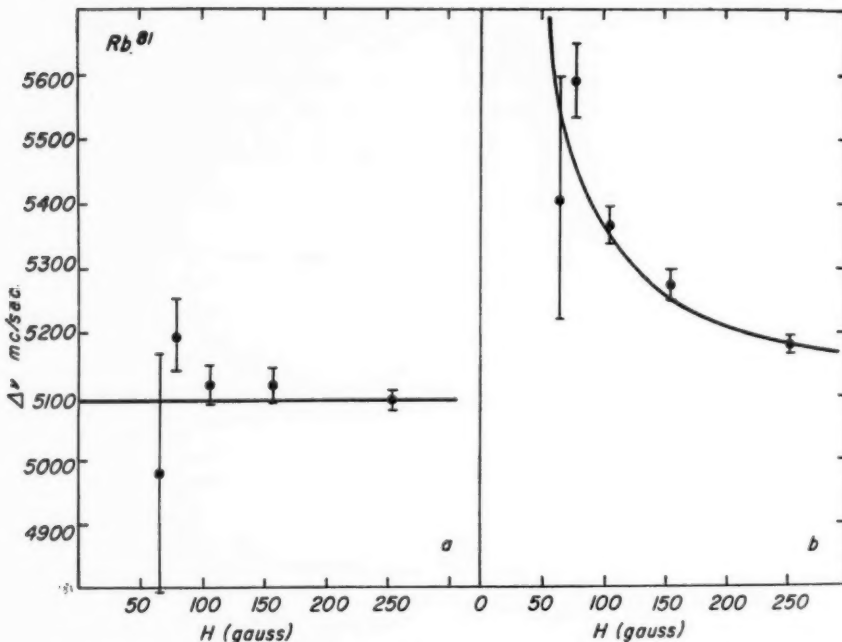


FIG. 14. Each observed resonance yields a value of the hyperfine interval, $\Delta\nu$. If $\Delta\nu$ of Rb⁸¹ is computed on the assumption that $g_I > 0$, and then plotted versus the H at which the measurement is made, the curve of Figure 14a results. If g_I is assumed negative, the curve of Figure 14b results. Clearly the g_I of Rb⁸¹ is positive.

varies well outside of experimental limits, and the drawn curve is the predicted variation for the wrong sign of g_I . If a more accurate value of $\Delta\nu$ is desired, a direct transition $\Delta F = \pm 1$ is now possible, because the determination has been reduced in error to the point where a search procedure can be minimized. However, unless a hyperfine anomaly measurement is desired, the present state of nuclear theory does not warrant precisions better than one per cent in the measurement of nuclear g -factors, except for the very lightest nuclei.

Table III is included as a summary of all spins and magnetic moments as derived from hyperfine ratios obtained by the method of atomic beams.

TABLE III
ATOMS INVESTIGATED BY THE TECHNIQUES OF ATOMIC
AND MOLECULAR BEAMS

The following table is intended to illustrate the variety of elements which have been investigated in atomic and molecular beam apparatus. The values of the nuclear magnetic moments and quadrupole moments are taken, for the most part, from the tables of Walchli (143) and Ramsey (144) and are rounded to three significant figures. The error in the last significant figure is given in parentheses. While some of the nuclear spins were originally measured by other means and very precise values of the magnetic moment result from other techniques, only representative references to atomic and molecular beam experiments are given. For information concerning the original measurements of nuclear spins and the more precise moment values obtained by other experimental methods, see Ramsey (144, 145) and Walchli (143, 146).

Half life	Z	A	<i>I</i> (units of \hbar)	μ n.m.	$Q(10^{-24}$ cm. ²)	References
13 min.	0 n	1	1/2	-1.91		(147 to 172)
stable	1 e	0	1/2	-1 bohr magneton		
stable	1 H	1	1/2	+2.79		
stable	1 H	2	1	+.857	+.0027	(159, 160, 161, 163, 164, 165, 169 to 179)
12.3 years	1 H	3	1/2	+2.98		(180, 181)
stable	2 He	3	1/2	-2.13		(182, 183, 184, 185)
stable	2 He	4	[0]	~0		(186, 187, 188)
stable	3 Li	6	1	+.822	+.023(2)	(189 to 199)
					XQ of Li ⁷	
stable	3 Li	7	3/2	+3.26		(163, 189, 193 to 202)
stable	4 Be	9	3/2	-1.18		(203)
stable	5 B	10	3	+1.80	+.074	(204)
stable	5 B	11	3/2	+2.69	+.036	(204, 205)
stable	6 C	13	1/2	+.702		(206, 207)
stable	7 N	14	1	+.404	+.02	(208)
stable	7 N	15	1/2	-.283		(209)
stable	9 F	19	1/2	+2.63		(160, 162, 193, 194, 195)
stable	10 Ne	20	[0]	$\leq 2 \times 10^{-4}$		(186, 210)
stable	10 Ne	22	[0]	$\leq .05$		(186)
2.6 years	11 Na	22	3	+1.75		(211, 212)
stable	11 Na	23	3/2	+2.22	+.10(1)	(162, 189, 198, 208, 213 to 218)
15.0 hr.	11 Na	24	4	+1.69(1)		(219, 244)
stable	13 Al	27	5/2	+3.64	+.149	(221 to 224)
stable	17 Cl	35	3/2	+.822	-.078	(225 to 233)
stable	17 Cl	37	3/2	+.684	-.062	(225 to 229, 231, 232, 234)
stable	18 A	40	[0]	$\leq .05$		(186)

TABLE III—*continued*

Half life	Z	A	I (units of \hbar)	μ n.m.	$Q(10^{-24}$ cm. ²)	References
stable	19 K	39	3/2	+.391	+.07(2)	(189, 196, 198, 208, 235 to 239, 329)
10 ⁶ years	19 K	40	4	-1.30		(211, 240, 241, 242)
stable	19 K	41	3/2	+.215	+1.22 $\times Q$ of K ³⁹	(189, 192, 196, 236, 237, 238, 243)
12.5 hr.	19 K	42	2	-1.14(1)		(244)
stable	24 Cr	52	[0]			(245)
stable	25 Mn	55	5/2	+3.47		(246)
3.3 hr.	29 Cu	61	3/2			(247)
stable	29 Cu	63	3/2	+2.23	-.16(1)	(248)
12.8 hr.	29 Cu	64	1	$\pm .216(3)$		(249, 250)
stable	29 Cu	65	3/2	+2.38	-.15(1)	(248)
9.8 hr.	31 Ga	66	[0]	$\leq 10^{-3}$		(251, 320)
78 hr.	31 Ga	67	3/2	+1.84(2)	+23(1)	(251)
68 min.	31 Ga	68	1			(321)
stable	31 Ga	69	3/2	+2.02	+.19	(252 to 257)
stable	31 Ga	71	3/2	+2.56	+.15	(252 to 257)
14 hr.	31 Ga	72	3			(322)
27 hr.	33 As	76	2			(323)
stable	35 Br	79	3/2	+2.11	+.33(2)	(258, 259, 260)
stable	35 Br	81	3/2	+2.27	+.28(2)	(258 to 260)
stable	36 Kr	83	9/2	-.969	+.15	(261)
4.7 hr.	37 Rb	81	3/2	+2.05(2)		(262 to 267)
31.5 min.	37 Rb	81 ^m	9/2			(268, 269)
6.3 hr.	37 Rb	82	5	+1.50(2)		(264, 266, 267)
83 days	37 Rb	83	5/2	+1.42(2)		(264, 266, 267)
33 days	37 Rb	84	2	-1.32(2)		(264, 266, 267)
stable	37 Rb	85	5/2	+1.35	+.31	(198, 201, 215, 225, 226, 270 to 274)
18.6 days	37 Rb	86	2	-1.69(1)		(220, 244, 275)
10 ¹⁰ years	37 Rb	87	3/2	+2.75	+.15	(198, 201, 215, 225, 226, 270 to 274, 276)
40 days	47 Ag	105	1/2			(277)
8.3 d.	47 Ag	106	6			(324)
stable	47 Ag	107	1/2	-.114		(278)
stable	47 Ag	109	1/2	-.131		(278)
253 d.	47 Ag	110 ^m	6			(324)
7.5 days	47 Ag	111	1/2	-.146(2)		(150, 249, 250, 279, 280)
stable	49 In	113	9/2	+5.52	+.82	(150, 281 to 283, 331, 332)
1.73 hr.	49 In	113 ^m	1/2	$\pm .217(2)$		(284)
49 days	49 In	114 ^m	5	+4.7		(285)
10 ¹⁶ years	49 In	115	9/2	+5.53	+.83	(150, 282, 283, 286 to 289, 331, 332)

TABLE III—*continued*

Half life	<i>Z</i>	<i>A</i>	<i>I</i> (units of \hbar)	μ n.m.	$Q(10^{-24}$ $\text{cm.}^2)$	References
54 min.	49 In	116 ^m	5	+4.4		(290)
13 hr.	53 I	123	5/2			(325)
stable	53 I	127	5/2	+2.81	-.59(20)	(291)
6.2 hr.	55 Cs	127	1/2	+1.41(4)		(292, 293)
8 d.	53 I	131	7/2			(325)
31 hr.	55 Cs	129	1/2	+1.47(4)		(292, 293)
30 min.	55 Cs	130	1	$\pm 1.5(3)$		(292, 294)
9.7 days	55 Cs	131	5/2	+3.48(4)		(244, 295)
7.1 days	55 Cs	132	2	+2.22(2)		(294, 295)
stable	55 Cs	133	7/2	+2.58	-.003(2)	(198, 201, 208, 215, 270, 276, 296, 297, 298, 327)
2.3 years	55 Cs	134	4	+2.95(1)		(244, 299, 300)
3.1 hr.	55 Cs	134 ^m	8	+1.10(1)		(301 to 305)
10 ⁶ years	55 Cs	135	7/2	+2.74		(212, 300, 306)
30 years	55 Cs	137	7/2	+2.85		(212, 300, 306, 307)
stable	56 Ba	135	3/2	+.836(3)		(207, 308)
stable	56 Ba	137	3/2	+.932(3)		(207, 308)
stable	59 Pr	141	5/2	+3.8(3)	-.054	(309, 310)
stable	57 La	139	7/2	+2.78		(311)
40 hr.	79 Au	194	1	$\pm .07(1)$		(326, 330)
stable	79 Au	197	3/2	+.14(2)		(278)
2.7 days	79 Au	198	2	$\pm .50(4)$		(312)
3.2 days	79 Au	199	3/2	$\pm .24(2)$		(312)
2.8 hr.	81 Tl	197	1/2			(313)
5 hr.	81 Tl	198 ^m	7			(313, 314)
7.4 hr.	81 Tl	199	1/2			(313, 314)
stable	81 Tl	203	1/2	+1.61		(257, 315, 316)
4.1 years	81 Tl	204	2	$\pm .089(3)$		(275, 313, 314, 317)
stable	81 Tl	205	1/2	+1.63		(257, 315, 316)
10 ¹⁷ years	83 Bi	209	9/2	+4.08		(318)
10 ⁶ years	83 Bi	210	1			(319)
10 ⁴ yr.	94 Pu	239	1/2			(328)

PARAMAGNETIC RESONANCE ABSORPTION

The relatively recent application of paramagnetic resonance absorption in crystals to nuclear problems and its success in the measurement of the spins and the static moments of nuclei require discussion in some detail at this writing. The subject is very well represented in the literature (77) due to its importance in the analysis of crystalline interatomic fields, its applications to low temperature research (78), and its possibilities in microwave amplifier development (masers). As a result, the literature is very complete with the detailed discussion of the crystalline fields, and it is the aim of this

article to condense the discussion of the method to its application to nuclear moment measurements.

In the atomic beam problem, the atomic electrons (valence electrons usually) are thought of as supplying the magnetic field and derivatives of the electric field that interact with the nuclear moments. The applied magnetic field removes degeneracy in total angular momentum in such a way as to yield a typical Breit-Rabi diagram (Figs. 2a, b, c). The remaining degeneracy is $2J+1$, where J is the largest value of the quantized projection of the angular momentum of the atom along an arbitrary direction. The direction is arbitrary (with vanishing external fields because of the rotational invariance of the system). The quantum number J is usually well known from spectroscopic and chemical evidence, and where there is doubt, the number of possibilities is very small. Similarly, a very close estimate of g_J can be made by use of Russell-Saunders coupling and the Landé g -factor in most cases. (Bi is an interesting exception.) If the same atom (ion) is in a crystal, however, the description is more complicated for several reasons. The first is that there exists a strong anisotropic electric field at the position of the ion. This field varies widely, so a uniform description of the state of the ion for all cases is not possible. Normally, the field-free ion will have both $\mathbf{L} = \sum_i \mathbf{l}_i$ and $\mathbf{S} = \sum_i \mathbf{s}_i$ as constants of the motion. This is customarily known as Russell-Saunders coupling, and the energy differences associated with different L -values and different S -values owe their origins to the electrostatic forces between the electrons and to the Pauli principle. The remaining degeneracy is removed by the magnetic spin-orbit forces giving rise to differences in energy between states of different J . These latter differences in energy are generally much smaller than the former. If the interaction of the internal electric field is weak compared to these energy differences, the low lying energy levels of the ion are similar to those of the free ion. Clearly two other cases are possible: one where the crystalline field interaction is enough to break the $\mathbf{L} \cdot \mathbf{S}$ interaction and remove J as a constant of the motion, but not affect either \mathbf{L} or \mathbf{S} ; and the other is where the interaction is enough to decouple the valence electrons from one another and then neither \mathbf{L} nor \mathbf{S} or J are constants of the motion.

All of these cases (including intermediate situations) exist in practice, and the complete description of the low lying ionic levels and their multiplicities is clearly a very difficult, albeit very interesting, problem. For the purposes of measuring nuclear properties, however, certain physical points have been made clear by Abragam & Pryce (79), following the physical principles described above, that are quite general for all ions in crystal fields. The first is that no matter what the crystal, there is a low lying level which is separated from its nearest upper neighbor by an amount no less than a typical fine structure term difference for the free ion ($100 \text{ cm.}^{-1} - 20,000 \text{ cm.}^{-1}$). Therefore, at ordinary temperatures (certainly at 4°K. , where many experiments are performed) only the lowest level is appreciably populated. Secondly, there will be a degeneracy $2S'+1$ associated with the ground state, which

can be removed by the application of an external magnetic field, due to the crystal symmetries. The symbol S' is primed to denote that, in general, it has only an indirect relation to any spin or orbital angular momentum of the free ion. In the presence of the external magnetic field the magnetic energy of this state can be represented (for illustration) by

$$W = -g_s \mu_0 H M, \quad M = S', S' - 1, \dots - S'_i.$$

This is an oversimplification of a tensorial interaction which will be discussed more fully later. The purpose now is to assign some orders of magnitude to the results. The constant g_s , which would be the Landé g -factor for the free ion, can, in a crystal, range over values $g_s \sim 0$ to $g_s \sim 7$, compared to the "spin only" value of 2 for an ion with $L=0$. The wide variation in g_s stems from the special mixture of wave functions required to satisfy the symmetry demands of the crystalline field. The source of these large g -factors is not obvious, nor is it helpful to say that it arises from the "quenching" of the orbital angular momentum, since it is difficult to imagine a mechanism that will quench the orbital angular momentum and not its magnetic moment. It must be true that, in those cases where $g_s \gg 2$, the connection between S' and the total angular momentum is very remote.

A more reasonable physical picture can be employed that can lead to a heuristic derivation of the Abragam-Pryce Hamiltonian. In the argument leading to the formulation of the Breit-Rabi Hamiltonian (Eq. 28), the fact that the matrix elements (diagonal in J) of any vector must be proportional to J itself led to the relation that $\mathbf{y} = c_J J$ for those matrix elements. This relation stemmed from the rotational invariance of the free atom as a whole (in the absence of nuclear moments). In the present case, this invariance does not exist and the most general connection between corresponding matrix elements is

$$\mu_i = \mu_0 \sum_{j=1}^3 g_{ij} S'_j, \quad g_{ij} = g_{ji}, \quad 32a.$$

where now μ_i and S'_j are the Cartesian components of the vectors \mathbf{y} and \mathbf{S}' respectively, and the g -factor has become a tensor. It is this equation that gives meaning to the vector \mathbf{S}' . The \mathbf{y} operator is known to exist for the ion in the crystal, but its matrix elements must be in some tensorial relation to the crystal. Furthermore the degeneracy of the ionic level must be taken into account, since for a nondegenerate level, the expectation values of \mathbf{y} will vanish. Higher order magnetic interactions could be considered in principle that require correspondingly larger values of S' and are always too small to be observed. The interaction Hamiltonian of the magnetic moment with an external field is, therefore,

$$\mathcal{H}_1 = - \sum_i \mu_i H_i = - \mu_0 \sum_{i,j} g_{ij} H_i S'_j. \quad 32b.$$

Similarly, if there is a magnetic field due to the electronic motion at the position of the nucleus, this field is

$$(H_0)_i = \sum_j C_{ij} S_j', \quad C_{ij} = C_{ji}, \quad 33.$$

and the interaction of nuclear magnetic moment with this field gives

$$\mathcal{H}_2 = - \sum_{i,j} g_i \mu_0 C_{ij} I_i S_j' = \sum_{i,j} A_{ij} I_i S_j', \quad 34.$$

where now the A_{ij} are proportional to g_i of the nucleus and I_i are the Cartesian components of the nuclear spin. This is the generalization of the cosine interaction of the atomic case. That the quadratic forms of Eqs. 32b and 34 can be diagonalized by choosing appropriate coordinates is well known. Since the symmetry of these forms must derive from the crystal itself, it is reasonable to assume that the same choice of space coordinates will diagonalize both simultaneously. The combined Hamiltonian then reads

$$\mathcal{H} = - \mu_0 \sum_i g_i H_i S_i' + \sum_i A_i I_i S_i'. \quad 35.$$

By extending this argument to the other possible interacting terms, the full Abragam-Pryce Hamiltonian is obtained,

$$\begin{aligned} \mathcal{H} = & - \mu_0 \sum_i g_i H_i S_i' + \sum_i A_i I_i S_i' + D[S_z'^2 - \frac{1}{2}S'(S'+1)] + E(S_x'^2 - S_y'^2) \\ & + P[I_z^2 - \frac{1}{2}I(I+1)] + P'[I_x^2 - I_y^2] - g_i \mu_0 \mathbf{I} \cdot \mathbf{H}. \end{aligned} \quad 36.$$

The third and fourth terms contain the remaining effects of the crystalline electric field that have been ignored until now. This is the Stark splitting of the \mathbf{S}' states that can remove some (though not all) of the degeneracy. This is second order in \mathbf{S}' , since it is well known that the first order Stark effect vanishes. The parameters D and E vary widely up to values of the order of 1 cm^{-1} . The fifth and sixth terms are nuclear in origin and represent the interaction of the nuclear electric quadrupole moment with the gradient of the electric field at its position. This gradient is of the order of e^2/a^3 , where a is the distance of an effective point charge from the nucleus in question. A simple calculation shows that contributions from neighboring atoms in the lattice are small compared to those from the valence electrons. In the free ion case, the orientation of \mathbf{J} , as well as \mathbf{I} will affect the value of this term. However, in the crystalline fields, the change in value of S_z' is generally not accompanied by a change in charge distribution, and therefore will not affect this term. This last remark seems very extreme and the overall picture would indicate that the wave functions are "locked-in" by the crystalline field with respect to the charge distribution, but not the current distribution, and therefore the effect of local and applied magnetic fields will involve the degeneracy vector \mathbf{S}' , but the local electric fields will not. This seems somewhat unsatisfactory in view of the desirability of having a completely general Hamiltonian to fit the experimental data and it would seem that terms of the following general form should be included:

$$P''[S_z'^2 - \frac{1}{2}S'(S'+1)][I_z^2 - \frac{1}{2}I(I+1)],$$

in analogy with the atomic case (Eq. 27) (off-diagonal terms should be included as well). In the limit of very strong crystalline fields this term would

undoubtedly be negligible compared to that involving P . However, for intermediate or weak fields where the behavior tends to that of a free ion, the existence of terms like P'' should be anticipated. In actual practice, few nuclear quadrupole terms have been observed, and, due to the relative smallness of these terms *in toto*, it is difficult to assess the desirability of including this term. The last term is the one that contains the direct nuclear interaction with the external field. This term is generally too small to be directly observed in paramagnetic absorption measurements in crystals. If it could be observed, even crudely, the sign of the nuclear magnetic moment could be determined. It will be neglected in the following discussion.

The experimental procedure involves the determination of the energy level differences by paramagnetic absorption. The observed frequencies are used to determine S' , I , g_x , g_y , g_z , A_x , A_y , A_z , D , E , P , and P' . This can be done, in general, by using different magnetic fields and by reorienting the crystal with respect to the applied magnetic field. The constants A_x , A_y , A_z give a good value of g_I if the resonance can be compared to one for a previously known isotope. If not, it can be estimated by a suitable choice of valence electron wave functions and a computation of $(1/r^3)$ and known angular factors. This last method gives crude estimates of g_I . The determination of the energy levels of the general Hamiltonian is a rather complicated procedure, but fortunately there is a strong simplifying possibility. The crystal can be oriented so that the magnetic field is parallel to either the x , y , or z axis. Furthermore, there is often an axial symmetry in the crystal for one of these axes and then the terms involving E and P' vanish. If $I = \frac{1}{2}$, the P term will vanish as for the field free atom; if $S' = \frac{1}{2}$, the D term vanishes.

The general method of paramagnetic resonance absorption in crystals was brought to its present state of effectiveness by Bleaney (80) and his co-workers in a long series of papers. They treated the rare earth and iron elements fairly systematically and some of the uranic and transuranic elements as well. At the present time the static moments of approximately 45 isotopes have been measured and Table IV at the end of this section lists those moments that have been measured. For the sake of illustration, Co⁵⁶ and Co⁶⁰ (both radioactive nuclei with $T_{1/2} = 72$ d and 5.2 y respectively) will be discussed in some detail (81, 82). Figure 15 is a block diagram of a typical experimental setup. The sample, in the form of some suitable single crystal salt is in a microwave cavity. The absorption is measured at a fixed frequency, while sweeping the magnetic field through the absorption region. Almost all experiments to date have been done at X band frequencies (10 kMc./sec.) or at K band frequencies (25 kMc./sec.). The appropriate magnetic fields vary between 1000 and 12,000 gauss, depending on the g-factor of S' and the crystal orientation. Most experiments have been performed under conditions where the hyperfine structure has been completely decoupled. This is because the signal-to-noise ratio in this type of experiment improves as the square of the frequency, so the highest frequency conveniently available must be used within the detector's noise limitations. The

TABLE IV

NUCLEAR SPINS AND MOMENTS OBTAINED BY PARAMAGNETIC RESONANCE

This table contains the results of moment measurements by paramagnetic resonance in crystals. The magnetic moments are in nuclear magnetons. The quadrupole moment Q is in 10^{-24} cm.². Since the absolute magnetic and quadrupole moments are not as well known as their ratios when these are measured, the ratios are also included in the form A_x/A_y , or P_x/P_y where A_y and P_y will be those of a stable isotope. The signs of the moments do not appear in this table because they are not measured.

Element	$T_{1/2}$	I	μ (n.m.)	Q	Ratio	Reference
$^{15}\text{P}^{31}$	—	1/2				(129)
$^{15}\text{P}^{32}$	14 days	1	-0.252		A^{32}/A^{31} = .1118	(333)
$^{23}\text{V}^{49}$	300 days	7/2	4.46		A^{49}/A^{51} = 0.87 ± 0.01	(142)
V^{50}	—	6	3.35		A^{50}/A^{51} = 0.38	(98) (138)
V^{51}	—	7/2	5.14*			(104, 139, 141)
$^{24}\text{Cr}^{53}$	—	3/2	0.5 ± 0.1			(105, 123)
$^{25}\text{Mn}^{55}$	$\sim 10^6$ years	7/2	5.05		A^{55}/A^{55} = 1.04	(125)
Mn^{55}	—	5/2	3.46*			(106, 141)
$^{27}\text{Co}^{56}$	72 days	4	3.86		$A^{59}/A^{56} = 1.38$	(99, 135)
Co^{57}	270 days	7/2	4.65		A^{57}/A^{59} = 1.00 ± 0.01	(100, 101, 136)
Co^{58}	72 days	2	4.05		$A^{58}/A^{59} = 1.53$	(126)
Co^{59}	—	7/2	4.64*			(107, 144)
Co^{60}	5.3 years	5	3.80		$A^{60}/A^{59} = 0.57$	(127)
$^{29}\text{Cu}^{63}$	—	3/2	†	-0.16	P^{63}/P^{65} = 1.08 ± 0.02	(108, 109, 110)
Cu^{65}	—	3/2	†	-0.15	$A^{65}/A^{63} = 1.07$	(108, 109, 110)
$^{33}\text{As}^{75}$	—	3/2	1.43			(129)
$^{33}\text{As}^{76}$	27 hours	2	-0.906		A^{76}/A^{75} = .474	(334)
$^{42}\text{Mo}^{95}$	—	5/2				(131)
Mo^{97}	—	5/2				(131)
$^{44}\text{Ru}^{99}$	—	5/2				(132)
Ru^{101}	—	5/2			A^{101}/A^{99} = 1.09 ± 0.03	(132)

* Value of μ measured by nuclear induction; diamagnetic correction is included. Value of μ for radio-isotope is usually obtained by taking the measured value of hfs ratio (neglecting the hfs anomaly) and the nuclear induction value of μ for the stable isotopes.

† The moments of Cu^{63} and Cu^{65} are known most accurately from measurements of nuclear resonance.

TABLE IV—continued

Element	$T_{1/2}$	I	μ (n.m.)	Q	Ratio	Reference
$_{51}\text{Sb}^{121}$	—	5/2	3.36		(130)	
Sb^{123}	—	7/2	2.55		(130)	
$_{58}\text{Ce}^{141}$	33 days	7/2	0.89 ± 0.09		(97)	
$_{59}\text{Pr}^{141}$	—	5/2	3.9 ± 0.2		(111, 112)	
$_{60}\text{Nd}^{143}$	—	7/2	1.03	<1	A^{143}/A^{145} = 1.61	(113, 114, 115)
Nd^{145}	—	7/2	0.64	<1		(113, 114, 115)
Nd^{147}	11 days	5/2	0.56 ± 0.06		$B^{147}/B^{149} = 0.76$	(97)
$_{62}\text{Sm}^{147}$	—	7/2	0.83	<0.7	A^{147}/A^{149} = 1.22 ± 0.01	(115, 122)
Sm^{149}	—	7/2	0.68	<0.7		(115, 122)
$_{63}\text{Eu}^{151}$	—	5/2	3.6		A^{151}/A^{149} = 2.23 ± 0.04	(116)
$_{63}\text{Eu}^{152}$	13 years	3	2.0		A^{152}/A^{151} = .465	(335)
Eu^{153}	—	5/2	1.6			(116)
Eu^{154}	16 years	3	2.1		A^{154}/A^{153} = 1.09	(137)
$_{64}\text{Gd}^{155}$	—	3/2	0.24		A^{155}/A^{157} = 0.75 ± 0.07	(140)
Gd^{157}	—	3/2	0.32			(140)
$_{65}\text{Tb}^{159}$	—	3/2	1.5 ± 0.4			(102)
$_{66}\text{Dy}^{161}$	—	5/2	0.38 ± 0.05			(124)
Dy^{163}	—	5/2	0.53 ± 0.05		A^{163}/A^{161} = 1.41 ± 0.02	(124)
$_{67}\text{Ho}^{165}$	—	7/2	3.29 ± 0.17			(103)
$_{68}\text{Er}^{167}$	—	7/2	0.48	9.4		(115, 117)
$_{70}\text{Yb}^{171}$	—	1/2	0.43 ± 0.05			(124)
Yb^{173}	—	5/2	0.60 ± 0.05		A^{173}/A^{171} = 0.28	(124)
$_{75}\text{Re}^{186}$	—	5/2				(131)
Re^{187}	—	5/2				(131)
$_{77}\text{Ir}^{191}$	—	3/2				(131)
Ir^{193}	—	3/2				(131)
$_{92}\text{U}^{233}$	$\sim 1.6 \times 10^6$ years	5/2	0.51	3.4	P^{235}/P^{233} = 0.56 ± 0.1	(128)
U^{235}	$\sim 7 \times 10^8$ years	7/2	0.34	4.0	A^{235}/A^{233} = 0.47	(118, 133)
$_{93}\text{Np}^{237}$	$\sim 2 \times 10^6$ years	5/2	6.0 ± 2.5			(119)
$_{93}\text{Np}^{239}$	2.3 days	1/2	0.3		A^{239}/A^{237} = 0.304	(336)
$_{94}\text{Pu}^{239}$	$\sim 2.4 \times 10^4$ years	1/2	0.4 ± 0.2			(120, 134)
Pu^{241}	~ 14 years	5/2	1.5 ± 0.6		A^{241}/A^{239} = 0.71	(120, 121)

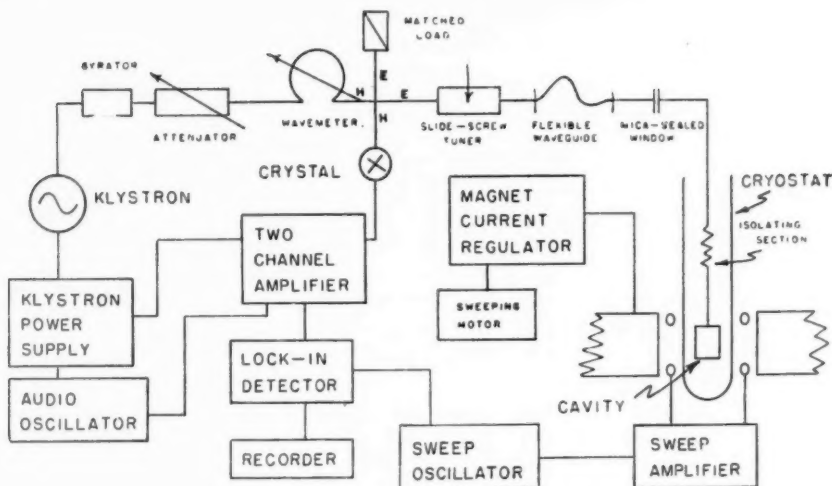


FIG. 15. A block diagram of a typical paramagnetic resonance setup.

noise is also a function of the sweep rate. In experiments on Co^{60} an 80c./sec. chopping rate was initially used to observe the spectrum on approximately 10^{15} atoms of Co^{60} . Since that time, experiments (83) using lock-in amplifiers at a 100 kc./sec. chopping rate have been used and this seems to improve the signal-to-noise ratio by about a factor of 20. In other words, this would seem to indicate that a sample of 10^{13} atoms is quite feasible. This compares very favorably with the atomic beam method. There are difficulties, however, in treating radioisotopes of half-lives less than several days. The first is the time lost in growing the crystal. The second is loss of crystal structure due to the radiation damage. These combined difficulties will undoubtedly prevent the method from becoming useful for the very short-lived isotopes. In the cobalt experiments, a magnetically dilute Tutton salt was used: $\text{Co}(\text{NH}_4)_2(\text{SO}_4)_2 \cdot 6\text{D}_2\text{O}$. The ground state of the Co ion is a Kramers doublet with $S' = \frac{1}{2}$. For this special value of S' the Hamiltonian is

$$\mathcal{H} = -\mu_0 [g_{\parallel} H_x S_z' + g_{\perp} (H_x S_x' + H_y S_y')] + A I_x S_z' + B [I_x S_x' + I_y S_y']. \quad 37.$$

The crystal has axial symmetry in the sense that the x direction is equivalent to the y direction. For that reason, $A_y = A_x = B$, $A_z = A$, $g_z = g_{\parallel}$, $g_x = g_y = g_{\perp}$, and the P' term vanishes. Since $S' = \frac{1}{2}$, all quadratic terms in S' vanish. The P term is present in principle but is not included, because its occurrence for Co in this crystal was not observed for the stable isotopes at the resolution available. Presumably the Q , or the field gradient, or both, are too small. There is a large anisotropy ($g_{\perp} \ll g_{\parallel}$) and $A \neq B$, but, for the purpose of measuring the nuclear spin and nuclear moment, it is simplest to line up the crystal so that \mathbf{H} is parallel to \mathbf{z} . The Hamiltonian is quite simple for this case, yielding

$$\mathfrak{H} = -\mu_0 g_{||} H_z S_z' + A I_z S_z' + B (I_x S_x' + I_y S_y'). \quad 38.$$

This is especially simple because it can be diagonalized explicitly as for the corresponding Breit-Rabi case. This is generally true if the crystal is axially symmetric, for then the Hamiltonian is rotationally invariant about the z -axis. This means that m , the quantum number of $I_z + S_z'$, is a good quantum number, even though F (corresponding to $\mathbf{F} = \mathbf{I} + \mathbf{S}'$) never is, even for $H=0$. There is little value in diagonalizing, however, because the experiments are always performed in the Paschen-Back region for the reasons explained above. If the decoupling is not complete, a second order perturbation correction could and usually is applied. The energy levels of Eq. 38 are, to first order:

$$W_{m_I m_{S'}} = -g_{||}\mu_0 H m_{S'} + A m_I A m_{S'} + O(H^2),$$

where $H = H_z$. The transitions are observed only between states corresponding to $\Delta m_{S'} = \pm 1$, because these are the only states which have appreciable

PARAMAGNETIC RESONANCE hfs OF Co⁶⁴



FIG. 16. The observed trace of the Co⁶⁴ paramagnetic resonance derivative absorption ($I=4$) with the inevitable Co⁵⁹ ($I=7/2$) absorption. The Co⁶⁴ resonances are numbered with primes.

population differences at liquid He temperatures, and because these are the high frequency transitions which are favored by the v^2 law. Within this restriction, $\Delta m_{S'} = \pm 1$, the selection rules for first order observable transitions are $\Delta m_I = 0$. The transitions corresponding to $\Delta m_I = \pm 1$ in the completely decoupled region require $\sim(2000)^2$ more perturbing field for the transitions. This possibility can be neglected. It is possible to observe some of these transitions because of the slight state mixing that takes place due to residual coupling. This point is of no importance here, but it will be referred to later in the discussion on nuclear polarization by paramagnetic resonance. The allowed transitions, $\Delta m_{S'} = \pm 1$, $\Delta m_I = 0$, therefore give rise to $2I+1$ equally spaced lines of equal intensity, corresponding to $g_{||}\mu_0 H + IA$, $g_{||}\mu_0 H + (I-1)A$, ..., $g_{||}\mu_0 H - IA$. The number of lines observed yields the spin, and the total interval yields a quantity proportional to the nuclear moment. Figure 16 is an excellent example of such an observation taken from Jones, Dobrowolski, & Jeffries (82). The applied H is parallel to the crystalline electric field. There are two sets of absorption lines, those due to the previously known Co⁵⁹ and those due to the radioactive Co⁶⁴. The Co⁵⁹ shows eight lines, consistent with a spin of $7/2$, the Co⁶⁴ shows nine lines consistent with a spin of four. This is an unusually good example, in that the carrier

isotope signal is about the same as that of the radioisotope. It happens more frequently that the carrier dominates the sample, in which case the overlap of lines makes the spin assignment somewhat more difficult. The line splitting, itself, must be proportional to g_I , which is just μ_I/I . Since there are $2I$ intervals, the overall width of the spectrum is proportional to $2\mu_I$. Therefore the ratio of the spectral extents of the Co^{60} to the Co^{64} is the ratio of the respective μ_I . Since Co^{64} is known from nuclear resonance experiments, the determination of the g-factor for Co^{60} is simple. In principle, the sign of the moment can be determined in a manner similar to that for the $J = \frac{1}{2}$ state of atomic beams. However, the resolution and the approximate nature of the Hamiltonian contrive to make this procedure impractical.

An interesting variation on this method has been recently proposed by Jeffries (85). The purpose of the method is to employ paramagnetic resonance to induce a nuclear polarization and then observe this nuclear polarization by the asymmetry of the nuclear radiation which is induced. Aside from its intrinsic interest, the method allows a separation of the radioactive isotope signal from the carrier in those cases where the carrier spectrum is dominant. Very little has been said here about the general relaxation process which takes place in these resonance experiments. In the atomic beam case, it is virtually nonexistent. The transitions are observed by the physical separation of the magnetic substates in the apparatus. In solid state resonance, there is a relaxation process that supplies the Boltzmann differential population in the first instance. This relaxation process competes with the rf applied power. That is, at a resonance, enough rf power can be fed in to make the difference in population between two levels vanish despite the relaxation process which tends toward a differential population. Figure 17 is the level diagram for a nuclear spin of one and an axial symmetric crystal for which $S' = \frac{1}{2}$. These are the lowest values of both parameters for which a nuclear anisotropic effect can be obtained and are chosen for simplicity in discussion. The overall selection rules are $\Delta m_{S'} = \pm 1, 0$, $\Delta m_I = \pm 1, 0$, and $\Delta(m_{S'} + m_I) = \pm 1, 0$. The transitions $\Delta m_{S'} = 0$ are never observed in resonance, although they will contribute some depolarizing effects in relaxation processes. In the diagram, the transitions $\Delta m_{S'} = \pm 1, \Delta m_I = 0$ are shown as solid lines. The transitions $\Delta m_{S'} = \pm 1, \Delta m_I = \mp 1$ are shown as dashed lines, and are first forbidden in the sense that the matrix elements squared for these transitions go as $|A/\mu_0 g \| H|^2$, compared to the direct transitions. This matrix element is a measure of the mixing of the pure Paschen-Back states due to incomplete decoupling by the applied magnetic field. There are still higher order transitions which will be ignored. The relaxation processes are strong for the allowed transitions and weak for the forbidden transitions for the same reasons as for the rf-induced transitions; i.e., they are caused by interactions with the fluctuating crystalline magnetic fields.

In the absence of the applied rf field, the $m_{S'} = \frac{1}{2}$ and the $m_{S'} = -\frac{1}{2}$ levels will differ in population in the ratio $\exp(-g\| \mu_0 H / kT)$ the small differences between the different m_I states being neglected). If a first for-

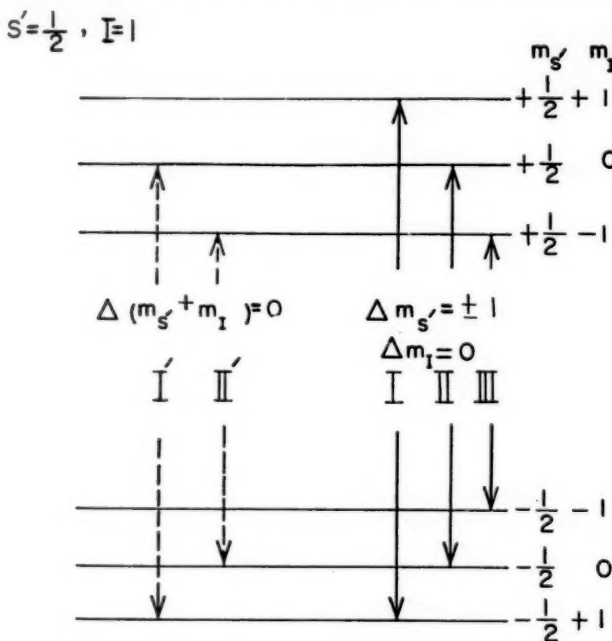


FIG. 17. The relative spacings of $S' = \frac{1}{2}, I = 1$ paramagnetic ion levels in a strong magnetic field.

bidden line (such as I') is saturated by the rf, the populations of the corresponding levels ($m_{S'} = \frac{1}{2}, m_I = 0; m_{S'} = -\frac{1}{2}, m_I = 1$) are forced to equality. Since the thermally allowed transitions are operating, the level ($m_{S'} = \frac{1}{2}, m_I = 1$) will be in the ratio of $\exp(-g\mu_0 H/kT)$ with respect to the level ($m_{S'} = -\frac{1}{2}, m_I = +1$). The net effect, therefore, is a decrease in the population of the $m_I = 1$ states with respect to the remaining m_I states, thus resulting in a partial nuclear polarization. This polarization is observed in the following manner. Two counters are so placed as to see the γ -rays emerging parallel to and perpendicular to the field. As the external magnetic field is varied through each of the $2I$ resonances consecutively, a change in the fractional difference in counting should be observed. This effect has been observed (86) in Co^{60} and Mn^{62} . Figure 18 is the experimental trace for Co^{60} . This trace shows ten lines, as is expected for $I = 5$. It is shown in comparison with the paramagnetic absorption spectrum of Co^{60} taken simultaneously. The Co^{60} sample is so weak that no trace of its paramagnetic absorption is seen. The Mn^{62} counting anisotropy trace was seen, but in an electronic state where $S' = 5/2$, and such a large number of lines was observed that the resolution made it difficult to interpret. This method has the disadvantage that no effect at all can be observed for $I = \frac{1}{2}$ and $I = 0$. Reversing a spin of $\frac{1}{2}$ the only change allowable in this case does not change the γ -ray pattern from parity

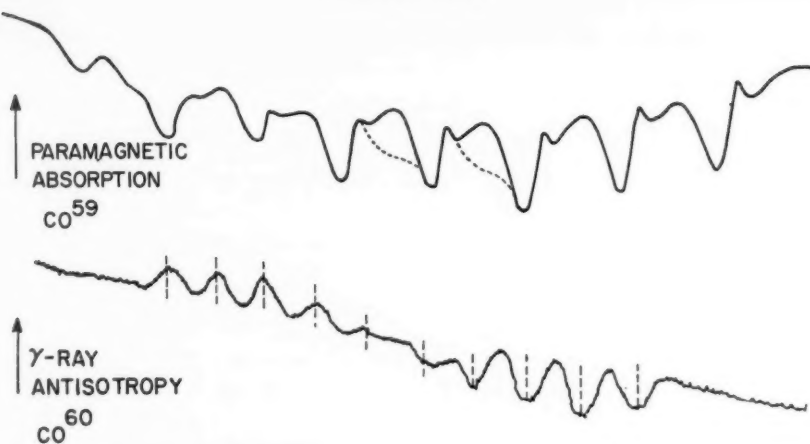


FIG. 18. The variation in the ratio of the counting rate of Co^{60} as the sample undergoes paramagnetic absorption in an applied field goes through ten resonances which is consistent with $I=5$. The upper curve is the normal paramagnetic absorption trace of the Co^{60} carrier.

conservation. However, this difficulty with spin $\frac{1}{2}$ may be removed in those cases where β 's are emitted in violation of parity restrictions if the β -particles are observed in the experiment. Table IV is included as a summary of all spins and moments measured by the method of paramagnetic absorption.

NUCLEAR g-FACTORS OF SHORT-LIVED EXCITED STATES

Following a suggestion of Brady & Deutsch (87), an entirely new technique is available for the measurement of spins and g -factors of excited states of nuclei. The general principle is the observation of the effect of an external magnetic field on the angular correlation between the emission of two successive particles in radioactive decay. This method has been successfully applied to γ - γ correlations in the measurement of the nuclear g_I of Cd^{111} , the first such moment having been observed by Aeppli, *et al.* (88) followed by measurements on (89) Ta^{181} and on (90, 91) Pb^{204} . α - γ correlation has been used to measure the g_I of the second excited state of F^{19} after inelastic scattering by protons (92). The complete theory of angular correlation, including polarization effects is extremely complicated and has been thoroughly discussed in the literature (93). The technique in practice is not nearly as unambiguous for the determination of nuclear spins as the methods previously discussed. In general, the spin assignments depend on the details of the decay scheme, as well as on the observed angular correlation. The determination of the g_I are not subject to these restrictions, and the measurements depend only on the experimental difficulties due to local fields and quadrupole effects but these effects have been successfully treated in all cases studied so far.

A simple discussion of these measurements can be made that is sufficient for the details of nuclear g -factor measurements. In its simplest and usual aspects, there are two particle detectors so placed that the straight lines connecting each detector to the radioactive sample make an angle θ . The two counters and the sample define a plane (see Fig. 19). When the magnetic field is applied, it is perpendicular to the plane because the change in the angular correlation is greatest for this geometry. On quite general grounds, the relative probability that one particle be detected in one of the counters and another particle be detected in the other must be

$$W(\theta) = A_0 + A_2 P_2(\cos \theta) + A_4 P_4(\cos \theta) + \dots \quad 39.$$

The reason for the absence of the odd Legendre polynomials is not obvious, and it depends upon the assumption that parity is conserved in the processes

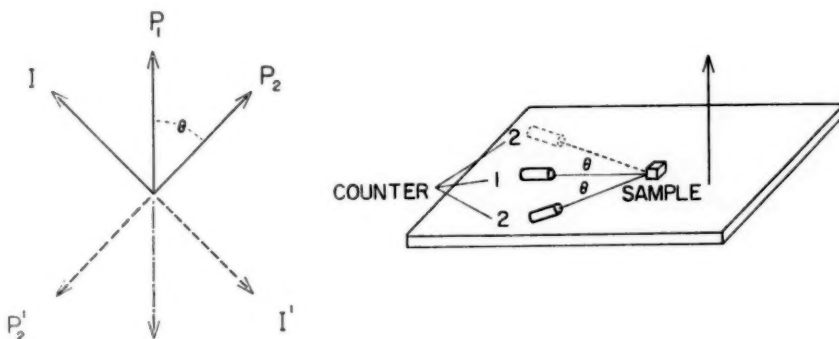


FIG. 19. A schematic arrangement of the radioactive sample, the counters and the magnetic field for an angular correlation setup for measuring g_I of a nucleus in an intermediate state.

governing the emission of the particles in the angular correlation experiment.⁴ First, the correlation function is a function of $\cos \theta$ only, since there is rotational symmetry about the direction of emission, and therefore replacing θ by $-\theta$ should have no effect. Second, that the correlation function is dependent upon parity conservation may be understood by reference to Fig. 19 and the following argument. If in an experiment a first particle, P_1 , is observed moving in a given direction, this implies that the spin of the resultant or intermediate nuclear state is in some preferred direction \mathbf{I} (in a right circular cone about P_1). The second particle, P_2 , is observed to emerge in a direction making an angle θ with respect to the first. If coordinate inversion through the origin is considered, the pseudo-vector \mathbf{I} is replaced by the inverted vector \mathbf{I}' , the vectors \mathbf{P} and \mathbf{P}' remaining as they were. Since by parity conservation the inferred position of the nuclear spin \mathbf{I}' is just

⁴ The author is greatly indebted to Professor E. Segrè for suggesting the reasoning on which this argument is based.

as likely as \mathbf{I} , given the momentum of \mathbf{P}_1 , the vector \mathbf{P}_2' of the direction of emission of the second particle which is determined by reversing the direction of \mathbf{P}_2 is equally likely. Inasmuch as the entire diagram is invariant to a rotation about the direction of \mathbf{P}_1 , it is seen that a correlation angle of $\pi - \theta$ is as likely as one of θ , and hence the odd Legendre polynomials disappear. It is interesting that this is a strong condition in the sense that only the P_1 process need be parity conserving for this result to hold. Furthermore, in a cascade involving an intermediate state of lifetime τ_1 , where a particle (or radiation) of angular momentum l_1 has been emitted in reaching this excited state and which emits a particle (or radiation) of angular momentum l_2 on decaying, and whose spin is I , the largest order of Legendre polynomial that can appear is the smallest of the three numbers $2l_1$, $2l_2$, or $2I$. This can be justified on exactly the same grounds as was the form for the general hyperfine structure of a free atom. Upon application of a magnetic field, the spin of the nucleus in its intermediate state will precess at its Larmor frequency, $g\mu_0 H/\hbar = \omega_L$, in a right circular cone about the \mathbf{H} direction as an axis. According to a simple and well known theorem on gyromagnets, the same physical situation will result if the observer will look at the experiment from a coordinate system rotating about the \mathbf{H} axis at the Larmor frequency but with the magnetic field set equal to zero. In this system, the spin direction is invariant, but the particle detectors go by in the opposite direction. If a signal is received in one counter, and, if after a time t , a signal is received in the second counter, its position relative to the first counter has changed by an angle $\omega_L t$. Now, many variations of this technique are possible, but the simplest is to assume that the resolving time for coincidences is large compared to the lifetime of the intermediate state (but short compared to accidentals). The correlation function is modified by the presence of the magnetic field and the new function is

$$W(H, \theta) = \int_0^\infty e^{-t/\tau_1} W(\theta - \omega_L t) dt / \tau_1. \quad 40.$$

This is most simply evaluated by writing the $W(\theta)$ in complex form (later to take the real part) with real coefficients as

$$W(\theta) = a_0 + a_2 e^{2i\theta} + a_4 e^{4i\theta} + \dots + a_n e^{ni\theta}. \quad 41.$$

The a_p are known linear combinations of the A_p . A typical integral evaluates to $a_p e^{ip\theta} / (1 + ip\omega_L \tau_1)$ and the real part is $a_p (1 + p^2 \omega_L^2 \tau_1^2)^{-1/2} \cos p(\theta - \theta_p)$, where $\theta_p = 1/p \tan^{-1} p\omega_L \tau_1$. The final formula is, then,

$$W(H, \theta) = a_0 + \frac{a_2}{(1 + 4\omega_L^2 \tau_1^2)^{1/2}} \cos 2(\theta - \theta_2) + \frac{a_4}{(1 + 16\omega_L^2 \tau_1^2)^{1/4}} \cos 4(\theta - \theta_4) + \dots \quad 42.$$

This represents a combined rotation and damping of the pattern. In most experiments to date, there has been no need to consider higher terms than the second. There are still a number of possible experimental variations. If the two counters are equally sensitive to both radiations, then the correlation function is half the sum of two terms of the form of Eq. 42, one with

θ replaced by $-\theta$. This is because there are two correlation functions, one for each counter detecting the first particle. The resultant $W(H, \theta)$ is then (94, 95, 96)

$$W(H, \theta) = a_0 + \frac{a_2 \cos 2\theta \cos 2\theta_2}{(1 + 4\omega_I^2 \tau_1^2)^{1/2}}, \quad 43.$$

or

$$W(H, \theta) = a_0 + \frac{a_2 \cos 2\theta}{1 + 4\omega_I^2 \tau_1^2}.$$

This pattern cannot give the sign of g_I . The observation was first made by the Zürich group (90) on the excited state of Cd¹¹¹ by observing $W(H, \theta)$, as a function of H at a fixed θ . The coefficient of H , $|g_I| \mu_0 \tau_1 / h$, was evaluated by a best fit. Since the value of τ_1 was known, g_I could be calculated. If a fixed delay could be introduced, then the first count is referred to a definite counter and the sense of rotation inferred (Eq. 42, with a small correction for the delay). Another method could be the use of counters with different efficiencies for the two radiations. The latter method was actually employed to demonstrate the negative moment of excited Cd¹¹¹. Typical accuracies are of the order of 3 per cent, and since the sign of the moment is also determined, this is more than satisfactory for the nuclear theorist. This method only yields g_I ; the magnetic moment, μ_I , can only be calculated if the spin of the intermediate is known. The method is limited to values of $\tau_1 > 10^{-8}$ sec. by the values of magnetic field available. $2\omega_I \tau_1$ should be of the order of unity. For 10^{-8} sec. this implies a frequency of about 8 Mc./sec., which corresponds to a field of 10,000 gauss for a nuclear $g_I \sim 1$. An upper limit of $\tau_1 < 10^{-5}$ or 10^{-6} sec. is set by the coincidence conditions. Accidental counts, because of the intensity required, cause difficulty. In addition, there is also the depolarization due to internal magnetic and electric field effects (the latter due to the nuclear quadrupole term).

The nuclear quadrupole effects, in general, are very complicated and, in the simplest cases where qQ , the product of the electric field gradient and the quadrupole moment, could be measured, q has been impossible to evaluate. The demonstrated effects are very beautiful examples of experimental physics and involve the theory of the solid state and liquid state, but have so far not yielded any direction information on the static nuclear moments. A very instructive example of this general technique is provided by the experiments of Lehmann, Leveque, & Pick (92). The magnetic moment of the second excited state of F¹⁹ was measured by noting the rotation of the anisotropic pattern of γ -rays that are emitted after bombardment by 5 Mev protons. Two counters are placed symmetrically on either side of the proton beam so that the radius vectors connecting them to the sample are in the same plane with the beam, and the angle between them is 2θ . Initially, the counting rates are the same. The sample is in the form of KF in a water solution. As a magnetic field is applied, a difference appears in the counting

rate of the two counters due to the Larmor precession of the spin of the intermediate state. This method is simpler than that involving angular correlation and permits a wider range of lifetimes, since coincidences in counting are not required. The answer can be reported in the form of the ratio of the counting rates versus applied magnetic field. If the counting rate ratios are normalized to unity for $H=0$, then intuitively the ratio will go to some maximum with increasing field, as the anisotropic γ -ray pattern is rotated at the Larmor frequency for the nucleus in the excited state, but it will lose coherence because of the natural radioactive decay. In addition, there is a precession of the nuclear spin because of the nuclear electric quadrupole interaction with the gradients of electric fields in its environment. The case of a liquid is relatively simple. The very rapid reorientations of the electric field in the neighborhood of the KF molecule makes the process stochastic. The F^{19} nucleus in its excited state will lose its polarization coherence before emitting a γ -ray with an exponential decay rate of mean life τ_2 . A safer surmise is that τ_2 is not only proportional to the electric quadrupole moment of the nucleus, but inversely to the viscosity as well. In the F^{19} experiments, two runs were made at two different dilutions, and the effect on the observed Larmor frequency was less than 5 per cent, corresponding to a systematic error of no more than $2\frac{1}{2}$ per cent.

Following the line of reasoning used to establish Eq. 42, the relative probability governing the counting rate of a counter, whose scattering angle is θ to the forward proton, is

$$W(\theta, H) = \int_0^\infty \{1 + a_2 e^{-t/\tau_2} P_2[\cos(\theta - \omega_I t)]\} e^{-t/\tau_1} dt / \tau_1. \quad 44.$$

ω_I is the Larmor frequency $g_I \mu_H H / \hbar$ of the nucleus in the field H . The quadrupole damping factor e^{-t/τ_2} is applied to the angular term only, since it has the effect of making the γ -ray distribution spherically symmetric in time but not the effect of reducing the total number of atoms in the excited state. After evaluation, the integral yields

$$W(\theta, H) = 1 + \frac{a_2}{4\tau_1} \left[\frac{3 \cos 2(\theta - \delta)}{(\omega^2 + 4\omega_I^2)^{1/2}} + \frac{1}{\omega} \right]; \quad 45.$$

where

$$\omega = \frac{1}{\tau_1} + \frac{1}{\tau_2}, \quad \text{and} \quad \delta = \frac{1}{2} \tan^{-1} 2\omega_I / \omega.$$

If $\theta = \pm 45^\circ$, that is, the scattering directions are perpendicular to one another, $W(\theta, H)$ has the particularly simple form

$$W(\pm 45^\circ, H) = 1 + \frac{a_2}{4\tau_1 \omega} \left[\pm \frac{6\xi}{1 + 4\xi^2} + 1 \right]; \quad \xi = \omega_I / \omega. \quad 46.$$

The ratio $W(+45^\circ, H)/W(-45^\circ, H)$ has a maximum for $\xi = \frac{1}{2}$, or

$$\omega_I = \frac{1}{2} \left(\frac{1}{\tau_1} + \frac{1}{\tau_2} \right).$$

This experiment was successfully completed for F^{19} , the maximum was observed to occur at about 600 gauss. The effect of τ_2 is absorbed by putting a possible $2\frac{1}{2}$ per cent systematic error by extrapolating the results at different viscosities. The simplicity of the method is appealing. The proton beam defines the axis of the system in the same sense as the first particle in an angular correlation experiment.

The author would like to express his deep appreciation to Professors N. Kurti and C. D. Jeffries; and Messrs. H. A. Shugart, R. W. Kedzie, M. Abraham and W. B. Ewbank for valuable help in the preparation of this manuscript.

LITERATURE CITED

1. (a) Nierenberg, W. A., Shugart, H. A., Silsbee, H. B., and Sunderland, R. J., *Phys. Rev.*, **104**, 1380 (1956); (b) Hubbs, J. C., Nierenberg, W. A., Shugart, H. A., and Silsbee, H. B., *Phys. Rev.*, **104**, 757 (1956)
2. Aeppli, H., Bishop, A. S., Frauenfelder, H., Walter, M., and Zunti, W., *Phys. Rev.*, **82**, 550 (1951)
3. Hobson, J. P., Hubbs, J. C., Nierenberg, W. A., Silsbee, H. B., and Sunderland, R. J., *Phys. Rev.*, **104**, 101 (1956)
4. Uretsky, J. (Private communication)
5. Breit, G., and Rabi, I. I., *Phys. Rev.*, **38**, 2082 (1931)
6. Kusch, P., Millman, S., and Rabi, I. I., *Phys. Rev.*, **57**, 765 (1940)
7. Zacharias, J. R., *Phys. Rev.*, **61**, 270 (1942)
8. Lemonick, A., Pipkin, F. M., and Hamilton, D. R., *Rev. Sci. Instr.*, **26**, 1112 (1955)
9. Bellamy, E. H., and Smith, K., *Phil. Mag.*, **44**, 33 (1953)
10. Lemonick, A., and Pipkin, F. M., *Phys. Rev.*, **95**, 1356 (1954)
11. Gilbert, D. A., and Cohen, V. W., *Phys. Rev.*, **97**, 243 (1955)
12. Goodman, L. S., and Wexler, S., *Phys. Rev.*, **99**, 192 (1955)
13. Hobson, J. P., Hubbs, J. C., Nierenberg, W. A., and Silsbee, H. B., *Phys. Rev.*, **104**, 101 (1956)
14. Millman, S., *Phys. Rev.*, **47**, 739 (1935)
15. (a) Ramsey, N. F., *Molecular Beams* (Oxford Press, London, England, 466 pp., 1956); (b) King, J. G., and Zacharias, J. R., *Advances in Electronics and Electronic Physics*, VIII (Academic Press, New York, N. Y., 1956)
16. Bleaney, B., *Phys. Rev.*, **78**, 214 (1950)
17. Bleaney, B., *Proc. Roy. Soc. (London)* [A], **204**, 203 (1950)
18. Dobrowolski, W., Jones, R. V., and Jeffries, C. D., *Phys. Rev.*, **101**, 1001 (1956)
19. Hutchison, C. A., Jr., Llewellyn, P. M., Wong, E., and Dorain, P., *Phys. Rev.*, **102**, 292 (1956)
20. Pryce, M. H. L., *Proc. Phys. Soc. (London)* [A], **63**, 25 (1950)
21. Lew, H., *Phys. Rev.*, **91**, 619 (1953)
22. (a) Kastler, A., *J. Phys. Radium*, **11**, 255 (1950); (b) *Proc. Roy. Soc. A*, **67**, 853. (1954)
23. Wittke, J. P., and Dicke, R. H., *Phys. Rev.*, **96**, 530 (1954)
24. Sagalyn, P. L., *Phys. Rev.*, **94**, 885 (1954)
25. Beringer, R., and Castle, J. G., Jr., *Phys. Rev.*, **81**, 82 (1951)
26. Jaccarino, V. (Private communication)
27. (a) Feher, G., *Phys. Rev.*, **103**, 500 (1956); (b) **103**, 834 (1956)

28. Steenland, M. J., and Tolhoek, H. A., *Progress in Low Temperature Physics*, II, (Gorter, C. J., Ed.), Interscience Publishers, New York, N. Y., 1957)
29. (a) Daniels, J. M., Grace, M. A., Robinson, F. N. H., *Nature*, **168**, 780 (1951);
 (b) Ambler, E., Grace, M. A., Halban, H., Kurti, N., Durand, H., Johnson, C. E., and Lemmer, H. R., *Phil. Mag.*, **44**, 216 (1953)
30. (a) Dabbs, J. W. T., Roberts, L. D., and Bernstein, S., *Phys. Rev.*, **98**, 1512 (1955); (b) Roberts, L. D., Dabbs, J. W. T., Parker, G. W., and Ellison, R. D., *Bull. Am. Phys. Soc.* [II], **1**, 207 (1956)
31. Overhauser, A., *Phys. Rev.*, **89**, 689 (1953); **92**, 411 (1953)
32. Abragam, A., *Compt. rend.*, **242**, 1720 (1956)
33. Abragam, A., and Proctor, W. G., *Experiments on Spin Temperature* (In press)
34. Jeffries, C. D., *Phys. Rev.*, **106**, 164 (1957)
35. Manning, T. E., Fred, M., and Tomkins, F. S., *Phys. Rev.*, **102**, 1108 (1956)
36. Jackson, D. A., *Phys. Rev.*, **103**, 1738 (1956)
37. Conway, J. G., and McLaughlin, R. D., *Phys. Rev.*, **94**, 498 (1954)
38. Speck, D. R., and Jenkins, F. A., *Phys. Rev.*, **101**, 1831 (1956)
39. Hubbs, J. C., et al., *Phys. Rev.* (To be published)
40. Fletcher, P., Ambler, E., *Bull. Am. Phys. Soc.*, [II], **2**, 30 (1957)
41. (a) Rabi, I. I., *Phys. Rev.*, **87**, 379 (1952); (b) Buck, P., Rabi, I. I., and Senitzky, B., *Phys. Rev.*, **104**, 553 (1956)
42. Gould, G., *Phys. Rev.*, **101**, 1828 (1956)
43. Fermi, E., *Z. Physik*, **60**, 320 (1930)
44. Schwartz, C., *Phys. Rev.*, **97**, 380 (1955)
45. Kramers, H. A., *Proc. Roy. Acad. (Amsterdam)*, **34**, 965 (1931)
46. (a) Casimir, H. B. G., *On the Interaction between Atomic Nuclei and Electrons* (Teyler's Tweede Genootschap, Haarlem, The Netherlands, 1936); (b) Casimir, H. B. G., and Karreman, G., *Physica IX*, **5**, 494 (1938)
47. Schwinger, J., *On Angular Momentum* (Nuclear Development Associates, Inc., White Plains, 73 pp., 1952)
48. Nafe, J. E., Nelson, E. B., and Rabi, I. I., *Phys. Rev.*, **71**, 914 (1947)
49. Kusch, P., *Phys. Rev.*, **100**, 1188 (1955)
50. Bloch, F., *Phys. Rev.*, **51**, 994 (1936)
51. Stroke, H. H., Jaccarino, V., Edmonds, D. S., Jr., and Weiss, R., *Phys. Rev.*, **87**, 676 (1952)
52. Kusch, P., (Unpublished data).
53. Bohr, A., and Weisskopf, V. F., *Phys. Rev.*, **77**, 94 (1950)
54. Stroke, H. H., Jaccarino, V., Edmonds, D. S., Jr., and Weiss, R., *Phys. Rev.*, **105**, 590 (1957)
55. Jaccarino, V., Bederson, B., and Stroke, H. H., *Phys. Rev.*, **87**, 676 (1952)
56. Nierenberg, W. A., Shugart, H. A., Silsbee, H. B., and Sunderland, R. J., *Phys. Rev.*, **104**, 1380 (1956)
57. Nierenberg, W. A., Rabi, I. I., and Slotnick, M. M., *Phys. Rev.*, **73**, 1430 (1948)
58. Nierenberg, W. A., *Phys. Rev.*, **80**, 1102 (1950)
59. Kusch, P., and Eck, T. G., *Phys. Rev.*, **94**, 1799 (1954)
60. (a) Jaccarino, V., King, J. G., Satten, R. A., and Stroke, H. H., *Phys. Rev.*, **94**, 1798 (1954); (b) Daly, R. T., Jr., and Holloway, J. H., *Phys. Rev.*, **96**, 539 (1954)
61. Davis, L., Feld, B. T., Zabel, C. W., and Zacharias, J. R., *Phys. Rev.*, **76**, 1076 (1949)

62. Kusch, P., and Foley, H. M., *Phys. Rev.*, **74**, 250 (1948)
63. Phillips, M., *Phys. Rev.*, **86**, 595 (1952)
64. Clendenin, W. W., *Phys. Rev.*, **94**, 1590 (1954)
65. Huffman, E. H. (Private communication)
66. (a) Reynolds, J. B., Karraker, D. G., and Templeton, D. H., *Phys. Rev.*, **75**, 313 (1949); (b) Karraker, D. G., and Templeton, D. H., *Phys. Rev.*, **80**, 646 (1950)
67. (a) Caird, R. S., and Mitchell, A. C. G., *Phys. Rev.*, **89**, 573 (1953); (b) Welker, J. P., and Perlman, M. L., *Phys. Rev.*, **100**, 74 (1955)
68. Majorana, E., *Nuovo Cimento*, **9**, 43 (1932)
69. Hubbs, J. C., Nierenberg, W. A., Shugart, H. A., Silsbee, H. B., and Sunderland, R. J., *Phys. Rev.* (To be published)
70. Silsbee, H. B., Nierenberg, W. A., and Shugart, H. A., *Bull. Am. Phys. Soc.*, [II], **2**, 30 (1957)
71. Nierenberg, W. A., Shugart, H. A., and Silsbee, H. B., *Bull. Am. Phys. Soc.*, [II], **2**, 200 (1957)
72. Silsbee, H. B., Nierenberg, W. A., Shugart, H. A., and Strom, P. O., *Bull. Am. Phys. Soc.*, **1**, 389 (1956)
73. Brink, G. O., Hubbs, J. C., Nierenberg, W. A., and Worcester, J. L., *Phys. Rev.*, **107**, 189 (1957)
74. Lipworth, E. (Private communication)
75. Silsbee, H. B., *University of California Radiation Laboratory Report UCRL 3723* (1957)
76. Smith, K. F., *Molecular Beams*, 101 (Methuen and Co., London, England, 133 pp., 1955)
77. (a) Bleaney, B., and Stevens, K. W. S., *Repts. Progr. Phys.*, **16**, (1953); (b) Bowers, K. D., and Owen, J., *Repts. Progr. Phys.*, **18**, 304 (1955)
78. Steenland, M. J., and Tolhoek, H. A., *Progress in Low Temperature Physics*, II, (Gorter, C. J., Ed., Interscience Publishers, New York, N. Y., 1957)
79. Abragam, A., and Pryce, M. H. L., *Proc. Roy. Soc. (London)* [A], **205**, 135 (1951)
80. (a) Bleaney, B., and Bowers, K. D., *Proc. Phys. Soc. (London)* [A], **64**, 1135 (1951); (b) Bleaney, B., Elliott, R. J., Scovil, H. E. D., and Trenam, R. S., *Phil. Mag.*, **42**, 1062 (1951)
81. Dobrowolski, W., Jones, R. V., and Jeffries, C. D., *Phys. Rev.*, **101**, 1001 (1956)
82. Jones, R. V., Dobrowolski, W., and Jeffries, C. D., *Phys. Rev.*, **102**, 738 (1956)
83. Baker, J. M., Bleaney, B., Llewellyn, P. M., *Proc. Roy. Soc. (London)* [A], **69**, 353 (1956)
84. Proctor, W. G., and Yu, F. C., *Phys. Rev.*, **81**, 20 (1951)
85. Jeffries, C. D., *Phys. Rev.*, **106**, 164 (1957)
86. Abraham, M., Kedzie, R. W., and Jeffries, C. D., *Phys. Rev.*, **106**, 165 (1957)
87. Brady, E. L., and Deutsch, M., *Phys. Rev.*, **78**, 558 (1950)
88. Aeppli, H., Albers-Schönberg, H., Bishop, A. S., Frauenfelder, H., and Heer, E., *Phys. Rev.*, **84**, 370 (1951)
89. Raboy, S., and Krohn, V. E., *Phys. Rev.*, **95**, 1689 (1954)
90. (a) Krohn, V. E., and Raboy, S., *Phys. Rev.*, **95**, 608 (1954); (b) Frauenfelder, H., Lawson, J. S., Jr., and Jentschke, W. K., *Phys. Rev.*, **93**, 1126 (1954)
91. Krohn, V. E., Novey, T. B., and Raboy, S., *Phys. Rev.*, **98**, 1187(A) (1955)
92. Lehmann, P., Leveque, A., and Pick, R., *Phys. Rev.*, **104**, 411 (1956)

93. Frauenfelder, H., *Beta- and Gamma-Ray Spectroscopy*, 531 (K. Seigbahn, Ed. North-Holland Publishing Company, Amsterdam, The Netherlands, 1955)
94. Alder, K., *Phys. Rev.*, **84**, 369 (1951)
95. Goertzel, G., *Phys. Rev.*, **70**, 897 (1946)
96. Abragam, A., and Pound, R. V., *Phys. Rev.*, **89**, 1306 (1953)
97. Abraham, M., Kedzie, R. W., and Jeffries, C. D. (To be published)
98. Baker, J. M., and Bleaney, B., *Proc. Phys. Soc. (London)* [A], **65**, 952 (1952)
99. Baker, J. M., Bleaney, B., Llewellyn, P. M., and Shaw, P. F. D., *Proc. Phys. Soc. (London)* [A], **69**, 353 (1956)
100. Baker, J. M., Bleaney, B., Bowers, K. D., Shaw, P. F. D., and Trenam, R. S., *Proc. Phys. Soc. (London)* [A], **66**, 305 (1953)
101. Baker, J. M., Bleaney, B., Llewellyn, P. M., and Shaw, P. F. D., *Proc. Phys. Soc. London* [A], **69**, 352 (1956)
102. Baker, J. M., and Bleaney, B., *Proc. Phys. Soc. (London)* [A], **68**, 257 (1955)
103. Baker, J. M., and Bleaney, B., *Proc. Phys. Soc. (London)* [A], **68**, 1090 (1955)
104. Bleaney, B., Ingram, D. J. E., and Scovil, H. E. D., *Proc. Phys. Soc. (London)* [A], **64**, 601 (1951)
105. Bleaney, B., and Bowers, K. D., *Proc. Phys. Soc. (London)* [A], **64**, 1135 (1951)
106. Bleaney, B., and Ingram, D. J. E., *Proc. Roy. Soc. (London)* [A], **205**, 336 (1951)
107. Bleaney, B., and Ingram, D. J. E., *Proc. Roy. Soc. (London)* [A], **208**, 143 (1951)
108. Bleaney, B., Penrose, R. P., and Plumpton, B. I., *Proc. Roy. Soc. (London)* [A], **198**, 406 (1949)
109. Bleaney, B., Bowers, K. D., and Ingram, D. J. E., *Proc. Phys. Soc. (London)* [A], **64**, 758 (1951); *Proc. Soc. (London)* [A], **228**, 147 (1955)
110. Bleaney, B., Bowers, K. D., and Pryce, M. H. L., *Proc. Roy. Soc. (London)* [A], **228**, 166 (1955)
111. Bleaney, B., and Scovil, H. E. D., *Phil. Mag.*, **43**, 999 (1952)
112. Bleaney, B., and Baker, J. M., *Proc. Phys. Soc. (London)* [A], **68**, 936 (1955)
113. Bleaney, B., and Scovil, H. E. D., *Proc. Phys. Soc. (London)* [A], **63**, 1369 (1950)
114. Bleaney, B., Scovil, H. E. D., and Trenam, R. S., *Proc. Roy. Soc. (London)* [A], **223**, 15 (1954)
115. Bleaney, B., and Baker, J. M., *Proc. Phys. Soc. (London)* [A], **68**, 937 (1955)
116. Bleaney, B., and Low, W., *Proc. Phys. Soc. (London)* [A], **68**, 55 (1955)
117. Bleaney, B., and Scovil, H. E. D., *Proc. Phys. Soc. (London)* [A], **64**, 204 (1951)
118. Bleaney, B., Hutchison, C. A., Jr., Llewellyn, P. M., and Pope, D. E. F., *Proc. Phys. Soc. (London)* [B], **68**, 1167 (1956)
119. Bleaney, B., Llewellyn, P. M., Pryce, M. H. L., and Hall, G. R., *Phil. Mag.*, **45**, 992 (1954)
120. Bleaney, B., Llewellyn, P. M., Pryce, M. H. L., and Hall, G. R., *Phil. Mag.*, **45**, 773 (1954)
121. Bleaney, B., Llewellyn, P. M., Pryce, M. H. L., and Hall, G. R., *Phil. Mag.*, **45**, 991 (1954)
122. Bogle, G. S., and Scovil, H. E. D., *Proc. Phys. Soc. (London)* [A], **65**, 368 (1952)
123. Bowers, K. D., *Proc. Phys. Soc. (London)* [A], **65**, 860 (1952)
124. Cooke, A. H., and Park, J. G., *Proc. Phys. Soc. (London)* [A], **69**, 282 (1956)
125. Dobrowolski, W., Jones, R. V., and Jeffries, C. D., *Phys. Rev.*, **104**, 1378 (1956)
126. Dobrowolski, W., and Jeffries, C. D. (Unpublished data)
127. Dobrowolski, W., Jones, R. V., and Jeffries, C. D., *Phys. Rev.*, **101**, 1001 (1956)
128. Dorain, P., Hutchison, C. A., Jr., and Wong, E., *Phys. Rev.*, **105**, 1307 (1957)

129. Fletcher, R. C., Yager, W. A., Pearson, G. L., Holden, R. B., Read, T., Jr., and Merritt, F. R., *Phys. Rev.*, **94**, 1392 (1954)
130. Fletcher, R. C., Yager, W. A., Pearson, G. L., and Merritt, F. R., *Phys. Rev.*, **95**, 844 (1954)
131. Griffiths, J. H. E., Owen, J., and Ward, I. M., *Proc. Roy. Soc. (London)* [A], **219**, 526 (1953)
132. Griffiths, J. H. E., and Owen, J., *Proc. Phys. Soc. (London)* [A], **65**, 951 (1952)
133. Hutchison, C. A., Jr., Llewellyn, P. M., Wong, E., and Dorain, P., *Phys. Rev.*, **102**, 292 (1956)
134. Hutchison, C. A., Jr., and Lewis, W. B., *Phys. Rev.*, **95**, 1096 (1954)
135. Jones, R. V., Dobrowolski, W., and Jeffries, C. D., *Phys. Rev.*, **102**, 738 (1956)
136. Jones, R. V., Dobrowolski, W., and Jeffries, C. D. (Unpublished data)
137. Kedzie, R. W., Abraham, M., and Jeffries, C. D., *Bull. Am. Phys. Soc.*, [II], **1**, 390 (1956)
138. Kikuchi, C., Sirvetz, M. H., and Cohen, V. W., *Phys. Rev.*, **92**, 109 (1953)
139. Knight, W. D., and Cohen, V. W., *Phys. Rev.*, **76**, 1421 (1949)
140. Low, W., *Phys. Rev.*, **103**, 1309 (1956)
141. Proctor, W. G., and Yu, F. C., *Phys. Rev.*, **81**, 20 (1951)
142. Weiss, M. M., Walter, R. I., Gillium, O. R., and Cohen, V. W., *Bull. Am. Phys. Soc.*, [II], **2**, 31 (1957)
143. Walchli, H. E., *Oak Ridge National Laboratory 1469 Suppl. 2*, (Feb. 1, 1955)
144. Ramsey, N. F., *Molecular Beams* (Oxford University Press, London, England, 466 pp., 1956)
145. Ramsey, N. F., *Nuclear Moments* (John Wiley and Sons, Inc., New York, N. Y., 169 pp., 1953)
146. Walchli, H. E., *Oak Ridge National Laboratory*, **1469** (April 1, 1953)
147. Alvarez, L. W., and Bloch, F., *Phys. Rev.*, **57**, 111 (1940)
148. Foley, H. M., and Kusch, P., *Phys. Rev.*, **73**, 412 (1948)
149. Kusch, P., and Foley, H. M., *Phys. Rev.*, **74**, 250 (1948)
150. Mann, A. K., and Kusch, P., *Phys. Rev.*, **76**, 163 (1949)
151. Mann, A. K., and Kusch, P., *Phys. Rev.*, **77**, 435 (1950)
152. Koenig, S. H., Prodell, A. G., and Kusch, P., *Phys. Rev.*, **83**, 687 (1951)
153. Koenig, S. H., Prodell, A. G., and Kusch, P., *Phys. Rev.*, **88**, 191 (1952)
154. Estermann, I., and Stern, O., *Z. Physik*, **85**, 17 (1933)
155. Estermann, I., Simpson, O. C., and Stern, O., *Phys. Rev.*, **52**, 535 (1937)
156. Frisch, R., and Stern, O., *Z. Physik*, **85**, 4 (1933)
157. Rabi, I. I., Kellogg, J. M. B., and Zacharias, J. R., *Phys. Rev.*, **45**, 761 (1934)
158. Rabi, I. I., Kellogg, J. M. B., and Zacharias, J. R., *Phys. Rev.*, **46**, 157 (1934)
159. Kellogg, J. M. B., Rabi, I. I., and Zacharias, J. R., *Phys. Rev.*, **50**, 472 (1936)
160. Kellogg, J. M. B., Rabi, I. I., Ramsey, N. F., and Zacharias, J. R., *Phys. Rev.*, **55**, 595 (1939)
161. Kellogg, J. M. B., Rabi, I. I., Ramsey, N. F., and Zacharias, J. R., *Phys. Rev.*, **56**, 728 (1939)
162. Millman, S., and Kusch, P., *Phys. Rev.*, **60**, 91 (1941)
163. Nafe, J. E., Nelson, E. B., and Rabi, I. I., *Phys. Rev.*, **71**, 914 (1947)
164. Nafe, J. E., and Nelson, E. B., *Phys. Rev.*, **73**, 718 (1948)
165. Nagle, D. E., Julian, R. S., and Zacharias, J. R., *Phys. Rev.*, **72**, 971 (1947)
166. Lamb, W. E., and Rutherford, R. C., *Phys. Rev.*, **72**, 241 (1947)
167. Taub, H., and Kusch, P., *Phys. Rev.*, **75**, 1481 (1949)

168. Kolsky, H. G., Phipps, T. E., Ramsey, N. F., and Silsbee, H. B., *Phys. Rev.*, **79**, 883 (1950)
169. Kolsky, H. G., Phipps, T. E., Ramsey, N. F., and Silsbee, H. B., *Phys. Rev.*, **87**, 395 (1952)
170. Prodell, A. G., and Kusch, P., *Phys. Rev.*, **79**, 1009 (1950)
171. Prodell, A. G., and Kusch, P., *Phys. Rev.*, **88**, 184 (1952)
172. Bray, P. J., Barnes, R. G., and Harrick, N. J., *Phys. Rev.*, **87**, 229 (1952)
- 172a. Estermann, I., and Stern, O., *Phys. Rev.*, **45**, 761 (1934)
173. Rabi, I. I., Kellogg, J. M. B., and Zacharias, J. R., *Phys. Rev.*, **45**, 769 (1934)
174. Rabi, I. I., Kellogg, J. M. B., and Zacharias, J. R., *Phys. Rev.*, **46**, 163 (1934)
175. Kellogg, J. M. B., Rabi, I. I., Ramsey, N. F., and Zacharias, J. R., *Phys. Rev.*, **55**, 318 (1939)
176. Kellogg, J. M. B., Rabi, I. I., Ramsey, N. F., and Zacharias, J. R., *Phys. Rev.*, **57**, 677 (1940)
177. Kolsky, H. G., Phipps, T. E., Ramsey, N. F., and Silsbee, H. B., *Phys. Rev.*, **80**, 483 (1950)
178. Kolsky, H. G., Phipps, T. E., Ramsey, N. F., and Silsbee, H. B., *Phys. Rev.*, **81**, 1061 (1951)
179. Kolsky, H. G., Phipps, T. E., Ramsey, N. F., and Silsbee, H. B., *Phys. Rev.*, **82**, 322 (1951)
180. Nelson, E. B., and Nafe, J. E., *Phys. Rev.*, **75**, 1194 (1949)
181. Prodell, A. G., and Kusch, P., *Phys. Rev.*, **106**, 87 (1957)
182. Hughes, V., Tucker, G., Rhoderick, E., and Weinreich, G., *Phys. Rev.*, **91**, 828 (1953)
183. Weinreich, G., Grosof, G. M., and Hughes, V., *Phys. Rev.*, **91**, 195 (1953)
184. Weinreich, G., and Hughes, V. W., *Phys. Rev.*, **95**, 1451 (1954)
185. Novick, R., and Commins, E., *Phys. Rev.*, **103**, 1897 (1956)
186. Kellogg, J. M. B., and Ramsey, N. F., *Phys. Rev.*, **53**, 331 (1938)
187. Hughes, V., and Tucker, G., *Phys. Rev.*, **82**, 322 (1951)
188. Tucker, G., Hughes, V., Rhoderick, E., and Weinreich, G., *Phys. Rev.*, **86**, 618 (1952)
189. Fox, M., and Rabi, I. I., *Phys. Rev.*, **48**, 746 (1935)
190. Manley, J. H., and Millman, S., *Phys. Rev.*, **50**, 380 (1936)
191. Manley, J. H., and Millman, S., *Phys. Rev.*, **51**, 19 (1937)
192. Gorham, J. E., *Phys. Rev.*, **53**, 331 (1938)
193. Millman, S., *Phys. Rev.*, **55**, 628 (1939)
194. Rabi, I. I., Millman, S., Kusch, P., and Zacharias, J. R., *Phys. Rev.*, **53**, 495 (1938)
195. Rabi, I. I., Millman, S., Kusch, P., and Zacharias, J. R., *Phys. Rev.*, **55**, 526 (1939)
196. Kusch, P., Millman, S., and Rabi, I. I., *Phys. Rev.*, **57**, 765 (1940)
197. Kusch, P., *Phys. Rev.*, **75**, 887 (1949)
198. Kusch, P., and Taub, H., *Phys. Rev.*, **75**, 1477 (1949)
199. Kusch, P., and Mann, A. K., *Phys. Rev.*, **76**, 707 (1949)
200. Fox, M., Millman, S., and Rabi, I. I., *Phys. Rev.*, **47**, 801 (1935)
201. Millman, S., and Zacharias, J. R., *Phys. Rev.*, **51**, 1049 (1937)
202. Kusch, P., *Phys. Rev.*, **76**, 138 (1949)
203. Kusch, P., Millman, S., and Rabi, I. I., *Phys. Rev.*, **55**, 666 (1939)
204. Millman, S., Kusch, P., Rabi, I. I., *Phys. Rev.*, **56**, 165 (1939)
205. Wessel, G., *Phys. Rev.*, **92**, 1581 (1953)

206. Hay, R. H., *Phys. Rev.*, **58**, 180 (1940)
207. Hay, R. H., *Phys. Rev.*, **60**, 75 (1941)
208. Kusch, P., Millman, S., and Rabi, I. I., *Phys. Rev.*, **55**, 1176 (1939)
209. Zacharias, J. R., and Kellogg, J. M. B., *Phys. Rev.*, **57**, 570 (1940)
210. Weinreich, G., Tucker, G., and Hughes, V., *Phys. Rev.*, **87**, 229 (1952)
211. Davis, L., *Phys. Rev.*, **74**, 1193 (1948)
212. Davis, L., Nagle, D. E., Zacharias, J. R., *Phys. Rev.*, **76**, 1068 (1949)
213. Rabi, I. I., and Cohen, V. W., *Phys. Rev.*, **43**, 582 (1933)
214. Rabi, I. I., and Cohen, V. W., *Phys. Rev.*, **46**, 707 (1934)
215. Millman, S., and Kusch, P., *Phys. Rev.*, **58**, 438 (1940)
216. Logan, R. A., and Kusch, P., *Phys. Rev.*, **81**, 280 (1951)
217. Perl, M. L., Rabi, I. I., and Senitzky, B., *Phys. Rev.*, **97**, 838 (1955)
218. Perl, M. L., Rabi, I. I., and Senitzky, B., *Phys. Rev.*, **98**, 611 (1955)
219. Smith, K. F., *Nature*, **167**, 942 (1951)
220. Bellamy, E. H., *Nature*, **168**, 556 (1951)
221. Millman, S., and Kusch, P., *Phys. Rev.*, **56**, 303 (1939)
222. Lew, H., *Phys. Rev.*, **74**, 1550 (1948)
223. Lew, H., *Phys. Rev.*, **76**, 1086 (1949)
224. Lew, H., and Wessel, G., *Phys. Rev.*, **90**, 1 (1953)
225. Kusch, P., and Millman, S., *Phys. Rev.*, **55**, 680 (1939)
226. Kusch, P., and Millman, S., *Phys. Rev.*, **56**, 527 (1939)
227. Davis, L., Feld, B. T., Zabel, C. W., and Zacharias, J. R., *Phys. Rev.*, **73**, 525 (1948)
228. Davis, L., and Zabel, C. W., *Phys. Rev.*, **74**, 1211 (1948)
229. Davis, L., Feld, B. T., Zabel, C. W., and Zacharias, J. R., *Phys. Rev.*, **76**, 1076 (1949)
230. Jaccarino, V., and King, J. G., *Phys. Rev.*, **83**, 209 (1951)
231. Jaccarino, V., and King, J. G., *Phys. Rev.*, **83**, 471 (1951)
232. King, J. G., and Jaccarino, V., *Phys. Rev.*, **84**, 852 (1951)
233. King, J. G., and Jaccarino, V., *Phys. Rev.*, **87**, 228 (1952)
234. Shrader, E. F., Millman, S., and Kusch, P., *Phys. Rev.*, **58**, 925 (1940)
235. Millman, S., Fox, M., and Rabi, I. I., *Phys. Rev.*, **46**, 320 (1934)
236. Millman, S., *Phys. Rev.*, **47**, 739 (1935)
237. Millman, S., Fox, M., and Rabi, I. I., *Phys. Rev.*, **47**, 801 (1935)
238. Ochs, S., Logan, R. A., and Kusch, P., *Phys. Rev.*, **78**, 184 (1950)
239. Franken, P., and Koenig, S. H., *Phys. Rev.*, **88**, 199 (1952)
240. Zacharias, J. R., *Phys. Rev.*, **60**, 168 (1941)
241. Zacharias, J. R., *Phys. Rev.*, **61**, 270 (1942)
242. Eisinger, J. T., Bederson, B., and Feld, B. T., *Phys. Rev.*, **86**, 73 (1952)
243. Manley, J. H., *Phys. Rev.*, **49**, 921 (1936)
244. Bellamy, E. H., and Smith, K. F., *Phil. Mag.*, **44**, 33 (1953)
245. Brix, P., Eisinger, J. T., Lew, H., and Wessel, G., *Phys. Rev.*, **92**, 647 (1953)
246. Woodgate, A. K., and Martin, J. S., *Proc. 2nd Conf. Molecular Beams* (Brookhaven, National Lab., Upton, N. Y., October, 1956)
247. Nierenberg, W. A., Shugart, H. A., and Silsbee, H. B., *Bull. Am. Phys. Soc.*, [II], **2**, 200 (1957)
248. Ting, Y., and Lew, H., *Phys. Rev.*, **105**, 581 (1957)
249. Hamilton, D. R., Lemonick, A., Pipkin, F. M., and Reynolds, J. B., *Phys. Rev.*, **95**, 1356 (1954)
250. Lemonick, A., and Pipkin, F. M., *Phys. Rev.*, **95**, 1356 (1954)

251. Hubbs, J. C., Nierenberg, W. A., Shugart, H. A., and Worcester, J. L., *Phys. Rev.*, **105**, 1928 (1957)
252. Renzetti, N. A., *Phys. Rev.*, **57**, 753 (1940)
253. Kusch, P., and Foley, H. M., *Phys. Rev.*, **72**, 1256 (1947)
254. Becker, G. E., and Kusch, P., *Phys. Rev.*, **73**, 584 (1948)
255. Daly, R. T., Jr., and Holloway, J. H., *Phys. Rev.*, **96**, 539 (1954)
256. Lurio, A., and Prodell, A. G., *Phys. Rev.*, **99**, 613 (1955)
257. Lurio, A., and Prodell, A. G., *Phys. Rev.*, **101**, 79 (1956)
258. Brody, S. B., Nierenberg, W. A., and Ramsey, N. F., *Phys. Rev.*, **72**, 258 (1947)
259. King, J. G., and Jaccarino, V., *Phys. Rev.*, **91**, 209 (1953)
260. King, J. G., and Jaccarino, V., *Phys. Rev.*, **94**, 1610 (1954)
261. Kellogg, J. M. B., and Millman, S., *Rev. Modern Phys.*, **18**, 323 (1946)
262. Hobson, J. P., Hubbs, J. C., Nierenberg, W. A., and Silsbee, H. B., *Phys. Rev.*, **96**, 1450 (1954)
263. Hobson, J. P., Hubbs, J. C., Nierenberg, W. A., and Silsbee, H. B., *Phys. Rev.*, **99**, 612 (1955)
264. Hobson, J. P., Hubbs, J. C., Nierenberg, W. A., Silsbee, H. B., and Sunderland, R. J., *Phys. Rev.*, **104**, 101 (1956)
265. Hubbs, J. C., Hobson, J. P., Nierenberg, W. A., and Silsbee, H. B., *Phys. Rev.*, **99**, 612 (1955)
266. Hubbs, J. C., Nierenberg, W. A., Shugart, H. A., and Silsbee, H. B. (To be published)
267. Sunderland, R. J., Hubbs, J. C., Nierenberg, W. A., and Silsbee, H. B. *Bull. Am. Phys. Soc.* [II], **1**, 252 (1956)
268. Hubbs, J. C., Nierenberg, W. A., Shugart, H. A., and Silsbee, H. B., *Phys. Rev.*, **104**, 757 (1956)
269. Shugart, H. A., Hubbs, J. C., Lipworth, E., Nierenberg, W. A., and Silsbee, H. B., *Bull. Am. Phys. Soc.* [II], **1**, 253 (1956)
270. Millman, S., and Fox, M., *Phys. Rev.*, **50**, 220 (1936)
271. Hughes, V., and Grabner, L., *Phys. Rev.*, **79**, 314 (1950)
272. Bederson, B., and Jaccarino, V., *Phys. Rev.*, **87**, 228 (1952)
273. Ochs, S., and Kusch, P., *Phys. Rev.*, **85**, 145 (1952)
274. Senitzky, B., Rabi, I. I., and Perl, M. L., *Phys. Rev.*, **98**, 1537 (1955)
275. Bennewitz, H. G., Paul, W., and Toschek, P., *Z. Naturforsch.*, **11a**, 956, (1956)
276. Daly, R. T., Jr., and Zacharias, J. R., *Phys. Rev.*, **91**, 476 (1953)
277. Silsbee, H. B., Nierenberg, W. A., Shugart, H. A., and Strom, P. O., *Bull. Am. Phys. Soc.* [II], **1**, 389 (1956)
278. Wessel, G., and Lew, H., *Phys. Rev.*, **92**, 651 (1953)
279. Woodgate, G. K., and Hellwarth, R. W., *Nature*, **176**, 395 (1955)
280. Woodgate, G. K., and Hellwarth, R. W., *Proc. Phys. Soc. (London)* [A], **69**, 581 (1956)
281. Hardy, T. C., and Millman, S., *Phys. Rev.*, **60**, 167 (1941)
282. Hardy, T. C., and Millman, S., *Phys. Rev.*, **61**, 459 (1942)
283. Mann, A. K., and Kusch, P., *Phys. Rev.*, **77**, 427 (1950)
284. Childs, W. J., and Goodman, L. S., *Bull. Am. Phys. Soc.* [II], **1**, 342 (1956)
285. Goodman, L. S., and Wexler, S., *Phys. Rev.*, **100**, 1245 (1955)
286. Millman, S., Rabi, I. I., and Zacharias, J. R., *Phys. Rev.*, **53**, 384 (1938)
287. Hamilton, D. R., *Phys. Rev.*, **56**, 30 (1939)
288. Hardy, T. C., *Phys. Rev.*, **59**, 686 (1941)

289. Kusch, P., and Eck, T. G., *Phys. Rev.*, **94**, 1799 (1954)
290. Goodman, L. S., and Wexler, S., *Phys. Rev.*, **100**, 1796 (1955)
291. Jaccarino, V., King, J. G., Satten, R. A., and Stroke, H. H., *Phys. Rev.*, **94**, 1798 (1954)
292. Nierenberg, W. A., Shugart, H. A., Silsbee, H. B., and Sunderland, R. J., *Phys. Rev.*, **104**, 1380 (1956)
293. Silsbee, H. B., Nierenberg, W. A., Shugart, H. A., and Sunderland, R. J., *Bull. Am. Phys. Soc.*, [II], **2**, 30 (1957)
294. Nierenberg, *et al.*, *Magnetic Moments of Cs¹³⁰ and Cs¹³²* (To be published)
295. Nierenberg, W. A., Hubbs, J. C., Shugart, H. A., Silsbee, H. B., and Strom, P. O., *Bull. Am. Phys. Soc.*, [II], **1**, 343 (1956)
296. Kusch, P., and Millman, S., *Phys. Rev.*, **55**, 596 (1939)
297. Sherwood, J. E., Lyons, H., McCracken, R. H., and Kusch, P., *Phys. Rev.*, **86**, 618 (1952)
298. Essen, L., and Parry, J. V. L., *Nature*, **176**, 280 (1955)
299. Jaccarino, V., Bederson, B., and Stroke, H. H., *Phys. Rev.*, **87**, 676 (1952)
300. Stroke, H. H., Jaccarino, V., Edmonds, D. S., Jr., and Weiss, R., *Phys. Rev.*, **105**, 590 (1957)
301. Cohen, V. W., and Gilbert, D. A., *Phys. Rev.*, **95**, 569 (1954)
302. Goodman, L. S., and Wexler, S., *Phys. Rev.*, **95**, 570 (1954)
303. Goodman, L. S., and Wexler, S., *Phys. Rev.*, **97**, 242 (1955)
304. Goodman, L. S., and Wexler, S., *Phys. Rev.*, **99**, 192 (1955)
305. Gilbert, D. A., and Cohen, V. W., *Phys. Rev.*, **97**, 243 (1955)
306. Nagle, D. E., *Phys. Rev.*, **76**, 847 (1949)
307. Davis, L., *Phys. Rev.*, **76**, 435 (1949)
308. Hay, R. H., *Phys. Rev.*, **59**, 686 (1941)
309. Lew, H., *Phys. Rev.*, **89**, 530 (1953)
310. Lew, H., *Phys. Rev.*, **91**, 619 (1953)
311. Ting, Y., and Lew, H. (Private communication, 1957)
312. Reynolds, J. B., Christensen, R. L., Hamilton, D. R., Lemonick, A., Pipkin, F. M., and Stroke, H. H., *Phys. Rev.*, **99**, 613 (1955)
313. Brink, G. O., Hubbs, J. C., Nierenberg, W. A., and Worcester, J. L., *Phys. Rev.*, **104**, 189 (1957)
314. Brink, G. O., Hubbs, J. C., Nierenberg, W. A., and Worcester, J. L., *Bull. Am. Phys. Soc.*, [II], **1**, 343 (1956)
315. Berman, A., Kusch, P., and Mann, A. K., *Phys. Rev.*, **77**, 140 (1950)
316. Berman, A., *Phys. Rev.*, **86**, 1005 (1952)
317. Brink, G. O., Hubbs, J. C., Nierenberg, W. A., and Worcester, J. L., *Bull. Am. Phys. Soc.*, [II], **2**, 200 (1957)
318. Smith, K. F., *Proc. 2nd Conf. Molecular Beam* (Brookhaven National Lab., Upton, N. Y., October, 1956)
319. Smith, K. F., reported by Wu, C. S., *1954 Glasgow Conf. Nuclear and Meson Physics* (Pergamon Press, Ltd., London, England, 1955)
320. Worcester, J. L., Hubbs, J. C., and Nierenberg, W. A., *Bull. Am. Phys. Soc.*, [II], **2**, 316 (1957)
321. Worcester, J. L., Hubbs, J. C., and Marrus, R. (Private communication)
322. Childs, W. J., and Goodman, L. S. (Private communication)
323. Christensen, R. L., Bennewitz, H. G., Hamilton, D. R., Reynolds, J. B., and Stroke, H. H. (To be published)

324. Ewbank, W. B., Nierenberg, W. A., Shugart, H. A., and Silsbee, H. B., *Bull. Am. Phys. Soc.*, [II], **2**, 317 (1957)
325. Lipworth, E., and Garvin, H. L., *Bull. Am. Phys. Soc.*, [II], **2**, 316 (1957)
326. Reynolds, J. B., Christensen, R. L., Hooke, W. M., Hamilton, D. R., Stroke, H. H., Ewbank, W. B., Nierenberg, W. A., Shugart, H. A., and Silsbee, H. B., *Bull. Am. Phys. Soc.*, [II], **2**, 317 (1957)
327. Hauns, R. D., Jr., and Zacharias, J. R., *Phys. Rev.*, **107**, 107 (1957)
328. Hubbs, J. C., Marrus, R., Nierenberg, W. A., and Worcester, J. L., *Bull. Am. Phys. Soc.*, [II], **2**, 316 (1957)
329. Buck, P., Rabi, I. I., Senitzky, B., *Phys. Rev.*, **104**, 553 (1956)
330. Reynolds, J. B., *et al.* (Private communication)
331. Eck, T. G., Lurio, A., and Kusch, P., *Phys. Rev.*, **106**, 954 (1957)
332. Eck, T. G., and Kusch, P., *Phys. Rev.*, **106**, 958 (1957)
333. Feher, G., Fuller, C. S., and Gere, E. R. (To be published)
334. Pipkin, F. M., and Culvahouse, J. W., *Phys. Rev.*, **106**, 1102 (1957)
335. Abraham, M., Kedzie, R. W., and Jeffries, C. D., *Phys. Rev.* (To be published)
336. Abraham, M., Jeffries, C. D., Kedzie, R. W., and Wallman, J. C., *Phys. Rev.*, **106**, 1357 (1957)

HYPERONS AND HEAVY MESONS (SYSTEMATICS AND DECAY¹)

BY MURRAY GELL-MANN

*Department of Physics, California Institute of Technology,
Pasadena, California*

AND

ARTHUR H. ROSENFELD

*Department of Physics and Radiation Laboratory, University of California
Berkeley, California*

1. INTRODUCTION

We attempt, in this article, to summarize the information now available, both experimental and theoretical, on the classification and decays of hyperons and heavy mesons. Our principal emphasis is on the "weak interactions" responsible for the slow decays of these particles. The "strong interactions" involved in production and scattering phenomena form a separate topic, which we do not discuss at length. We do, however, mention the hyperfragments, the study of which bears on both kinds of interactions.

In Section 2 we take up some general features of elementary particle phenomena—the families of particles, the types of interactions, and some symmetry principles. The systematics of hyperons and heavy mesons is treated in Section 3 according to the "strangeness" theory. Section 4 is devoted to the weak interactions, not only of hyperons and heavy mesons, but also of the more familiar particles; we emphasize especially the recent work on non-conservation of parity and the classification of all weak processes. The detailed phenomenology of hyperon and heavy meson decays is discussed in Sections 5 and 6 respectively.

A great deal of the theoretical material is presented in a rather dogmatic way. We take for granted, for example, the correctness of charge independence, the strangeness theory, and the two-component neutrino, because we feel that an adequate discussion of the present experimental evidence on these questions would lead us too far afield. The reader must bear in mind that some of these theoretical principles may ultimately be proved wrong, although there is no doubt that they have been very useful so far.

In the phenomenological work we make extensive use of further hypotheses such as CP invariance, spin 0 for the heavy mesons, and spin $\frac{1}{2}$ for the hyperons. In the case of these assumptions, however, we give some discussion of the relevant experimental evidence, either in the text or in an appendix.

Most of the experimental data in the article are presented in the form of tables. In many cases, the numbers represent weighted averages of the results of many groups, and references to the individual experimental papers

¹ The survey of literature pertaining to this review was completed in July, 1957.

are to be found in the footnotes to the tables. We restrict ourselves, however, principally to the most recent work, and references to earlier research, including many pioneering experiments, must be looked for in the later papers. In particular, we apologize for having slighted the cosmic ray experiments, in which most of the salient features of the new particle field were first revealed.

Many references to theoretical papers are lacking also. An extensive list of these is given by Dalitz (R3). We present, at the beginning of the bibliography, six references to useful review articles and compilations of information on strange particles (R1 to R6).

2. ELEMENTARY PARTICLES

2.1. Field theory.—We are at present very far from having a satisfactory theory of the elementary particles. The enumeration of the particles, with their spins, their masses, and the nature and strength of their couplings must be taken wholly or largely from experiment. If we are given this information, we can attempt a detailed description of particle phenomena by means of the quantum theory of fields, which is, in fact, the only apparatus we have for such a description. It is not known, however, whether field theory, with its strict requirements of microscopic causality and relativistic invariance, is applicable to phenomena at very small distances, say $\sim 10^{-14}$ cm.²

At larger distances, field theory has scored some success. Quantum electrodynamics is in excellent accord with experiment; the Yukawa theory, especially in the simplified form studied by Chew and collaborators, gives a semi-quantitative description of the nucleon-pion system; and the Fermi theory of β -decay, later extended to other weak processes, has been very useful. It may be worthwhile to apply the methods of field theory to the new particles as well, but we do not attempt anything of the kind in this section. Let us refer, however, to one or two very general results of field theory.

2.2. Particle and antiparticle; CPT invariance.—The connection between spin and statistics is an example of a general principle that can be proved from the basic structure of field theory. Particles of integral spin must obey Bose-Einstein statistics and are called "bosons"; those of odd half-integral spin obey Fermi-Dirac statistics and are called "fermions."

Recently (1) attention has been called to another general property of present-day field theory:

For every particle there exists an antiparticle (which may or may not be identical with the particle itself). For every possible state Ψ of a system of particles, there is a possible state Ψ' of the corresponding system of antiparticles which looks just like the state Ψ with space and time inverted.

We may restate the result in terms of invariance. We define an operation

² We use the symbol \sim for "is of the order of magnitude of," \approx for "is approximately equal to," and \propto for "is proportional to."

C (called "charge conjugation") that carries each particle into its anti-particle without disturbing space-time, an operation P that reflects space coordinates, and an operation T that reverses time. Then what we are discussing is the automatic invariance of field theories under the product of these operations, CPT.³

The behavior of the electromagnetic field is such that particle and anti-particle have equal and opposite electric charge. Thus charged particles like π^+ and p have antiparticles distinct from themselves (π^- and \bar{p} , respectively). A neutral particle may be identical with its antiparticle (e.g., π^0 or the photon γ) or distinct from its antiparticle (e.g., n and \bar{n}).

From CPT invariance it follows that the spins, for example, of particle and antiparticle are the same and that their masses are exactly equal; if they are unstable, their lifetimes are equal as well (2).

In field theory, the destruction of a particle and the creation of its anti-particle are described by the same field operator and are closely related phenomena. In fact, we may say that scattering of a particle and the production and annihilation of particle-antiparticle pairs are all different forms of the same process. (For example, they are all described by the same Feynman diagram.)

2.3. Types of interaction.—All the known interactions of the elementary particles appear to fall into three categories: (a) The strong interactions, typified by the virtual Yukawa process $N \leftrightarrow N + \pi$ principally responsible for nuclear forces; here, N represents a nucleon (n or p). The strength of this process may be measured by the dimensionless coupling constant $g^2/4\pi\hbar c \approx 15$, or alternatively by the constant

$$f^2/4\pi\hbar c = \left(\frac{m_\pi}{2m_N} \right)^2 g^2/4\pi\hbar c \approx .08.$$

In general, the strong couplings are characterized by coupling constants of the order of unity. (b) The electromagnetic interaction, through which a photon may be virtually emitted or absorbed by any charged particle, real or virtual. Here the universal parameter of strength is the fine structure constant $e^2/4\pi\hbar c \approx 1/137$. (c) The weak interactions, of which the classic example is the β -decay coupling that induces the decay $n \rightarrow p + e^- + \bar{\nu}$.⁴ The Fermi constant C that measures the strength of β -decay⁵ is $\sim 10^{-49}$ erg cm.³ and can be written in dimensionless form only if a length is specified. For our purposes a convenient length is the Compton wave-length of the

³ The CPT invariance of field theory arises essentially from the Hermiticity of the Hamiltonian, which is necessary to insure positive probabilities. Roughly speaking, the operation CPT for a conventional field theory Hamiltonian is equivalent to Hermitian conjugation.

⁴ We use heavy arrows to denote strong or electromagnetic processes, whether real or virtual, for example, $n \leftrightarrow p + \pi^-$, $\pi^0 \leftrightarrow 2\gamma$. Light arrows indicate weak processes: $n \rightarrow p + e^- + \bar{\nu}$, etc.

⁵ There are really several such constants C ; they are defined in 4.1.

charged pion $\hbar/m_\pi c$; in terms of this we have $C \sim 10^{-7} \hbar c (\hbar/m_\pi c)^2$. Actually the probability of β -decay is proportional to C^2 and we may therefore take as a reasonable dimensionless measure of the strength of the weak couplings a value like 10^{-14} . That this estimate works not only for β -decay but for all the known weak interactions is a remarkable law of nature, the "universality of strength" of the weak couplings (see 4.1).

2.4. Families of particles.—The known elementary particles can be classified in the following way (see Table I): (a) The photon, which is coupled to all charged particles by the electromagnetic interaction. No other coupling of the photon is known except this familiar interaction with charges and currents; the apparent absence of other couplings is sometimes referred to as the principle (3) of "minimal electromagnetic interaction."

Thus the "anomalous moments" of proton and neutron, for example, are attributed not to a special magnetic coupling of these particles but to the ordinary interaction of the electromagnetic field with the charges and currents of the meson cloud. (b) Baryons and antibaryons, which are fermions possessing strong couplings and satisfying a rigorous conservation law, the "conservation of baryons." This is the law responsible for the stability of nuclei; it states that baryons (such as the proton) cannot be created or destroyed except in baryon-antibaryon pair production and annihilation. However, one baryon may be transformed into another, as when a neutron turns into a proton in β -decay. The word "hyperon" means an elementary particle heavier than the nucleon. In fact, all the known hyperons are baryons: they are fermions and they are made from nucleons and ultimately decay into nucleons. The antihyperons have not yet been observed, but the recent discovery of the antiproton and antineutron makes it virtually certain that antihyperons exist also, as required by CPT invariance. (c) Mesons, which in our terminology are bosons possessing strong couplings. (We do not call the muon a meson, but a lepton.) Unlike baryons, mesons can be created or destroyed; they are radiated or absorbed in the course of baryon transformations much as photons are radiated or absorbed by charged particles. The lightest known meson is the pion. The term " K particle" is applied in principle to any particle intermediate in mass between pion and nucleon. In fact, the known K particles are "mesons," in our sense of the word. (d) Leptons, which are fermions possessing no strong couplings. (Strictly speaking, we should distinguish, as in Table I, between leptons and antileptons, but the nature of this distinction is only now becoming clear. See 4.4.)

The known leptons, all with spin $\frac{1}{2}$, are the electron and positron e^- and e^+ , the negative and positive muon μ^- and μ^+ , and the neutrino and antineutrino. The last two we shall denote by ν and $\bar{\nu}$ respectively or else, for convenience, by $+\nu$ and $-\nu$ respectively. Thus instead of writing " $\pi^+ \rightarrow \mu^+ + \nu$ " and " $\pi^- \rightarrow \mu^- + \bar{\nu}$ " we shall write " $\pi^\pm \rightarrow \mu^\pm \pm \nu^\pm$ ".

2.5. Nonconservation of parity; hypothesis of CP invariance.—We have mentioned in 2.2 the automatic invariance under CPT of field theories, for which one need assume only invariance under Lorentz transforma-

TABLE I
MASSES AND LIFETIMES OF ELEMENTARY PARTICLES

	Particle	Spin	Mass (Errors represent standard deviation) (Mev)	Mass difference (Mev)	Mean life (sec)	Decay rate (number per second)
Photons	γ	1	0		stable	0.0
Leptons and antileptons	$\nu, \bar{\nu}$ e^-, e^+ μ^-, μ^+	$\frac{1}{2}$	0 0.510976* $105.70 \pm 0.06^*$		stable stable $(2.22 \pm 0.02) \times 10^{-6}^*$	0.0 0.0 0.45×10^6
Mesons	π^\pm π^0 K^\pm K^0	0	$139.63 \pm 0.06^*$ $135.04 \pm 0.16^*$ 494.0 ± 0.20 (a) 493 ± 5 (Th)	4.6* 1 \pm 5	$(2.56 \pm 0.05) \times 10^{-8}^*$ $(0.0 < \tau < 0.4) \times 10^{-15}$ (O) $(1.224 \pm 0.013) \times 10^{-8}$ (b) $K_1: (0.95 \pm .08) \times 10^{-10}$ (P) $K_t: (3 < \tau < 100) \times 10^{-8}$ (L)(P)	0.39×10^8 $> 2.5 \times 10^{16}$ 0.815×10^8 1.05×10^{10} $(> 0.01 < 0.3) \times 10^8$
Baryons†	p n Λ Σ^+ Σ^- Ξ^0 Ξ^- Ξ^0	$\frac{1}{2}$ $\frac{1}{2}$ $\frac{1}{2}$? $\frac{1}{2}$? $\frac{1}{2}$? $\frac{1}{2}$? ?	$938.213 \pm 0.01^*$ $939.506 \pm 0.01^*$ 1115.2 ± 0.13 (B) 1189.3 ± 0.35 (B) 1196.4 ± 0.5 (B) 1188.8 ± 2 (g)		stable $(1.04 \pm 0.13) \times 10^{+8}^*$ $(2.77 \pm 0.15) \times 10^{-10}$ (d) $(0.78 \pm 0.074) \times 10^{-10}$ (e) $(1.58 \pm 0.17) \times 10^{-10}$ (f) $(< 0.1) \times 10^{-10}$ (A) theoretically $\sim 10^{-19}$ $(4.6 \pm \tau < 200) \times 10^{-10}$ (Tr) ?	0.0 0.96×10^{-8} 0.36×10^{10} 1.28×10^{10} 0.64×10^{10} $> 10 \times 10^{10}$ theoretically $\sim 10^{19}$ $(> 0.005, < 0.2) \times 10^{10}$

* From compilations by Cohen, Crowe, and DuMond, *Nuovo cimento*, **5**, 541 (1957), and "Fundamental Constants of Physics," to be published by Interscience, New York, 1957. They include all data available before January 1, 1957.

† Antibaryons have the same spin, mass, and mean life as baryons.

(A) Alvarez, Bradner, Falk-Vairant, Gow, Rosenfeld, Solmitz, and Tripp, K^- Interactions in Hydrogen, UCRL-3775, May 1957.

(B) Barkas and Rosenfeld UCRL-8030, (1957).

(L) Lande, Booth, Impeduglia, Lederman, and Chinowsky, *Phys. Rev.*, **103**, 1901 (1956).

(O) Orear, Harris, and Taylor, *Bull. Am. Phys. Soc.*, **2**, 26.

(P) Plano, Samios, Schwartz, and Steinberger, *Phys. Rev.* (to be published) 1957.

(Th) Thompson, Burwell, and Huggett, Supplement 2 *Nuovo cimento*, **4**, 286 (1956).

(Tr) G. H. Trilling and G. Neugebauer, *Phys. Rev.*, **104**, 1688 (1956).

(W) R. S. White, compilation of all emulsion data available from all laboratories, prepared for 7th Rochester Conference (private communication).

(a) $m_{K^\pm} = 3m_\pi \pm Q_T$, where Q_T is the weighted average from Heckman, Smith, and Barkas, *Nuovo cimento*, **4**, 51 (56); from Roy Haddock, *Nuovo cimento*, **4**, 240 (56); and from Bacchella, Berthelot, et al., *Nuovo cimento*, **4**, 1529 (56). We have assumed that the K^- is the antiparticle of the K^+ and shares the same mass and lifetime. The present experimental mass of the K^- is consistent with this assumption, namely 493.4 ± 0.5 Mev (W).

(b) Weighted average of

1.227 ± 0.015 (Alvarez, Crawford, Good, and Stevenson, *Phys. Rev.* (to be published)).

1.211 ± 0.026 (V. Fitch and R. Motley, *Phys. Rev.*, **101**, 496 (1956); *Phys. Rev.*, **105**, 265 (1957); and private communication). The quoted errors are statistical only. We have assumed that the K^- is the antiparticle of the K^+ and shares the same mean life. The present experimental mean life is consistent with this assumption, namely $\tau_{K^-} = 1.25 \pm 0.11$ (W. H. Barkas, Seventh Rochester Conference).

(d) Weighted average of

1.9 ± 0.4 (Graves, Brown, Glaser, and Perl, *Bull. Am. Phys. Soc.*, **2**, 221 (1957)).

2.77 ± 0.2 (Eisler, Plano, Samios, Steinberger, and Schwartz, *Bull. Am. Phys. Soc.*, **2**, 221 (1957)).

3.1 ± 0.5 (A)

$3.25 \pm 0.33^*$

(e) Weighted average of

0.95 ± 0.30 (Graves, Brown, Glaser, and Perl, *Bull. Am. Phys. Soc.*, **2**, 221 (1957)).

0.69 ± 0.1 (A)

0.89 ± 0.12 (compilation of all emulsion data available from all laboratories, prepared for 7th Rochester Conference by G. Snow (private communication)).

(f) Weighted average of

1.5 ± 0.35 (Eisler, Plano, Samios, Steinberger, and Schwartz, *Bull. Am. Phys. Soc.*, **2**, 221 (1957)).

1.6 ± 0.2 (A)

(g) Combined result from Alvarez et al., K^- Interactions in Hydrogen, UCRL-3583, Nov. 1956, and a private communication from M. Schwartz and R. Plano giving $Q = 73.5 \pm 3.5$ for $\Xi^0 \rightarrow \Lambda + \gamma + Q$.

tions (those not involving space or time inversion). Until recently it was thought that the laws of physics were also invariant under C, P, and T separately. (For the strong and electromagnetic interactions, this still appears to be true. See 3.10.)

Let us discuss in particular invariance under P, which is equivalent to the conservation of the quantum number called parity (also denoted by P). If parity is exactly conserved, then physical laws do not distinguish between right and left: the mirror reflection of any state of a system of particles is also a possible state of the same system of particles. The conservation of parity is now known to be violated by the weak interactions. This was first suspected in K particle decay (see Section 6). It was then suggested by Lee and Yang (4) that nonconservation of P be looked for in nuclear β -decay and in the decays of π^\pm and μ^\pm . Their conjectures were brilliantly confirmed by a series of experiments early in 1957 (see Section 4). As an example, we may take the β^- -decay of oriented Co^{60} . The spinning nucleus emits electrons preferentially "down," where "up" is defined by the nuclear spin using the right hand rule. The angular distribution of electrons is of the form $1+a \cos \theta$ with a around -1 for the fastest electrons (5); the "up-down" ratio is then $(1+a)/(1-a)$. Clearly parity is not conserved; the mirror image of decaying Co^{60} is not a possible state of Co^{60} .

Does this mean that the microscopic laws of nature do define a right hand? Not necessarily. There is still the possibility that physical laws are exactly invariant under CP, i.e., that the mirror reflection of a state of a system of particles is always a possible state of the corresponding system of antiparticles. For example, the β^+ -decay of anti- Co^{60} would then have an angular distribution exactly the opposite of that of Co^{60} , namely $1-a \cos \theta$. We could then not define a right hand by means of β -decay unless we specified that we were talking about matter and not antimatter. But there would be no intrinsic way to tell matter from antimatter except the very handedness we are trying to define.

Exact invariance under CP was predicted by Landau (6). So far all the experiments on nonconservation of parity are consistent with this hypothesis, but further tests of its validity are still required.⁶ In Appendix A we discuss the possibility of interpreting present information without CP invariance, but in the text we shall make extensive use of the hypothesis.

Let us emphasize here that if CP invariance should fail in β -decay, then for a nucleus like Ag^{111} , if it could be oriented, the β^- angular distribution would be, say, $1+b \cos \theta$ and yet the β^+ angular distribution of oriented

⁶ Given nonconservation of P the conservation of CP implies, of course, nonconservation of C. The nonconservation of C has been verified spectacularly in all of the parity experiments involving neutrinos, which suggest that the neutrino is always right circularly polarized, while its charge conjugate, the antineutrino, is always left circularly polarized. (See Section 4.) This is evidently a clear-cut violation of C invariance.

anti-Ag^{III} would be $1 - b' \cos \theta$ with b' different from b .⁷ This difference would permit an absolute definition of matter and antimatter and of right and left.

2.6. Consequences of CP invariance; T invariance.—If CP is an exact symmetry of nature, then isolated matter and antimatter differ only in handedness. The decay schemes of particle and antiparticle are always exactly the same and their decays mirror images of each other. (We assume here that particle and antiparticle always decay into different final states, as π^+ and π^- do because of conservation of charge or as n and \bar{n} do because of conservation of baryons. When particle and antiparticle can decay into the same final states, we have a quite different situation like the one described in 3.9.)

Just as P invariance would be equivalent to the conservation of the quantum number P, so CP invariance is equivalent to the conservation of a quantum number CP. However, CP is less directly useful as a quantum number than P would be, since a system of particles can be in an eigenstate of CP only when it is neutral, has equal numbers of baryons and antibaryons, etc. For example, a deuteron cannot be in an eigenstate of CP, since charge conjugation would turn it into an antideuteron.

However, a neutral pair of pions $\pi^+ + \pi^-$ or $2\pi^0$ in their center of mass system *are* in an eigenstate⁸ of CP with eigenvalue +1. In 3.9 we shall use this result, together with the assumption of exact CP invariance, to prove that a particle (K_2^0) with $CP = -1$ cannot decay into two pions, even through the weak interactions.

If CP is exactly conserved, then the CPT invariance of field theory guarantees exact symmetry under time reversal T. Now T invariance does not correspond directly to a conservation law. Instead, it determines the *phases* of transition matrix elements (7a, 7b). The contrast between the behavior of T and that of other symmetry operators, such as CP or angular momentum, can be appreciated if we introduce the famous unitary operator

⁷ We have chosen Ag^{III} rather than Co⁶⁰ as an example here because the difference between b' and b probably vanishes for Co⁶⁰, while it must be non-zero for Ag^{III} if CP invariance is violated in β -decay and if the two-component theory of the neutrino is correct. This can be shown, using scalar and tensor (or vector and axial vector) interactions (and assuming that nuclear matrix elements do not accidentally vanish), from the fact that the transition is of the form $\frac{1}{2}^+ \rightarrow \frac{1}{2}^-$. The difference $b' - b$ arises from a Coulomb effect.

⁸ For two identical bosons such as $2\pi^0$, the wave function must be symmetric under the operator X that exchanges the two particles, i.e., $X = +1$. For π^+ and π^- , which are not identical, we can define a generalized wave function by including a charge coordinate that distinguishes π^+ and π^- . This generalized wave function must again be symmetric under the exchange operator X, since boson field operators commute.

Now for either case, $2\pi^0$ or $\pi^+ + \pi^-$, the operator X is identical with CP in the center of mass system, because CP interchanges both charge and position for the two particles. Thus $CP = X = +1$.

S . Often called the S matrix, it transforms initial into final states in a collision problem. The law of conservation of CP may be written in the form $CPS = SCP$ and this implies that the eigenvalue of CP is the same before and after the collision. In the case of time reversal, however, the initial and final states must be interchanged, so that T invariance implies $TS = S^{-1}T$. This relation does not give selection rules; but when it is combined with the unitarity of S , it gives conditions on the phases of S matrix elements. For example, in the photopion effect $\gamma + N \rightarrow \pi + N$ there is the following familiar result (7b). The phase of the matrix element leading to a final state of given energy, angular momentum, parity, and isotopic spin is given by the phase shift for the scattering $\pi \leftrightarrow N + \pi + N$ in the same state. (Strictly speaking, this particular statement is true only to lowest order in the fine structure constant.)

Landau (6) has pointed out that CP or T invariance forbids the existence of static electric dipole moments for elementary particles, even when P invariance is violated. Consider the neutron, for example. A tiny fraction of the time it is virtually dissociated into proton, electron, and antineutrino. The wave function ψ of this system contains both even and odd parity terms ψ_e and ψ_o , respectively, since P is not conserved in β -decay. We might therefore expect that the electric dipole moment operator D could have a small expectation value $(\psi_e, D\psi_o) + (\psi_o, D\psi_e)$ for the neutron. However, it can be shown that T invariance requires ψ_e and ψ_o to be 90° out of phase, so that the expectation value of the real operator D is zero.

Of course if two elementary particles with spin were degenerate with each other and electromagnetic transitions were allowed between them, then a static electric dipole moment might arise (approximately as it does for molecules.) No such situation is known, however, among the particles.

3. THE NEW PARTICLES; STRANGENESS THEORY

3.1. Charge independence.—A striking property of the strong interactions and the particles that possess them (baryons, antibaryons, and mesons) is the principle of *charge independence* or *conservation of isotopic spin* (8).

Each strongly coupled particle belongs to a charge multiplet with an isotopic spin quantum number I and multiplicity $2I+1$. The components of the multiplet are characterized by values of I_z ranging from $-I$ to I ; corresponding to the variation of I_z there is a variation in the electric charge which increases in steps of e as I_z increases in steps of one. These properties are illustrated in Figure 1 and by Eq. 1 below. Each multiplet carries an isotopic spin vector I and the charge independence of the strong interactions means that they conserve the total I in any process. Similarly, the strong interactions leave all charge multiplets rigorously degenerate.

Electromagnetic interactions are manifestly charge dependent. They violate the conservation of isotopic spin and remove the degeneracy of the charge multiplets. For example, the $n-n$ and $p-p$ forces are identical as far as the strong interactions are concerned, but the Coulomb force obviously destroys the equality. Similarly, electromagnetic effects presumably give

rise to the mass difference between neutron and proton. (See 3.5.)

3.2. *Conservation of strangeness.*—Although it violates conservation of I , the electromagnetic interaction does not affect the conservation of I_s . We can understand this on the basis of "minimal electromagnetic interaction." The photon is coupled only through the charge; since the charge is a function of I_s , we see that the electromagnetic coupling transforms in isotopic spin space like a function of I_s and commutes with the total I_s .

The conservation of I_s is usually restated in a more convenient form. We write the relation between charge and I_s for the members of a multiplet as follows:

$$Q/e = I_s + \frac{1}{2}Y \quad 1.$$

Here $\frac{1}{2}Y$ is the center of charge, or average charge, of the multiplet; it is indicated by a fulcrum in Figure 1. Since Q/e is always integral, we see that Y is an even integer when I is integral and an odd integer when I is half-integral. Since Q is rigorously conserved, the conservation of I_s is the same as the conservation of Y .

A still more convenient notation can be used if we introduce the quantity

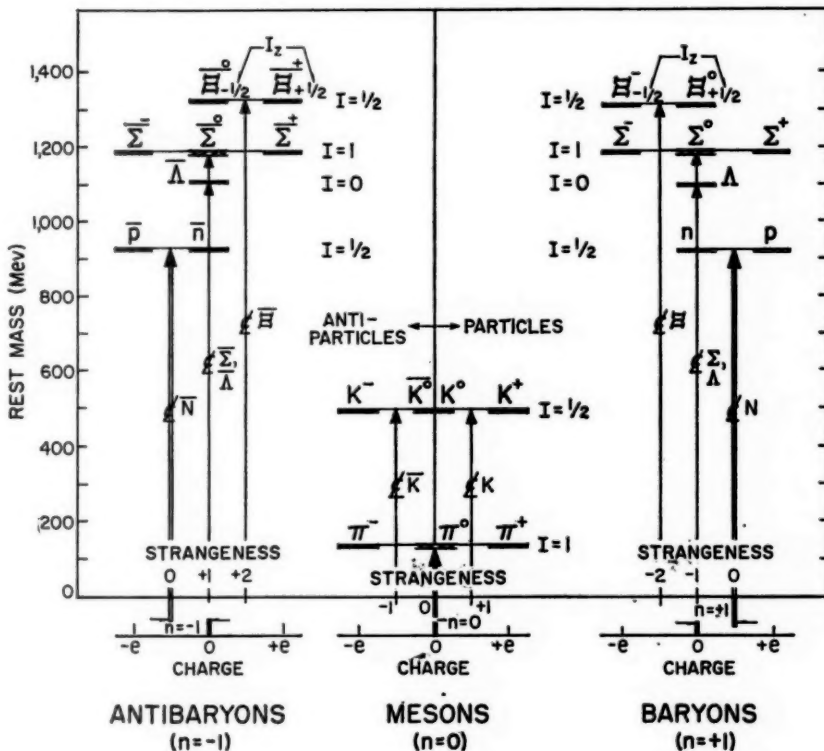


FIG. 1. Strongly interacting particles (SIPs). Particles unstable against electromagnetic decay are represented with a dotted bar; the rest are drawn solid.

n , the number of baryons minus the number of antibaryons. The law of conservation of baryons then states that the "baryon number" n is rigorously conserved. For the nucleon, antinucleon, and pion the center of charge $\frac{1}{2}Y$ is just equal to $\frac{1}{2}n$; that is, it is $+\frac{1}{2}$ for the nucleon, and $-\frac{1}{2}$ for the antinucleon, and 0 for the pion. We can measure the displacement of the center of charge from its familiar values, therefore, by writing $Y=n+S$ or

$$Q/e = I_z + \frac{1}{2}n + \frac{1}{2}S \quad 2.$$

S is then an integer, conserved whenever I_z is, and zero in the case of nucleon (N), antinucleon (\bar{N}), and π . It is called "strangeness" and the strongly coupled particles for which $S \neq 0$ are "strange" particles. The quantum number S is conserved by both strong and electromagnetic interactions; since these conserve I_z ; only the weak interactions can violate *conservation of strangeness* (3, 9, 9a).

3.3. *The strange particles.*—The known hyperons are all strange baryons and the known K particles are strange mesons (right-hand column of Fig. 1.)

Let us consider the baryons first. The nucleon N , of course, is a doublet with $S=0$, consisting of the proton p and the neutron n . The strange baryons are, in order of increasing mass: Λ , a singlet with $S=-1$ (Λ). Σ , a triplet with $S=-1$ (Σ^+ , Σ^0 , Σ^-). Ξ , a doublet with $S=-2$. (Ξ^0 , Ξ^- . The Ξ^0 is so far hypothetical.)

The antibaryons (left-hand column of Fig. 1) follow the same pattern, but with the signs of charge, strangeness, and I_z all reversed.⁹ So far only the antinucleons have been detected experimentally.

Finally we have the mesons (middle column of Fig. 1). The pion is a triplet with $S=0$ (π^+ , π^0 , π^-). The strange mesons are a pair of doublets: K^+ and K^0 , with $S=+1$, and \bar{K}^0 and K^- with $S=-1$. We shall speak of the first doublet collectively as K and the second as \bar{K} ; this notation emphasizes that K and \bar{K} are each other's antiparticles.

In principle the symbol K should be reserved for the class of all particles with masses between m_π and m_N . However, this causes no difficulty at present since the specific particles we call K and \bar{K} are the only members of the class now known.

3.4. *Conservation of S and I in particle reactions.*—The rule that $\Delta S=0$ in strong and electromagnetic processes gives not only particle stability, as discussed in 3.2, but also severe restrictions on particle reactions. For example, in all collisions of nucleons, pions, and antinucleons the initial strangeness is zero. If in such collisions a strange particle is produced ($S \neq 0$), it must be accompanied by at least one other strange particle; this is the famous law of "associated production." However, the conservation of strangeness is much more stringent than the requirement of associated production. For example, processes like $\pi+N \Rightarrow \bar{K}+\Sigma$ or $N+N \Rightarrow \Lambda+\Lambda$ are forbidden while $\pi+N \Rightarrow K+\Sigma$ and $\gamma+N \Rightarrow K+\Lambda$ are allowed.

⁹ We can see that this arrangement is necessary since production and annihilation of particle-antiparticle pairs must be possible without violating conservation laws. (See 2.2.)

Besides the conservation of I_s , or strangeness, we must take into account conservation of total I (or charge independence) in strong processes involving the new particles. Of course the latter law requires corrections from electromagnetic effects, which the former does not.

Charge independence tells us, for example, that the force between Λ and the proton is the same as between Λ and the neutron. It gives us also intensity rules like the following (3, 10):

$$d\sigma(K^- + d \Rightarrow \Lambda + n + \pi^0) = \frac{1}{2} d\sigma(K^- + d \Rightarrow \Lambda + p + \pi^-) \quad 3.$$

and

$$d\sigma(K^- + d \Rightarrow \Sigma^0 + \pi^- + p) = d\sigma(K^- + d \Rightarrow \Sigma^- + \pi^0 + p). \quad 4.$$

The electromagnetic corrections to such rules are small (perhaps of the order of the fine structure constant ~ 1 per cent in amplitude) and the rules are therefore quite useful. These rules have not yet been tested in experiments with strange particles, but they can easily be checked by stopping K^- in a deuterium bubble chamber.

3.5. Electromagnetic mass differences. Apart from the Coulomb force, the most striking effect of the electromagnetic violation of charge independence is the removal of degeneracy of charge multiplets. The neutron-proton mass difference of 1.3 Mev has, of course, been known for a long time. Its electromagnetic origin was long in doubt, since it was hard to understand why the neutron should be heavier. Recently Feynman & Speisman (11) have shown, by means of a crude model, that electromagnetic effects could give a heavier neutron. However, we have no quantitative theory of the mass differences, and we shall restrict ourselves to the experimental facts. (See Table I.)

The mass difference between charged and neutral K particles is very poorly known; the mass of K^+ has been accurately determined but we know about the mass of K^0 only that it is the same to within ~ 5 Mev. The mass difference of charged and neutral pions (4.6 Mev) is best measured by means of the Panofsky effect: $\pi^- + p \Rightarrow \pi^0 + n$ for captured π^- .

Next the baryons—we have mentioned the nucleon above; we have no information about Ξ since Ξ^0 has never been detected; Λ is a singlet; thus we have only the Σ triplet to discuss. The difference in mass of Σ^+ and Σ^- (7.2 ± 0.1 Mev with Σ^- heavier, see Table I) has been determined as follows by emulsion workers. About 1 per cent of the K^- which come to rest in emulsion are captured by free protons to give the reactions $K^- + p \Rightarrow \Sigma^\pm + \pi^\mp$. The difference in the Σ ranges $R_- - R_+$ leads to an accurate determination of the mass difference. The difference in mass between the charged and neutral Σ cannot be measured with such an accurate tool as emulsions, and at present we know only that Σ^0 and Σ^+ have the same mass within ± 3 Mev: Σ^- particles have been captured by protons in a hydrogen bubble chamber, yielding $\Sigma^0 + n$, followed by the decay sequence $\Sigma^0 \Rightarrow \gamma + \Lambda$, $\Lambda \rightarrow p + \pi^-$. However only three such complete sequences have been seen (11a) and a more accurate though less direct value for m_{Σ^0} has been obtained with a propane bubble chamber by observing the gamma ray in the sequence of

processes $\pi^- + p \Rightarrow \Sigma^0 + K^0$, $\Sigma^0 \Rightarrow \gamma + \Lambda$ (12). The mass of Σ^0 can then be determined with respect to that of Λ , which is known to about $\frac{1}{2}$ Mev.

3.6. Stability and electromagnetic decay.—In the presence of strong and electromagnetic interactions only, the particles we have listed would, with three exceptions, all be stable. Although allowed by conservation of S , such decays as $N \Rightarrow P + \pi^-$ or $\Lambda \Rightarrow P + K^-$ or $\Sigma^+ \Rightarrow \Lambda + \pi^+$ are forbidden by conservation of energy. Energetically possible decays like $\Lambda \Rightarrow p + \pi^-$ or $K^+ \Rightarrow \pi^+ + \pi^0$ are forbidden by conservation of strangeness.

The exceptions are the particles π^0 , Σ^0 and $\bar{\Sigma}^0$. Each of these would be stable under strong interactions only, but they can all decay electromagnetically. The π^0 meson, like the vacuum, has zero charge and zero strangeness and thus the transition $\pi^0 \Rightarrow$ vacuum can occur with the emission of two γ rays. The necessary change of I by one unit is easily accomplished by the electromagnetic coupling.¹⁰ This process $\pi^0 \Rightarrow 2\gamma$ is known experimentally to have a mean life of $\lesssim 10^{-15}$ sec. (See Table I.)

In a similar way, the transition $\Sigma^0 \Rightarrow \Lambda + \gamma$ requires no change in charge or strangeness and a change of I by only one unit. A rough theoretical estimate of the lifetime can be obtained if we assume a magnetic dipole transition between particles of spin $\frac{1}{2}$, with a transition magnetic moment of the same order as the neutron magnetic moment. We then obtain a Σ^0 lifetime $\tau \sim 5 \times 10^{-20}$ sec. Such a mean life is rather inaccessible to experiment. It is not long enough to permit Σ^0 to go a measurable distance before decaying ($c\tau = 1.5 \times 10^{-9}$ cm.); nor is it short enough to produce a measurable width of the Σ^0 state ($\hbar/\tau = 10$ Kev). There are no direct measurements of this width (even the mass is unknown to ± 3 Mev). In fact, the present experimental limits on the mean life of Σ^0 are roughly analogous to a determination that the moon is closer than the sun and farther than the ceiling.

3.7. Decay through the weak interactions.—So far we have ignored the effects of the weak interactions. It is very difficult to observe their effects in collision processes, because of the extremely small cross-sections involved. To date only one such experiment has been successful: the search (12) for inverse β -decay $\bar{\nu} + p \rightarrow e^+ + n$, with a cross-section around 4×10^{-44} cm.² (averaged over the spectrum of high-energy neutrinos from a pile).

In collisions involving strange particles, violations of the strangeness selection rules by the weak interactions should be of the order of one part in 10^{13} or 10^{14} , since this is the magnitude of the dimensionless strength parameter of Section 2.3.

Thus the weak interactions manifest themselves almost exclusively in

¹⁰ The electromagnetic interaction is proportional to charge Q and therefore linear in I_z (see Eq. 1). In other words, it transforms in isotopic spin space like a scalar plus the z -component of a vector. Therefore, each time the electromagnetic coupling occurs (in the sense of perturbation theory) it can change the total isotopic spin either by zero or by one unit ($|\Delta I| = 0$ or 1). A first order electromagnetic process (first order in e in the amplitude) can change I by as much as one unit, a second order process by as much as two units, etc.

decay processes.¹¹ We have seen that most mesons and baryons are stable in the absence of the weak interactions; they "wait," so to speak, for the weak couplings to induce their decay. A typical lifetime for weak decay can be estimated by taking a "nuclear time" like $(\hbar/m_\pi c^2) \sim \frac{1}{2} \times 10^{-22}$ sec. and multiplying it by 10^{13} or 10^{14} . In fact the lifetimes do range mostly from 10^{-8} to 10^{-10} sec. Of course, severely limited phase space in the final state can vastly increase the lifetime, as in the case of the neutron, which has a mean life of about 1040 sec.

All the baryons, antibaryons, and mesons that are stable under strong and electromagnetic effects disintegrate by means of the weak interactions, with the exception of the proton and antiproton, which are absolutely stable since they are the lightest baryon and antibaryon, respectively.

Let us refer to baryons, antibaryons, and mesons as "strongly interacting particles" or *SIPs*. The disintegration products in the weak decay of a *SIP* are either: (a) *SIPs* alone, as in the case $\Lambda \rightarrow p + \pi^-$, or (b) a lepton-antilepton pair, with or without *SIPs*, as in the decays $n \rightarrow p + e^- + \bar{\nu}$, $K^+ \rightarrow \mu^+ + \nu$, $K^+ \rightarrow \mu^+ + \nu + \pi^0$, etc.

There are also decays involving both weak and electromagnetic interactions. These "weak electromagnetic decays" may be either inner bremsstrahlung processes or else decays in which a γ -ray is essential.

3.8. Decay into strongly interacting particles; possible selection rules.—The weak interactions are known to induce the following decays of *SIPs* into *SIPs*, in violation of conservation of strangeness: Baryons— $\Xi \rightarrow \Lambda + \pi$, $\Sigma^\pm \rightarrow N + \pi$, $\Lambda \rightarrow N + \pi$. Antibaryons—presumably the corresponding processes. Mesons— $K \rightarrow 2\pi$, $K \rightarrow 3\pi$, $\bar{K} \rightarrow 2\pi$, $\bar{K} \rightarrow 3\pi$.

These are all the energetically possible decays of this kind allowed by conservation of baryons, with one exception: the unobserved decay $\Xi \rightarrow N + \pi$. Since only about a dozen Ξ events have been observed, all in cosmic rays, it is by no means clear that this process is absent. However, if it is indeed forbidden, it is significant that it involves a change in strangeness of two units, while all the others involve a change of only one unit. It may be, then (9a), that there is a rule $\Delta S = \pm 1$ for weak decays of *SIPs* into *SIPs* or, what is the same thing, a rule $\Delta I_z = \pm \frac{1}{2}$. It is important that this rule be checked by a further search for decays of the form $\Xi^- \rightarrow \pi^- + n$ or $\Xi^0 \rightarrow \pi^- + p$.

In the decays we are discussing, not only strangeness but isotopic spin too is defined in initial and final states. It has been suggested that there may be a further rule (9a) that $|\Delta I| = \frac{1}{2}$. This would, of course, be subject to electromagnetic corrections. In Sections 5 and 6 we discuss the evidence for and against the rule.

A convenient formal device for treating the rule $|\Delta I| = \frac{1}{2}$ was introduced

¹¹ The absorption of μ^- by nuclei is, of course, a weak process and well known experimentally, although not a decay. However, the absorption always takes place from the ground state of a muonic atom, which would be stable in the absence of the absorption. The situation is therefore just like that of a decaying particle.

by Wentzel (R1). In a weak decay of an *SIP* into *SIPs*, we imagine that an additional particle is emitted or absorbed that carries no energy or momentum or charge, but does carry an isotopic spin of $\frac{1}{2}$, with whichever z -component ($\pm \frac{1}{2}$) is needed to balance I_z in the reaction. This particle is aptly named the "spurion." With the spurion included, we then assume that I is conserved in the decay process. Such an assumption is clearly equivalent to the rule $|\Delta I| = \frac{1}{2}$. For applications of the spurion method, see for example 5.6 and 5.7.

3.9. Decay of neutral K particles; K_1^0 and K_2^0 .—The weak decays of the strange particles K^0 and \bar{K}^0 are subject to some interesting special considerations. The reader will note that in Table I we do not list lifetimes for K^0 and \bar{K}^0 . The reason is that neither of these particles has a unique lifetime. Instead, we must consider two linear combinations of the states representing K^0 and \bar{K}^0 ; these combinations are called K_1^0 and K_2^0 and it is they that are characterized by unique lifetimes τ_1 and τ_2 respectively. This situation was predicted theoretically (14) on the basis of the strangeness theory and has since been confirmed in several respects by experiment (15).

In our discussion we assume, as before, the exact conservation of CP, or, what is equivalent, exact symmetry under time reversal T. (In the original treatment (14), exact conservation of C was taken for granted even for the weak interactions; the old argument can, however, be modernized if we replace C by CP. The possibility of nonconservation of CP is taken up in Appendix A.)

In the production of a neutral K particle, the conservation of strangeness brings about a sharp distinction between K^0 and \bar{K}^0 . Only K^0 , for example, can be produced in the reaction $\pi^- + p \rightarrow K^0 + \Lambda^0$; only \bar{K}^0 in the reaction $K^- + p \rightarrow \bar{K}^0 + n$. However, in the subsequent decay of an isolated K^0 or \bar{K}^0 , strangeness is not conserved and plays no important role. We must consider instead the quantum number CP, which is conserved in the decay.

For convenience, let us take K to be spinless. Denote by $|K^0\rangle$ the state of a K^0 meson at rest and by $|\bar{K}^0\rangle$ the state of a \bar{K}^0 meson at rest. These are eigenstates of strangeness with eigenvalues +1 and -1, respectively. In each of the reactions mentioned above, the produced meson, in its own rest frame, is in one of these states. Now under CP these two states evidently go into each other, since K^0 and \bar{K}^0 are antiparticles. We can adjust the relative phase of the states so that CP $|K^0\rangle = |\bar{K}^0\rangle$ and CP $|\bar{K}^0\rangle = |K^0\rangle$.

In treating the decay, we must form eigenstates of CP instead of strangeness: we define $|K_1^0\rangle \equiv 2^{-1/2}(|K^0\rangle + |\bar{K}^0\rangle)$ and $|K_2^0\rangle \equiv 2^{-1/2}(|K^0\rangle - |\bar{K}^0\rangle)$. Then $|K_1^0\rangle$ corresponds to the eigenvalue +1 and $|K_2^0\rangle$ to the eigenvalue -1 of CP. We may refer to these states as even and odd respectively under CP. The equations defining $|K_1^0\rangle$ and $|K_2^0\rangle$ may be inverted so that the original states $|K^0\rangle$ and $|\bar{K}^0\rangle$ are expressed in terms of them: $|K^0\rangle = 2^{-1/2}(|K_1^0\rangle + |K_2^0\rangle)$ and $|\bar{K}^0\rangle = 2^{-1/2}(|K_1^0\rangle - |K_2^0\rangle)$.

We may say, then, that the production of a K^0 meson (or a \bar{K}^0 meson) corresponds to the production, with equal probability and prescribed relative phase, of a " K_1^0 meson" or a " K_2^0 meson." Each particle K_1^0 or K_2^0 is

its own antiparticle, the former being even under CP and the latter odd under CP. Since CP is assumed conserved in the decay, some decay modes are available to K_1^0 that are forbidden to K_2^0 and vice versa. Thus these two particles must have different lifetimes.

For example, consider the familiar decay into two pions $\pi^+ + \pi^-$ or $\pi^0 + \pi^0$; this final state is even under CP, as we have mentioned in 2.6. Thus decay into two pions is allowed for K_1^0 and forbidden for K_2^0 . Now in fact two neutral K particles have been observed. One of these decays nearly always into 2π and has a lifetime of about 10^{-10} sec.; it is to be identified with the theoretical K_1^0 meson. The other has a much longer lifetime (at least 300 times longer) and does not appear to give 2π ; it must be the K_2^0 meson. Apparently the 2π decay has a much higher rate than other possible modes for either K_1^0 or K_2^0 .

Suppose now we generate a "beam" of 1000 K^0 mesons, for example, by the reaction $\pi^- + p \Rightarrow \Lambda^0 + K^0$. In terms of K_1^0 and K_2^0 , we have 500 of each. After around 10^{-9} sec. (in the rest system of the mesons), nearly all the K_1^0 have decayed, mostly into 2π ; very few of the K_2^0 have decayed, however. Our "beam" now contains about 500 K_2^0 . These are not in a pure state of strangeness. They have with equal probability $S = +1$ and $S = -1$. In striking matter, half of them (around 250) are capable of reactions like $K^0 + p \Rightarrow K^+ + n$ characteristic of $S = +1$ and the other half are capable of reactions like $\bar{K}^0 + n \Rightarrow K^- + p$ or $\bar{K}^0 + p \Rightarrow \Sigma^+ + \pi^0$ characteristic of $S = -1$ (15). This behavior of the "stale beam" is to be contrasted with that of the "fresh beam" of 1000 K^0 mesons, all of which had strangeness +1.

This thought-experiment illustrates the characteristic feature of the situation, that K^0 and \bar{K}^0 are the important entities in strong processes but K_1^0 and K_2^0 in decay.

We may note that since K_1^0 and K_2^0 have different lifetimes (and therefore different "level widths") they must also have different values of the tiny self-energy due to virtual weak decays. In other words, the weak interactions should give rise to a mass difference between K_1^0 and K_2^0 ; this difference cannot be calculated at the present time but we may crudely estimate it to be of the same order of magnitude as the level width of the K_1^0 state which is $\hbar/\tau_1 \approx 6 \times 10^{-12}$ Mev. Despite the smallness of this quantity, there is a chance that it can be measured (see 6.9).

3.10. Invariance under C; parity conservation.—In Section 3 up to this point we have emphasized one special property of the strong interactions, namely charge independence. We have seen that one aspect of charge independence, the conservation of S , applies also to electromagnetism, although not to the weak interactions.

We have mentioned in Section 2 the existence of another conservation law that seems to be valid for the strong and electromagnetic interactions and violated by the weak ones. We have referred to this law as the conservation of parity P. However, we have adopted in 2.5 the point of view of Landau that the symmetry of nature between right and left is manifested in the exact invariance of physical laws under CP, even for weak interactions. (Of

course this must still be checked by further experiments.) From this viewpoint, conservation of parity P and of charge conjugation C imply each other.

Can we find any way of connecting the separate conservation of C and P with the conservation of S , which has the same domain of validity? Perhaps so, if we concentrate our attention on C invariance and regard P invariance merely as a consequence of it. The point is that C invariance may be thought of as related to symmetry under reflection in isotopic spin space,¹² while conservation of S is related to conservation of I_z or symmetry under rotations about the z -axis in isotopic spin space.

There is a difficulty in this formulation, however. The separate conservation of C and P applies not only to baryons, antibaryons, and mesons, but also to the electromagnetic coupling of electrons and muons, for which isotopic spin and strangeness have, so far as we know, no useful meaning.

The conservation of parity by electromagnetism is established experimentally down to about one part in 10^6 in intensity by the validity of selection rules in atomic transitions (4). In the case of strong interactions, the best evidence seems to be the experiment of Tanner (17), which indicates that parity is conserved by nuclear forces down to one part in 10^7 in intensity. (He has investigated the reaction $p + F^{19} \Rightarrow \alpha + O^{16}$, which would have a resonance corresponding to a known 1^+ state of Ne^{20} if parity were not conserved. The resonance is not observed.)

The consequences of the separate conservation of C and P are well known. It may be instructive, however, to give an example of the sort of interaction that is forbidden by C or P invariance, although allowed by CP invariance, charge independence, and all other known symmetries. Let us use the notation of field theory and denote by the same symbol a particle and the field operator that destroys it. Then consider a coupling term of the form¹³

¹² We may consider in place of C the operator G introduced by Yang and Lee (16) in discussing nucleon-antinucleon annihilation; G is the product of C by rotation in isotopic spin space of 180° about the y -axis. It commutes with I but carries baryons into antibaryons and K into \bar{K} ; the pion field changes sign under G . The operator G behaves in every way like a reflection of all three coordinates in isotopic spin space, and it might be useful to interpret it in that way. We may then regard C invariance of the strong interactions as an extension of charge independence—the interactions are invariant under reflection G as well as under rotations in isotopic spin space. When we “turn on” the electromagnetic coupling of the photon with charged particles, conservation of C , like that of strangeness, remains exact.

¹³ The reader may wonder why we have used nucleons, hyperons, and K particles for our counterexample rather than electrons and photons, or nucleons and pions. The reason is that in these latter systems there seems to be no simple coupling (for instance, bilinear in the fermion fields and not involving gradients) that violates separate C and P invariance while obeying CP conservation and the other known laws.

In a sense, therefore, hyperon phenomena will provide a more stringent test of parity conservation than the more familiar reactions. Still, we do not expect a spectacular violation of the law by the strong couplings of hyperons, since such a violation should probably have shown up, by means of virtual processes, in Tanner's experiment on nuclei (15).

$$\bar{p}(g_s + g_p \gamma_5) \Lambda K^+ + \bar{n}(g_s + g_p \gamma_5) \Lambda K^0 + \text{Herm. conj.},$$

where g_s and g_p are required to be real by CP invariance. (We assume Λ has spin $\frac{1}{2}$ and K spin 0.) If g_s and g_p were both $\neq 0$, then this coupling would violate C and P invariance. It would introduce a handedness into hyperon production phenomena; for example, in $\pi^- + p \Rightarrow \Lambda + K^0$ the Λ would be, in general, longitudinally polarized.

With C and P separately conserved by the strong interactions, either g_s or g_p must be zero; the K -particle must have a unique parity relative to N and Λ , as far as strong and electromagnetic processes are concerned.

4. THE WEAK INTERACTIONS

4.1. Four-fermion couplings; the Puppi triangle.—Let us begin our detailed discussion of the weak interactions by reviewing the general properties we have mentioned in the previous sections: (a) They exhibit an apparent universality of strength—around 10^3 times weaker in intensity than the strong couplings (18). (b) They violate conservation of strangeness S and the separate conservation of parity P and charge conjugation C. (c) They manifest themselves mostly in the decay of systems that would be stable under strong and electromagnetic processes alone.

We must now attempt to list in some coherent fashion the known weak processes. Before the discovery of the strange particles the situation could be summarized by means of the Puppi triangle shown in Figure 2. At each vertex is a pair of spin $\frac{1}{2}$ particles, one charged and one neutral. The sides of the triangle represent interactions between one such pair and another. For simplicity only the positive pair is indicated at each vertex, for example $p\bar{n}$; of course $n\bar{p}$ is coupled, too.

The line C connecting $p\bar{n}$ and $e^+\nu$ stands for the β -decay interaction responsible for the following observed processes: $n \rightarrow p + e^- + \bar{\nu}$ (β^- -decay of the free neutron or a neutron in a nucleus); $p \rightarrow n + e^+ + \nu$ (β^+ -decay of a proton in a nucleus); $e^- + p \rightarrow n + \nu$ (K -capture by a proton in a nucleus); $\bar{\nu} + p \rightarrow n + e^+$ (detection of the antineutrino). These reactions can, of course, be derived from one another by two fundamental operations: reversing a

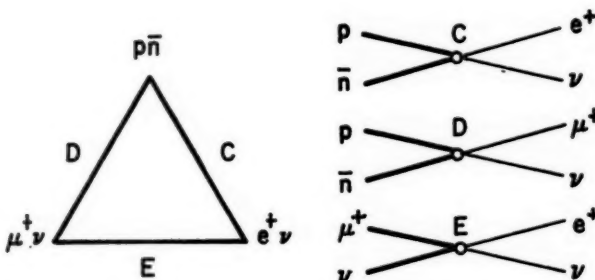


FIG. 2. Puppi triangle representing four-fermion interactions of positively charged pairs. Equivalent Feynman diagrams are drawn to the right. Leg C represents the β -decay interaction; leg D, muon capture, and leg E, muon decay.

reaction arrow and transposing a particle from one side of the arrow to the other while replacing it by its antiparticle. By convention, the antineutrino is the particle emitted in neutron decay along with the electron.

According to Fermi's theory of β -decay and its subsequent generalizations, we describe the coupling $e^+\nu$ and $p\bar{n}$ as a point interaction or δ function potential (with charge exchange). In the language of field theory, we write the interaction Lagrangian density in some such form as this (19):

$$C_V(\bar{p}\gamma_\alpha n)(\bar{e}\gamma_\alpha \nu) + C_V^*(\bar{n}\gamma_\alpha p)(\bar{\nu}\gamma_\alpha e).$$

Here ν is the field operator that destroys a neutrino or creates an antineutrino; e destroys an electron or creates a positron, etc. Correspondingly, the operator $\bar{\nu}$ creates a neutrino or destroys an antineutrino; mathematically, $\bar{\nu} = \nu^\dagger \gamma_4$, where ν^\dagger is the Hermitian conjugate of ν . There are similar relationships for the other fields. Thus the second term is the Hermitian conjugate of the first; the first term induces, for example, the β^- -decay of the neutron and the second the β^+ -decay of the proton.

Each operator is a spinor, of course, with four components, and each pair of spinors has a Dirac matrix sandwiched in between. In this case we have used the vector operator γ_α and constructed the vector interaction V . The nonconservation of parity in β -decay permits us to couple $\bar{p}\gamma_\alpha n$ also to the axial vector quantity $\bar{e}\gamma_\alpha \gamma_\beta \nu$ to form an additional "vector" interaction

$$C_V'(\bar{p}\gamma_\alpha n)(\bar{e}\gamma_\alpha \gamma_\beta \nu) + \text{Herm. conj.}$$

Eight more point interactions are possible: two forms each of the scalar interaction (S), the tensor (T), the axial vector (A) and the pseudoscalar (P). (The labels S , T , etc. describe the Dirac matrix for the nucleons.) The total β -decay coupling is then a linear combination of these ten forms:

$$\begin{aligned} \mathcal{L} = & C_S(\bar{p}n)(\bar{e}\nu) + C_S'(\bar{p}n)(\bar{e}\gamma_\beta \nu) \\ & + C_V(\bar{p}\gamma_\alpha n)(\bar{e}\gamma_\alpha \nu) + C_V'(\bar{p}\gamma_\alpha n)(\bar{e}\gamma_\alpha \gamma_\beta \nu) \\ & + \frac{1}{2}C_T(\bar{p}\sigma_{\alpha\beta} n)(\bar{e}\sigma_{\alpha\beta} \nu) + \frac{1}{2}C_T'(\bar{p}\sigma_{\alpha\beta} n)(\bar{e}\sigma_{\alpha\beta} \gamma_\beta \nu) \\ & - C_A(\bar{p}\gamma_\alpha \gamma_\beta n)(\bar{e}\gamma_\alpha \gamma_\beta \nu) - C_A'(\bar{p}\gamma_\alpha \gamma_\beta n)(\bar{e}\gamma_\alpha \nu) \\ & + C_P(\bar{p}\gamma_\alpha n)(\bar{e}\gamma_\beta \nu) + C_P'(\bar{p}\gamma_\alpha n)(\bar{e}\nu) \\ & + \text{Herm. conj.} \end{aligned} \quad 5.$$

If CP or T invariance holds, then all the coefficients C are real.

The line D connecting $p\bar{n}$ with $\mu^+\nu$ in Figure 2 represents a coupling analogous to β -decay but with the electron replaced by the muon. In this case, the only observed process is the capture of μ^- by a proton in a nucleus: $\mu^- + p \rightarrow n + \nu$. (We write ν rather than $\bar{\nu}$ for reasons discussed in 4.4. The other processes coupled by line D , $n \rightarrow p + \mu^- + \bar{\nu}$ and $p \rightarrow n + \mu^+ + \nu$, analogous to neutron and proton β -decay, are forbidden by conservation of energy and the reaction $\bar{\nu} + p \rightarrow n + \mu^+$ requires an intense source of high energy antineutrinos that is unavailable today.) Again there are ten possible forms of point interaction, such as $D_V(\bar{p}\gamma_\alpha n)(\bar{\mu}\gamma_\alpha \nu) + \text{Herm. conj.}$ The total " μ -capture coupling" is presumed to be some linear combination of these.

The third leg E of the Puppi triangle connects $\mu^+\nu$ and $e^+\nu$. Here the

observed process is the decay of the muon $\mu^\pm \rightarrow e^\pm + \nu + \bar{\nu}$. The point interaction Lagrangian again may consist of ten different terms, such as $E_V(\bar{\nu}\gamma_\mu\mu)(\bar{e}\gamma_\mu\nu) + \text{Herm. conj.}$, $E_V'(\bar{\nu}\gamma_\mu\mu)(\bar{e}\gamma_\mu\gamma_5\nu) + \text{Herm. conj.}$, etc. The actual form of the coupling is taken up in 4.5.

The phenomenon of "universality of strength" can now be appreciated if we calculate the rates of three weak processes corresponding to the three legs of the triangle and compare these with experiments. The rate of decay of the free neutron is given, with neglect of recoil and of "Fierz terms," by the formula

$$\Gamma_n = \frac{0.47}{60\pi^3} c^4 \hbar^{-7} \Delta^5 (C_S^2 + C_{S'}^2 + C_V^2 + C_{V'}^2 + 3C_T^2 + 3C_{T'}^2 + 3C_A^2 + 3C_{A'}^2), \quad 6.$$

where Δ is the difference in rest mass of the neutron and proton. The number 0.47 is computed from the ratio m_e/Δ and would be unity if the electron were massless; we may call it the "blocking factor" because the finite electron mass blocks up phase space. The rate of decay of the muon is given by the formula (20)

$$\Gamma_\mu = \frac{1}{1536\pi^3} c^4 \hbar^{-7} m_\mu^5 (E_S^2 + E_{S'}^2 + 4E_V^2 + 4E_{V'}^2 + 6E_T^2 + 6E_{T'}^2 + 4E_A^2 + 4E_{A'}^2 + E_P^2 + E_{P'}^2), \quad 7.$$

where m_e/m_μ has been neglected. The rate of capture of μ^- from a 1s atomic orbit around a free proton is given, with neglect of recoil, by the formula

$$\Gamma = \frac{1}{2\pi^2} \left(\frac{1}{137} \right)^3 c^4 \hbar^{-7} m_\mu^5 [(D_S + D_V)^2 + (D_{S'} + D_{V'})^2 + 3(D_T + D_A)^2 + 3(D_{T'} + D_{A'})^2] 8.$$

Now in Table I we find Γ_n and Γ_μ in sec.⁻¹ and Δ and m_μ in Mev, which we may convert to grams. Then we obtain, substituting into Eqs. 5 and 6, the results

$$\begin{aligned} C_S^2 + \dots &\approx 10.4 \times (10^{-49} \text{ erg cm}^3)^2 \\ &= 2.62 \times 10^{-13} \hbar^2 c^2 \left(\frac{\hbar}{m_e c} \right)^4 \end{aligned} \quad 9.$$

and

$$\begin{aligned} E_S^2 + \dots &\approx 16.1 \times (10^{-49} \text{ erg cm}^3)^2 \\ &= 4.06 \times 10^{-13} \hbar^2 c^2 \left(\frac{\hbar}{m_e c} \right)^4 \end{aligned} \quad 9a.$$

The similarity in strength is striking. We have, for simplicity, used the Compton wave length of the charged pion to put the constants in dimensionless form. The third quantity Γ has not been measured but can be roughly estimated by extrapolating results on μ^- capture in nuclei. The result for $(D_S + D_V)^2 + \dots$, is then of the same order of magnitude as the quantities in Eqs. 9 and 9a.

4.2. The two-component or longitudinal neutrino.—The discovery of non-conservation of parity in weak processes has permitted an important advance in the theory of the neutrino. This particle seems to have the unique

property of possessing no couplings but weak ones; it is possible, therefore, for the neutrino to be governed completely by laws that violate separate P and C invariance.

Such a possibility has been welcomed by theoretical physicists who have long felt that the idea of a massless neutrino is repugnant unless there is some principle guaranteeing the masslessness. In the case of the photon, the principle is gauge invariance. For the neutrino, there was such a principle available, but it violated conservation of parity! With the removal of this obstacle, however, it became possible to justify the masslessness of the neutrino. The theory that we shall set forth here has been proposed by Landau (6), Salam (21), and Lee & Yang (22).

Let us postulate that all physical laws are invariant under the replacement of the neutrino operator ν by $e^{ia\nu}\gamma_5\nu$, where $e^{ia\nu}$ is some fixed phase factor. Then the Dirac equation for a free neutrino¹⁴

$$\left(\gamma_\mu \frac{\partial}{\partial x_\mu} + m_\nu \right) \psi_\nu = 0, \quad 10.$$

where ψ_ν is the neutrino wave function, must be invariant under $\psi_\nu \rightarrow e^{ia\nu}\gamma_5\psi_\nu$. But γ_5 and γ_μ anticommute, so we have, multiplying Eq. 10 by $e^{ia\nu}\gamma_5$, the result

$$\left(\gamma_\mu \frac{\partial}{\partial x_\mu} - m_\nu \right) e^{ia\nu}\gamma_5\psi_\nu = 0 \quad 11.$$

The invariance is possible only if $m_\nu = 0$. We have guaranteed masslessness.

We must ask what happens to other fields under the transformation that affects the neutrino field as we have described. For the fermions, for example, it must not introduce multiplication by γ_5 , for then these particles too would be massless. It must not carry one particle into another, for then the masses of these would be equal, and so forth. The only effect of the transformation on other fields than the neutrino can be multiplication of each one by some phase factor e^{ia} characteristic of the field.

Now let us apply the principle of invariance under this transformation to the Lagrangian (Eq. 5) of the β -decay interaction. The effect of the transformation is to interchange the roles of the primed and unprimed couplings and to multiply the whole interaction by $e^{i(a_\nu + a_n - a_e - a_p)}$. But according to the invariance principle the interaction must be unchanged by the transformation. There are then only two possibilities:

- (a) $C_S = -C'_S, \quad C_T = -C'_T, \text{ etc. and } e^{i(a_\nu + a_n - a_e - a_p)} = -1$
- (b) $C_S = +C'_S, \quad C_T = +C'_T, \text{ etc. and } e^{i(a_\nu + a_n - a_e - a_p)} = +1.$

Let us examine one of these alternatives, say (a), according to which the neutrino field in β -decay occurs only in the combination $(1 - \gamma_5)\nu$ (and its Hermitian conjugate). Physically this means, as we shall see, that neutrinos can be created or destroyed in one spin state only—that in which the spin

¹⁴ For the rest of this section we set $\hbar = c = 1$.

vector is aligned with the direction of motion (and antineutrinos, correspondingly, can be created or destroyed only in the case of spin aligned opposite to the direction of motion). It is physically clear why such a condition is coupled with rigorous masslessness of the neutrino—if there were any rest mass, the particle could be at rest, and the requirement that spin σ and momentum p be always aligned would have no meaning.

We must still show that coupling through $(1 - \gamma_5)\nu$ corresponds to the interaction of right-handed neutrinos only. The wave function ψ_ν of the neutrino in β -decay occurs multiplied by $(1 - \gamma_5)$. With $m_\nu = 0$ the Dirac equation (Eq. 10) for ψ_ν can be written in the form

$$i \frac{\partial \psi_\nu}{\partial t} = \frac{1}{i} \alpha \cdot \nabla \psi_\nu, \quad 12.$$

where Dirac's α is related to the spin σ by the relation $\alpha = -\gamma_5 \sigma = -\sigma \gamma_5$. For $(1 - \gamma_5)\psi_\nu$, therefore, we have the equation

$$i \frac{\partial}{\partial t} (1 - \gamma_5)\psi_\nu = \frac{1}{i} \sigma \cdot \nabla (1 - \gamma_5)\psi_\nu, \quad 13.$$

or, in Fourier transform, frequency $= \sigma \cdot p$. For the positive frequency solution, which represents the neutrino, we have $+p = \sigma \cdot p$ or righthanded longitudinal polarization. The negative frequency solution has $-p = \sigma \cdot p$ or left-handed polarization; using the "hole theory" approach, we may say that the antineutrino is a hole in the sea of such "left-handed" negative frequency neutrinos. The hole has the opposite spin and momentum; the antineutrino is therefore left-handed.

In this theory, then, two states out of four have been eliminated from the interaction—the neutrino state with left polarization and the antineutrino state with right polarization. It is possible, therefore, to write the Dirac equation with a new wave function consisting of only two components instead of four. Hence the name "two-component theory." It is easier, however, to retain the four-component Dirac spinor together with the matrix $(1 - \gamma_5)$ that strikes out any coupling of the two forbidden states.

We have looked so far at possibility (a) above, $(1 - \gamma_5)\nu$, which couples right-handed ν and left-handed $\bar{\nu}$. Possibility (b), which is $(1 + \gamma_5)\nu$, couples the other two states instead. We shall see below that (b) is excluded by experiment, while (a) is strongly supported. We may therefore discuss the longitudinal neutrino in terms of (a) only [see, however, (46)].

Now the question arises how this theory is to be applied to interactions other than β -decay. That depends, evidently, on the phase factors e^{ia_p} , e^{ia_n} , e^{ia_e} , e^{ia_μ} , etc. One possible situation is that these factors are equal to unity for all fields except the neutrino. (According to (a) e^{ia_ν} must then be -1 .) In that case, it is always $(1 - \gamma_5)\nu$ that occurs in the interaction, no matter what the process is (β -decay, μ -absorption, μ -decay, etc.). This is the simplest situation and seems, so far, to fit the facts. The other physically distinct possibility is that the product of phase factors is sometimes -1 and some-

times +1, depending on the particles involved. In that case, it is sometimes the right-handed ν and left-handed $\bar{\nu}$ that are coupled but other times the left-handed ν and right-handed $\bar{\nu}$. Fortunately, it has not been necessary to invoke this complicated alternative. We shall consider only the simple form of the longitudinal theory in which the same two neutrino states are involved in all processes. This is the true "two-component" theory.

The theory, then, can be summarized in this way: The neutrino field always occurs in the combination $(1 - \gamma_5)\nu$ and its Hermitian conjugate, which couple right-handed ν and left-handed $\bar{\nu}$ only. We shall explore some experimental consequences in the next few paragraphs.

4.3. The longitudinal neutrino in β -decay. We have seen that the Fermi theory of β -decay may be described in terms of the ten parameters C_S , $C_{S'}$, C_V , $C_{V'}$, etc., and that CP invariance requires these to be real. In the longitudinal neutrino picture, there are only five independent constants since we have the relations $C_{S'} = -C_S$, $C_{V'} = -C_V$, etc.

The obsolete form of the theory, in which C and P are separately conserved, could be expressed by setting the coefficients $C_{S'}$, $C_{V'}$, etc. equal to zero; this would leave only "parity conserving" terms in the coupling.

Considerable support for the longitudinal neutrino theory was provided by the same experiment that first established the nonconservation of parity in β -decay: the work of Wu, *et al.* (5), who investigated the asymmetry in the angular distribution of electrons emitted by oriented Co⁶⁰ nuclei. As we mentioned in 2.5, the angular distribution has the form $1 - a(E) \cos \theta$ where E is the electron energy and θ is the angle between the electron momentum \mathbf{p} and the spin direction $\langle \mathbf{J} \rangle / J$ of the decaying nucleus. (For simplicity we consider the idealized case of fully oriented nuclei.)

Let us defer until later the comparison of the experimental result with the two-component theory. For the moment, we wish to emphasize that the novel feature of the experiment was the measurement of a pseudoscalar quantity. The probability of decay per unit solid angle and per unit electron energy may be written $I(E, \theta) = S(E)[1 - a(E) \cos \theta] = S(E) - S(E)a(E)(\mathbf{p}/p) \cdot (\langle \mathbf{J} \rangle / J)$. The first term $S(E)$ is the electron spectrum (averaged over the direction of \mathbf{p} or $\langle \mathbf{J} \rangle$) and is evidently a scalar. The second term, which contains the asymmetry, is a pseudoscalar, the dot product of a polar vector \mathbf{p} and an axial vector $\langle \mathbf{J} \rangle$ times a constant. (With CP invariance, the constant in such a formula always has the opposite sign for the antinucleus and the symmetry of space between left and right is preserved.)

Now in any intensity formula in β -decay, we can divide the terms into scalar ones (such as those giving spectrum and reciprocal lifetime and $e - \nu$ angular correlation) and pseudoscalar ones (such as those giving electron asymmetry or longitudinal electron polarization). In the old theory with parity conserved, all the pseudoscalar quantities vanish. In a general theory with ten coupling constants, they arise from interference between "parity conserving" and "parity nonconserving" terms in the coupling; they depend on $C_S C_{S'}$, $C_V C_{V'}$, $C_S C_T + C_T C_{S'}$, etc. In the longitudinal theory, of course, these become $-C_S^2$, $-C_V^2$, $-2C_S C_T$, etc.

The scalar quantities were the only ones measured until 1957. The formulas for scalars, unlike those for pseudoscalars, are essentially the same in the old theory and in the longitudinal theory. One need merely replace C_S^2 by $C_S^2 + C_{S'}^2 = 2C_S^2$, $C_S C_V$ by $C_S C_V + C_{S'} C_{V'} = 2C_S C_V$, etc. (Even this doubling is, of course, a matter of definition of the constants C .)

The conclusions about the form of the β -decay coupling that are based on the measurements of these scalar quantities over the past several years should thus be essentially unchanged. It was concluded that S and T interactions are both present, with $|C_S|$ and $|C_T|$ of comparable magnitude, and $|C_V|$ and $|C_A|$ much smaller or zero (23). (The pseudoscalar interaction P is difficult to detect in β -decay since the operator γ_5 vanishes in the non-relativistic limit and nucleons are not highly relativistic in the nucleus. In 4.6 we shall argue on other grounds that C_P is small or zero.)

We shall assume in what follows that the β -decay interaction does consist primarily of S and T . However, current experiments have cast some doubt on these time-honored assignments. In 4.6, we shall therefore discuss also the remote but attractive possibility that the interaction is instead a mixture of V and A .

Let us now return to the discussion of the Co^{60} decay. The initial and final nuclear spins are 5 and 4 respectively and the parities the same. This corresponds to an "allowed Gamow-Teller" transition in which only tensor and axial vector interactions are effective; since the latter is supposed to be absent (or nearly so) in the β -decay coupling, we are dealing with a transition induced purely by T . The longitudinal theory with $C_T = -C_{T'}$ then predicts a unique value for the asymmetry parameter a :

$$a = -v/c,$$

where v is the electron velocity. [This is in good agreement with the results of ref. (5).] If we had made the opposite choice of the neutrino spin direction ($C_T = +C_{T'}$) the sign of a would be changed. The measurement on Co^{60} thus confirmed the longitudinal theory and established the sign of the neutrino polarization.

Another important pseudoscalar quantity that has now been measured is the longitudinal polarization of the β -rays themselves. In a decay induced purely by the tensor interaction, the longitudinal theory predicts a fractional polarization $(-v/c)$ (the sign means the electrons are spinning to the left). It is clear that the polarization must vanish at zero electron velocity, since there is then no vector for the spin to point along. We can also see that the polarization must be -100 per cent for $v/c \approx 1$, by the following argument. In the longitudinal theory the tensor coupling has the form

$$[\bar{e}\sigma_{\alpha\beta}(1-\gamma_5)e][\bar{\nu}\sigma_{\alpha\beta}\nu] + \text{Herm. conj.}$$

We will recall that $\bar{e} = e^\dagger \gamma_4$ and that γ_5 commutes with $\sigma_{\alpha\beta}$ and anticommutes with γ_4 . Thus we have, for the lepton factor in the coupling, the form $e^\dagger(1+\gamma_5)\gamma_4\sigma_{\alpha\beta}\nu$, or, in the Hermitian conjugate, the form $\nu^\dagger\sigma_{\alpha\beta}\gamma_4(1+\gamma_5)e$. Now when $v/c \approx 1$, the electron is effectively massless. Thus the expression $(1+\gamma_5)e$ is perfectly analogous to the expression $(1-\gamma_5)\nu$ that gives us a

right-handed neutrino. We have a left-handed electron, i.e., polarization -100 per cent. The expression (v/c) for the polarization of the electrons in the decay of Co^{60} has been verified to an accuracy of around 20 per cent by Frauenfelder *et al.* (R2).

We have discussed the polarization in the case of a transition involving T only. The value at $v/c = 1$ can be obtained for other interactions by the same argument we have used above for T . Since γ_5 commutes with 1 just as it does with $\sigma_{\alpha\beta}$, S and T behave alike. The operators γ_α and $\gamma_5\gamma_\alpha$ anticommute with γ_5 , and thus the polarization of β^- in the case of V or A coupling is $+100$ per cent at $v/c, \approx 1$ whereas it is -100 per cent for S or T . If the true interaction really contains S and T only, then the polarization must be -100 per cent at $v/c \approx 1$ in all β^- transitions. The fact that the value -100 per cent is approximately verified for "Gamow-Teller" transitions like $\text{Co}^{60} \rightarrow \text{Ni}^{60}$ confirms, within the framework of the longitudinal theory with T dominant, that there is very little A compared to T . Current experiments on β -polarization in "Fermi" and "mixed" transitions, where S and V play a role, will reveal similarly whether or not there is a considerable admixture of V , assuming S dominant.

Note that for a given coupling the polarization of β^+ is opposite to that of β^- .

4.4. Conservation of leptons.—In our description of the weak couplings covered by the Puppi triangle (4.1), we made explicit assumptions about the roles of neutrino and antineutrino, which we promised to justify here. In the decay of the muon, we chose the scheme $\mu^- \rightarrow e^- + \nu + \bar{\nu}$ rather than $\mu^- \rightarrow e^- + \nu + \nu$ or $\mu^- \rightarrow e^- + \bar{\nu} + \bar{\nu}$ (with corresponding schemes for the positive muon). In the absorption of μ^- we assumed that a neutrino rather than an antineutrino is emitted. We must now discuss the motivation of these choices, which have been made possible by the success of the two-component theory, with its sharp physical distinction between ν and $\bar{\nu}$.

The electron spectrum in μ decay, according to a point interaction theory such as was discussed in 4.1, is characterized by a single parameter ρ , introduced by Michel (20). In general, ρ varies between 0 and 1 for the scheme $\mu^- \rightarrow e^- + \nu + \bar{\nu}$ employed in 4.1; if, instead, two neutrinos or two antineutrinos are emitted, ρ varies between 0 and $\frac{1}{2}$. The two-component theory removes all this freedom; it turns out that in this theory ρ must equal zero if the electron is accompanied by $\nu + \nu$ or $\bar{\nu} + \bar{\nu}$, while in the case of $\nu + \bar{\nu}$ the value of ρ is $\frac{1}{2}$ (21). Now the experimental value, corrected for inner bremsstrahlung effects, is 0.68 ± 0.02 (24), which selects the decay scheme $\mu^- \rightarrow e^- + \nu + \bar{\nu}$ and at the same time provides a check on the longitudinal theory of the neutrino, although there is still a discrepancy between $.68$ and $.75$ to be explained.

At this point an important theoretical principle should be introduced, the law of conservation of leptons. This law has not yet been fully established, but seems a very attractive hypothesis at the present time. It is exactly analogous to the law of conservation of baryons, discussed in 2.4; it states that the number of leptons minus the number of antileptons is a conserved

quantity in all processes. The law is obviously incomplete, however, without a specification of which particles are leptons and which antileptons. To start with, we may certainly define the electron to be a lepton, as a matter of convention; the positron is then an antilepton. Next, we have defined the antineutrino to be the particle emitted along with the electron in neutron decay; we may say, then, that the antineutrino is an antilepton and the neutrino a lepton. (The neutron and proton are assumed to have the same lepton content, which we take to be zero.)

The nontrivial question is the assignment of the muon. Is the negative muon a lepton like e^- and ν or an antilepton like e^+ and $\bar{\nu}$? If leptons are really conserved, the answer is determined by the decay scheme for the muon that was established above: $\mu^- \rightarrow e^- + \bar{\nu} + \nu$. The negative muon must be a lepton like the negative electron. Our assignments are summarized in Table I, where ν , e^- , μ^- are labeled "leptons" and $\bar{\nu}$, e^+ , μ^+ , are labelled "antileptons." Finally, these assignments give for muon capture $\mu^- + p \rightarrow n + \nu$. The conservation of leptons requires that the particle on the right be ν rather than $\bar{\nu}$. This has not yet been tested experimentally.

All the assignments of ν and $\bar{\nu}$ in the reactions associated with the Puppi triangle have been justified. But it is clearly desirable to have more experimental tests of lepton conservation. One reaction that can be used for such a test is the decay of the charged pion. In 4.7 we shall speculate about the mechanism of this decay, but here we may simply refer to the experimental fact that it yields a muon and a neutrino or antineutrino. Conservation of leptons then requires that we have $\pi^- \rightarrow \mu^- + \bar{\nu}$ and $\pi^+ \rightarrow \mu^+ + \nu$, with consequences as described below. Another test of lepton conservation is the decay $K^\pm \rightarrow \mu^\pm \pm \nu$. Experiment (57) shows that the neutrino assignment is the same for K and π -decay (see 4.5).

4.5. Polarization and decay of the muon.—Consider the decay of a positive pion in its own rest frame and assume conservation of leptons. Since π^+ is spinless and the decay products μ^+ and ν travel in opposite directions, the neutrino's angular momentum of $+\frac{1}{2}$ about its direction of motion must be balanced by μ^+ also carrying an angular momentum of $+\frac{1}{2}$ about its direction of motion. In other words, μ^+ from the decay of π^+ is 100 per cent right polarized as a consequence of the longitudinality of the neutrino. Similarly μ^- from π^- decay is 100 per cent left polarized.

Eventually the sense of polarization of these muons will probably be measured "directly" (i.e., without recourse to the muon decay) but this has not yet been done. In order to understand the present evidence that the μ^+ is right polarized we shall discuss the decay $\mu^+ \rightarrow e^+ + \nu + \bar{\nu}$, using the two-component theory of the neutrino.

The Fermi type theory of μ -decay described in 4.1 contains ten parameters, but these are reduced to two in the two-component picture. Requiring that ν always occur in the combination $(1 - \gamma_5)\nu$ and, correspondingly, $\bar{\nu}$ always occur in the combination $\bar{\nu}(1 + \gamma_5)$, yields the conditions $E_\nu = -E_{\bar{\nu}} = -E_A = E'_A$, $E_S = -E_{S'} = -E_P = E'_{P'}$, and $E_T = E'_{T'} = 0$. Thus the complete interaction may be written in the form

$$E_V[\bar{\nu}(1 + \gamma_b)\gamma_a\mu][\bar{e}\gamma_a(1 - \gamma_b)\nu] + E_S[\bar{\nu}(1 + \gamma_b)\mu][\bar{e}(1 - \gamma_b)\nu] + \text{Herm. conj.} \quad 14.$$

The two coupling constants E_V and E_S are real in a theory invariant under CP.

If we now calculate the distribution of the angle θ between the spin direction $\hat{\delta}_\mu$ of a stationary μ and the direction \hat{p}_e of its decay electron, we find it to be given by the formula of Landau (6) and Lee & Yang (22),

$$I(\theta) \propto 1 \pm \lambda (\hat{\delta}_\mu^\pm \cdot \hat{p}_e^\pm)(2\epsilon - 1)(3 - 2\epsilon)^{-1}, \quad 15.$$

where ϵ is the electron energy in units of the maximum electron energy and λ is $(E_S^2 - E_V^2)/(E_S^2 + E_V^2)$. Note that for a μ^- with the same spin direction, the coefficient of $\hat{\delta} \cdot \hat{p}$ changes sign.

Now the quantity $\hat{\delta} \cdot \hat{p}$ of Eq. 15 is not directly observable, since the muon spin direction has not yet been measured. Instead, let us consider the $\pi \rightarrow \mu \rightarrow e$ chain, with conservation of leptons. We want to rewrite 15 in terms of the observable angle $\varphi = \cos^{-1} \hat{p}_\mu \cdot \hat{p}_e$. We remember that when a π^+ decays at rest, the μ^+ emitted is fully right polarized; if the μ^+ is now brought to rest, it is still polarized in the same direction. There may, however, be some depolarization, in an amount depending on the medium. Say the muon retains a fraction $|P|$ of its polarization along its former direction of motion. Then the angular distribution of the decay positrons relative to this direction is

$$I(\varphi) \propto 1 + |P| \lambda (\hat{p}_\mu \cdot \hat{p}_e)(2\epsilon - 1)(3 - 2\epsilon)^{-1}. \quad 16.$$

For the negative $\pi \rightarrow \mu \rightarrow e$ chain, there are two changes of sign in this formula. In the first place, μ^- is accompanied by $\bar{\nu}$ instead of ν and μ^- is therefore fully left polarized. In the second place, the $\hat{\delta} \cdot \hat{p}$ term in Eq. 15 (for the electron distribution relative to the spin direction) changes sign as we go from μ^+ to μ^- . The two sign changes cancel each other and we are left with the same formula (Eq. 16) for $\pi \rightarrow \mu \rightarrow e$ whether the charge is positive or negative. Of course the factor $|P|$ depends on the sign of charge; experimentally μ^- is depolarized much more than μ^+ .

The historic experiments confirming the asymmetry in the $\pi \rightarrow \mu \rightarrow e$ chain were carried out by two groups: Friedman & Telegdi (25) looked at $\pi^+ \rightarrow \mu^+ \rightarrow e^+$ decays in emulsion; Garwin, Lederman & Weinrich (26) stopped μ^\pm in many materials and counted the decay electrons with scintillation counters, verifying approximately the energy dependence of Eq. 16. For both μ^+ and μ^- the highest energy decay electrons ($\epsilon = 1$) come off preferentially backwards (i.e., the distribution for $\epsilon = 1$ is of the form $1 + |P|\lambda \hat{p}_\mu \cdot \hat{p}_e$ with $|P|\lambda < 0$). Because μ^- are depolarized while making atomic transitions before they decay, their asymmetry coefficient $|P\lambda|$ is never > 10 per cent, but for μ^+ stopping in many materials it is nearly unity ($|P|\lambda \approx -1$). We can then say that for these materials there is little depolarization ($|P| \approx 1$) and that the muons from π decay are fully polarized. Moreover, λ is then roughly -1 ; since we know $\lambda = (E_S^2 - E_V^2)/(E_S^2 + E_V^2)$, we have established that μ decay proceeds predominantly through a vector-axial vector interaction.

Now that we know the form of the interaction ($E_V^2 \gg E_S^2$) we can finally calculate the direction of polarization of the electron in μ decay and compare it with experiment. We proceed just as in 4.3 where we calculated the polarization of nuclear β -rays. In Eq. 1, the E_V term contains e in the combination $\bar{e}\gamma_a(1-\gamma_b) = e^+\gamma_4\gamma_a(1-\gamma_b) = e^+(1-\gamma_b)\gamma_4\gamma_a$ since γ_b anticommutes with both γ_4 and γ_a . Thus this vector-axial vector interaction involves e coupled only through $(1-\gamma_b)e$, which corresponds to electrons spinning to the right and positrons spinning to the left.

At the time of writing, the positron polarization is in the process of being measured (27); and it seems to be coming out lefthanded, consistent with conservation of leptons in $\pi \rightarrow \mu$ decay. Let us emphasize that if the decay scheme of π^+ were $\pi^+ \rightarrow \mu^+ + \bar{\nu}$, in violation of conservation of leptons, the result would be the opposite: the positrons from μ^+ decay would be spinning to the right. The point is that Eq. 15, giving the angular distribution of positrons from muons of known spin direction, is independent of the pion decay and would still hold; however, in Eq. 16, where we have expressed the angle in terms of the initial muon momentum, we have made use of the decay scheme $\pi^+ \rightarrow \mu^+ + \nu$. If it were $\bar{\nu}$ instead, μ^+ would be left polarized instead of right and the coefficient of $\hat{p}_e \cdot \hat{p}_\mu$ in Eq. 16 would change sign. The experimental asymmetry of $\pi \rightarrow \mu \rightarrow e$ decay would then indicate $\lambda = +1$ or scalar-pseudoscalar interaction. Now 1 and λ_5 both commute with γ_b , as opposed to γ_a and $\gamma_4\gamma_a$, which anticommute with it. Thus the positron polarization would change sign.

We conclude our discussion of the $\pi\mu e$ chain by repeating that if leptons are conserved then the $K\mu e$ chain must give the same μ polarization; consequently the \hat{p}_μ/\hat{p}_e asymmetry must again be given by Eq. 16. This asymmetry has recently been experimentally verified at Berkeley (57). It was mentioned at the end of 4.4 that conservation of leptons must eventually pass three experimental tests. This experiment is the only unambiguous positive result so far reported.

4.6. The "universal Fermi interaction."—Since the "universality of strength" of the three sides of the Puppi triangle was remarked (18), there has been speculation that the form of the interaction might also be "universal." Such a situation seems to be ruled out if the β -decay coupling is primarily S and T and the μ decay coupling V and A , as we have stated in 4.3 and 4.5 respectively. Since the β -decay picture is somewhat confused at the moment, let us discuss briefly the possibility that we may have V and A there too, instead of S and T with a possible admixture of V . We may call this V, A hypothesis the "last stand" of the UFI (universal Fermi interaction) (28).

We must first of all disregard much of the evidence on $e\nu$ angular correlation in β -decay, especially the result of Rustad & Ruby (29) on He^6 , which clearly indicates T rather than A . This is already a very serious objection to the UFI.

The evidence from β -decay spectra and rates is perfectly consistent with

V and A , as well as with S and T . That exhausts the information available from scalar quantities. We must go on, therefore, to discuss the recent measurements of pseudoscalars. The results of Wu *et al.* (5) and Fraunfelder *et al.* (R2) on the electron asymmetry and longitudinal polarization respectively in the decay of Co^{60} are also perfectly consistent with A instead of T in Gamow-Teller transitions provided the sign of neutrino polarization is changed in the longitudinal theory. We recall from 4.3 that the electron polarization changes sign if we replace T by A ; if we also replace $(1-\gamma_b)\nu$ by $(1+\gamma_b)\nu$, i.e., we have left-handed ν instead of right-handed ν , then the sign of the electron polarization changes back to the observed one.

With a longitudinal but left-handed neutrino and a V, A coupling, all β^- polarizations are -100 per cent ν/c , just as they are for S, T coupling with a right-handed neutrino. As we mentioned in 4.3, current experiments are testing this in "Fermi transitions" where S and V are important. If -100 per cent ν/c polarization is confirmed, it will still not distinguish between pure S, T with right-handed ν and pure V, A with left-handed ν . If it is not confirmed, then there must be an admixture of V in the former case or of S in the latter case. For the moment, let us suppose that the β^- polarization is always -100 per cent ν/c and continue to explore the consequences of a universal V, A coupling with left-handed ν and right-handed $\bar{\nu}$.

The value of the spectrum parameter ρ in muon decay still requires the scheme $\mu^\pm \rightarrow e^\pm + \nu + \bar{\nu}$, as in 4.4, and the assignments of lepton and anti-lepton are unchanged. In pion decay, the conservation of leptons still gives $\pi^+ \rightarrow \mu^+ + \nu$ and $\pi^- \rightarrow \mu^- + \bar{\nu}$. However, μ^+ must now be left polarized and μ^- right polarized instead of the other way around. In Eq. 15 for the electron angular distribution from muons of given spin direction, the sign of the asymmetry term must be changed; this is because in Eq. 14 for the coupling, the parity nonconserving term changes sign when we replace $(1-\gamma_b)\nu$ by $(1+\gamma_b)\nu$ and $\bar{\nu}(1+\gamma_b)$ by $\bar{\nu}(1-\gamma_b)$, while the parity conserving term is unchanged. Thus in Eq. 16 for the asymmetry in the $\pi \rightarrow \mu \rightarrow e$ chain, we have two changes in sign which cancel each other; one from the muon spin direction and one from Eq. 15. Thus the experiments on the $\pi \rightarrow \mu \rightarrow e$ chain still show that $\lambda \equiv (E_S^2 - E_V^2)/(E_S^2 + E_V^2)$ is about -1 and that the muon coupling has the form V, A . However, the positron polarization in $\pi^+ \rightarrow \mu^+ \rightarrow e^+$ is now predicted to be positive (right-handed) rather than negative as in 4.5. The positive polarization is in disagreement with preliminary experimental results (27).

In 4.7 we shall see that there is one more piece of evidence against the UFI: the very small or vanishing branching ratio of $(\pi^+ \rightarrow e^+ + \nu) / (\pi^+ \rightarrow \mu^+ + \nu)$.

Despite all of the objections to it at the present time, the UFI hypothesis with V, A coupling seems so attractive that it should perhaps be borne in mind until definitely disproved by experiment. It would correspond to a coupling

$$E_V [\bar{\nu} \gamma_\alpha (1 + \gamma_b) \mu] [\bar{e} \gamma_\alpha (1 + \gamma_b) \nu] + \text{Herm. conj. in muon decay},$$

$$C_V [\bar{\nu} \gamma_\alpha (1 + \gamma_b) n] [\bar{e} \gamma_\alpha (1 + \gamma_b) \nu] + \text{Herm. conj. in } \beta\text{-decay, and}$$

$$D_V [\bar{\nu} \gamma_\alpha (1 + \gamma_b) n] [\bar{\mu} \gamma_\alpha (1 + \gamma_b) \nu] + \text{Herm. conj. in muon capture}.$$

The coefficients C_V and D_V would have to be equal, but they could differ somewhat from E_V since the C and D interactions may be subject to corrections from pion effects in the nucleon. Using Eqs. 9 and 9a, we find, with the couplings listed above,

$$|E_V| m_\pi^2 \approx 1.6 \times 10^{-7} \quad \text{and} \quad |C_V| m_\pi^2 = |C_A| m_\pi^2 \approx 1.6 \times 10^{-7}.$$

The scheme that we have used previously for β -decay, with roughly equal amounts of S and T and a right-handed neutrino, yields in the same way $|C_S| m_\pi^2 \approx |C_T| m_\pi^2 \approx 1.6 \times 10^{-7}$. The result for the muon decay is of course the same as above, $|E_V| m_\pi^2 \approx 1.6 \times 10^{-7}$.

4.7. Mechanism of pion decay.—We have sketched so far the present theory of β -decay, μ -decay, and μ -absorption, based on four-fermion contact interactions as indicated schematically by the Puppi triangle. Experiments to date are consistent with CP invariance, the longitudinality of the neutrino and conservation of leptons, although these principles must be subjected to further experimental tests. More experimental work is needed also to determine the values of the five independent real coupling constants in μ -absorption, the five in β -decay (of which two or three may well be zero), and the two in Eq. 14 for μ -decay (of which one, E_S , may be zero). It is known, as mentioned in 4.1, that all three legs of the triangle have about the same strength, but the present experimental situation, indicating S and T (and perhaps V) for β -decay and V and A for μ decay, is hardly suggestive of any universality of form for the four-fermion couplings, unless the β -decay evidence should change, as discussed in 4.6, so as to permit a universal coupling of the V , A type.

We must now take up the question of other weak processes and how they fit into the scheme we have outlined. Let us discuss first the decay of the charged pion, which we have referred to extensively as a source of polarized muons.

An obvious explanation of the decay $\pi^+ \rightarrow \mu^+ + \nu$ is available within the framework of the Puppi triangle: we may suppose that the virtual Yukawa process $\pi^+ \rightarrow p + \bar{n}$ is followed by the virtual weak process $p + \bar{n} \rightarrow \mu^+ + \nu$ induced by the coupling responsible for μ -absorption. (See the top Feynman Diagram of Fig. 3, sect. 4.9.) Let us use this possible explanation as the starting point of our discussion.

It is important to notice that only two of the five possible μ absorption couplings can induce the decay of the pseudoscalar pion: these are the pseudoscalar coupling

$$D_P [\bar{\rho} \gamma_5 n] [\bar{\mu} \gamma_5 (1 - \gamma_5) \nu] + \text{Herm. conj.}$$

and the axial vector coupling

$$-D_A [\bar{\rho} \gamma_\alpha \gamma_5 n] [\bar{\mu} \gamma_\alpha \gamma_5 (1 - \gamma_5) \nu] + \text{Herm. conj.}$$

For the other three couplings (scalar, vector, and tensor) the decay of the charged pion is forbidden (apart from electromagnetic corrections). We can derive this result by means of field theory. Imagine the most general Feynman diagram for the process $\pi^+ \Rightarrow p + \bar{n} \Rightarrow ? \Rightarrow p + \bar{n} \rightarrow \mu^+ + \nu$, where the

question mark stands for all the possible strong processes that may intervene between the creation of the virtual ($p\bar{n}$) pair by the pion at some space-time point x and its annihilation into leptons at another space-time point y . No matter what these intervening processes are, they give an effective coupling between the pion destroyed at x and the nucleon-antinucleon operator at y that is involved in the interaction with leptons. This effective coupling is nonlocal, but can depend on only one vector in space-time, namely $(x-y)$. From the pseudoscalar pion field and one four-vector, the only couplings we can form are the pseudoscalar P and the axial vector A , as was stated above.

In the following discussion, we shall ignore the UFI hypothesis of 4.6 and adopt the point of view of 4.1-4.5 that there is no universality of form.

It is not yet known experimentally whether or not the μ capture interaction contains appreciable amounts of P or A . Suppose, for the moment, that a large fraction of the μ capture interaction is A . Then $|D_A| \sim (10^{-7}/m_\pi^2)$. We may then try to estimate (very roughly) the rate of $\pi \rightarrow \mu\nu$ decay through the axial vector coupling by treating the Yukawa process in the lowest order of perturbation theory. The result is logarithmically divergent and must be cut off at some virtual mass λ :

$$\Gamma_\pi \approx \frac{1}{2\pi^4} m_\pi [D_A m_\pi^2]^2 \frac{g^2}{4\pi} \left(\ln \frac{\lambda}{m_N} \right)^2 \left(\frac{m_N}{m_\pi} \right)^2 \left(\frac{m}{m_\pi} \right)^2 \left(1 - \frac{m_\mu^2}{m_\pi^2} \right)^2 \approx 7 \times 10^8 / \text{sec.} \quad 17.$$

if we estimate D_A as above and $\ln \lambda/m_N$ as unity. (We recall that $g^2/4\pi \approx 15$.) This result is about 15 times greater than the experimental rate in Table I. Such a discrepancy is not surprising in view of the extreme crudity of the calculation, and we have no particular reason, therefore, for discarding the simple explanation of $\pi \rightarrow \mu\nu$ decay. If the μ capture interaction contains P , the formula corresponding to Eq. 17 contains a quadratic divergence, and the argument is even less reliable.

We must, of course, understand not only the occurrence of the decay $\pi^\pm \rightarrow \mu^\pm \pm \nu$ but also the absence or extreme rarity of the analogous process $\pi^\pm \rightarrow e^\pm \pm \nu$, for which the branching ratio is quoted experimentally as $< 10^{-5}$ (30). We have mentioned in 4.3 that there seems to be little or no A in the β -decay coupling but that essentially no information is available about P . If P and A are both lacking in β -decay, then $\pi^\pm \rightarrow e^\pm \pm \nu$ is forbidden. At the moment, this seems the likeliest explanation of the situation. The forbidden process $\pi^\pm \rightarrow e^\pm \pm \nu$ can still occur through electromagnetic effects: the virtual proton or antiproton emits a virtual photon that is absorbed by the final electron. The rate of the decay is then expected to be so small that it is inaccessible to present experimental techniques.

There is, however, another electromagnetic process that should occur more rapidly, in which the virtual proton or antiproton emits a real photon. The decay scheme is $\pi^\pm \rightarrow e^\pm \pm \nu + \gamma$. This is allowed, for example, for the tensor interaction in β -decay. Again we may estimate the rate using first order perturbation theory for the Yukawa process, and again the result is logarithmically divergent:

$$\begin{aligned}\Gamma_{\pi \rightarrow \mu\nu\gamma} &\approx \frac{C_T^2 m_\pi^5}{384\pi^5} \frac{e^2}{4\pi} \frac{g^2}{4\pi} \left(\ln \frac{\lambda}{m_N} \right)^2 \\ &\approx 5 \times 10^3/\text{sec.}\end{aligned}\quad 18.$$

using the value $|C_T| m_\pi^2 \approx 1.6 \times 10^{-7}$ given by β -decay phenomenology and estimating $\ln \lambda/m_N$ as unity as before. Experimental upper limits for the rate of the process are given by Cassels (31) and by Lokanathan (32) as $4 \times 10^2/\text{sec.}$ and $10^3/\text{sec.}$, respectively. Just as for $\pi^\pm \rightarrow \mu^\pm \pm \nu$, the crude calculation has overestimated the rate by at least a factor of ten, but the general theoretical picture does not seem to be in serious trouble. Of course, if further measurements show that the rate of the radiative decay is even lower, we may have to revise the theory.

Besides the obvious objections to a calculation using a cutoff and perturbation theory in a strong interaction, there is an additional point to be made about the theory. The pion (say π^+) may dissociate virtually not only into $p + \bar{n}$ but also into the following baryon-antibaryon pairs: $\Sigma^+ + \bar{\Lambda}$, $\Sigma^+ + \bar{\Sigma}^0$, $\Lambda + \Sigma^-$, $\Sigma^0 + \Sigma^-$, and $\Xi^0 + \Xi^-$. All of these processes are allowed by charge independence and can presumably be induced by the strong interactions. It may easily turn out that these baryons are particles of spin $\frac{1}{2}$ and possess weak couplings to the pairs $\mu\nu$ and $e\nu$ analogous to the μ -absorption and β -decay couplings of the nucleons. In the Puppi triangle, we would have to replace the label " $(p\bar{n})$ " at one vertex by the label " $(p\bar{n}), (\Sigma^+\bar{\Lambda})$, etc." In the decay of the pion, then, all six of these baryon-antibaryon pairs may appear as intermediate states and interfere with one another. If the interference should turn out to be destructive, it might help to explain the overestimates obtained in Eqs. 17 and 18. However, the calculations are so crude that at present this is pure speculation.

We have ignored completely the possibility of a direct coupling of π to μ and ν , relying entirely on four-fermion interactions to explain the decay of the charged pion. Such a point of view may, of course, be wrong. However, there is not much practical difference between the two theories. We have seen that a pseudoscalar or axial vector coupling of $p\bar{n}$ to $\mu^+\nu$ implies an effective coupling of π to $\mu\nu$. Conversely a direct coupling of π to $\mu\nu$ implies an effective pseudoscalar or axial vector interaction in μ capture. Experiment cannot distinguish one theory from the other without reliable calculations involving the strong interactions in virtual baryon-antibaryon pair states, and such calculations are far from possible at the present time.

Practically the same situation applies to the weak interactions of the strange particles. We shall therefore discuss all weak interactions in terms of four-fermion couplings, leaving in abeyance the question of whether direct weak couplings of mesons exist as well.

Let us now return briefly to the hypothesis of the UFI with V, A coupling, as treated in 4.6. We promised to show that the experimental ratio $(\pi^+ \rightarrow e^+ + \nu) / (\pi^+ \rightarrow \mu^+ + \nu) < 10^{-5}$ is inconsistent with the hypothesis. With V, A as the coupling, only A is effective in inducing the decays. We may refer to Eq. 17 for the $\pi \rightarrow \mu\nu$ rate using A . The $\pi \rightarrow e\nu$ rate is given by the same formula with m_μ replaced by m_e , so that the ratio is

$$\frac{\Gamma(\pi^+ \rightarrow e^+ + \nu)}{\Gamma(\pi^- \rightarrow \mu^- + \nu)} = \frac{m_e^2}{m_\mu^2} \frac{\left(1 - \frac{m_e^2}{m_\pi^2}\right)^2}{\left(1 - \frac{m_\mu^2}{m_\pi^2}\right)^2} \approx 1.3 \times 10^{-4}.$$

This result was remarked by Ruderman & Finkelstein (33), who showed that it is exact to all orders in the strong couplings.

4.8. Classification of weak interactions; the tetrahedron.—What changes must we make in the Puppi triangle in order to accommodate all known weak processes?

In 4.6 we have already suggested that it may be necessary to modify the vertex $p\bar{n}$ by adding some or all of the five additional baryon pairs $\Sigma^+\bar{\Lambda}$, $\Sigma^+\bar{\Sigma}^0$, etc. It is difficult to test whether or not this replacement is necessary, since interconversion among all these baryon-antibaryon pairs is possible by means of the strong couplings. For example, if someone should observe an event $\Sigma^+ \rightarrow \Lambda + e^+ + \nu$, this might be interpreted either as caused by a direct coupling of these four particles or else as proceeding indirectly through the usual β -decay coupling by means of the virtual reactions $\Sigma^+ \leftrightarrow \Lambda + p + \bar{n} \rightarrow \Lambda + e^+ + \nu$. In the absence of quantitative arguments, we must regard the above-mentioned six baryon-antibaryon pairs as a class and not attempt at the moment to resolve the class into its individual members. Let us call it Class I of baryon-antibaryon pairs.

The observed weak processes not accounted for by the Puppi triangle all involve strange particles. We may start with the decay $K^\pm \rightarrow \mu^\pm \pm \nu$. (We assume conservation of leptons.) The selection rules obeyed by the strong interactions allow K^\pm to dissociate into any of the following six charged pairs of baryons and antibaryons: $p+\bar{\Lambda}$, $p+\bar{\Sigma}^0$, $n+\bar{\Sigma}^-$, $\Lambda+\bar{\Xi}^-$, $\Sigma^++\bar{\Xi}^0$, $\Sigma^0+\bar{\Xi}^-$. Let us refer to these as Class II and again not attempt to distinguish carefully among them. If some or all of the pairs of Class II are coupled by appropriate four-fermion couplings to μ and ν , then the decay of the charged K into muon and neutrino can be understood. By "appropriate," we mean, of course, "consistent with selection rules"; for example, if K is pseudoscalar relative to Λ and N , then we refer to a pseudoscalar or axial vector coupling of $p\bar{\Lambda}$ to $\mu^+\nu$ as "appropriate." (The situation is then exactly analogous to that in $\pi^\pm \rightarrow \mu^\pm \pm \nu$ decay.)

The decay $K^\pm \rightarrow \pi^0 + \mu^\pm \pm \nu$ also requires couplings of Class II to μ and ν , although here the selection rules on the form of the coupling are different. (See 4.9.) The point is that any of the virtual baryons or antibaryons can easily emit a π^0 .

Similarly the decay $K^\pm \rightarrow \pi^0 + e^\pm \pm \nu$ corresponds to four-fermion couplings between Class II and the electron-neutrino pair. So does the unobserved decay $K^\pm \rightarrow e^\pm \pm \nu$, but this can be forbidden, like the analogous decay of the pion, by omitting some of the possible forms of the coupling.

The purely pionic decays of K particles can be understood in terms of four-fermion couplings between Class I and Class II. For example, the

process $K^+ \rightarrow \pi^+ + \pi^0$ can be thought of in terms of the sequence of virtual steps $K^+ \Rightarrow p + \bar{\Lambda} \rightarrow p + \bar{n} \Rightarrow p + \bar{n} + \pi^0 \Rightarrow \pi^+ + \pi^0$ or else, say, $K^+ \Rightarrow \Lambda^0 + \bar{\Xi}^- \rightarrow \Sigma^+ + \bar{\Sigma}^0 \rightarrow \Sigma^+ + \bar{\Sigma}^0 + \pi^0 \Rightarrow \pi^+ + \pi^0$, etc.

The reader may now satisfy himself that all of the weak decays of strange particles listed in Tables II and VI are accounted for by the interactions we have just listed; namely, those of Class II with $e\nu$, $\mu\nu$, and Class I. Let us give some further examples. For the decay $\Sigma^+ \rightarrow p + \pi^0$ we may have a chain like $\Sigma^+ \rightarrow \Sigma^0 + p + \bar{\Lambda} \Rightarrow p + \pi^0$. For $\Xi^- \rightarrow \Lambda + \pi^-$ one possibility is $\Xi^- \rightarrow \Lambda + n + \bar{p} \Rightarrow \Lambda + \pi^-$, and so forth.

A number of so far unobserved processes are predicted also. For example, the coupling of Class II to $e\nu$ leads to at least one of the following leptonic decays of hyperons: $\Lambda^0 \rightarrow p + e^- + \bar{\nu}$, $\Sigma^0 \rightarrow p + e^- + \bar{\nu}$ (undetectable because of competition from $\Sigma^0 \Rightarrow \Lambda^0 + \gamma$), $\Sigma^- \rightarrow n + e^- + \bar{\nu}$, $\Xi^- \rightarrow \Lambda^0 + e^- + \bar{\nu}$, $\Xi^- \rightarrow \Sigma^0 + e^- + \bar{\nu}$, and $\Xi^0 \rightarrow \Sigma^+ + e^- + \bar{\nu}$. We discuss these hypothetical processes further in 4.9.

The picture we have outlined is summarized in Figure 2a. The Puppi triangle is replaced by a tetrahedron, with vertices occupied by $e^+\nu$, $\mu^+\nu$, Class I and Class II, respectively. We may think of the K particles as attached by means of strong interactions to the Class II vertex (for example through $K^+ \Leftrightarrow p + \Lambda$), while one or more pions are similarly attached to the Class I vertex (for example through $\pi^+ \Leftrightarrow p + \bar{n}$).

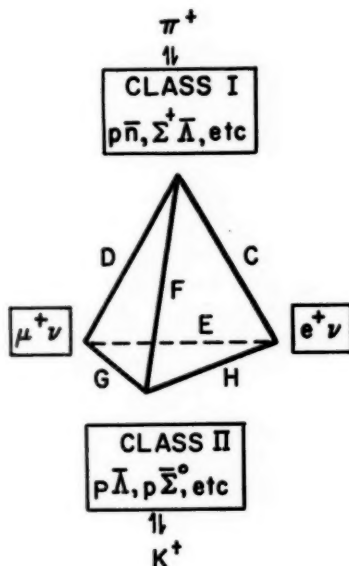


FIG. 2a. Tetrahedron representation of four-fermion interaction of positively charged pairs. Legs C, D, and E form the Puppi triangle of Fig. 2. Strange particles are introduced at the Class II vertex; their decays are represented by legs F, G, and H.

The physical ideas behind the tetrahedron scheme have been put forward by Dalla porta and collaborators (34) and by Gell-Mann (R1).

In our subsequent discussion of the weak decays of strange particles, we shall refer to Figure 2a and to the rough theory that it represents. Let us therefore make clear what is involved in such a description of the weak couplings.

We have already emphasized that it is not worth while at the present moment to quibble about whether some of the four-fermion interactions should be replaced by, say, boson-fermion interactions, nor about which members of Classes I and II actually possess direct weak couplings. We have seen, moreover, that the tetrahedron expresses the general features of the experimental situation. In 4.9 we shall discuss the "universality of strength" of the six edges of the tetrahedron. The principal point to be clarified, therefore, is the nature of the conceivable weak processes not included in Figure 2a.

In effect, by restricting the weak interactions to the *minimal set* (those represented in Fig. 2a) that can explain known processes, we are constructing an elaborate set of selection rules forbidding other weak couplings. Some of these additional couplings are known to be absent or nearly so, others can be looked for in the near future, while still others are inaccessible to investigation with present techniques. Let us list some of the more interesting hypothetical couplings omitted from the tetrahedron: (a) The processes $\mu^\pm \rightarrow e^\pm + e^\pm + e^\mp$, $\mu^\pm \rightarrow e^\pm + \gamma$, and $\mu^- + p \rightarrow e^- + p$ have been searched for and found to be very rare or absent (35). Nothing in the tetrahedron is known to induce these. In fact the only interaction in our scheme that couples μ and e together is the muon decay interaction. (In Table VI an experimental upper limit is given for the rate of the hypothetical decay $K^+ \rightarrow \mu^\pm + e^\mp + \pi^\pm$, a typical reaction in which μ and e might occur together.) (b) The muon decay interaction is also the only one listed that couples a neutrino-antineutrino pair. Now it is conceivable that other systems also can decay by $\nu - \bar{\nu}$ pair emission. For example, weak virtual processes like $n \rightarrow n + \nu + \bar{\nu}$ or $p \rightarrow p + \nu + \bar{\nu}$ might exist. They are completely undetectable at present, however, because in the decay of nuclear excited states or the decay of π^0 , where such couplings might show up, they are overwhelmingly dominated by electromagnetic decays. Other decays involving $\nu - \bar{\nu}$ pairs could be detected if they exist: For example, $K^\pm \rightarrow \pi^\pm + \nu + \bar{\nu}$ or $\Sigma^+ \rightarrow p + \nu + \bar{\nu}$ could be distinguished from other decay schemes, and all competing processes, moreover, are weak. An upper limit for the rate of the former process is given in Table VI. The decays $K_1^0 \rightarrow \nu + \bar{\nu}$ and $K_2^0 \rightarrow \nu + \bar{\nu}$, it is interesting to note, are forbidden by conservation of angular momentum if K is spinless and the neutrino longitudinal. (c) It is convenient to introduce a Class III of baryon-antibaryon pairs that might form an additional fifth vertex of our figure that was first a triangle and then a tetrahedron. This class consists of the two pairs $\Sigma^+ \bar{n}$ and $\Xi^0 \bar{\Sigma}^-$; these are the pairs into which a hypothetical meson of positive charge but negative strangeness might dissociate. (We recall that Classes I

and II are the possible dissociation products of π^+ and K^+ , respectively.) We may now generate a group of weak couplings excluded from the tetrahedron: we couple the pairs of Class III to $e\nu$ or to $\mu\nu$. This will lead to such decays as $\Sigma^+ \rightarrow n + \mu^+ + \nu$ and $\Xi^0 \rightarrow \Sigma^- + e^+ + \nu$, which are forbidden in the tetrahedron scheme.

A subtle point now arises in connection with the leptonic decay of K^0 and \bar{K}^0 . We note that in the tetrahedron picture we can have only $\bar{K}^0 \rightarrow e^- + \bar{\nu} + \pi^+$, or $\mu^- + \bar{\nu} + \pi^+$, $K^0 \rightarrow e^+ + \nu + \pi^-$ or $\mu^+ + \nu + \pi^-$. These processes are essentially implied by the corresponding decays of K^- and K^+ .

The hypothetical couplings of Class III to the $e\nu$ and $\mu\nu$ vertices would lead to the additional processes $\bar{K}^0 \rightarrow e^+ + \nu + \pi^-$ or $\mu^+ + \nu + \pi^-$, and $K^0 \rightarrow e^- + \bar{\nu} + \pi^+$ or $\mu^- + \bar{\nu} + \pi^+$.

The subtlety enters when we remember that the decay of neutral K mesons must be discussed as in 3.9, in terms of K_1^0 and K_2^0 , which are linear combinations of K^0 and \bar{K}^0 . We shall return to this very interesting question in 6.9. (d) If we introduce Class III as above and couple it to Class II, we obtain interactions involving SIPS only, but with ΔS not restricted to ± 1 . Such processes as $\Xi^- \rightarrow n + \pi^-$, involving $|\Delta S| = 2$, become possible. In 3.8, we have mentioned that there is some evidence against such decays. (e) The tetrahedron excludes also decays of Ξ into N with lepton pair emission, such as $\Xi^- \rightarrow n + e^- + \bar{\nu}$.

In concluding this survey, let us call attention to one further set of possible weak interactions of the four-fermion type, a set which is suggested by the tetrahedron scheme although not included in it as we have described it so far. These are couplings of the four vertices to themselves. For example, we may have such interactions as $[\bar{e}(1 - \gamma_5)\nu][\bar{\nu}(1 + \gamma_5)e]$ or $(\bar{p}n)(\bar{n}p)$ or $(\bar{p}\Lambda)(\bar{\Sigma}^0 p)$.

The first one represents electron-neutrino scattering and may be experimentally detectable by means of the recoils of atomic electrons struck by the antineutrinos from a large nuclear reactor. The cross section should be slightly smaller than the cross section for the reaction $\bar{\nu} + p \rightarrow e^+ + n$, which has been observed (12). It should be noted that in the longitudinal theory the neutrino possesses no magnetic or electric moments and any neutrino-electron scattering that may be observed is presumably to be ascribed to the interaction we are discussing.

A weak coupling of the pair $\bar{p}n$ to itself might some day be detectable to the extent that it violates conservation of parity. If it is of the same strength as other weak couplings, it could give a violation of parity conservation by one part in 10^{13} or 10^{14} in intensity in a nuclear experiment such as Tanner's (17) (mentioned in 3.10). Present measurements exclude any violation by more than one part in 10^7 . If no coupling of Class I (or Class II) to itself exists, then parity may be conserved in nuclear processes to one part in 10^{26} or 10^{28} . At this level, second order weak processes come into play such as virtual β -decay followed by virtual inverse β -decay.

4.9. *Decay rates of strange particles.*—We have sketched in 4.8 the tetra-

hedron scheme that provides a minimal set of four-fermion couplings that can account for known weak processes. Three of the six edges of the tetrahedron are simply the three sides of the Puppi triangle. The remaining three edges correspond to the coupling of Class II ($p\bar{\Lambda}$, etc.) to $e^+\nu$, $\mu^+\nu$, and Class I ($p\bar{n}$, etc.); these three are the ones responsible for strange particle decays. We shall now present some crude estimates of the rates of decay of strange particles on the assumption that these edges have about the same strength as those in the Puppi triangle. The estimates are in reasonable accord with experiment.

We have supposed that the baryons have spin $\frac{1}{2}$. Let us further suppose that the spin of K is zero. (Experimental evidence for this is adduced in 6.1.) The relative parity of Λ and N is not a determinate quantity, since any process such as $\Lambda \rightarrow \pi + N$, by means of which it might be measured, is weak and need not conserve parity. However, as pointed out in 3.10, the parity of K relative to Λ and N is unique if parity is conserved by the strong interactions. Let us therefore define the parity of Λ to be the same as that of N and call K scalar or pseudoscalar according to its coupling to Λ and N . (It is in the same spirit that we conventionally define the parities of p and n to be the same and call π^\pm pseudoscalar because of its pseudoscalar coupling to p and n .)

For simplicity let us consider in Class I only the pair $p\bar{n}$ and in Class II only the pair $p\bar{\Lambda}$. In this way we discard many interesting effects, especially possible cancellations among the various members of a class, but we are concerned here only with very rough estimates.

Let us look first at the decays of Λ . The coupling of $p\bar{\Lambda}$ and $p\bar{n}$ can lead to the decays $\Lambda \rightarrow p + \bar{p} + n \Rightarrow p + \pi^-$ and $\Lambda \rightarrow p + \bar{p} + n \Rightarrow n + \pi^0$, which have been observed. The couplings of $p\bar{\Lambda}$ to $e^+\nu$ and to $\mu^+\nu$ give the processes $\Lambda \rightarrow p + e^- + \bar{\nu}$ and $\Lambda \rightarrow p + \mu^- + \bar{\nu}$ respectively; these have never been detected with certainty and seem to form $\lesssim 2$ per cent of all decays of Λ (Table II). We must, of course, try to account for this situation.

The absolute rates of the leptonic decays are easily estimated. There is a direct analogy between these processes and the decay of the neutron, $n \rightarrow p + e + \bar{\nu}$. We may refer to Eq. 6 for the rate of neutron decay. Assuming that $C_e^2 + C_{e'}^2 + \dots$ is about the same for Λ couplings as for the neutron, we see that the only differences are these: Δ , which is now the mass difference of Λ and p , is 177 Mev instead of 1.293 Mev; and the blocking factor is 1 for $\Lambda \rightarrow p + e^- + \bar{\nu}$ and 0.16 for $\Lambda \rightarrow p + \mu^- + \bar{\nu}$. With the couplings roughly the same, therefore, we have for the rates

$$\Gamma(\Lambda \rightarrow p + e^- + \bar{\nu}) = \left(\frac{177}{1.293} \right)^5 \frac{1}{.47} \Gamma_n \sim 10^8/\text{sec.}$$

$$\Gamma(\Lambda \rightarrow p + \mu^- + \bar{\nu}) \sim .16 \Gamma(\Lambda \rightarrow p + e^- + \bar{\nu}) \sim .16 \times 10^8/\text{sec.}$$

Here Γ_n is, of course, the rate of neutron decay. We have neglected recoil effects, which may reduce these estimates by as much as a factor of two. The experimental upper limit on the rate of leptonic decays (Table II) is in

the vicinity of 10^8 /sec. If these rates are really not much lower, the theory is not in trouble.

We must somehow understand, however, why the pionic decays go much faster. Let us try to estimate the rate of $\Lambda \rightarrow p + \pi^-$. We might simply use the lowest order of perturbation theory for the strong couplings in the process $\Lambda \rightarrow p + n + \bar{p} \Rightarrow p + \pi^-$. It is helpful to note, however, the similarity between the decays $\Lambda \rightarrow p + \pi^-$ and $\pi^\pm \rightarrow \mu^\pm \pm \nu$, exhibited in the lowest order Feynman diagrams for these two processes (Fig. 3). We must recall that in 4.7, when we treated the pion decay using an axial vector coupling of typical strength, we found that the nucleon-antinucleon loop in the lowest order Feynman diagram gave rise to a logarithmic divergence. When we estimated

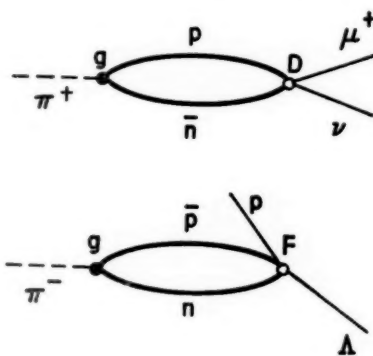


FIG. 3. Feynman diagrams for $\pi^+ \rightarrow \mu^+ + \nu$ and $\Lambda \rightarrow p + \pi^-$. The solid circles labeled g represent the strong πN interaction. The open circles labeled D and F represent the weak four-fermion interactions (legs D and F of the tetrahedron).

the logarithm by means of a cutoff in the vicinity of the nucleon mass, we found that the rate of pion decay came out too high by a factor of about 15.

In view of the many uncertainties in the pion decay calculation (perturbation theory, cutoff, possible contributions of other pairs in Class I, etc.) it is probably wisest to let the rate of $\pi^+ \rightarrow \mu^+ + \nu$ serve as an experimental calibration of the effect of the nucleon-antinucleon loop. We mentioned in 4.7 that the loop gives rise to an effective nonlocal interaction of π with the pair $\mu\nu$. Actually, since the mass of the nucleon pair in the loop is much greater than the mass of the pion, we may approximate this by a local coupling. Thus the axial vector interaction

$$\mathcal{L}_A = - D_A [\bar{\mu} \gamma_\alpha \gamma_\beta \mu] [\bar{\nu} \gamma_\alpha \gamma_\beta (1 - \gamma_5) \nu] + \text{Herm. conj.} \quad 19.$$

of 4.7 gives rise effectively to a direct interaction of the form

$$\mathcal{L}_{\text{eff.}} = \frac{id}{m_\pi} \frac{\partial \pi}{\partial x_\alpha} [\bar{\mu} \gamma_\alpha \gamma_\beta (1 - \gamma_5) \nu] + \text{Herm. conj.} \quad 20.$$

where we have formed an axial vector by taking the gradient of the pseudo-

scalar pion field operator π that destroys π^- or creates π^+ . The Hermitian conjugate operator π^\dagger destroys π^+ or creates π^- . In 4.7, we tried to calculate d from the loop. Now let us take it from experiment. The rate of charged pion decay, with the coupling of Eq. 20, is

$$\Gamma_\pi = \frac{d^2}{4\pi} \frac{m_\mu^2}{m_\pi^2} \left(1 - \frac{m_\mu^2}{m_\pi^2}\right)^2. \quad 21.$$

Using the known rate Γ_π , we find $(d^2/4\pi) \approx 1.8 \times 10^{-15}$.

Suppose we try a coupling of $p\bar{n}$ to $p\bar{\Lambda}$ analogous to Eq. 19 for $p\bar{n}$ to $\mu^+\nu$. In the case of $p\bar{\Lambda}$, we have no longitudinal theory that forces us to the expression $(1-\gamma_5)$; the "parity conserving" and "parity nonconserving" terms need not have equal strength. Let us therefore imagine an interaction like

$$-F_A[\bar{p}\gamma_\alpha\gamma_\beta n][\bar{\Lambda}\gamma_\alpha\gamma_\beta p] - F_A'[\bar{p}\gamma_\alpha\gamma_\beta n][\bar{\Lambda}\gamma_\alpha p] + \text{Herm. conj.}$$

Then the effective coupling analogous to Eq. 20 will be

$$\frac{if}{m_\pi} \frac{\partial\pi}{\partial x_\alpha} [\bar{\Lambda}\gamma_\alpha\gamma_\beta p] + \frac{if'}{m_\pi} \frac{\partial\pi}{\partial x_\alpha} [\bar{\Lambda}\gamma_\alpha p] + \text{Herm. conj.} \quad 22.$$

The first (parity conserving) term gives rise to $\Lambda \rightarrow p + \pi^-$ with the pion in a p state and the second (parity nonconserving) term gives $\Lambda \rightarrow p + \pi^-$ with the pion in an s state. (Remember we have defined the parities of Λ and p to be the same.) Using Eq. 22, we may calculate the rates of decay of Λ into $p + \pi^-$ in an s or a p state respectively, neglecting recoil for simplicity:

$$\Gamma_{\Lambda^s \rightarrow p + \pi^-} = \frac{f'^2}{4\pi} \cdot 2p_\Lambda \left(\frac{m_\Lambda - m_p}{m_\pi}\right)^2, \quad 23.$$

$$\Gamma_{\Lambda^p \rightarrow p + \pi^-} = \frac{f^2}{4\pi} \cdot 2p_\Lambda \left(\frac{p_\Lambda}{m_\pi}\right)^2, \quad 24.$$

where p_Λ is the momentum of the emitted pion (see Table III). If the order of magnitude of $F_A'^2$ and D_A^2 is the same, then we should expect $f'^2/4\pi \approx (d^2/4\pi)$; similarly, if F_A^2 and D_A^2 are comparable, so are $f^2/4\pi$ and $d^2/4\pi$. Under the former assumption, using our experimental value of $d^2/4\pi$, we find $\Gamma_{\Lambda \rightarrow p + \pi^-} \sim 10^9/\text{sec}$. If $(f^2/4\pi) \sim (d^2/4\pi)$, we have $\Gamma_{\Lambda \rightarrow p + \pi^-} \sim 3 \times 10^8/\text{sec}$. The experimental value of the total rate of $\Lambda \rightarrow p + \pi^-$ is $\approx 2 \times 10^9/\text{sec}$. (see Table II), in excellent and probably fortuitous agreement with the calculated values.

If we had used pseudoscalar rather than axial vector coupling, the agreement would have been somewhat worse and the ratio of s to p wave emission would have been much larger for equivalent coupling constants.

Let us regard our discussion of Λ as typical of the situation for hyperons, and turn to the decays of K particles. The process $K^+ \rightarrow \mu^+ + \nu$ is also analogous to $\pi^+ \rightarrow \mu^+ + \nu$, although here the analogy is of a different nature. The Feynman diagrams to lowest order in the strong couplings are shown in Figure 4. In the pion decay, the loop is composed of, say, nucleon and anti-nucleon, while in K^+ decay it is, say, a $p\bar{\Lambda}$ loop. The coupling of K to $\bar{\Lambda}$ and N need not have precisely the same strength as that of π to N and \bar{N} ; in

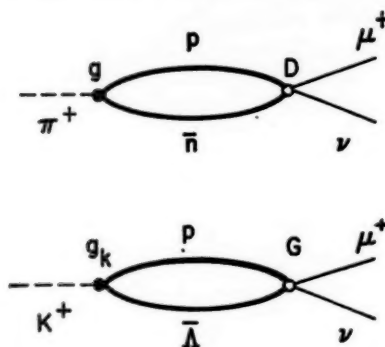


FIG. 4. Feynman diagrams for $\pi^+ \rightarrow \mu^+ + \nu$ and $K^+ \rightarrow \mu^+ + \nu$. The solid circles labeled g represent the strong meson-nucleon interactions. The open circles represent weak four-fermion interactions (legs D and G of the tetrahedron).

fact, K might be scalar rather than pseudoscalar so that the coupling would even have a different form. Also the K mass is greater than that of π and not nearly so negligible compared to baryon masses.

These differences are in addition to possible differences between the weak coupling of $p\bar{\Lambda}$ to $\mu^+\nu$ and that of $p\bar{n}$ to $\mu^+\nu$. Say we write the former as

$$G_S[\bar{p}\Lambda][\bar{\mu}(1-\gamma_5)\nu] + G_V[\bar{p}\gamma_{\alpha}\Lambda][\bar{\mu}\gamma_{\alpha}(1-\gamma_5)\nu] + \dots + \dots + \text{Herm. conj. } 25.$$

where the labels S , V , etc., refer to the Dirac matrices for the baryons. We have assumed the two component theory of the neutrino and conservation of leptons. Supposing that the coefficients G are of the same order of magnitude as the constants D in the muon capture interaction, let us pursue our rough analogy between $K^\pm \rightarrow \mu^\pm \pm \nu$ and $\pi^\pm \rightarrow \mu^\pm \pm \nu$.

If K , like π , is pseudoscalar, then only the P and A interactions can induce the decay $K^\pm \rightarrow \mu^\pm \pm \nu$. (The reason is the same as that given in 4.7 for the pion case.) By the same argument, if K is scalar, only the S and V interactions can induce it. Suppose that the interaction responsible for the decay is A (for a pseudoscalar K) or V (for a scalar K). This corresponds to our assumption of an A interaction in treating the pion decay. The $p\bar{\Lambda}$ loop will produce an effective coupling of K to $\mu\nu$ analogous to the effective coupling between π and $\mu\nu$ displayed in Eq. 20. The coefficient of the effective interaction is called d/m_π in Eq. 20; for the K particle let us call the corresponding coefficient γ/m_K . Then in place of Eq. 21 for the pion decay rate we have for the rate of $K^\pm \rightarrow \mu^\pm \pm \nu$ the expression

$$\Gamma_{K \rightarrow \mu\nu} = \frac{\gamma^2}{4\pi} m_K \frac{m_\mu^2}{m_K^2} \left(1 - \frac{m_\mu^2}{m_K^2}\right)^2 \quad 26.$$

Since experimentally $\Gamma_{K \rightarrow \mu\nu} \approx \Gamma_{\pi \rightarrow \mu\nu}$, we see that $\gamma^2/m_K^2 \approx 1/17 d^2/m_\pi^2$. Why is the effective coupling in K decay apparently much smaller than that in π decay if the weak four-fermion couplings have about the same strength? The explanation may be that the strong coupling of K to Λ , N is somewhat

weaker than the Yukawa coupling of π to the nucleon. Experiments on the photo- K effect ($\gamma + p \Rightarrow \Lambda + K^+$) should soon decide whether this is the case.

As in pion decay, we must understand why $\mu^\pm \pm \nu$ is preferred over $e^\pm \pm \nu$. The experimental upper limit on the ratio $(K^\pm \rightarrow e^\pm \pm \nu)/(K^\pm \rightarrow \mu^\pm \pm \nu)$ is only 0.02 (Table VI) as compared with 10^{-5} for the pion, but the problem still exists. We mentioned in discussing the UFI (4.6) that with identical couplings of Class I to $\mu^+\nu$ and $e^+\nu$ the lowest ratio $(\pi^\pm \rightarrow e^\pm \pm \nu)/(\pi^\pm \rightarrow \mu^\pm \pm \nu)$ is attained for the A interaction, namely

$$\frac{\Gamma(\pi \rightarrow e + \nu)}{\Gamma(\pi \rightarrow \mu + \nu)} = \frac{m_e^2}{m_\mu^2} \frac{\left(1 - \frac{m_e^2}{m_\pi^2}\right)^2}{\left(1 - \frac{m_\mu^2}{m_\pi^2}\right)^2} \approx 1.3 \times 10^{-4}.$$

Since according to Anderson and Lattes (30) the actual ratio is less than 10^{-5} , we must apparently give up the idea of identical couplings.

This result makes speculation about identical couplings of Class II to $e^+\nu$ and $\mu^+\nu$ seem rather unprofitable. For purposes of orientation, however, we may remark that for equal A couplings the ratio $(K^\pm \rightarrow e^\pm \pm \nu)/(K^\pm \rightarrow \mu^\pm \pm \nu)$ would be $\approx 2.5 \times 10^{-6}$ while for equal P couplings it would be ≈ 1 . (We are taking K to be pseudoscalar.) Probably the best we can say at the moment is the following: The coupling of Class II to $\mu^+\nu$ contains P and/or A while the coupling to $e^+\nu$ probably lacks P but may or may not contain A . If K is scalar, we must replace P by S and A by V in this statement.

The decays $K \rightarrow \pi + e^\pm \pm \nu$ and $K \rightarrow \pi + \mu^\pm \pm \nu$ occur with about equal frequency. This is in no sense a paradox, despite the smallness of the ratio $(K^\pm \rightarrow e^\pm \pm \nu)/(K^\pm \rightarrow \mu^\pm \pm \nu)$, since it turns out that the leptonic decay with single pion emission occurs through just those interactions that cannot induce plain leptonic decay. For a pseudoscalar K , the processes $K \rightarrow \pi + \text{leptons}$ are induced by S , T , and V ; for a scalar K , by P , T , and A .

The rate of $K^\pm \rightarrow \pi^0 + \mu^\pm \pm \nu$ is about 15 times smaller than that of $K^\pm \rightarrow \mu^\pm \pm \nu$. Simple considerations of available phase space may explain this qualitatively. The uncertainties in quantitative arguments seem to be so great as to make a detailed calculation not worthwhile.

The same applies to the rates of $K \rightarrow 3\pi$ and $K \rightarrow 2\pi$, which occur through the coupling of Class I with Class II in the tetrahedron scheme. We shall see in 6.5 that for a spinless K the 3π are in a 0^- state of angular momentum and parity, while the 2π are in a 0^+ state. For a pseudoscalar K , then, the former decay is induced by the "parity conserving" terms in the coupling and the latter by the "parity nonconserving" terms. For a scalar K , the reverse is true.

5. THE WEAK DECAYS OF HYPERONS

5.1. General features—In Table II we show what is known about hyperon decays. We have already referred to the principal features of the situation. Let us review them here.

TABLE II
BRANCHING RATIOS AND DECAY RATES OF Λ AND Σ^\pm

Mode	Branching ratio (%)	Rate* (number per sec)	Momentum $p\uparrow$ (Mev/c)	$h\Gamma/2pc\ddagger$
$\Lambda \rightarrow p + \pi^+$	65 ± 5 (a)	0.234×10^{10}	99.9	0.78×10^{-14}
$\rightarrow n + \pi^0$	35 ± 5 (a)	0.126×10^{10}	103.3	0.41×10^{-14}
$\rightarrow p + \left\{ \begin{array}{l} e \\ \mu \end{array} \right\}^- + \bar{\nu}$	< 2 (a)	($< 0.007 \times 10^{10}$)		
	100	0.36×10^{10}		1.19×10^{-14}
$\Sigma^+ \rightarrow p + \pi^0$	46 ± 6 (b)	0.59×10^{10}	189.0	1.04×10^{-14}
$\rightarrow n + \pi^+$	54 ± 6 (b)	0.69×10^{10}	185.0	1.24×10^{-14}
$\rightarrow n + \left\{ \begin{array}{l} e \\ \mu \end{array} \right\}^+ + \nu$	< 3 (b)	($< 0.04 \times 10^{10}$)		
	100	1.28×10^{10}		2.28×10^{-14}
$\Sigma^- \rightarrow n + \pi^-$	100	0.64×10^{10}	192.1	1.06×10^{-14}
$\rightarrow n + \left\{ \begin{array}{l} e \\ \mu \end{array} \right\}^- +$	< 5 (b)	($< 0.04 \times 10^{10}$)		
	100	0.64×10^{10}		1.06×10^{-14}

* The decay rates are based on the mean lives given in Table I.

† From Table III.

‡ $h\Gamma/2pc = |S|^2 + |P|^2$, the sum of the squares of the amplitudes, as defined in 5.3 and 5.6.

(a) Plano, Samios, Schwartz, and Steinberger, *Nuovo cimento* 5, 1700 (1957).

(b) Alvarez, Bradner, Falk-Vairant, Gow, Rosenfeld, Solmitz, and Tripp, *Interactions of K- Mesons in Hydrogen*, UCRL-3775, May 1957; see also *Nuovo cimento*, 5, 1026 (1957).

This branching ratio $f_0^+ = 46 \pm 6\%$ comes from 58 Σ^+ decays in a hydrogen bubble chamber ($27 \rightarrow \pi^0$, $31 \rightarrow \pi^+$). Six times as many Σ^+ decays have been seen in emulsion, namely 291 Σ^+ decays from rest ($137 \rightarrow \pi^0$, $154 \rightarrow \pi^+$), giving $f_0^+ = (47 \pm 3)\%$, where the 3% is based on statistical errors only. However, the true uncertainty in f_0^+ is no smaller than that for the bubble chamber events, because in emulsion the detection efficiency for $\Sigma^+ \rightarrow n + \pi^+$ is probably 10% less than for $\Sigma^+ \rightarrow p + \pi^0$. A correction for this bias of $(10 \pm 10)\%$ against $\Sigma^+ \rightarrow p + \pi^0$ reduces f_0^+ from emulsion to $(45 \pm 5)\%$. The emulsion events were gathered from all laboratories by G. Snow (private communication) for presentation to the Seventh Rochester Conference.

(a) Leptonic Decays. So few leptonic decays have been reported (36) that it is hard to say that any has ever been identified with certainty. We have seen in 4.9 that an estimate of the rate of $\Lambda \rightarrow p + e^- + \bar{\nu}$ on the basis of the tetrahedron is roughly equal to the experimental upper limit (Table II) for this rate. A similar estimate for $\Sigma^- \rightarrow n + e^- + \bar{\nu}$ yields the same conclusion. The decay $\Sigma^+ \rightarrow n + e^+ + \nu$ has a comparable upper limit experimentally; of course it may be absent as in the tetrahedron scheme. However, in the case of Λ and Σ^- , it is difficult to conceive that the leptonic modes could be absent, since even without the tetrahedron they could proceed by the virtual emission of K^- , which is known to undergo leptonic decay. Of course such an indirect process might give lower rates.

We have mentioned in 4.8 that the decays of strange particles present an opportunity to test the forbiddenness of $\nu\bar{\nu}$ and $\mu^\pm e^\mp$ lepton pair emission.

However, the K particle decays, in which at least *charged* lepton pairs occur frequently, are probably a better place to look for such an effect.

(b) Decays into *SIPs*. All energetically possible pionic decays of hyperons have been observed, except three: the decay of Ξ into π and N , which involves a change in strangeness of two units; the weak decay of Σ^0 that is unobservable because it cannot compete with the electromagnetic process $\Sigma^0 \rightarrow \Lambda + \gamma$; and the decay of the so-far unseen Ξ^0 , presumably into π^0 and Λ .

The rates of the known pionic decays of Σ and Λ are given in Table II and are all of the same order of magnitude; if we try to make a small correction for the available phase space by dividing out the pion momentum as in the fourth column, the effective strengths come out even closer. It seems that the intrinsic strengths of the weak couplings involved are very similar. We do not know, however, exactly what the law of variation of the strength is, neither between Σ and Λ nor even with the charge multiplet Σ . The law of variation within a multiplet is not charge independence, of course, since it is precisely by violating charge independence that the weak couplings induce these decays. It has been suggested, as we mentioned in 3.8, that the violation of isotopic spin conservation in weak decays of *SIPs* into *SIPs* may be subject to limitations, for example $|\Delta I| = \frac{1}{2}$.

No suggestion has yet been made of a possible law of variation of the decay rate from multiplet to multiplet.

5.2. *Spins of Λ and Σ* .—We shall assume that both Λ and Σ have spin $\frac{1}{2}$. The experimental evidence to date by no means either confirms or contradicts this assumption.

An argument in favor of spin $\frac{1}{2}$ for the Λ , based on the decay of hyperfragments, has been given by Ruderman & Karplus (37); it is taken up in Appendix D.

For both Λ and Σ the remaining evidence concerns the absence of anisotropy in the decay of these particles. Appendix B contains a description of the anisotropies and asymmetries to be expected under various assumptions. It also summarizes the present experimental evidence.

5.3. *Decay of Λ* .—The pionic decay of Λ can take place through four channels. There are two charge states, which we may list as $\pi^- + p$ and $\pi^0 + n$ or as eigenstates of isotopic spin with $I = \frac{1}{2}$ and $I = \frac{3}{2}$. There are also two states of pion orbital angular momentum: the final pion-nucleon system with angular momentum $J = \frac{1}{2}$ can be in either a ${}^2S_{1/2}$ or a ${}^2P_{1/2}$ state. These have opposite parity, but presumably parity need not be conserved in the decay.

Let us define amplitudes for the decays into the four channels. For the ${}^2S_{1/2}$ state with $I = \frac{1}{2}$, call the amplitude S_3 ; for the ${}^2P_{1/2}$ state with $I = \frac{1}{2}$, call it P_1 , etc. To make the amplitudes dimensionless, let us normalize them so that the decay rate into a given channel, say ${}^2S_{1/2}$ with $I = \frac{1}{2}$, is given by

$$\Gamma({}^2S_{1/2}, I = 1/2) = \frac{2\rho_{\Lambda c}}{\hbar} | S_3 |^2. \quad 27.$$

TABLE III
KINEMATICS OF HYPERON DECAYS

Decay mode	Momentum, \not{p} (Mev/c)	Total energy, $w = T + mc^2$ (Mev)	Available kinetic energy, Q (Mev)
p (mass = 938.21 ± 0.01 Mev) n (mass = 939.51 ± 0.01 Mev)			
Λ (mass = $1115.2 \pm .14$ Mev)	99.9	$w_p = 943.5$ $w_\pi = 171.7$	37.2
$\Lambda \rightarrow p + \pi^-$			
$\Lambda \rightarrow n + \pi^0$	103.3	$w_n = 945.2$ $w_\pi = 170.0$	40.5
Σ^0 (mass = 1188.8_{-3}^{+2} Mev)	71.2	$w_\Lambda = 1117.3$	73.5
$\Sigma^0 \rightarrow \Lambda + \gamma$			
Σ^+ (mass = $1189.3 \pm .25$ Mev)	189.0	$w_p = 957.1$ $w_\pi = 232.2$	116.1
$\Sigma^+ \rightarrow p + \pi^0$			
$\Sigma^+ \rightarrow n + \pi^+$	185.0	$w_n = 957.5$ $w_\pi = 231.8$	110.2
Σ^- (mass = $1196.4 \pm .5$ Mev)	192.2	$w_n = 958.9$ $w_\pi = 237.5$	117.3
$\Sigma^- \rightarrow n + \pi^-$			
Ξ^- (mass = 1321 ± 3.5 Mev)	139.4	$w_\Lambda = 1123.6$ $w_\pi = 197.3$	66.4
$\Xi^- \rightarrow \Lambda + \pi^-$			

Here \not{p}_Λ is the momentum of the pion emitted in Λ decay, about 100 Mev/c. (See Table III.) (Comparing Eq. 27 with Eqs. 23 and 24, we see that the quantities $|S|^2$ and $|P|^2$ are related to the "effective coupling constants" $f'^2/4\pi$ and $f^2/4\pi$ introduced in 4.9.) Evidently the total rate of pionic decay of Λ is

$$\Gamma(\Lambda \rightarrow N + \pi) = \frac{2\not{p}_\Lambda c}{\hbar} \{ |S_1|^2 + |S_3|^2 + |P_1|^2 + |P_3|^2 \} \quad 28.$$

and, neglecting possible rare additional modes of decay, we may equate this to the reciprocal lifetime of Λ (Table II) and obtain

$$|S_1|^2 + |S_3|^2 + |P_1|^2 + |P_3|^2 \approx 1.2 \times 10^{-14}. \quad 29.$$

We may expand the states $\pi^- + p$ and $\pi^0 + n$ as linear combinations of the isotopic spin eigenstates. The coefficients are given in Table IV which displays a real, unitary matrix of Clebsch-Gordan coefficients. Say the

TABLE IV
CLEBSCH-GORDAN COEFFICIENTS*

s Component of isotopic spin		Mode	$I = \frac{1}{2}$ (S_1 or P_1)	$I = \frac{3}{2}$ (S_3 or P_3)
$-\frac{1}{2}$	Λ	$\pi^- + p$ (S_- or P_-)	$\sqrt{\frac{2}{3}}$	$\sqrt{\frac{1}{3}}$
		$\pi^0 + n$ (S_0 or p_0)	$-\sqrt{\frac{1}{3}}$	$\sqrt{\frac{2}{3}}$
$+\frac{1}{2}$	Σ^+	$\pi^0 + p$ (S_0^+ or P_0^+)	$\sqrt{\frac{1}{3}}$	$\sqrt{\frac{2}{3}}$
		$\pi^+ + n$ (S_+^+ or P_+^+)	$-\sqrt{\frac{1}{3}}$	$\sqrt{\frac{1}{3}}$
$-\frac{3}{2}$	Σ^-	$\pi^- + n$ (S_-^- or P_-^-)	0	1

* Taken from E. U. Condon and G. H. Shortley, "Theory of Atomic Spectra" (Cambridge University Press, Cambridge, England, 1953), Table 2², p. 76.

s-wave amplitudes for final states $\pi^- + p$ and $\pi^0 + n$ are S_- and S_0 respectively; for the *p*-waves we have P_- and P_0 . Then we have the formulae

$$S_- = \sqrt{\frac{2}{3}} S_1 + \sqrt{\frac{1}{3}} S_3, \quad P_- = \sqrt{\frac{2}{3}} P_1 + \sqrt{\frac{1}{3}} P_3, \text{ etc.}$$

The unitarity of the Clebsch-Gordan matrices means that

$$|S_1|^2 + |S_3|^2 = |S_-|^2 + |S_0|^2 = \Gamma_S \frac{\hbar}{2p_{\Lambda} c}$$

and the same for the *P*'s.

The fraction of all pionic decays leading to $\pi^- + p$ is then

$$f_- = \frac{|S_-|^2 + |P_-|^2}{\Gamma_A \frac{\hbar}{2p_{\Lambda} c}} = \frac{|\sqrt{\frac{2}{3}} S_1 + \sqrt{\frac{1}{3}} S_3|^2 + |\sqrt{\frac{2}{3}} P_1 + \sqrt{\frac{1}{3}} P_3|^2}{|S_1|^2 + |S_3|^2 + |P_1|^2 + |P_3|^2} \quad 30.$$

Experiments on associated production of the $\Lambda - K^0$ pairs show that the fraction of all Λ 's decaying by this mode is 0.65 ± 0.05 (Plano 57); if the residue is virtually all $\pi^0 + n$, then we may say that $f_- \sim \frac{2}{3}$.

5.4. *Up-down asymmetry in the decay of Λ .*—The decay rates of Eqs. 27 or 28 involve the *S* and *P* amplitudes incoherently. An experiment that involves them coherently is one that explicitly tests the nonconservation of parity. Suppose that we have produced Λ particles in a reaction that leaves them polarized in the *x* direction. For example, in a two-body collision the

x -axis would be normal to the plane of production. In the center of mass system of the collision, let the Λ come off at an angle θ to the z -axis, which is along the direction of the incident beam that produces the reaction. Say that at this angle the amount of polarization in the x -direction is $p(\theta) \neq 0$. Then nonconservation of parity in the decay of Λ permits the existence of an "up-down" asymmetry of the decay pions. Let us write the intensity $W_-(\theta, \xi)$ of negative decay pions (coming from Λ produced at angle θ) as a function of $\xi = \cos \psi$, where ψ is the angle (in the rest system of Λ) between the momentum of the decay pion and the x -axis. We have

$$W_-(\theta, \xi) d\Omega d\xi = f_- I(\theta) d\Omega \frac{1}{2} [1 + \alpha_- p(\theta) \xi] d\xi, \quad 31.$$

where $I(\theta) d\Omega$ is the intensity of Λ production in the element of solid angle $d\Omega$ and α_- is the parameter of up-down asymmetry, which can range from -1 to 1. For neutral decay pions we replace f_- by $1-f_-$ and α_- by the corresponding parameter α_0 .

If we regard the production reaction as a polarizer of Λ 's then α measures the efficiency of the decay asymmetry as an analyzer. It is easy to express each α in terms of the S and P amplitudes (38):

$$\alpha_- = \frac{2 \operatorname{Re} S_-^* P_-}{|S_-|^2 + |P_-|^2}; \quad \alpha_0 = \frac{2 \operatorname{Re} S_0^* P_0}{|S_0|^2 + |P_0|^2}. \quad 32.$$

So far the S and P amplitudes are complex numbers of unknown phase. If CP or T invariance holds, then the phases are determined (see 2.6) in terms of pion-nucleon phase shifts. We can take

$$S_1 = |S_1| e^{i\delta_1}, \quad S_3 = \pm |S_3| e^{i\delta_3}, \quad P_1 = \pm |P_1| e^{i\delta_{11}}, \quad P_3 = \pm |P_3| e^{i\delta_{31}}, \quad 33.$$

where the δ 's are the $\pi-N$ phase shifts at center-of-mass momentum p_Λ in the states $(S_{1/2}, I = \frac{1}{2})$, $(S_{1/2}, I = \frac{3}{2})$, $(P_{1/2}, I = \frac{1}{2})$, and $(P_{1/2}, I = \frac{3}{2})$ respectively. The \pm signs in Eq. 33 are all independent. Experimental values of the phase shifts are given in Table V. Since all these phases are quite small, it is a fair approximation to take all of the S and P amplitudes real, assuming T invariance.

An up-down asymmetry has indeed been observed by the Berkeley hydrogen bubble chamber group (58). They have produced Λ by bombarding protons with pions according to the reactions $\pi^- + p \Rightarrow \Lambda + K^0$. Preliminary results indicate a large positive value of α_- . We can see from Eq. 32 that the search for up-down asymmetry represents a measurement of the extent to which one parity state (s - or p -wave) predominates over the other. The large asymmetry thus shows that neither s - or p -wave emission is dominant. However in Appendix D on hyperfragments we mention some evidence that $|P_-/S_-|^2 \leq 1/2$.

5.5. Possible rule $|\Delta I| = \frac{1}{2}$ in Λ decay.—We have mentioned in 3.8 that a selection rule on the change of isotopic spin has been suggested for the decay of SIPs into SIPs, namely $|\Delta I| = \frac{1}{2}$ (apart from electromagnetic corrections).

TABLE V

 $\pi - N$ PHASE SHIFTS AT THE MOMENTA OF Λ AND Σ DECAY

Momentum and type of decay	Phase shift			
	δ_1	δ_3	δ_{11}	δ_{31}
99.5 Mev/c (Λ)	+8°	-4°	≈ 0	≈ 0
189.0 Mev/c (Σ)	+8°	-14°	-3°	-3°

The subscripts used for the phase shifts are explained below, Eq. 33.

All the phase shifts except the underscored ones are taken from H. L. Anderson, Sixth Rochester Conference, 1956. The underscored numbers come from the more recent compilation of Anderson and Davidon, *Nuovo cimento*, **5**, 1238 (1957).

For decay of Λ , which has $I=0$, the consequences of this rule are extremely simple. It requires that the decay leave pion and nucleon in the $I=\frac{1}{2}$ state, so that both amplitudes P_3 and S_3 must vanish; according to Table IV we then have $S_- = -\sqrt{2}S_0$ and $P_- = -\sqrt{2}P_0$. Eq. 30 then tells us that the fraction f_- of charged decays must be $\frac{1}{2}$, which is in good agreement with experiment (see Table II).

The rule has the further consequence (as we see from Eq. 32) that the asymmetry parameters α_- and α_0 are equal. Of course α_0 is intrinsically difficult to deal with because only neutral particles are involved, and there is no experimental information on this point at present. Nevertheless, it is perhaps interesting to remark that the ratio α_-/α_0 can be determined without a knowledge of the Λ polarization $p(\theta)$.

5.6. *The decay of Σ^\pm .*—Just as we described the pionic decay of Λ in terms of four parameters, we can use six to describe the decay of Σ^+ and Σ^- .

In Σ^+ decay there are again four channels corresponding to s - and p -waves and to $I=\frac{1}{2}$ and $I=\frac{3}{2}$. We may call the corresponding amplitudes S_1^+ , S_3^+ , P_1^+ , and P_3^+ in an obvious notation. If we use the alternative description in terms of the states $\pi^0 + p$ and $\pi^+ + n$ (see Table IV) we must use (say in the s -state) the amplitudes S_0^+ and S_+^+ respectively, given by the relations

$$S_0^+ = \sqrt{\frac{1}{3}}S_1^+ + \sqrt{\frac{2}{3}}S_3^+, \quad S_+^+ = -\sqrt{\frac{2}{3}}S_1^+ + \sqrt{\frac{1}{3}}S_3^+. \quad 34.$$

In Σ^- decay the only possible final state is $\pi^- + n$ with $I=\frac{3}{2}$. Thus we have only two amplitudes $S_3^- = S_-^-$ and $P_3^- = P_-^-$.

The normalization of the S and P amplitudes will be as in Eq. 27 for the Λ case, except that here in place of p_Λ we use $p_\Sigma \approx 200$ Mev/c, the momentum of a pion in Σ decay. The quantities $|S_0^+|^2 + |P_0^+|^2 = \hbar\Gamma_0^+/2p_\Sigma c$, $|S_+^+|^2 + |P_+^+|^2 = \hbar\Gamma_+^+/2p_\Sigma c$, and $|S_-^-|^2 + |P_-^-|^2 = \hbar\Gamma_-^-/2p_\Sigma c$ are displayed in Table II; they are all approximately equal.

For each of the three decay modes we can define an asymmetry parameter α as we did in Eq. 32 for the Λ . Let us call these $\alpha_-^-, \alpha_0^+, \alpha_+^+$, where as usual the upper index is the charge of the Σ and the lower one is the charge of the emitted pion. In each case we have as before

$$\alpha = \frac{2 \operatorname{Re} (S^* P)}{|S|^2 + |P|^2}, \quad 35.$$

where S and P carry the same indices as α .

Associated production experiments with bubble chambers have shown an up-down asymmetry for Λ , (as mentioned above) but not for Σ . However most of the experiments have used negative pion beams, and we must remember that $\pi^- + p$ can yield $\Sigma^- + K^+$, but not $\Lambda^+ + K^-$. We conclude that the asymmetry is small for $\Sigma^- \rightarrow \pi^- + n$, and we must look elsewhere for information on the two decay modes of Σ^+ . Now in nuclear emulsion many K^- have been brought to rest and captured from atomic orbits according to the reaction $K^- + p \Rightarrow \Sigma^\pm + \pi^\mp$. The Σ and π tracks are in general not collinear for at least two reasons: first, the proton p is in motion in the nucleus; second, the Σ may be scattered before it leaves the nucleus. Thus one can define a "production plane" and its normal, $\hat{n} = \hat{p}_\Sigma \times \hat{p}_\pi$. Now consider the decay $\Sigma \rightarrow N + \pi'$, and classify it "up" if $\hat{p}_\pi \cdot \hat{n} > 0$. The present data are: $\Sigma^+ \rightarrow p + \pi^0$, 48 up and 69 down; $\Sigma^\pm \rightarrow n + \pi^\pm$, 67 up and 88 down. In the first process there seems to be an effect.¹⁵

If T invariance holds, the quantities S_1^+, P_1^+ , etc. have determined phases as before (compare Eq. 33). The relevant phase-shifts at the energy of Σ decay are given in Table V along with the corresponding ones for the Λ decay energy. Even at the higher energy the phase shifts are small enough so that in a rough approximation all S and P amplitudes are real.

5.7. *The $|\Delta I| = \frac{1}{2}$ rule in Σ^\pm decay.*—We shall now examine the restrictions imposed on the experimental quantities by the proposed selection rule $|\Delta I| = \frac{1}{2}$. We employ the "spurion" notation of Wentzel. (See 3.8.)

In $\Sigma \rightarrow N + \pi$, the value of I_z decreases by $\frac{1}{2}$; we can say that a spurion with $I = \frac{1}{2}$, $I_z = -\frac{1}{2}$ is absorbed by Σ^+ or Σ^- , which has $I = 1$ and $I_z = +1$ or -1 respectively, to give $\pi + N$, which can have $I = \frac{3}{2}$ or $I = \frac{1}{2}$.

We then have the following Clebsch-Gordan coefficients:

$\Sigma^+ + \text{Spurion}$	$I = 1/2$	$I = 3/2$
	$(S_1 \text{ and } P_1)$	$(S_3 \text{ and } P_3)$
$\Sigma^- + \text{Spurion}$	$-\sqrt{\frac{2}{3}}$	$\sqrt{\frac{1}{3}}$
	0	1

In our treatment of hyperon decays so far we have defined, for each isotopic spin state, a pair of amplitudes S and P corresponding to the two

¹⁵ This possible source of polarized Σ 's was pointed out to us by R. Gatto and R. D. Tripp and by M. Ceccarelli in private communications. The data have been supplied by many emulsion groups.

values of orbital angular momentum. Here we shall find it more convenient to define for the $I = \frac{1}{2}$ state, say, a vector \mathbf{N}_1 with components S_1 and P_1 along orthogonal "s" and "p" axes (see Fig. 5). In this notation the rule $|\Delta I| = \frac{1}{2}$ gives us the restriction

$$\mathbf{N}_3^- = \sqrt{3}\mathbf{N}_3^+, \quad 35a.$$

as we can see from the Clebsch-Gordan coefficients above. There is no restriction on \mathbf{N}_1^+ . We define analogous vectors \mathbf{N}_0 , \mathbf{N}_+ , and \mathbf{N}_- , where as usual the subscript refers to the charge of the emitted pion and where we have dropped the redundant superscript giving the charge of Σ . Using Table IV we can then write:

$$\begin{aligned} \mathbf{N}_0 &= -\sqrt{\frac{1}{3}}\mathbf{N}_1^+ + \sqrt{\frac{2}{3}}\mathbf{N}_3^+; & |\mathbf{N}_0|^2 &= \frac{\hbar}{2p_{2c}}\Gamma_0 \\ \mathbf{N}_+ &= -\sqrt{\frac{2}{3}}\mathbf{N}_1^+ + \sqrt{\frac{1}{3}}\mathbf{N}_3^+ & |\mathbf{N}_+|^2 &= \frac{\hbar}{2p_{2c}}\Gamma_+ \\ \mathbf{N}_- &= 0 + \sqrt{3}\mathbf{N}_3^+ & |\mathbf{N}_-|^2 &= \frac{\hbar}{2p_{2c}}\Gamma_- \end{aligned} \quad 36.$$

and the identity

$$\sqrt{2}\mathbf{N}_0 + \mathbf{N}_+ = \mathbf{N}_-. \quad 37.$$

In other words, if the rule $|\Delta I| = \frac{1}{2}$ is valid the three vectors $\sqrt{2}\mathbf{N}_0$, \mathbf{N}_+ and \mathbf{N}_- must form a triangle as shown in Figure 5. We assume at this point CP or T invariance and neglect the $\pi - N$ phase shifts, so that our "vectors" are real. Table II shows that the experimental rates are all equal (within about 10 per cent) so let us take $|\mathbf{N}_-| = |\mathbf{N}_0| = |\mathbf{N}_+|$. We see that our triangle must have sides in the ratio $\sqrt{2}:1:1$. Such a $(45^\circ, 45^\circ, 90^\circ)$ triangle of course can be constructed, and so the $|\Delta I| = \frac{1}{2}$ rule is consistent with the rates of the three Σ^\pm decays.

In Fig. 5 we have drawn \mathbf{N}_- at an unknown angle ν_- with the *s*-axis indicating that we have so far put no restrictions on $P_-/S_- = \tan \nu_-$.

We can now write the asymmetry coefficients α_- , α_0 and α_+ (Eq. 35) in terms of the three known sides of the triangle and of the unknown P_-/S_- ratio. We note that the expression for α_- can be rewritten in terms of the angle ν_- :

$$\alpha_- = \sin 2\nu_-. \quad 38.$$

We can see by inspection that the angles of \mathbf{N}_0 and \mathbf{N}_+ in *s-p* space are $\nu_0 = \nu_- \pm 45^\circ$ and $\nu_+ = \nu_- \pm 90^\circ$. (The signs arise because the triangle could equally well have been drawn reflected about \mathbf{N}_-). Asymmetry expressions like Eq. 38 obviously apply for all three modes of decay, so we have

$$\alpha_0 = \sin 2(\nu_- \pm 45^\circ) = \pm \cos 2\nu_-, \quad 39.$$

$$\alpha_+ = \sin 2(\nu_- \pm 90^\circ) = -\sin 2\nu_-. \quad 39a.$$

Eqs. 38, 39, and 39a give us all three asymmetries in terms of the angle ν_- . For example, if ν_- is near 0° or near 90° (pure *s*- or *p*-wave in the Σ^- decay),

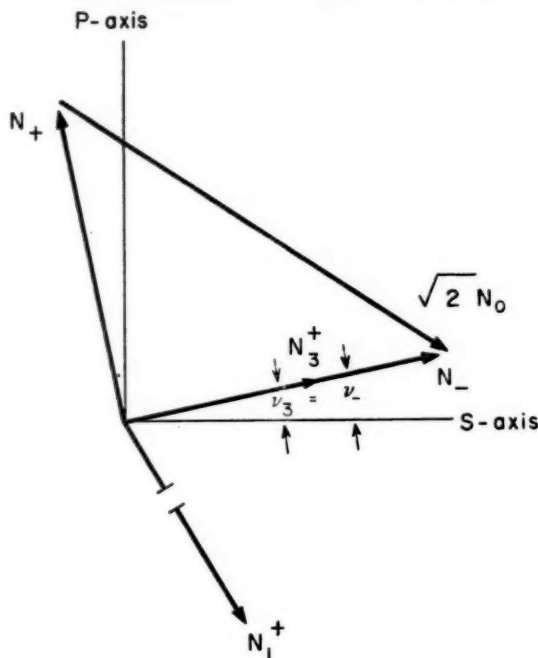


FIG. 5. Triangle representing the restrictions imposed on Σ decay by the $|\Delta I| = \frac{1}{2}$ rule.

then α_- and α_+ are small and α_0 is maximal. (Such a situation could describe the data presented below Eq. 35, if they were taken seriously.) There is no value of ν_- for which all three asymmetry parameters α can be small.

5.8. *The decay of Ξ .*—Very little is known about the Ξ particle. If pionic decay really predominates here, too, then there is only one principal mode of decay for each charge state: the known process $\Xi^- \rightarrow \pi^- + \Lambda$ and the hypothetical process $\Xi^0 \rightarrow \pi^0 + \Lambda$.

If the rule $|\Delta I| = \frac{1}{2}$ applies, then the rate of pionic decay of Ξ^- is twice that of Ξ^0 .

As mentioned earlier, it is important to know whether the decay into $\pi + N$ with $|\Delta S| = 2$ is really forbidden.

6. K MESON DECAY

6.1. *The spin of the K meson.*—There is considerable evidence in favor of spin zero for the K meson. First of all there are two indications that the spin is even: (a) The spectrum of the decay $K^+ \rightarrow \pi^+ + \pi^+ + \pi^-$ seems to be inconsistent with odd spin, although quite consistent with spin zero or two (see 6.5). (b) A neutral mode of decay of K_1^0 has been discovered that is probably $K_1^0 \rightarrow \pi^0 + \pi^0$ (39). Since the neutral pions are identical bosons,

this would rule out odd spin. Then there are three arguments for spin 0 rather than 2, 4, etc.: (a) If the spin were 4 or greater, it would seem that the decay of K_1^0 should be delayed by centrifugal barrier effects and should not proceed with a typical hyperonic lifetime of about 10^{-10} sec. Even spin 2 seems unlikely for this reason. (b) For any spin greater than zero, Dalitz (40) has estimated that the decay $K^+ \rightarrow \pi^+ + \gamma$ should compete rather favorably with other modes. Experiment, however, indicates that not more than a few per cent of K^+ , if any, decay in this way. For a spinless K meson, of course, the decay into $\pi^+ + \gamma$ is strictly forbidden, since it is then a $0 \Rightarrow 0$ transition. (c) Finally, there is the argument based on the absence of anisotropy in the decay of K^+ mesons.¹⁶

6.2. *Modes of decay of K mesons.*—In Table VI we list the decay modes and branching ratios for K^\pm , K_1^0 , and K_2^0 , as far as they are known at present. Table VII gives the momenta and energies of the decay products.

The most rapid decay is $K_1^0 \rightarrow 2\pi$ with a rate of around $10^{10}/\text{sec}$. No competing process has been detected with certainty in the case of K_1^0 . In the case of K_2^0 , the decay into two pions seems to be rare or lacking. (CP invariance would forbid it altogether, as we saw in 3.9.) The lifetime is correspondingly much longer and the much slower processes $K \rightarrow 3\pi$ and $K \rightarrow \text{leptons} + \pi$ are observed.

In the decay of K^\pm , the 2π mode is somehow inhibited; the rate of 2π decay is smaller than in the case of K_1^0 by a factor of around 500. As in K_2^0 decay, the modes 3π and leptons + π have a chance to compete. In the case of the charged K , however, an additional leptonic mode is available, $K^\pm \rightarrow \mu^\pm \pm \nu$ (with no π^0). This is, in fact, the most frequent mode of disintegration of the charged K . As we mentioned in 4.9, the analogous decays $K^\pm \rightarrow e^\pm \pm \nu$ are rare or absent. Experiments on K^+ stopping in emulsion with the emission of e^+ indicate that the ratio $(e^+ + \nu)/(\mu^+ + \nu)$ is probably less than 2 per cent and could be zero.

In 4.8 we mentioned that no decays by neutrino-pair emission are known (except for the ambiguous case of μ^+ -decay) but that they might exist, so far as we know. Presumably the best test of neutrino-pair emission would be the hypothetical decay $K^+ \rightarrow \pi^+ + \nu + \bar{\nu}$. Experiments to date rule out a

¹⁶ Barring accidents, we should expect some polarization in a K^+ beam if the spin is greater than zero. If there is polarization then there must be anisotropy in the decay $K^+ \rightarrow \pi^+ + \pi^0$ (and if the K has a spin > 2 also for the mode $K \rightarrow \mu + \nu$). In general the decay $K \rightarrow \mu + \nu$ should not only be anisotropic, but should also exhibit an up-down asymmetry with respect to the plane of production of K . About one thousand decays of stopped " K_L " mesons have been analyzed to detect asymmetry or anisotropy of the emitted charged particle (K^+ decays which exhibit a single fast track are called " K_L "; nearly $\frac{2}{3}$ of the secondary tracks are from $K \rightarrow \mu + \nu$, $\frac{1}{3}$ from $K \rightarrow \pi + \pi$). Since $K \rightarrow \pi + \pi$ can exhibit anisotropy but not asymmetry it cannot wash out an asymmetry of the $K \rightarrow \mu + \nu$ mode. The 1000 K_L decays show evidence for neither asymmetry nor anisotropy. 600 decays of $K \rightarrow 3\pi$ are also isotropic (41, 42).

TABLE VI
BRANCHING RATIOS AND DECAY RATES IN K DECAY

K^+ decay mode			K^0 decay mode		
	Branching ratio (%)	Decay rate* (number/sec.)		Branching ratio (%)	Decay rate* (number/sec.)
<i>Identified</i>					
$(\theta^+) \rightarrow \pi^+ + \pi^0$	25.6 ± 1.7	20.9 ± 10^8	$\begin{cases} K_1^0 \rightarrow \pi^+ + \pi^- \\ K_1^0 \rightarrow \pi^0 + \pi^0 \end{cases}$ (a)	86 ± 6 14 ± 6	0.9×10^{10} 0.15×10^{10}
$(\tau) \rightarrow \pi^+ + \pi^0 + \pi^-$	5.66 ± 0.30	4.62×10^8	$K_1^0 \rightarrow \pi^+ + \pi^- + \pi^0$	~ 30	1.05×10^{10}
$(\tau') \rightarrow \pi^+ + \pi^0 + \pi^0$	1.70 ± 0.32	1.38×10^8	no analogue		$\sim 3 \times 10^8$ (c)
$(K_\mu) \rightarrow \mu^+ + \nu$	58.8 ± 2.0	48.0×10^8	$K_1^0 \rightarrow e^\pm \pm \nu + \pi^\mp$	~ 30	$\sim 3 \times 10^8$ (c)
$(K_\beta) \rightarrow e^+ + \nu + \pi^0$ (b)	4.19 ± 0.42	3.42×10^8	$K_1^0 \rightarrow \mu^\pm \pm \nu + \pi^\mp$	~ 30	$\sim 3 \times 10^8$ (c)
$(K_\mu) \rightarrow \mu^+ + \nu + \pi^0$	4.0 ± 0.77	3.26×10^8		100	$\sim 10 \times 10^8$ (c)
	100	81.6×10^8			
<i>Missing (perhaps rigorously forbidden)</i>					
$K^+ \rightarrow \pi^+ + \gamma$	<2.0	Forbidden because: Spinless K	$K_1^0 \rightarrow \pi^+ + \pi^-$	<5	Forbidden because: CP invariance
$K^+ \rightarrow \nu + \bar{\nu} + \pi^+$	<2.0	Neutrino pair emission	$K_1^0 \rightarrow \pi^0 + \gamma$	<10	spinless K
$K^+ \rightarrow \mu^+ + e^- + \pi^+$ etc.	<0.01	$\mu - e$ pair emission	$K_1^0 \rightarrow \nu + \nu$	<10	spinless K
$K_1^0 \rightarrow e^\pm + \mu^\mp$			$K_1^0 \rightarrow e^\pm + \mu^\mp$	<5	$\mu - e$ pair emission
<i>Missing (rare but perhaps allowed)</i>					
$K^+ \rightarrow e^+ + \nu$	<1.0		$K_1^0 \rightarrow \pi^\pm + \pi^0 + \mu^\mp \nu$, etc.		
$K^+ \rightarrow \pi^+ + \pi^- + \mu^+ + \nu$, etc.	<0.01		$K_1^0 \rightarrow e^\pm + \pi^\mp$, etc.		

Analogous identified modes of decay of K^+ and K^0 are shown on the same horizontal line. The symbols (θ), (τ), etc., are older names used to describe the 2π , 3π , etc. decay modes of the K^+ .

The branching ratios of the K^+ are a weighted average of the data of the Berkeley and Dublin emulsion groups [G. Alexander, R. H. W. Johnston, C. O'Ceallaigh, private communication (*Nuovo cimento*, **6**, 478 (1957)); and Birge, Perkins, Peterson, Stork, and Whitehead, *Nuovo cimento*, **4**, 834 (1956)]. For the τ and τ' we have also included the following branching fractions, τ , (5.1 ± 0.3)%; τ' , (1.5 ± 0.2)% supplied by Harris, Orear, and Taylor (private communication).

The branching ratio for the K_1^0 have been determined by the Steinberger propane chamber group studying associated production of strange particles by π^- [Plano, Samios, Schwartz, Steinberger, *Phys. Rev.* (to be published, 1957)]. They find that <2% of K_1^0 undergo 3-body decay with charged particles.

The qualitative data on the K_1^0 have been given by the Columbia cloud chamber group [Lande, Lederman, and Chinowsky, *Phys. Rev.*, **105**, 1925 (1957)].

* The decay rates are based on the mean lives in Table I.

- (a) This mode has not been definitely identified as $K \rightarrow 2\pi^0$; it is known only that some gammas are associated with the decay. Nevertheless the assignment $K \rightarrow 2\pi^0$ is suggested by the energy spectrum of these gammas and is otherwise very plausible (see Sect. 6.5).
- (b) The π^0 has not yet been identified, but is suggested by the presence of the analogous charged π 's seen in K^0 decay. Dalitz pairs have not yet been seen in association with $K^+ \rightarrow e^+ + \nu + \pi^0$; they have been identified in association with $K^+ \rightarrow \mu^+ + \nu + \pi^0$ (and with $K^+ \rightarrow \pi^+ + \pi^0 + \pi^0$).
- (c) There is a large uncertainty in this rate (see Table I).

TABLE VII
KINEMATICS OF MESON DECAYS

Decay mode	Momentum, \not{p} (Mev/c)*	Total energy $w = T + mc$ (Mev)*	Available kinetic energy, Q (Mev)
e^\pm (mass = 0.510976 Mev)	stable	stable	stable
μ^\pm (mass = $105.70 \pm .06$ Mev)	$\not{p}^m = 52.85$	$w_e^m = 52.85$	105.19
$\mu^\pm \rightarrow e^\pm + \nu + \bar{\nu}$			
π^\pm (mass = $139.63 \pm .06$ Mev)	$\not{p} = 29.81$	$w_\mu = 109.82$	33.93
$\pi^\pm \rightarrow \mu^\pm \pm \nu$			
π^0 (mass = $135.04 \pm .16$ Mev)	$\not{p} = 67.52$	$w_\gamma = 67.52$	135.04
$\pi^0 \rightarrow \gamma + \gamma$			
K^+ (mass = 494.0 ± 0.14 Mev)	$\not{p} = 205.3$	$w_{\pi^+} = 248.25$	219.33
$K_{\pi^2} \rightarrow \pi^+ + \pi^0$			
$K_\tau \rightarrow \pi^+ + \pi^+ + \pi^-$	$\not{p}_{\pi^m} = 125.5$	$w_{\pi^m} = 187.8$	75.11
$K_{\tau'} \rightarrow \pi^+ + \pi^0 + \pi^0$	$\not{p}_{\pi^{+m}} = 133.1$ $\not{p}_{\pi^{0m}} = 132.3$	$w_{\pi^{+m}} = 192.9$ $w_{\pi^{0m}} = 189.0$	84.29
$K_{\mu 2} \rightarrow \mu^+ + \nu$	$\not{p} = 235.7$	$w_\mu = 258.3$	388.3
$K_{\mu 3} \rightarrow \mu^+ + \pi^0 + \nu$	$\not{p}_{\mu^m} = 215.2$ $\not{p}_{\pi^0m} = 215.3$	$w_{\mu^{+m}} = 239.8$ $w_{\pi^{0m}} = 254.1$	253.26
$K_{e 2} \rightarrow e^+ + \pi^+ + \nu$	$\not{p}_e^m = 228.5$ $\not{p}_{\pi^m} = 228.5$	$w_{e^{+m}} = 228.5$ $w_{\pi^m} = 265.4$	358.45
$K_{e 2} \rightarrow e^+ + \nu$ not observed	$\not{p} = 247.0$	$w_e^+ = 247.0$	493.49
$K_{\pi \gamma} \rightarrow \pi^+ + \gamma$ not observed	$\not{p} = 227.2$	$w_\pi^+ = 266.7$	354.37
K^0 (mass = 493 ± 5 Mev)	$\not{p} = 203.1$	$w = 246.5$	213.7
$K^0 \rightarrow \pi^+ + \pi^-$			
$\rightarrow \pi^0 + \pi^0$	$\not{p} = 206.2$	$w = 246.5$	222.9
$\rightarrow \pi^+ + \pi^- + \pi^0$	$\not{p}_{\pi^{\pm m}} = 128.4$	$w_{\pi^{\pm m}} = 189.7$	78.7
$\rightarrow \mu^\pm + \pi^\mp \pm \nu$	$\not{p}_{\mu^m} = 213.2$ $\not{p}_{\pi^m} = 213.2$	$w_{\mu^m} = 238.0$ $w_{\pi^m} = 254.9$	247.7
$\rightarrow e^\pm + \pi^\mp \pm \nu$	$\not{p}_{\pi^m} = 226.6$ $\not{p}_e^m = 226.6$	$w_{\pi^m} = 266.2$ $w_e^m = 226.7$	352.9

* The momentum and total energy are given in the rest frame of the decaying particle. In three-body decays, the maximum momentum and energy possible for each of the products is given, as indicated by the superscript m .

branching ratio of more than a few per cent for this process. If it can be shown with much greater accuracy that this process is absent, our speculation that neutrino pair emission never occurs would be supported.

6.3. *The modes $K \rightarrow 2\pi$.*—We have seen that K_1^0 decays into two pions with a rate comparable to those of hyperon decays. For K_2^0 this mode is absent (or nearly so), but that can be explained either by CP invariance or possibly otherwise. (See Appendix A.) We then must deal with the fact that K^+ decays into two pions about 500 times slower than K_1^0 . Let us apply the proposed isotopic spin selection rule $|\Delta I| = \frac{1}{2}$.

The rule requires that the final state differ in isotopic spin from the original one by $\frac{1}{2}$. Since the initial state has $I = \frac{1}{2}$, the final one must have $I = 0$ or 1 . After the decay of a spinless K particle, the two pions are in an s -state. Since they obey Bose-Einstein statistics, the complete wave function must be symmetric; thus the isotopic spin function must be symmetric. When we combine two unit isotopic spins in a symmetrical way we get $I = 0$ or $I = 2$. Here only $I = 0$ is permitted. Thus, to the extent that charge independence is rigorous apart from the weak coupling and to the extent that the weak coupling obeys the rule $|\Delta I| = \frac{1}{2}$, we have:

(a) K^+ is forbidden to decay into two pions (clearly $\pi^+ + \pi^0$ cannot have $I = 0$, since $I_Z = +1$).

(b) In the decay $K_1^0 \rightarrow 2\pi$ we have the branching ratio characteristic of $I = 0$; the fraction f of decays into neutral pions is $\frac{1}{2}$.

Now experimentally the first result is nearly true; the decay $K^+ \rightarrow \pi^+ + \pi^0$ is practically forbidden, and the $|\Delta I| = \frac{1}{2}$ rule has given an explanation of the fact. However, the decay does occur, albeit slowly, and so we must look for corrections to the rule, either from electromagnetic violations of charge independence or from a slight failure of the rule in the weak interaction itself.

The second result is that

$$= \frac{K_1^0 \rightarrow 2\pi^0}{K_1^0 \rightarrow 2\pi}$$

is $\frac{1}{2}$; this is in disagreement with the present experimental value (39) of 0.14 ± 0.06 . This discrepancy is discussed in 6.4.

6.4. *Validity of the rule $|\Delta I| = \frac{1}{2}$.*—Let us summarize the evidence on the rule $|\Delta I| = \frac{1}{2}$. We have seen in Section 5 that the rule is in agreement with hyperon results so far and scores a success in predicting the branching ratio of Λ decay. In 6.5 we shall see that it is not far from agreement with results on the decay $K \rightarrow 3\pi$. We have just noted that, apart from requiring a small correction, it explains the slowness of $K^+ \rightarrow \pi^+ + \pi^0$. But the branching ratio in K_1^0 decay appears to require a larger correction.

It is certainly worthwhile, therefore, to discuss the possibility that the $|\Delta I| = \frac{1}{2}$ rule is approximately correct. In order to get a nonzero rate of decay for $K^+ \rightarrow \pi^+ + \pi^0$ we must put in some contribution from $|\Delta I| = \frac{3}{2}$ and/or $|\Delta I| = \frac{5}{2}$. Say we introduce these with complex amplitudes ϵ_3 and ϵ_5 respectively relative to that for $|\Delta I| = \frac{1}{2}$. Then the ratio Γ^+/Γ^0 of the decay

rates $K^+ \rightarrow 2\pi$ and $K_1^0 \rightarrow 2\pi$ and the fraction f of K_1^0 that give $2\pi^0$ are given by the relations:

$$\frac{\Gamma^+}{\Gamma^0} = \frac{1}{3} \frac{|3/2\epsilon_3 - \epsilon_5|^2}{1 + |\epsilon_3 + \epsilon_5|^2} \text{ instead of } 0,$$

$$f = \frac{1}{3} \frac{|1 - \sqrt{2}(\epsilon_3 + \epsilon_5)|^2}{1 + |\epsilon_3 + \epsilon_5|^2} \text{ instead of } 1/3.$$

If CP invariance holds, then ϵ_3 and ϵ_5 have the same phase $\delta_2 - \delta_0$, where δ_I is the s-wave pion-pion phase shift in the state with isotopic spin I at the energy of the final two-pion system. This phase shift is, of course, unknown at present.

Let us put $\Gamma^+/\Gamma^0 \approx 1/500$ as indicated by the experiments. Then if we use only ϵ_3 (admixture of $|\Delta I| = \frac{1}{2}$) only (42a) the fraction f must lie between 0.28 and 0.38, which is still in disagreement with 0.14 ± 0.06 . If we use both ϵ_3 and ϵ_5 then we can fit $f = 0.14$ with $\epsilon_3 \approx 12$ per cent and $\epsilon_5 \approx 11$ per cent or with $\epsilon_3 \approx 6$ per cent and $\epsilon_5 \approx 17$ per cent. Similarly we can fit $f = 0.20$ with $\epsilon_3 \approx 9$ per cent and $\epsilon_5 \approx 6$ per cent or with $\epsilon_3 \approx 3$ per cent and $\epsilon_5 \approx 12$ per cent. Making the parameters ϵ complex will, in general, require them to be still larger in magnitude.

Can such large corrections come from electromagnetic violations of charge independence? It seems unlikely, since electromagnetic effects are of the order of the fine structure constant and moreover attempts to estimate them theoretically for this problem have not given anomalously large answers.

We are led, then, to say that the $|\Delta I| = \frac{1}{2}$ rule may be approximately valid, but if so it seems to be approximate for the weak interactions themselves, with corrections of the order of 5 or 10 per cent; i.e., it is hard to blame the electromagnetic field for these corrections.

6.5. The decay $K^+ \rightarrow \pi^+ + \pi^+ + \pi^-$.—The 3π mode of decay of K has been most extensively studied in the case $K^+ \rightarrow \pi^+ + \pi^+ + \pi^-$ which accounts for only some 5 per cent of all K^+ decays, but is spectacular in photographic emulsion, cloud chambers, or bubble chambers.

The distribution in energy and angle of the emitted pions has been carefully investigated and is notable for having provided, together with the decay $K^+ \rightarrow \pi^+ + \pi^0$, the first evidence that parity is not conserved by the weak interactions. The 3π mode shows a distribution (see below) characteristic of even angular momentum and odd parity for the final state (0^- for a spinless K). In the 2π mode, the final state cannot have odd parity if it has even angular momentum; for a spinless K the state of the two pions is, of course, 0^+ .

There was the suggestion (43) that two particles might be involved, one with even parity called the θ and one with odd parity called the τ and that these were degenerate because of a new kind of symmetry. The discovery of nonconservation of parity has made such a complication unnecessary.

The analysis of the “ τ ” events $K^+ \rightarrow 3\pi$ has been carried out by the method of Dalitz (44). The Q-value is 75.11 Mev, shared among the three pions, which we may roughly assume to be nonrelativistic in the rest system of K^+ .

Let the kinetic energies of the two π^+ and the π^- be called T_1, T_2, T_3 respectively, with $T_1+T_2+T_3=Q$. A decay event is then described by two independent variables, for which Dalitz chose $x \equiv \sqrt{3}(T_1-T_2)/Q$ and $y \equiv (3T_3-Q)/Q$. In Appendix C we show why these variables were chosen, namely that x^2+y^2 runs between 0 and 1 and the element of volume in phase space is just proportional to $dxdy$. Thus if we plot individual events inside the unit circle in the $x-y$ plane the density of events as a function of x and y is proportional to $|M|^2$, the square of the decay matrix element. Since the two π^+ are identical, M is an even function of x and thus the circle can be folded across the y -axis to form a semicircle. The Dalitz plot of "τ" events to date appears in Figure 6. Each event is a dot inside the semicircle. Relativistic effects slightly distort the semicircle into the dashed curve (45).

Figure 6 shows that the population of events is fairly uniform. Proceeding naively, we may simply conclude that the matrix element M is practically a constant, independent of the pion momenta, so that the three pions are essentially in an overall s -state with a totally symmetric wave function. The spin of K must then be zero. In fact we accept these conclusions, although they are not rigorous consequences of the data in Figure 6. That the K spin is even, however, we may now show with considerable confidence just on the basis of the Dalitz plot.

The spin S of the K^+ meson is equal to the sum of the two independent angular momenta l and L , defined as follows: the two π^+ revolve about their mutual center of mass with orbital angular momentum l , while the $2\pi^+$ system and the π^- revolve around the three-body center of mass with orbital angular momentum L . We have $S=l+L$, where l , of course, is even. Simultaneous eigenstates of l^2 and L^2 may be described by the symbol (L, l) . We want to show that amplitudes of the type $(0, l)$ are present, so that $S=l+0$ is even.

We must assume that the K particle has some reasonable "radius" R and consider π^- of such low energy $T_3=\hbar^2 k_3^2/2m_\pi$ that $k_3 R \lesssim 1$. For $T_3 < 10$ Mev, we need only suppose that $R \lesssim 5\hbar/m_\pi c$. Then for $L > 0$ the existence of a centrifugal barrier would make $|M|^2$ approach zero as $(k_3 R)^{2L}$ for small $k_3 R$, which corresponds to the bottom of the semicircle in Figure 6. But the uniform population of dots in this region shows (46) that an appreciable part of the matrix element does not tend to zero for small $k_3 R$ and must correspond to $L=0$. We cannot, however, exclude the presence of some $L>0$. In any case S is even. (Furthermore, the parity is -1 for any $L=0$ configuration of the three pseudoscalar pions.)

Inspection of the upper corner of the semicircle, where the relative momentum of the two π^+ is very small, shows in a similar way that there is a large amplitude with $l=0$.

These arguments do not exclude the possibility of spin 2, with a wave function for the pions composed largely of $(0, 2)$ and $(2, 0)$. However, we have seen in 6.1 that there are strong arguments for a K spin of zero and we shall continue the discussion on that basis.

With $S=0$, the pion wave function is composed of $(0, 0)$ $(2, 2)$, etc.

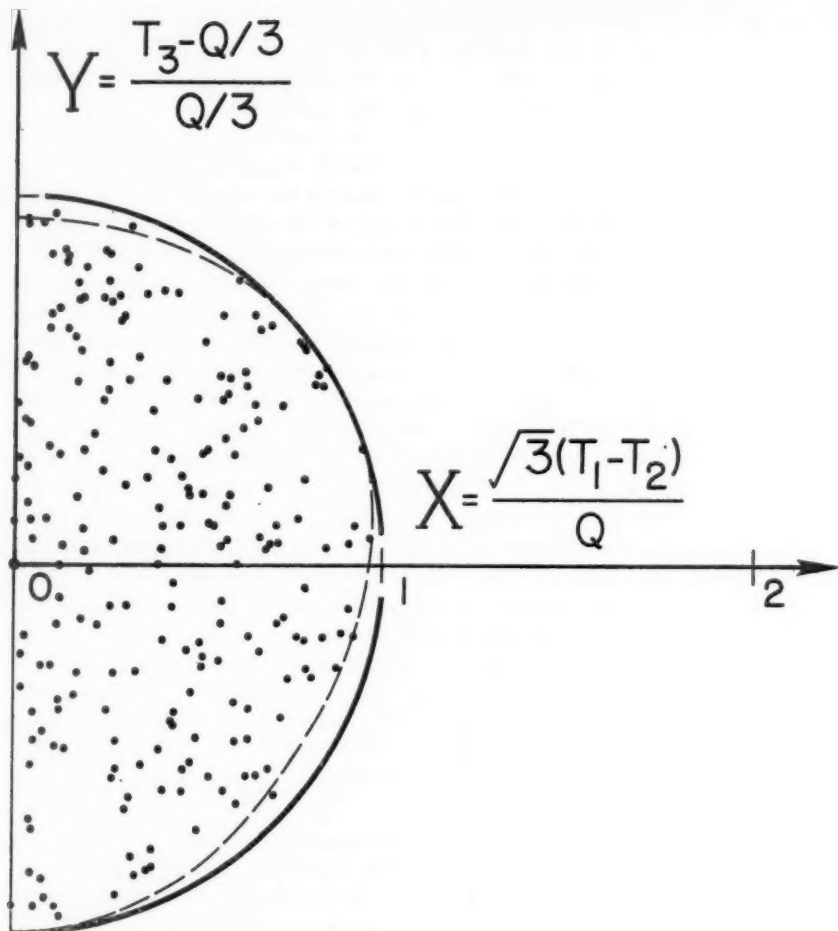


FIG. 6. Dalitz plot of the distribution of pion energies in the "r" decay $K^+ \rightarrow \pi_1^+ + \pi_2^+ + \pi_3^-$. If the problem is treated nonrelativistically the semicircle represents the boundary of the region allowed by conservation of momentum. Relativistic treatment gives the dashed curve. The 219 events (from Berkeley, Columbia, and MIT) were compiled by Orear, Harris, and Taylor, *Phys. Rev.*, **102**, 1676 (1956).

(Note the parity of each of these configurations is -1 .) For any reasonable radius R , we may expect centrifugal barrier effects to suppress $(2, 2)$ and higher amplitudes relative to $(0, 0)$. Moreover, the matrix element corresponding to $(0, 0)$ should be a constant plus terms of order $(kR)^2$, where k is the wave number of any of the pions. All of this is perfectly consistent with the appearance of Figure 6. In fact, we can try expanding the matrix element M in a power series in x and y ; note odd terms in x must be absent

because of the identity of the two π^+ . A good fit to the data, obtained from a plot given by Dalitz (R3), is obtained with

$$M \propto 1 + \frac{1}{10} y. \quad 40.$$

The term 1 is of course totally symmetric in the three pions, while the term $1/10y$ is not. We can thus obtain a rough estimate, useful in 6.6, of the fraction of τ decays into nonsymmetric states of the three pions. We square the amplitude M and average the resulting intensity over the semicircle. Since the average of y^2 is $\frac{1}{4}$, the nonsymmetric term $1/10y$ contributes a fraction $\frac{1}{4}(1/10)^2 = 1/400$ of the total intensity.¹⁷

6.6. Charge dependence of the decay $K \rightarrow 3\pi$; the neutral 3π mode.—There is another charge state of three pions into which K^+ can decay: $\pi^+ + 2\pi^0$. Let us try to predict the ratio of these two modes by means of the $|\Delta I| = \frac{1}{2}$ rule. The isotopic spin of K is $\frac{1}{2}$, and so in the final state we would have $I=1$ or $I=0$. However, in the decay of K^+ the final state has $I_Z = +1$ and thus only $I=1$ is possible. Now there are two ways of combining three unit isotopic spins to make $I=1$, just as there are two ways of constructing a vector trilinear in three vectors a , b , and c . One of these (corresponding to $a \cdot bc + a \cdot cb + b \cdot ca$) gives an isotopic spin function totally symmetric in the three pions. Since the pions are bosons, this must be associated with a matrix element totally symmetric in the pion momenta, like the constant term in Eq. 40. The other kind of isotopic spin function is not totally symmetric (and corresponds to a vector like $a \times [b \times c]$). It is associated with a non-symmetric matrix element like the term $1/10y$ in Eq. 40. Since the first kind of term seems to predominate in the decay, we can, as a good approximation, use the totally symmetric isotopic spin function. The ratio $(\pi^+ + 2\pi^0) / (\pi^+ + \pi^- + \pi^0)$ is then uniquely determined to be $\frac{1}{3}$ (47). The experiments (as in Table VI) indicate the value 0.33 ± 0.07 . More data are necessary to determine whether there is a serious disagreement with the "predicted" ratio 0.25. In any case, we know from the $K_{\pi 2}$ decay that the $|\Delta I| = \frac{1}{2}$ rule is not exact.

Let us now turn to the " τ " decays of neutral K mesons. If CP invariance holds, we can draw strong conclusions about the decay of K_1^0 and K_2^0 into 3π . We have seen in 6.5 that there is no 0^+ state of 3π ; with a spinless K , therefore, the final 3π system has $P = -1$. There are two charge states: $3\pi^0$ and $\pi^+ + \pi^- + \pi^0$. Now π^0 is well-known to be even under charge conjugation (for example, it decays into 2γ) and thus a state of any number of π^0 mesons has $C = +1$. We see, then, that the final $3\pi^0$ system has $CP = -1$ and is a possible decay product of K_2^0 but not of K_1^0 if CP is conserved.

In the case of $\pi^+ + \pi^- + \pi^0$, we cannot conclude that $C = +1$ and $CP = -1$

¹⁷ We have assumed a real coefficient of y in our empirical formula 40 for M . With CP invariance, the phase of the coefficient is specified, but unfortunately in terms of unknown phase shifts of the final three-pion system. Fitting the data with a complex coefficient of y might increase somewhat our estimate of the nonsymmetric fraction.

without some knowledge of the wave function. But to the extent that the matrix element is symmetric in π^+ and π^- , the conclusion does hold. Now in the case of charged τ decay we have seen that the matrix element is practically a constant and that the fraction of decays into totally symmetric pion states is probably >99 per cent. If we make the reasonable assumption that the neutral τ decays behave the same way, then we can say that the rate of $K_1^0 \rightarrow \pi^+ + \pi^- + \pi^0$ is at least ~ 100 times less than that of $K_2^0 \rightarrow \pi^+ + \pi^- + \pi^0$. Moreover, the lifetime of K_1^0 is at least 300 times shorter than that of K_2^0 and therefore the fraction of K_1^0 decays into $\pi^+ + \pi^- + \pi^0$ should be at least 3×10^4 smaller than the corresponding fraction for K_2^0 .

Experimentally, the fraction of K_2^0 decays into 3π is quite appreciable (see Table VI). We can calculate the rates of these decays if we assume the validity of the $|\Delta I| = \frac{1}{2}$ rule and the practically total symmetry of the 3π wave function. The result is that the total rate of $K_2^0 \rightarrow 3\pi$ should equal the total rate of $K^+ \rightarrow 3\pi$ ($6 \times 10^6/\text{sec.}$ in Table VI), while the ratio $K_2^0 \rightarrow 3\pi^0 / K_2^0 \rightarrow \pi^+ + \pi^- + \pi^0$ should be $3/2$.

6.7. *The decay $K^\pm \rightarrow \mu^\pm \pm \nu$.*—The fact that a large fraction of K^\pm decay into $\mu^\pm \pm \nu$ makes possible an experiment on asymmetry in the $K \rightarrow \mu \rightarrow e$ chain analogous to those for the $\pi \rightarrow \mu \rightarrow e$ chain described in 4.5.

If K is spinless and if the longitudinal theory of the neutrino and conservation of leptons are both correct, then the two chains must behave exactly alike. The forward-backward asymmetry and the polarizations of μ and e must be identical for $K \rightarrow \mu \rightarrow e$ and $\pi \rightarrow \mu \rightarrow e$. As mentioned in 4.5, this has been borne out experimentally (57).

The rate of the decay $K^\pm \rightarrow \mu^\pm \pm \nu$ and the rarity or absence of $K^\pm \rightarrow e^\pm \pm \nu$ have been discussed in 4.9.

Assuming, as in the tetrahedron scheme, that $\nu\bar{\nu}$ and $\mu^\pm e^\mp$ pair emission can never occur, we see that the purely leptonic decay of K^\pm has no neutral counterpart.

6.8. *The modes $K \rightarrow \pi + \text{leptons}; \text{ spectra}$.*—The decays of K mesons into $\pi + \text{leptons}$ have been referred to briefly toward the end of 4.9. We remarked that they are induced by different interactions from those that lead to $K^\pm \rightarrow \text{leptons}$ alone. For example, for a pseudoscalar K , the couplings we have labeled S , V , and T are responsible for decay into $\pi + \text{leptons}$, while P and A can induce pure leptonic decay. In Eq. 25 we have given a somewhat special definition of these couplings, employing the tetrahedron scheme and forming S , for example, by coupling $\bar{\mu}(1 - \gamma_5)\nu$ to $\bar{p}\Lambda$. More generally, in order to form S for the muon and neutrino, we might couple $\bar{\mu}(1 - \gamma_5)\nu$ to other scalar field operators with the same strangeness properties as $\bar{p}\Lambda$, but let us continue to use Eq. 25 to fix our ideas. For the electron and neutrino, of course, we have similar definitions of the couplings with $\bar{\mu}(1 - \gamma_5)\nu$ replaced by $\bar{e}(1 - \gamma_5)\nu$, etc.

A complete discussion of the decays $K \rightarrow \pi + \text{leptons}$ involves 18 amplitudes. We must distinguish: (a) the electron and muon. (b) the three different processes $K^\pm \rightarrow \pi^0 + e^\pm \pm \nu$, $K_1^0 \rightarrow \pi^\mp + e^\pm \pm \nu$ and $K_2^0 \rightarrow \pi^\mp + e^\pm \pm \nu$ (likewise

for the muon), and (c) the three types of interaction: S , V , and T for a pseudoscalar K or P , A , and T for a scalar K . The product of $2 \times 3 \times 3$ is 18.

(a) The relation between and muon couplings is unknown. The rates of decay into $\pi + e^\pm \pm \nu$ and $\pi + \mu^\pm \pm \nu$ seem to be about equal for both charged and neutral K mesons (see Table VI) but we have no idea whether the couplings are identical in form for electron and muon.

(b) If the lifetime of K_2^0 is around 10^{-7} sec., then the rates of $K^\pm \rightarrow \pi + \text{leptons}$ and $K_2^0 \pi + \text{leptons}$ are comparable (see Table VI); however, the present limits on the K_2^0 lifetime are rather far apart (see Table I). The process $K_1^0 \rightarrow \pi + \text{leptons}$ has not yet been established. If its rate is comparable with that of $K_2^0 \rightarrow \pi + \text{leptons}$, that still corresponds to a very small fraction of K_1^0 decays ($\lesssim 0.1$ per cent). Assuming that both K_1^0 and K_2^0 give $\pi + \text{leptons}$ with similar rates, we must discuss those rare events in which neutral K mesons decay into $\pi + \text{leptons}$ after $\lesssim 10^{-10}$ sec. in terms of interference between K_1^0 and K_2^0 . This phenomenon is treated theoretically in 6.9, but has not been observed.

(c) Let us consider a particular decay, say $K_2^0 \rightarrow \pi^\mp + e^\pm \pm \nu$, and compare the effects of various couplings. For simplicity we take the K pseudoscalar and use S , V , and T . (The same consequences would hold for a scalar K if we used P , A , and T .) Also we neglect the electron mass.

Following Pais & Treiman, (48) we may introduce three effective coupling parameters b_S , b_V , and b_T corresponding to the three interactions. Assuming CP invariance and neglecting tiny coulomb effects in the final state, we can take these to be real. In principle the b 's may depend on the pion total energy w ; however, if the decays really proceed through baryon-anti-baryon loops this dependence is probably rather weak. Let $p(w)$ equal the pion momentum and $x(w)$ equal $p(w)/(m_K - w)$; let θ be the angle between e and π . Then the distribution of decays per unit energy and unit solid angle is proportional to (48)

$$\frac{(1-x^2)^2(m_K-w)^2}{(1+x\cos\theta)^4} p \left\{ b_V^2 x^2 \sin^2 \theta + \left[b_S(1+x\cos\theta) + \frac{b_T p}{m_K}(x+\cos\theta) \right]^2 \right\}. \quad 41.$$

(Here and in the rest of the Section, we put $\hbar = c = l$.)

An analysis of a large number of three-body decays using this formula should permit the identification of the couplings involved. The longitudinal neutrino theory predicts that the electrons corresponding to the V term are 100 per cent longitudinally polarized in one sense and those corresponding to the S , T term 100 per cent polarized in the opposite sense. Using conservation of leptons and a right-handed neutrino, we see that the V interaction gives right-polarized electrons and left-polarized positrons, as in β -decay, μ -decay, etc.

The analogue of Eq. 41 for the muon case is more complicated; [it is given in ref. (48)]. There is longitudinal polarization of the muons also, again slightly more complicated because of the finite muon mass. This polarization can be detected by means of the asymmetry of $\mu \rightarrow e$ decay.

If CP invariance holds, there should be no appreciable transverse muon polarization, i.e., perpendicular to the plane of the K decay. (See Appendix A.)

6.9. *Interference phenomenon in K decay.*—We have referred in 6.8 to the possibility that both K_1^0 and K_2^0 decay into $\pi^\mp + e^\pm \pm \nu$ and/or $\pi^\mp + \mu^\pm \pm \nu$. In a "fresh" beam of neutral K mesons (see 3.9), out of which the K_1^0 , component has not yet largely decayed, a small fraction (perhaps ~ 0.1 per cent) of the decay products will be $\pi +$ leptons. These events will arise from interference of K_1^0 and K_2^0 (49). (In a "stale" beam, of course, the decays into $\pi +$ leptons are to be attributed to K_2^0 alone.)

For simplicity let us treat a definite model of the interference, namely that supplied by the tetrahedron scheme, in which $K^0 \rightarrow \pi^- + e^+ + \nu$ and $\bar{K}^0 \rightarrow \pi^+ + e^- + \bar{\nu}$ are allowed, but $K^0 \rightarrow \pi^+ + e^- + \bar{\nu}$ and $\bar{K}^0 \rightarrow \pi^- + e^+ + \nu$ are forbidden, and likewise for the muon (see 4.8).

We must recall the relations, given in 3.9, between K^0 , \bar{K}^0 and K_1^0 , K_2^0 :

$$\begin{aligned} |K^0\rangle &= \frac{1}{\sqrt{2}} |K_1^0\rangle + \frac{1}{\sqrt{2}} |K_2^0\rangle, \\ |\bar{K}^0\rangle &= \frac{1}{\sqrt{2}} |K_1^0\rangle - \frac{1}{\sqrt{2}} |K_2^0\rangle. \end{aligned} \quad 42.$$

Let Γ_1 and Γ_2 stand for the reciprocal lifetimes of K_1^0 and K_2^0 respectively, while m_1 and m_2 are their masses, which are presumed to differ by something like 10^{-11} Mev. We may then write the state of a neutral K meson as

$$|\Psi(t)\rangle = a_1 |K_1^0\rangle e^{-im_1 t} e^{-\Gamma_1 t/2} + a_2 |K_2^0\rangle e^{-im_2 t} e^{-\Gamma_2 t/2}. \quad 43.$$

Suppose we are dealing with a beam that initially is pure K^0 , i.e., has pure strangeness +1. Then $a_1 = a_2 = 1/\sqrt{2}$ and we have

$$|\Psi(t)\rangle = \frac{1}{\sqrt{2}} |K_1^0\rangle e^{-im_1 t} e^{-\Gamma_1 t/2} + \frac{1}{\sqrt{2}} |K_2^0\rangle e^{-im_2 t} e^{-\Gamma_2 t/2}. \quad 44.$$

The quantity $|\langle K^0 | \Psi(t) \rangle|^2$ will now give the fraction of the original K^0 that remain in the beam after time t , while $|\langle \bar{K}^0 | \Psi(t) \rangle|^2$ gives the fraction of the original K^0 that have been turned into \bar{K}^0 . The sum of these fractions keeps decreasing with increasing t as mesons decay. We have

$$|\langle K^0 | \Psi(t) \rangle|^2 = \left| \frac{1}{2} e^{-im_1 t} e^{-\Gamma_1 t/2} + \frac{1}{2} e^{-im_2 t} e^{-\Gamma_2 t/2} \right|^2 \quad 45.$$

and

$$|\langle \bar{K}^0 | \Psi(t) \rangle|^2 = \left| \frac{1}{2} e^{-im_1 t} e^{-\Gamma_1 t/2} - \frac{1}{2} e^{-im_2 t} e^{-\Gamma_2 t/2} \right|^2 \quad 46.$$

Let us now impose the condition implied by the tetrahedron scheme, that $K^0 \rightarrow \pi^- +$ leptons and $\bar{K}^0 \rightarrow \pi^+ +$ leptons are allowed, with a common rate Γ_1 (common because of CP invariance), while $\bar{K}^0 \rightarrow \pi^- +$ leptons and $K^0 \rightarrow \pi^+ +$ leptons are forbidden. Then the number of leptonic decays per second per original K^0 in the beam is

$$\begin{aligned} L_- &= \Gamma_1 |\langle K^0 | \Psi(t) \rangle|^2 \text{ for } \pi^- + \text{ leptons and} \\ L_+ &= \Gamma_1 |\langle \bar{K}^0 | \Psi(t) \rangle|^2 \text{ for } \pi^+ + \text{ leptons.} \end{aligned}$$

Using Eqs. 45 and 46, we obtain

$$L_- = \frac{\Gamma_l}{4} \{e^{-\Gamma_1 t} + e^{-\Gamma_2 t} + 2e^{-(\Gamma_1+\Gamma_2)t/2} \cos (m_1 - m_2)t\}, \quad 47.$$

$$L_+ = \frac{\Gamma_l}{4} \{e^{-\Gamma_1 t} + e^{-\Gamma_2 t} - 2e^{-(\Gamma_1+\Gamma_2)t/2} \cos (m_1 - m_2)t\}, \quad 48.$$

$$L \equiv L_+ + L_- = \frac{\Gamma_l}{2} \{e^{-\Gamma_1 t} + e^{-\Gamma_2 t}\}. \quad 49.$$

Eq. 49 is perfectly straightforward. Both K_1^0 and K_2^0 can decay into leptons at the same rate Γ_l ; initially we have 50 per cent of each, but each decays out according to its own lifetime.

The equations for L_- and L_+ separately are rather peculiar, however. L_- starts out at Γ_l and then decreases, while L_+ starts out at 0 and then increases at first. If $|m_1 - m_2| \geq \Gamma_l$, a striking oscillation phenomenon sets in, with a frequency corresponding to the very small mass difference. If $|m_1 - m_2|$ is too small, the oscillations are badly damped and would be hard to detect. If $|m_1 - m_2|$ is much larger than Γ_l , the oscillations are very rapid compared to the time of traversal of experimental apparatus and may be difficult to detect. If it should turn out, though, that $|m_1 - m_2|$ and Γ_l are comparable, then a measurement could be made of a mass difference $\sim 10^{-11}$ Mev.

APPENDIX A

Possible Noninvariance under CP and T.—It may still turn out that separate invariance under CP and T fails for weak couplings. We have pointed out in 2.5 that an absolute definition of right and left and of matter and antimatter would then be possible. Moreover, as we discussed in 2.6, the phases of transition matrix elements in weak processes would not be theoretically determined. Despite its unattractiveness, noninvariance under CP and T is a perfectly tenable hypothesis; present experimental evidence does not really distinguish between invariance and noninvariance.

The well-known equality of mass and lifetime for particle-antiparticle pairs like π^\pm , μ^\pm , etc. is guaranteed by CPT invariance alone (2, 50) and is thus not evidence for CP invariance. The remarkable behavior of K_1^0 and K_2^0 , which we have explained in the text on the basis of CP invariance, has been discussed by Lee, Oehme, & Yang (50) on the assumption that this principle fails. They show that without the invariance principle one may arrive at a rather similar picture of K_1^0 and K_2^0 , and that experimental data so far are consistent with either situation.

In a specific field-theoretic model of the weak couplings, like the theory of four-fermion interactions treated in Section 4, CP or T invariance is equivalent to the (relative) reality of the coupling parameters C , D , E , etc. In the text we have written all the formulas for rates, longitudinal polariza-

tions, and angular distributions in weak decays on the assumption that these coefficients are real. To obtain the corresponding formulas in the case of noninvariance under CP, we must replace C_S^2 by $|C_S|^2$, $2C_S C_T$ by $2 \operatorname{Re} C_S^* C_T$, etc., apart from certain corrections (50a).

These corrections are introduced by interactions among the decay products, for example the Coulomb force in β -decay, and they vanish for cases like $\mu^\pm \rightarrow e^\pm + \nu + \bar{\nu}$, where there are no (appreciable) final state interactions. They take the form of terms in $\operatorname{Im} C_T^* C_A$, $\operatorname{Im} C_S^* C_T$, etc., which are zero if CP invariance holds.

Let us consider, for instance, the formula for the asymmetry parameter a in the decay of Co^{60} (see 2.5 and 4.3) under the assumption that both T and A interactions are present and that the neutrino is right-handed:

$$a = \frac{v}{e} \frac{|C_A|^2 - |C_T|^2}{|C_A|^2 + |C_T|^2 + \frac{2m}{E} \operatorname{Re} C_A^* C_T} - \frac{Zm}{137E} \frac{2 \operatorname{Im} C_T^* C_A}{|C_A|^2 + |C_T|^2 + \frac{2m}{E} \operatorname{Re} C_A^* C_T}. \quad \text{A-1}$$

The term in $\operatorname{Im} C_T^* C_A$ occurs only in the Coulomb correction.

Now there is a class of measurable quantities that follow the reverse pattern: the leading term is proportional to $\operatorname{Im} C_S^* C_T$, say, while only the correction due to final state interactions involves $\operatorname{Re} C_S^* C_T$, etc. Such quantities, unlike the ones previously considered, are odd under the reversal of time (50b).

We note that momenta \mathbf{p} and angular momenta \mathbf{J} or $\mathbf{\sigma}$ change sign under time reversal. The asymmetry parameter a of Eq. A-1 multiplies $(\mathbf{J} \cdot \mathbf{p})$ in an angular distribution; such a term is evidently even under T . Similarly the longitudinal polarization of electrons is the coefficient of $\mathbf{\sigma} \cdot \mathbf{p}$, again even under T . To obtain a scalar or pseudoscalar that is odd under T , we must use at least three momenta and/or angular momenta, for example $\mathbf{\sigma} \cdot \mathbf{p}_1 \times \mathbf{p}_2$. In the decay of polarized neutrons, \mathbf{p}_1 may stand for the electron momentum and \mathbf{p}_2 for the proton momentum.

Experiments are in progress to measure this angular correlation between the spin direction and the plane of decay of polarized neutrons. The coefficient γ of $\mathbf{\sigma}_n \cdot \mathbf{p}_e \times \mathbf{p}_p$ is proportional to

$$\operatorname{Im} (C_S^* C_T - C_V^* C_A) - \frac{m}{137 p_e} \operatorname{Re} (C_S^* C_A - C_V^* C_T) \quad \text{A-2}$$

if the neutrino is longitudinal.

The contrast between Eq. A-2 for a time-odd quantity and Eq. A-1 for a time-even quantity is what we have stressed. The measurement of a time-odd quantity can provide a clear-cut test of time reversal invariance. Consider the measurement of γ in neutron decay. Whether the nuclear β -decay coupling is S , T or V , A , there must be a large effect if T invariance is violated appreciably in β -decay. If T invariance holds, there should be no effect, or at most a tiny Coulomb term.

A similar experiment is possible involving the decay $K_2^0 \rightarrow \pi^\mp + \mu^\pm \pm \nu$, namely a search for a correlation $\delta_\mu \cdot p_\mu \times p_\pi$, where δ_μ is measured by the asymmetry of $\mu \rightarrow e$ decay. If T invariance holds, there can be no such transverse muon polarization, except through a Coulomb effect. Longitudinal polarization of the muons is expected, however (see 6.8) and can be detected in the same experiment.

APPENDIX B: POLARIZATION AND ASYMMETRY; SYMMETRIC ALIGNMENT AND ANISOTROPY

We wish to discuss and contrast two different sorts of spin alignments of particles produced in a strong, parity conserving reaction such as

$$\pi + p \Rightarrow \Lambda + K. \quad B-1$$

We assume the target protons are unpolarized and call the π and Λ momenta p_1 and p_2 respectively.

B.1. Polarization and "up-down" asymmetry.—First we take up polarization, by which we mean a nonzero expectation value of the Λ spin along the direction $n = p_1 \times p_2$ normal to the production plane containing p_1 and p_2 . Our reason for picking the particular direction n and ignoring all others stems from considerations of parity. When we measure the polarization $p(\theta)$ we are actually measuring $\langle \delta \cdot p_1 \times p_2 \rangle$. This expression is P-invariant, but no other combination of δ with p_1 and p_2 can be found which is P-invariant.

Since the target protons were originally unpolarized, the Λ cannot be polarized unless the interaction is capable of distinguishing between spin-up and spin-down by means of some spin-dependent operator like $L \cdot \delta$. Thus if reaction B1 takes place so close to threshold that it proceeds overwhelmingly through s-wave, there can be no polarization. More precisely, polarization takes place through the interference between two partial waves.

Let us next consider the decay of a polarized particle. If the decay proceeds through two states of opposite parity (thus violating conservation of P) then we may expect the decay products to exhibit an "up-down" asymmetry with respect to the production plane.

B.2. Symmetric alignment and "polar vs. equatorial" anisotropy.—For particles with spin $> \frac{1}{2}$ the spin can still be aligned even in the absence of polarization: we may call this "symmetric alignment," meaning "symmetric about the production plane." As an example we discuss Λ production at 0° or 180° by reaction B.1. Let us assume that K is spinless (like the π) and choose the z-axis along the beam direction. The symmetric alignment is introduced by the fact that a particle can have no component of orbital angular momentum along its direction of motion, i.e., $L_z = 0$ both before and after collision. For unpolarized target protons the two spin states $S_z = \pm \frac{1}{2}$ are equally probable, and the same must then apply for Λ . Now if Λ had spin $> \frac{1}{2}$ this restriction to $S_z = \pm \frac{1}{2}$ would mean that S tended to be perpendicular to the z-axis. Thus, as Adair has pointed out (51), we would have a beam of

Λ with their spins aligned symmetrically fore and aft with respect to the z -axis.

The angular distribution of decay products from such *aligned* Λ must exhibit a (fore-aft) symmetry with respect to the z -axis (i.e., must contain no odd terms in $\cos \theta$) but it will in general be *anisotropic* in a "polar vs. equatorial" sense (i.e., will contain terms in $\cos^2 \theta$, etc.). For instance suppose that Λ has spin $3/2$ and is produced at 0° or 180° . It is then easy to show that the angular distribution of its decay is

$$d\sigma/d\Omega \propto 1/3 + \cos^2 \theta. \quad \text{B-2}$$

Another reaction that will yield the same symmetric anisotropy is the absorption of K^- from an atomic s -state of hydrogen according to



Since $L_z = L = 0$ in the initial state this example is entirely equivalent to the one already discussed, and the distribution of the angle of decay is given by Eq. B2 (52).

B.3. General Remarks.—For spin $\frac{1}{2}$ particles alignment necessarily means polarization; "symmetric alignment" is meaningless. In the decay of spin $\frac{1}{2}$ particles the only possible deviation from isotropy is an "up-down" asymmetry resulting from polarization in production followed by lack of parity conservation in the decay.

For particles with spin $>\frac{1}{2}$ we have so far contrasted polarization with symmetric spin alignment. Of course in general when two or more partial waves interfere in a reaction we expect both polarization and symmetric alignment.

B.4. Hyperon spins: associated production.—Adair has recommended the use of reaction B.1 and Eq. B2 as a test of the Λ spin (or of the Σ spin if we use a reaction like $\pi^\pm + p \Rightarrow \Sigma^\pm + K^\mp$). Of course one cannot in practice restrict oneself to Λ or Σ produced exactly at 0° or 180° ; however, as Adair suggests, the effect should not wash out very much if we restrict ourselves to angles within $1/L_{\max}$ radians of the forward and backward directions, where L_{\max} is the largest important orbital angular momentum in the final state. Even far away from the forward and backward directions, we may expect some polar vs. equatorial anisotropy in the distribution of the decay angle if the hyperon has spin $>\frac{1}{2}$. At production angles comparable to or large compared with $1/L_{\max}$, however, the effect could accidentally vanish or be small, whereas near 0° or 180° it must exist in full strength.

The present experimental situation is that less than 1000 hyperon decays have been observed following associated production and only a few tens of these satisfy Adair's condition. Neither the unselected events nor those satisfying Adair's condition permit any useful conclusion about the spin of Λ or Σ ; however there is another reaction, Eq. B3, which we now discuss.

B.5. Hyperon spins: K^- capture from rest.—Bubble chamber and emulsion groups have reported the decay of nearly 500 hyperons coming from

reaction B.3. Table BI shows that the numbers of polar and equatorial decays are almost equal. If we know that the (spinless) K^- cascaded down all the way to an atomic s -state before capture this near-isotropy would surely establish that both Λ and Σ have spin $\frac{1}{2}$. We are not sure, however, that capture from p -states is unimportant, and so it can only be said that the data are consistent with spin $\frac{1}{2}$ but also with spin $3/2$.

TABLE BI
POLAR VS EQUATORIAL DECAYS OF Λ AND Σ FROM K^- CAPTURES AT REST

	$n_{\text{polar}}/n_{\text{total}}$
Λ from $K^- + P^*$	$\frac{31}{58} = 0.53 \pm .06$
Σ^\pm from $K^- + P^*$	$\frac{87}{159} = 0.55 \pm .04$
Σ^\pm from $K^- + \text{emulsion}^\dagger$	$\frac{237}{432} = 0.55 \pm .024$

n_{polar} includes those events with $|\cos \theta| > 1/2$. For an isotropic distribution of decays, $n_{\text{polar}}/n_{\text{total}}$ should be $1/2$.

* Alvarez *et al.*, UCRL-3774 (1957) and *Nuovo cimento*, 5, 1026 (1957).

† Compilation of all emulsion data available from all laboratories ($\approx 90\% \Sigma^+$, $10\% \Sigma^-$) compiled by G. Snow for the Seventh Rochester Conference.

APPENDIX C. CONSTRUCTION OF THE DALITZ PLOT AND DENSITY OF STATES IN τ DECAY

In order to find a convenient representation for the " τ " decay $K \rightarrow 3\pi$, Dalitz has taken advantage of the fact that if a point α is plotted inside an equilateral triangle (Fig. 7) and from it perpendiculars of length T_1 , T_2 , T_3 are dropped to its three sides, then the sum $T_1 + T_2 + T_3$ of these lengths is equal to the height Q of the triangle. If the pions are treated nonrelativistically, it can be shown that the momentum condition $\not{p}_1 + \not{p}_2 + \not{p}_3 = 0$ forces the point α to lie within the inscribed circle. Inspection of the figure gives the Cartesian coordinates x and y in terms of the kinetic energies T ; the normalization is chosen so that the circle has unit radius ($0 \leq x^2 + y^2 \leq 1$).

We shall now show that unit area $dxdy$ on the Dalitz plot is proportional to unit volume in phase space, even if the τ decay is treated relativistically.

A familiar expression for the decay rate Γ for $K \rightarrow 3\pi$ is

$$\Gamma = \frac{2\pi}{\hbar} \frac{\Omega^2}{(2\pi\hbar)^6} \int d^3p_1 \int d^3p_2 \int d^3p_3 \delta \left(\sum_i \not{p}_i \right) \delta \left(m_K c^2 - \sum_i w_i \right) |R|^2 \quad \text{C-1.}$$

where R is the transition matrix element, \not{p}_i is the momentum of the i th pion, and w_i its total energy. The normalization volume is Ω . Because of the constraints on energy and momentum and the angular symmetries of the

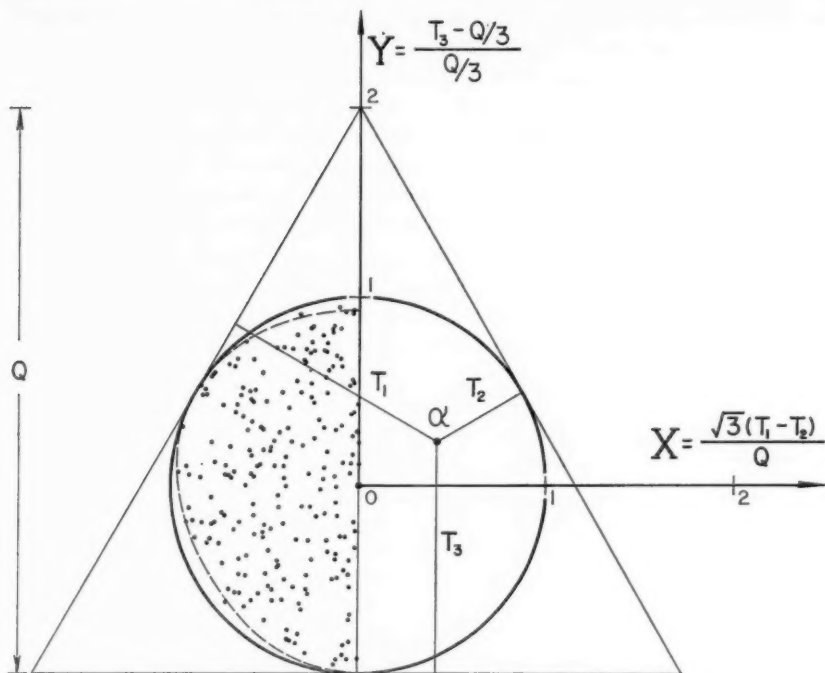


FIG. 7. Dalitz triangular construction for the distribution of pion energies in the "τ" decay $K \rightarrow \pi_1^+ + \pi_2^+ + \pi_3^-$.

problem, the matrix element R depends on only two variables, which we may choose to be w_1 and w_2 . Thus we may write

$$\Gamma = \frac{2\pi}{\hbar} \int \int dW_1 dW_2 |R(W_1, W_2)|^2 \frac{\Omega^2}{(2\pi\hbar)^6} \rho(W_1, W_2), \quad C-2.$$

where

$$\rho(W_1, W_2) = \int \int \int d^3 p_1 d^3 p_2 d^3 p_3 \delta(\sum p_i) \delta(m_K c^2 - \sum w_i) \delta(w_1 - W_1) \delta(w_2 - W_2). \quad C-3.$$

Now we can reduce C-3 to the simple form

$$\rho(W_1, W_2) = \frac{8\pi^2}{c^6} W_1 W_2 W_3; \quad (W_3 = m_K c^2 - W_1 - W_2) \quad C-4.$$

by proceeding as follows:

We integrate out the momentum p_3 and all angles except the angle θ between p_1 and p_2 , obtaining

$\rho(W_1, W_2)$

$$= \int 4\pi p_1^2 dp_1 \int 2\pi p_2^2 dp_2 \int d(\cos \theta) \delta(m_K c^2 - \sum w_i) \delta(w - W_1) \delta(w_2 - W_2). \quad C-5.$$

Now we can put

$$w_3^2 = (cp_3)^2 + (m_\pi c^2)^2 = (cp_1)^2 + (cp_2)^2 + 2c^2 p_1 p_2 \cos \theta + (m_\pi c^2)^2 \quad C-6.$$

and, taking the differential of both sides with p_1 and p_2 fixed, we find

$$2w_3 dw_3 = 2c^2 p_1 p_2 d(\cos \theta). \quad C-7.$$

Using C-7 and the relation $p_i dw_i = w_i dw_i / c^2$, we have in place of C-5

$$\rho(W_1, W_2) = \frac{8\pi^2}{c^6} \int \int \int w_1 dw_1 w_2 dw_2 w_3 dw_3 \delta(w_1 - W_1) \delta(w_2 - W_2) \delta(w_3 - W_3), \quad C-8.$$

which immediately gives C-4.

It is convenient to factor out of the R matrix element the product

$$\sqrt{N} = \prod \frac{1}{\sqrt{2w_i}}$$

that comes from the creation of three pions. We are then left with the Feynman matrix element $M = R/\sqrt{N}$, which is a world-scalar (53). In the non-relativistic limit, N is a constant and M and R are simply proportional. Relativistically, it is $|M|^2$ that is proportional to the population of dots in the Dalitz plot, as we now show.

We use C-2, C-4, and the definition of M to obtain

$$\Gamma = \frac{2\pi}{\hbar} \int \int dw_1 dw_2 |M(w_1, w_2)|^2 \cdot \frac{\pi^2}{c^6} \frac{\Omega^2}{(2\pi\hbar)^6} \quad C-9.$$

We see immediately that if $dw_1 dw_2$ is the element of area in the Dalitz plot, then the density of dots is proportional to $|M|^2$. We must show that $dxdy \propto dw_1 dw_2$, where x and y are the Dalitz coordinates of Figures 6 and 7. Clearly $dw_1 dw_2 = dT_1 dT_2$, since $w_i = T_i + m_\pi c^2$. But x and y are related to T_1 and T_2 by a linear transformation with constant Jacobian, and so $dxdy \propto dT_1 dT_2$.

APPENDIX D

Hypernuclei.—Nuclear matter can bind Λ to form systems stable for a time comparable with the Λ mean life. Such systems are well known and are called hypernuclei or hyperfragments. This topic has been treated thoroughly by Dalitz in his forthcoming review (R3). Experimental data have recently been surveyed by Levi-Setti, Slater, and Telegdi (54).

Mesonic vs. nonmesonic decay.—In the decay of a bound Λ we have two competing processes: the mesonic decay, for example the mode

$$\begin{aligned} \Lambda &\rightarrow p + \pi^-_{\text{real}} \text{ at a rate } \Gamma_{\text{real}} \\ (|\not{p}_{\text{real}, \pi}| &= 99.8 \text{ Mev}/c), \end{aligned} \quad D-1.$$

and the nonmesonic mode. These competing rates can be compared most conveniently by assuming a simple model in which the nonmesonic mode arises principally from the "internal conversion" of a virtual π , for example

$$\begin{aligned} \Lambda &\rightarrow p_1 + \pi^-_{\text{virt}}, \pi^-_{\text{virt}} + p_2 \Rightarrow n, \text{ rate } \Gamma_{\text{virtual}} \\ (|\not{p}_{\text{virt}, \pi}| &\approx |\not{p}_n| \approx 380 \text{ Mev}/c). \end{aligned} \quad D-2.$$

TABLE DI
RATIOS OF NON- π^- -MESONIC TO π^- -MESONIC DECAYS

I Hyperfragment	II $\frac{\text{non-}\pi^-\text{-mesonic}}{\pi^-\text{-mesonic}}$	III $\frac{\text{nonmesonic}}{\pi^-\text{-mesonic}}$	IV $Q^{(-)}$ Estimated from data	V Theoretical $Q^{(-)}$
Hydrogen	$\frac{0}{6}$	$\frac{0}{6}$	$\frac{0}{6} = 0$	0.5
Helium	$\frac{18}{7}$	$\frac{16}{7}$	$\frac{11}{7} = 1.5$	1.1
Lithium	$\frac{31}{2}$	$\frac{31}{2}$	$\frac{20}{2} = 10$	—
$Z > 3$	$\frac{140}{2}$	$\frac{140}{2}$	$\frac{93}{2} = 46$	50.0

Table DI: Internal Conversion Data for Hyperfragments; Col. II [from Schneps, Fry & Swami (56)] is observed "directly" when hyperfragments decay in emulsion. To calculate $Q^{(-)}$ one must go through two steps. First we get from Col. II, which lists "non- π^- -mesonic" to Col. III, which lists "nonmesonic," by estimating the number of decays in which an unseen π^0 escaped. To get Col. IV one must multiply the numerators by $\frac{2}{3}$ to correct for the fact that about $\frac{1}{3}$ of the nonmesonic decays result from conversion of virtual neutral pions (see Table II). (We assume that the probability for a π^0 to be absorbed by either protons or neutrons equals the probability for π^- to be absorbed by protons only.) The purpose of the quotation marks around the word "directly" is to emphasize the considerable uncertainties introduced by scanning bias and experimental ambiguities arising from the fact that it is relatively easy to identify mesonic decays, whereas nonmesonic decays can look like π^- captures, nuclear interactions, etc., Col. V gives the calculated $Q_a^{(-)}$ of Ruderman & Karplus (55).

The momentum involved is estimated by dividing the available energy between two nucleons.

Just as in the case of the internal conversion of a nuclear γ ray, the internal conversion coefficient $Q = \Gamma_{\text{virt}}/\Gamma_{\text{real}}$ is a very sensitive function of the orbital angular momentum carried by the (real or virtual) pion. Using the simple model mentioned above, and assuming the pions have angular momentum l , Ruderman & Karplus (55) have shown that Q_l is proportional to the relative probability of penetrating an angular momenta barrier, i.e.,

$$Q_l^{(-)}(Z) = Q_0^{(-)}(Z)(p_{\text{virt}}/p_{\text{real}})^{2l} = Q_0^{(-)}(Z) \times 15^l. \quad \text{D-3.}$$

$Q_0^{(-)}$ is proportional to the density of protons near the Λ in a nucleus of charge Z . In heavy nuclei $Q_0^{(-)}(Z)$ must also be corrected for many complications such as the Pauli exclusion principle and self-absorption of real π^- before they escape from the nucleus. The subscript $(-)$ means we consider only the decay mode $p + \pi^-$ (real or virtual).

Cols. II of Table D1 gives data obtained with nuclear emulsion and Cols. III and IV convert the data into an experimental estimate of $Q^{(-)}$. Col. V gives the Ruderman-Karplus estimate of $Q_0^{(-)}$. We see that the experimental $Q^{(-)}$ agrees with the theoretical $Q_0^{(-)}$ (i.e., for $l=0$), and disagrees badly with $Q_l^{(-)}$ for $l>0$ (Eq. D-3). Even though Ruderman & Karplus claim that their calculation of $Q_0^{(-)}$ is reliable only within a factor three, the argument for at least some decay amplitude through $l=0$, and therefore the evidence for a Λ spin $S_\Lambda = \frac{1}{2}$, is impressive.

Let us next try to get quantitative (and less reliable) information from the data, namely to estimate $x_- \equiv |S_-/P_-|^2$ where S_- and P_- are the relative amplitudes of s - and p -wave in the decay $\Lambda \rightarrow p + \pi^-$ as defined by Eq. 27. Eq. D-3 generalizes, in the case of mixed s - and p -waves, to

$$Q^{(-)} = 1.1 \left(\frac{1 + 15x_-}{1 + x_-} \right) \quad \text{D-4.}$$

If we took this equation and the data perfectly seriously we would find $x_- < 1/7$. If we assume the value $Q_0 = 1.1$ is uncertain by no more than a factor 3 and also allow for the experimental uncertainty, we still find $x_- < \frac{1}{2}$. Despite the uncertainties the argument does show that the p -wave channel is not dominant. Of course if x_- is as large as $\frac{1}{2}$, $|P/S|$ is $1/\sqrt{2}$, and the asymmetry parameter α_- of Eq. 32 can be nearly unity.

LITERATURE CITED

- Rochester Conferences on High-Energy Physics, Interscience, New York
- R1. Proceedings of Sixth Conference (1956)
 - R2. Proceedings of Seventh Conference (1957)
 - R3. Dalitz, R. H., *Reports in Progress in Physics* (To be published by the Physical Society, London, 1957)
 - R4. Franzinetti, C., and Morpurgo, G., *Nuovo cimento Suppl.* (To be published 1957)
 - R5. Gell-Mann, M., and Rosenbaum, E. P., *Sci. American*, **197**, 72 (1957)
 - R6. Okun, L., *Uspekhi Fiz. Nauk*, **61**, 535 (1957)
- 1. Schwinger, J., *Phys. Rev.*, **82**, 914 (1951); Lüders, R., *Kgl. Dansk. Videnskab. Selskab., Mat fys. Medd.*, **28**, No. 5 (1954); Pauli, W., *Niels Bohr and the Development of Physics* (Pergamon Press, London, England, 195 pp., 1955), p. 30
 - 2. Lüders, G., and Zumino, B., *Phys. Rev.*, **106**, 385 (1957)
 - 3. Gell-Mann, M., to *Nuovo cimento*, **4**, Suppl. 2, 848 (1956)
 - 4. Lee, T. D., and Yang, C. N., *Phys. Rev.*, **104**, 254 (1956)
 - 5. (a) Postma, H., Huiskamp, W. J., Miedema, A. R., Steenland, M. J., Tolhoek, H. A., and Gorter, C. J., *Physica*, **23**, 259 (1957); (b) Wu, C. S., Ambler, E., Hayward, R. W., Hopkins, D. D., and Hudson, R. P., *Phys. Rev.*, **105**, 1413 (1956); (c) (To be published, 1957)
 - 6. Landau, L., *Nuclear Phys.*, **3**, 127 (1957)
 - 7. (a) Coester, F., *Phys. Rev.*, **89**, 619 (1953); (b) Fermi, E., *Nuovo cimento*, **2**, Suppl. 1, 54 (1955); (c) Gell-Mann, M., and Watson, K. M., *Ann. Rev. Nuclear Sci.*, **5**, 219-70 (1954)
 - 8. Bethe, H. A., and de Hoffman, F., *Mesons and Fields*, II, Sect. 3.1 (Row, Peter-
son and Co., Evanston, Ill., 434 pp. 1955)
 - 9. Gell-Mann, M., *Phys. Rev.*, **92**, 833 (1953); Nakano, T., and Nishijima, K., *Progr. Theoret. Phys. (Kyoto)*, **10**, 581 (1953); Nishijima, K., *Progr. Theoret. Phys. (Kyoto)*, **13**, 285 (1955)
 - 9a. Gell-Mann, M., and Pais, A., *Proceedings of the International Conference on High-Energy Physics* (Pergamon Press, London, England, 350 pp., 1955)
 - 10. Lee, T. D., *Phys. Rev.*, **99**, 337 (1955)
 - 11. Feynman, R. P., and Speisman, G., *Phys. Rev.*, **94**, 500 (1951)
 - 11a. Alvarez, L. W., Bradner, H., Falk-Vairant, F., Gow, J. D., Rosenfeld, A. H., Solmitz, F., and Tripp, R. D., UCRL-3775 (unpublished 1957); *Nuovo cimento*, **5**, 1026 (1957)
 - 12. Plano, R., Samios, N., Schwartz, M., and Steinberger, J., *Nuovo cimento*, **5**, 203 (1957)
 - 13. Reines, F., and Cowan, C. L., (Private communication, 1957); *CERN Symposium*, (1956); *Phys. Rev.*, **92**, 830 (1953)
 - 14. Gell-Mann, M., and Pais, A., *Phys. Rev.*, **97**, 1387 (1955)
 - 15. Lande, K., Lederman, L. M., and Chinowsky, W., *Phys. Rev.*, **105**, 1925 (1957); Fowler, W. B., Lander, R. L., and Powell, W. M., *Bull. Am. Phys. Soc.*, **2**, 236 (1957); [See also two papers on nuclear interactions of K_2^0 with emulsion; Baldo-Ceolin *et al.* and Ammar *et al.*, both submitted to *Nuovo cimento*, (1957)]
 - 16. Lee, T. D., and Yang, C. N., *Nuovo cimento*, **3**, 49 (1956)
 - 17. Tanner, N., *Phys. Rev.*, (In press, 1957)
 - 18. Puppi, G., *Nuovo cimento*, **5**, 505 (1948); Klein, O., *Nature*, **161**, 897 (1948);

- Lee, T. D., Rosenbluth, M., and Yang, C. N., *Phys. Rev.*, **75**, 905 (1949);
 Tiomno, J., and Wheeler, J. A., *Rev. Modern Phys.*, **21**, 144 (1949)
19. Blatt, J. M., and Weisskopf, V. F., *Theoretical Nuclear Physics* (John Wiley, New York, N. Y., 863 pp., 1952); Konopinski, E. J., and Langer, L. M., *Ann. Rev. Nuclear Sci.*, **2**, 261-304
20. Michel, L., *Proc. Phys. Soc.*, **A63**, 514, 1371 (1950)
21. Salam, A., *Nuovo cimento*, **5**, 299 (1957)
22. Lee, T. D., and Yang, C. N., *Phys. Rev.*, **105**, 1671 (1957)
23. Kofod-Hansen, O., and Winther, A., *Kgl. Danske Videnskab Selskab, Mat. fys. Medd.*, **30**, (2) (1956)
24. The following ρ values have been reported: 0.68 ± 0.02 —Crowe, K. M., *Bull. Am. Phys. Soc.*, **2**, 234 (1957); 0.72 ± 0.05 —Dudziak, W., and Sagane, R., reported by Barkas, W. H., Seventh Rochester Conference on High-Energy Physics (Interscience Publishers, New York, To be published, 1957); 0.68 ± 0.05 —Sargent, C. P., Rinehart, M., Lederman, L. M., and Rogers, K. C., *Phys. Rev.*, **99**, 885 (1955); 0.67 ± 0.05 —Rosenson, L., *Momentum Spectrum of Positrons from the Decay of μ^+ Mesons*, Doctoral Thesis, University of Chicago, 1957 (Unpublished data)
25. Friedman, J. I., and Telegdi, V. L., *Phys. Rev.*, **105**, 1681 (1957)
26. Garwin, R. L., Lederman, L. M., and Weinrich, M., *Phys. Rev.*, **105**, 1415 (1957)
27. Coffin, T., Berley, D., Garwin, R. L., Lederman, L., and Weinrich, M. (Private communication, 1957)
28. (a) Sudarshan, G., and Marshak, R. (To be published, 1957) (b) Feynman, R. P., and Gell-Mann, M. (To be published, 1957)
29. Rustad, B. M., and Ruby, S. L., *Phys. Rev.*, **97**, 991 (1955)
30. Anderson, H. L., and Lattes, C. M. G., *Nuovo cimento* (To be published, 1957) (Find $\Gamma(\pi \rightarrow e + \nu)/\Gamma_\pi = 0.04 \pm 0.9 \times 10^{-5}$, and $\Gamma(\pi \rightarrow e + \nu + \gamma)/\Gamma_\pi = -2 \pm 1.6 \times 10^{-4}$)
31. Cassels, J. M., *Proc. 7th Rochester Conf. High-Energy Phys.* (To be published, 1957); finds a branching fraction of $(3 \pm 7) \times 10^{-6}$ for the radiative decay $\pi^+ \rightarrow e^+ + \nu + \gamma$, assuming tensor coupling
32. Lokanathan, S., *Nevis*, **30** (Unpublished, 1957)
33. Ruderman, M. A., and Finkelstein, R. J., *Phys. Rev.*, **76**, 1458 (1949)
34. Dallaporta, N., *Nuovo cimento*, **1**, 962 (1953); Costa, G., and Dallaporta, N., *Nuovo cimento*, **2**, 519 (1955)
35. The branching fraction $\mu \rightarrow e + \gamma$ is $< 2 \times 10^{-5}$, according to Steinberger, J., and Wolfe, H. B., *Phys. Rev.*, **98**, 240 (1955). The branching fraction for the μ^- capture mode $\mu^- + N \rightarrow N + e^-$ is $< 5 \times 10^{-4}$, according to Lokanathan S., and Steinberger, J., *Phys. Rev.*, **100**, 1490 (1955).
36. Hornbostel, J., and Salant, E. O., *Phys. Rev.*, **102**, 502 (1956)
37. Ruderman, M. A., and Karplus, R., *Phys. Rev.*, **102**, 247 (1956)
38. Lee, T. D., Steinberger, J., Feinberg, G., Kabir, P. K., and Yang, C. N., *Possible Detection of Parity Non-Conservation in Hyperon Decay* (To be published, 1957)
39. Plano, R., Samois, N., Schwartz, M., and Steinberger, J. (To be published, 1957)
40. Dalitz, R. H., *Phil. Mag.*, **44**, 1068 (1953); *Phys. Rev.*, **99**, 915 (1955)
41. Brucker, E. B., and Fazio, G., *Bull. Am. Phys. Soc.*, **2**, 236 (1957), also Birge, R., and Barkas, W. H. (Private communication, 1957)
42. Ritson, D. M. (Private communication, 1957)
- 42a. Gell-Mann, M., *Nuovo cimento*, **5**, 76 (1957)

43. Lee, T. D., and Yang, C. N., *Phys. Rev.*, **102**, 290 (1956); Gell-Mann, M., *Proc. 7th Rochester Conf. High-Energy Phys.* (To be published, 1957)
44. Dalitz, R. H., *Phil. Mag.*, **44**, 1068 (1953)
45. Fabri, E., *Nuovo cimento*, **11**, 479 (1954)
46. Orear, J., *Phys. Rev.*, **106**, 834 (1957)
47. Wentzel, G., *Phys. Rev.*, **101**, 1215 (1956)
48. Pais, A., and Treiman, S. B., *Phys. Rev.*, **105**, 1616 (1957)
49. Treiman, S. B., and Sachs, R. G., *Phys. Rev.*, **103**, 1545 (1956)
50. Lee, T. D., Oehme, R., and Yang, C. N., *Phys. Rev.*, **106**, 340 (1957)
- 50a. Jackson, J. D., Treiman, S. B., and Wyld, H. W., Jr., *Phys. Rev.*, **106**, 517 (1957)
- 50b. Jackson, J. D., Treiman, S. B., and Wyld, H. W., Jr., *Phys. Rev.* (To be published)
51. Adair, R. K., *Phys. Rev.*, **100**, 1540 (1955)
52. Treiman, S. B., *Phys. Rev.*, **101**, 1216 (1956)
53. Feynman, R. P., *Phys. Rev.*, **84**, 108, Sect. 10 (1951)
54. Levi-Setti, R., Slater, W. E., and Telegdi, V. L., *A World Survey of Hypernuclei* (To be published, 1957); Telegdi, V. L., *Proc. 7th Rochester Conf. on High-Energy Physics* (To be published, 1957)
55. Ruderman, M. A., and Karplus, R., *Phys. Rev.*, **102**, 247 (1956); (Private communication, 1957)
56. Schneps, J., Fry, W. F., and Swami, M. S., *Phys. Rev.*, **106**, 1062 (1957)
57. Coombes, C. A., Cork, B., Galbraith, W., Lambertson, G., and Wenzel, W. A., (Private communication, Sept., 1957); *Phys. Rev.* (To be published)
58. (a) Alvarez, L. W., *et al.* (Private communication, Sept., 1957); (b) Crawford, F. S., Cristi, M., Good, M. L., and Ticho, H., *Phys. Rev.* (To be published, 1957)

AUTHOR INDEX

A

Abashian, A., 311, 328, 344
 Abbott, J. D., 135, 145, 148
 Abbott, J. D., 147
 Abragam, A., 352, 382, 395
 Abraham, M., 387, 391
 Acheson, L. K., Jr., 278, 281
 Ackerman, G. A., 166
 Ackermann, I. B., 148
 Adair, R. K., 469
 Adler, H. I., 66, 68
 Aepli, H., 349, 392
 Agodi, A., 327
 Akeson, A., 96
 Akita, K., 101
 Alaga, G., 225
 Albers-Schönberg, H., 392
 Alder, K., 186, 188, 190, 211,
 214, 225, 395
 Alderman, I. M., 138, 148, 150
 Alei, E. F., 324, 325
 Alexander, H. D., 125
 Alexander, H. E., 70
 Alexander, P., 119
 Alfinslater, R., 148
 Alimarin, I. P., 340, 341
 Allen, A. C., 147
 Allen, A. J., 178
 Allen, K. R., 304
 Ally, M. S., 172
 Alm, R. S., 33
 Alpen, E. P., 141
 Alter, T., 73, 113, 114, 115
 Alston, M. H., 335
 Alter, A. J., 177
 Altman, K. I., 92, 99
 Alvarez, L. W., 5, 379, 417, 451
 Alvarez, W., 26
 Amaldi, E., 264, 272, 280, 301
 Ambler, E., 1, 352, 353, 412, 428
 Ammar, I. A., 420
 Amphlett, C. B., 32
 Andersen, R. S., 114
 Anderson, E. C., 83
 Anderson, H. L., 319, 321,
 323, 324, 325, 326, 436, 446
 Anderson, N. G., 74
 Anderson, R. E., 171
 Andrews, G. A., 175
 Andrews, J. S., 125
 Andrews, N. L., 144
 Angel, C. W., 51
 Angell, C. E., 323, 325
 Anger, H. O., 178
 Annis, M., 26
 Apperly, A., 49
 Araujo, J. A., 215, 216
 Ard, W. B., 119
 Arehart, R. A., 33

Arima, A., 221
 Armstrong, D. E., 38
 Armstrong, W. D., 95
 Arnold, A., 176
 Aronson, D. L., 103, 106
 Arvey, L., 167, 168
 Asanovich, G., 53, 54
 Ashkin, J., 318, 319, 321, 323,
 324, 325, 327, 328
 Asprey, L. B., 38
 Auerbach, C., 122
 Austin, M. K., 145

B

Bachofen, C. S., 79, 115
 Baclesse, F., 122
 Bacq, Z. M., 94, 99, 117, 121,
 135, 146, 150
 Baggett, E. R., 38
 Bagnall, K. W., 48, 49, 51
 Bailey, O. T., 177
 Bailey, P., 176
 Baiukov, Iu. D., 334, 335, 337,
 338
 Baker, B. L., 169
 Baker, E. W., 338, 341
 Baker, J. M., 386, 387
 Baker, W. F., 328, 329
 Baldo-Ceolin, 420
 Baldwin, T. H., 109
 Baldwin, W. H., 40
 Ball, W. P., 342, 344
 Ballin, J. C., 164
 Baranov, V. I., 340, 341
 Baranova, V. T., 340, 341
 Barhorst, R. R., 149
 Barkas, W. H., 3, 26, 430,
 456
 Barker, C. F., 221
 Barner, H. D., 68, 69
 Barnes, D. W. H., 122, 146,
 148, 149, 165, 166
 Barnes, R. G., 379
 Barr, T. A., 137
 Barrer, R. M., 32
 Barron, E. S. G., 103
 Barshay, S., 326
 Barth, G., 167
 Bartlett, J. H., 276
 Bartz, M. H., 51, 53, 54, 55
 Basson, J. K., 144
 Batson, A. P., 331, 332, 333,
 335
 Batzer, H., 126
 Baum, S. J., 145, 166
 Bauman, W. C., 39
 Baxendale, J. H., 111, 120
 Baxi, A. J., 124
 Baxter, C. F., 96, 146

Baxter, R. C., 152
 Bayard, R. T., 277
 Beadle, A. B., 40
 Beam, C. A., 63, 77
 Beattie, J. W., 136
 Beatty, A. V., 110
 Beaumarriage, M., 94
 Becker, G. E., 380
 Bederson, B., 357, 380, 381
 Behrends, R. E., 13
 Bekkum, D. W. van, 100, 101,
 118, 148, 150
 Belcher, E. H., 95, 96, 146
 Belenki, S. Z., 337
 Beljanski, M., 66, 68, 69
 Bell, J. S., 187
 Bell, V. L., 91
 Bell, W. E., 13
 Bellamy, E. H., 350, 366, 380,
 381
 Bellamy, W. D., 109, 113
 Bellios, N. C., 166
 Benedict, W. H., 173, 178
 Beneventano, M., 327
 Benford, F. J., 48
 Bennett, G., 54
 Bennett, J., 65
 Bennett, L. R., 110
 Bennewitz, H. G., 380, 381
 Benson, R. E., 150
 Berg, R. A., 208, 209
 Berger, M. J., 137
 Bergquist, L., 148
 Beringer, R., 351
 Berkhouit, U. M., see Meyer-
 Berkhouit, U.
 Berley, D., 433, 434
 Berlin, N. I., 152
 Berman, A., 381
 Bernardini, G., 327, 338, 339,
 340
 Bernardini, M., 303, 327
 Bernheim, F., 91
 Bernstein, M. H., 109
 Bernstein, S., 352
 Bertani, G., 82
 Berthard, W. F., 123
 Bethe, H. A., 1, 186, 209, 239,
 241, 245, 246, 248, 255, 271,
 324, 425, 414
 Bethell, F. H., 145, 146, 169,
 173
 Betz, H., 172
 Biegel, A. C., 178
 Biel, S. J., 310
 Bigelow, R. B., 175
 Billen, D., 121, 123
 Biller, W. F., 340, 341
 Billings, M. S., 138
 Binford, F. T., 31

AUTHOR INDEX

- Bink, N., 149
 Birge, R., 456
 Birkner, R., 176
 Birnbaum, W., 3
 Bishop, A. S., 349, 392
 Bissell, O. M., 56
 Bitter, F., 279
 Bivins, R., 342
 Blackford, M. E., 117, 121
 Blair, H. A., 137, 140, 144, 147, 151, 152
 Blankenbecler, R., 259, 266, 267
 Blaser, J. P., 318, 319, 321, 323, 324, 325, 327, 328
 Blasius, E., 40
 Blatt, J. M., 218, 225, 257, 258, 424
 Blau, M., 330
 Bleaney, B., 351, 381, 385, 386, 387
 Blin-Stoyle, R. J., 214, 221
 Bloch, F., 356, 379
 Blomgren, R. A., 51, 53, 54, 55
 Bloom, W., 79, 163, 164
 Bludman, S. A., 16
 Boag, J. W., 100
 Bock, K., 171
 Bodansky, D., 321, 323, 325
 Boddington, P., 49
 Bodmer, A. R., 279
 Bogle, G. S., 387
 Bogoliubov, N. P., 331, 332, 333
 Bogoliubov, N. N., 326
 Bohlin, N. B., 49
 Bohlin, N. J. G., 51
 Bohr, A., 186, 188, 190, 193, 196, 203, 204, 211, 214, 221, 222, 225, 233, 357
 Bohr, D. F., 146, 169, 173
 Boiffard, J. A., 167, 168
 Boiron, M., 99
 Bond, V. P., 135-62; 135, 136, 137, 138, 139, 140, 141, 142, 143, 144, 145, 146, 147, 148, 149, 150, 152, 165, 166, 167
 Bondurant, J. H., 145
 Bonet-Maury, P., 120
 Bonetti, A., 13
 Bonnichsen, R., 96
 Boone, I. U., 144
 Booth, E. T., 338, 339, 340, 342
 Bora, K. C., 143
 Borg, D. C., 136, 137, 138, 139, 140, 141, 142
 Born, M., 234
 Borstel, R. C. von, 65, 67
 Borthwick, H. A., 64
 Boss, W. R. F., 95
 Botkin, A. L., 175
 Bouchard, J., 176
 Bovy, R., 40
 Bowers, K. D., 7, 381, 385, 386
 Brace, K. C., 144
 Bradner, H., 417
 Brady, E. L., 392
 Bragina, T. V., 340, 341
 Bralove, A. L., 49
 Brandenburg, W., 176
 Brandt, C. L., 65, 67, 69, 74
 Brauer, R. W., 152
 Bray, P. J., 379
 Brecher, G., 138, 140, 144, 145, 148
 Breit, G., 350
 Brenner, S., 257, 280, 292
 Bressee, J. C., 33, 56
 Brick, I. B., 170, 171, 172
 Bridges, A. E., 80
 Bridgforth, E. B., 138
 Bright, H. A., 38
 Brin, M., 91, 99
 Brink, G. O., 376, 381
 Brinton, C., 82
 Brix, P., 380
 Broda, E., 31
 Brody, S. B., 380
 Brohult, A., 124, 125
 Brohult, S., 120
 Brooks, D., 167
 Brooks, P. M., 169
 Brovett, P., 303
 Brown, B., 277
 Brown, D. V. L., 178
 Brown, E. D., 38
 Brown, G. E., 257, 280, 292
 Brown, J. B., 169
 Brown, K. B., 33
 Brown, M. B., 165
 Brown, W. M. C., see Court Brown, W. M.
 Brownell, G. L., 136, 139, 143
 Browning, L. E., 135, 137, 140, 166
 Bruce, A. K., 95
 Bruce, F. R., 31
 Bruce, V. G., 69
 Brucer, M., 137, 175
 Brucker, E. B., 456
 Brueckner, K. A., 186, 189, 200, 208, 209, 320, 328, 334
 Brues, A. M., 146, 153
 Buchanan, D. J., 138
 Buck, P., 353, 380
 Buechner, W. W., 247, 277
 Buffa, N. T., 80
 Buckley, R. J., 208
 Buley, H. M., 167, 168
 Bumiller, F., 310
 Bunney, L. R., 33, 40
 Burbridge, G. R., 23
 Burg, C., 91
 Burhop, E. H. S., 310
 Burk, C., 51
 Burn, J. H., 100
 Burnett, G. W., 170
 Burnett, W. T., Jr., 188, 172
 Burnham, J. B., Jr., 51, 53, 54, 55
 Burns, V. W., 74
 Burrill, E. A., 277
 Burstell, F. H., 37
 Burstone, M. S., 170
 Buser, W., 31, 39
 Bush, S., 150
 Bustad, L. K., 175
 Busygina, A. A., 39
 Butler, C. K., 37
 Butler, J. A. V., 73, 105, 114
 Buu-Hoi, N. P., 120
 Buzzell, A., 69, 81
- C
- Caird, R. S., 372
 Caldecott, R., 119
 Calkins, G. D., 51, 53, 54
 Cammermeyer, J., 176
 Campbell, E. C., 34
 Campo, R. D., 147
 Cantelow, H. P., 51
 Capps, R. N., 325, 326, 327
 Caretto, A. A., 338, 341
 Carleson, G., 37
 Carlson, T. A., 33
 Carlson, W. D., 53
 Carpender, J. W. J., 173
 Carroll, H. W., 152
 Carsten, A. L., 151
 Carswell, D. J., 39
 Carter, R. E., 136, 138, 144, 145
 Casarett, G., 137, 148, 152
 Case, K. M., 17
 Casimir, H. B. G., 353, 358
 Cassels, J. M., 437
 Caster, W. O., 95
 Castillejo, L., 320, 322
 Castle, J. G., Jr., 351
 Castner, S. V., 51
 Cater, D. B., 121
 Cathers, G. I., 32
 Catsch, A., 137, 150
 Caulton, M., 330
 Caverly, M. R., 51, 53
 Ceolin, B., see Baldo-Ceolin
 Chambers, E. E., 252, 253, 263, 269, 270, 308
 Chambers, F. W., Jr., 136, 138, 139, 141, 142
 Chandler, V. L., 80
 Chang, J. J., 103
 Chaplin, C. E., 68
 Chapman, E. M., 175
 Chapman, K. R., 277
 Chapman, W. H., 138, 145
 Charles, R. L., 68
 Charlesby, A., 119
 Chastain, S. M., 110
 Chen, F. F., 331, 332, 333, 342, 344
 Chen, I., 144
 Chen, T., 39
 Chen, Y., 39
 Cheng, A. L. S., 148
 Cherrier, N., 70
 Chevallier, A., 91
 Chew, G. F., 319, 320, 322, 327

- Child, R. G., 82
 Childs, W. J., 380
 Chinowsky, W., 420, 422
 Chippa, S., 167
 Choppin, G. R., 36, 38, 40
 Christenberry, K. W., 173, 178
 Christensen, E., 65, 69, 72
 Christensen, R. L., 380, 381
 Christian, E. J., 146
 Christopherson, E. W., 51
 Christy, R. F., 4, 18
 Cibis, P. A., 178
 Cini, M., 327
 Clark, D., 323, 325, 326, 327
 Clark, G. M., 79
 Clark, J. W., 143, 145, 147, 149
 Clark, W. G., 138, 147
 Clementel, E., 253
 Clendenin, W. W., 362
 Cochran, K. W., 99
 Coester, F., 198, 221, 413
 Coffin, T., 2, 10, 433, 434
 Cogan, D. G., 178
 Cohen, E. R., 3, 25
 Cohen, J. A., 101
 Cohen, S. S., 67, 79
 Cohen, V. W., 350, 370, 379, 381, 386
 Cohn, P., 105
 Cohn, S. H., 135, 137, 140, 166
 Cole, L. J., 109, 148, 149, 165, 166, 173
 Coleman, C. F., 33
 Coleman, J. S., 38
 Coleman, S., 125
 Collins, V. P., 140
 Collinson, E., 90
 Comar, C. L., 139
 Commins, E., 379
 Conard, R. A., 135, 137, 140, 145, 148, 167
 Conboy, J. T., 52
 Conforto, A. M., 27
 Congdon, C. C., 135, 150, 165, 166, 172
 Conger, A. D., 116
 Coniglio, J. G., 90
 Constant, M., 150
 Conte, F. P., 137, 143
 Conway, B. E., 114
 Conway, J. G., 352
 Cook, E. S., 136, 138, 140
 Cook, G. B., 40
 Cook, L. G., 49
 Cooke, A. H., 387
 Cool, R., 311, 323, 325, 326, 327, 328, 344
 Coombe, D. C., 38
 Coombes, C. A., 431, 433
 Coon, J. M., 140
 Cooper, L. N., 4, 23, 311
 Coor, T., 331, 333, 342
 Copeland, M. M., 169
 Coplan, B. V., 52, 55
 Corben, H. C., 22
- Cork, B., 431, 433
 Cormier, M. J., 103
 Cornish, F. W., 40
 Corp, M. J., 148, 149
 Costa, G., 440
 Cotter, G. J., 111, 120
 Cotzias, G. C., 98
 Court Brown, W. M., 147
 Cowing, R. F., 174
 Cox, H. R., 82
 Cox, R. A., 120
 Crathorn, A. R., 105
 Crawford, F. S., 451
 Crew, J. E., 326
 Crewe, A. V., 335
 Cristi, M., 451
 Cronin, J., 328, 344
 Cronin, J. W., 311
 Cronkite, E. P., 135, 136, 137, 138, 139, 140, 141, 142, 143, 144, 145, 146, 147, 148, 149, 150, 167
 Crouch, E. A. C., 40
 Crouch, M. F., 1
 Crouse, D. J., 33
 Crowe, K. M., 3, 25, 430
 Crummett, W. B., 37
 Culvahouse, J. W., 386
 Culwick, B., 311, 332, 333, 335
 Cumming, J. B., 338, 341
 Cunningham, J. G., 40
 Curr, R. M., 277, 304
 Curtis, H., 143
 Cuypers, Y., 121
 Czech, H., 175
- D
- Dabbs, J. W. T., 352
 Dahl, A. H., 141
 Dailey, M. E., 175
 Dale, W. M., 97
 Dalitz, R. H., 234, 310, 320, 322, 408, 456, 460, 463, 473
 Dallaporta, N., 440
 Dallenbach, F., 144
 Dalton, J. C., 34
 Daly, R. T., Jr., 359, 380, 381
 Damgaard, E., 167, 168
 Damodaran, K. K., 277
 Danielli, J. F., 74
 Daniels, E. W., 75
 Daniels, J. M., 352
 Darby, W. J., 90, 138
 Darwin, C. G., 284
 Dauer, M., 140
 David, L., 379
 David, P. W., 172
 Davidon, W. C., 319, 321, 323, 324, 325, 326, 327
 Davids, J. A., 148
 Davison, J. P., 187
 Davies, C. W., 37
 Davis, L., 360, 380, 381
 Davydoff, S., 83
 Day, E. J., 125
- Day, R. A., 38
 De Benedetti, S., 3
 Debley, V., 170
 De Borde, A. H., 23
 de Groot, J., 118
 de Hoffmann, F., see Hoffmann, F. de
 Deitz, V. R., 31, 32
 Delihas, N., 143
 Demeur, M., 23
 Denham, W., 175
 De Pagter, J. K., 26
 De Shryver, A., 150
 de Shalit, A., see Shalit, A. de
 Detrick, L. E., 170
 Detwiler, C. G., 49
 Deuel, H., 31, 32
 Deuel, H. J., Jr., 148
 Deutsch, M., 392
 Devik, F., 121, 167, 168, 169
 Devine, R. L., 112
 Dewell, E., 49
 Dhar, S., 258, 259, 262, 263, 264, 308
 Diamond, R. M., 37
 Dicke, R. H., 351
 Dimaggio, F. L., 152
 Dirac, P. A. M., 282
 Dismuke, S., 48
 Doan, C., 49
 Dobrowolski, W., 351, 385, 386
 Dobson, R. L., 170
 Dobyns, B. M., 175
 Dockum, N. L., 175
 Doe, W. B., 51, 52
 Doggett, J. A., 137, 278, 304
 Doherty, D. G., 118
 Domen, S. R., 136
 Donaldson, D. D., 178
 Dorain, P., 351, 387
 Dorfman, R. I., 105
 Doty, D. M., 126
 Doudney, C. O., 118, 123
 Doull, J., 99, 138
 Dowben, R. M., 145
 Dowdy, A. H., 110
 Dowlen, R. N., 104
 Downs, B. W., 303, 304, 309
 Doyle, B., 64, 120
 Draper, L. R., 149
 Drell, S. D., 267, 303
 Drew, R., 109
 Drungis, A., 177, 178
 Drutz, E., 165
 Dubois, K. P., 98, 99, 138
 Ducoff, H. S., 75
 Dudziak, W. F., 13, 26, 430
 Dugger, G. S., 176
 Dulbecco, R., 82
 Du Mond, J. W. M., 3, 25
 Dunham, C. L., 135, 137, 140, 166
 Dunjic, A., 145, 149, 150
 Dunster, H. J., 51, 54
 Duplan, J. F., 120
 Durand, H., 352

AUTHOR INDEX

- Durham, N. N., 72
 Duyckaerts, G., 40
 Dwyer, F. M., 92
 Dykes, F. W., 51, 53, 54
 Dyson, F. J., 320, 322, 325
 Dzhelepov, V. P., 329, 331, 332, 333
- E
- Early, J. C., 93
 Easterday, O. D., 143, 144, 152
 Ebert, M., 116, 135, 152
 Eck, T. G., 359, 380
 Edelman, A., 95, 135, 147, 175
 Eden, R. J., 186, 187
 Edgerly, R. H., 168
 Edington, C. W., 80
 Edlund, T., 124
 Edmonds, A. R., 194, 196
 Edmonds, D. S., Jr., 357, 362, 381
 Efner, J. A., 90, 138
 Eguchi, T., 16
 Ehrenberg, H., 274, 275, 304, 308, 310
 Ehrenberg, L., 119
 Fhret, C. F., 64, 67, 79
 Eichel, H. J., 99
 Eisinger, J. T., 380
 Ejdjarn, L., 118, 119
 Eldred, E., 137
 Ellenberg, J. Y., 33
 Ellinger, F., 136, 138, 139, 140, 141, 142
 Elliott, A. M., 79
 Elliott, J. P., 194
 Elliott, R. J., 385
 Ellis, F., 97, 107
 Ellis, G., 177
 Ellis, M. E., 109, 149, 165, 173
 Ellison, R. D., 352
 Elton, L. R. B., 257, 280, 292, 304, 305, 310
 Emmons, A. H., 51
 English, J. A., 98, 145, 170
 Entenman, C., 90, 92, 93
 Epstein, H. T., 73
 Eriksen, E., 22
 Errera, M., 67, 70, 99
 Eschenbrenner, A. B., 173
 Essen, L., 381
 Estermann, I., 379, 380
 Evans, J., 4
 Evans, R. D., 231
 Evans, T. C., 111, 144, 164, 177, 178
 Evans, W. H., 335
 Evrard, E., 121
 Ewbank, W. B., 380, 381
- F
- Fabri, F., 461
- Falconer, J. D., 32
 Falk-Variant, F., 417
 Faraghan, W. G., 165
 Faris, J. P., 40
 Farmakes, J. R., 51
 Farmansfarmaian, A., 65
 Farr, R. S., 135, 137, 140, 167
 Farris, G., 187
 Faucher, J. A., 32
 Faxen, H., 278
 Fazio, G., 456
 Fechner, H. R., 273, 308
 Fedorov, N. A., 97
 Feenberg, E., 185, 187, 209, 272
 Feher, G., 352, 386
 Feinberg, G., 451
 Feinberg, V. I., 328
 Feiner, F., 318, 319, 321, 323, 324, 325, 327, 328
 Feinstein, R. N., 98, 111, 120
 Feirstein, H. E., 51
 Feld, B. T., 325, 360, 379, 380
 Feldman, D., 332
 Feldman, M. J., 52
 Fenn, W. O., 150
 Ferguson, K. R., 54, 55
 Fermi, E., 321, 323, 324, 325, 335, 353, 413
 Fernbach, S., 328, 342
 Ferrari, G., 321, 324, 325
 Ferrell, R. A., 272, 301, 302
 Ferretti, L., 321, 324, 325
 Ferroni, S., 303, 309
 Feshbach, H., 185, 247, 264, 267, 277, 278, 279, 280, 304
 Feynman, R. P., 417, 433, 473
 Ficq, A., 67
 Fidecaro, G., 264, 272, 280, 301
 Field, R. E., 53
 Fields, T. H., 331, 332
 Filippov, A. I., 330
 Finkelstein, R. J., 13, 438
 Finlay, E. A., 304
 Finston, H. L., 34
 Fischer, P., 92, 94
 Fisher, D. J., 52, 53
 Fisher, R. W., 53
 Fishler, M. C., 147, 165
 Fitch, F., 149
 Fitch, F. W., 98
 Fitch, V. L., 2, 3, 4, 22, 23, 24, 25, 26
 Fitzpatrick, J. P., 49
 Flanders, P. H., see Howard-Flanders, P.
 Flandry, J. R., 56
 Fleming, J., 90
 Flesher, A. M., 150
 Fletcher, G. H., 140
 Fletcher, G. L., 98
 Fletcher, J. M., 31
 Fletcher, P., 353
 Fletcher, R. C., 386, 387
- Fletcher, R. D., 51, 53, 54
 Flowers, B. H., 185
 Fluke, D. J., 64, 106
 Fogg, L. C., 174
 Foldy, L. L., 220, 250, 255, 271
 Foley, H. M., 362, 379, 380
 Folmar, G. D., Jr., 138
 Foltz, J. R., 51, 53, 55
 Fonner, R. L., 150
 Foraker, A. G., 175
 Ford, C. E., 122, 146, 166
 Ford, K. W., 1, 22, 23, 24, 209, 220, 221, 222, 280, 292, 309
 Forrest, P. J., 37
 Forsblom, S., 40
 Forsling, W., 38
 Forssberg, A., 90, 91, 92, 96, 105, 121, 124, 135, 145, 148
 Fowler, E., 333, 336, 337
 Fowler, G. N., 4, 279
 Fowler, W. B., 331, 332, 333, 335, 336, 337, 420, 422
 Fox, B. W., 170, 172
 Fox, J. G., 331, 332
 Fox, M., 379, 380, 381
 Frajola, W. J., 166
 Francis, N. C., 186, 187
 Franken, P., 380
 Franklin, J., 326
 Franzinetti, C., 408
 Fraser, M. J., 103
 Frauenfelder, H., 349, 392, 395
 Fred, M., 352
 Frederick, E. J., 51, 54
 Freedman, J. I., 12
 Fregeau, J. H., 272, 274, 295, 302, 308, 309
 Freiling, E. C., 33, 40
 Fremlin, J. H., 40
 Freund, H., 38
 Freymann, J. G., 75
 Fricke, H., 93
 Frickey, P., 83
 Friedberg, W., 150
 Friedell, H. L., 121, 150
 Friedlander, G., 338, 341, 342
 Friedman, F. L., 185
 Friedman, H., 16
 Friedman, J. I., 432
 Friedman, N. B., 165, 170, 171
 Frisch, R., 379, 380
 Fritz-Niggli, H., 76, 102
 Fröman, P. O., 225
 Fryer, M. P., 169
 Frysinger, G. R., 31
 Fubini, S., 303, 309, 327
 Fudge, A. J., 34
 Fuert, C. R., 83, 84
 Fuger, J., 40
 Fuller, C. S., 386
 Fuller, J. B., 144
 Fung, S. C., 26

- Furchner, J. E., 143, 144, 165
 Furth, J., 163, 172, 173
- G**
- Gabe, M., 167, 168
 Gaines, G. L., Jr., 32
 Gaither, N., 79, 80, 111, 124
 Galbraith, W., 431, 433
 Gallone, S., 209, 210
 Galperin, H., 70
 Gammel, J. L., 332
 Gardella, J. W., 103
 Garden, N. B., 47-62; 48, 49,
 51, 53, 54
 Gardiner, V., 73
 Gardner, W. J., 51, 53, 55
 Garvin, H. L., 381
 Garwin, R. L., 1, 2, 10, 11,
 12, 432, 433, 434
 Gaston, E. O., 123, 149
 Gatha, K. M., 273
 Gatto, R., 272, 305, 306
 Gaulden, M. E., 106
 Geisseloder, J. L., 94
 Gell-Mann, M., 407-77; 318,
 338, 339, 340, 342, 408, 409,
 413, 416, 417, 419, 420, 433,
 460
 Genge, J. A. R., 39
 Gengozian, N., 150
 Genna, S., 136
 George, E. P., 4
 Gere, E. R., 386
 Gerebtzoff, M. A., 117
 Gershbein, L. L., 172
 Gerstner, H. B., 140, 168,
 169, 177
 Gessaroli, R., 321, 324, 325
 Gessert, C. F., 150
 Ghiorso, A., 40
 Giese, A. C., 65, 67, 69, 72,
 74
 Gifford, J. F., 53
 Gilbert, C. W., 96, 151
 Gilbert, D. A., 350, 370, 381
 Gilbert, D. L., 150
 Gilbert, I. G. F., 95, 146
 Giles, N. H., 110
 Giles, P. C., 26
 Gillis, J., 40
 Gillum, O. R., 386
 Gillman, T., 167
 Ginell, W. S., 32
 Ginoza, W., 66, 81
 Glass, R., 40
 Glassgold, A. E., 279, 287,
 288
 Glauber, R. J., 328
 Gleiser, C. A., 137
 Glen, H. J., 56
 Glenn, J. L., 95
 Glicksman, M., 319, 321, 323,
 324
 Glover, K. M., 40
 Glucksman, A., 165, 171
 Glueckauf, E., 33, 34
- Goertz, R. C., 51, 53
 Goertzel, G., 395
 Goff, J. L., 178
 Gold, S. S., 49
 Goldberger, M. L., 325, 326,
 327, 338, 339, 340, 342
 Golden, R., 137
 Goldfeder, A., 102
 Goldgraber, M. R., 170
 Goldhaber, G., 26
 Goldhaber, G. S., see
 Scharff-Goldhaber, G.
 Goldhaber, M., 220, 221
 Goldin, L. L., 190, 225
 Goldman, A. S., 65, 67
 Goldstone, J., 186, 209
 Goldwasser, E. L., 327
 Goldwater, W. H., 90
 Gofland, I. A., 328
 Golovin, B. M., 331, 333
 Gomberg, H. J., 51
 Gonshery, L., 138
 Good, M. L., 451
 Goode, J. H., 56
 Goodman, C., 208
 Goodman, L. S., 350, 370,
 380, 381
 Gordon, E. P., 100
 Gordon, L., 38
 Gordon, S. A., 105
 Gordy, W., 119
 Gorham, J. E., 379, 380
 Gorman, J. G., 318, 319, 323,
 325, 327, 328
 Gorter, C. J., 412, 428, 434
 Gotlieb, T., 82
 Gottfried, K., 211
 Gottlieb, D., 80
 Goucher, C. R., 66, 71, 77
 Gould, G., 353
 Gould, J. R., 48
 Gould, R. G., 90, 91
 Goutier-Pitotte, M., 99
 Gow, J. D., 417
 Gowen, J. W., 153
 Grabner, L., 380
 Grace, M. A., 352
 Graf, P., 31
 Grahn, D., 136, 137, 138, 141,
 146, 145
 Graves, E., 178
 Gray, L. H., 63, 79, 90, 97,
 116, 121, 164
 Green, A. E. S., 208, 218
 Green, D. E., 126
 Greenfield, M. A., 138
 Greenman, V., 149
 Greschman, R., 150
 Gricouroff, G., 163, 171
 Griessbach, R., 31
 Griffin, J., 192
 Griffith, H. D., 167, 169
 Griffith, W. H., 125
 Griffiths, J. H. E., 386, 387
 Grigoriev, E. L., 330
 Grim, R. E., 32
 Grosoff, G. M., 379
- Grossman, B. J., 173
 Grutter, W. F., 31
 Gualandi, C., 38
 Gude, W. D., 167, 168
 Guest, G. H., 49
 Giuliano, R., 96
 Gunter, S. E., 76, 77, 136
 Gurian, J. M., 73
 Gurnami, S. U., 124
 Guth, E., 247, 255, 278
 Gwatkin, B., 80
- H**
- Haase, J., 176
 Haberland, G. L., 92
 Habermeyer, J. G., 148, 149,
 166
 Haber-Schaim, U., 327
 Hagemann, F., 54
 Hagen, U., 118, 120
 Hague, J. L., 38
 Hahn, B., 273, 280, 292, 294,
 295, 297, 298, 299, 303, 308,
 309, 328
 Hahn, E., 70
 Haigh, M. V., 96, 138, 144,
 151
 Haik, G. M., 177
 Halban, H., 352
 Hale, D. B., 187
 Hale, D. K., 32, 34
 Haley, T. J., 140, 150, 153,
 170
 Hall, B. V., 116
 Hall, G. R., 387
 Ham, W. T., Jr., 177
 Hamerton, J. L., 122, 166
 Hamilton, D. R., 350, 380,
 381
 Hamilton, K. F., 137, 148
 Hämerling, J., 67
 Hampton, M. M., 111, 120
 Hancher, C. W., 33
 Hancock, F. E., 51
 Handen, D. T., 94
 Hannan, R. S., 125, 126
 Hansen, O. K., see Kofoed-
 Hansen, O.
 Hanson, A. O., 278
 Hardy, T. C., 380
 Harm, W., 82
 Harrick, N. J., 379
 Harrington, R., 56
 Harris, D. C., 92
 Harris, D. H., 140
 Harris, G., 26
 Harris, P. F., 145, 166
 Harris, P. S., 143, 144, 147,
 164, 170
 Harris, E. B., 96, 146
 Harsh, G. R., 3rd, 177
 Harter, J. A., 137
 Hartinger, L., 40
 Hartman, P. E., 66
 Hartree, D. R., 310
 Harvey, B. G., 36, 38, 40

AUTHOR INDEX

- Harvey, E. N., 103
 Harvey, R. A., 136, 144
 Hatch, L. P., 32
 Hauns, R. D., Jr., 381
 Haxel, O., 185
 Hay, R. H., 379, 381
 Hayakawa, S., 325
 Haymaker, W., 176
 Hayward, R. W., 1, 412, 428
 434
 Hearon, J. Z., 111
 Hecht, F., 38
 Hechter, H. H., 136
 Heckman, H. H., 26
 Heer, E., 392
 Heite, H. J., 169
 Heitler, W., 234, 236, 239
 Hellwarth, R. W., 380
 Helm, R. H., 262, 295, 296,
 297, 302, 309
 Hempelmann, L. H., 92, 93,
 99, 100, 122, 135, 140
 Henderson, W. J., 136, 144
 Hendricks, S. B., 64
 Henley, E. M., 23
 Hennessey, T. J., 95
 Henriques, F. W., Jr., 167,
 168
 Henry, V. P., 26
 Henshaw, P. S., 140
 Hensley, P. N., 137
 Herber, R. H., 38
 Herve, A., 121
 Hevesy, G., 90, 91, 92, 96,
 105, 145, 148
 Heyde, W., 171
 Heydenburg, N. P., 187, 189,
 191, 221, 224
 Heyningen, R. van, 100
 Hicks, S. P., 144, 176
 Higby, D., 170
 Higgins, I. R., 32, 33, 40
 Hill, D. A., 331, 333, 342
 Hill, D. L., 1, 22, 23, 24, 185,
 186, 192, 209, 280, 292, 309
 Hill, E. L., 167, 169
 Hill, R. D., 326
 Hine, G. H., 136, 139, 143
 Hinks, E. P., 13
 Hirokawa, S., 4, 18
 Hirsch, B. B., 165
 Hirst, G. K., 82
 Hiuskamp, W. J., 412, 428,
 434
 Hoak, C., 164, 170, 171, 173,
 176
 Hoang, T. F., 26
 Hobson, J. P., 349, 350, 363,
 380
 Hochstetler, S. K., 165
 Hoffman, D. C., 40
 Hoffman, J. C., 93
 Hoffman, J. G., 73, 75, 135,
 140
 Hoffmann, F. de, 1, 239, 246,
 248, 321, 324, 325, 414
 Hofstadter, R., 231-316; 231,
- 241, 244, 249, 250, 252, 255,
 261, 263, 264, 265, 266, 267,
 268, 269, 270, 271, 272, 273,
 274, 275, 280, 281, 292, 294,
 295, 297, 298, 299, 301, 302,
 303, 308, 309, 310, 311, 328
 Höhne, G., 105, 122
 Hoi, N. P. B., see Buu-Hoi,
 N. P.
 Hokin, L. E., 105
 Hokin, M. R., 105
 Holden, R. B., 386
 Hollaender, A., 76, 118, 120,
 121, 123, 124, 135
 Holleck, L., 40
 Hollis, R. F., 33
 Holloway, J. H., 359, 380
 Holmberg, J., 124
 Holmes, B. E., 89-134; 63,
 80, 105, 135
 Holrody, A., 39
 Holtzman, J., 278
 Honda, M., 37, 39
 Hooke, W. M., 381
 Hoppe, D. D., 1, 412, 428,
 434
 Horgan, V. J., 112
 Horie, H., 221
 Horn, F., 54
 Hornbostel, J., 26, 447
 Hornsey, S., 76, 116, 122
 Hornyak, W., 331, 333, 342
 Horton, A. D., 36
 Houtermans, T., 80
 Howard, A., 76, 106, 107, 135,
 152
 Howard-Flanders, P., 113,
 117
 Howlett, L. N., 53
 Howland, J. W., 138, 150
 Huang, K. C., 145
 Hubbs, J. C., 349, 350, 353,
 357, 361, 363, 375, 376, 380,
 381
 Hudis, J., 338, 341
 Hudson, G. W., 90, 138
 Hudson, R. P., 1, 412, 428,
 434
 Huff, R. L., 95
 Huffman, E. H., 38, 40, 367
 Hug, O., 73, 104
 Hughes, D. C., 52, 53
 Hughes, I. S., 331, 332, 333,
 335
 Hughes, L. B., 168
 Hughes, V., 379, 380
 Hughes, W. F., Jr., 177, 178
 Hull, H. L., 53
 Hungerford, H. E., 137
 Hunter, J. A., 36, 38
 Hunter, K. R., 52
 Hursh, J. B., 137, 148, 152
 Hurst, G. S., 137, 143
 Hushfar, F., 326
 Hutchison, J. M., 33
 Hutchison, C. A., Jr., 351,
 387
 Hutschneker, K., 31, 32
 Huus, T., 186, 188, 190, 211,
 214
 Hyatt, E. C., 49
 Hyde, E. K., 31, 36
 Hyman, H. H., 31
- I
- Ignatenko, A. E., 318, 319,
 323, 325, 327, 328, 330
 Imirie, G., 136, 137, 138,
 139, 140, 141, 142
 Inglis, D. R., 211, 212, 216,
 217
 Ingraham, F. D., 177
 Ingram, D. J. E., 386
 Inman, F. W., 26
 Irvine, J. W., Jr., 38
 Irving, C. C., 92
 Ishimori, T., 36, 37
 Itzhaki, S., 107
 Ivanov, V. G., 329
 Ivy, A. C., 170, 172
- J
- Jaccarino, V., 352, 357, 359
 362, 379, 380, 381
 Jackson, D. A., 352
 Jackson, J. D., 468
 Jacobsen, E. M., 145, 166
 Jacobsohn, B. A., 24
 Jacobson, H. G., 135, 139
 Jacobson, L. E., 147
 Jacobson, L. O., 149, 123,
 166
 Jagger, J., 81
 Jagger, J. J., 71
 James, A. P., 68
 James, R. H., 34
 Jankus, V. Z., 254, 256, 257,
 265, 266, 267
 Jaroslow, B. N., 149
 Jean, M., 220, 222
 Jeffries, C. D., 351, 352, 385,
 386, 387, 390, 391
 Jehotte, J., 172
 Jenkins, E. N., 34
 Jenkins, F. A., 353
 Jennings, F. L., 118, 148
 Jensen, J. H. D., 185
 Jentschke, W. K., 392, 395
 Jentsch, D., 36
 Jerry, G. H., 135, 139
 Johansson, S. A. E., 190
 Johnson, B. C., 125
 Johnson, C. E., 352
 Johnson, J. S., 33
 Jones, D. C., 141
 Jones, D. R., 26, 27
 Jones, H. B., 108, 153
 Jones, L. W., 26
 Jones, M. D., 175
 Jones, M. E., 52, 53, 60
 Jones, R. V., 351, 385, 386
 Jongefrier, H. J., 101

- Jordan, D. L., 143, 145, 147, 149
 Jordan, H. S., 49
 Jordan, R. T., 81
 Julian, R. S., 379
 Jungerman, J. A., 340, 341
 Jury, S. H., 33
- K
- Kabir, P. K., 451
 Kallman, R. F., 136, 138, 141, 148, 149, 174
 Kamei, I., 66, 77
 Kane, J. A., 331, 332
 Kaplan, C., 72
 Kaplan, H. S., 165
 Kaplan, M. F., 26
 Kaplan, R. W., 72
 Kaplan, S. N., 27
 Karplus, R., 326, 448, 474
 Karreman, G., 353, 358
 Kastler, A., 351
 Kasue, T., 101
 Katrakis, G., 167
 Katz, J. J., 31
 Kaufman, B. P., 109
 Kaulitz, D. C., 51
 Kawaguchi, M., 325
 Kay, R. E., 92, 93
 Kasarinov, I. M., 331, 333
 Kedzie, R. W., 387, 391
 Keenan, T. K., 38
 Keilima, R. Y., 92
 Keller, M. E., 170
 Kelley, M. T., 36, 52, 53
 Kellogg, J. M. B., 380
 Kelly, L. S., 108
 Kelman, L. M., 51
 Kelner, A., 71
 Kember, N. F., 34, 37
 Kempe, L. L., 81
 Kendall, D. G., 74
 Kent, S. P., 178
 Kereiakes, J. G., 146, 147
 Kerman, A., 220
 Kertesz, Z. I., 125
 Kessler, D., 4
 Kessler, P., 4
 Kikuchi, C., 386
 Kimball, R. F., 76, 79, 80, 111, 120, 124, 139
 Kimeldorf, D. J., 145, 151, 166
 Kimura, K., 40
 Kimura, S. F., 178
 Kinderman, E. M., 48, 52
 King, J. G., 351, 353, 359, 379, 380, 381
 Kinoshita, T., 13
 Kittle, J. H., 51
 Klein, G., 74, 150
 Klein, J. R., 105, 145
 Klein, O., 423, 433
 Klein, P. D., 94
 Knight, W. D., 386
 Knisely, R. M., 175
- Knouff, R. A., 166
 Knowlton, N. P., 122
 Koch, R., 117, 118, 120, 137
 Kocholaty, W., 66, 71, 77
 Koenig, S. H., 379, 380
 Kofoed-Hansen, O., 311, 429
 Koh, W. Y., 80
 Kohler, G. D., 137
 Kohn, H. I., 76, 77, 136, 138, 141, 148, 149, 174
 Kojima, M., 37, 38
 Kolsky, H. G., 379
 Komori, H., 4, 18
 Konecci, E. B., 120
 Konopinski, E. J., 424
 Kordik, P., 100
 Korkisch, J., 38
 Korson, R., 175
 Koslov, S., 3, 25
 Kowlessar, O. D., 99
 Kovacs, J. S., 337
 Kozodaev, M. S., 329, 330, 334, 335, 337, 338
 Kramers, H. A., 353
 Kraus, K. A., 31-46; 31, 32, 33, 36, 38, 39, 40
 Krause, F. T., 150
 Kraushaar, J. J., 220
 Krebe, A. T., 150, 151
 Krebs, H. A., 97, 146
 Krebs, J. S., 152
 Krohn, L. H., 152
 Krohn, V. E., 392, 395
 Kroll, N. M., 22
 Kroning, F., 167, 176
 Kruse, U. E., 319, 321, 323, 324, 325, 326, 331, 332
 Kryder, G. D., 148
 Kuhn, U. S. G., 3rd, 153
 Kulwin, M. H., 167, 168
 Kumta, U. S., 124
 Kundu, D. N., 188, 203
 Kunin, R., 31
 Kunkel, H. A., 105, 122
 Kurti, N., 352
 Kusaka, S., 4, 18
 Kusch, P., 350, 356, 357, 359, 362, 379, 380, 381
- L
- Lacassagne, A., 120, 122, 163, 171
 La Fague, J., 176
 Laird, D., 150
 Lajtha, L. G., 97, 107
 Lamas, L. E., 38
 Lamb, E., 56
 Lamb, W. E., 379
 Lambertson, G., 431, 433
 Lamerton, L. F., 95, 96, 146
 Lamson, B. G., 139
 Landau, L., 1, 7, 12, 412, 414, 426, 432
 Lande, K., 420, 422
 Lander, R. L., 420, 422
 Landman, W., 93
- Lane, J. J., 138, 153
 Langer, L. M., 424
 Langendorff, H., 137
 Langendorff, N., 150
 Langham, W. H., 83, 143, 144, 164, 170
 Lanvin, M., 125
 Lanzele, E. F., 170
 Laqueur, G. L., 176
 Laser, H., 103, 112, 113
 Laskowski, W., 69
 Latarjet, R., 66, 68, 69, 70, 71, 112
 Latta, J. S., 167
 Lattes, C. M. G., 436, 446
 Laufer, M. A., 81
 Laughlin, J. S., 77, 136, 139, 143, 144, 176
 Lauson, F. A., 148
 Lavatelli, L., 326
 Lawrence, W., Jr., 169
 Lawson, J. S., Jr., 392, 395
 Lawton, E. J., 113
 Lazarus, A. J., 3
 Lea, D. E., 73
 Leavitt, C., 331, 332, 333, 342, 344
 LeBlond, C. P., 170
 Leddicote, G. W., 33
 Lederer, E., 31
 Lederer, M., 31, 34
 Lederman, L. M., 1, 2, 10, 11, 12, 13, 14, 328, 420, 430, 432, 433, 434
 Lee, I. L., 37
 Lee, K., 208
 Lee, R. H., 138, 145
 Lee, T. D., 1, 7, 12, 412, 417, 422, 423, 426, 432, 451, 460, 467
 Lefort, M., 119
 Lehmann, P., 392, 395
 Leidy, G., 70
 Leigh, K. E., 144, 176
 Leinfelder, P. J., 144, 177, 178
 Leipuner, L., 3
 Leith, C. E., Jr., 342, 344
 Leith, W. H., 53
 Lelièvre, P., 172
 Lemmer, H. R., 352
 Lemonick, A., 350, 380, 381
 Lenard, A., 13
 Leonard, S. J., 323, 325
 Leone, C. A., 93
 Lepore, J. V., 337
 Lerner, M., 39
 Leskin, G. A., 331, 332, 333
 Leveque, A., 392, 395
 Leviner, J. S., 271
 Levinson, C. A., 186, 200, 220
 Levi-Setti, R., 473
 Levy, B., 138
 Levy, M. M., 237, 246, 250, 251, 261, 262, 264
 Lew, H., 351, 379, 380, 381

AUTHOR INDEX

- Lewis, A. E., 138
 Lewis, R. B., 169
 Lewis, R. R., 305
 Lewis, W. B., 387
 Lewis, Y. S., 93
 Libby, T. L., 49
 Lichtlter, E. J., 103
 Lilly, E. H., 91
 Lilly, R. C., 38
 Lin, C., 39
 Lindenbaum, S. J., 317-48; 318,
 320, 322, 323, 325, 326, 328,
 329, 333, 335, 336, 337, 338,
 339, 340, 342
 Lindsay, S., 175
 Lindsley, D. L., 166
 Linman, J. W., 145
 Linn, J. G., 178
 Lipkin, H. J., 204, 205, 207,
 212
 Lipsicas, M., 304
 Lipworth, E., 376, 380, 381
 Lisco, H., 93
 Littman, A., 170, 172
 Llewellyn, P. M., 351, 386,
 387
 Lloyd, J. L., 4
 Lock, W. O., 331, 332, 333,
 335, 338, 339, 340
 Loeffler, R. K., 140
 Loevinger, R., 147
 Logan, R. A., 379, 380
 Loiseleur, J., 115
 Lokanathan, S., 16, 437, 440
 Lomon, E. L., 281, 210
 Lorenz, E., 135, 138, 165, 166
 Loriers, J., 40
 Lothe, F., 121
 Lott, J. R., 147
 Loureau, M., see Loureau-Pitres, M.
 Loureau-Pitres, M., 92
 Loutit, J. F., 122, 146, 148,
 149, 165, 166
 Lovrukhanina, A. P., 340, 341
 Low, F. E., 319, 320, 322
 Low, W., 387
 Lüders, G., 409, 477
 Lüders, R., 215, 408, 409, 477
 Luippold, H. E., 116
 Lumbert, A. R., 54
 Lunden, L., 40
 Lurio, A., 380, 381
 Lush, E. C., 53, 54
 Lushbaugh, C. C., 163-84; 164,
 165, 167, 168, 169, 170, 171,
 173, 176
 Luxton, R. W., 173
 Lyman, E. M., 278
 Lyon, H. W., 145, 170
 Lyons, H., 381
- M
- Maaløe, O., 69
 Maass, H., 105, 122
 McAllister R. W., 249, 250,
- 261, 263, 270, 271, 281, 308,
 310
 McArthur, C. K., 33
 McCormick, D. D., 90
 McCormick, W. G., 153
 McCracken, R. H., 381
 McCulloh, E. F., 153
 McDiarmid, I. B., 4
 MacDonald, J. E., 177, 178
 McDonald, L. A., 32
 McDonald, M. R., 106, 109
 Macdonald, P. J., 37
 McElhinney, J., 136
 McGinnis, C. L., 188, 203
 McIntyre, J. A., 258, 259,
 262, 263, 264, 273, 308
 McIsaac, L. D., 40
 Mack, E. W., 288
 McKeaque, R., 338, 339, 340
 McKee, R. W., 91, 99
 McKenna, J. M., 150
 McKinley, W. A., Jr., 274,
 277
 Mackinney, G., 125
 McLaughlin, R. D., 352
 McLaurin, R. L., 177
 MacLennan, W. D., 169
 McManus, H., 338, 339, 340,
 342
 MacNevin, W. M., 37
 McReynolds, A. W., 331, 332,
 333
 Madden, S. G., 139
 Mahlman, H. A., 33
 Main, J. M., 148, 149, 166
 Maisin, H., 145, 149, 150
 Maisin, J., 145, 149, 150
 Major, D., 304
 Majorana, E., 372
 Makinodan, T., 150, 166
 Maldaque, P., 145, 149, 150
 Malenka, B. J., 281, 305
 Maloff, F., 175
 Manaresi, E., 321, 324, 325
 Manley, J. H., 380
 Mann, A. K., 379, 380, 381
 Mann, M. G., see Gell-Mann, M.
 Manning, T. E., 352
 Manowitz, B., 32, 33
 March, P. V., 331, 332, 333,
 335, 338, 339, 340
 Marcovich, H., 77
 Marcus, P. I., 77
 Margulies, R. S., 324
 Mariani, F., 264, 272, 280,
 301
 Mariani, J., 301
 Marios, M., 122
 Marks, E. K., 123, 149
 Marks, S., 175
 Marrus, R., 380
 Marshak, R. E., 1, 332, 433
 Marshall, J., 331, 332
 Marshall, L., 331, 332
 Marston, R. Q., 138
 Martin, J. J., 32
- Martin, J. S., 380
 Martin, R., 321, 323, 324
 Martinovich, M. M., 94
 Marty, C., 193, 199, 222,
 223
 Marumori, T., 208
 Masek, G. E., 3
 Mason, B. T., 145
 Mason, C. J., 26
 Mason, H. C., 145
 Massey, B. W., 170
 Massey, H. S. W., 245, 283,
 284, 286, 287, 304
 Mateyko, G. M., 175
 Matheson, J., 83
 Mathews, J., 17
 Matsuda, H., 101
 Matsukawa, E., 277
 Maurer, H. J., 176
 Maury, P. B., see Bonet-Maury, P.
 Mayer, M. G., 185
 Mayer, S. W., 40
 Mayfield, R. M., 52
 Mead, J. F., 79, 125
 Meadors, O. L., 51
 Medak, H., 170
 Medved, S. V., 331, 332, 333
 Mee L. K., 103, 105, 106
 Mefford, R. B., 146
 Meinke, W. W., 51
 Meldolesi, G. E., 184
 Meloche, V. W., 40
 Mendelsohn, M. L., 115
 Meredith, W. J., 97
 Merrison, A. W., 334
 Merritt, F. R., 386, 387
 Merwin, R. M., 167, 169
 Meschan, I., 167
 Meshcheriakov, M. G., 331,
 332, 333, 334, 335, 337, 338
 Mesh Kovshki, A. G., 334,
 335, 337, 338
 Metropolis, N., 73, 324, 325,
 342
 Meyer, A. J., 14, 15
 Meyer, H. U., 70
 Meyer-Berkhout, U., 274,
 275, 308, 310
 Miceli, R., 95
 Michaelson, S. M., 138, 150
 Michel, L., 9, 425, 430
 Michie, R. W., 152
 Mickelwait, A. B., 22
 Miedema, A. R., 412, 428,
 434
 Milford, F. J., 220
 Miller, C., 145, 170
 Miller, C. C., 36, 38
 Miller, E. R., 175
 Miller, J. D., 26
 Miller, J. M., 342
 Miller, L. F., 48, 52
 Miller, L. S., 140
 Miller, M., 145
 Miller, R. C., 305
 Millman, S., 350, 379, 380,

- 381
 Mills, W. A., 137, 143
 Milsted, J., 40
 Minami, S., 325
 Miner, F. J., 38
 Miskel, J., 34
 Mitchell, A. C. G., 372
 Mitchell, D. D., 175
 Mitchell, J. S., 135
 Mitchell, R. N., 49
 Mitchison, N. A., 148
 Mitin, N. A., 330
 Mittelstaedt, P., 208
 Miyatake, O., 208
 Miyazawa, H., 326
 Miyazima, T., 198
 Moldauer, P. A. 17
 Mole, R. H., 100, 144, 145,
 151, 153
 Moller, C., 243
 Monk, G. S., 64
 Montagna, W., 170, 171
 Moore, D., 113, 117
 Moore, E. C., 106
 Moore, F. L., 33
 Moore, G. E., 36, 38
 Moos, W. S., 144, 145
 Morehouse, C. T., 80
 Morehouse, M. G., 90
 Morgan, B. H., 125
 Morgan, J. E., 136, 138, 139,
 140, 141, 142
 Morgan, J. R., 52
 Morgan, R. H., 139
 Moritz, A. R., 167, 168
 Morpurgo, G., 272, 301, 302,
 408
 Morrison, G. C., 338, 339,
 340, 342
 Mortimer, R. K., 63, 77
 Moser, H., 65, 67
 Moses, C., 178
 Moshman, J., 173
 Moskoloev, V. I., 331, 332,
 333
 Moszkowski, S. A., 210, 212
 Motley, R., 26
 Mott, N. F., 245, 274, 283,
 284, 286, 287
 Mott, W. E., 331, 332
 Motta, V. C., 125
 Mottleson, B. R., 186, 188,
 190, 191, 211, 214, 225
 Mottram, J. C., 110
 Mouhasseb, A., 216, 217
 Moulthrop, H. A., 51
 Moyer, A. W., 82
 Moyer, B. J., 27, 342, 344
 Mudd, S., 66
 Muirhead, H., 331, 332, 333,
 335, 338, 339, 340, 342
 Mukhin, A. I., 318, 319, 321,
 323, 324, 325, 327, 328
 Muller, E., 173
 Muller, J., 147
 Mullin, C. J., 255
 Munoz, C. M., 177, 178
 Murden, C. H., 152
 Murin, A. N., 340, 341
 Myers, L. S., 79
 N
 Nachod, F. C., 31
 Nafe, J. E., 356, 362, 379
 Nagai, S., 100
 Nagle, D. E., 321, 323, 324,
 379, 381
 Nakao, Y., 76, 100, 115, 122
 Nakano, T., 416
 Nataf, R., 198, 204, 207
 Nauta, W. J. H., 176
 Neal, F. E., 149
 Nedzel, V. A., 331, 332, 342
 Neel, J. V., 135, 141
 Neganov, B. S., 331, 332, 333,
 334, 335, 337, 338
 Negwer, M., 40
 Nelson, E. B., 356, 362, 379
 Nelson, F., 31-46; 31, 33, 34,
 36, 38, 39, 40
 Nelson, W., 149
 Nerli, A., 167, 169
 Nerurka, M. K., 124
 Nerurka, M. V., 124
 Nervik, W. E., 33
 Nettleship, A., 167
 Neufeld, J., 137, 142
 Neumann, M., 337
 Newcombe, H. B., 72, 79
 Newton, R. G., 303
 Nickols, N. A., 26
 Nickson, J. J., 169
 Nielsen, E., 48, 50, 53
 Nielsen, H. H., 200
 Nierenberg, W. A., 349-406;
 349, 350, 357, 358, 363, 375,
 376, 380, 381
 Nieuwerkerk, H. T. M., 101
 Niggli, H. F., see Fritz-
 Niggli, H.
 Nikishov, A. I., 337
 Nilsson, S. G., 210, 211
 Nims, L. F., 94
 Nishijima, K., 416
 Nodi, F., 167
 Noonan, T. R., 151, 152
 Norman, A., 81, 138
 Novey, T. B., 392
 Novick, R., 379
 Novikova, G. I., 190, 225
 Nowell, P. C., 148, 149, 166,
 173
 Nozareda, C. S., 165
 Nybom, N., 121
 O
 Oakberg, E. F., 173, 174
 Ochs, S., 380
 Odell, T. T., Jr., 166
 Oehme, R., 1, 326, 467
 Ogawa, S., 16
 Ogg, J. E., 66, 68
 Okada, S., 98, 100
 Okun, L., 408
 Okuno, H., 36, 37
 Oliver, A. R., 330
 Oliver, R., 97, 107
 Olivia, L., 167
 Olivo, J. P., 80
 Oneda, S., 16
 O'Neill, T., 150
 O'Neill, T. A., 147
 Ord, M. G., 102, 108, 110
 Ord, M. J., 74
 Orear, J., 26, 324, 325, 427,
 461
 Orear, J., Jr., 323, 324, 325
 Osborne, J. W., 170, 171,
 172
 Osipenkov, V. T., 329
 Osipova, V. E., 38, 39
 Oth, A., 99
 Ottolenghi, A., 91
 Oughterson, A. W., 135, 141
 Osborn, G. H., 31
 Osborn, G. K., 151
 Osborne, J. W., 145
 Oswalt, R. L., 38, 40
 Ovadia, J., 77
 Overand, W. G., 120
 Overhauser, A., 352
 Owen, B. D. R., 37
 Owen, J., 381, 386, 387
 Owen, M. E., 77
 Ozawa, S., 4, 18
 Ozerov, E. B., 318, 319, 321,
 323, 324, 327, 328
 P
 Page, J. E., 33
 Painter, E., 137
 Pais, A., 416, 419, 420, 465
 Palmer, L. E., 146, 169, 173
 Palmer, W. L., 170
 Panetti, M., 13
 Panofsky, W. K. H., 3, 253,
 281, 310
 Paolletti, C., 99
 Paris, W. N., 150
 Park, J. G., 387
 Parker, G. W., 32, 33, 40,
 352
 Parker, K., 304, 305
 Parker, M. W., 64
 Parkes, A. S., 151
 Parr, W., 150
 Parr, W. H., 146
 Parry, J. V. L., 381
 Pauli, W., 408
 Parzen, G., 278, 304
 Paschke, G., 93
 Patel, N. J., 273
 Patel, R. F., 273
 Paterson, E., 96, 137, 138,
 144, 150
 Patt, H. M., 110, 116, 117,
 121, 164
 Patti, F., 120

AUTHOR INDEX

- Paul, W. 380, 381
 Pauli, W., 1, 7, 248
 Pauling, L. 284
 Paulissen, L. J., 150
 Pavlovitch, R., 94
 Payne, J. I., 66
 Paysinger, J. R., 153
 Peacocke, A. R., 120
 Pearson, G. L., 386, 387
 Peaslee, D. C., 337
 Peierls, R. E., 192, 194, 255
 Pelc, S. R., 76, 100, 106
 Pencharz, R., 94, 176
 Penman, S., 2, 10
 Penn, J., 167
 Penneman, R. A., 38
 Penrose, R. P., 386
 Pepper, R. E., 80
 Perkins, R. W., 34
 Perkinson, J. D., 92
 Perl, M. L., 379, 380
 Perlman, M. L., 372
 Perry, J. P., 323, 325
 Perry, M. F. C., 84
 Petermann, A., 2, 10, 17
 Peters, B., 255
 Petersen, D. F., 98
 Peterson, J. R., 26
 Petrov, N. I., 329
 Pettersson, T., 167, 168
 Pevsner, A., 26, 328, 329
 Pfeiffer, V. G., 177, 178
 Pfirsich, D., 209
 Philip, J. F., 167
 Phillips, A. F., 116, 121
 Phillips, A. W., 66
 Phillips, G., 40
 Phillips, H. O., 32, 33
 Phillips, K., 304
 Phillips, M., 362
 Phillips, P. H., 150
 Phillips, R. H., 3
 Philpot, J. St. L., 112
 Phipps, T. E., 379
 Piccioni, O., 323, 325, 326, 327
 Pick R., 392, 395
 Pickering, J. E., 178
 Piez, K. A., 33
 Pihl, A., 118, 119
 Pincus, G., 105
 Pipkin, F. M., 350, 380, 381, 386
 Pirie, A., 98, 100, 101, 105
 Pirotte, M. G., see Goutier-Pirotte, M.
 Piskarev, E. V., 331, 332, 333
 Pitoy, S., 176
 Pitres, M. L., see Loureau-Pitres, M.
 Pittman, D. D., 77
 Plano, R., 418, 441, 455, 459
 Pligin, Iu. S., 334, 335, 337, 338
 Plumpton, B. L., 386
 Pollard, E. C., 81, 82
 Pontekorvo, B. M., 318, 319, 321, 323, 324, 325, 327, 328
 Pontius, G. V., 171
 Pope, D. E. F., 387
 Popjak, G., 91
 Poppe, E., 177, 178
 Poppel, M. H., 135, 139
 Poriskola, L. V., 328
 Porter, C., 185
 Postma, H., 412, 428, 434
 Potter, J. C., 142
 Pottinger, M. A., 115
 Pound, R. V., 395
 Povlotskaya, F. I., 340, 341
 Powell, J. E., 40
 Powell, W. F., 64, 81
 Powell, W. M., 420, 422
 Powers, E. L., 87, 79, 83
 Prehn, R. T., 148, 149, 165
 Preobrazhensky, B. K., 340, 341
 Preston, W. M., 338
 Preuss, A. F., 40
 Proctor, W. G., 352, 386
 Prodell, A. G., 379, 380, 381
 Prodi, G., 95
 Prosser, C. L., 137, 139
 Pryce, M. H. L., 185, 351, 382, 386, 387
 Puck, T. T., 77
 Pullman, I., 136, 139, 143
 Puntenney, I., 177
 Puppi, G., 321, 324, 325, 327, 423, 433
 Pyle, R. V., 27
- Q
- Quarenj, G., 321, 324, 325
 Quastler, H., 145, 170, 171
- R
- Rabi, I. L. 2, 350, 353, 356, 357, 362, 379, 380
 Raboy, S., 392, 395
 Radivojivitch, D. V., 94
 Rainwater, J., 1-30; 2, 3, 4, 16, 22, 23, 24, 25, 185, 187, 328, 329
 Rajewsky, B., 135
 Ramsey, N. F., 331, 332, 351, 353, 380, 386, 397
 Ranadive, N. S., 124
 Ranzi, A., 321, 324, 325
 Rarita, W., 333
 Rathgen, G. H., 105
 Ravenhall, D. G., 237, 246, 250, 251, 261, 262, 264, 272, 279, 280, 281, 286, 288, 289, 290, 291, 292, 293, 294, 295, 298, 299, 302, 303, 306, 309, 328
 Raventos, A., 148
 Rawitscher, G. H., 3
 Rayleigh, Lord, B., 278
 Read, J., 110
 Read, T. Jr., 386
 Redhead, M. L. G., 310
- Redlich, M. G., 196
 Regan, W. H., 32
 Reignier, J., 279
 Rein, J. E., 51, 53, 54
 Reinhardt, P. W., 137
 Renzetti, N. A., 380
 Ressovsky, N. W. T., see Timoféeff-Ressovsky, N. W.
 Restivo, S. R., 146
 Rutherford, R. C., 379
 Reynolds, H. W., 52
 Reynolds, J. B., 380, 381
 Reynolds, M. B., 52
 Reynolds, S. A., 40
 Rhoderick, E., 379
 Rhody, R. B., 137, 144
 Richards, P., 54
 Richards, R. D., 144
 Richardson, L. R., 125
 Richardson, R. E., 342, 344
 Richey, E. O., 169
 Richman, C., 255
 Riddiford, L., 331, 332, 333, 335
 Rieck, A. F., 71
 Rieman, W., 39
 Rieser, P., 93, 169
 Riley, E. F., 144, 177, 178
 Riley, H. P., 110
 Rinehart, M., 13, 430
 Ring, F., Jr., 51
 Ritchie, A. B., 49
 Ritson, D. M., 26, 456
 Roake, W. E., 51
 Roan, P. L., 148, 166
 Roberts, C. J., 54, 141
 Roberts, J. T., 32, 33, 40
 Roberts, L. D., 352
 Robertson, H. H. 310
 Robertson, J. S., 135-62; 136, 137, 138, 139, 140, 141, 142, 143, 144, 152
 Robinson, C. S., 305
 Robinson, F. N. H., 352
 Robson, H. H., 67
 Robson, M. J., 123, 149
 Rockmore, R., 23, 328
 Rockwell, T., 3rd, 54
 Rogers, B. S., 144
 Rogers, K. C., 13, 328, 430
 Romanini, A., 167
 Rondell, P. A., 146, 169, 173
 Root, S. W., 175
 Rose, M. E., 6, 255, 278
 Rose, P. H., 277
 Rose, R. G., 174
 Rosen, F. D., 51, 53, 55
 Rosenbaum, E. P., 408
 Rosenbluth, M. N., 248, 251, 423, 433
 Rosenfeld, A. H., 407-77; 334, 417
 Rosenfeld, G., 105
 Rosenfeld, L., 279
 Rosenson, L., 13, 430
 Rosenthal, R. L., 140
 Rosenzweig, W., 137

- Ross, M., 16
 Ross, S. W., 137
 Rosser, W. G. V., 338, 339,
 340, 342
 Rossi, B., 1
 Rossi, G., 13
 Rossi, H. H., 137
 Rotenberg, M., 186, 200, 208
 Rothermel, S. M., 144, 164,
 170
 Roux, M., 167
 Rozenaai, H. M., 109
 Rubin, B. A., 84, 170
 Ruby, S. L., 433
 Ruderman, M. A., 16, 267, 303,
 326, 438, 448, 474
 Rudich, E. C., 71
 Rugh, R., 138, 174, 178
 Rupp, A. F., 48
 Ruehle, W. G., Jr., 48, 53, 54
 Rusakov, V. A., 329
 Rush, R. M., 36
 Russell, E. S., 148
 Rust, J. H., 138, 139, 153
 Rustad, B. M., 433
 Rustgi, M. L., 271
 Ruth, H. J., 138, 150
 Rutman, R. J., 93
 Rupp, A. F., 31
 Ryabchikov, D. I., 38, 39
 Ryan, N., 148
 Rylander, E. W., 51, 53, 54,
 55
- S
- Sacher, G., 136, 138, 141, 146,
 153
 Sachs, A., 2, 10, 321, 323, 325
 Sachs, R. G., 466
 Sagalyn, P. L., 351
 Sagane, R., 13, 430
 Sahasrabudhe, M. B., 124
 Said, A. S., 34
 Salam, A., 1, 7, 12, 325, 326,
 426, 430
 Salant, E. O., 26, 447
 Salerno, P. R., 121, 150
 Salmon, J. E., 39
 Salmon, W. D., 125
 Salvetti, C., 209, 210
 Salzman, G., 250
 Sammon, D. C., 32
 Samios, N., 418, 441, 455, 459
 Samuelson, O., 31, 40
 Sandler, O. E., 124
 Sandmann, H., 37
 Sapadin, L., 138
 Sard, R. D., 1, 26, 27
 Sargent, C. P., 13, 430
 Sargent, J. A., 165
 Sasaki, Y., 36
 Satten, R. A., 359, 381
 Sauberlich, H. E., 125
 Saxon, D., 342, 343, 344
 Scadden, E. M., 40
 Schaim, U. H., see Haber-
- Schaim, U.
 Scharff-Goldhaber, G., 203,
 220
 Scheraga, H. A., 94
 Scherbakov, I. A., 330
 Schiff, L. I., 234, 237, 255,
 257, 281, 301, 302, 305, 306,
 310
 Schiller, J., 176
 Schindewolf, U. 31
 Schjeide, O. A., 79
 Schlesinger, M. J., 148
 Schlüter, R., 26
 Schoch, D., 177
 Schoenborn, H. W., 70
 Scholes, G., 114
 Schönberg, H. A., see Albers-
 Schönberg, H.
 Schönfeld, T., 31
 Schoolman, H. M., 170, 172
 Schubert, J., 31, 34
 Schull, W. J., 135, 141
 Schrader, W., 169
 Schraadt, J. H., 51
 Schramm, K., 40
 Schreier, K., 92
 Schuck, A. B., 52
 Schulze, H. F., 49
 Schuman, R. P., 52, 53, 60
 Schwartz, C., 353, 359
 Schwartz, E. S., 51
 Schwartz, M., 418, 441, 455,
 459
 Schweber, S. S., 239, 246,
 248
 Schweigert, B. S., 126
 Schweitzer, W. H., 174
 Schwinger, J., 281, 310, 353,
 408
 Scott, M. B., 278
 Scott, O. C. A., 116
 Scovil, H. E. D., 385, 386,
 387
 Scully, N. J., 64
 Seaborg, G. T., 36, 37, 38,
 40
 Searcy, R. L., 90
 Selvin, G. J., 54
 Semenov, M. M., 331, 333
 Sempoux, D., 149
 Senitsky, B., 353, 379, 380
 Serber, R., 22, 328, 333, 342
 Setlow, J., 81
 Setlow, R. B., 64, 65, 67, 120
 Setti, R. L., 13
 Setti, R. L., see Levi-Setti,
 R.
 Seymour, P. H., 136, 138,
 144, 145
 Shabudin, A. F., 334, 335,
 337, 338
 Shaditch, G. S., 94
 Shafer, W. G., 169
 Shaffer, R. N., 167
 Shalit, A. de, 204, 207, 212,
 220, 221
- Shalomov, Ia. Ia., 334, 335,
 337, 338
 Shank, R. C., 51, 53, 54
 Shapiro, A. M., 26, 331, 332,
 333, 342, 344
 Shapiro, G., 77
 Sharp, W. T., 338, 339, 340,
 342
 Shaver, S. L., 173, 174
 Shaw, P. F. D., 386
 Shebanov, V. A., 334, 335,
 337, 338
 Scheemeister, I. L., 149
 Shefner, D., 83
 Shellabarger, C. J., 144
 Shepard, D. C., 65, 74
 Shepherd, H. J., 125
 Shepard, W. D., 326
 Sheppard, C. W., 95
 Sherman, B. F., 302
 Sherman, F. G., 92
 Sherman, N., 278
 Sherwood, J. E., 381
 Shields, H., 119
 Shively, J. N., 138
 Shrader, E. F., 379
 Shrek, R., 165
 Shuck, A. B., 51
 Shugart, H. A., 349, 357, 375,
 380
 Shulman, N. R., 135, 137,
 140, 167
 Shumway, B. W., 137
 Shutt, R. P., 333, 336, 337
 Sidorov, V. M., 334, 335, 337,
 338
 Siegel, A., 66
 Sigmund, R., 167
 Signell, P. S., 332
 Sigoloff, S. C., 137
 Silsbee, H. B., 349, 350, 357,
 363, 375, 376, 379, 380
 Silva, R. J., 40
 Silverman, M. S., 144, 145,
 146, 149
 Silvester, A. G., 54
 Simons, C. S., 139
 Simons, E. L., 123
 Simpson, O. C., 379, 380
 Sirlin, A., 13
 Sirvetz, M. H., 386
 Six, E., 65, 67
 Sjöstrom, E., 40
 Skinner, R. S., 204
 Skyrme, T. H. R., 187, 194,
 197
 Slater, M., 137
 Slater, W. E., 473
 Slotnik, M. M., 357
 Smith, C. L., 103, 106, 135
 Smith, D. E., 95, 117, 148
 Smith, D. J., 52, 55
 Smith, E. L., 33
 Smith, E. S., 93
 Smith, F., 148
 Smith, F. M., 3, 26
 Smith, G. W., 33, 40

AUTHOR INDEX

- Smith, H. L., 40
 Smith, J. H., 240, 255, 306,
 310
 Smith, K., 350, 366
 Smith, K. F., 376, 379, 380,
 381
 Smith, L., 331, 333, 342
 Smith, L. J., 148
 Smith, L. W., 331, 332, 333
 Smith, S. A., 168
 Smith, S. C., 53
 Smith, W. W., 138, 148, 150
 Smithies, D. H., 111
 Smythe, W. R., 258
 Snow, G., 331, 332, 333, 342
 Snyder, M. D., 51, 53
 Snyder, W. S., 137, 142
 Sobottka, S., 241, 244, 274,
 308
 Soetens, R., 121
 Solmitz, F., 417
 Sommers, S. C., 172
 Sondhaus, C. A., 136, 137, 138,
 139, 140, 141, 142
 Soroko, L. M., 331, 332, 333
 Spalding, J. F., 83, 167, 168,
 173, 174
 Speck, D. R., 353
 Spedding, F. H., 40
 Speisman, G., 417
 Spencer, L. V., 278
 Sperduto, A., 277
 Spiegelmeyer, I. M., 67
 Spiers, F. W., 100
 Spragg, W. T., 48, 49, 51
 Stadler, J., 153
 Stahl, F. W., 84
 Stallwood, R. A., 331, 332
 Stang, L. G., Jr., 53, 54
 Stanghellini, A., 321, 324, 325,
 327
 Stannard, J. N., 95, 152
 Stapleton, G. E., 76, 80, 121,
 123, 124
 Steadman, L. T., 92
 Stearner, P. S., 146
 Stearns, B. F., 26
 Stearns, M., 3, 23
 Stearns, M. B., 3, 23
 Stearns, R. F., 51, 53
 Steenland, M. J., 352, 361, 412,
 438, 434
 Steffansen, D., 110
 Stein, G., 103
 Stein, J., 135, 139
 Stein, W., 69
 Steinberger, J., 14, 16, 321,
 323, 325, 418, 441, 440, 451,
 455, 459
 Steiner, N. M., 340, 341
 Stent, G. S., 83, 84
 Stern, M. O., 318, 319, 321,
 323, 324, 325, 327, 328
 Stern, O., 379, 380
 Sternheimer, R. M., 326, 328,
 335, 336, 337
 Stevens, C. E., 170
 Stevens, K. W. S., 381
 Stevens, L. G., 163
 Stewardson, E. A., 277
 Stewart, D. C., 40
 Stickley, E. E., 137, 143, 144,
 152
 Stocken, L. A., 102, 108, 110
 Stohlmeyer, F., 144
 Storer, J. B., 122, 143, 144,
 146, 147, 150, 164, 165, 167,
 168, 169, 170
 Stork, D. H., 323, 325
 Storm, M., 342
 Stoyle, R. J. B., see Blin-
 Stoyle, R. J.
 Stratford, J. G., 176
 Straub, R. L., 117
 Straube, R. L., 121
 Strauss, B. S., 83
 Street, K., Jr., 37
 Streher, B. L., 103
 Streib, J. F., 273, 308
 Streisinger, G., 66
 Strickland, G., 54
 Stroke, H. H., 357, 359, 362,
 380, 381
 Strom, P. O., 375, 380, 381
 Strom, C. P. A., 145, 148
 Strong, V. G., 144
 Stroud, A. N., 75, 83, 164
 Stuy, J. H., 71, 81
 Suchowsky, G., 176
 Sudarshan, G., 433
 Suess, H. E., 185
 Sugimura, T., 122
 Suit, H. D., 97
 Suito, E., 34
 Sulairov, R. M., 330
 Sullivan, L. O., 51, 53
 Sulzberger, W. B., 167, 168
 Sunderland, R. J., 349, 357,
 363, 375, 380
 Sunyar, A. W., 224
 Surlis, J. P., Jr., 38
 Sussdorf, P. H., 149
 Süssman, G., 208
 Sutton, E., 94
 Sutton, R. B., 331, 332
 Suura, H., 2, 10, 17, 281, 310
 Svedberg, T., 120
 Swallow, A. J., 90, 103, 110
 Swanson, A. A., 178
 Swartout, J. A., 49
 Swiatecki, W. J., 208
 Swick, R. W., 94
 Swift, M. N., 137, 142, 145,
 146, 147
 Swift, M. W., 171
 Swindell, G. E., 167
 Symanzik, K., 326
- T
- Tabachnik, J., 99
 Taft, E. B., 71
 Taft, H., 321, 324, 325
 Tahmisan, T. N., 104, 112
 Tait, J. H., 137
 Takeda, G., 325, 326, 327
 Taketa, S. T., 142, 145, 146,
 171
 Taliaferro, L. G., 149
 Taliaferro, W. H., 149
 Talmadge, P., 103
 Talmi, I., 204, 207, 212
 Tamm, I. E., 328
 Tamura, T., 198, 204, 207
 Tanaka, R., 208
 Tanner, N., 422, 441
 Tappel, A. L., 125
 Tassie, L. J., 272, 237, 301
 Tau, L., 327
 Taub, H., 379, 380, 381
 Tausche, F. G., 166
 Tautfest, G. W., 253, 281,
 310
 Taylor, S., 26
 Taylor, T. B., 328, 342
 Taylor, W. F., 120
 Tazima, Y., 122
 Teem, J. M., 331, 332
 Teichner, H., 38
 Teir, H., 165
 Teleghi, V. L., 12, 432, 473
 Temmer, G. M., 187, 189,
 191, 221, 214
 Terwilliger, K. M., 26
 Tessman, E. S., 67
 Tessmer, C. F., 118
 Thaler, R. M., 332
 Thanassi, F. Z., 84
 Thaxter, M. D., 51
 Thie, J. A., 255
 Thoday, J. M., 110
 Thomas, A., 40
 Thomas, H. C., 31, 32
 Thomas, S. F., 94, 176
 Thomason, P. F., 36
 Thomlinson, R. H., 116
 Thompson, E. C., 144
 Thompson, H. E., 92
 Thompson, P., 77
 Thompson, S. G., 36, 38, 40
 Thompson, W. M., 53
 Thomson, J. F., 135, 137,
 139, 146
 Thonnard, A., 99
 Thorndike, A. M., 1, 333,
 336, 337
 Tiapkin, A. A., 334, 335, 337,
 338
 Ticho, H., 451
 Till, J. E., 82
 Tillotson, G. W., 174
 Timoféeff-Ressovsky, H. W.,
 73
 Ting, Y., 380, 381
 Tiomno, J., 1, 13, 423
 Tisellius, A., 33
 Tobias, C. A., 73, 77, 178
 Toch, P., 185
 Tochilin, E., 137
 Tokiyama, K., 34
 Tolhoek, H. A., 352, 376, 412

- 428, 434
 Tomansini, G., 13
 Tomkins, F. S., 352
 Tomkins, P. C., 48, 56
 Tomonaga, S., 198
 Toropova, V. F., 39
 Toschek, P., 380, 381
 Tourtellotte, W. W., 139
 Trautman, J., 176
 Treiman, S. B., 16, 465, 466,
 468, 470
 Trenam, R. S., 385, 386, 387
 Trentin, J. J., 148, 149
 Tretyakov, E. F., 190, 225
 Tripp, A. M., 53
 Tripp, R. D., 418
 Trkula, D., 81
 Trowbridge, W. V., 137
 Trowell, O. A., 164
 True, W. W., 220
 Trujillo, T. T., 122
 Trum, B. F., 138, 139, 153
 Truran, W. H., 52
 Tubiana, M., 99
 Tubis, M., 49
 Tucker, G., 379
 Tullis, J. F., 139
 Turk, E. H., 51, 53, 54
 Turkevich, A., 342
 Tuttle, L. W., 125
 Tyam, E., 176
 Tyree, E. B., 77, 95, 148
- U
- Uehling, E. A., 22
 Uncapher, R. P., 147
 Ungar, F., 105
 Ungar, G., 167, 168
 Upham, H. C., 170
 Uphoff, D., 138, 165
 Upton, A. C., 137, 143, 163,
 167, 172, 173, 178
 Urban, P., 277
 Uretsky, J., 210, 349
 Uretz, R. B., 79
 Uri, N., 111
 Uyeki, E., 121, 150
- V
- Vaharu, T., 83
 Valatin, T. J., 213
 Valk, H. S., 280
 van Bekkum, D. W., see
 Bekkum, D. W. van
 Van de Graff, R. J., 247, 277
 van Heyningen, R., see
 Heyningen, R.
 Van Hove, L., 310
 van Lieshout, R., 188, 203
 Van Sallman, L., 177, 178
 Van Slyke, F., 152
 van Wagendonk, W. J., see
 Wagendonk, W. J. van
 Variant, F. F., see Falk-
 Variant, F.
- Vasilev, A. M., 39
 Vazquez, J. J., 138
 Vedder, J., 13
 Venturello, G., 38
 Veomett, R., 150
 Vickery, A. L., 175
 Villars, F., 185-230; 192, 198,
 200, 214
 Villi, C., 253
 Vincent, J., 150
 Vinogradov, A. P., 340, 341
 Visscher, W. M., 272, 301,
 302
 Vitale, B., 327
 Vogel, F. S., 164, 176
 Vogel, H. H., Jr., 143, 145,
 147, 149
 von Borstel, R. C., see
 Borstel, R. C. von
 Von Gierke, G., 335
 Von Massenbach, W., 175
 Vos, O., 148
 Voss, R. G. P., 342, 343, 344
 Vzorov, I. K., 331, 332, 333,
 334, 335, 337, 338
- W
- Wachsmann, F., 167
 Wachter, J. F., 126
 Wacker, R. E., 40
 Wada, W., 208, 209
 Waggener, R. E., 167
 Wagendonk, W. J. van, 64
 Walnright, T., 304
 Wakasa, A., 16
 Walchli, H. E., 379
 Walker, J., 331, 332, 333,
 335
 Walker, J. K., 104, 145
 Walker, W. D., 326
 Wall, J. G. L., 39
 Wallenmeyer, W. A., 333, 336,
 337
 Waller, I., 310
 Wallman, J. C., 387
 Walter, M., 349
 Walter, R. I., 386
 Walton, H., 136, 138, 141,
 146
 Ward, I. M., 386, 387
 Warren, S., 135, 141, 172,
 174
 Warshaw, I. M., 169
 Watanabe, Y., 205
 Watson, C. D., 55, 56
 Watson, G. N., 285
 Watson, J. S., 56
 Watson, K. M., 318, 334, 413
 Watson, R. E., 276
 Waugh, R. L., 177
 Way, K., 188, 203
 Weatherwax, R. S., 70
 Weber, J., Jr., 49
 Wehrle, R. B., 53
 Weigle, J. J., 82
 Weinreich, G., 379
- Weinrich, M., 1, 2, 10, 11,
 12, 14, 432, 433, 434,
 Weiss, C., 99
 Weiss, J., 114
 Weiss, M. M., 386
 Weiss, R., 357, 362, 381
 Weisskopf, V. F., 185, 209,
 216, 218, 225, 257, 258, 372,
 424
 Welch, C., 178
 Welch, G. A., 34
 Welker, J. P., 372
 Wellnitz, J. M., 174
 Wells, R. A., 34, 37
 Wenener, J., 203, 220
 Wentzel, G., 199, 221, 463
 Wenzel, W. A., 431, 433
 Wessel, G., 379, 380, 381
 Wexler, B. C., 94, 176
 Wexler, S., 350, 370, 380,
 381
 Weyzen, W. W., 148
 Wheatcroft, M. G., 145, 170
 Wheaton, R. M., 39
 Wheeler, J. A., 1, 13, 23,
 185, 186, 191, 192, 423
 Wheelwright, E. J., 40
 White, J., 172
 Whittemore, W. L., 333, 336,
 337
 Whitney, J. E., 51
 Wichmann, E., 22
 Wichmann, E. H., 2, 10, 17
 Wickbold, R., 37
 Widgoff, M., 26
 Wigner, E. P., 196
 Wihilm, H., 64
 Wijsman, R. A., 73
 Wilbur, K. M., 91
 Wildermuth, K., 208
 Wilde, W. S., 95
 Wilding, J. L., 139, 147
 Wildman, S. G., 66
 Willets, L., 24, 208, 209, 220,
 222
 Wilkins, H. C., 26
 Wilkinson, R. W., 114
 Wilkinson, W. D., 51
 Wilkowski, L. J., 171
 Wilks, S. S., 120
 Willcocks, R. G. W., 38
 Williams, F., 167, 168
 Williams, J. P., 33
 Williams, L. A., 38
 Williams, R. E., 328, 329
 Williams, R. W., 328, 342,
 343
 Williams, R. F., 114
 Wilson, C. W., 100
 Wilson, E. B., 284
 Wilson, J. E., 150
 Wilson, J. W., 170, 171
 Wilson, R., 342, 343, 344
 Wilson, R. N., 280, 281, 283,
 286, 288, 292, 293
 Wilson, R. R., 140, 152
 Wilson, S., 120

AUTHOR INDEX

- Wilson, S. M., 80, 124
 Winders, G. R., 53
 Winkler, C., 93
 Winsche, W. E., 54
 Winther, A., 186, 188, 190,
 211, 214, 429
 Wish, L., 40
 Wissler, R. W., 149
 Witten, V. H., 167, 168
 Wittke, J. P., 351
 Wolf, L., 104
 Wolfe, H. B., 14, 440
 Wolfe, R. G., 77
 Wolfendale, A. W., 4
 Wolfenstein, L., 332
 Wolff, I., 73
 Wolff, J., 178
 Wolff, S., 116
 Wolfgang, R., 338, 341
 Wong, E., 351, 387
 Wood, L., 177
 Wood, T. H., 81
 Woodard, H. Q., 100
 Woodburg, D. H., 124
 Woodgate, A. K., 380
 Woodgate, G. K., 380
 Woodhead, J. L., 34
 Woods, R. D., 342, 343, 344
 Woodward, W. W., 310
 Woodward, K. T., 144, 164,
 170
 Woodworth, P., 125
- Worcester, J. L., 376, 380,
 381
 Wright, B. J., 104
 Wright, E. A., 113, 117
 Wright, K. A., 144, 176
 Wu, C. S., 1, 412, 428, 434
 Wyld, H. W., Jr., 16, 468
 Wyss, O., 72
- Y
- Yadav, H. N., 277, 304
 Yager, W. A., 386, 387
 Yakovlev, Yu. V., 340, 341
 Yamada, E., 208
 Yang, C. N., 1, 7, 12, 324,
 412, 422, 423, 426, 432, 451,
 460, 467
 Yearian, M. R., 268, 269, 270,
 310
 Yekutieli, G., 26
 Yennie, D. R., 237, 246, 250,
 251, 257, 261, 262, 264, 279,
 280, 281, 283, 286, 288, 289,
 290, 291, 292, 293, 303, 309,
 310
 Yoccoz, J., 192, 194
 Yodh, G. B., 310
 Yoe, J. H., 36
 Yoffey, J. M., 166
 Yokimov, M. A., 340, 341
 Yost, H. T., 67
- Youngquist, C. H., 51, 53
 Yoshino, Y., 36, 37, 38
 Yntema, J. L., 277
 Yu, F. C., 386
 Yuan, L. C. L., 318, 319, 320,
 322, 323, 325, 333, 335, 336,
 337, 338
 Yukawa, J., 208
 Yunker, R., 150
 Yutlandov, I. A., 340, 341
- Z
- Zabel, C. W., 360, 379
 Zacharias, J. R., 350, 351,
 353, 360, 363, 379, 381
 Zamenhoff, S., 70
 Zelle, M. R., 66, 68
 Zeller, J. H., 139
 Zendle, B., 136
 Zharkov, G. F., 328
 Zimmer, K. G., 73
 Zimmerman, L. N., 68
 Zirkle, R. E. 73, 135,
 137, 138, 140, 141, 164
 166
 Zorn, G. T., 26
 Zrelov, V. P., 334, 335, 337,
 338
 Zumino, B., 409, 477
 Zunti, W., 349
 Zweifach, B. W., 150

SUBJECT INDEX

A

Adrenal cortex
radiosensitivity of, 175-76
Alpha particles
electron scattering by, 271
Amines
as ion exchangers, 33
Angular correlation, 392-97
Anion Exchange
see Ion exchange
Antineutrino
see Neutrino
Antiparticles, 408-10
Ascorbic acid
in irradiated tissues, 94
Atomic beams, 350, 363-78
Atomic bombs
effects of, 138-41
see also Fall-out

B

Baryon number, 416
Baryons, 410
see Mesons, pi; mu
Beryllium
electron scattering by, 273
pion reaction with, 328-30
proton reaction with, 338
Beta decay
theory of, 423-35
Biochemistry
in food sterilization, 125-27
irradiation effects and, 89-127
see also Chemistry
Bone marrow
radiosensitivity of, 165-67
syndrome, 144-47
Brain
radiosensitivity of, 176
Burns, radiation, 167-69

C

Cage effect, 148
Capillaries, radiosensitivity of, 169
Carbon
electron scattering by, 241
244, 273, 302
pion reaction with, 328-30
see also Graphite
Carbon monoxide
in radiation protection, 120
Cascades, 339, 342
Cataracts, radiation, 177-78
Cation exchange, see Ion exchange
Cell division

and haemoglobin formation, 96
radiation effects on, 74-80

Cells, radiosensitivity of, 164-65

Cellular radiobiology, 63-84
cell division studies in, 74-80

target theory in, 73
temperature effects in, 80-81, 122

theoretical approach in, 73-74

and ultraviolet irradiation, 63-72

Cesium isotopes
spins, masses of, 350, 357, 375

Charge conjugation, 12, 409, 412, 467

Charge conservation, 334, 414
Charge distribution, nuclear, 307-9

Chemistry, hot
equipment for, 47-58

ion exchange separations
in, 32-41
see also Biochemistry

Clay minerals
as ion exchangers, 32

Clebsch-Gordan coefficients, 450

Cobalt isotopes
spins, moments of, 385-92

Collective model, 185-227
Bohr-Mottelson model, 217-25

Inglis model, 211-17
magnetic moments in, 191

moments of inertia in, 195
nuclear potential and, 186-88

quadrupole moments in, 189, 197

rotational levels in, 188, 195, 201

spheroidal independent model and, 208-11

theory of, 191-208

Computers
in radiobiology studies, 74

Concrete, as radiation shield, 54

Connective tissues

radiosensitivity of, 167-69

Contamination barrier, 48-52

Copper, electron scattering by, 290-94

Cosmic rays
mu mesons and, 4, 18

Cysteamine
in radiation protection, 117, 121

D

Dalitz plot, 471

Dark recovery, 68-70

Deoxyribonucleic acid synthesis, radiation effect on, 106-10

Deuterons
electrodisintegration of, 264-67

electron scattering by, 254-67

fusion of, 5

interaction with pions, 327
interaction with protons, 333-34

Digestive system,
radiosensitivity of, 169-70

Dosimetry, radiation, 136-37, 141

E

E2 transitions, 189

Electrons
from muon decay, 12, 14, 16

Electrons, high-energy
correlation effects in
scattering of, 305
deuteron scattering of, 254-72

heavy nuclei scattering of, 276-96

kinematics of scattering of, 231-33

nuclear scattering of, 231-312

point nucleus scattering of, 237-39

polarization studies and, 303

proton scattering of, 249-54

p-shell nuclei scattering of, 273-76

Emulsions, nuclear
pion reaction with, 330
proton reaction with, 339

Endocrine glands,
radiosensitivity of, 175-76

Enzymes
in irradiated foods, 126
irradiation effects and, 97-106, 114, 120

SUBJECT INDEX

- and ultraviolet sensitivity, 66
E
 Eye, radiosensitivity of, 177-78
F
 Fall-out, atomic bomb, 139-41, 167
 Fat metabolism and whole body irradiation, 90-94
 Fats, irradiation of, 126
 Feynman diagram, 423
 Field theory of elementary particles, 408
Fission
 with high-energy protons, 341-42
 theory of, 191
Fission products
 separation of, 40
 Food sterilization, 125-27
Fusion, nuclear muon catalysis of, 5
- G**
Gamma rays
 dose units for, 137
 shielding from, 54
Gastrointestinal tract, radiosensitivity of, 170-72
Gauge invariance, 426
Generative system radiosensitivity of, 173-75
Genetic constitution and ultraviolet sensitivity, 66, 71
Glass
 high density types, 55
 radiation damage to, 56
Gold
 electron scattering by, 290-94
Graphite
 muon interaction with, 12
 see also Carbon
Gut syndrome, 144-47
- H**
Hazards, radiation in radiochemical processes, 47-58
Hematopoietic system radiosensitivity of, 165-67
Hibernation and radiation protection, 122-23
Hoods, 49-51
Hot laboratory equipment for, 47-58
Hydration in radiation protection, 119
Hydrofluoric acid
- and ion exchange separations, 38
Hydrogen peroxide in irradiated bacteria, 111
Hyperfine structure, 352, 376-78
Hyperfragments, 473-75
Hypernuclei, 473-75
Hyperons
 stability of, 418
 and strangeness, 416
 systematics and decay of, 407-75
 weak decays of, 446-55
 and weak interactions, 421-46
- I**
Independent particle model, 185
Inorganic chemistry
 ion exchange in, 31-41
Intestines, radiosensitivity of, 170-72
Invariance postulates, 467-69
Ion exchange
 acid salts in, 32-33
 amines in, 33
 cation versus anion, 35
 chloride separation and, 36-38
 column theory and, 35
 complexing and, 35
 cyanide solutions and, 39
 with HCl-HF mixtures, 36-39
 in HI, HBr solutions, 38
 hydrous oxides in, 32
 mineral clays in, 32
 in nitrate solutions, 38-39
 organic ligands and, 39
 organic resins and, 32
 radiochemical separation by, 31-41
 rapidity of, 34
 separations in, 34-41
 in sulfate solutions, 39
 techniques in, 33-34
 thiocyanate complexing and, 38
 and various inorganic ions, 38-39
Isotopic spin
 conservation of, 414
 in p-p, n-p reactions, 333
- K**
Kidneys, radiosensitivity of, 173
K-Mesons, see Mesons, K
- L**
Leptons, 410
 see Mesons, mu
- Lethal chromosome change theory**, 78
Lethal dose
 factors affecting, 141-50
 survival and, 152
 tabulation of, 137-41
Lifetimes of elementary particles, 411
Light recovery, 70-72
Linear energy transfer, 73
Liquid drop nuclear model, 218
Lithium
 electron scattering by, 273
 pion reaction with, 328-30
Liver, radiosensitivity of, 172
- M**
Macromolecules radiosensitivity of, 82
Magnetic moments, nuclear 191, 349-97
Mammals lethal dose for, 137-41
Manipulators in radiochemical processing, 50, 52-54
Masses of elementary particles, 411
Meats, irradiation of, 126
Mesons and nuclear structure, 267-71
Mesons, heavy stability of, 418
 and strangeness, 416
 systematics and decay of, 407-75
 and weak interactions, 421-46, 455-67
Mesons, K, 25-26
 decay of, 411, 444, 455-67
 masses, lifetimes, 411
Mesons, mu, 1-27
 cobalt-60 decay and, 1
 and cosmic ray bursts, 4
 decay of, 13-16, 411, 430
 graphite reaction with, 12
 and K mesons, 25-26
 lifetime in matter of, 13-16
 mass of, 3, 411
 in nuclear fusion, 5
 nuclear interaction of, 3-4
 and parity, 1-2, 6-13
 polarization of, 10-13
 spin of, 17, 411
 theory of decay of, 6-13
Mesons, pi
 and CP invariance, 413
 decay of, 6-13, 16, 411, 435
 deuteron interaction with, 327-28

electron scattering of, 328-32
inelastic scattering of, 328-32
from K-meson decay, 455-67
mass, 3, 411
production of, 333-39
proton interaction with, 318-27
Michel parameter, 12-14
Moment of inertia, nuclear, 195, 224
Moments, nuclear, 349-97
atomic beam method, 363-78
measurement of, 349-53
paramagnetic resonance method, 381-92
of short lived excited states, 392-97
tabulation of, 379-81, 386-87
theoretical aspects of, 353-63
Monte Carlo problem, 74
Mortality, post-irradiation, 137, 152-54
Mumesic atoms, 4-5
x-rays from, 17
Muonium, 12
Muons, see Mesons, mu

N

Neighboring nuclei, 297
Nephritis, radiation, 173
Nervous system, radiosensitivity of, 176-77
Neutrinos, 1, 2, 411, 425-33
Neutrons
decay of, 423-25
dose units for, 137
electron scattering by, 254-71
muon production of, 26-27
and radiation cataracts, 178
RBE of, 143-44
structure of, 267-71
Nuclear models
collective, 185-227
Nuclear shape, 185
form factor for, 240, 307
and nucleon-nucleon collisions, 343-44
Nuclear size
and mumesic x-rays, 2-3, 17-25
from muon experiments, 14, 124
summary of data on, 308-9
Nuclear spins, see Spins, nuclear
Nuclei
electron scattering by, 231-312
Nucleons, see Neutrons,

P
Protons
Nucleoproteins, 106-10
Nutrition
and radiosensitivity, 148

O

Oral tissues, radiosensitivity of, 169-70
Organic resins, 32
Ovary, radiosensitivity of, 174
Oxygen
electron scattering, 274-76
and radiosensitivity, 77, 89, 110-17, 120-22, 145-51

P

Pancreas, radiosensitivity of, 172-73
Paramagnetic resonance, 351-52, 381-92
Parity conservation, 1, 6-13, 392, 394, 409, 412, 421, 467-69
Particle theory, 408-14
Photochemistry, 63-72
Photoreactivation of ultraviolet irradiated materials, 70-72
Pions, see Mesons, pi
Pituitary, radiosensitivity of, 175
Plastics
as corrosion barrier, 55-58
Polarization, nuclear, 352
Positrons
from muon decay, 12, 14, 16
scattering of, 302-5
Protein synthesis
ultraviolet effects on, 68
Protons
deuteron reaction with, 333-34
electron scattering by, 231-312
inelastic scattering of, 339-42
neutron reaction with, 333-37
and nuclear emulsions, 339
pion production and, 333-39
pion reaction with, 318-27, 469
proton reaction with, 332-37
size of, 252-54, 261-64
Pupill triangle, 423

Q

Quadrupole moments, nuclear, 189, 195-201, 224

R

Rad, 136

Radiation damage
in radiochemical processing, 55-56
Radiation protection, 117-23
Radiation recovery, 123-27
Radiation therapy, 145-51, 165-67, 179
Radiobiology
biochemical effects in, 89-127
cellular enzymes and, 97-106
food sterilization and, 125-27
nucleic acid metabolism in, 106-10
oxygen effects in, 110-17
radiation protection and, 117-23
radiation recovery and, 123-25
theoretical, 73-74
whole-body irradiation in, 90-97

Radiobiology, cellular
see Cellular radiobiology
Radiobiology, vertebrate
see Vertebrate radiobiology
Radiochemical processes
contamination area in, 48-52
corrosion resistant materials in, 56-57
design of equipment for, 47-48
equipment for, 47-58
operation equipment and, 57-58
radiation damage in, 55-56
shielding in, 52-55
viewing and, 52-55
Radiochemical separations, 31-41

Radiodermatitis, 167-69
Radioenteritis, 170
Radioisotopes
in cellular systems, 82-84
spins of, 349-97
static moments of, 349-97
Radiology, 141
Radiopathology, 163-79
Radiosensitivity, definition of, 165

RBE, 143-44
Reciprocity
in biological irradiations, 63-65

Renal system, radiosensitivity of, 173

Resins
as ion exchange materials, 32
Roentgen, 136
Rotational levels, nuclear, 168, 195
Rubidium isotopes
spins, moments of, 366-75

SUBJECT INDEX

S

Salivary glands, radiosensitivity of, 170
 Scintillation telescope, 2
 Shielding
 in radiochemical processes, 52-55
 Silicon
 in hyperfine structure studies, 352
 Skin, radiosensitivity of, 167-69
 Solid state
 and nuclear moments, 352, 381-92
 Spallation, 341-42
 Spectrograph, ultraviolet, 64
 Spinal cord, radiosensitivity of, 176
 Spins
 of mesons, 17, 411
 Spins, nuclear, 349-97
 atomic beam method, 363-78
 measurements of, 349-53
 paramagnetic resonance method, 381-92
 of short-lived excited states, 392-97
 tabulation of, 379-81, 386-87
 theoretical aspects of, 353-63
 Spleen, radiosensitivity of, 165-67
 Spurion, 453
 Stars, nuclear emulsion pion induced, 330-32
 proton induced, 339
 Stomach, radiosensitivity of, 170-72
 Strange particles, 416
 Strangeness, conservation of, 415
 Sulphydryl compounds
 in radiation protection, 117, 121
 Survival curves, 73, 152

T

Target theory

in radiobiology, 73
 Teflon, radiosensitivity of, 56
 Testis, radiosensitivity of, 173-74
 Thiocyanates
 in ion exchange separations, 38
 Thyroid, radiosensitivity of, 175
 Time reversal, 12, 409, 413, 467
 Tracers, identification of, 41
 Tumors, ultraviolet-induced, 71

U

Ultraviolet radiation
 biological effects of, 63-72
 action spectrum and, 64
 cytoplasm damage by, 65-67
 dark recovery and, 68-70
 enzymes and, 66
 light recovery and, 70-72
 and low temperatures, 64-65
 spectrograph for, 64
 strain differences and, 66-67
 Universal Fermi Interaction, 433
 Uterus, radiosensitivity of, 174-75

V

Vertebrate radiobiology, 135-54, 163-79
 and capillaries, 169
 cellular radiosensitivity in, 164-65
 and connective tissues, 167-69
 and digestive system, 169-70
 dosimetry in, 136-37
 and endocrine glands, 175-76

and eyes, 177-78
 factors involved in, 141-50
 and gastrointestinal tract, 170-72
 and generative system, 173-75
 gram roentgen concept in, 145
 and hematopoietic system, 165-67
 irradiation recovery and, 151-52
 late effects in, 152-54
 lethal actions in, 135-54
 lethal dose values, 137-41
 and liver, 172
 and nervous system, 176-77
 and pancreas, 172-73
 pre-protection in, 150-51
 radiopathology and, 163-71
 and renal system, 173
 Viruses
 radiosensitivity of, 81-82
 ultraviolet inactivation of, 64
 Vitamins
 and irradiation of foods, 125

W

Waste disposal, radiochemical, 51-55

X

x-rays
 dose units for, 137
 mumesonic, 2-3, 17-25
 in radiobiology studies, 74-76, 80-81, 141

Z

Zirconium oxide
 hydrous
 as ion exchanger, 32

